EDUARDO ROCHETE ROPELLE

Caracterização da Transmissão do Sinal da Insulina e da Leptina em Hipotálamo de Roedores Durante a Anorexia Induzida pelo Câncer.

CAMPINAS

2010

EDUARDO ROCHETE ROPELLE

Caracterização da Transmissão do Sinal da Insulina e da Leptina em Hipotálamo de Roedores Durante a Anorexia Induzida pelo Câncer.

Tese de Doutorado apresentada à Pós-Graduação da Faculdade de Ciências Médicas da Universidade Estadual de Campinas para obtenção do título de Doutor em Fisiopatologia médica, área de concentração em Ciências básicas.

Orientador: *Prof. Dr José Barreto Campello Carvalheira*

CAMPINAS

2010

FICHA CATALOGRÁFICA ELABORADA PELA
BIBLIOTECA DA FACULDADE DE CIÊNCIAS MÉDICAS DA UNICAMP
Bibliotecário: Sandra Lúcia Pereira – CRB-8ª / 6044

R681c

Ropelle Eduardo Rochete
Caracterização da transmissão do sinal da insulina e da leptina em hipotálamo de roedores durante a anorexia induzida pelo câncer / Eduardo Rochete Ropelle. Campinas, SP : [s.n.], 2010.

Orientador : José Barreto Campello Carvalheira
Tese (Doutorado) Universidade Estadual de Campinas. Faculdade de Ciências Médicas.

1. Insulina. 2. Leptina. 3. Anorexia. 4. Câncer. I. Carvalheira, José Barreto Campello. II. Universidade Estadual de Campinas. Faculdade de Ciências Médicas. III. Título.

Título em inglês : Chraracterization of insulin and leptin signaling in the hypothalamus of rodents during cancer induced anorexia

Keywords:
- Insulin
- Leptin
- Anorexia
- Hypothalamus

Titulação: Doutor em Fisiopatologia Médica
Área de concentração: Medicina Experimental

Banca examinadora:

Prof. Dr. José Barreto Campello Carvalheira
Prof. Dr. Luiz Guilherme Siqueira Branco
Prof. Dr. Antonio Carlos Boschero
Profa. Dra. Silvana Auxiliadora Bordin
Prof. Dr. Gabriel Forato Anhe

Data da defesa: 05-03-2010

Banca examinadora da tese de Doutorado

Eduardo Rochete Ropelle

Orientador(a) : Prof(a). Dr(a). José Barreto Campello Carvalheira

Membros:

1. Prof(a). Dr(a). José Barreto Campello Carvalheira
2. Prof(a). Dr(a). Luiz Guilherme Siqueira Branco
3. Prof(a). Dr(a). Antonio Carlos Boschero
4. Prof(a). Dr(a). Silvana Auxiliadora Bordin
5. Prof(a). Dr(a). Gabriel Forato Anhe

Curso de pós-graduação em Fisiopatologia Médica da Faculdade de Ciências Médicas da Universidade Estadual de Campinas.

Data: 05/03/2010

DEDICATÓRIA

À Eloize Chiarreotto Ropelle,
ao meu filho João Otávio,
aos meus pais e à minha irmã
pelo estímulo e carinho.

AGRADECIMENTOS

Ao meu orientador Dr. José Barreto Campello Carvalheira por acreditar na minha capacidade, pela orientação competente e pelo exemplo como pesquisador e ser humano.

Ao professor Dr. Mário José Aballa Saad pelos ensinamentos e por toda a estrutura oferecida para a realização deste e de outros trabalhos.

Ao Dr. Lício Augusto Velloso pela atenção e pelo conhecimento compartilhado.

Ao Dr. Sigisfredo Luiz Brenelli oportunidade oferecida.

Ao Dr. José Rodrigo Pauli e Dr. Dennys Cintra pela amizade, capacidade, seriedade e dedicação. Muito obrigado monstros.

Ao Dr. Cláudio Teodoro de Souza pela amizade e conhecimentos compartilhados.

Ao Guilherme Rocha e Marília Dias pela dedicação e amizade.

À Dioze Guadagnini pelo trabalho competente.

Aos colegas de laboratório que me ajudaram durante a realização deste trabalho:

Alexandre Gabarra, Andréia M. Caricilli, Bruno Carvalho, Carlos Kiyoshi, Fabrício Camargo, Felipe C. Osório, Joseane Morari, Karina Zecchin, Marcelo Flores, Marco Antonio C. Filho, Maria Carolina Mendes, Mirian Ueno, Patrícia de O. Prada, Patty Karol Picardi e Tiago Araújo.

Apoio técnico:

Jósimo Pinheiro, Luiz Janeri, Márcio P. da Cruz, Sr. António, Sr. José e Sr. Luís.

Apoio financeiro:

Fundação de Amparo à Pesquisa do Estado de São Paulo (FAPESP).

SUMÁRIO

Pág.

LISTA DE ABREVEATURAS

α-MSH- Hormônio estimulador de melanócito alfa

ACTH- Hormônio adenocorticotrófico

AgRP- Proteína relacionada ao Agouti

AMP- Adenosina monofosfato

AMPK- Proteína quinase ativada por AMP

ARC- Núcleo arqueado do hipotálamo

ASOPTP1B- Oligonucleotídeo anti-sense contra Proteína tirosina Fosfatase 1B

ATP- Adenosina trifosfato

BAT- Tecido adiposo marrom

CART- *cocaine-and anphetamine–regulated transcription*

COBEA- Colégio brasileiro de experimentação animal

db/db- Camundongo deficiente do receptor de leptina

DMH- Núcleo dorsomedial do hipotálamo

EDTA- Ácido etilenodiaminotetracético

ELISA- *Enzyme Linked Immuno Sorbent Assay*

Foxo1- Fator de transcrição 1 da família *Forkhead box*

i.c.v.- Intracerebroventricular

IFN-γ- Interferon gama

IL-1R1- Receptor 1 de interleucina 1

IL-1β- Interleucina 1 beta

IL-6- Interleucina 6

IR- Receptor de insulina

IRS-1- Substrato do receptor de insulina-1

IRS-2- Substrato do receptor de insulina-2

Jak2- Proteína Janus quinase 2

LH- Hipotálamo lateral

LLC- Células de câncer de pulmão de Lewis

MC3R- Receptor de Melanocortina 3

MC4R- Receptor de Melanocortina 4

MIC-1 Citocina inibidora de macrófago-1

mRNA- Ácido ribonucleico (mensageiro)

Na_3VO_4- Ortovanadato de sódio

$Na_4P_2O_7$- Pirofosfato de sódio

NaCl- Cloreto de sódio

NaF- Fluoreto de sódio

NF-κB- Fator nuclear kappa B

NPY- Neuropeptídeo Y

ob/ob- Camundongo deficiente de leptina

OBR- Receptor de leptina

OBR_L- Receptor de leptina de forma longa

OBR_S- Receptor de leptina de forma curta

PC-3- Células de câncer de próstata

PI 3-K- fosfatidilinositol 3-quinase

PKC- Proteína quinase C

POMC- Proopiomelanocortina

PTP1B- Proteína Tirosina Fosfatase 1B

PVN- Núcleo paraventricular do hipotálamo

RAI- Radio-imuno ensaio

RNA- Ácido ribonucleico

S.E.M.- Erro padrão

SNC- Sistema nervoso central

SOCS-3- Supressor da sinalização de citocinas-3

STAT-3- Transdutor de sinal e ativador de transcrição 3

TNF-α- Fator de necrose tumoral

Tris- Tri (hidroximetil)-aminometano

UCP-1- Proteína desacopladora-1

VMH- Núcleo ventromedial do hipotálamo

W-256- Tumor de Walker-256

RESUMO

A síndrome anorexia-caquexia é observada em cerca de 80% dos pacientes com câncer em estágio avançado e contribui diretamente para o aumento da morbidade e mortalidade desses pacientes. Postula-se que a patogênese da anorexia do câncer seja mediada por persistentes sinais anorexigênicos no hipotálamo, contribuindo com a redução da ingestão alimentar e do peso corporal. No presente estudo, demonstramos que as vias anorexigênicas mediadas pela insulina e pela leptina no hipotálamo estão hipersensíveis durante a anorexia induzida por tumor em roedores. Identificamos que a expressão proteína tirosina fosfatase 1B (PTP1B), proteína que modula negativamente a via de transmissão do sinal da insulina e da leptina, está significativamente reduzida no tecido hipotalâmico em diferentes modelos de anorexia induzida pelo câncer, contribuindo assim para o aumento dos sinais anorexigênicos mediados principalmente pela STAT-3. Evidenciamos que mediadores pró-inflamatórios clássicos, como a IL-1 β e o TNF-α, participam do controle da expressão e atividade da PTP1B em neurônios. Demonstramos que a infusão central do anticorpo anti-IL-1 β ou do inibidor específico do TNF-α, o Infliximab, restaurou a atividade da PTP1B, reduzindo a sensibilidade à insulina e à leptina, aumentando a ingestão alimentar, peso corporal e a sobrevida em animais com tumor. Inversamente, as injeções do recombinante da IL-1 β ou do TNF-α diretamente no terceiro ventrículo hipotalâmico foram capazes de suprimir a expressão PTP1B neuronal e aumentar a sensibilidade à insulina e à leptina em animais controle. Finalmente, a redução seletiva da expressão da PTP1B em áreas em torno do terceiro ventrículo hipotalâmico através do uso do oligonucleotídeo antisense contra a PTP1B (PTP1B ASO), provocou anorexia, perda de peso corporal severa e morte em ratos controle e ainda inibiu os efeitos do anticorpo anti-IL-1 β e do Infliximab em ratos com anorexia. Coletivamente, estes dados mostram que a PTP1B hipotalâmica é proteína chave para o controle da ingestão alimentar e do peso corporal em roedores e representa um potencial avo terapêutico para o tratamento da anorexia induzida pelo câncer.

ABSTRACT

The anorexia-cachexia syndrome is observed in 80% of patients with advanced cancer and contributes directly to increased morbidity and mortality of these patients. It is postulated that the pathogenesis of cancer anorexia is mediated by persistent anorexigenic signs in the hypothalamus, contributing to the reduction of food intake and body weight. In this study, we demonstrated that the anorexigenic pathways mediated by insulin and leptin in the hypothalamus are hypersensitive during tumor-induced anorexia in rodents. We found that the expression protein tyrosine phosphatase 1B (PTP1B), a protein that negatively modulates the route of signal transmission of insulin and leptin, is significantly reduced in the hypothalamic tissue in different models of cancer-induced anorexia, contributing to the increase in anorexigenic signals mediated by STAT-3. We showed that classical pro-inflammatory cytokines, such IL-1β and TNF-α modulate PTP1B activity in neurons. We have shown that central infusion of, anti-IL-1β antibody or specific inhibitor of TNF-α, Infliximab, restored the PTP1B activity, reducing insulin and leptin sensitivity, increasing food intake, body weight and survival in tumor-bearing animals. Conversely, intracerebroventricular injections of recombinant IL-1β or TNF-α were able to suppress the PTP1B expression and increase the central insulin and leptin sensitivity in control animals. Finally, the selective reduction of PTP1B expression in areas around the third ventricle of the hypothalamus using the antisense oligonucleotide against PTP1B (PTP1B ASO), evoked anorexia, severe weight loss and death in control rats, in addition, PTP1B ASO blunted the effects of anti-IL-1β antibody or Infliximab in anorectic rats. Collectively, these data show that the hypothalamic PTP1B is key protein in the control of food intake and body weight in rodents and presents an attractive opportunity for the treatment of cancer-induced anorexia.

1-INTRODUÇÃO

A incidência de câncer no Brasil e no mundo.

Atualmente as neoplasias figuram entre as doenças com maior taxa de mortalidade em todo o mundo. Em 2005, de um total de 58 milhões de mortes ocorridas no mundo, os óbitos por câncer somaram 7,6 milhões, o que representou 13% de todas as mortes. O câncer de pulmão foi o que apresentou maior mortalidade, seguido pelos tumores de estômago, fígado, cólon e mama (WHO, 2009). Estima-se que no final da aproxima década ocorram cerca de 15 milhões de novos casos por ano (WHO, 2009). No Brasil, as estimativas mais recentes apontam que, a cada ano ocorram cerca de 466.000 casos novos de câncer (INCA, 2009). Os tipos mais incidentes, à exceção do câncer de pele do tipo não melanoma, são os cânceres de próstata e de pulmão, no sexo masculino, e os cânceres de mama e de colo do útero, no sexo feminino, acompanhando o mesmo perfil da magnitude observada no mundo (INCA, 2009). Diante de tal cenário, fica clara a necessidade de novos investimentos e estratégias para o controle do câncer, nos diferentes níveis de atuação como: na promoção da saúde, na detecção precoce, na assistência aos pacientes, na vigilância, na formação de recursos humanos, na comunicação e mobilização social e no desenvolvimento científico e tecnológico.

Durante as últimas décadas, importantes avanços científicos e tecnológicos aumentaram a capacidade de detecção precoce do câncer e aumentaram a eficácia dos esquemas de tratamento antineoplásicos. Esses avanços proporcionaram aumento da expectativa de vida e maior chance de cura em diversos tipos câncer. Consequentemente, o cuidado paliativo é cada vez mais importante no manejo de pacientes com câncer. Atualmente, oncologistas visam cada vez mais influenciar positivamente a qualidade de vida, o estado nutricional, bem como a sobrevivência (Laviano 2003). Os principais cuidados paliativos em pacientes oncológicos estão relacionados aos sintomas mais frequentes da doença, como, dor, fadiga e anorexia, (Laviano 2003). Em especial, a anorexia vem ganhando destaque nos últimos anos por influenciar diretamente a qualidade de vida dos pacientes e por ser considerada fator determinante para piora do prognóstico dos pacientes oncológicos (Bruera, 1997; Tisdale, 1997; Larkin, 1998).

Desenvolvimento da síndrome anorexia-caquexia em pacientes com câncer

O crescimento tumoral é frequentemente associado com o desenvolvimento de uma síndrome conhecida como, síndrome da anorexia-caquexia. Etimologicamente, o termo anorexia deriva do grego “an”, deficiência ou ausência de, e “orexis”, apetite. Desta forma, a anorexia pode ser definida como a perda do desejo de comer. A anorexia é um relevante problema no manejo clínico de pacientes com câncer, uma vez que afeta o curso clínico da doença e está diretamente associada ao aumento da morbidade e mortalidade dos pacientes (Bruera, 1997; Tisdale, 1997; Larkin, 1998).

A anorexia é um dos principais indutores de caquexia, embora o padrão de perda de peso observado na caquexia difira daquele observado na restrição alimentar (Tisdale, 1997). A chamada síndrome anorexia-caquexia é observada em cerca de 80% dos pacientes com câncer em estágio avançado (Ramos *et al.*, 2004). A caquexia é um estado involuntário de perda de peso encontrado em doenças neoplásicas, infecciosas e inflamatórias que contribui diretamente para a mortalidade dessas moléstias.

A palavra caquexia deriva do grego “kakos” que significa “mal” e “hexis” que quer dizer “condição” (Tisdale, 1997). Aproximadamente metade dos pacientes com câncer desenvolve caquexia, caracterizada por anorexia e diminuição do tecido adiposo e da massa muscular. Geralmente, pacientes com tumores sólidos têm uma maior frequência de caquexia (Bruera, 1997). No momento do diagnóstico, aproximadamente 80% dos pacientes com câncer do trato gastrointestinal e 60% dos pacientes com câncer de pulmão têm perda de peso significativa. A caquexia é mais comum em crianças e idosos e se torna mais pronunciada com a evolução da neoplasia. Pacientes oncológicos com perda ponderal maior que 10% do peso corporal possuem menor sobrevida quando comparado a pacientes com o mesmo tipo e estádio da doença que se mantém eutróficos (Whitman, 2000). Evidências obtidas em estudo clínico apontam ainda que o hipermetabolismo e a perda de peso significativa predispõem a menor sobrevida, enquanto o aumento da ingestão energética foi associado ao aumento da sobrevida (Bosaeus *et al.*, 2002).

O hipotálamo no controle da anorexia induzida pelo câncer.

A síndrome anorexia-caquexia é desencadeada por uma inter-relação complexa de variáveis metabólicas e comportamentais que se correlacionam com prognósticos ruins e comprometimento da qualidade de vida (Bruera, 1997; Tisdale, 1997; Larkin, 1998). Apesar da etiologia da caquexia não ser bem definida, várias hipóteses têm sido exploradas incluindo a participação de citocinas, hormônios circulantes, neuropeptídeos, neurotransmissores e fatores derivados dos tumores (Schwartz *et al.*, 1995; Plata-Salaman, 1997; Larkin, 1998). Entretanto, a hipótese de que a síndrome anorexia-caquexia seja causada pela ação das citocinas potencializando os sinais anorexigênicos no sistema nervoso central (SNC) tem ganhado destaque nos últimos anos.

Postula-se que numerosas citocinas (TNF-α, IL-1, IL-6, IFN-γ) participem da síndrome anorexia-caquexia observada em pacientes com câncer. As citocinas podem ser produzidas pelo tumor, liberadas na circulação e transportadas para o cérebro através da barreira hematoencefálica e órgãos circunventriculares (áreas que permitem a passagem mais fácil de moléculas na barreira hematoencefálica). Uma vez no tecido hipotalâmico, estas citocinas induzem potentes sinais anorexigênicos, resultando em menor ingestão alimentar, maior gasto energético (Figura 1).

Figura 1

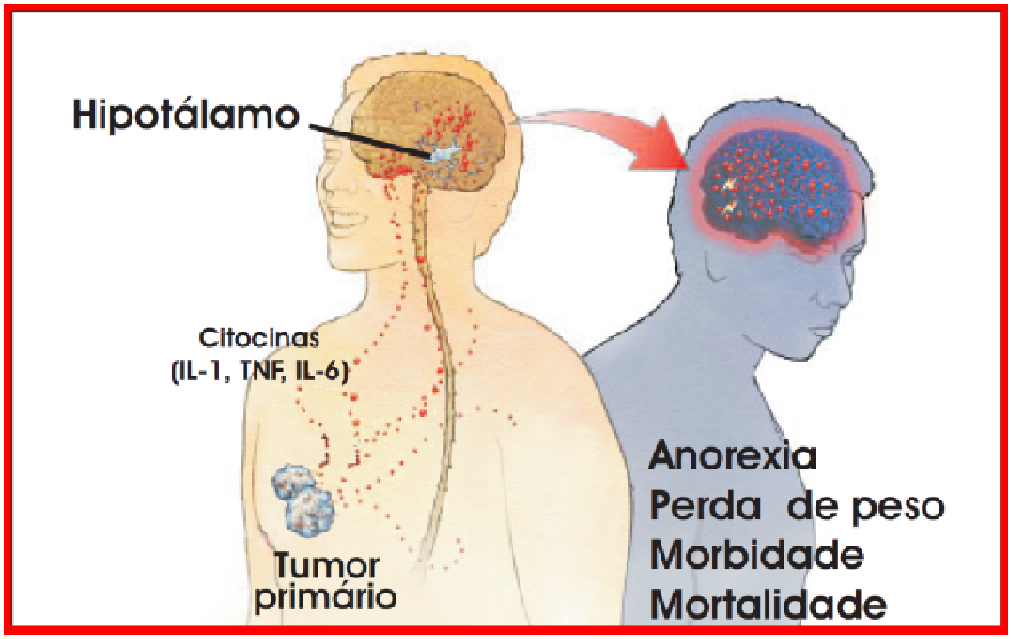

Figura 1- *Mecanismo de ação das citocinas inflamatórias na indução de anorexia mediada por tumor.*

Por outro lado, as citocinas também são produzidas por neurônios e células da glia do sistema nervoso central, em resposta ao aumento das citocinas periféricas (Hopkins & Rothwell, 1995; Rothwell & Hopkins, 1995; Licinio & Wong, 1997; Sternberg, 1997; Haslett, 1998; Mantovani *et al.*, 1998). Embora o local da síntese de citocinas no sistema nervoso central seja dependente da natureza do estímulo, as doenças sistêmicas parecem influenciar predominantemente a atividade hipotalâmica, área com a maior densidade de receptores para a maioria das citocinas (Hopkins & Rothwell, 1995).

A administração crônica dessas citocinas pró-inflamatórias, tanto isoladamente como em conjunto são capazes de reduzir a ingestão alimentar e reproduzir as diferentes características da síndrome anorexia-caquexia (Gelin *et al.*, 1991; Moldawer *et al.*, 1992; Matthys & Billiau, 1997b; Tisdale, 1997; Mantovani *et al.*, 1998). Outras evidências do envolvimento dessas citocinas na regulação do peso corporal no hipotálamo foram adquiridas através de estudos com neutralização específica das diversas citocinas através de anticorpos (Sherry *et al.*, 1989; Noguchi *et al.*, 1996; Matthys & Billiau, 1997a). Recentemente descrevemos que a *AMP-activated protein kinase* (AMPK) neuronal pode

desempenhar papel antiinflamatório importante durante a anorexia induzida pelo câncer. A administração intracerebroventricular, intraperitoneal ou oral de diferentes ativadores da AMPK, foi capaz de reduzir a expressão de moléculas inflamatórias e modular neuropeptídeos envolvidos do controle da ingestão alimentar, atenuando a anorexia e aumentando a sobrevida em ratos com anorexia induzida por tumor (Ropelle *et al.*, 2007).

Alguns estudos apontam que, os sinais anorexigênicos gerados pelas citocinas pró-inflamatórias no hipotálamo ocorram em virtude da ativação de uma sub-população de neurônios especializada na propagação de sinais anorexigênicos. Esses sinais podem ser mediados principalmente pelos receptores de melanocortinas 3 e 4 MC3R e MC4R (Laviano *et al.*, 2008). Além disso, postula-se que as citocinas pró-inflamatórias possam também induzir anorexia através da complexa rede neural que envolve vias de sinalização responsáveis pela transmissão de sinais anorexigênicos mediados por hormônios como insulina e leptina. Estudos conduzidos em ratos demonstraram que a administração intracerebroventricular de interleucina-6 (IL-6) é capaz de potencializar os efeitos anorexigênicos mediado pela leptina e pela insulina no hipotálamo (Flores *et al.*, 2006; Ropelle *et al.*, 2008), sugerindo uma relação sinérgica entre esta citocina e a transmissão do sinal desses dois hormônios na supressão do apetite. Adicionalmente, Johnen e colaboradores identificaram que a proteína *Macrophage inhibitory cytokine-1* (MIC-1) produzida e liberada na circulação a partir do desenvolvimento tumoral, é capaz de alcançar o sistema nervoso central e induzir anorexia através da ativação da proteína distal da via de sinalização da leptina a *Signal Transducers Activators of Transcription 3* (STAT3), modulando neuropeptídeos hipotalâmicos envolvidos no controle da saciedade (Johnen *et al.*, 2007). Coletivamente, esses dados sugerem que as vias de transmissão dos sinais mediados por insulina e leptina no sistema nervoso central têm participação crucial na perpetuação de sinais anorexigênicos durante o desenvolvimento tumoral, entretanto, os mecanismos moleculares que envolvem a ação de citocinas sobre sinalização da leptina e insulina no hipotálamo no desenvolvimento da anorexia induzida pelo tumor ainda são desconhecidos.

Transmissão do Sinal de Insulina e Leptina em Hipotálamo de Ratos: Inter-relações e Implicações Fisiopatológicas

A leptina é expressa principalmente no tecido adiposo e em menores quantidades no epitélio gástrico e placenta (Maffei *et al.*, 1995; Masuzaki *et al.*, 1997; Bado *et al.*, 1998). A proteína do gene *ob* está presente no plasma de camundongos normais, como um monômero com peso molecular de 16 kDa, não foi detectada em plasma de camundongos *ob/ob*, e foi observada em concentrações elevadas em camundongos *db/db* (Halaas *et al.*, 1995). A administração de leptina a camundongos *ob/ob* resulta em diminuição da ingestão alimentar, perda de peso e redução dos níveis glicêmicos (Campfield *et al.*, 1995), além de aumentar a atividade simpática em tecido adiposo marrom, com conseqüente aumento do gasto energético (Pelleymounter *et al.*, 1995). Entretanto, o mesmo resultado não foi observado quando este hormônio foi injetado nos animais *db/db*.

Os níveis séricos de leptina correlacionam-se de forma positiva com o índice de massa corporal na grande maioria das populações estudadas (Frederich *et al.*, 1995; Maffei *et al.*, 1995; Considine *et al.*, 1996; Havel *et al.*, 1998). A secreção desse hormônio diminui com o jejum prolongado e estímulo β-adrenérgico (Ahima *et al.*, 1996) e aumenta em resposta à administração de insulina e glicocorticóides (De Vos *et al.*, 1995; Saladin *et al.*, 1995). A leptina é secretada de forma pulsátil e inversamente relacionada à atividade do eixo ACTH-Cortisol, ou seja, ocorre diminuição da secreção de leptina ao amanhecer e aumento no final da tarde (Licinio *et al.*, 1997). A leptina produzida pelo tecido adiposo informa o estado nutricional do indivíduo a centros hipotalâmicos, que regulam a ingestão alimentar e o gasto energético. Assim, a redução da quantidade de tecido adiposo leva a diminuição dos níveis circulantes de leptina, estimulando a ingestão alimentar e reduzindo o gasto energético. Contrariamente, o aumento do estoque de tecido adiposo está associado à elevação dos níveis séricos de leptina, diminuindo a ingestão alimentar e aumentando o gasto energético.

O receptor de leptina (OBR) é membro da família gp130 da classe I dos receptores de citocinas (Tartaglia *et al.*, 1995). É encontrado em muitos tecidos com várias formas de *splicing*, sendo as mais encontradas a forma curta (OBRs), expressa em vários tecidos, que apresenta domínios intracelulares truncados, e a forma longa (OBRL), que apresenta domínios intracelulares longos e é expressa principalmente no hipotálamo (núcleos paraventricular, arqueado, ventromedial e dorsomedial (Mercer *et al.*, 1996; Woods *et al.*,

1996). O OBRs não tem sua função bem definida, mas parecem influir no transporte da leptina através da barreira hematoencefálica.

A homologia do receptor de leptina à classe I dos receptores de citocinas forneceu informações importantes para a descoberta dos possíveis mediadores intracelulares da ação da leptina. Os receptores da classe I das citocinas agem através das famílias das proteínas Jak (*Janus Kinase*) e STAT (*Signal Transducers Activators of Transcription*) (Heldin, 1995). Tipicamente, as proteínas Jak estão constitutivamente associadas com sequências de aminoácidos dos receptores, e adquirem sua atividade tirosina quinase após a ligação do hormônio a seu receptor. Uma vez ativada, a proteína Jak fosforila o receptor induzindo a formação de um sítio de ligação para as proteínas STAT, as quais são ativadas após terem se associado ao receptor e serem fosforiladas pela Jak. As proteínas STATs ativadas, são translocadas para o núcleo e estimulam a transcrição gênica (Figura 2). No entanto a homologia do receptor de leptina à classe I dos receptores de citocinas, permite que várias outras citocinas amplifiquem a transmissão do sinal da leptina. Assim as proteínas subsequentes ao receptor de leptina (Jak e STAT) podem exercer uma interface no controle da ingestão alimentar, regulando fatores de saciedade e adiposidade à longo prazo (através da própria leptina) ou desenvolvendo sinais anorexigênicos patológicos (através de citocinas) (Plata-Salaman, 1996).

O receptor de leptina é capaz de estimular outras vias de sinalização além da Jak/STAT, tais como a via da proteína quinase ativadora de mitose (MAPK) e a via de fosfatidilinositol 3-quinase (PI 3-K) (Heldin, 1995), e é possível que a capacidade do OBR controlar o peso dependa também destas vias de sinalização (Tartaglia, 1997; Niswender *et al.*, 2001).

Após a ativação dos receptores de leptina no cérebro e das proteínas envolvidas na transmissão do sinal desse hormônio, respostas neuronais integradas são necessárias para modular a ingestão alimentar e o gasto energético. Alguns neurotransmissores importantes para o funcionamento dessa rede neuronal estimulam a ingestão alimentar como o neuropeptídeo Y (NPY) (Stephens *et al.*, 1995) e o *Agouti related peptide* (AGRP) (Shutter *et al.*, 1997), enquanto outros provocam redução da ingestão alimentar como o *cocaine-and*

anphetamine–regulated transcription (CART) (Kristensen *et al.*, 1998) e o *melanocyte stimulating hormone* (α-MSH) (Fan *et al.*, 1997). A leptina regula o balanço energético diminuindo os níveis de neuropeptídeos anabólicos NPY e AGRP e aumentando a concentração de neuropeptídeos catabólicos CART e α-MSH. Os neurônios que expressam esses neuropeptídeos interagem com cada outro e com sinais advindos da periferia (como a insulina, leptina, grelina, etc), atuando na regulação do controle e do gasto energético (Flier, 2004). A localização precisa dos receptores neurais para cada sinal orexigênico e anorexigênico não esta totalmente compreendida. Sabe-se, no entanto, que os receptores para estes sinais estão presentes principalmente no núcleo arqueado (ARC) e paraventricular (PVN) hipotalâmico, mas eles não estão restritos a estas áreas (Wynne *et al.*, 2005).

Assim como a leptina, a insulina também é considerada um hormônio que sinaliza ao hipotálamo o estoque de tecido adiposo e modula a ingestão alimentar (Woods *et al.*, 1979; Woods *et al.*, 1985). A insulina circula em níveis proporcionais ao conteúdo de tecido adiposo e atravessa a barreira hematoencefálica via um sistema de transporte saturável em níveis proporcionais aos plasmáticos (Baura *et al.*, 1993). Os receptores de insulina são expressos por neurônios envolvidos na ingestão alimentar (Baskin *et al.*, 1988; Cheung *et al.*, 1997; Baskin *et al.*, 1999). A administração de insulina no sistema nervoso central reduz a ingestão alimentar e diminui o peso corporal, enquanto a deficiência desse hormônio causa hiperfagia (Sipols *et al.*, 1995).

A correlação dos níveis séricos de insulina com o conteúdo de gordura corporal é consequência da resistência à insulina induzida pelo aumento da gordura corporal (Schwartz *et al.*, 1997). Assim, à medida que o peso corporal aumenta a insulina deve aumentar para compensar a resistência à insulina e manter a homeostase de glicose (Polonsky *et al.*, 1988; Kahn *et al.*, 1993). A sinalização intracelular da insulina em tecidos insulino-sensíveis inicia-se com a ligação do hormônio a um receptor específico de membrana, uma proteína heterotetramérica com atividade quinase, composta por duas subunidades α e duas subunidades β. A ligação da insulina à subunidade α estimula a autofosforilação da região intracelular da subunidade β do receptor. Uma vez ativado, o receptor de insulina fosforila vários substratos protéicos em tirosina incluindo membros da

família dos substratos dos receptores de insulina (IRS-1/2/3), Shc, Gab-1 e Cbl. A fosforilação em tirosina das proteínas IRS cria sítios de reconhecimento para moléculas contendo domínios com homologia à Src 2 (SH2). Dentre estas se destaca a PI 3-quinase. A fosforilação das proteínas IRSs cria sítios de ligação para a PI 3-K, promovendo a sua ativação (Figura 2). Atualmente, a PI 3-K é a única molécula intracelular inequivocamente considerada essencial para o transporte de glicose (Czech & Corvera, 1999). As proteínas alvo conhecidas dessa enzima são a Akt e as isoformas atípicas da PKC (ζ e λ), porém a função dessas proteínas no transporte de glicose ainda não está bem estabelecida (Kohn *et al.*, 1996; Bandyopadhyay *et al.*, 1997; Kitamura *et al.*, 1998; Kotani *et al.*, 1998; Kim *et al.*, 1999).

Dentre os alvos da Akt, destaca-se a *forkhead transcriptional factor subfamily forkhead box O1* (Foxo-1 ou FKHR), que atua como fator de transcrição. A fosforilação da Akt induz a fosforilação e a manutenção da Foxo1 no meio citplasmático, inibindo sua atividade transcricional (Figura 2). Por outro lado, a baixa fosforilação desta proteína é correlacionada com o aumento da sua expressão e atividade transcricional no núcleo celular. A Foxo1 está presente em neurônios POMC e AgRP, tendo sua região promotora em região adjacente à região promotora da STAT3 nestes neurônios, promovendo uma constante competição pela região promotora (Kim *et al.*, 2006; Kitamura *et al.*, 2006). A hiperexpressão da Foxo1 em neurônios é responsável por inibir a ação anorexigênica da leptina, aumentando a ingestão alimentar e o peso corporal em camundongos (Kitamura *et al.*, 2006). Desta forma a Foxo1 pode ser considerada principal proteína, distal à via da insulina, responsável pelo controle da homeostase energética. O esquema abaixo representa as vias de sinalização da insulina e leptina no controle da ingestão alimentar (Figura 2).

Figura 2

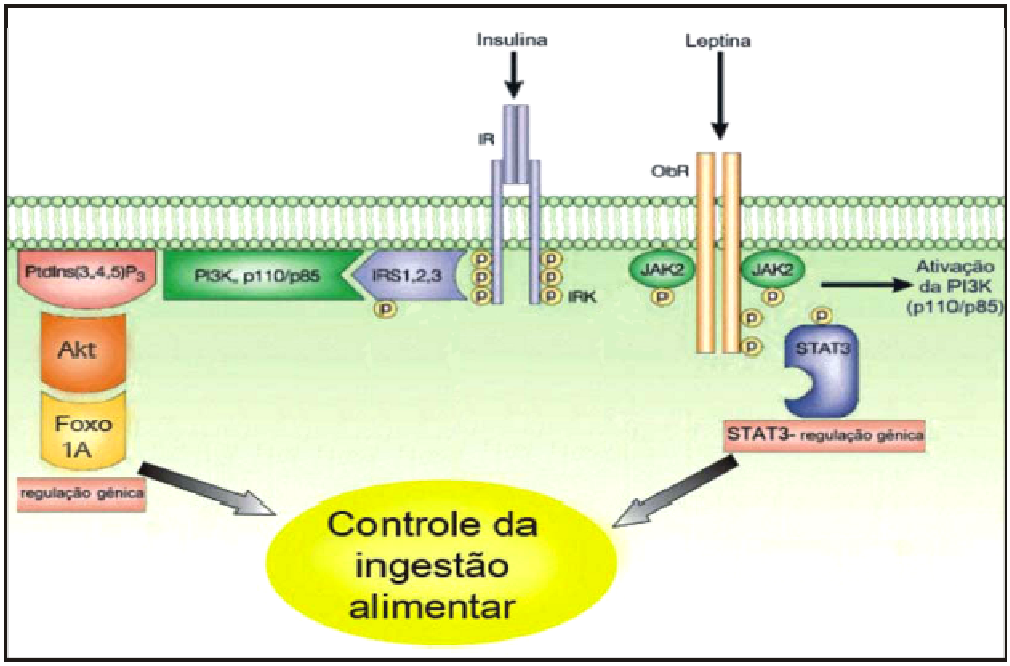

Figura 2*- Esquema representativo das vias de sinalização da insulina (à esquerda) e da leptina (à direita) no controle da ingestão alimentar em células neuronais.*

A PTP1B neuronal no controle da ingestão alimentar.

O balanço entre a fosforilação e a desfosforilação de proteínas é a base para o controle de diversos eventos biológicos disparados por efetores extracelulares, como hormônios, agentes carcingênicos, citocinas, neurotransmissores e substâncias ou metabólicos tóxicos (Harrison *et al.*, 1999). Estima-se que 30% das proteínas intracelulares são fosfoproteínas e que cerca de 4% do genoma eucariótico codifique proteínas quinases e proteínas fosfatases (Hunter, 1995). As atividades de proteínas quinases e fosfatases são minuciosamente reguladas *in vivo*. Modificações na atividade dessas enzimas podem proporcionar consequências graves, que incluem neoplasias, diabetes, inflamação e doenças resultantes de defeitos imunológicos (Harrison *et al.*, 1999). Recentemente a descrição da atividade da Proteína Tirosina Fosfase 1B (PTP1B) no sistema nervoso central ajudou a elucidar como ocorrem as alterações do *status* de fosforilação das proteínas envolvidas na transmissão do sinal da insulina e da leptina no tecido hipotalâmico de roedores obesos.

A PTP1B é a principal proteína tirosina fosfatase implicada na regulação da ação da insulina e da leptina (Seely *et al.*, 1996; Elchebly *et al.*, 1999). Evidências genéticas e bioquímicas demonstram um importante papel da PTP1B como um regulador negativo da fosforilação da tirosina de componentes principais da via de sinalização da insulina e da leptina. Diversos estudos examinaram a expressão PTP1B em roedores e seres humanos com a resistência à insulina, diabetes e obesidade, relatando aumento da expressão e / ou atividade da PTP1B nestes estados (Ahmad & Goldstein, 1995; Dadke *et al.*, 2000; Venable *et al.*, 2000; Ropelle *et al.*, 2006).

Essa fosfatase é expressa em diferentes tecidos sensíveis à insulina e à leptina e diferentes estudos em cultura de células e em roedores, indicam que esta enzima se associa ao receptor de insulina (IR) e aos substratos 1 e 2 do receptor de insulina (IRS-1 e IRS-2) promovendo a desfosforilação dessas proteínas atenuando o sinal da insulina (Goldstein *et al.*, 2000; Di Paola *et al.*, 2002; Hirata *et al.*, 2003). De forma semelhante, a PTP1B também regula negativamente a transmissão do sinal da leptina através da interação direta com a proteína Jak2 (Cheng *et al.*, 2002; Johnson *et al.*, 2002). A figura 3 demonstra o mecanismo de ação da PTP1B nas vias de sinalização da insulina e leptina (Figura 3).

Figura 3

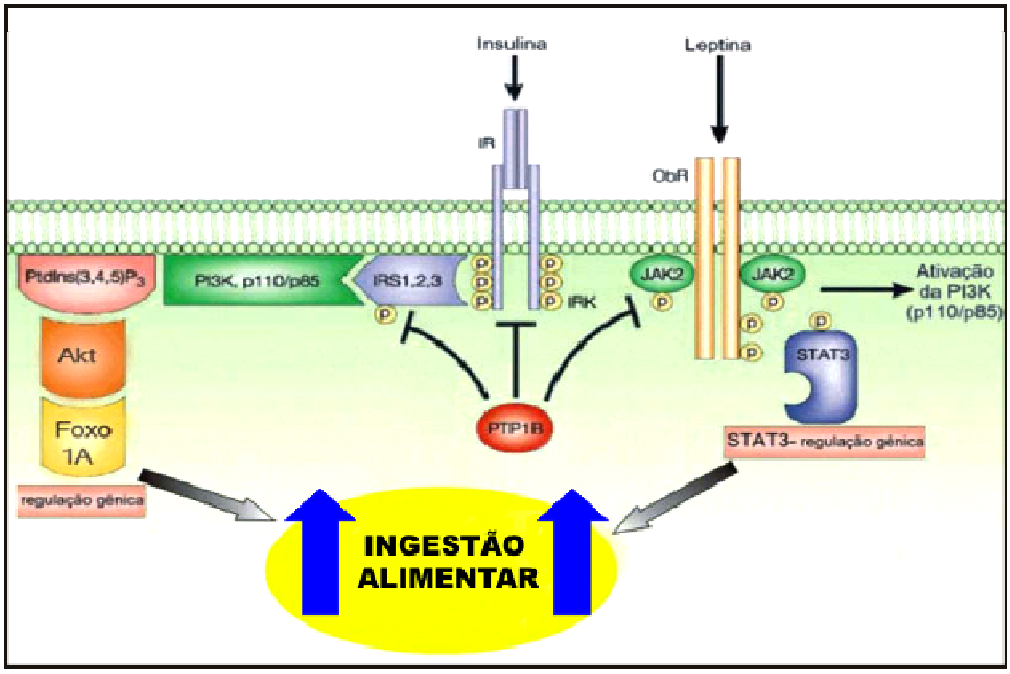

Figura 3*- A Proteína tirosina fosfatase 1B (PTP1B) tem a capacidade de se associar ao receptor de insulina (IR), ao substrato do receptor de insulina-1 (IRS-1) e à Janus quinase 2 (Jak2). A ligação à estas proteínas é acompanhada da desfosforilação de resíduos de tirosina e atenuação da transdução dos mediados pela insulina e pela leptina. Em neurônios hipotalâmicos o aumento da atividade da PTP1B resulta em aumento da ingestão alimentar.*

Um único estudo conduzido em cultura de células embrionárias de rim humano (HEK) 293 demonstrou e que a PTP1B também é capaz de desfosforilar a STAT3, reduzindo sua capacidade transcricional (Lund *et al.*, 2005). No entanto, a ação da PTP1B sobre a atividade da STAT3 necessita de novos estudos.

O papel da PTP1B hipotalâmica no controle dos sinais de saciedade passou a ser explorado apenas nos últimos 7 anos. A primeira evidência de que essa fosfatase poderia induzir resistência à leptina em neurônios, partiu de um estudo realizado em uma linhagem de células hipotalâmicas de camundongos, GT1-7. A hiperexpressão da PTP1B nestas células atenuou a transmissão do sinal da leptina reduzindo a ativação da via Jak/STAT

(Kaszubska *et al.*, 2002). Posteriormente, estudos em modelo experimental de obesidade evidenciaram que roedores submetidos à dieta rica em gordura apresentaram elevados níveis de PTP1B no tecido hipotalâmico, em paralelo à menor sensibilidade à insulina e leptina (Picardi *et al.*, 2008; White *et al.*, 2009).

Neste sentido, Picardi e colaboradores estabeleceu que a redução da expressão da PTP1B em neurônios que controlam o apetite é capaz de atenuar a resistência central à insulina e à leptina em hipotálamo de animais obesos, reduzindo o peso corporal. Para tal, os autores utilizaram a infusão intracerebroventricular do oligonucleotídeo antisense contra a PTP1B. O tratamento durante 4 dias consecutivos foi suficiente para a reduzir a expressão da PTP1B e restabelecer a ativação das vias PI3-K/Akt e Jak/STAT no hipotálamo (Picardi *et al.*, 2008). Adicionalmente, recente estudo demonstrou que a ausência da PTP1B hipotalâmica está envolvida no aumento da sinalização anorexigênica em camundongos. Bence e colaboradores observaram que a animais gerados com ausência da PTP1B, especificamente no hipotálamo, apresentaram hipersensibilidade a leptina e aumento considerável do gasto energético evidenciando a importância da participação desta proteína em neurônios hipotalâmicos para o controle dos sinais anorexigênicos em roedores (Bence *et al.*, 2006).

Coletivamente, esses dados apontam que a PTP1B neuronal é proteína chave no controle da homeostase energética, de forma que, o aumento da sua atividade se relaciona estreitamente com a prevalência da hiperfagia e obesidade, por outro lado, sua ausência proporciona aumento dos sinais anorexigênicos e maior gasto energético. Embora alguns estudos tenham centrado esforços para investigar o papel da PTP1B no desenvolvimento da obesidade, evidências da participação desta fosfatase no sistema nervoso central no desenvolvimento da anorexia são inexistentes.

2-OBJETIVOS

2.1 Objetivo geral

Caracterizar as vias de transmissão de sinal da insulina e da leptina em hipotálamo de roedores com anorexia induzida por tumor, bem como, evidenciar papel da PTP1B neuronal neste contexto.

2.2 Objetivo específico

- Caracterizar a sensibilidade à insulina e à leptina em hipotálamo de amimais com anorexia induzida por tumor.
- Investigar o papel de diferentes moduladores da via de sinalização da insulina e da leptina, como a SOCS-3, SH-PTP2 e a PTP1B, no hipotálamo durante anorexia induzida por tumor.
- Investigar os efeitos da infusão intracerebroventricular de mediadores antiinflamatórios sobre a expressão da PTP1B hipotalâmica, sobre a sensibilidade à insulina e à leptina, ingestão alimentar, gasto energético e sobrevida em animais com anorexia induzida por câncer.
- Determinar os efeitos da infusão intracerebroventricular do recombinante da Interleucina-1 Beta (IL-1β) e do Fator de Necrose Tumoral Alfa (TNF-α) sobre a expressão da PTP1B hipotalâmica e sobre a sensibilidade à insulina e à leptina em ratos controle.
- Avaliar os efeitos da infusão intracerebroventricular do oligonucleotídeo antisense contra a PTP1B (ASOPTP1B) sobre a sensibilidade à insulina e à leptina, ingestão alimentar, gasto energético e sobrevida em ratos controle.

3-CAPÍTULO

3.1 - Artigo 1

PTP1B: A Key Phosphatase in Cancer-Induced Anorexia.

Ropelle ER[1], Rocha GZ[1], Cintra DE[1], Marin RM[1], Dias MM[1], Pauli JR[1], Picardi PK[1], Prada PO[1], Zecchin KG[2], Velloso LA[1], Saad MJA[1], Carvalheira JBC[1].

[1-] Department of Internal Medicine, FCM, State University of Campinas (UNICAMP), Campinas, São Paulo, Brazil.

[2-] Department of Clinical Pathology, FCM, State University of Campinas (UNICAMP), Campinas, São Paulo, Brazil.

Please address correspondence to:

José B. C. Carvalheira, MD.
Department of internal medicine
FCM - State University of Campinas (UNICAMP)
13081-970 - Campinas, SP, Brazil.
Fax: + 55 19 3521-8950
E-mail: carvalheirajbc@uol.com.br

ABSTRACT

Cancer anorexia-cachexia syndrome is observed in 80% of patients in the advanced stages of cancer and is a strong independent risk factor for mortality. Accumulating evidence indicates that the pathogenesis of cancer anorexia is mediated by persistent anorexigenic signals into the hypothalamus. Here, we show that neuronal Protein Tyrosine Phosphatase 1B (PTP1B) represents a core modulator of food intake and energy expenditure during cancer-induced anorexia. Hypothalamic PTP1B expression is markedly reduced in different models of cancer-induced anorexia in rodents, contributing to anorexigenic signals mediated by STAT-3. Furthermore, we found that classical pro-inflammatory mediators are able to suppress neuronal PTP1B expression. A selective transient reduction of PTP1B expression in areas surrounding the third ventricle of the hypothalamus, driven by antisense oligonucleotide (ASO PTP1B), evoked anorexia, severe weight loss and death in control rats. Intrahypothalamic infusion of recombinant IL-1β or TNF-α reduces the PTP1B expression in the hypothalamus of control rats. Conversely, central infusion of anti-IL-1β antibody or the specific TNF-α inhibitor, Infliximab, restored PTP1B activity, increasing food intake, body weight and survival in tumor-bearing animals. Conversely, forced reduction in PTP1B expression, using an intrahypothalamic infusion of ASOPTP1B blunts the effects of anti-IL-1β antibody or Infliximab on increased food intake and survival in tumor-bearing rats. Collectively, these data show that hypothalamic PTP1B activity links the central inflammation and the anorexigenic signals during cancer-induced anorexia.

INTRODUCTION

Anorexia and weight loss are part of the wasting syndrome of late-stage cancer and are a major cause of morbidity and mortality in cancer (1, 2). Anorexic cancer patients often report early satiety, which together with a reduced appetite has been postulated to be caused by the production of factors by the tumor that exerts their effects by acting on hypothalamic cells, amplifying the anorexigenic signals (3, 4). The pro-inflammatory cytokines such as tumor necrosis factor-α (TNF-α), interleukin 1 (IL-1β), and interferon gamma (IFN γ) are the major products secreted by the tumor proposed to play a role in the etiology of cancer-induced anorexia (3). Distinct neuron subpopulations of the arcuate nucleus of the hypothalamus act as the sensors for the energy stores in the body and coordinate a complex network of neurons that, in due course, control the balance of hunger versus satiety, and pro- versus anti-thermogenesis (5, 6). These first-order neurons are equipped with receptors and intracellular molecular systems capable of detecting subtle or chronic changes in the levels of hormones and nutrients present in the bloodstream (6).

It is well established that Protein Tyrosine Phosphatase 1B (PTP1B), a negative modulator of leptin and insulin signaling, is a key phosphatase involved in the control of food intake and energy expenditure by acting in the hypothalamus (7, 8). PTP1B is localized to the cytoplasmic face of the endoplasmic reticulum and is expressed ubiquitously (9). This phosphatase can associate with and dephosphorylate activated insulin receptor (IR), insulin receptor substrates (IRS), Jak2 and STAT3 (10-14). Thus, once activated, hypothalamic PTP1B activity induces insulin and leptin resistance, as demonstrated in an animal model of obesity (8, 15), and leptin resistance in aging rats (16).

Conversely, previous studies have demonstrated that the selective ablation of neuronal PTP1B induces hypersensitivity to insulin and leptin in rodents (7, 8). In addition, specific neuronal PTP1B knockout mice have reduced body weights, adiposity and increased energy expenditure.

To date, increased PTP1B activity has been implicated in the development of central insulin and leptin resistance and obesity, whereas the impact of PTP1B on the development of anorexia has not been addressed. Thus, we examined the role of hypothalamic PTP1B on the control of food intake and energy expenditure in different models of cancer-induced anorexia in rodents.

MATERIALS AND METHODS

Reagents for SDS-PAGE and immunoblotting were from Bio-Rad Laboratories (Hercules, CA). Tris, aprotinin, ATP, dithiothreitol, phenylmethylsulfonyl fluoride, Triton X-100, Tween 20, glycerol, and BSA (fraction V) were from Sigma Chemical Co. (St. Louis, MO). Nitrocellulose paper (BA85, 0.2 mm) was from Schleicher & Schuell (Keene, NH). Ketamine hydrochloride was from Cristália (Itapira SP, Brazil). Anti-phospho- Jak2 antibody was from Upstate Biotechnology (Charlottesville, VA, USA). Anti-Jak2, anti-STAT3, anti-phospho-IRβ, anti-IRβ, anti-phospho-IRS-1, anti-IRS-1, anti-FOXO1, anti-IL-1β, anti-UCP-1 and anti-PGC-1α antibodies were from Santa Cruz Biotechnology, Inc. Anti -phospho- STAT3 (rabbit, anti-phospho-Akt, anti-phospho-FOXO1, anti-beta tubulin and anti-Akt were from Cell Signalling Technology (Beverly, MA, USA). Recombinant IL-1β, TNF-α and leptin were from Calbiochem (San Diego, CA, USA). Human recombinant insulin (Humulin R) was from Lilly (Indianapolis, IN, USA). The anti-TNF-α monoclonal antibody, Infliximab, was from Centocor (Horsham, PA). Routine reagents were purchased from Sigma Chemical Co. (St. Louis, MO), unless otherwise specified. The doses administrated in each experimental group are given below.

Animals and surgical procedures

Adult male Wistar rats (250-300 g), C57BL6/J (21-23 g) and SCID (18-22 g), were used in all of the experiments in accordance with the guidelines of the Brazilian College for Animal Experimentation; the Ethics Committee at the State University of Campinas approved experiments. Room temperature was maintained (28 ± 1° C), and rats were housed in individual cages, subjected to a standard light-dark cycle (0600–1800/1800–0600

h) and provided with standard rodent chow and water *ad libitum*. After an overnight fast, the rats were anesthetized with ketamine hydrochloride (100 mg/kg, ip) and positioned on a Stoelting stereotaxic apparatus. The implantation of an intracerebroventricular (i.c.v.) catheter into the third ventricle has been previously described (17). After a 5-day recovery period, cannula placement was confirmed by a positive drinking response after administration of angiotensin II (40 ng per 2 µl), and animals that did not drink 5 ml of water within 15 min after treatment were not included in the experiments.

Cell culture

The human prostate cancer cell line, PC-3, and Lewis lung carcinoma (LLC) were obtained from ATCC, Philadelphia, PA, USA and the Walker-256 tumor cell line (originally obtained from the Christ Hospital Line, National Cancer Institute Bank, Cambridge, UK). Cells were cultured in RPMI containing 10% fetal bovine serum and glutamine without addition of antibiotics or fungicides; they were maintained at 37°C, 5% CO2.

Tumor xenograft models

Male SCID mice were implanted with 1.0×10^6 PC-3 cells as previously described (18), and male C57BL6/J mice were implanted with 5.0×10^5 LLC cells into the dorsal subcutis of the right flank. About 30-35 days after the injections, PC-3 or LLC cells induced anorexia in mice. Four days after the onset of anorexia, the mice were killed, the hypothalamic tissue was excised and mice were weighed with and without tumor.

Walker-256 tumor cells were obtained from the ascitic fluid of the peritoneal cavity of Wistar rats, 5 days after the intraperitoneal injection of 20 x 10^6 carcinoma cells. After cell harvesting, the percentage of viable cells was determined by using 1% Trypan blue solution in a Neubauer chamber. Tumor cells (2 x 10^6 cells in 1 mL saline solution) were injected in the right flank after the surgical implantation of the intracerebroventricular (i.c.v.) cannula.

Definition of cancer anorexia and treatments

Each animal's individual baseline 24-h food intake was defined as the average daily food intake over a period of 3 consecutives days. Subsequent food intake data are expressed as individual percentages and baseline daily food intake. In tumor-bearing animals, cancer anorexia was defined as a single value of less than 70% of baseline occurring after a steady decline of at least 3 days duration, as previously described (19).

Intracerebroventricular treatments

When criteria for anorexia had been met, tumor-bearing animals were daily treated with i.c.v. injection (2 µl bolus injection), anti-IL-1β antibody (25ng), Infliximab (0.3 µg) or its vehicles. These treatments were performed for 4 days before Western blot and cumulative food intake analysis and the daily chronic treatment were conducted for survival curve determination. Water intake was not altered by these treatments, compared with the respective control group (data not shown).

Control rats were acutely injected with i.c.v. (2 µl bolus injection) of recombinant IL-1β (2.5ng) or TNF-α (10^{-6}M) or vehicle at 18:00h and the hypothalamus was obtained 0,

1, 3 and 6 hours after each injection for Western blot analysis and food intake was measured 24-hours later.

For insulin and leptin sensitivity, hypothalami samples were obtained 15 minutes after insulin (200mU) or leptin (10^{-6}M) infusion.

Dissection of the hypothalamic regions

Rats were killed by decapitation and hypothalamic nuclei were quickly dissected and frozen in liquid nitrogen. Later on, each region of the hypothalamus was dissected from 1 mm thick sagittal sections of fresh brain. PVH, ARH, and VMH plus DMH were dissected from the first sections from the midline of the brain, and LH was dissected from the next lateral sections. Coordinates for each hypothalamic region are as follows; PVH: square area with anterior margin (posterior region of anterior commisure), dorsal margin (border with thalamus), ventral margin, and posterior margin (white matter separating PVH/anterior hypothalamus and VMH/DMH); VMH plus DMH: triangular area with anterior margin (white matter separating PVH/anterior hypothalamus and VMH/DMH), posterior margin (border with mammilary body), and ventral margin (border with ARH); ARH: ventral part of the medial hypothalamus with anterior and dorsal margin and posterior margin (border with mammilary body).

Physiological and metabolic parameters

After 6 h of fasting, the animals, tumors and epididymal fat were weighted. RIA was used to measure serum insulin, according to a previous description (20). Leptin

concentrations were determined using a commercially available ELISA kit (Crystal Chem Inc., Chicago, IL).

Morphological analysis of brown adipose tissue.

Brown adipose tissue (BAT) depots were fixed by immersion in 4% formaldehyde in 0.1 mM phosphate buffer, pH 7.4, dehydrated, cleared, and then embedded in paraffin. Serial sections (5.0 μm thick) were obtained and then stained by hematoxylin and eosin to assess the morphology by light microscopy.

Body composition determination.

The carcass (without the gastrointestinal tract) was weighed and stored at −20°C for analysis of body composition. Carcass water was determined as the difference between the dry and wet weights. Total fat was extracted with petroleum ether using a Soxhlet apparatus. The carcass without fat was dried to determine the lean mass.

Proinflammatory-cytokine determination

Cytokine levels (IL-1β and TNF-α) were determined in samples of hypothalamic protein extracts (2.0 mg/ml) as well as serum TNF- α using ELISA kits (Pierce Endogen, Rockford, IL), according to the manufacturer's instructions.

Phosphorthioate-modified oligonucleotide treatment

The sequences of sense and antisense (ASO) phosphorthioate oligonucleotides, specific for PTP1B (sense, 5'-AAA GTG CTG TTG G-3' and antisense, 5'-CCA ACA GCA

CTT T-3'), were selected among three unrelated pairs of oligonucleotides on the basis of their ability to block PTP1B protein expression, as evaluated by immunoblotting total protein extracts of hypothalamus using specific anti-PTP1B antibodies. The antisense oligonucleotide sequences were submitted to BLAST analyses (www.ncbi.nlm.nih.gov) and matched only for the Rattus norvegicus PTP1B coding sequence. Control and tumor-bearing rats were cannulated, housed in individual cages and treated with sense oligonucleotide (PTP1B-Sense) or PTP1B antisense oligonucleotide (PTP1B-ASO). Sense and antisense PTP1B oligonucleotides were diluted in TE buffer (10 mM Tris-HCl, 1 mM EDTA) and treatment was achieved by icv infusions, twice a day (0800 h/1800 h) with a total vol. of 2.0 µl/ dose (4.0 nmol/µl) for 4 days and the hypothalamus was excised 4 hours after the last injection. In tumor-bearing rats, the treatment was administered twice a day when the criteria of anorexia had been met.

Protein tyrosine phosphatase activity assay

The hypothalami were removed and homogenized in the solubilization buffer containing (mm): Tris 20 (pH 7.6), EDTA 5, PMSF 2, EGTA 1 and NaCl 130, and 0.1 mg aprotinin ml−1 and 1% Triton X-100. The lysates were centrifuged (15 000 g for 25 min at 4°C) and the supernatants were collected for immunoprecipitation. Immunoprecipitates were washed in PTP assay buffer containing (mm): Hepes 100 (pH 7.6), EDTA 2, DTT 1 and NaCl 150, and 0.5 mg ml−1 bovine serum albumin. The pp60c-src C-terminal phosphoregulatory peptide (TSTEPQpYQPGENL; Biomol) was added to a final concentration of 200 µm in a total reaction volume of 60 µl in a PTP assay buffer for the immunoprecipitation. The reaction was then allowed to proceed for 1 h at 30°C. At the end

of the reaction, 40 µl aliquots were placed into a 96-well plate, 100 µl Biomol Green reagent (Biomol) was added, and absorbance was measured at 630 nm.

Confocal microscopy

Paraformaldehyde-fixed hypothalami were sectioned (5 µm). The sections were obtained from the hypothalami of six rats per group in the same localization (antero-posterior = −1.78 from bregma) and used for regular single- or double-immunofluorescence staining using DAPI, anti-PTP1B, anti-IL-1β receptor, anti-TNF-α receptor, Jak2 and STAT3 (1:200; Santa Cruz Biotechnology) antibodies, according to a previously described protocol (21). Analysis and photodocumentation of results were performed using a LSM 510 laser confocal microscope (Zeiss, Jena, Germany). The anatomical correlations were made according to the landmarks given in a stereotaxic atlas.

Immunoblotting

Four days after the respective treatments, animals were anesthetized with sodium amobarbital (15 mg/kg body weight, ip) and used as soon as anesthesia was assured by the loss of pedal and corneal reflexes. Samples from liver, gastrocnemius muscle and BAT were obtained, thereafter, rats were killed and the basal diencephalon, including the preoptic area and the hypothalamus, was removed at the time points indicated, minced coarsely, and homogenized immediately in solubilization buffer containing (mM) 100 Tris (pH 7.6), 1% Triton X-100, 10 Na3VO4, 100 NaF, 10 Na4P2O7, 4 EDTA, 150 NaCl, 0.1 mg aprotinin, and 35 mg phenylmethylsulfonyl fluoride per milliliter, using a polytron PTA 20S generator (model PT 10/35; Brinkmann Instruments, Westbury, NY) operated at

maximum speed for 30 seconds and clarified by centrifugation. Hypothalami (200 µg protein) were used for immunoblotting followed by Western blot analysis with the indicated antibodies. Blots were exposed to preflashed XAR film (Kodak, Rochester, NY) with Cronex Lightning Plus intensifying screens at –80° C for 12–48 h. Band intensities were quantitated by optical densitometry (Scion Image software; Scion Corp., Frederick, MD).

Statistical analysis

The survival curves were estimated using Kaplan-Meier's estimates, and curves were compared using the log-rank test and the level of significance was set at $P < 0.001$. Where appropriate, results are expressed as the means ± SEM, accompanied by the indicated number of rats used in experiments. Comparisons among groups were made using parametric one-way ANOVA; where F ratios were significant, further comparisons were made using the Bonferroni test. The level of significance was set at $P < 0.05$. The results of blots are presented as direct comparisons of bands in autoradiographs and quantified by densitometry.

RESULTS

Down regulation of hypothalamic PTP1B expression during cancer-induced anorexia in rats.

To evaluate the hypothalamic PTP1B expression during cancer induced-anorexia, Walker-256 tumor cells (W-256) were injected in the subcutaneous tissue of male wistar rats and induced to severe anorexia (Figures 1A), decreasing the cumulative food intake during by 75% four days after the onset of anorexia (Figure 1B) and weight loss (Figure 1C), and reducing fat and lean mass, by 50 and 35%, respectively (Figure 1D). In addition, we determined the energy expenditure by monitoring the brown adipose tissue (BAT) profile in control and tumor-bearing rats. The macroscopic characteristics of BAT were clearly modified four days after the onset of anorexia. Its reddish color was more intense (Figure 1E) and its relative mass was significantly increased (Figure 1F) in the W-256 group. Under light microscopy examination, the fat droplets were reduced and nuclei were more densely distributed, suggesting a reduction in mean cell size (Figure 1G). The Western blot assay revealed that the expression of UCP1, a key protein involved in BAT thermogenesis, was increased in BAT obtained from W-256 group (Figure 1 H). In addition, the expression of PGC1α, an important protein involved in the mitochondrial biogenesis was increased in the BAT of W-256 group (Figure 1H).

Using Western blotting and protein tyrosine phosphatase assays, we observed that PTP1B expression and activity were reduced by 65 and 62%, respectively, in the hypothalami samples obtained from the W-256 group at four days after the onset of anorexia (Figures 1I and J). Consistent with a decreased PTP1B activity, hypothalamic

Jak/STAT signaling was increased in the W-256 group, as indicated by Jak2 and STAT3 tyrosine phosphorylation (Figure 1 K). We also observed that the expression of other negative modulators of leptin signaling, such as, SH-PTP2 and SOCS3, were not altered in the hypothalamus of anorectic rats (Figure Supplementary 1A).

Thereafter, the accuracy of the dissection of the hypothalamus was assessed by measuring the expression of PTP1B in specific hypothalamic nuclei. We observed abundant PTP1B expression in the arcuate nucleus when compared to DMH/VMH, PVN and LH I control rats (Figure 1L). Thus, we examined PTP1B expression and activation of Jak/STAT signaling in the arcuate nuclei of control and anorectic rats. Figure 1M shows that PTP1B expression was reduced and Jak2 and STAT3 tyrosine phosphorylation were increased in the arcuate nuclei of the W-256 group, when compared to the control (Figure 1M). In addition, immunohistochemistry with anti-PTP1B-specific antibody showed that PTP1B is expressed in the majority of neurons in the arcuate nuclei of control animals (Figure 1N-left panel). Double-staining confocal microscopy showed that most neurons expressing PTP1B in the arcuate nucleus were shown to possess Jak2 and STAT3 in control rats (Figure 1N-right panel).

Neuronal PTP1B expression is reduced in different models of cancer-induced anorexia.

To extend our hypothesis, we investigated hypothalamic PTP1B expression in other models of cancer-induced anorexia. Lewis lung carcinoma (LLC) and human prostate cancer (PC3) cell were injected in the subcutaneous of C57BL6/J and SCID mice, respectively. LLC and PC-3 induced anorexia and cachexia, reducing the cumulative food

intake (Figures 2A and E) and inducing weight loss (Figure 2B and F) in these mice. As observed in Wistar rats with Walker tumor, hypothalamic expression of PTP1B was reduced in LLC and PC-3 injected mice by about 50 and 35%, respectively, compared to the control group (Figure 2C and G). The statuses of Jak2 and STAT3 tyrosine phosphorylation were higher in the hypothalamus of both strains of mice during the anorexia period when compared to control animals (Figures 1D and H). The hypothalamic expressions of SH-PTP2 and SOCS3 were similar between tumor-bearing mice, when compared to respective control groups (Figure Supplementary 1B and C). These data indicated that hypothalamic PTP1B expression was reduced in different models of cancer-induced anorexia.

Up regulation of insulin and leptin sensitivity in the hypothalamus of rats during cancer-induced anorexia.

We next evaluate whether the reduction of hypothalamic PTP1B during anorexia modulates central insulin and leptin signaling, four days after the onset of anorexia, tumor-bearing rats and the respective control group were fasted during six hours and injected with insulin (200 mU) or leptin (10^{-6} M) or vehicle into the third ventricle and the hypothalamus were removed then fifteen minutes after each injection. Hypothalami samples from insulin or vehicle-treated rats were submitted to Western blot analysis. Insulin, induced increases in IRβ and IRS-1 tyrosine phosphorylation and Akt and Foxo1 serine phosphorylation in hypothalamus from both control and anorectic rats, but the levels of IRβ and IRS-1 tyrosine phosphorylation and Akt and Foxo1 serine phosphorylation were ~ 50% higher in the hypothalamus of rats during anorexia, when compared to control animals injected with

insulin (Figure 3 A-D- upper panels). The expressions of IRβ, IRS-1, Akt and Foxo1 were similar between the groups (Figure 3 A-D- lower panels).

Leptin, induced increases in Jak2 and STAT3 tyrosine phosphorylation in hypothalamus from both control and anorectic rats, but the levels of Jak2 and STAT3 tyrosine phosphorylation were 55 and 50% higher, respectively, in the hypothalamus of rats during anorexia, when compared to control animals injected with leptin (Figure 3 E and F- upper panels). The expressions of Jak2 and STAT3 were similar between the groups (Figure 3 E and F- lower panels).

Interestingly, the serum levels of fasting insulin and leptin were drastically reduced in tumor-bearing rats, when compared to control rats (Figures 3G and H).

Central inflammation modulates PTP1B activity.

Several studies have shown that proinflammatory cytokines such as IL-1β and TNF-α are involved in the anorectic response during cancer-induced anorexia (19, 22-24). Thus, we investigated the role of the inflammatory response in PTP1B activity, insulin and leptin sensitivity and food intake in tumor-bearing rats. Four days after anorexia onset, we found high levels of TNF-α and IL-β in the hypothalamus of the W-256 group (Figure 4A and Supplementary Figure 2A). We tested whether the inhibition of TNF-α modulates PTP1B activity and insulin and leptin signaling. After the onset of anorexia had been met, the specific TNF-α inhibitor, Infliximab (0.6 μg) or its vehicle were injected into third cerebral ventricle of tumor-rearing rats during 4 days. The Infliximab treatment was able to increase the PTP1B protein expression (48%) and PTP1B activity (28%) in the hypothalamus of the

W-256 group when compared to the W-256 group treated with vehicle (Figures 4B and C). Infliximab treatment also reduced the Jak2 and STAT3 tyrosine phosphorylation in the hypothalamus of rats bearing the W-256 tumor, whereas, this treatment did not change the Jak/STAT signaling in control animals (Figure 4 D). Moreover, insulin and leptin sensitivity were reduced by about 60% in the hypothalamus of tumor-bearing rats after Infliximab treatment, as detected by Akt serine and STAT3 tyrosine phosphorylation after insulin or leptin intrahypothalamic infusion, respectively (Figures E and F). Infliximab treatment also increased the cumulative food intake (49%) and body weight (18%) in the W-256 group (Figures 4G and H).

We also performed a chronic Infliximab treatment to evaluate the survival in tumor-bearing rats. As shown in the Kaplan-Maier graphs, a daily intrahypothalamic infusion of Infliximab statistically prolonged the survival in the W-256 group when compared to the vehicle treatment, whereas, the median survival of the W-256 group treated with vehicle was 7.5 days, while the median survival of the W-256 group treated with Infliximab was 10 days ($p<0.0214$) (Figure 4I).

Additionally, intrahypothalamic treatment with the anti-IL-1β antibody increased the expression and activity of neuronal PTP1B, reduced the Jak2 and STAT3 tyrosine phosphorylation in the hypothalamus, reduced the insulin and leptin signaling and increased the food intake and body weight and survival in tumor-bearing rats by the same magnitude as that promoted by Infliximab treatment (Supplementary Figures 2B-I).

To further investigate the isolated roles of TNF-α and IL-1β in PTP1B activity, we injected recombinant TNF-α or IL-1β into the third cerebral ventricle of control rats. As

expected, acute intrahypothalamic infusion of recombinant TNF-α (10^{-6} M) reduced the food intake in control rats (Figure 5A). In addition, we observed that central infusion of recombinant TNF-α reduced PTP1B expression in a time-dependent manner and, conversely, the STAT3 tyrosine phosphorylation increased in a time-dependent manner after TNF-α infusion (Figure 5B). We also observed that recombinant TNF-α infusion into the hypothalamus of control rats increased the anorexigenic effects mediated by insulin or leptin (Figures 5C and D)and increased the insulin and leptin sensitivity, as determined by Akt and STAT3 tyrosine phosphorylation (Figures 5E and F). Similar results were found when we injected recombinant IL-1β (5.0 ng) (Figure Supplementary 3A-F).

Despite the high levels of PTP1B in the arcuate nucleus, we sought to determine whether the IL-1 receptor (IL-1R) and the TNF receptor (TNFR) are co-localized with PTP1B in the arcuate nucleus in control animals. Figure 5G shows that both IL-1R and TNFR, are localized in the same specific neuronal subtypes that possess PTP1B.

Neuronal PTP1B disruption evokes anorexia, weight loss and death in control rats.

Next, we sought to investigate whether the reduction of hypothalamic PTP1B expression modulates the food intake and body weight, independently of tumor development. We generated a selective, transient reduction in PTP1B by intrahypothalamic infusion of an antisense oligonucleotide (ASOPTP1B) designed to blunt the expression of PTP1B in rat hypothalamic areas surrounding the third ventricle in control rats. Two daily doses of ASOPTP1B during 4 days reduced hypothalamic PTP1B expression in a dose-dependent manner (Figure 6A). The treatment with ASOPTP1B (4.0 nM) during 4 days did

not change PTP1B expression in other brain areas such as cortex and cerebellum and did not affect the PTP1B expression in peripheral tissues such as, skeletal muscle and hepatic tissue (Figure 6B). Intrahypothalamic ASOPTP1B treatment also reduced the hypothalamic PTP1B activity (60%) when compared to sense treatment (Figure 6C). Furthermore, we observed that the intrahypothalamic infusion of ASOPTP1B activated Jak/STAT signaling in animals (Figure 6D). We did not observe differences in the expression of SOCS3 and SH-PTP2 in the hypothalamus after ASOPTP1B treatment (Figure 6E). In addition, although ASOPTP1B treatment reduced the serum levels of insulin and leptin, we observed an increased insulin and leptin sensitivity in the hypothalamus (Supplementary Figure 4A-H).

Next, we examined the effects of the disruption of hypothalamic PTP1B, mediated by central ASOPTP1B treatment, on food intake and body weight. ASOPTP1B treatment dramatically reduced the food intake in control rats (Figures 6F), reducing the cumulative food intake by about 75%, when compared to sense treatment (Figure 6G). We found that wistar rats presented severe anorexia during treatment with ASOPTP1B, but rapidly recovered food consumption after the termination of the treatment (Figure 6F), indicating that ASOPTP1B does not induces a persistent state of anorexia. Four days of ASOPTP1B treatment were sufficient to induces weight loss (Figure 6H), reducing fat and lean mass by 55 and 30%, respectively, in control rats (Figure 6I). The macroscopic characteristics of BAT were modified four days after the ASOPTP1B treatment. Its reddish color was more intense (Figure 6J) and its relative mass was significantly increased (Figure 6K) in ASOPTP1B treated animals. Under light microscopy examination, the fat droplets were reduced and nuclei were more densely distributed, suggesting a reduction in mean cell size

(Figure 6L). The Western blot assay revealed that the expression of UCP1 and PGC1α was increased in BAT obtained after intrahypothalamic ASOPTP1B treatment (Figure 6M).

Thereafter, we examined the effects of chronic ASOPTP1B treatment in control rats. Interestingly, we found that chronic ASOPTP1B treatment induced death in control animals, whereas the survival median was 6 days (Figure 6N).

ICV anti-inflammatory treatments require hypothalamic PTP1B expression to increase food intake and lifespan in tumor-bearing rats.

Next, we investigate whether the anti-inflammatory approaches to restoring food intake in tumor-bearing animals are dependent on PTP1B expression. To address this question, we injected anti-IL-1β antibody or Infliximab during cancer-induced anorexia at the same time that we forced low levels of hypothalamic PTP1B using daily intrahypothalamic ASOPTP1B injections in control animals. While intrahypothalamic infusion of anti-IL-1β antibody increased the cumulative food intake and reduced STAT3 tyrosine phosphorylation in the hypothalamus of tumor-bearing rats, the treatment with ASOPTP1B blunted all these effects mediated by anti-IL-1β antibody treatment (Figures 7A and B). In addition, the treatment with anti-IL-1β antibody did not increase the lifespan in W-256 group during ASOPTP1B treatment, p=0.756 (Figures 7C). Similar results were found during central infusion of Infliximab (Figures 7D-F). These results indicate that the anti-inflammatory strategies to restore food intake are dependent upon the increase in PTP1B hypothalamic levels.

DISCUSSION

Approximately 80% of cancer patients at advanced stages of the disease suffer from anorexia, which leads to significant weight loss and progressive cachexia, an important factor that contributes to death. Cancer anorexia may be a result of an imbalance between orexigenic signals and anorexigenic signals into the hypothalamus (25). It has been postulated that hypothalamic PTP1B, a negative regulator of insulin and leptin signaling, modulates food intake and energy expenditure in control and obese animals (7, 8, 15). In the present study, we expand the knowledge of these data, showing that PTP1B is a crucial phosphatase that regulates the aberrant anorexigenic signal in different models of cancer-induced anorexia.

In recent years genetic and biochemical evidences have shown an important activity of PTP1B as a negative regulator of tyrosine phosphorylation of the main components of the insulin and leptin pathway signaling. Several studies have examined the PTP1B expression in rodents and humans with insulin resistance, diabetes and obesity and many reports have shown increased expression and/or activity of PTP1B in these states (13, 26, 27). Conversely, our data demonstrate that, during anorexia, PTP1B expression was markedly reduced in the hypothalamus of rodents, increasing STAT3 tyrosine phosphorylation and central insulin and leptin sensitivity and energy expenditure. Our data show that different tumor cell xenografts in the subcutaneous of rodents induced severe anorexia, weight loss and death, in parallel; we observed an expressive down regulation of hypothalamic PTP1B expression and activity. This finding is consistent with the increase of hypothalamic insulin and leptin sensitivity, and even low levels of serum insulin and leptin in anorectic animals are able to regulate the food intake in a low magnitude hypothalamic

set point. The increased leptin sensitivity in the hypothalamus may help to understand why circulating concentrations of leptin are inversely related with the inflammatory response and depend only on the total amount of fat in anorectic patients, despite the decreased food intake observed in these individuals (28-30).

Amounting evidence has shown that central infusion of pro-inflammatory cytokines induces anorexia and weight loss in rodents (23, 24, 31). Interestingly, in the present study, we observed that by blocking TNF-α or IL1-β in the central nervous system, PTP1B expression and activity was restored, decreasing STAT3 phosphorylation, and increasing food intake and body weight in anorectic rats. Furthermore, the infusion of recombinant IL-1β or TNF-α decreased PTP1B expression and increased the anorexigenic effects of insulin and leptin. These data demonstrate that the inflammatory response observed in tumor-bearing animals modulates the hypothalamic PTP1B activity. Conversely, some studies have suggested that inflammation up-regulates PTP1B expression in the hypothalamus; thus, in these studies, low doses of TNF α increase PTP1B mRNA and protein levels and induce insulin and leptin resistance (32, 33). Pro-inflammatory signaling in the hypothalamus play a dual role in the control of feeding and thermogenesis, in some cases promoting anorexia and catabolism (1, 34) and in other cases precipitating hyperphagia and obesity (35, 36), and in both cases PTP1B has a central role. Thus, PTP1B plays a crucial role in the control of food intake during hyperphagic or anorectic response, but the signaling network that the pro-inflammatory molecules use to control PTP1B expression remains unsolved and deserves further investigations.

In cachexia, both the reduction in caloric intake and the increase in energy expenditure, mostly due to increased thermogenesis, act in synergy to accelerate body mass depletion. Weight loss in cancer patients is due to a dramatic reduction in total body fat and an important skeletal muscle wasting (37). Interestingly, the exclusive disruption of PTP1B in the central nervous system was able to; induces anorexia, severe weight loss and death, as observed in tumor-bearing animals. In accordance to our data, the neuronal PTP1B knockout mice, shows reduced food consumption, weight and adiposity, and increased energy expenditure (7), however these animals are viable suggesting that PTP1B knockout mice develops alternative pathways that counter-balance the potent effect of hypothalamic PTP1B blockade. In line with this idea our data show that; Firstly, intrahypothalamic PTP1B blockade increased energy expenditure in control animals, as determined by BAT analysis, reduced fat mass. Secondly, as previously demonstrated, and by a similar fashion to tumor-bearing animals we also observed an increased insulin and leptin sensitivity in the hypothalamus submitted to PTP1B knockdown (8). Finally, we observed that different anorexigenic cytokines converge their signals to PTP1B, since the use of anti-inflammatory agents failed to increase the food intake during central PTP1B knockdown.

Traditionally, the lean body mass loss observed during cachexia has been considered to be dependent on humoral factors, including pro-inflammatory cytokines. Surprisingly, we observed that neuronal PTP1B disruption reduced the lean weight in control animals in a similar magnitude as observed in tumor-bearing rats. These data are in accordance with Wisse and colleagues that showed that reduction of food intake by LPS administration depends upon central, rather than peripheral inflammatory signals (38).

Thus, altogether these data suggest a direct role of the central nervous system in the control of lean mass.

In summary, our data provide important insights into the control of food intake during anorexia. Decreased PTP1B expression in the CNS during anorexia, despite a reduction in fuel and nutrients, could produce a reduction in nutrient intake, at the level of stored fat and lean mass. These findings support the hypothesis that PTP1B links the central inflammation and anorexigenic signals during cancer-induced anorexia.

ACKNOWLEDGMENTS

This study was supported by grants from Fundacão de Amparo à Pesquisa do Estado de São Paulo (FAPESP) and Conselho Nacional de desenvolvimento científico e tecnológico (CNPq).

We thank Mr. Luiz Janeri for technical assistance and Nicola Conran for English language editing.

REFERENCES

1. Laviano, A., Meguid, M.M., Inui, A., Muscaritoli, M., and Rossi-Fanelli, F. 2005. Therapy insight: Cancer anorexia-cachexia syndrome--when all you can eat is yourself. *Nat Clin Pract Oncol* 2:158-165.

2. Mantovani, G., Maccio, A., Massa, E., and Madeddu, C. 2001. Managing cancer-related anorexia/cachexia. *Drugs* 61:499-514.

3. Laviano, A., Meguid, M.M., and Rossi-Fanelli, F. 2003. Cancer anorexia: clinical implications, pathogenesis, and therapeutic strategies. *Lancet Oncol* 4:686-694.

4. Tisdale, M.J. 1997. Biology of cachexia. *J Natl Cancer Inst* 89:1763-1773.

5. Flier, J.S., and Maratos-Flier, E. 1998. Obesity and the hypothalamus: novel peptides for new pathways. *Cell* 92:437-440.

6. Schwartz, M.W., Woods, S.C., Porte, D., Jr., Seeley, R.J., and Baskin, D.G. 2000. Central nervous system control of food intake. *Nature* 404:661-671.

7. Bence, K.K., Delibegovic, M., Xue, B., Gorgun, C.Z., Hotamisligil, G.S., Neel, B.G., and Kahn, B.B. 2006. Neuronal PTP1B regulates body weight, adiposity and leptin action. *Nat Med* 12:917-924.

8. Picardi, P.K., Calegari, V.C., Prada Pde, O., Moraes, J.C., Araujo, E., Marcondes, M.C., Ueno, M., Carvalheira, J.B., Velloso, L.A., and Saad, M.J. 2008. Reduction of hypothalamic protein tyrosine phosphatase improves insulin and leptin resistance in diet-induced obese rats. *Endocrinology* 149:3870-3880.

9. Frangioni, J.V., Beahm, P.H., Shifrin, V., Jost, C.A., and Neel, B.G. 1992. The nontransmembrane tyrosine phosphatase PTP-1B localizes to the endoplasmic reticulum via its 35 amino acid C-terminal sequence. *Cell* 68:545-560.

10. Asante-Appiah, E., and Kennedy, B.P. 2003. Protein tyrosine phosphatases: the quest for negative regulators of insulin action. *Am J Physiol Endocrinol Metab* 284:E663-670.

11. Johnson, T.O., Ermolieff, J., and Jirousek, M.R. 2002. Protein tyrosine phosphatase 1B inhibitors for diabetes. *Nat Rev Drug Discov* 1:696-709.

12. Lund, I.K., Hansen, J.A., Andersen, H.S., Moller, N.P., and Billestrup, N. 2005. Mechanism of protein tyrosine phosphatase 1B-mediated inhibition of leptin signalling. *J Mol Endocrinol* 34:339-351.

13. Venable, C.L., Frevert, E.U., Kim, Y.B., Fischer, B.M., Kamatkar, S., Neel, B.G., and Kahn, B.B. 2000. Overexpression of protein-tyrosine phosphatase-1B in adipocytes inhibits insulin-stimulated phosphoinositide 3-kinase activity without altering glucose transport or Akt/Protein kinase B activation. *J Biol Chem* 275:18318-18326.

14. Zabolotny, J.M., Bence-Hanulec, K.K., Stricker-Krongrad, A., Haj, F., Wang, Y., Minokoshi, Y., Kim, Y.B., Elmquist, J.K., Tartaglia, L.A., Kahn, B.B., et al. 2002. PTP1B regulates leptin signal transduction in vivo. *Dev Cell* 2:489-495.

15. White, C.L., Whittington, A., Barnes, M.J., Wang, Z., Bray, G.A., and Morrison, C.D. 2009. HF diets increase hypothalamic PTP1B and induce leptin resistance through both leptin-dependent and -independent mechanisms. *Am J Physiol Endocrinol Metab* 296:E291-299.

16. Morrison, C.D., White, C.L., Wang, Z., Lee, S.Y., Lawrence, D.S., Cefalu, W.T., Zhang, Z.Y., and Gettys, T.W. 2007. Increased hypothalamic protein tyrosine phosphatase 1B contributes to leptin resistance with age. *Endocrinology* 148:433-440.

17. Ropelle, E.R., Fernandes, M.F., Flores, M.B., Ueno, M., Rocco, S., Marin, R., Cintra, D.E., Velloso, L.A., Franchini, K.G., Saad, M.J., et al. 2008. Central

exercise action increases the AMPK and mTOR response to leptin. *PLoS One* 3:e3856.

18. Oliveira, J.C., Souza, K.K., Dias, M.M., Faria, M.C., Ropelle, E.R., Flores, M.B., Ueno, M., Velloso, L.A., Saad, S.T., Saad, M.J., et al. 2008. Antineoplastic effect of rapamycin is potentiated by inhibition of IRS-1 signaling in prostate cancer cells xenografts. *J Cancer Res Clin Oncol* 134:833-839.

19. Ropelle, E.R., Pauli, J.R., Zecchin, K.G., Ueno, M., de Souza, C.T., Morari, J., Faria, M.C., Velloso, L.A., Saad, M.J., and Carvalheira, J.B. 2007. A central role for neuronal adenosine 5'-monophosphate-activated protein kinase in cancer-induced anorexia. *Endocrinology* 148:5220-5229.

20. Scott, A.M., Atwater, I., and Rojas, E. 1981. A method for the simultaneous measurement of insulin release and B cell membrane potential in single mouse islets of Langerhans. *Diabetologia* 21:470-475.

21. Araujo, E.P., Amaral, M.E., Souza, C.T., Bordin, S., Ferreira, F., Saad, M.J., Boschero, A.C., Magalhaes, E.C., and Velloso, L.A. 2002. Blockade of IRS1 in isolated rat pancreatic islets improves glucose-induced insulin secretion. *FEBS Lett* 531:437-442.

22. Laviano, A., Inui, A., Marks, D.L., Meguid, M.M., Pichard, C., Rossi Fanelli, F., and Seelaender, M. 2008. Neural control of the anorexia-cachexia syndrome. *Am J Physiol Endocrinol Metab* 295:E1000-1008.

23. Marks, D.L., Ling, N., and Cone, R.D. 2001. Role of the central melanocortin system in cachexia. *Cancer Res* 61:1432-1438.

24. Scarlett, J.M., Jobst, E.E., Enriori, P.J., Bowe, D.D., Batra, A.K., Grant, W.F., Cowley, M.A., and Marks, D.L. 2007. Regulation of central melanocortin signaling by interleukin-1 beta. *Endocrinology* 148:4217-4225.

25. Davis, M.P., Dreicer, R., Walsh, D., Lagman, R., and LeGrand, S.B. 2004. Appetite and cancer-associated anorexia: a review. *J Clin Oncol* 22:1510-1517.

26. Dadke, S.S., Li, H.C., Kusari, A.B., Begum, N., and Kusari, J. 2000. Elevated expression and activity of protein-tyrosine phosphatase 1B in skeletal muscle of insulin-resistant type II diabetic Goto-Kakizaki rats. *Biochem Biophys Res Commun* 274:583-589.

27. Ropelle, E.R., Pauli, J.R., Prada, P.O., de Souza, C.T., Picardi, P.K., Faria, M.C., Cintra, D.E., Fernandes, M.F., Flores, M.B., Velloso, L.A., et al. 2006. Reversal of diet-induced insulin resistance with a single bout of exercise in the rat: the role of PTP1B and IRS-1 serine phosphorylation. *J Physiol* 577:997-1007.

28. Brown, D.R., Berkowitz, D.E., and Breslow, M.J. 2001. Weight loss is not associated with hyperleptinemia in humans with pancreatic cancer. *J Clin Endocrinol Metab* 86:162-166.

29. Simons, J.P., Schols, A.M., Campfield, L.A., Wouters, E.F., and Saris, W.H. 1997. Plasma concentration of total leptin and human lung-cancer-associated cachexia. *Clin Sci (Lond)* 93:273-277.

30. Takahashi, M., Terashima, M., Takagane, A., Oyama, K., Fujiwara, H., and Wakabayashi, G. 2009. Ghrelin and leptin levels in cachectic patients with cancer of the digestive organs. *Int J Clin Oncol* 14:315-320.

31. Bernstein, I.L., Taylor, E.M., and Bentson, K.L. 1991. TNF-induced anorexia and learned food aversions are attenuated by area postrema lesions. *Am J Physiol* 260:R906-910.

32. Romanatto, T., Cesquini, M., Amaral, M.E., Roman, E.A., Moraes, J.C., Torsoni, M.A., Cruz-Neto, A.P., and Velloso, L.A. 2007. TNF-alpha acts in the hypothalamus inhibiting food intake and increasing the respiratory quotient--effects on leptin and insulin signaling pathways. *Peptides* 28:1050-1058.

33. Zabolotny, J.M., Kim, Y.B., Welsh, L.A., Kershaw, E.E., Neel, B.G., and Kahn, B.B. 2008. Protein-tyrosine phosphatase 1B expression is induced by inflammation in vivo. *J Biol Chem* 283:14230-14241.

34. Matthys, P., and Billiau, A. 1997. Cytokines and cachexia. *Nutrition* 13:763-770.

35. De Souza, C.T., Araujo, E.P., Bordin, S., Ashimine, R., Zollner, R.L., Boschero, A.C., Saad, M.J., and Velloso, L.A. 2005. Consumption of a fat-rich diet activates a proinflammatory response and induces insulin resistance in the hypothalamus. *Endocrinology* 146:4192-4199.

36. Zhang, X., Zhang, G., Zhang, H., Karin, M., Bai, H., and Cai, D. 2008. Hypothalamic IKKbeta/NF-kappaB and ER stress link overnutrition to energy imbalance and obesity. *Cell* 135:61-73.

37. Fearon, K.C. 1992. The Sir David Cuthbertson Medal Lecture 1991. The mechanisms and treatment of weight loss in cancer. *Proc Nutr Soc* 51:251-265.

38. Wisse, B.E., Ogimoto, K., Tang, J., Harris, M.K., Jr., Raines, E.W., and Schwartz, M.W. 2007. Evidence that lipopolysaccharide-induced anorexia depends upon central, rather than peripheral, inflammatory signals. *Endocrinology* 148:5230-5237.

FIGURE LEGENDS

Figure 1. PTP1B expression in the hypothalamus of control and tumor-bearing rats. Walker-256 tumor cells (20 x 10^6) were injected in to the subcutaneous of wistar rats to evaluate food intake, body weight, energy expenditure and hypothalamic PTP1B expression. (A) Curve of food intake (B) cumulative food intake four days after the onset of anorexia. (C) Total body weight (excluding the tumor). (D) Body weight composition. (E) Typical BAT macroscopic features from right portion, representative of 5 independent experiments. (F) Total BAT mass/whole body mass. (G) Histological analysis of BAT stained with hematoxilin and eosin. (H) UCP1 and PGC1α expression from BAT samples. (I) Hypothalamic PTP1B expression, representative Western blot of 4 independent experiments. (J) PTPase activity in PTP1B immunoprecipitates from hypothalamic samples. (K) Hypothalamic Jak2 and STAT3 tyrosine phosphorylation. (L) PTP1B expression in the medio basal, lateral hypothalamus and cortex in control rats. (M) PTP1B expression and Jak2 and STAT3 tyrosine phosphorylation in the arcuate nucleus from control and anorectic rats. (N) Confocal microscopy was performed using anti-PTP1B-specific antibody (green) and DAPI (blue), with 50x magnification (left panel) and co-localization of PTP1B (green) and Jak2 and STAT3 (red) in the arcuate nuclei of control rats, with 200x magnification. Bars represent means ± S.E.M. of n = 6–8 rats. *$P < 0.05$, versus control rats and #$P < 0.05$, versus DMH/VMH, PVN and LH.

Figure 2. Reduced hypothalamic PTP1B expression in different models of cancer-induced anorexia. Male C57BL6/J and SCID mice were implanted with 5.0×10^5 LLC cells or 1.0×10^6 PC-3 cells, respectively into the dorsal subcutis of right flank. (A and E) cumulative food intake four days after the onset of anorexia. (B and F) Total body weight

(excluding the tumor). (C and G) Hypothalamic PTP1B expression, representative of 4 independent experiments (n=5). (D and H) Hypothalamic Jak2 and STAT3 tyrosine phosphorylation. Bars represent means ± S.E.M. of n = 6–8 mice. *$P < 0.05$, versus control mice.

Figure 3. Hypothalamic insulin and leptin sensitivity during cancer-induced anorexia. Four days after onset of anorexia, hypothalamic extract from tumor-bearing and control rats were obtained 15 minutes after i.c.v. insulin or leptin infusion. Tissue extracts were immunoblotted (IB) with specific antibodies to evaluate the levels of (A) IRβ, (B) IRS1, (C) Akt (D) Foxo1 (E) Jak2 and (F) STAT3 phosphorylation. (G) Fasting insulin and (H) leptin levels. The results of scanning densitometry were expressed as arbitrary units. Bars represent means ± S.E.M. of n = 6–8 rats. *$P < 0.05$, versus control rats.

Figure 4. The effects of Infliximab on hypothalamic PTP1B activity in tumor-bearing rats. (A) Hypothalamic levels of TNF-α in control and tumor-bearing rats during cancer-induced anorexia period. The effects of daily intrahypothalamic treatment with Infliximab (0.6 μg) on (B) hypothalamic PTP1B protein expression and (C) protein tyrosine phosphatase activity of PTP1B. (D) Hypothalamic extracts from tumor-bearing and control rats were obtained at 60 minutes after the last infusion of Infliximab to evaluate Jak2 and STAT3 tyrosine phosphorylation. (E and F) One hour after the last infusion of rabbit pre-immune serum (RPIS) or Infliximab, tumor-bearing rats received intrahypothalamic infusion of insulin or leptin for evaluation of hypothalamic Akt and STAT3 phosphorylation, respectively. (G) Cumulative food intake and (H) body weight of control and tumor-bearing rats during cancer-induced anorexia period after RPIS or Infliximab

treatment. (I) Representative survival curves demonstrating the effect of chronic administration of central Infliximab treatment on the life span of tumor-bearing animals. The survival curves were estimated using Kaplan-Meier's estimates, and curves were compared using the log-rank test, $P = 0.0214$ (n = 10). Bars represent means ± S.E.M. of n = 6–8 rats. *$P < 0.05$, versus control rats and #$P < 0.05$, versus W-256 plus vehicle.

Figure 5. The effects of TNF-α on PTP1B activity and insulin and leptin sensitivity in the hypothalami of control animals. (A) Effects of intrahypothalamic infusion of recombinant TNF-α (10^{-6} M) on food intake in control animals. (B) Time-course representing STAT3 tyrosine phosphorylation and PTP1B expression in the hypothalamus of control rats injected with recombinant TNF-α. (C and D) Food intake was determined after central TNF-α infusion plus insulin or leptin in control animals. (E and F) Three hours after TNF-α infusion, insulin or leptin was injected for evaluation of Akt and STAT3 phosphorylation, respectively. The results of scanning densitometry were expressed as arbitrary units. Bars represent means ± S.E.M. of n = 5–6 animals. *$P < 0.05$, versus control animals and § $P < 0.05$, versus pSTAT3. (G) Confocal microscopy was performed using anti-PTP1B-specific antibody (green) and DAPI (blue), with 50x magnification (left panel) and co-localization of PTP1B (green) and TNFR and IL-1R (red) in the arcuate nuclei of control rats, with 200x magnification.

Figure 6. Effects of intrahypothalamic infusion of ASOPTP1B in control rats. Antisense oligonucleotide (ASOPTP1B) designed to blunt the hypothalamic expression of PTP1B of control rats. (A) Dose course (0.5-1.0 nM) of ASOPTP1B on hypothalamic PTP1B expression (B) PTP1B expression in different tissues after intrahypothalamic

infusion of ASOPTP1B. (C) PTPase activity in PTP1B immunoprecipitates from hypothalamic samples. (D) Hypothalamic Jak2 and STAT3 tyrosine phosphorylation. (E) Hypothalamic SOCS3 and SH-PTP2 protein expression after ASOPTP1B infusion. (F) Food intake during ASOPTP1B infusion. (G) Cumulative food intake during four days of ASOPTP1B treatment. (H) Total body weight. (I) Body weight composition. (J) Typical BAT macroscopic features from right portion, representative of 5 independent experiments. (K) Total BAT mass/whole body mass. (L) Histological analysis of BAT stained with hematoxilin and eosin. (M) UCP1 and PGC1α expression from BAT samples after sense or ASOPTP1B treatments. Bars represent means ± S.E.M. of n = 6–8 rats. *$P < 0.05$, versus control rats. (N) Representative survival curves demonstrating the effect of chronic administration of sense and ASOPTP1B treatments on life span of control animals. The survival curves were estimated using Kaplan-Meier's estimates, and curves were compared using the log-rank test, $P < 0.0001$ versus sense treatment (n = 10).

Figure 7. Anti-inflammatory strategies require hypothalamic PTP1B expression to reverse anorexia. Antisense oligonucleotide (ASOPTP1B) and anti-IL-1β antibody or Infliximab were injected in the hypothalamus after anorexia onset, in tumor-bearing animals. (A) Cumulative food intake during four days of ASOPTP1B (4.0 nM) and/or anti-IL-1β antibody (50 ng) treatments. (B) Hypothalamic STAT3 tyrosine phosphorylation. (C) Representative survival curves demonstrating the effect of chronic administration of anti-IL-1β or anti-IL-1β plus ASOPTP1B treatments on life span of tumor-bearing animals, p=0.756, n = 10. (D) Cumulative food intake during four days of ASOPTP1B (4.0 nM) and/or Infliximab (0.6 μg) treatments. (E) Hypothalamic STAT3 tyrosine phosphorylation. Bars represent means ± S.E.M. of n = 5–6 rats. *$P < 0.05$, versus control rats. (F)

Representative survival curves demonstrating the effect of chronic administration of Infliximab and Infliximab plus ASOPTP1B on life span of tumor-bearing animals, p=0.427, n = 10. The survival curves were estimated using Kaplan-Meier's estimates, and curves were compared using the log-rank test.

Figure 1

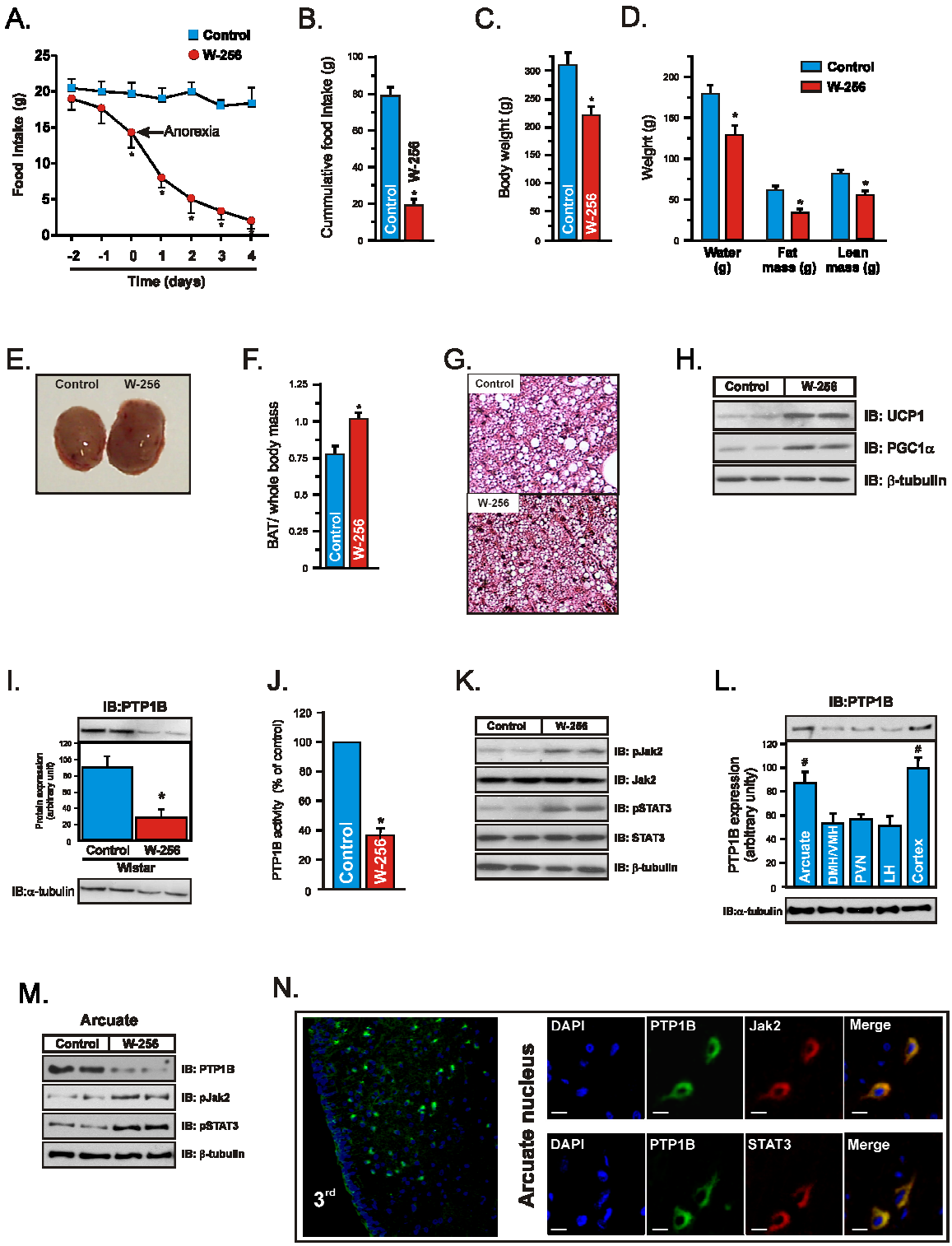
A.
Control
W-256
Food Intake (g)
Anorexia
Time (days)
B.
Cummulative food intake (g)
Control
W-256
C.
Body weight (g)
Control
W-256
D.
Weight (g)
Control
W-256
Water (g)
Fat mass (g)
Lean mass (g)
E.
Control
W-256
F.
BAT/ whole body mass
Control
W-256
G.
Control
W-256
H.
Control
W-256
IB: UCP1
IB: PGC1α
IB: β-tubulin
I.
IB:PTP1B
Protein expression (arbitrary unit)
Control
W-256
Wistar
IB:α-tubulin
J.
PTP1B activity (% of control)
Control
W-256
K.
Control
W-256
IB: pJak2
IB: Jak2
IB: pSTAT3
IB: STAT3
IB: β-tubulin
L.
IB:PTP1B
PTP1B expression (arbitrary unity)
Arcuate
DMH/VMH
PVN
LH
Cortex
IB:α-tubulin
M.
Arcuate
Control
W-256
IB: PTP1B
IB: pJak2
IB: pSTAT3
IB: β-tubulin
N.
3rd
Arcuate nucleus
DAPI
PTP1B
Jak2
Merge
DAPI
PTP1B
STAT3
Merge

Figure 2

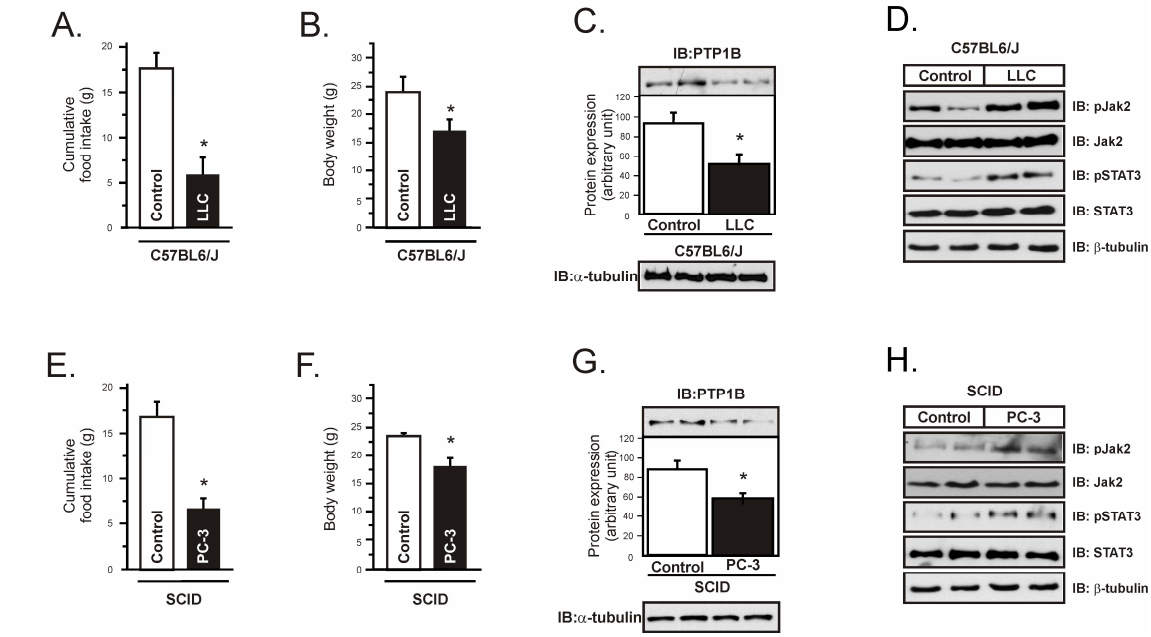
A.
Cumulative food intake (g)
Control
LLC
C57BL6/J
B.
Body weight (g)
Control
LLC
C57BL6/J
C.
IB:PTP1B
Protein expression (arbitrary unit)
Control
LLC
C57BL6/J
IB:α-tubulin
D.
C57BL6/J
Control
LLC
IB: pJak2
IB: Jak2
IB: pSTAT3
IB: STAT3
IB: β-tubulin
E.
Cumulative food intake (g)
Control
PC-3
SCID
F.
Body weight (g)
Control
PC-3
SCID
G.
IB:PTP1B
Protein expression (arbitrary unit)
Control
PC-3
SCID
IB:α-tubulin
H.
SCID
Control
PC-3
IB: pJak2
IB: Jak2
IB: pSTAT3
IB: STAT3
IB: β-tubulin

Figure 3

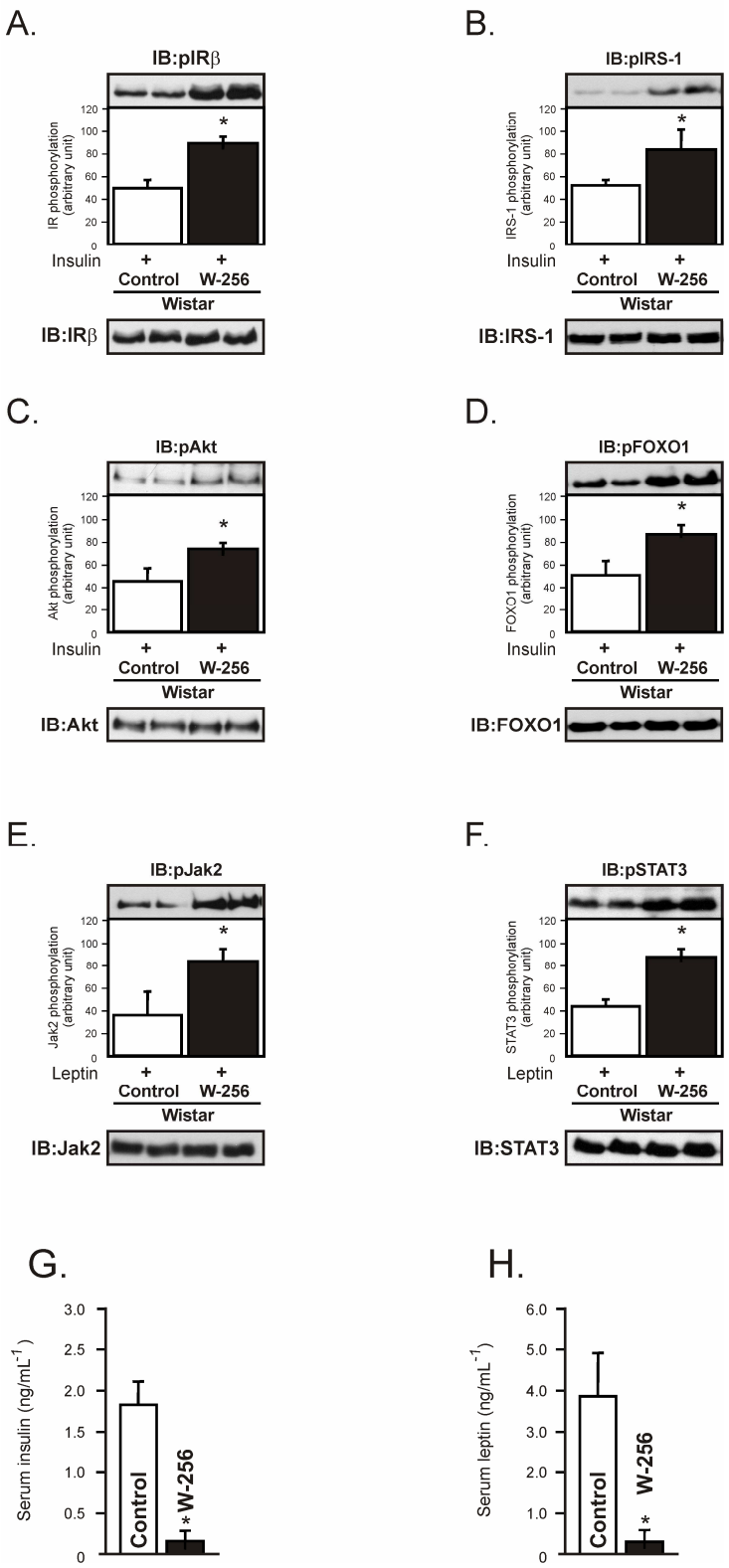
A.
IB:pIRβ
IR phosphorylation (arbitrary unit)
Insulin
Control
W-256
Wistar
IB:IRβ
B.
IB:pIRS-1
IRS-1 phosphorylation (arbitrary unit)
IB:IRS-1
C.
IB:pAkt
Akt phosphorylation (arbitrary unit)
IB:Akt
D.
IB:pFOXO1
FOXO1 phosphorylation (arbitrary unit)
IB:FOXO1
E.
IB:pJak2
Jak2 phosphorylation (arbitrary unit)
Leptin
IB:Jak2
F.
IB:pSTAT3
STAT3 phosphorylation (arbitrary unit)
IB:STAT3
G.
Serum insulin (ng/mL-1)
H.
Serum leptin (ng/mL-1)

Figure 4

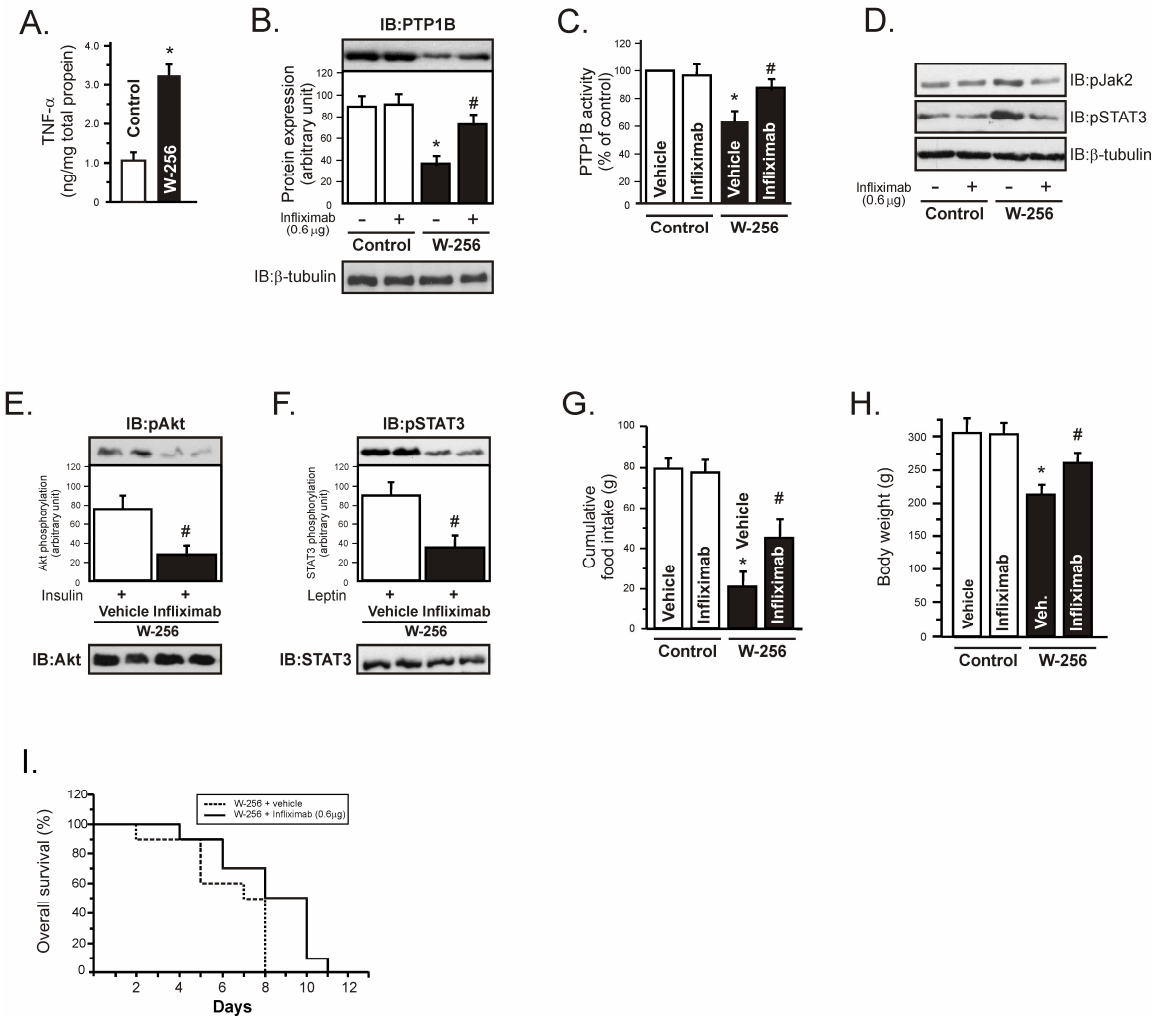
A.
TNF-α (ng/mg total propein)
Control
W-256
B.
IB:PTP1B
Protein expression (arbitrary unit)
Infliximab (0.6 μg)
Control
W-256
IB:β-tubulin
C.
PTP1B activity (% of control)
Vehicle
Infliximab
Control
W-256
D.
IB:pJak2
IB:pSTAT3
IB:β-tubulin
Infliximab (0.6 μg)
Control
W-256
E.
IB:pAkt
Akt phosphorylation (arbitrary unit)
Insulin
Vehicle Infliximab
W-256
IB:Akt
F.
IB:pSTAT3
STAT3 phosphorylation (arbitrary unit)
Leptin
Vehicle Infliximab
W-256
IB:STAT3
G.
Cumulative food intake (g)
Vehicle
Infliximab
Control
W-256
H.
Body weight (g)
Vehicle
Infliximab
Veh.
Infliximab
Control
W-256
I.
Overall survival (%)
W-256 + vehicle
W-256 + Infliximab (0.6μg)
Days

Figure 5

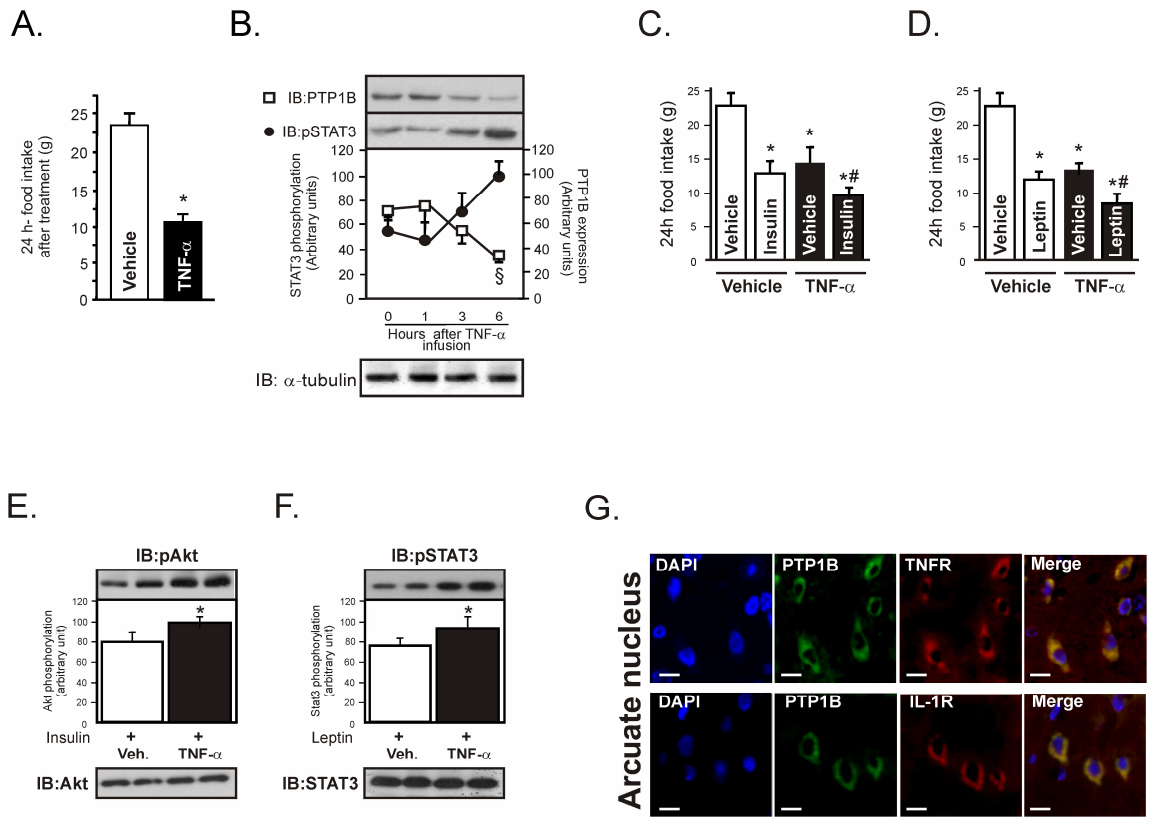
A.
B.
C.
D.
24 h- food intake after treatment (g)
Vehicle
TNF-α
IB:PTP1B
IB:pSTAT3
STAT3 phosphorylation (Arbitrary units)
PTP1B expression (Arbitrary units)
Hours after TNF-α infusion
IB: α-tubulin
24h food intake (g)
Insulin
Leptin
Vehicle
TNF-α
E.
F.
G.
IB:pAkt
Akt phosphorylation (arbitrary unit)
Insulin
Veh.
IB:Akt
IB:pSTAT3
Stat3 phosphorylation (arbitrary unit)
Leptin
IB:STAT3
Arcuate nucleus
DAPI
PTP1B
TNFR
IL-1R
Merge

Figure 6

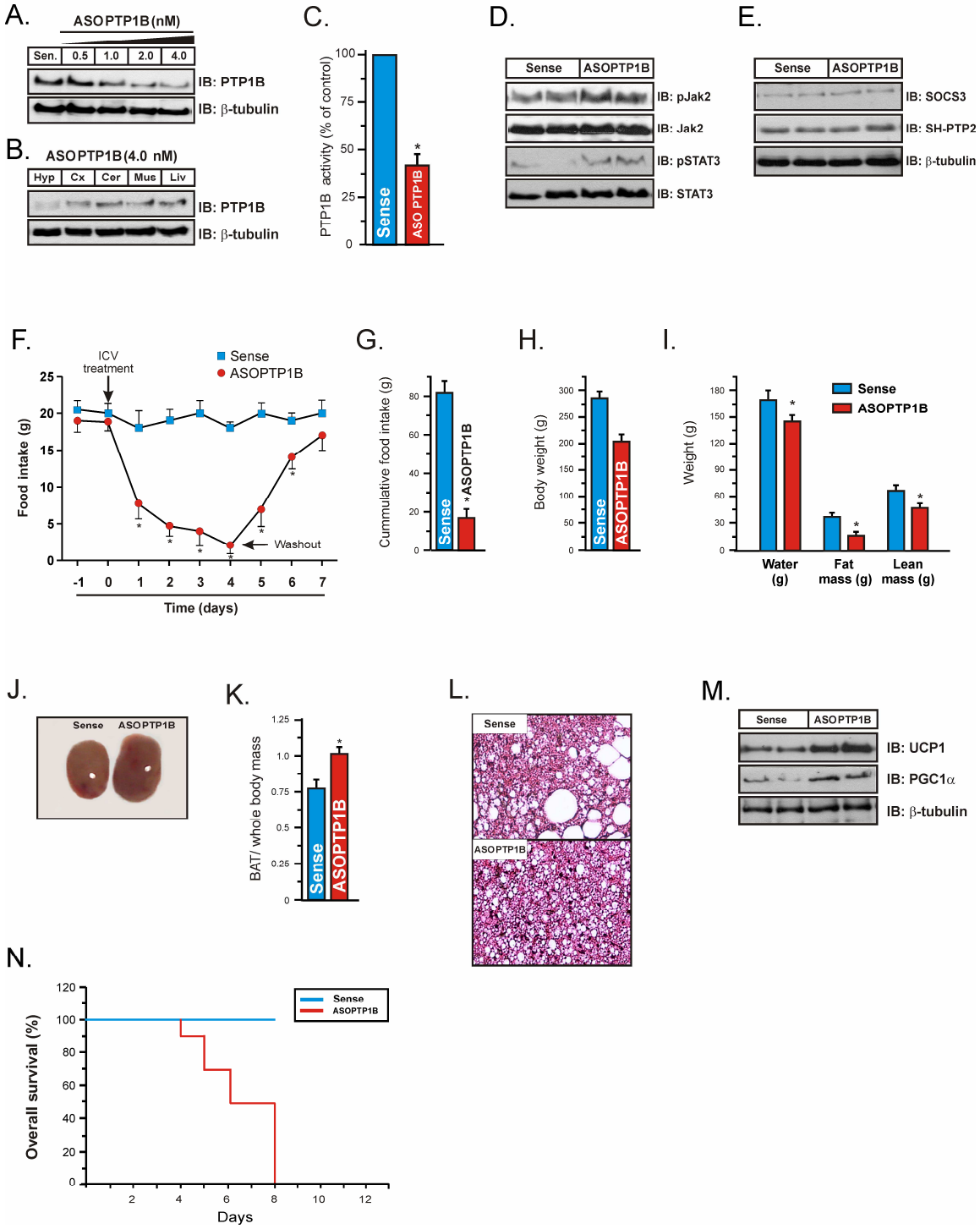
A.
ASOPTP1B(nM)
Sen.
0.5
1.0
2.0
4.0
IB: PTP1B
IB: β-tubulin
B.
ASOPTP1B(4.0 nM)
Hyp
Cx
Cer
Mus
Liv
IB: PTP1B
IB: β-tubulin
C.
PTP1B activity (% of control)
Sense
ASO PTP1B
D.
Sense
ASOPTP1B
IB: pJak2
IB: Jak2
IB: pSTAT3
IB: STAT3
E.
Sense
ASOPTP1B
IB: SOCS3
IB: SH-PTP2
IB: β-tubulin
F.
ICV treatment
Sense
ASOPTP1B
Food intake (g)
Washout
Time (days)
G.
Cummulative food intake (g)
Sense
ASOPTP1B
H.
Body weight (g)
Sense
ASOPTP1B
I.
Weight (g)
Sense
ASOPTP1B
Water (g)
Fat mass (g)
Lean mass (g)
J.
Sense
ASOPTP1B
K.
BAT/ whole body mass
Sense
ASOPTP1B
L.
Sense
ASOPTP1B
M.
Sense
ASOPTP1B
IB: UCP1
IB: PGC1α
IB: β-tubulin
N.
Overall survival (%)
Sense
ASOPTP1B
Days

Figure 7

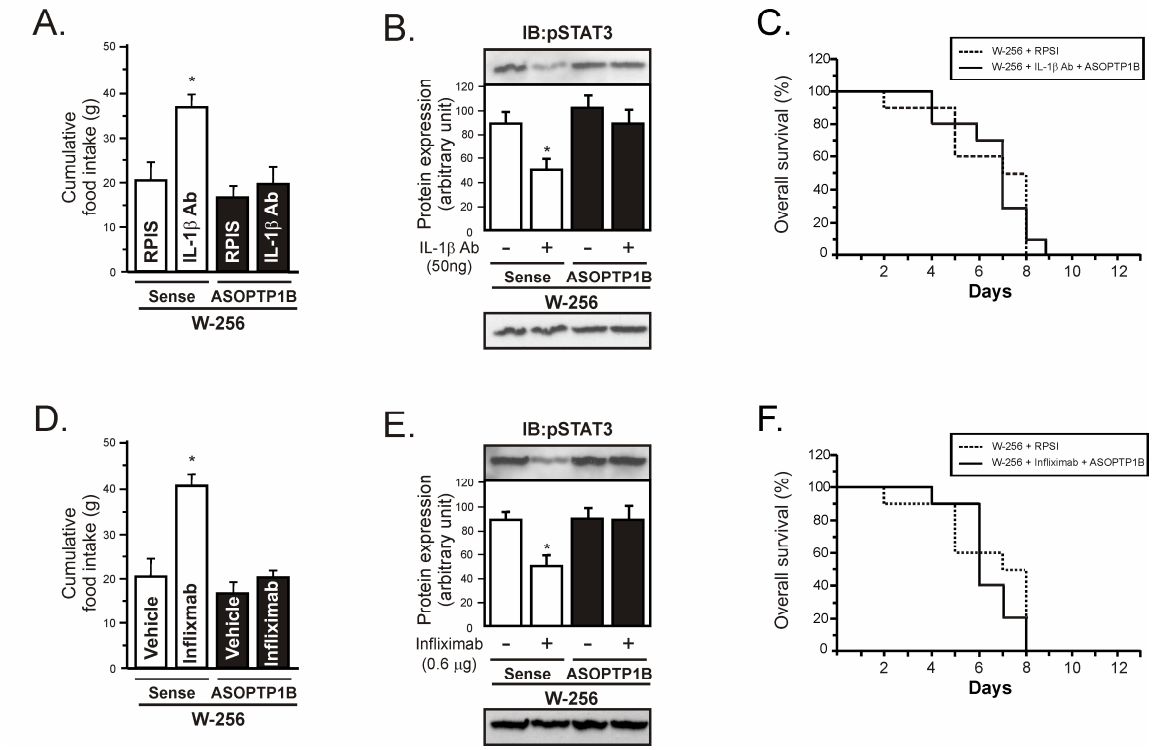
A.
Cumulative food intake (g)
RPIS
IL-1β Ab
RPIS
IL-1β Ab
Sense
ASOPTP1B
W-256
B.
IB:pSTAT3
Protein expression (arbitrary unit)
IL-1β Ab (50ng)
Sense
ASOPTP1B
W-256
C.
W-256 + RPSI
W-256 + IL-1β Ab + ASOPTP1B
Overall survival (%)
Days
D.
Cumulative food intake (g)
Vehicle
Infliximab
Vehicle
Infliximab
Sense
ASOPTP1B
W-256
E.
IB:pSTAT3
Protein expression (arbitrary unit)
Infliximab (0.6 μg)
Sense
ASOPTP1B
W-256
F.
W-256 + RPSI
W-256 + Infliximab + ASOPTP1B
Overall survival (%)
Days

Supplementary Figures 1

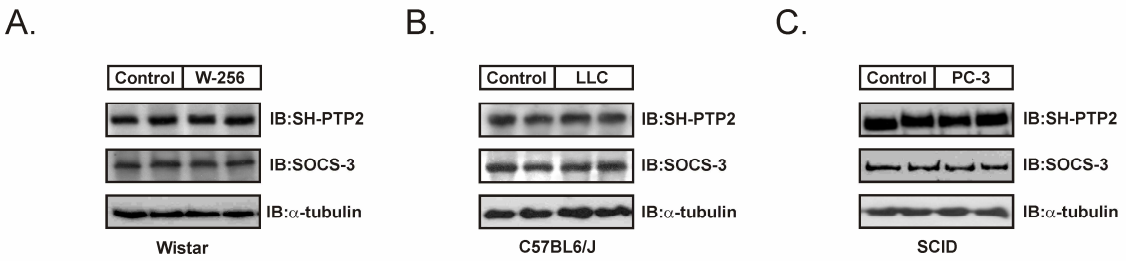

Supplementary Figure 1. SOCS3 and SH-PTP2 expression in the hypothalamus of anorectic rodents. (A) Hypothalamic SOCS3 and SH-PTP2 expression, in Walker-256 tumor-bearing rats. (B) Male C57BL6/J mice were implanted with 5.0×10^5 LLC cells into the dorsal subcutis and hypothalami samples were removed to evaluation of SOCS3 and SH-PTP2 expression. (C) Male SCID mice were implanted with 1.0×10^6 PC-3 cells into the dorsal subcutis and hypothalami samples were removed to evaluation of SOCS3 and SH-PTP2 expression.

Supplementary Figures 2

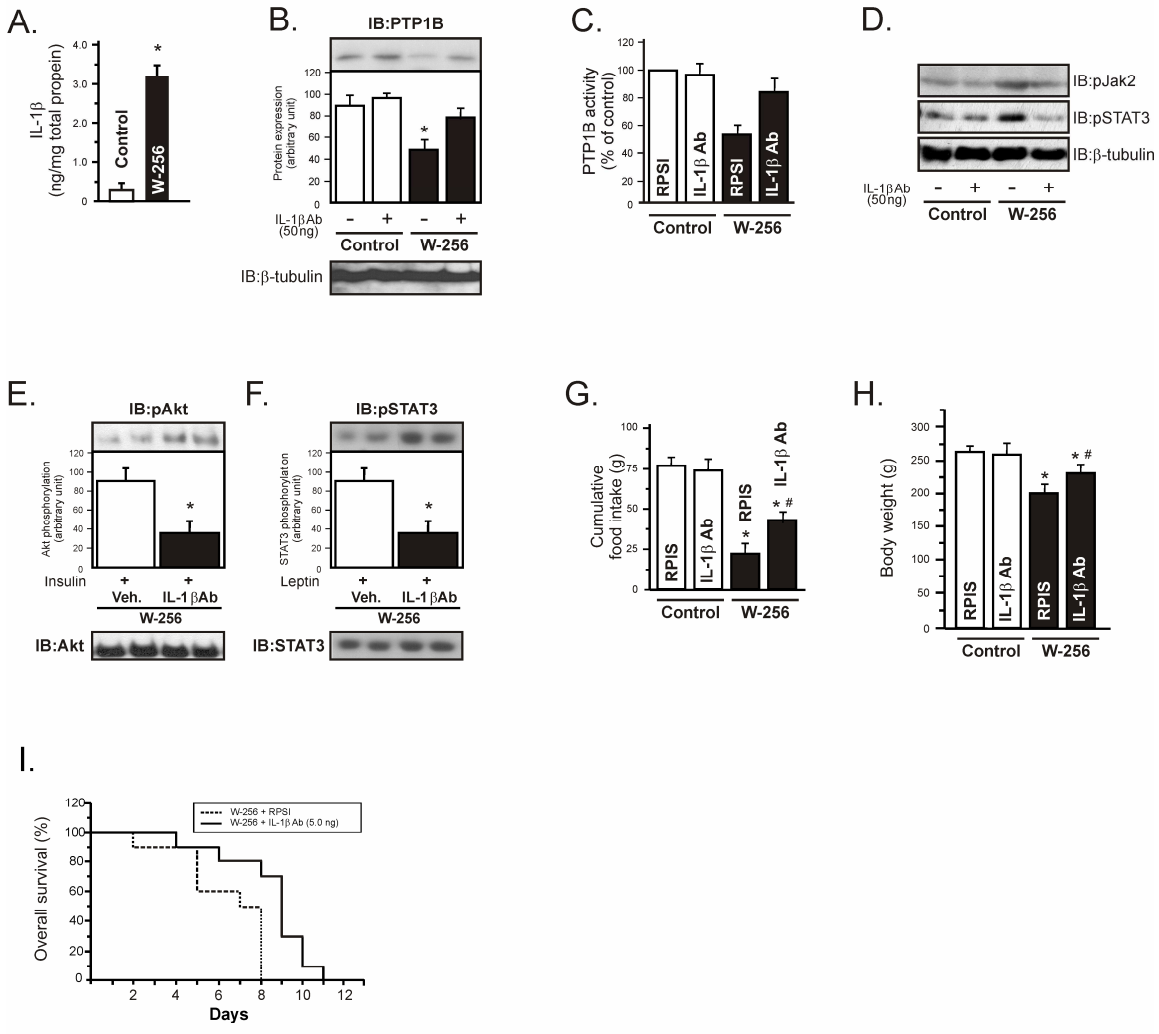

Supplementary Figure 2. The effects of anti-IL-1 antibody on hypothalamic PTP1B activity in tumor-bearing rats. (A) IIypothalamic levels of TNF-α in control and tumor-bearing rats during cancer-induced anorexia period. The effects of daily i.c.v. treatment with anti-IL-1β antibody (50 ng) on (B) hypothalamic PTP1B protein expression and (C) Protein tyrosine phosphatase activity of PTP1B. (D) Hypothalamic extract from tumor-bearing and control rats were obtained 60 minutes after the last i.c.v. anti-IL-1β antibody infusion to evaluate Jak2 and STAT3 tyrosine phosphorylation. (E and F) One hour after the last i.c.v. rabbit pre-immune serum (RPIS) or anti-IL-1β antibody infusion, tumor-bearing rats received i.c.v. insulin or leptin infusion to evaluation of hypothalamic Akt and STAT3 phosphorylation, respectively. (G) Cumulative food intake and (H) body weight of control and tumor-bearing rats during cancer-induced anorexia period after RPIS or anti-IL-1β antibody treatment. (I) Representative survival curves demonstrating the effect of chronic administration of anti-IL-1β antibody on life span of tumor bearing-animals. The survival curves were estimated using Kaplan-Meier's estimates, and curves were compared using the log-rank test, $P < 0.001$ (n = 10).

Supplementary Figures 3

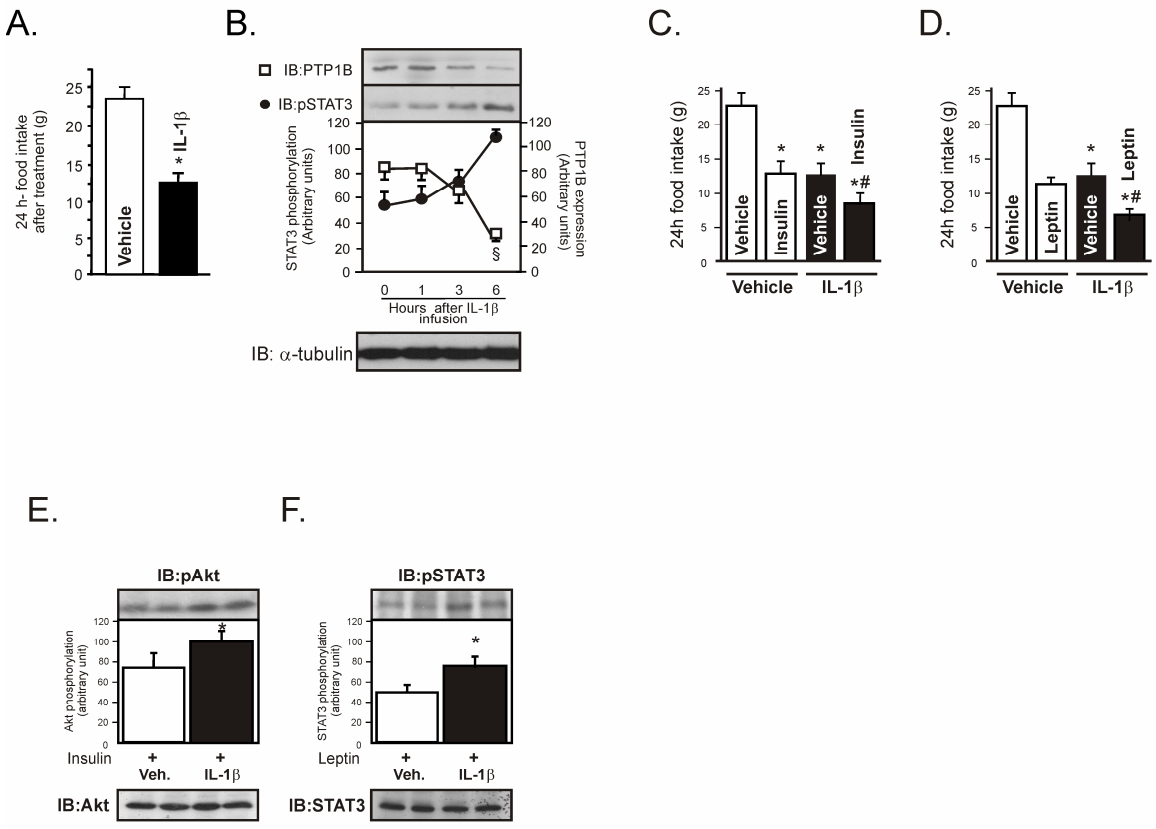

Supplementary Figure 3. The effects of IL-1b on PTP1B activity and insulin and leptin sensitivity in hypothalamus of control animals. (A) Effects of i.c.v. infusion of recombinant IL-1β (5.0 ng) infusion on food intake in control animals. (B) Time-course representing STAT3 tyrosine phosphorylation and PTP1 expression in the hypothalamus of control rats injected with recombinant IL-1β . (C and D) Food intake was determine after i.c.v. IL-1β infusion plus insulin or leptin in control animals. (E and F) Three hours after IL-1β infusion, insulin or leptin was injected to evaluation of Akt and STAT3 phosphorylation, respectively. The results of scanning densitometry were expressed as arbitrary units. Bars represent means ± S.E.M. of n = 56 animals. **P* < 0.05, versus control animals and §*P* < 0.05, versus pSTAT3.

Supplementary Figures 4

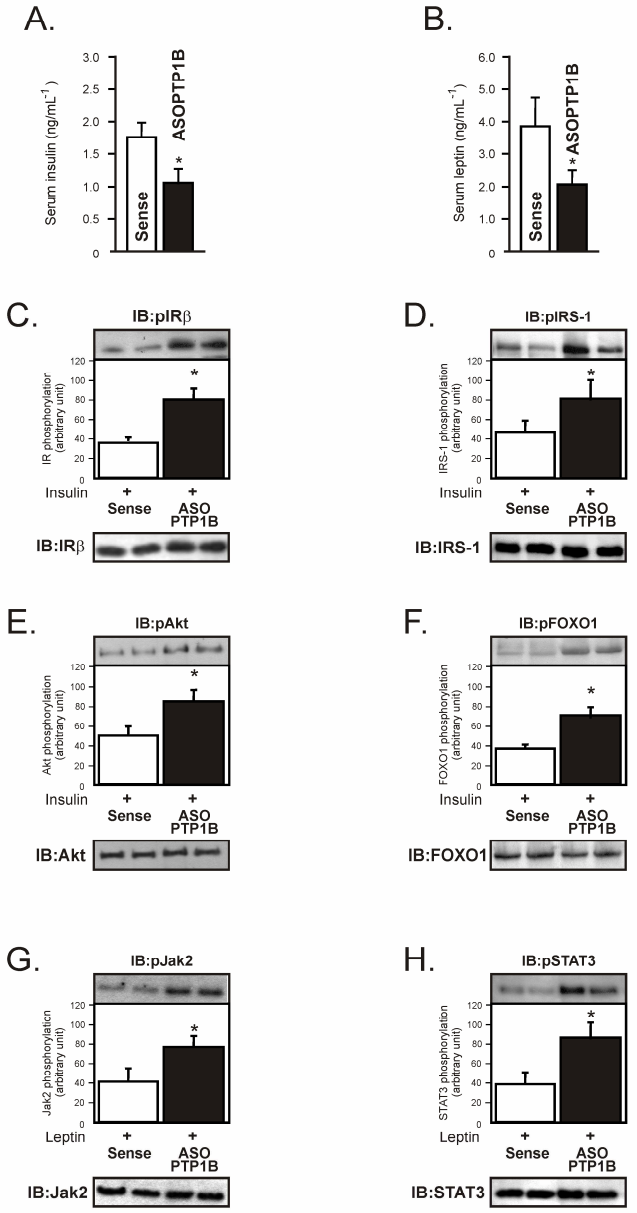

Supplementary Figure 4. Intrahypothalamic infusion of ASOPTP1B increase insulin and leptin sensitivity in rats. Four days after ASOPTP1B (4.0nM) treatment, reduced serum insulin and leptin levels (A and B) as determined by ELISA assays. hypothalamic extract were obtained 15 minutes after i.c.v. insulin or leptin infusion. Tissue extracts were immunoblotted (IB) with specific antibodies to evaluate the levels of © IRβ, (D) IRS1, (E) Akt (F) Foxo1 (G) Jak2 and (H) STAT3 phosphorylation. The results of scanning densitometry were expressed as arbitrary units. Bars represent means ± S.E.M. of n = 68 rats. *$P < 0.05$, versus control rats.

4-CONCLUSÃO

O presente estudo caracterizou as vias de transmissão dos sinais de saciedade promovidos pela insulina e pela leptina no hipotálamo de roedores durante a anorexia induzida pelo desenvolvimento tumoral e documentou a importância da expressão da PTP1B neuronal no controle da anorexia. Demonstramos que as vias anorexigênicas mediadas pela insulina e pela leptina no hipotálamo estão hipersensíveis durante a anorexia induzida por tumor em consequência da baixa expressão da PTP1B hipotalâmica. Evidenciamos ainda que a infusão central de agentes antiinflamatórios como o anticorpo anti-IL-1 β ou o Infliximab, foi capaz de restaurar a expressão e a atividade PTP1B em neurônios, reduzindo a sensibilidade à insulina e à leptina, aumentando a ingestão alimentar, peso corporal e de sobrevida em animais com tumor. Inversamente, a injeção intracerebroventricular do recombinante da IL-1 β ou do TNF-α reduziu a expressão PTP1B neuronal e aumentou a sinalização anorexigênica modulada pela à insulina e pela leptina em animais controle. Finalmente, infusão central do oligonucleotídeo antisense contra a PTP1B (PTP1B ASO), provocou anorexia, perda de peso corporal severa e morte em ratos controle. Assim, estes dados sugerem que a PTP1B neuronal é fosfatase chave para o controle dos sinais anorexigênicos e representa um potencial alvo terapêutico para o tratamento da anorexia em pacientes com câncer.

5-ARTIGOS RELACIONADOS

O sistema nervoso central é responsável por perceber e identificar as condições ambientais externas, bem como as condições reinantes dentro do próprio corpo e elaborar respostas que adaptem a essas condições, no intuito de manter a homeostase. Acredita-se que não haja função no organismo humano que, direta ou indiretamente, não seja controlada pelo hipotálamo (Cross, 1964) (The hypothalamus in mammalian homeostasis). Desta forma, as funções hipotalâmicas desempenham papel determinante para a manutenção da saúde. Dentre estas funções o controle da ingestão alimentar tem sido o principal alvo de investigação a mais de meio século.

Além do desenvolvimento tumoral outros distúrbios metabólicos podem interferir diretamente no funcionamento do hipotálamo e alterar sensivelmente a homeostase energética. Dentre estes distúrbios metabólicos, destaca-se a obesidade. Diversos grupos em todo o mundo se propuseram a entender como os hormônios, os nutrientes e a atividade física estão envolvidos no controle da ingestão alimentar.

Mediante a este cenário, além do trabalho anteriormente apresentado, outros estudos com base no controle da ingestão alimentar mediado pelo hipotálamo foram conduzidos durante o período de doutoramento. A seguir, descrevo um breve resumo de cada trabalho, bem como os artigos publicados na íntegra (em Apêndices).

5.1- ARTIGO 2

Um extenso acumulado de evidências aponta que distúrbios funcionais do hipotálamo participam de forma importante da gênese da obesidade. Tais distúrbios podem em algumas circunstancias decorrer de defeitos genéticos que levam a expressão anômala de proteínas com funções centrais no controle da fome e da termogênese. Entretanto, distúrbios hipotalâmicos gerados por fatores ambientais têm maior relevância epidemiológica no desenvolvimento da obesidade.

Dentre as diversas vias de sinalização neuronais envolvidas no controle da ingestão alimentar, as vias intracelulares moduladas pela insulina e pela leptina ganharam maior destaque nos últimos anos. Embora os mecanismos de transdução dos sinais gerados pela insulina e pela leptina sejam considerados complexos, parece haver um consenso de que fatores de transcrição como a *forkhead transcriptional factor subfamily forkhead box O1* (Foxo1), que participa da transmissão do sinal insulínico, e a *Signal Transducer and Activator of Transcription-3* (STAT-3), que é proteína distal da via de sinalização da leptina, são moléculas importantes para o controle da fome e da saciedade em mamíferos.

Desta forma o trabalho intitulado "*Inhibition of hypothalamic Foxo1 expression reduced food intake in diet-induced obesity rats*" publicado em 2009, foi conduzido em modelo experimental de obesidade induzida por dieta e aponta que a inibição da Foxo1 em neurônios hipotalâmicos é capaz de reduzir a ingestão alimentar e o peso corporal em ratos e desta forma representa um potencial alvo terapêutico para o combate à obesidade (artigo **APÊNDICE I**).

5.2- ARTIGO 3

Desde a teoria glicostática de Mayer e a teoria lipostática de Kennedy, acreditava-se que os nutrientes possuíam a capacidade de modular o apetite por ações no sistema nervoso central (Mayer *et al.*, 1952; Christophe & Mayer, 1960; Hales & Kennedy, 1964). Estudos desenvolvidos principalmente na última década revelaram que a glicose e ácidos graxos têm capacidade de modular a ingestão alimentar através de redes neurais específicas localizadas no hipotálamo. No ano de 2006, Cota e colaboradores descreveram pela primeira vez, que além da glicose e dos ácidos graxos, os aminoácidos também sinalizam para o sistema nervoso central e controlam a ingestão alimentar. Os autores demonstraram que a proteína *mammalian Target of Rapamycin* (mTOR) é capaz de modular a ingestão alimentar integrando sinais hormonais (leptina) e nutricionais (leucina) no tecido hipotalâmico (Cota *et al.*, 2006).

Mais recentemente, o estudo desenvolvido em nosso laboratório intitulado "*A central role for neuronal AMP-activated protein kinase (AMPK) and mammalian target of rapamycin (mTOR) in high-protein diet-induced weight loss*", publicado em 2008 na revista *Diabetes*, demonstrou que a via AMPK/mTOR é sensibilizada pela dieta rica em proteínas, e que a leucina é o principal aminoácido presente na dieta hiperproteica responsável pela modulação da via AMPK/mTOR no hipotálamo. A inibição da AMPK e a ativação da mTOR mediada pela leucina são essenciais para o controle da ingestão alimentar e do peso corporal, tanto em ratos normais como em modelo de camundongo diabético. Além disso, este trabalho demonstra a estreita relação existente entre a AMPK e a mTOR em neurônios contribuindo diretamente para o controle da homeostase energética, evidenciando a capacidade de aminoácidos específicos em modular circuitos neuronais responsáveis pela ingestão alimentar. Esses achados ampliam as teorias criadas por Mayer e Kennedy, colocando os aminoácidos como nutrientes centrais no controle da ingestão alimentar (**APÊNDICE II**).

5.3- ARTIGO 4

A atividade física é uma das pedras angulares tanto na prevenção como no tratamento de doenças associadas à obesidade como diabetes tipo 2 e doenças cardiovasculares. O dispêndio energético proporcionado tanto por exercícios aeróbicos como pelos exercícios resistidos é um dos fatores mais importantes na redução do peso ponderal. No entanto, recentes evidências demonstram que além de proporcionar maior gasto energético, a atividade física também é capaz de amplificar os sinais anorexigênicos no hipotálamo, contribuindo significativamente para a redução da ingestão alimentar e redução do *set point* para o peso corporal em roedores (Bi *et al.*, 2005; Flores *et al.*, 2006; Patterson *et al.*, 2009). A primeira evidência de que a atividade física poderia modular sinais anorexigênicos no sistema nervoso central foi descrita por Flores e colaboradores em 2006. Os autores descreveram que a citocinas IL-6 é a principal molécula, produzida durante a contração muscular, responsável por amplificar as ações anorexigênica em hipotálamo de ratos. Neste sentido investigamos se a atividade física, através da IL-6, poderia modular a via AMPK/mTOR no sistema nervoso central.

Identificamos que a IL-6 modulou a via AMPK/mTOR em neurônios hipotalâmicos através do aumento da razão AMP:ATP no sistema nervoso central, aumentando significativamente a sensibilidade desta via em resposta à leptina. O estudo intitulado "*Central exercise action increases the AMPK and mTOR response to leptin"* foi publicado na revista *PLoS One* em 2008 (artigo **APÊNDICE III**).

5.4- ARTIGO 5

Postula-se que o desenvolvimento de um processo inflamatório sub-clinico, decorrente da obesidade, seja a principal causa da resistência central a ação da leptina e da insulina no tecido hipotalâmico, resultando em hiperfagia e perpetuação da obesidade. Recentemente, a proteína IKKβ foi identificada como uma molécula chave na sinalização inflamatória responsável por atenuar os sinais anorexigênicos mediados pela insulina e leptina no tecido hipotalâmico (Zhang *et al.*, 2008; Milanski *et al.*, 2009). No entanto, a maioria das terapias antiinflamatórias testadas, tendo como alvo a proteína IKKβ, foram incapazes de concentrar seus efeitos especificamente no sistema nervoso central. Desta forma, elaboramos a hipótese de que a atividade física poderia ser uma importante estratégia para atenuar a inflamação no sistema nervoso central e restabelecer a transmissão dos sinais da insulina e da leptina em hipotálamo de animais obesos. O estudo intitulado "*IL-6 Anti-inflammatory Activity Links Exercise to Hypothalamic Insulin and Leptin Sensitivity through IKKβ and ER Stress Inhibition*", fornece evidências substanciais de que a atividade física promove uma resposta antiinflamatória no tecido hipotalâmico através do aumento da expressão das proteínas IL-6 e IL-10. Descrevemos que a IL-6 e IL-10 são importantes contribuintes fisiológicos produzidas pelo exercício, responsáveis por recuperar a sensibilidade à insulina e à leptina no hipotálamo e atenuar a hiperfagia em diferentes modelos de obesidade em roedores. Desta forma, a atividade física pode ser uma estratégia terapêutica para restaurar a sensibilidade central à insulina e leptina em indivíduos obesos desempenhando papel importante na manutenção em longo prazo do fenótipo magro. (artigo em fase de publicação na revista PLoS Biology- **APÊNDICE IV**)

5.5- ARTIGO 6

Por fim, à convite de um dos editores da revista *Neurologia*, elaboramos um artigo de revisão intitulado*"Brain regulation of food intake and expenditure energy: molecular action of insulin, leptin and physical exercise"*onde descrevemos muitos dos nossos achados, enfatizando principalmente a ação da IL-6 no controle da ingestão alimentar e do gasto energético. Além disso, evidenciamos as mais novas descobertas à respeito da sinalização da insulina e da leptina no sistema nervoso central, no que concerne a regulação da homeostase energética (**APÊNDICE V**).

6- DEMAIS ARTIGOS PUBLICADOS

Além dos artigos anteriormente mencionados, elaborei, executei e colaborei com o desenvolvimento de outros projetos com enfoque nos mecanismos de resistência à insulina em tecidos periféricos como músculo, fígado e tecido adiposo. Dentre estes trabalhos, destaco dois, nos quais sou primeiro autor de um e divido a primeira autoria do outro com a Dra. Patrícia Prada. Os artigos são:

- Acute exercise modulates the Foxo1/PGC-1alpha pathway in the liver of diet-induced obesity rats. Ropelle ER, Pauli JR, Cintra DE, Frederico MJ, de Pinho RA, Velloso LA, De Souza CT. ***J Physiol***. 2009. 587:2069-76. **(APÊNDICE VI)**.

- EGFR Tyrosine Kinase Inhibitor (PD153035) Improves Glucose Tolerance and Insulin Action in High-Fat Diet-Fed Mice. Prada PO, Ropelle ER, Mourão RH, de Souza CT, Pauli JR, Cintra DE, Schenka A, Rocco SA, Rittner R, Franchini KG, Vassallo J, Velloso LA, Carvalheira JB, Saad MJ. ***Diabetes***. 2009. 58(12):2910-19 **(APÊNDICE VII)**.

Por fim, relaciono os demais trabalhos que participei como co-autor durante o processo de doutoramento. São eles:

- Hypothalamic Actions of Tumor Necrosis Factor {alpha} Provide the Thermogenic Core for the Wastage Syndrome in Cachexia. Arruda AP, Milanski M, Romanatto T, Solon C, Coope A, Alberici LC, Festuccia WT, Hirabara SM, Ropelle E, Curi R, Carvalheira JB, Vercesi AE, Velloso LA. ***Endocrinology***. 2010. 151(2):683-94. **(APÊNDICE VIII)**

- Aspirin attenuates insulin resistance in muscle of diet-induced obese rats by inhibiting inducible nitric oxide synthase production and S-nitrosylation of IRbeta/IRS-1 and Akt. Carvalho-Filho MA, Ropelle ER, Pauli RJ, Cintra DE, Tsukumo DM, Silveira LR, Curi R, Carvalheira JB, Velloso LA, Saad MJ. ***Diabetologia***. 2009. 52(11):2425-34. **(APÊNDICE IX)**.

- Acute exercise reverses TRB3 expression in the skeletal muscle and ameliorates whole body insulin sensitivity in diabetic mice. Matos A, Ropelle ER, Pauli JR, Frederico MJ, de Pinho RA, Velloso LA, De Souza CT. ***Acta Physiol*** (Oxf). 2009 198(1):61-9. **(APÊNDICE X)**.

- New mechanisms by which physical exercise improves insulin resistance in the skeletal muscle. Pauli JR, Cintra DE, Souza CT, Ropelle ER. ***Arq Bras Endocrinol Metabol***. 2009. (4):399-408 **(APÊNDICE XI)**.

- Acute exercise reduces insulin resistance-induced TRB3 expression and amelioration of the hepatic production of glucose in the liver of diabetic mice. Lima AF, Ropelle ER, Pauli JR, Cintra DE, Frederico MJ, Pinho RA, Velloso LA, De Souza CT. ***J Cell Physiol***. 2009. 221(1):92-7. **(APÊNDICE XII).**

- Antineoplastic effect of rapamycin is potentiated by inhibition of IRS-1 signaling in prostate cancer cells xenografts. Oliveira JC, Souza KK, Dias MM, Faria MC, Ropelle ER, Flores MB, Ueno M, Velloso LA, Saad ST, Saad MJ, Carvalheira JB. ***J Cancer Res Clin Oncol***. 2008. 134(8):833-9. **(APÊNDICE XIII).**

- Statin modulates insulin signaling and insulin resistance in liver and muscle of rats fed a high-fat diet. Lalli CA, Pauli JR, Prada PO, Cintra DE, Ropelle ER, Velloso LA, Saad MJ. ***Metabolism***. 2008. 57(1):57-65. **(APÊNDICE XIV)**

- Acute physical exercise reverses S-nitrosation of the insulin receptor, insulin receptor substrate 1 and protein kinase B/Akt in diet-induced obese Wistar rats. Pauli JR, Ropelle ER, Cintra DE, Carvalho-Filho MA, Moraes JC, De Souza CT, Velloso LA, Carvalheira JB, Saad MJ. ***J Physiol***. 2008. 15;586(2):659-71. **(APÊNDICE XV)**

7-REFERÊNCIAS

Ahima RS, Prabakaran D, Mantzoros C, Qu D, Lowell B, Maratos-Flier E & Flier JS. (1996). Role of leptin in the neuroendocrine response to fasting. *Nature* **382,** 250-252.

Ahmad F & Goldstein BJ. (1995). Increased abundance of specific skeletal muscle protein-tyrosine phosphatases in a genetic model of insulin-resistant obesity and diabetes mellitus. *Metabolism* **44,** 1175-1184.

Bado A, Levasseur S, Attoub S, Kermorgant S, Laigneau JP, Bortoluzzi MN, Moizo L, Lehy T, Guerre-Millo M, Le Marchand-Brustel Y & Lewin MJ. (1998). The stomach is a source of leptin. *Nature* **394,** 790-793.

Bandyopadhyay G, Standaert ML, Zhao L, Yu B, Avignon A, Galloway L, Karnam P, Moscat J & Farese RV. (1997). Activation of protein kinase C (alpha, beta, and zeta) by insulin in 3T3/L1 cells. Transfection studies suggest a role for PKC-zeta in glucose transport. *J Biol Chem* **272,** 2551-2558.

Baskin DG, Breininger JF & Schwartz MW. (1999). Leptin receptor mRNA identifies a subpopulation of neuropeptide Y neurons activated by fasting in rat hypothalamus. *Diabetes* **48,** 828-833.

Baskin DG, Wilcox BJ, Figlewicz DP & Dorsa DM. (1988). Insulin and insulin-like growth factors in the CNS. *Trends Neurosci* **11,** 107-111.

Baura GD, Foster DM, Porte D, Jr., Kahn SE, Bergman RN, Cobelli C & Schwartz MW. (1993). Saturable transport of insulin from plasma into the central nervous system of dogs in vivo. A mechanism for regulated insulin delivery to the brain. *J Clin Invest* **92,** 1824-1830.

Bence KK, Delibegovic M, Xue B, Gorgun CZ, Hotamisligil GS, Neel BG & Kahn BB. (2006). Neuronal PTP1B regulates body weight, adiposity and leptin action. *Nat Med* **12,** 917-924.

Bi S, Scott KA, Hyun J, Ladenheim EE & Moran TH. (2005). Running wheel activity prevents hyperphagia and obesity in Otsuka long-evans Tokushima Fatty rats: role of hypothalamic signaling. *Endocrinology* **146,** 1676-1685.

Bosaeus I, Daneryd P & Lundholm K. (2002). Dietary intake, resting energy expenditure, weight loss and survival in cancer patients. *J Nutr* **132,** 3465S-3466S.

Bruera E. (1997). ABC of palliative care. Anorexia, cachexia, and nutrition. *Bmj* **315,** 1219-1222.

Campfield LA, Smith FJ, Guisez Y, Devos R & Burn P. (1995). Recombinant mouse OB protein: evidence for a peripheral signal linking adiposity and central neural networks. *Science* **269,** 546-549.

Cheng A, Uetani N, Simoncic PD, Chaubey VP, Lee-Loy A, McGlade CJ, Kennedy BP & Tremblay ML. (2002). Attenuation of leptin action and regulation of obesity by protein tyrosine phosphatase 1B. *Dev Cell* **2,** 497-503.

Cheung CC, Clifton DK & Steiner RA. (1997). Proopiomelanocortin neurons are direct targets for leptin in the hypothalamus. *Endocrinology* **138,** 4489-4492.

Christophe J & Mayer J. (1960). Glucose uptake as a function of food intake in normal and hypothalamic hyperphagic rats. *Metabolism* **9,** 932-937.

Considine RV, Sinha MK, Heiman ML, Kriauciunas A, Stephens TW, Nyce MR, Ohannesian JP, Marco CC, McKee LJ, Bauer TL & et al. (1996). Serum immunoreactive-leptin concentrations in normal-weight and obese humans. *N Engl J Med* **334,** 292-295.

Cota D, Proulx K, Smith KA, Kozma SC, Thomas G, Woods SC & Seeley RJ. (2006). Hypothalamic mTOR signaling regulates food intake. *Science* **312,** 927-930.

Cross BA. (1964). The hypothalamus in mammalian homeostasis. *Symp Soc Exp Biol* **18,** 157-193.

Czech MP & Corvera S. (1999). Signaling mechanisms that regulate glucose transport. *J Biol Chem* **274,** 1865-1868.

Dadke SS, Li HC, Kusari AB, Begum N & Kusari J. (2000). Elevated expression and activity of protein-tyrosine phosphatase 1B in skeletal muscle of insulin-resistant type II diabetic Goto-Kakizaki rats. *Biochem Biophys Res Commun* **274,** 583-589.

De Vos P, Saladin R, Auwerx J & Staels B. (1995). Induction of ob gene expression by corticosteroids is accompanied by body weight loss and reduced food intake. *J Biol Chem* **270,** 15958-15961.

Di Paola R, Frittitta L, Miscio G, Bozzali M, Baratta R, Centra M, Spampinato D, Santagati MG, Ercolino T, Cisternino C, Soccio T, Mastroianno S, Tassi V, Almgren P, Pizzuti A, Vigneri R & Trischitta V. (2002). A variation in 3' UTR of hPTP1B increases specific gene expression and associates with insulin resistance. *Am J Hum Genet* **70,** 806-812.

Elchebly M, Payette P, Michaliszyn E, Cromlish W, Collins S, Loy AL, Normandin D, Cheng A, Himms-Hagen J, Chan CC, Ramachandran C, Gresser MJ, Tremblay ML & Kennedy BP. (1999). Increased insulin sensitivity and obesity resistance in mice lacking the protein tyrosine phosphatase-1B gene. *Science* **283,** 1544-1548.

Fan W, Boston BA, Kesterson RA, Hruby VJ & Cone RD. (1997). Role of melanocortinergic neurons in feeding and the agouti obesity syndrome. *Nature* **385,** 165-168.

Flier JS. (2004). Obesity wars: molecular progress confronts an expanding epidemic. *Cell* **116,** 337-350.

Flores MB, Fernandes MF, Ropelle ER, Faria MC, Ueno M, Velloso LA, Saad MJ & Carvalheira JB. (2006). Exercise improves insulin and leptin sensitivity in hypothalamus of Wistar rats. *Diabetes* **55,** 2554-2561.

Frederich RC, Hamann A, Anderson S, Lollmann B, Lowell BB & Flier JS. (1995). Leptin levels reflect body lipid content in mice: evidence for diet-induced resistance to leptin action. *Nat Med* **1,** 1311-1314.

Gelin J, Moldawer LL, Lonnroth C, Sherry B, Chizzonite R & Lundholm K. (1991). Role of endogenous tumor necrosis factor alpha and interleukin 1 for experimental tumor growth and the development of cancer cachexia. *Cancer Res* **51,** 415-421.

Goldstein BJ, Bittner-Kowalczyk A, White MF & Harbeck M. (2000). Tyrosine dephosphorylation and deactivation of insulin receptor substrate-1 by protein-tyrosine phosphatase 1B. Possible facilitation by the formation of a ternary complex with the Grb2 adaptor protein. *J Biol Chem* **275,** 4283-4289.

Halaas JL, Gajiwala KS, Maffei M, Cohen SL, Chait BT, Rabinowitz D, Lallone RL, Burley SK & Friedman JM. (1995). Weight-reducing effects of the plasma protein encoded by the obese gene. *Science* **269,** 543-546.

Hales CN & Kennedy GC. (1964). Plasma glucose, non-esterified fatty acid and insulin concentrations in hypothalamic-hyperphagic rats. *Biochem J* **90,** 620-624.

Harrison S, Page CP & Spina D. (1999). Airway nerves and protein phosphatases. *Gen Pharmacol* **32,** 287-298.

Haslett PA. (1998). Anticytokine approaches to the treatment of anorexia and cachexia. *Semin Oncol* **25,** 53-57.

Havel PJ, Uriu-Hare JY, Liu T, Stanhope KL, Stern JS, Keen CL & Ahren B. (1998). Marked and rapid decreases of circulating leptin in streptozotocin diabetic rats: reversal by insulin. *Am J Physiol* **274,** R1482-1491.

Heldin CH. (1995). Dimerization of cell surface receptors in signal transduction. *Cell* **80,** 213-223.

Hirata AE, Alvarez-Rojas F, Carvalheira JB, Carvalho CR, Dolnikoff MS & Abdalla Saad MJ. (2003). Modulation of IR/PTP1B interaction and downstream signaling in insulin sensitive tissues of MSG-rats. *Life Sci* **73,** 1369-1381.

Hopkins SJ & Rothwell NJ. (1995). Cytokines and the nervous system. I: Expression and recognition. *Trends Neurosci* **18,** 83-88.

Hunter T. (1995). Protein kinases and phosphatases: the yin and yang of protein phosphorylation and signaling. *Cell* **80,** 225-236.

INCA (2009). Estimativa 2010: incidência de câncer no Brasil / Instituto Nacional de Câncer. – Rio de Janeiro

Johnen H, Lin S, Kuffner T, Brown DA, Tsai VW, Bauskin AR, Wu L, Pankhurst G, Jiang L, Junankar S, Hunter M, Fairlie WD, Lee NJ, Enriquez RF, Baldock PA, Corey E, Apple FS, Murakami MM, Lin EJ, Wang C, During MJ, Sainsbury A, Herzog H & Breit SN. (2007). Tumor-induced anorexia and weight loss are mediated by the TGF-beta superfamily cytokine MIC-1. *Nat Med* **13,** 1333-1340.

Johnson TO, Ermolieff J & Jirousek MR. (2002). Protein tyrosine phosphatase 1B inhibitors for diabetes. *Nat Rev Drug Discov* **1,** 696-709.

Kahn SE, Prigeon RL, McCulloch DK, Boyko EJ, Bergman RN, Schwartz MW, Neifing JL, Ward WK, Beard JC, Palmer JP & et al. (1993). Quantification of the relationship between insulin sensitivity and beta-cell function in human subjects. Evidence for a hyperbolic function. *Diabetes* **42,** 1663-1672.

Kaszubska W, Falls HD, Schaefer VG, Haasch D, Frost L, Hessler P, Kroeger PE, White DW, Jirousek MR & Trevillyan JM. (2002). Protein tyrosine phosphatase 1B negatively regulates leptin signaling in a hypothalamic cell line. *Mol Cell Endocrinol* **195,** 109-118.

Kim MS, Pak YK, Jang PG, Namkoong C, Choi YS, Won JC, Kim KS, Kim SW, Kim HS, Park JY, Kim YB & Lee KU. (2006). Role of hypothalamic Foxo1 in the regulation of food intake and energy homeostasis. *Nat Neurosci* **9,** 901-906.

Kim YB, Nikoulina SE, Ciaraldi TP, Henry RR & Kahn BB. (1999). Normal insulin-dependent activation of Akt/protein kinase B, with diminished activation of phosphoinositide 3-kinase, in muscle in type 2 diabetes. *J Clin Invest* **104,** 733-741.

Kitamura T, Feng Y, Kitamura YI, Chua SC, Jr., Xu AW, Barsh GS, Rossetti L & Accili D. (2006). Forkhead protein FoxO1 mediates Agrp-dependent effects of leptin on food intake. *Nat Med* **12,** 534-540.

Kitamura T, Ogawa W, Sakaue H, Hino Y, Kuroda S, Takata M, Matsumoto M, Maeda T, Konishi H, Kikkawa U & Kasuga M. (1998). Requirement for activation of the serine-threonine kinase Akt (protein kinase B) in insulin stimulation of protein synthesis but not of glucose transport. *Mol Cell Biol* **18,** 3708-3717.

Kohn AD, Summers SA, Birnbaum MJ & Roth RA. (1996). Expression of a constitutively active Akt Ser/Thr kinase in 3T3-L1 adipocytes stimulates glucose uptake and glucose transporter 4 translocation. *J Biol Chem* **271,** 31372-31378.

Kotani K, Ogawa W, Matsumoto M, Kitamura T, Sakaue H, Hino Y, Miyake K, Sano W, Akimoto K, Ohno S & Kasuga M. (1998). Requirement of atypical protein kinase clambda for insulin stimulation of glucose uptake but not for Akt activation in 3T3-L1 adipocytes. *Mol Cell Biol* **18,** 6971-6982.

Kristensen P, Judge ME, Thim L, Ribel U, Christjansen KN, Wulff BS, Clausen JT, Jensen PB, Madsen OD, Vrang N, Larsen PJ & Hastrup S. (1998). Hypothalamic CART is a new anorectic peptide regulated by leptin. *Nature* **393,** 72-76.

Larkin M. (1998). Thwarting the dwindling progression of cachexia. *Lancet* **351,** 1336.

Laviano A, Inui A, Marks DL, Meguid MM, Pichard C, Rossi Fanelli F & Seelaender M. (2008). Neural control of the anorexia-cachexia syndrome. *Am J Physiol Endocrinol Metab* **295,** E1000-1008.

Licinio J, Mantzoros C, Negrao AB, Cizza G, Wong ML, Bongiorno PB, Chrousos GP, Karp B, Allen C, Flier JS & Gold PW. (1997). Human leptin levels are pulsatile and inversely related to pituitary-adrenal function. *Nat Med* **3,** 575-579.

Licinio J & Wong ML. (1997). Pathways and mechanisms for cytokine signaling of the central nervous system. *J Clin Invest* **100,** 2941-2947.

Lund IK, Hansen JA, Andersen HS, Moller NP & Billestrup N. (2005). Mechanism of protein tyrosine phosphatase 1B-mediated inhibition of leptin signalling. *J Mol Endocrinol* **34,** 339-351.

Maffei M, Halaas J, Ravussin E, Pratley RE, Lee GH, Zhang Y, Fei H, Kim S, Lallone R, Ranganathan S & et al. (1995). Leptin levels in human and rodent: measurement of plasma leptin and ob RNA in obese and weight-reduced subjects. *Nat Med* **1,** 1155-1161.

Mantovani G, Maccio A, Lai P, Massa E, Ghiani M & Santona MC. (1998). Cytokine activity in cancer-related anorexia/cachexia: role of megestrol acetate and medroxyprogesterone acetate. *Semin Oncol* **25,** 45-52.

Masuzaki H, Ogawa Y, Sagawa N, Hosoda K, Matsumoto T, Mise H, Nishimura H, Yoshimasa Y, Tanaka I, Mori T & Nakao K. (1997). Nonadipose tissue production of leptin: leptin as a novel placenta-derived hormone in humans. *Nat Med* **3,** 1029-1033.

Matthys P & Billiau A. (1997a). Cytokines and cachexia. *Nutrition* **13,** 763-770.

Matthys P & Billiau A. (1997b). Cytokines and cachexia. *Nutrition* **13,** 763-770.

Mayer J, Bates MW & Van Itallie TB. (1952). Blood sugar and food intake in rats with lesions of the anterior hypothalamus. *Metabolism* **1,** 340-348.

Mercer JG, Hoggard N, Williams LM, Lawrence CB, Hannah LT & Trayhurn P. (1996). Localization of leptin receptor mRNA and the long form splice variant (Ob-Rb) in mouse hypothalamus and adjacent brain regions by in situ hybridization. *FEBS Lett* **387,** 113-116.

Milanski M, Degasperi G, Coope A, Morari J, Denis R, Cintra DE, Tsukumo DM, Anhe G, Amaral ME, Takahashi HK, Curi R, Oliveira HC, Carvalheira JB, Bordin S, Saad MJ & Velloso LA. (2009). Saturated fatty acids produce an inflammatory response predominantly through the activation of TLR4 signaling in hypothalamus: implications for the pathogenesis of obesity. *J Neurosci* **29,** 359-370.

Moldawer LL, Rogy MA & Lowry SF. (1992). The role of cytokines in cancer cachexia. *JPEN J Parenter Enteral Nutr* **16,** 43S-49S.

Niswender KD, Morton GJ, Stearns WH, Rhodes CJ, Myers MG, Jr. & Schwartz MW. (2001). Intracellular signalling. Key enzyme in leptin-induced anorexia. *Nature* **413,** 794-795.

Noguchi Y, Yoshikawa T, Matsumoto A, Svaninger G & Gelin J. (1996). Are cytokines possible mediators of cancer cachexia? *Surg Today* **26,** 467-475.

Patterson CM, Bouret SG, Dunn-Meynell AA & Levin BE. (2009). Three weeks of postweaning exercise in DIO rats produces prolonged increases in central leptin sensitivity and signaling. *Am J Physiol Regul Integr Comp Physiol* **296,** R537-548.

Pelleymounter MA, Cullen MJ, Baker MB, Hecht R, Winters D, Boone T & Collins F. (1995). Effects of the obese gene product on body weight regulation in ob/ob mice. *Science* **269,** 540-543.

Picardi PK, Calegari VC, Prada Pde O, Moraes JC, Araujo E, Marcondes MC, Ueno M, Carvalheira JB, Velloso LA & Saad MJ. (2008). Reduction of hypothalamic protein tyrosine phosphatase improves insulin and leptin resistance in diet-induced obese rats. *Endocrinology* **149,** 3870-3880.

Plata-Salaman CR. (1996). Leptin (OB protein), neuropeptide Y, and interleukin-1 interactions as interface mechanisms for the regulation of feeding in health and disease. *Nutrition* **12,** 718-719.

Plata-Salaman CR. (1997). Anorexia during acute and chronic disease: relevance of neurotransmitter-peptide-cytokine interactions. *Nutrition* **13,** 159-160.

Polonsky KS, Given BD & Van Cauter E. (1988). Twenty-four-hour profiles and pulsatile patterns of insulin secretion in normal and obese subjects. *J Clin Invest* **81,** 442-448.

Ramos EJ, Suzuki S, Marks D, Inui A, Asakawa A & Meguid MM. (2004). Cancer anorexia-cachexia syndrome: cytokines and neuropeptides. *Curr Opin Clin Nutr Metab Care* **7,** 427-434.

Ropelle ER, Fernandes MF, Flores MB, Ueno M, Rocco S, Marin R, Cintra DE, Velloso LA, Franchini KG, Saad MJ & Carvalheira JB. (2008). Central exercise action increases the AMPK and mTOR response to leptin. *PLoS One* **3,** e3856.

Ropelle ER, Pauli JR, Prada PO, de Souza CT, Picardi PK, Faria MC, Cintra DE, Fernandes MF, Flores MB, Velloso LA, Saad MJ & Carvalheira JB. (2006). Reversal of diet-induced insulin resistance with a single bout of exercise in the rat: the role of PTP1B and IRS-1 serine phosphorylation. *J Physiol* **577,** 997-1007.

Ropelle ER, Pauli JR, Zecchin KG, Ueno M, de Souza CT, Morari J, Faria MC, Velloso LA, Saad MJ & Carvalheira JB. (2007). A central role for neuronal adenosine 5'-monophosphate-activated protein kinase in cancer-induced anorexia. *Endocrinology* **148,** 5220-5229.

Rothwell NJ & Hopkins SJ. (1995). Cytokines and the nervous system II: Actions and mechanisms of action. *Trends Neurosci* **18,** 130-136.

Saladin R, De Vos P, Guerre-Millo M, Leturque A, Girard J, Staels B & Auwerx J. (1995). Transient increase in obese gene expression after food intake or insulin administration. *Nature* **377,** 527-529.

Schwartz MW, Dallman MF & Woods SC. (1995). Hypothalamic response to starvation: implications for the study of wasting disorders. *Am J Physiol* **269,** R949-957.

Schwartz MW, Prigeon RL, Kahn SE, Nicolson M, Moore J, Morawiecki A, Boyko EJ & Porte D, Jr. (1997). Evidence that plasma leptin and insulin levels are associated with body adiposity via different mechanisms. *Diabetes Care* **20,** 1476-1481.

Seely BL, Staubs PA, Reichart DR, Berhanu P, Milarski KL, Saltiel AR, Kusari J & Olefsky JM. (1996). Protein tyrosine phosphatase 1B interacts with the activated insulin receptor. *Diabetes* **45,** 1379-1385.

Sherry BA, Gelin J, Fong Y, Marano M, Wei H, Cerami A, Lowry SF, Lundholm KG & Moldawer LL. (1989). Anticachectin/tumor necrosis factor-alpha antibodies attenuate development of cachexia in tumor models. *Faseb J* **3,** 1956-1962.

Shutter JR, Graham M, Kinsey AC, Scully S, Luthy R & Stark KL. (1997). Hypothalamic expression of ART, a novel gene related to agouti, is up-regulated in obese and diabetic mutant mice. *Genes Dev* **11,** 593-602.

Sipols AJ, Baskin DG & Schwartz MW. (1995). Effect of intracerebroventricular insulin infusion on diabetic hyperphagia and hypothalamic neuropeptide gene expression. *Diabetes* **44,** 147-151.

Stephens TW, Basinski M, Bristow PK, Bue-Valleskey JM, Burgett SG, Craft L, Hale J, Hoffmann J, Hsiung HM, Kriauciunas A & et al. (1995). The role of neuropeptide Y in the antiobesity action of the obese gene product. *Nature* **377,** 530-532.

Sternberg EM. (1997). Neural-immune interactions in health and disease. *J Clin Invest* **100,** 2641-2647.

Tartaglia LA. (1997). The leptin receptor. *J Biol Chem* **272,** 6093-6096.

Tartaglia LA, Dembski M, Weng X, Deng N, Culpepper J, Devos R, Richards GJ, Campfield LA, Clark FT, Deeds J & et al. (1995). Identification and expression cloning of a leptin receptor, OB-R. *Cell* **83,** 1263-1271.

Tisdale MJ. (1997). Biology of cachexia. *J Natl Cancer Inst* **89,** 1763-1773.

Venable CL, Frevert EU, Kim YB, Fischer BM, Kamatkar S, Neel BG & Kahn BB. (2000). Overexpression of protein-tyrosine phosphatase-1B in adipocytes inhibits insulin-stimulated phosphoinositide 3-kinase activity without altering glucose transport or Akt/Protein kinase B activation. *J Biol Chem* **275,** 18318-18326.

White CL, Whittington A, Barnes MJ, Wang Z, Bray GA & Morrison CD. (2009). HF diets increase hypothalamic PTP1B and induce leptin resistance through both leptin-dependent and -independent mechanisms. *Am J Physiol Endocrinol Metab* **296,** E291-299.

Whitman MM. (2000). The starving patient: supportive care for people with cancer. *Clin J Oncol Nurs* **4,** 121-125.

WHO WORLD HEALTH ORGANIZATION (2009). World Cancer Report, 2008. International Agency for Research on Cancer, Lyon.

Woods SC, Chavez M, Park CR, Riedy C, Kaiyala K, Richardson RD, Figlewicz DP, Schwartz MW, Porte D, Jr. & Seeley RJ. (1996). The evaluation of insulin as a metabolic signal influencing behavior via the brain. *Neurosci Biobehav Rev* **20,** 139-144.

Woods SC, Lotter EC, McKay LD & Porte D, Jr. (1979). Chronic intracerebroventricular infusion of insulin reduces food intake and body weight of baboons. *Nature* **282,** 503-505.

Woods SC, Porte D, Jr., Bobbioni E, Ionescu E, Sauter JF, Rohner-Jeanrenaud F & Jeanrenaud B. (1985). Insulin: its relationship to the central nervous system and to the control of food intake and body weight. *Am J Clin Nutr* **42,** 1063-1071.

Wynne K, Stanley S, McGowan B & Bloom S. (2005). Appetite control. *J Endocrinol* **184,** 291-318.

Zhang X, Zhang G, Zhang H, Karin M, Bai H & Cai D. (2008). Hypothalamic IKKbeta/NF-kappaB and ER stress link overnutrition to energy imbalance and obesity. *Cell* **135,** 61-73.

8- APÊNDICES

APÊNDICE *I*

J Physiol 587.10 (2009) pp 2341–2351

The Journal of Physiology

Inhibition of hypothalamic Foxo1 expression reduced food intake in diet-induced obesity rats

Eduardo R. Ropelle[2], José R. Pauli[1], Patrícia Prada[2], Dennys E. Cintra[2], Guilherme Z. Rocha[2], Juliana C. Moraes[2], Marisa J. S. Frederico[3], Gabrielle da Luz[3], Ricardo A. Pinho[3], José B. C. Carvalheira[2], Licio A. Velloso[2], Mario A. Saad[2] and Cláudio T. De Souza[3]

[1]*Curso de Educação Física – Modalidade Saúde, Departamento de Biociências, UNIFESP, Santos, SP, Brazil*
[2]*Departamento de Clínica Médica, FCM, Universidade Estadual de Campinas, Campinas, SP, Brazil*
[3]*Programa de Pós-Graduação em Ciências da Saúde, PPGCS, Universidade do Extremo Sul Catarinense, Criciúma, SC, Brazil*

Insulin signalling in the hypothalamus plays a role in maintaining body weight. The forkhead transcription factor Foxo1 is an important mediator of insulin signalling in the hypothalamus. Foxo1 stimulates the transcription of the orexigenic neuropeptide Y and Agouti-related protein through the phosphatidylinositol-3-kinase/Akt signalling pathway, but the role of hypothalamic Foxo1 in insulin resistance and obesity remains unclear. Here, we identify that a high-fat diet impaired insulin-induced hypothalamic Foxo1 phosphorylation and degradation, increasing the nuclear Foxo1 activity and hyperphagic response in rats. Thus, we investigated the effects of the intracerebroventricular (I.C.V.) microinfusion of Foxo1-antisense oligonucleotide (Foxo1-ASO) and evaluated the food consumption and weight gain in normal and diet-induced obese (DIO) rats. Three days of Foxo1-ASO microinfusion reduced the hypothalamic Foxo1 expression by about 85%. I.C.V. infusion of Foxo1-ASO reduced the cumulative food intake (21%), body weight change (28%), epididymal fat pad weight (22%) and fasting serum insulin levels (19%) and increased the insulin sensitivity (34%) in DIO but not in control animals. Collectively, these data showed that the Foxo1-ASO treatment blocked the orexigenic effects of Foxo1 and prevented the hyperphagic response in obese rats. Thus, pharmacological manipulation of Foxo1 may be used to prevent or treat obesity.

(Received 29 January 2009; accepted after revision 25 March 2009; first published online 30 March 2009)
Corresponding author C. T. De Souza: Programa de Pós-Graduação em Ciências da Saúde, PPGCS, Universidade do Extremo Sul Catarinense, CEP 88806-000 – Criciúma, SC, Brazil. Email: ctsouza@unesc.net

Abbreviations AgRP, Agouti-related peptide; Akt, protein kinase B; ASO, antisense oligonucleotide; CBP, citrate binding protein; DIO, diet-induced obesity; DTT, dithiothreitol; EDTA, ethylenediamine tetraacetic acid; Foxo1, forkhead box protein; I.C.V., intracerebroventricular; IR, insulin receptor; IRS-1, insulin receptor substrate 1; IRS-2, insulin receptor substrate 2; Kitt, glucose disappearance rate; NPY, neuropeptide Y; PI3K, phosphatidylinositol-3-kinase; POMC, proopiomelanocortin; RIA, radioimmunossay; SDS-PAGE, sodium dodecyl sulfate polyacrylamide gel electrophoresis; STAT3, signal transducer-activated transcript-3; PMSF, phenylmethanesulphonylfluoride; RNA, ribonucleic acid.

Obesity is a major public health problem, associated with morbidity and mortality, and continues to increase worldwide (Zimmet *et al.* 2001). Food intake and energy expenditure are tightly regulated by complex physiological mechanisms, and a disturbance in these processes may lead to obesity (Spiegel *et al.* 2005). The hypothalamus is critical in the regulation of food intake-controlling neural circuits, which produce a number of peptides that influence food intake. The hypothalamus receives and integrates neural, metabolic and humoral signals from the periphery, such as insulin and leptin from pancreatic and adipose tissue, respectively (Schwartz *et al.* 2000). However, the underlying mechanisms by which these hormones regulate the food intake are unclear.

Insulin acts at the same hypothalamic areas as leptin to suppress feeding (Carvalheira *et al.* 2003). The insulin receptor (IR) is a protein with endogenous tyrosine kinase activity that, following activation by insulin, undergoes rapid autophosphorylation and, subsequently, phosphorylates intracellular protein substrates, including IRS-1 and IRS-2 (Cheatham & Kahn, 1995). After stimulation by insulin, IRS-1 and IRS-2 associate with

DOI: 10.1113/jphysiol.2009.170050

Table 1. Components of rat chow and high fat diet

Ingredients	Standard chow (g kg^{-1})	kcal kg^{-1}	High fat diet (g kg^{-1})	kcal kg^{-1}
Cornstarch (Q.S.P.)	397.5	1590	115.5	462
Casein	200	800	200	800
Sucrose	100	400	100	400
Dextrinated starch	132	528	132	528
Lard	—	—	312	2808
Soybean oil	70	630	40	360
Cellulose	50	—	50	—
Mineral mix	35	—	35	—
Vitamin mix	10	—	10	—
L-Cysteine	3	—	3	—
Choline	2.5	—	2.5	—
Total	1000	3948	1000	5358

several proteins, including phosphatidylinositol 3-kinase (PI3K) (Folli *et al.* 1992; Saad *et al.* 1993; Williamson *et al.* 2003). Downstream from PI3K, the serine threonine kinase, Akt, is activated and plays a pivotal role in the regulation of various biological processes, including apoptosis, proliferation, differentiation, and intermediary metabolism (Downward, 1998; Chen *et al.* 2001). Among the targets of activated Akt is forkhead transcriptional factor subfamily forkhead box O1 (Foxo1 or FKHR), which is inhibited by Akt-mediated phosphorylation (Tang *et al.* 1999).

It has been suggested that hypothalamic Foxo1 is an important regulator of food intake and energy balance (Kim *et al.* 2006; Kitamura *et al.* 2006). Nuclear Foxo1 expression stimulates the transcription of the orexigenic neuropeptide Y and Agouti-related protein and suppresses the transcription of anorexigenic proopiomelanocortin (POMC) by antagonizing the activity of signal transducer-activated transcript-3 (STAT3) (Kim *et al.* 2006; Kitamura *et al.* 2006). In addition, the PI3K/Akt signalling pathway can exclude the Foxo1 from the nucleus and lead Foxo1 to proteosomal degradation (Matsuzaki *et al.* 2003; Aoki *et al.* 2004). These molecular events can repress Foxo1-induced orexigenic signals in the hypothalamus. In the present study, we sought to determine the contribution of the hypothalamic Foxo1 on food intake and body weight in diet-induced obesity (DIO) rats. Moreover, we examined the effects of intracerebroventricular (I.C.V.) microinfusion of Foxo1 antisense oligonucleotide (Foxo1-ASO) in the hypothalamus of control and DIO rats and evaluated the food intake and body weight.

Methods

Experimental animals

Male 4-week-old Wistar rats from the University of Campinas Breeding Center were randomly divided into two groups: control, fed standard rodent chow *ad libitum*, and DIO, fed a fat-rich diet *ad libitum* (Table 1). This diet composition has been previously used (Ropelle *et al.* 2006; Pauli *et al.* 2008). For Western blot analysis, hypothalami and other tissues were obtained from six to eight rats of each group after 8 weeks of dieting. The University's Ethical Committee approved the protocols. The animals were maintained on a 12-h artificial light, 12-h dark cycle and kept in individual cages.

Physiological and metabolic parameters

After 6 h of fasting, control and DIO rats were submitted to an insulin tolerance test (1 U (kg body weight)$^{-1}$ of insulin). Rats were injected with insulin and blood samples were collected at 0, 4, 8, 12 and 16 min from the tail for serum glucose determination. The rate constant for plasma glucose disappearance was calculated using the formula 0.693/biological half life ($t_{1/2}$). The plasma glucose $t_{1/2}$ was calculated from the slope of last square analysis of the plasma glucose concentration during the linear phase of decline (Bonora *et al.* 1989). Plasma glucose was determined using a glucose meter (Roche Diagnostic, Rotkreuze, Switzerland), and RIA was used to measure serum insulin, according to a previous description (Scott *et al.* 1981). Following the experimental procedures, the rats were killed under anaesthesia (200 mg kg^{-1} thiopental) following the recommendations of the NIH.

Intracerebroventricular cannulation

The Wistar rats were stereotaxically instrumented under sodium amobarbital (15 mg (kg body weight)$^{-1}$) anaesthesia with chronic unilateral 26-gauge stainless steel indwelling guide cannulae, aseptically placed into the lateral ventricle (0.2 mm posterior, 1.5 mm lateral, and 4.2 mm ventral to bregma), as previously described

(Pereira-da-Silva *et al.* 2003). After a 1 week recovery period, all rats were submitted to experimental protocols.

Foxo1 antisense oligonucleotide (Foxo1-ASO)

Sense and antisense Foxo1 oligonucleotides were diluted in TE buffer (10 mM Tris-HCl, 1 mM EDTA) and injected (Hamilton syringe) twice a day at 08.00 h and 16.00 h, with a total volume of 2.0 μl per dose (final concentrations of 0.1, 0.2 and 0.4 nmol), 24, 48 and 72 h after the onset of the experimental period. Rats were randomly assigned to treatment conditions: rats without oligonucleotide treatment (control); rats with sense (5′GAT GCT GGA CAT GGG AGA T 3′) oligonucleotide treatment (Sense) and rats with antisense (5′ATC TCC CAT GTC CAG CAT C 3′) oligonucleotide treatment (ASO).

Treatments and measurement of food intake

Rats deprived of food for 6 h with free access to water were I.C.V. injected (2 μl) with saline or insulin (10^{-6} M). Thereafter standard chow was given and food intake was determined by measuring the difference between the weight of chow given and the weight of chow at the end of a 12 h period. Similar studies were carried out in rats that were initially injected I.C.V. with sense or Foxo1-ASO (4 nmol).

Protein analysis by immunoblotting

As soon as anaesthesia was assured by the loss of pedal and corneal reflexes, 2.0 μl of normal saline or insulin (10^{-6} M) was injected I.C.V. using a Hamilton syringe. Ten minutes after insulin injection, the cranium was opened and the basal diencephalon, including the preoptic area and hypothalamus, was excised. The hypothalami were pooled and 200 μg of protein was used as whole tissue extract. For evaluated insulin-induced Foxo1 expression, hypothalamus was excised 30 min after insulin injection, as shown for Kim and colleagues (Kim *et al.* 2006). Tissues were pooled, minced coarsely and homogenized immediately in extraction buffer (1% Triton X-100, 100 mM Tris, pH 7.4, containing 100 mM sodium pyrophosphate, 100 mM sodium fluoride, 10 mM EDTA, 10 mM sodium vanadate, 2 mM phenylmethanesulphonylfluoride (PMSF) and 0.1 mg ml^{-1} aprotinin) at 4°C with a Polytron PTA 20S generator (Brinkmann Instruments model PT 10/35) operated at maximum speed for 15 s. The extracts were centrifuged at 9 000 *g* and 4°C in a Beckman 70.1 Ti rotor (Palo Alto, CA, USA) for 45 min to remove insoluble material, and the supernatants of these tissues were used for protein quantification, using the Bradford method (Bradford, 1976). Proteins were denatured by boiling in Laemmli sample buffer (Laemmli, 1970) containing 100 mM DTT, run on SDS-PAGE, transferred to nitrocellulose membranes. Antibodies used for immunoprecipitation and immunoblotting were anti-phosphotyrosine, anti-IR, anti-IRS-2 anti-Akt, anti-phospho-Akt, anti-α-tubulin and anti-histone (Santa Cruz Biotechnology, Inc., CA, USA), anti-phospho-Foxo1 and anti-Foxo1 (Cell Signaling Technology, MA, USA). Blots were exposed to preflashed Kodak XAR film with Cronex Lightning Plus intensifying screens at −80°C for 12–48 h. Band intensities were analysed by optical densitometry (Scion Image software, ScionCorp, Frederick, MD, USA) of the developed autoradiographs.

Nuclear extraction

To characterize the expression and subcellular localization of Foxo1, a subcellular fractionation protocol was employed as described previously (Prada *et al.* 2006). The hypothalami from untreated rats or rats treated with Foxo1-ASO (0.4 nmol), according to the protocols described above, were minced and homogenized in 2 vol. of STE buffer (0.32 M sucrose, 20 mM Tris–HCl (pH 7.4), 2 mM EDTA, 1 mM DTT, 100 mM sodium fluoride, 100 mM sodium pyrophosphate, 10 mM sodium orthovanadate, 1 mM PMSF, and 0.1 mg ml^{-1} aprotinin) at 4°C with a Polytron homogenizer. The homogenates were centrifuged (1000 *g*, 25 min, 4°C) to obtain pellets. The pellets were washed once with STE buffer (1000 *g*, 10 min, 4°C) and suspended in Triton buffer (1% Triton X-100, 20 mM Tris-HCl (pH 7.4), 150 mM NaCl, 200 mM EDTA, 10 mM sodium orthovanadate, 1 mM PMSF, 100 mM NaF, 100 mM sodium pyrophosphate, and 0.1 mg ml^{-1} aprotinin), kept on ice for 30 min, and centrifuged (15 000 *g*, 30 min, 4°C) to obtain the nuclear fraction. The samples were used for immunoprecipitation with Foxo1 antibody and Protein A-Sepharose 6MB (Amersham Pharmacia Biotech UK Ltd). Thereafter they were treated with Laemmli buffer with 100 mM DTT and heated in a boiling water bath for 5 min, and aliquots (100 μg of protein) were subjected to SDS-PAGE and Western blotting with anti-CBP/p300 or Foxo1 antibodies, as described elsewhere (Gasparetti *et al.* 2003).

Statistical analysis

All numerical results are expressed as the means ± S.E.M. of the indicated number of experiments. The results of blots are presented as direct comparisons of bands in autoradiographs and quantified by densitometry using the Scion Image software. Data were analysed by ANOVA followed by *post hoc* analysis of significance (Bonferroni test) when appropriate, comparing experimental and control groups. The level of significance was set at $P < 0.05$.

Results

Metabolic parameters and energy intake of control and DIO rats

Figure 1 shows comparative data regarding control and DIO rats. Rats fed on the high-fat diet for 8 weeks had a greater body weight, epididymal fat pad weight and fasting serum insulin than age-matched controls. The glucose disappearance rate (Kitt) was decreased in DIO animals when compared to control groups (Fig. 1*A*–*D*). The fasting glucose concentration was similar between the groups (data not shown).

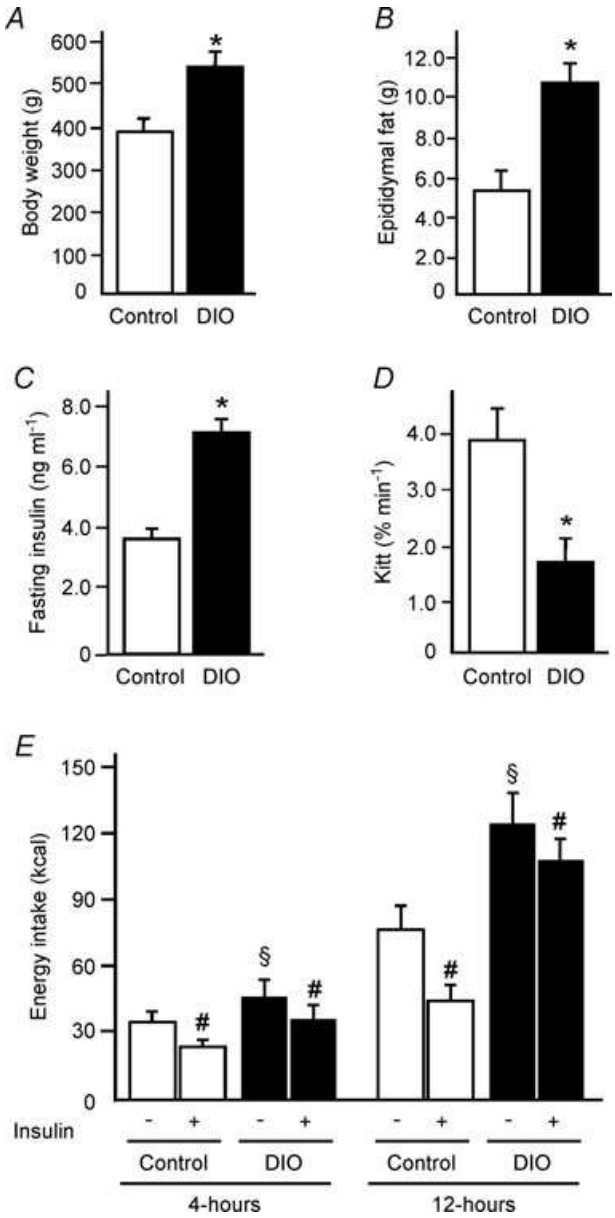

Figure 1. Metabolic parameters and energy intake of control and diet-induced obese (DOI) rats
A, total body weight. *B*, epididymal fat pad weight. *C*, fasting serum insulin. *D*, insulin tolerance test. *E*, energy intake 4 and 12 h after saline or insulin infusion in the hypothalamus of control and DOI rats. Bars represent means ± S.E.M. of eight rats. **P* < 0.004 *versus* control, #*P* < 0.04 *versus* respective saline groups, §*P* < 0.01 obese rats plus saline *versus* control plus saline.

Next, we evaluated the effect of insulin (2 μl, 10^{-6} M) or its saline vehicle on the control of food intake. In the control and DIO rats treated with saline, we observed that the energy intake was higher in DIO rats, 27% and 63% during 4 and 12 h, respectively, when compared to control animals. Insulin induced reductions in the 4 and 12 h of food intake of both control and DIO rats. In the control group, insulin reduced food intake by about 31% and 41% during 4 and 12 h, respectively, while in the obese rats the same dose induced reductions of about 21% and 14% respectively, indicating that insulin was much less effective in DIO rats (Fig. 1*E*).

Intracerebroventricular insulin activates the hypothalamic IR/IRS-2/Akt/Foxo1 pathway in control rats to a greater extent than in DIO rats

Insulin (2 μl, 10^{-6} M) I.C.V. induced increases in IR, IRS-2, Akt and Foxo1 phosphorylation in hypothalamus from both control and DIO rats. However, insulin was much less effective in inducing IR, IRS-2, Akt and Foxo1 phosphorylation in DIO rats when compared to control rats (Fig. 2*A*–*D*, upper panels). We did not observe differences in IR, IRS-2, Akt and Foxo1 phosphorylation between control and DIO groups treated with saline.

In addition, we evaluated the Foxo1 nuclear expression and the association between Foxo1 and CBP/p300 in control and DIO rats after insulin and saline injection. In the hypothalamus of control rats, insulin reduced Foxo1 expression in the nuclear fraction by 89%, compared with a 22% reduction in the hypothalamus from DIO rats (Fig. 2*E*, upper panel). Insulin also reduced Foxo1/CBP interaction by 89% in control rats and 29% in the hypothalamus of DIO rats (Fig. 2*F*, upper panel). We did not observe differences in Foxo1 nuclear expression and Foxo1/CBP binding between control and DIO groups treated with saline.

Insulin reduced Foxo1 expression in the hypothalamus of control but not in DIO rats

Previous studies suggested that insulin controlled the Foxo1 expression in the hypothalamus of lean mice (Kim *et al.* 2006). We sought to determine the effects of I.C.V. infusion of insulin on the expression of Foxo1 in the hypothalamus of control and DIO rats. First, we observed that insulin did not change the IR, IRS-2 and Akt protein expression in the hypothalamus of control and DIO rats (Fig. 3*A*). However, 30 min of insulin I.C.V. infusion reduced Foxo1 expression in the

hypothalamus of control rats by about 27%. Interestingly, in the hypothalamus of DIO rats, insulin did not change the Foxo1 expression (Fig. 3*B*). We did not observe differences in Foxo1 expression between control and DIO groups treated with saline.

Determining the dose–response and time course effects of I.C.V.-injected Foxo1 antisense upon hypothalamic Foxo1 expression

To evaluate the effect of Foxo1-ASO on Foxo1 expression in the hypothalamus, I.C.V.-cannulated control rats were treated for 1 day with antisense Foxo1 at low doses (0.1 and 0.2 nmol Foxo1-ASO) or at a high dose (0.4 nmol Foxo1-ASO). As shown in Fig. 4, a single infusion of Foxo1-ASO (0.4 nmol) induced a reduction of Foxo1 expression by about 50% in the hypothalamus of control animals. In addition, injection of a high dose (0.4 nmol) of Foxo1-ASO for 1, 2 and 3 days was able to reduce Foxo1 expression in a time-dependent manner. Three days after Foxo1-ASO treatment we observed a great reduction (85%) in the expression of Foxo1 in the hypothalamus of control rats (Fig. 4*B*). This treatment with Foxo1-ASO did not change the IR, IRS-2 and Akt protein expression in the hypothalamus of control rats (Fig. 4*D*, upper panels) and did not change the Foxo-1 protein expression in the peripheral tissues such as gastrocnemius muscle, liver and white adipose tissue (Fig. 4*C*).

Effects of Foxo1-ASO treatment on food intake and body weight in control and DIO rats

To determine the impact of Foxo1-ASO treatment on food intake and body weight, we injected Foxo1-ASO

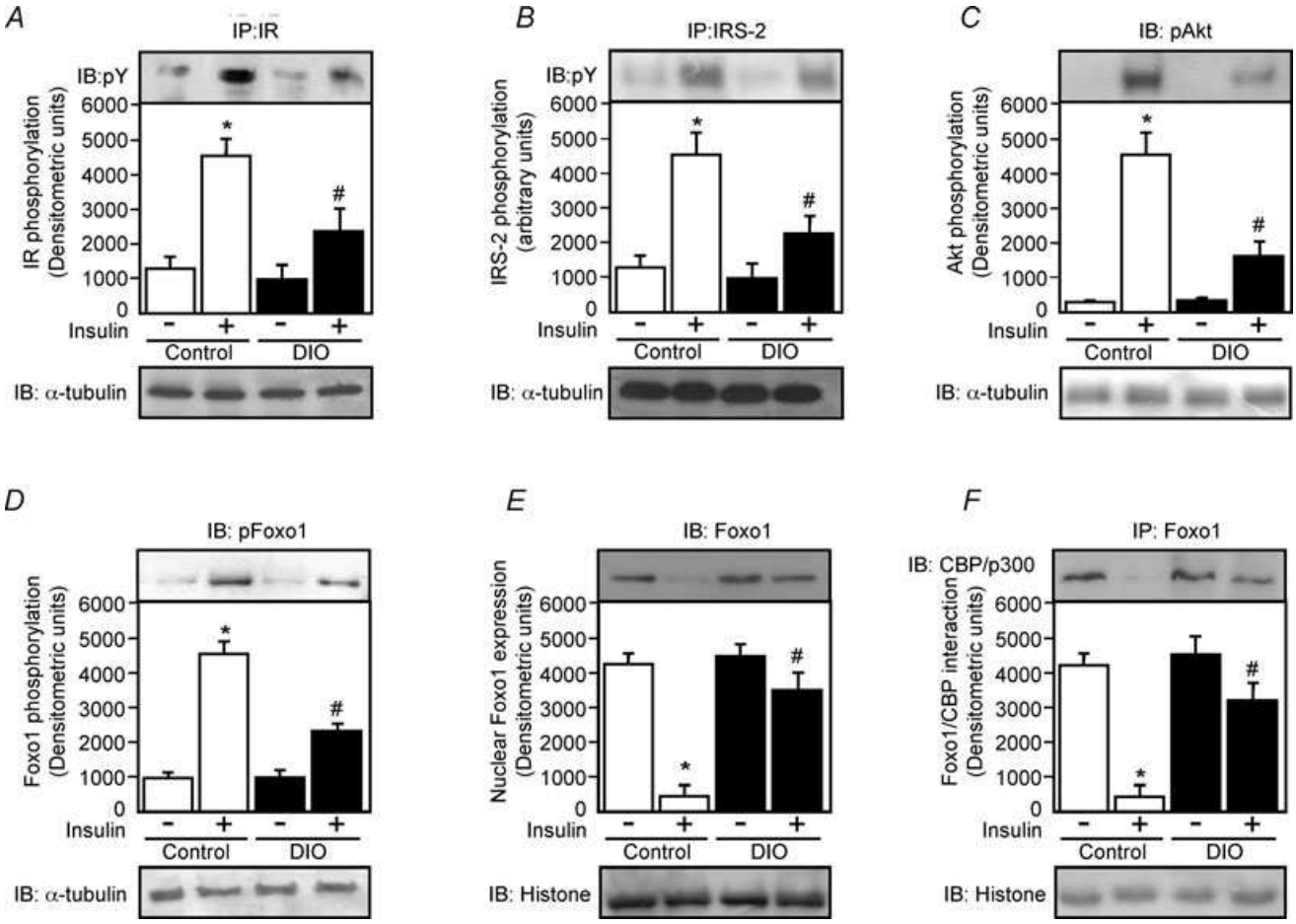

Figure 2. Effects of I.C.V. infusion of insulin on insulin signalling in the hypothalamus of control and DIO rats

A–D, upper panels, representative blots show the insulin-stimulated tyrosine phosphorylation of insulin receptor (IR; *A*), insulin receptor substrate-2 (IRS-2; *B*), Akt serine phosphorylation (*C*) and Foxo1 phosphorylation of control and DIO rats (*D*). *A–D*, lower panels, total protein expression of α-tubulin. The evaluation of nuclear Foxo1 expression (*E*) and the association between Foxo1 and CBP/p300 (*F*), were performed using nuclear extract of control and DIO rats as described in Methods. The results of scanning densitometry were expressed as arbitrary units. Bars represent means ± S.E.M. of six rats. $^*P < 0.001$ *versus* control plus saline, $\#P < 0.01$ *versus* DIO plus saline.

(0.4 nmol) in the hypothalamus of control and DIO rats during 3 days. Foxo1-ASO reduced Foxo1 expression in control and DIO rats in a time-dependent manner (Fig. 5*A*). The nuclear Foxo1 expression was reduced by about 71 and 64% in control and DIO rats, respectively, when compared to the respective control group treated with sense after 3 days (Fig. 5*B*). We also observed that Foxo1-ASO reduced Foxo1/CBP interaction by about 70% and 73% in control and DIO rats, respectively, when compared to the respective control group treated with sense after 3 days (Fig. 5*C*).

Three days after Foxo1-ASO treatment the cumulative food intake, body weight, epididymal fat pad weight, fasting insulin levels and insulin sensitivity were similar in control animals when compared to sense-injected control rats (Fig. 5*D–H*). However, 3 days after Foxo1-ASO treatment in DIO rats, there was a reduction in cumulative food intake (21%), body weight change (28%), epididymal fat pad weight (22%) and fasting serum insulin levels (19%) and an increase in insulin sensitivity (34%) when compared to sense-injected DIO rats (Fig. 5*D–H*). The fasting glucose concentration was similar between the groups (data not shown).

Discussion

During the last decade, advances have been made in the characterization of the role played by the hypothalamus in the coordination of food intake and energy expenditure (Friedman, 2000; Flier, 2004). Multiple hypothalamic neuronal signalling pathways and the cross talk between these pathways are involved in the control of energy intake (Schwartz *et al.* 2000; Minokoshi *et al.* 2004; Cota *et al.* 2006; Ropelle *et al.* 2007, 2008*b*). In addition to leptin, insulin is also able to reduce food intake (Schwartz *et al.* 2000; Carvalheira *et al.* 2001; Niswender *et al.* 2003). It has been demonstrated that the increased responsiveness of leptin and insulin action in the hypothalamus could be pathophysiologically important in the prevention of obesity (Picardi *et al.* 2008; Ropelle *et al.* 2008*a*) and Foxo1 is a distal protein of the insulin signalling that contributed to anorexigenic effects of insulin (Romanatto *et al.* 2007; Belgardt *et al.* 2008). In the present study, we demonstrate that intracerebroventricular (I.C.V.) microinfusion of insulin reduced Foxo1 expression in the hypothalamus of control but not in rats with diet-induced obesity (DIO). We showed that the injection of Foxo1 antisense oligonucleotide (Foxo1-ASO) in the hypothalamus leads to reduced Foxo1 expression in both control and DIO rats, and reduced food consumption and body weight gain in DIO but not in control rats.

As in peripheral tissues, neuronal insulin action involves the IR/IRS/phosphatidylinositol 3-kinase (PI3K) signal transduction pathway (Schwartz *et al.* 2000). The hypothalamic insulin signalling increases after either I.C.V. or systemic insulin administration (Niswender *et al.* 2003) and the inhibitory effect of I.C.V. insulin on both food intake (Carvalheira *et al.* 2001; Niswender *et al.* 2003) and the impairment in this pathway contribute to the hyperphagic response (Carvalheira *et al.* 2003; De Souza *et al.* 2005). On the other hand, the improvement in the hypothalamic IR/IRS-2/Akt pathway increases insulin-induced anorexigenic signals (Flores *et al.* 2006). Foxo1 is a downstream target of Akt. Activation of Akt phosphorylates Foxo1, leading to its nuclear exclusion and proteosomal degradation (Matsuzaki *et al.* 2003; Aoki

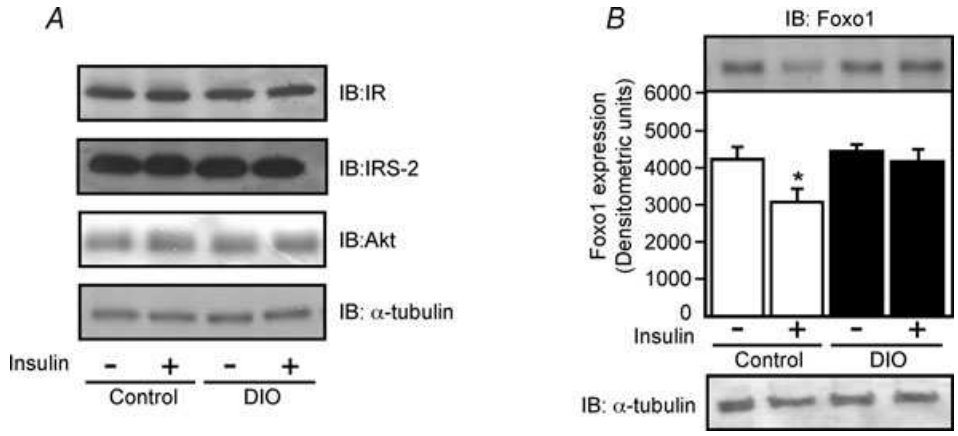

Figure 3. Effects of I.C.V. insulin infusion on Foxo1 expression in the hypothalamus of control and DIO rats

A, representative blots show the protein expression of insulin receptor (IR), insulin receptor substrate-2 (IRS-2) and Akt in the hypothalamus of control and DIO rats injected with saline (2.0 μl) or insulin (2.0 μl, 10^{-6} M). *B*, representative blots show the protein expression of Foxo1 in the hypothalamus of control and DIO rats injected with saline (2.0 μl) or insulin (2.0 μl, 10^{-6} M). The results of scanning densitometry were expressed as arbitrary units. Bars represent means ± S.E.M. of six rats. $^{*}P < 0.03$ *versus* control plus saline.

et al. 2004), and thereby inhibiting its anorexigenic actions. Here, we showed that I.C.V. insulin infusion increased the IR/IRS-2/Akt/Foxo1 phosphorylation in control rats to a greater extent than in DIO animals. This aberrant molecular signalling also reduced insulin-induced Foxo1 degradation in the hypothalamus of DIO rats compared with control rats. These data suggest that hypothalamic Foxo1 phosphorylation and degradation are required for the induction of anorexia by insulin, establishing a signalling pathway through which insulin acts in hypothalamus neurons to control food intake.

Foxo1 is expressed in cells in the hypothalamus, in POMC and Agouti-related protein (AgRP) neurons (Kitamura *et al.* 2006). In these neurons, Foxo1 stimulates the transcription of the orexigenic neuropeptide Y (NPY) and AgRP through the PI3K/Akt signalling pathway, and suppresses the transcription of anorexigenic POMC by antagonizing the activity of STAT3 in lean mice (Kim *et al.* 2006; Kitamura *et al.* 2006). Different groups have demonstrated that the hypothalamic Foxo1 expression controls food intake in rodents (Kim *et al.* 2006; Kitamura *et al.* 2006). It has been proposed that insulin and leptin decrease hypothalamic Foxo1 expression. In agreement with this, activation of insulin signalling by expression of PI3K and Akt or treatment with insulin and leptin inhibits Foxo1-stimulated NPY transcription (Kim *et al.* 2006).

In the present study, we sought to determine the effects of Foxo1-ASO in the hypothalamus of DIO rats. The I.C.V. treatment with Foxo1-ASO promoted reduction of Foxo1 protein expression in a time- and dose-dependent manner. Foxo1-ASO also reduced

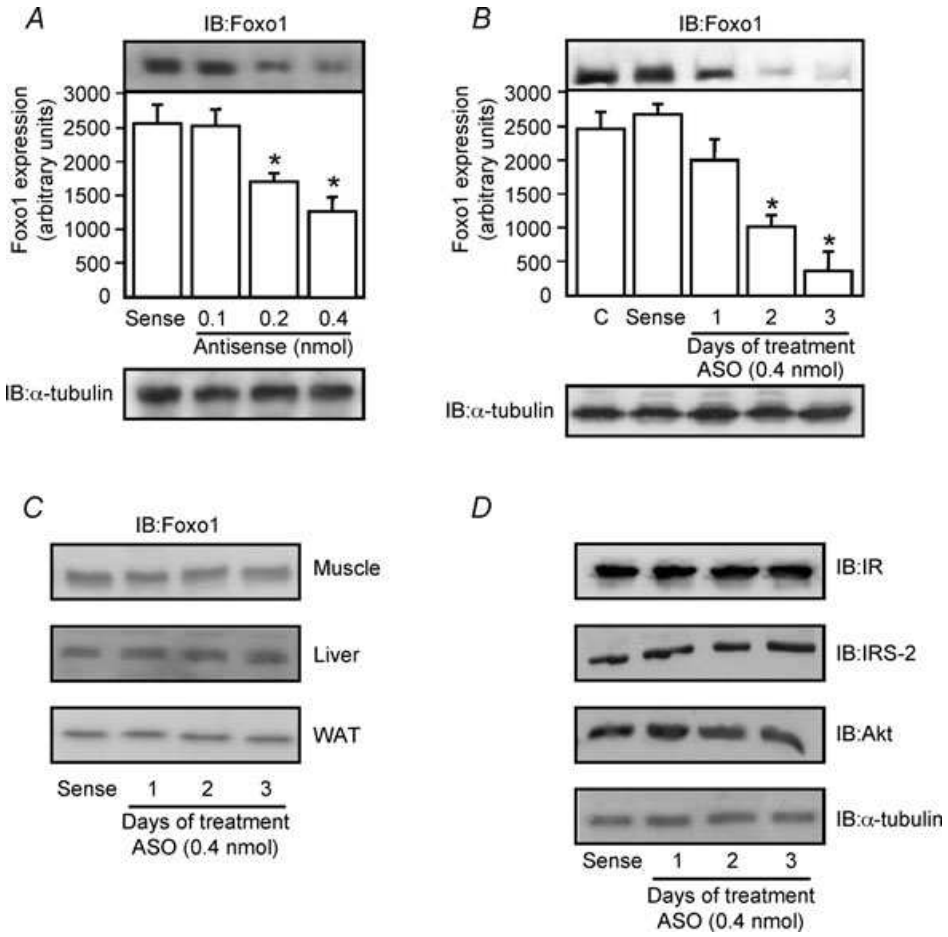

Figure 4. Effects of I.C.V. Foxo1-ASO injection in hypothalamic Foxo1 expression in lean rats
Representative Western blots demonstrating the dose-dependent effect of 24 h of treatment with saline, sense or Foxo1-ASO in lean rats (*A*) and hypothalamic Foxo1 expression in a time-dependent manner after central infusions of Foxo1-ASO in lean rats (*B*). *C*, representative Western blots show the protein expression of Foxo1 in the gastrocnemius muscle, hepatic tissue and white adipose tissue after I.C.V. infusion of Foxo1-ASO in lean rats during 3 days (0.4 nmol). *D*, representative Western blots show the protein expression of IR, IRS-2, Akt and α-tubulin in the hypothalamus of lean rats after I.C.V. infusion of Foxo1-ASO in lean rats during 3 days (0.4 nmol). The results of scanning densitometry were expressed as arbitrary units. Bars represent means ± S.E.M. of eight rats. $^{*}P < 0.01$ *versus* sense treatment.

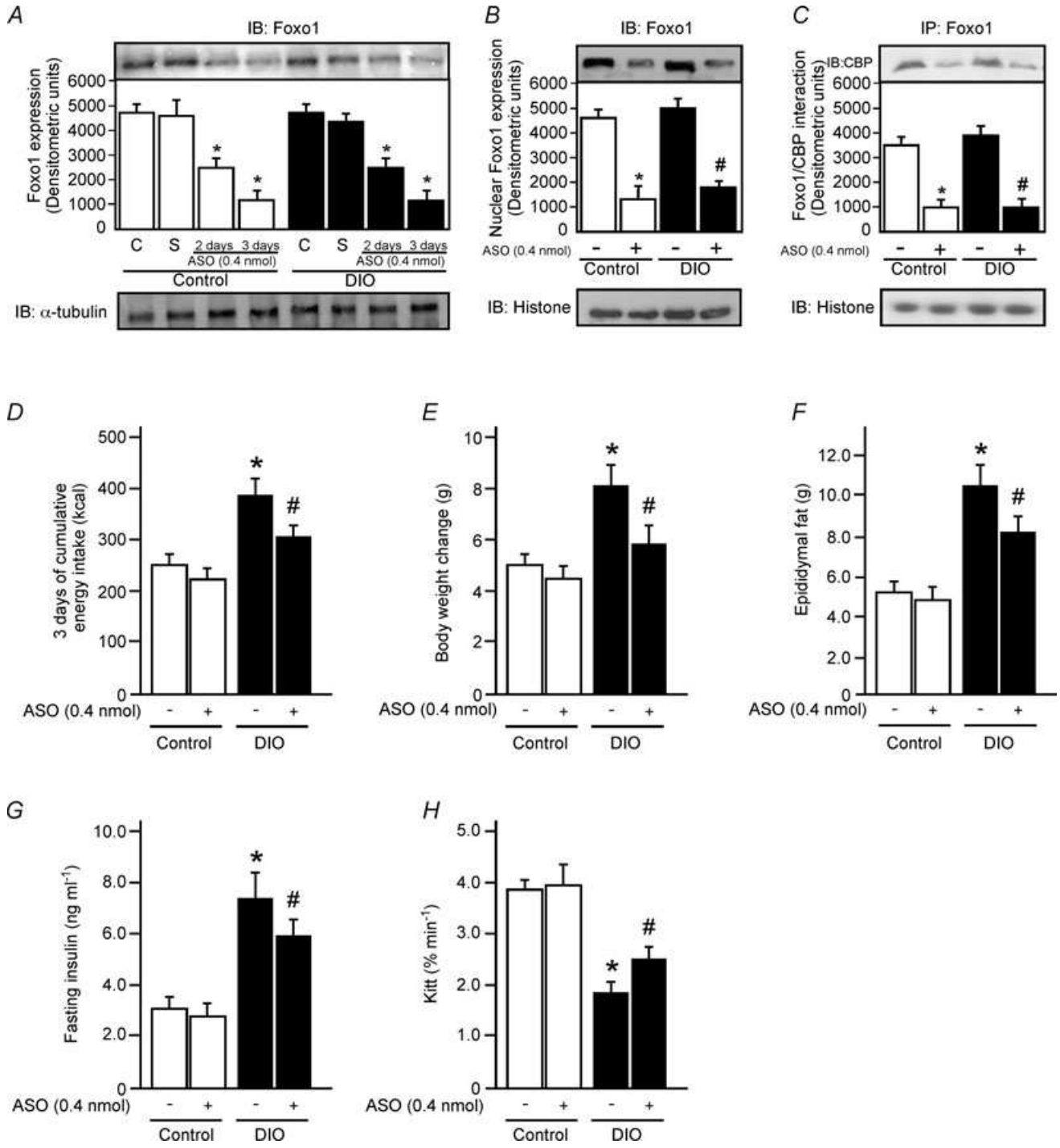

Figure 5. The effect of central infusion of Foxo1-ASO on total Foxo1 expression, food intake and body weight in control and DIO rats

Hypothalamic Foxo1 expression was evaluated after 72 h of central infusions of Foxo1-ASO in lean and DIO rats. Rats received I.C.V. saline (C), sense (S) or Foxo1-ASO (0.4 nmol) during 2 or 3 days (*A*). The evaluation of nuclear Foxo1 expression (*B*) and the association between Foxo1 and CBP/p300 (*C*) were performed using nuclear extract of control and DIO rats as described in Methods. Determination of 3 days of cumulative energy intake (*D*), body weight change (*E*), epididymal fat pad weight (*F*), fasting serum insulin (*G*) and insulin tolerance test (*H*) of control and DIO rats 3 days after Foxo1-ASO or sense I.C.V. infusion. Bars represent means ± S.E.M. of 6–8 rats; $^*P < 0.001$, ASO *versus* control plus sense; #$P < 0.03$, *versus* DIO plus sense.

nuclear interaction between Foxo1 and CBP/p300 in the hypothalamus of control and DIO rats. Three days of treatment with Foxo-ASO (4 nmol) reduced the cumulative energy intake, body weight gain and epididymal fat pad weight, fasting insulin levels and increased insulin sensitivity in DIO but not in control animals. Although Kim and colleagues showed that bilateral injection of the Foxo1 siRNA into the arcuate nucleus of hypothalamus decreased daily food intake and body weight in lean mice (Kim *et al.* 2006), our results showed that a daily infusion of Foxo1-ASO during 3 days reduced the cumulative food intake in DIO but not in control animals. Our data are in accordance with Kitamura and coworkers who explored the contribution of loss-of-function of Foxo1 on orexigenic signalling and food intake using two different approaches in lean mice. The injection of a dominant-negative of Foxo1 prevented induction of AgRP expression caused by fasting but the AgRP expression was similar in mice under normal conditions. Furthermore, in Foxo1 haploinsufficient mice (Foxo1$^{+/-}$), the food intake was similar under basal conditions when compared to wild-type littermate controls and the difference in food intake occurred only after I.C.V. leptin infusion in Foxo1$^{+/-}$ mice when compared to control mice (Kitamura *et al.* 2006). These apparent contradictory results in lean animals may be related to the different approaches and model of rodent and deserves further investigation.

The *in vivo* physiological importance of Foxo transcription factors in the brain has been reported. Several studies showed that Foxo1 is expressed in different areas of murine brain, including hippocampus, neocortex, hypothalamus and other areas (Fukunaga *et al.* 2005; Hoekman *et al.* 2006; Kitamura *et al.* 2006). In the hypothalamus of rodents, Foxo1 is expressed in a majority of cells in the arcuate nucleus, ventromedial hypothalamus and dorsomedial hypothalamus (Kitamura *et al.* 2006). Although the Foxo1-ASO injection into the third ventricle of rats reduced Foxo1 expression in a tissue-specific manner as demonstrated in Fig. 4, we cannot exclude the possibility that Foxo1-ASO reduced the Foxo1 expression in other areas of the brain.

Collectively, these data showed that central insulin resistance diminished insulin-induced Foxo1 phosphorylation and insulin-induced Foxo1 degradation. Thus, we identify that a high-fat diet impaired the hypothalamic Foxo1 phosphorylation and increased the nuclear activity, increasing the hyperphagic response in rats. Foxo1-ASO treatment blocked the orexigenic effects of hypothalamic Foxo1 and prevented the hyperphagic response in these animals. Thus, pharmacological manipulation of Foxo1 may be used to prevent or treat obesity.

References

Aoki M, Jiang H & Vogt PK (2004). Proteasomal degradation of the FoxO1 transcriptional regulator in cells transformed by the P3k and Akt oncoproteins. *Proc Natl Acad Sci U S A* **101**, 13613–13617.

Belgardt BF, Husch A, Rother E, Ernst MB, Wunderlich FT, Hampel B, Klockener T, Alessi D, Kloppenburg P & Bruning JC (2008). PDK1 deficiency in POMC-expressing cells reveals FOXO1-dependent and -independent pathways in control of energy homeostasis and stress response. *Cell Metab* **7**, 291–301.

Bonora E, Moghetti P, Zancanaro C, Cigolini M, Querena M, Cacciatori V, Corgnati A & Muggeo M (1989). Estimates of in vivo insulin action in man: comparison of insulin tolerance tests with euglycemic and hyperglycemic glucose clamp studies. *J Clin Endocrinol Metab* **68**, 374–378.

Bradford MM (1976). A rapid and sensitive method for the quantitation of microgram quantities of protein utilizing the principle of protein-dye binding. *Anal Biochem* **72**, 248–254.

Carvalheira JB, Ribeiro EB, Araujo EP, Guimaraes RB, Telles MM, Torsoni M, Gontijo JA, Velloso LA & Saad MJ (2003). Selective impairment of insulin signalling in the hypothalamus of obese Zucker rats. *Diabetologia* **46**, 1629–1640.

Carvalheira JB, Siloto RM, Ignacchitti I, Brenelli SL, Carvalho CR, Leite A, Velloso LA, Gontijo JA & Saad MJ (2001). Insulin modulates leptin-induced STAT3 activation in rat hypothalamus. *FEBS Lett* **500**, 119–124.

Cheatham B & Kahn CR (1995). Insulin action and the insulin signaling network. *Endocr Rev* **16**, 117–142.

Chen R, Kim O, Yang J, Sato K, Eisenmann KM, McCarthy J, Chen H & Qiu Y (2001). Regulation of Akt/PKB activation by tyrosine phosphorylation. *J Biol Chem* **276**, 31858–31862.

Cota D, Proulx K, Smith KA, Kozma SC, Thomas G, Woods SC & Seeley RJ (2006). Hypothalamic mTOR signaling regulates food intake. *Science* **312**, 927–930.

De Souza CT, Araujo EP, Bordin S, Ashimine R, Zollner RL, Boschero AC, Saad MJ & Velloso LA (2005). Consumption of a fat-rich diet activates a proinflammatory response and induces insulin resistance in the hypothalamus. *Endocrinology* **146**, 4192–4199.

Downward J (1998). Mechanisms and consequences of activation of protein kinase B/Akt. *Curr Opin Cell Biol* **10**, 262–267.

Flier JS (2004). Obesity wars: molecular progress confronts an expanding epidemic. *Cell* **116**, 337–350.

Flores MB, Fernandes MF, Ropelle ER, Faria MC, Ueno M, Velloso LA, Saad MJ & Carvalheira JB (2006). Exercise improves insulin and leptin sensitivity in hypothalamus of Wistar rats. *Diabetes* **55**, 2554–2561.

Folli F, Saad MJ, Backer JM & Kahn CR (1992). Insulin stimulation of phosphatidylinositol 3-kinase activity and association with insulin receptor substrate 1 in liver and muscle of the intact rat. *J Biol Chem* **267**, 22171–22177.

Friedman JM (2000). Obesity in the new millennium. *Nature* **404**, 632–634.

Fukunaga K, Ishigami T & Kawano T (2005). Transcriptional regulation of neuronal genes and its effect on neural functions: expression and function of forkhead transcription factors in neurons. *J Pharmacol Sci* **98**, 205–211.

Gasparetti AL, de Souza CT, Pereira-da-Silva M, Oliveira RL, Saad MJ, Carneiro EM & Velloso LA (2003). Cold exposure induces tissue-specific modulation of the insulin-signalling pathway in *Rattus norvegicus*. *J Physiol* **552**, 149–162.

Hoekman MF, Jacobs FM, Smidt MP & Burbach JP (2006). Spatial and temporal expression of FoxO transcription factors in the developing and adult murine brain. *Gene Expr Patterns* **6**, 134–140.

Kim MS, Pak YK, Jang PG, Namkoong C, Choi YS, Won JC, Kim KS, Kim SW, Kim HS, Park JY, Kim YB & Lee KU (2006). Role of hypothalamic Foxo1 in the regulation of food intake and energy homeostasis. *Nat Neurosci* **9**, 901–906.

Kitamura T, Feng Y, Kitamura YI, Chua SC Jr, Xu AW, Barsh GS, Rossetti L & Accili D (2006). Forkhead protein FoxO1 mediates Agrp-dependent effects of leptin on food intake. *Nat Med* **12**, 534–540.

Laemmli UK (1970). Cleavage of structural proteins during the assembly of the head of bacteriophage T4. *Nature* **227**, 680–685.

Matsuzaki H, Daitoku H, Hatta M, Tanaka K & Fukamizu A (2003). Insulin-induced phosphorylation of FKHR (Foxo1) targets to proteasomal degradation. *Proc Natl Acad Sci U S A* **100**, 11285–11290.

Minokoshi Y, Alquier T, Furukawa N, Kim YB, Lee A, Xue B, Mu J, Foufelle F, Ferre P, Birnbaum MJ, Stuck BJ & Kahn BB (2004). AMP-kinase regulates food intake by responding to hormonal and nutrient signals in the hypothalamus. *Nature* **428**, 569–574.

Niswender KD, Morrison CD, Clegg DJ, Olson R, Baskin DG, Myers MG Jr, Seeley RJ & Schwartz MW (2003). Insulin activation of phosphatidylinositol 3-kinase in the hypothalamic arcuate nucleus: a key mediator of insulin-induced anorexia. *Diabetes* **52**, 227–231.

Pauli JR, Ropelle ER, Cintra DE, Carvalho-Filho MA, Moraes JC, De Souza CT, Velloso LA, Carvalheira JB & Saad MJ (2008). Acute physical exercise reverses *S*-nitrosation of the insulin receptor, insulin receptor substrate 1 and protein kinase B/Akt in diet-induced obese Wistar rats. *J Physiol* **586**, 659–671.

Pereira-da-Silva M, Torsoni MA, Nourani HV, Augusto VD, Souza CT, Gasparetti AL, Carvalheira JB, Ventrucci G, Marcondes MC, Cruz-Neto AP, Saad MJ, Boschero AC, Carneiro EM & Velloso LA (2003). Hypothalamic melanin-concentrating hormone is induced by cold exposure and participates in the control of energy expenditure in rats. *Endocrinology* **144**, 4831–4840.

Picardi PK, Calegari VC, Prada PO, Moraes JC, Araujo E, Marcondes MC, Ueno M, Carvalheira JB, Velloso LA & Saad MJ (2008). Reduction of hypothalamic protein tyrosine phosphatase improves insulin and leptin resistance in diet-induced obese rats. *Endocrinology* **149**, 3870–3880.

Prada PO, Pauli JR, Ropelle ER, Zecchin HG, Carvalheira JB, Velloso LA & Saad MJ (2006). Selective modulation of the CAP/Cbl pathway in the adipose tissue of high fat diet treated rats. *FEBS Lett* **580**, 4889–4894.

Romanatto T, Cesquini M, Amaral ME, Roman EA, Moraes JC, Torsoni MA, Cruz-Neto AP & Velloso LA (2007). TNF-α acts in the hypothalamus inhibiting food intake and increasing the respiratory quotient – effects on leptin and insulin signaling pathways. *Peptides* **28**, 1050–1058.

Ropelle ER, Fernandes MF, Flores MB, Ueno M, Rocco S, Marin R, Cintra DE, Velloso LA, Franchini KG, Saad MJ & Carvalheira JB (2008*a*). Central exercise action increases the AMPK and mTOR response to leptin. *PLoS ONE* **3**, e3856.

Ropelle ER, Pauli JR, Fernandes MF, Rocco SA, Marin RM, Morari J, Souza KK, Dias MM, Gomes-Marcondes MC, Gontijo JA, Franchini KG, Velloso LA, Saad MJ & Carvalheira JB (2008*b*). A central role for neuronal AMP-activated protein kinase (AMPK) and mammalian target of rapamycin (mTOR) in high-protein diet-induced weight loss. *Diabetes* **57**, 594–605.

Ropelle ER, Pauli JR, Prada PO, de Souza CT, Picardi PK, Faria MC, Cintra DE, Fernandes MF, Flores MB, Velloso LA, Saad MJ & Carvalheira JB (2006). Reversal of diet-induced insulin resistance with a single bout of exercise in the rat: the role of PTP1B and IRS-1 serine phosphorylation. *J Physiol* **577**, 997–1007.

Ropelle ER, Pauli JR, Zecchin KG, Ueno M, de Souza CT, Morari J, Faria MC, Velloso LA, Saad MJ & Carvalheira JB (2007). A central role for neuronal adenosine 5′-monophosphate-activated protein kinase in cancer-induced anorexia. *Endocrinology* **148**, 5220–5229.

Saad MJ, Folli F, Kahn JA & Kahn CR (1993). Modulation of insulin receptor, insulin receptor substrate-1, and phosphatidylinositol 3-kinase in liver and muscle of dexamethasone-treated rats. *J Clin Invest* **92**, 2065–2072.

Schwartz MW, Woods SC, Porte D Jr, Seeley RJ & Baskin DG (2000). Central nervous system control of food intake. *Nature* **404**, 661–671.

Scott AM, Atwater I & Rojas E (1981). A method for the simultaneous measurement of insulin release and B cell membrane potential in single mouse islets of Langerhans. *Diabetologia* **21**, 470–475.

Spiegel A, Nabel E, Volkow N, Landis S & Li TK (2005). Obesity on the brain. *Nat Neurosci* **8**, 552–553.

Tang ED, Nunez G, Barr FG & Guan KL (1999). Negative regulation of the forkhead transcription factor FKHR by Akt. *J Biol Chem* **274**, 16741–16746.

Williamson D, Gallagher P, Harber M, Hollon C & Trappe S (2003). Mitogen-activated protein kinase (MAPK) pathway activation: effects of age and acute exercise on human skeletal muscle. *J Physiol* **547**, 977–987.

Zimmet P, Alberti KG & Shaw J (2001). Global and societal implications of the diabetes epidemic. *Nature* **414**, 782–787.

Author contributions

E.R.R.: conception and design, or analysis and interpretation of data, drafting the article or revising it critically for important intellectual content, final approval of the version to be published; J.R.P.: conception and design; P.P.: conception and design; D.E.C.: conception and design; G.Z.R.: conception and design; J.C.M.: conception and design; M.J.S.F.: conception and design;

G.d.L.: conception and design; R.A.P.: final approval of the version to be published; J.B.C.C.: drafting the article or revising it critically for important intellectual content; L.A.V.: drafting the article or revising it critically for important intellectual content; M.J.S.: drafting the article or revising it critically for important intellectual content; C.T.D.S: conception and design, or analysis and interpretation of data, drafting the article or revising it critically for important intellectual content, final approval of the version to be published.

Acknowledgements

These studies were supported by grants from Fundacão de Amparo à Pesquisa do Estado de São Paulo (FAPESP) and Conselho Nacional de desenvolvimento científico e tecnológico (CNPq).

APÊNDICE *II*

ORIGINAL ARTICLE

A Central Role for Neuronal AMP-Activated Protein Kinase (AMPK) and Mammalian Target of Rapamycin (mTOR) in High-Protein Diet–Induced Weight Loss

Eduardo R. Ropelle,[1] José R. Pauli,[1] Maria Fernanda A. Fernandes,[1] Silvana A. Rocco,[1] Rodrigo M. Marin,[1] Joseane Morari,[1] Kellen K. Souza,[1] Marília M. Dias,[1] Maria C. Gomes-Marcondes,[2] José A.R. Gontijo,[1] Kleber G. Franchini,[1] Lício A. Velloso,[1] Mario J.A. Saad,[1] and José B.C. Carvalheira[1]

OBJECTIVE—A high-protein diet (HPD) is known to promote the reduction of body fat, but the mechanisms underlying this change are unclear. AMP-activated protein kinase (AMPK) and mammalian target of rapamycin (mTOR) function as majors regulators of cellular metabolism that respond to changes in energy status, and recent data demonstrated that they also play a critical role in systemic energy balance. Here, we sought to determine whether the response of the AMPK and mTOR pathways could contribute to the molecular effects of an HPD.

RESEARCH DESIGN AND METHODS—Western blotting, confocal microscopy, chromatography, light microscopy, and RT-PCR assays were combined to explore the anorexigenic effects of an HPD.

RESULTS—An HPD reduced food intake and induced weight loss in both normal rats and *ob*/*ob* mice. The intracerebroventricular administration of leucine reduced food intake, and the magnitude of weight loss and reduction of food intake in a leucine-supplemented diet are similar to that achieved by HPD in normal rats and in *ob*/*ob* mice, suggesting that leucine is a major component of the effects of an HPD. Leucine and HPD decrease AMPK and increase mTOR activity in the hypothalamus, leading to inhibition of neuropeptide Y and stimulation of pro-opiomelanocortin expression. Consistent with a cross-regulation between AMPK and mTOR to control food intake, our data show that the activation of these enzymes occurs in the same specific neuronal subtypes.

CONCLUSIONS—These findings provide support for the hypothesis that AMPK and mTOR interact in the hypothalamus to regulate feeding during HPD in a leucine-dependent manner. ***Diabetes* 57:594–605, 2008**

From the [1]Department of Internal Medicine, Faculty of Medical Sciences, State University of Campinas (UNICAMP), Campinas, São Paulo, Brazil; and the [2]Department of Physiology and Biophysics of State University of Campinas (UNICAMP), Campinas, São Paulo, Brazil.

Address correspondence and reprint requests to José B.C. Carvalheira, MD, Department of Internal Medicine, FCM–State University of Campinas (UNICAMP), 13083-970, Campinas, SP, Brazil. E-mail: carvalheirajbc@uol.com.br.

Received for publication 26 April 2007 and accepted in revised form 16 November 2007.

Published ahead of print at http://diabetes.diabetesjournals.org on 5 December 2007. DOI: 10.2337/db07-0573.

2-DG, 2-deoxy-D-glucose; ACC, acetyl-CoA carboxylase; AMPK, AMP-activated protein kinase; ASO, antisense oligonucleotide; CSF, cerebrospinal fluid; HPD, high-protein diet; mTOR, mammalian target of rapamycin; NPY, neuropeptide Y; pACC, phosphorylated ACC; POMC, pro-opiomelanocortin.

Low-carbohydrate, high-protein diets (HPDs) have become increasingly popular, and many bestselling diet books have promoted this approach (1–3). However, only in recent years have studies begun to examine the effects of HPD on energy expenditure, subsequent energy intake, and weight loss, as compared with lower-protein diets (4–6). Currently, there is convincing evidence that a higher protein intake increases thermogenesis and satiety, compared with diets of lower protein content (7). The weight of evidence also suggests that high-protein meals lead to a reduced subsequent energy intake (7,8).

Recently, hypothalamic AMP-activated protein kinase (AMPK) signaling has become an important focus of interest in the control of food intake (9–11). AMPK is the downstream component of a kinase cascade that acts as a sensor of cellular energy charge, being activated by rising AMP coupled with falling ATP. Once activated, AMPK phosphorylates acetyl-CoA carboxylase (ACC) and switches on energy-producing pathways at the expense of energy-depleting processes (12). Another target molecule for the control of food intake and energy homeostasis is the mammalian target of rapamycin (mTOR) catalytic activity, which has been suggested to be affected by the phosphatidylinositol 3-kinase/Akt pathway (13). Activated signaling through mTOR phosphorylates the serine/threonine kinase p70S6K and the translational repressor eukaryotic initiation factor (eIF) 4E binding protein (4EBP1) (14). mTOR signaling is inhibited under conditions of low nutrients, such as glucose and amino acids, and low intracellular ATP levels (15). Whereas mTOR was presumed to serve as the direct cellular sensor for ATP levels (16), mounting evidence has implicated AMPK in the regulation of mTOR activity (17–19).

Leucine has been reported to more potently activate mTOR than other amino acids (20). Leucine may regulate mTOR signaling through the tuberous sclerosis complexes and Rheb (21). However, Xu et al. (22) recently proposed that leucine stimulates the mTOR pathway, in part, by serving both as a mitochondrial fuel through oxidative carboxylation and an allosteric activation of glutamate dehydrogenase. This hypothesis may support the idea that leucine modulates mTOR function, in part by regulating mitochondrial function and AMPK activity.

In this study, we sought to determine whether the response of the AMPK and mTOR pathways could contribute to the molecular effects of an HPD. We therefore

TABLE 1
Components of standard rodent chow, HPD, and leucine-supplemented diet

	Standard chow (g/kg diet)	HPD (g/kg diet)	Leucine-supplemented diet (g/kg diet)
Casein	202	593.5	202
Leucine	—	—	50
Sucrose	100	39	100
Cornstarch	397	150	347
Dextrinated starch	130.5	47	130.5
Soybean oil	70	70	70
Cellulose	50	50	50
Mineral mix AIN-93	35	35	35
Vitamin mix AIN-93	10	10	10
l-cystin	3	3	3
Choline	2.5	2.5	2.5
Total	1,000	1,000	1,000
Energy (kj/g)	15.9	15.8	15.9

examined the hypothalamic modulation of the AMPK/ACC and mTOR signaling pathways induced by HPD as well as the role of leucine in these signaling pathways.

RESEARCH DESIGN AND METHODS

2-Deoxy-D-glucose (2-DG) and L-leucine were from Sigma (St. Louis, MO). The amino acid mix consisted of all amino acids without leucine. Alanine, arginine, asparagine, aspartic, cysteine, glutamic, glutamine, glycine, histidine, isoleucine, lysine, methionine, phenylalanine, proline, serine, threonine, tryptophan, tyrosine, and valine were also from Sigma. The mTOR inhibitor, rapamycin, was from LC Laboratories (Woburn, MA). mTOR antisense oligonucleotide (ASO) was obtained from Invitrogen (Gaithersburg, MD). The sequence was obtained from NCBI Entrez Nucleotide Bank based on the *Mus musculus* mTOR mRNA complete code (sense 5′ GAACCTCAGGGCAAGAT 3′ and antisense 5′ ATCTTGCCCTGAGGTTC 3′). Routine reagents were purchased from Sigma, unless otherwise specified.

Animals and diets. Male 8-week-old Wistar-Hannover rats from the University of Campinas Breeding Center and male 10-week-old *ob*/*ob* and *db*/*db* mice (C57BL/6J background), originally imported from The Jackson Laboratory (Bar Harbor, ME), were used in accordance with the guidelines of the Brazilian College for Animal Experimentation (COBEA), and the ethics committee at the State University of Campinas approved experiments.

Control animals were fed standard rodent chow (Table 1), given ad libitum. Diets were designed to maintain similar contributions of energy from different macronutrients. The HPD consisted of a 50% protein-enriched diet (Table 1). The leucine-supplemented diet was obtained with leucine addition in place of an equivalent amount of casein used in an HPD (Table 1).

Physiological and metabolic parameters. After 6 h of fasting, rats were submitted to an insulin tolerance test (1 unit/kg body wt of insulin) as previously described (23). Plasma glucose was determined using a glucose meter (Roche Diagnostic, Rotkreuze, Switzerland), and radioimmunoassay was used to measure serum insulin, according to a previous description (24). Leptin concentrations were determined using an enzyme-linked immunosorbent assay kit (Crystal Chem, Chicago, IL). Cerebrospinal fluid (CSF) and plasma leucine were measured following the spectrophotometric methods described by Rosen (25).

Body composition determination. The carcass (without the gastrointestinal tract) was weighed and stored at −20°C for analysis of body composition. Carcass water was determined as the difference between the dry and wet weights. Total fat was extracted with petroleum ether using a Soxhlet apparatus. The carcass without fat was dried to determine the lean mass.

Taste reactivity test. The video cameras (JVC, Digital Still Camera GR-DVL557) were placed outside the chamber, 300 mm from the ring holding the food cup. The video signal was recorded on a conventional VHS tape at 50 frames/s using a recorder (Compact Super VHS, JVC: GR-SXM307). Videotapes were analyzed by slow-motion playback to count taste reactivity components. Taste reactivity components to HPD or leucine-supplemented diet were classified as hedonic, aversive, or neutral, as has previously been described (26).

Intracerebroventricular cannulation and cisterna magna puncture. The rats were anesthetized with intraperitoneal injection of a mix of ketamin (10 mg) and diazepam (0.07 mg) (0.2 ml/100 g body wt), after overnight fasting and positioning on a Stoelting stereotaxic apparatus. The implantation of an intracerebroventricular catheter into the third ventricle (27) and the method for liquor sampling (28) have been previously described.

Treatments. In acute treatments, rats were deprived of food for 6 h with free access to water and were injected intracerebroventricularly (3 μl bolus injection) with vehicle, rapamycin (15 μg), leucine (0.5, 2.0, or 4.0 mmol/l), mTOR ASO (1 mmol/μl), or amino acid mix (4.0 mmol/l for each amino acid). Chronic treatment with leucine (4.0 mmol/l) or mTOR ASO was performed by intracerebroventricular infusion every day between 5:00 and 6:00 P.M., during 1 or 3 weeks. Similar studies were carried out in rats that were initially pretreated with i.p. 2-DG, intracerebroventricular microinjection of rapamycin or either vehicles, and after 40 min with intracerebroventricular leucine (4.0 mmol/l) or vehicles, respectively.

Western blot analysis. After the diets and intraperitoneal, intravenous, and/or intracerebroventricular treatments, animals were anesthetized with an intraperitoneal injection and brown adipose tissue, gastrocnemius muscle, and hypothalamus were quickly removed, minced coarsely, and homogenized immediately. Western blot was performed as previously described (29).

The antibodies used for Western blot were as follows: anti-Akt phosphoserine 473-specific, anti-p70S6K phosphothreonine 389-specific, anti-p70S6K, anti-eIF4E phosphoserine 209-specific, and anti-eIF4E antibodies from Cell Signaling Technology (Beverly, MA); anti-UCP-1, anti-IR, anti-Akt, and antiphosphotyrosine antibodies from Santa Cruz Biotechnology (Santa Cruz, CA); and the anti-mTOR antibodies (mTAB1 and 2) from Upstate Biotechnology (Lake Placid, NY).

mRNA isolation and RT-PCR. mRNA isolation and RT-PCR were performed as previously described (30). The primers used were as follows: RPS-29 (NCBI: NM012876), sense: 5′-AGGCAAGATGGGTCACCAGC-3′, antisense: 5′-AGTCGAATCATCCATTCAGGTCG-3′; neuropeptide Y (NPY) (NCBI: NM012614), sense: 5′-AGAGATC CAGCCCT GAGACA-3′, antisense: 5′-AACG ACAACAAGGGAAATGG-3′; pro-opiomelanocortin (POMC) (NCBI: AF510391), sense: 5′-CTCCTGCTTCAGACCTCCAT-3′, antisense: 5′-TTGGGG TACACCTTCACAGG-3′.

Chromatography. Chromatographic analyses were carried out on a Waters Alliance equipment series 2695 (Milford, MA) equipped with a quaternary pump, an autosampler, a degasser, and a Waters 2475 fluorescence detector model. The fluorescence of derivatized compounds (ATP, ADP, and AMP) was monitored with excitation and emission wavelengths set at 280 and 420 nm, respectively, as previously described (31).

Light microscopy. Visceral (epididymal) white adipose tissue depots were dissected and assessed by light microscopy as previously described (32).

Confocal microscopy. Paraformaldehyde-fixed hypothalami were sectioned (5 μm) and used in regular single- or double-immunofluorescence staining using DAPI, anti-AMPK (1:200; Santa Cruz Biotechnology), anti-phospho-p70SK (1:200; Santa Cruz Biotechnology), anti-mTOR (1:200; ABCAM, Cambridge, MA), and anti–phospho-ACC (1:200; Cell Signaling Technology) antibodies, according to a previously described protocol (33). Analysis and photodocumentation of results were performed using a LSM 510 laser confocal microscope (Zeiss, Jena, Germany). The anatomical correlations were made according to the landmarks given in a stereotaxic atlas (34).

Statistical analysis. Where appropriate, the results are expressed as the mean ± SE accompanied by the indicated number of animals used in experiments. Comparisons among groups were made using parametric two-way ANOVA; where F ratios were significant, further comparisons were made using the Bonferroni test.

RESULTS

An HPD reduces food intake and body weight in rodents. We gave male Wistar rats and *ob*/*ob* mice standard rodent chow or HPD for 3 weeks. HPD significantly reduced food intake and body weight in Wistar rats and *ob*/*ob* mice (Fig. 1*A* and *B*). Next, we assessed whether these differences in weight were related to alterations in adiposity. Weight gain and expansion of fat mass was significantly attenuated in HPD-fed rats without changes in total water and lean body mass (Fig. 1*C*). The fat pad weights of Wistar rats and *ob*/*ob* mice after 3 weeks on an HPD showed a 50 and 35% decreased, respectively, compared with the respective control groups (Fig. 1*D*). In accordance, sections of adipose tissue from rats and mice submitted to HPD exhibit decreases in adipocyte size relative to controls (Fig. 1*E*). To evaluate the possibility

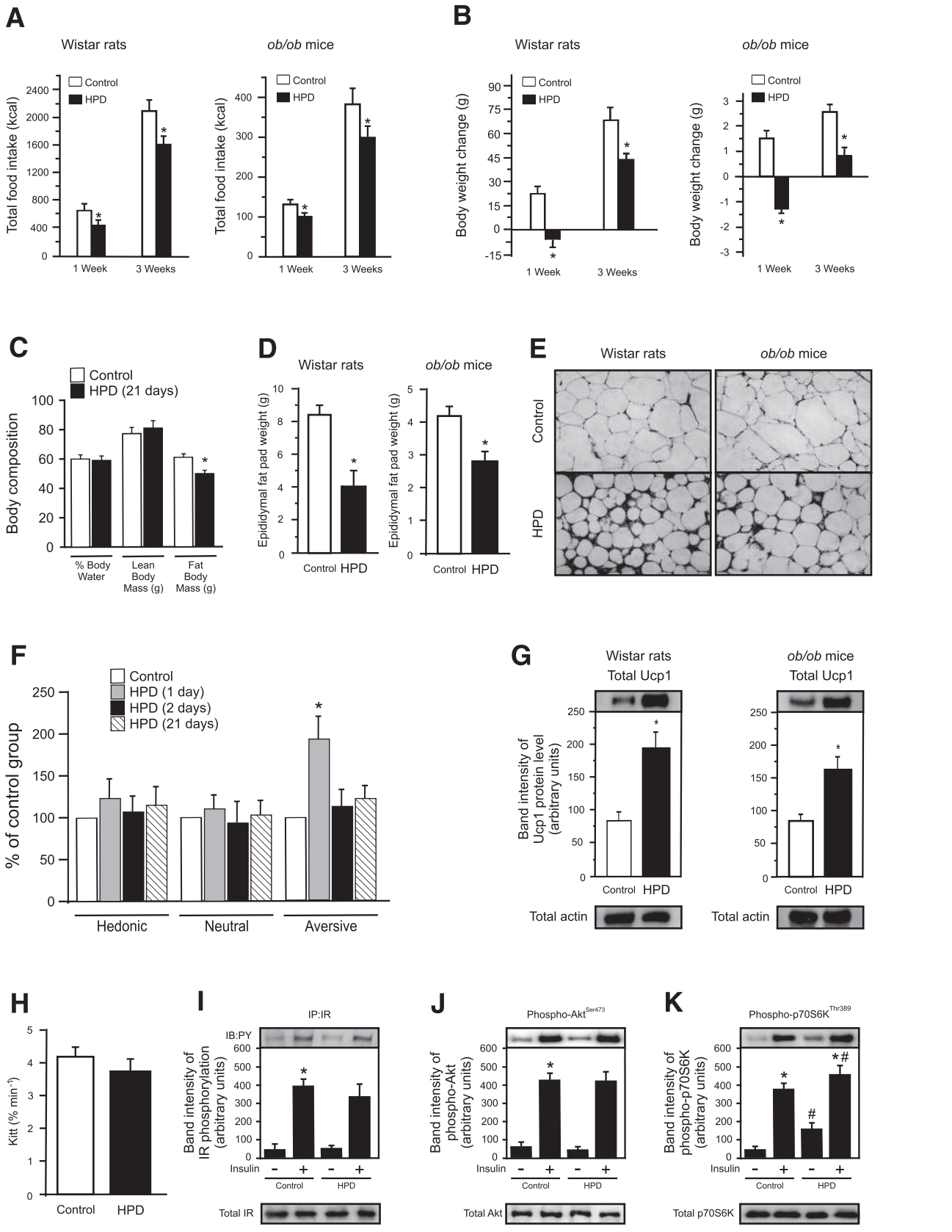

FIG. 1. HPD causes weight loss and anorexia in Wistar rats and *ob/ob* mice. Cumulative food intake (*A*) and body weight (*B*) of animals on an HPD and chow diet ($n = 6$) are shown. *C*: Body composition of HPD-fed Wistar rats ($n = 8$). *D*: Epididymal fat pad weights ($n = 6$). *E*: Histological sections of epididymal fat pads (original magnification ×50, $n = 6$). *F*: Evaluation of taste reactivity in Wistar rats on an HPD and chow diet ($n = 8$). *$P < 0.05$, HPD 1 day vs. control and 2 and 21 days. *G*: Western blot analysis of UCP-1 expression in brown adipose tissue ($n = 6$). *$P < 0.05$, HPD vs. control. *H*: Insulin tolerance test ($n = 8$). Western blot analysis of insulin receptor (IR), tyrosine phosphorylation (*I*), phospho-Akt^{Ser473}, serine-phosphorylated Akt (*J*), and phospho-p70S6K^{thr389} and threonine-phosphorylated p70S6K (*K*) ($n = 6$). *$P < 0.05$ vs. vehicle-injected rats; #$P < 0.05$ vs. the respective control group. IB, immunoblotted; IP, immunoprecipitated; Py, phosphotyrosine.

that the anorectic effect of HPD was caused by an aversive effect, we measured taste reactivity. As shown in Fig. 1*F*, the total numbers of hedonic and neutral reactions during the 15-min recording period remained the same; the aversive reactions were increased on the first day of HPD and returned to control levels thereafter.

Uncoupling protein (UCP-1) in brown adipose tissue is a chief regulator of energy expenditure in rodents (35). Normal rats and obese mice on HPD during 1 week demonstrated an increase of 2.2- and 1.9-fold, respectively, in UCP-1 protein expression in brown adipose tissue (Fig. 1*G*), indicating that weight loss on an HPD may also be associated with an increase in energy expenditure.

We also observed that 1 week of HPD did not alter plasma glucose in Wistar rats under fasting conditions, but increased insulin levels compared with standard rodent chow (1.82 ± 0.36 vs. 1.05 ± 0.17 ng/ml, respectively; $P < 0.05$) and reduced leptin levels (3.59 ± 1.43 vs. 5.43 ± 1.12 ng/ml, respectively; $P < 0.05$). In addition, 1 week of HPD promoted reduction in plasma glucose in *ob*/*ob* mice under fasting conditions when compared with the respective control group (166.7 ± 9.0 vs. 275.9 ± 8.8 mg/dl, respectively; $P < 0.05$) and increased insulin levels (13.1 ± 2.04 vs. 8.98 ± 2.56 ng/ml, respectively; $P < 0.05$). Despite the increased insulin levels, we did not observe changes in insulin tolerance test (Fig. 1*H*) and in insulin receptor (Fig. 1*I*) and Akt (Fig. 1*J*) phosphorylation in Wistar rats. The phosphorylated p70S6K was increased in HPD-fed rats at both basal and after insulin stimulation (Fig. 1*K*).

HPD modulates the hypothalamic AMPK/ACC signaling pathway. To assess the effect of HPD on hypothalamic AMPK signaling, we gave an HPD to Wistar rats and obese mice (*ob*/*ob*) for 3 weeks. HPD suppressed AMPK and ACC phosphorylation in the hypothalamus of Wistar rats in a time-dependent manner (Fig. 2*A*). Similar results were observed in *ob*/*ob* mice (Fig. 2*B*).

To further delineate the mechanism by which the HPD reduced the AMPK/ACC pathway, we analyzed ATP content and the AMP-to-ATP ratio in the hypothalami tissues of HPD-fed rats. The chromatographic analysis shows that 3 days of HPD changed the hypothalamic ATP, ADP, and AMP concentrations in Wistar rats (Fig. 2*C*). HPD markedly increased ATP content by ~35% (Fig. 2*D*) and reduced the AMP-to-ATP ratio by ~60% in the hypothalamus of Wistar rats (Fig. 2*E*).

HPD activates mTOR in the hypothalamus. We next examined whether HPD modulates mTOR activity in hypothalamus. HPD caused a significant increase in the phosphorylation of two downstream targets of mTOR—p70 ribosomal S6 kinase (p70S6K) and eukaryotic initiation factor 4E (eIF4E)—in a time-dependent manner in the hypothalamus of Wistar rats (Fig. 3*A*). Similar results were observed in *ob*/*ob* mice (Fig. 3*B*).

To determine whether mTOR is required for the HPD-dependent reduction of food intake, we chronically administered mTOR ASO in animals submitted to HPD. As shown in Fig. 3*C*, intracerebroventricularly administration of mTOR ASO reduced mTOR expression in a time-dependent manner and completely reversed the HPD-induced anorexia in Wistar rats (Fig. 3*D*). Moreover, while HPD-fed rats lost a significant amount of weight, the mTOR ASO treatment prevented the effect of HPD on body weight during the time frame observed (Fig. 3*E*). According to these data, treatment with mTOR ASO during 3 days prevents the increase in phosphorylation of p70S6K and eIF4E, both induced by HPD (Fig. 3*F* and *G*).

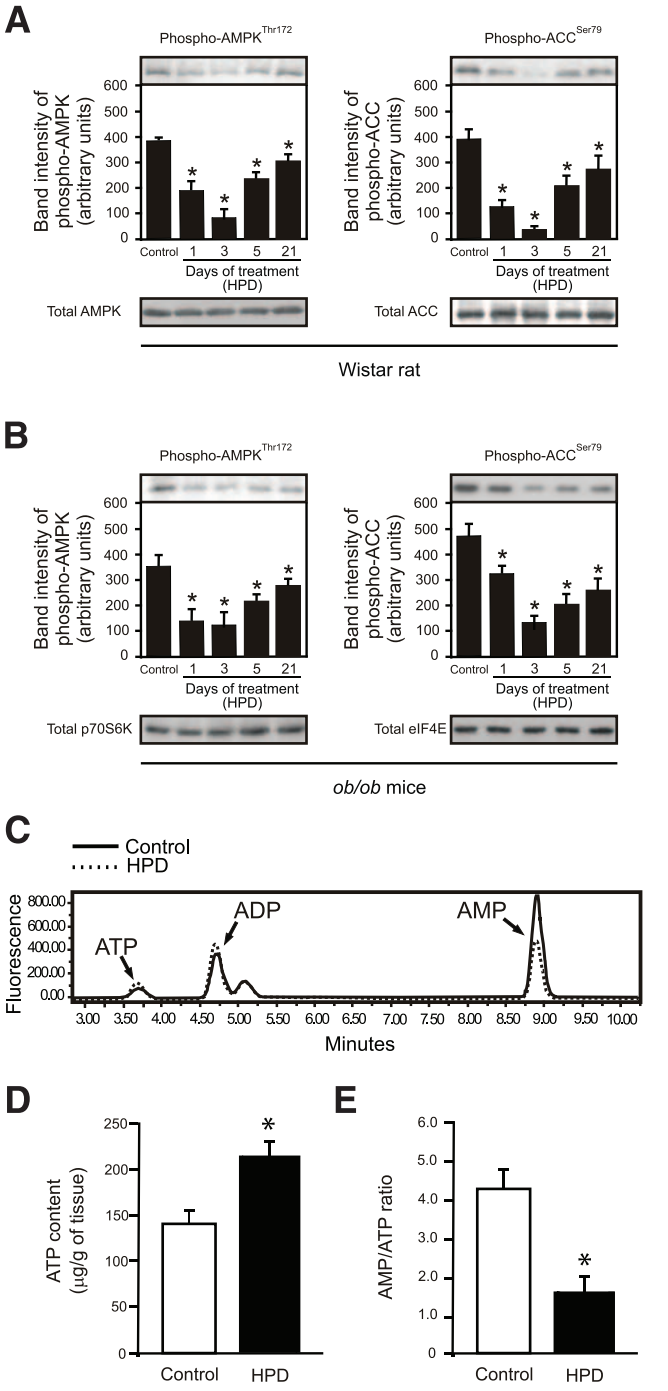

FIG. 2. Effects of HPD on hypothalamic AMPK activity and ATP content. Representative Western blots of six independent experiments showing hypothalamic lysates from Wistar rats (*A*) and *ob*/*ob* mice (*B*) and phospho-AMPK^{thr172}, threonine-phosphorylated AMPK, and phospho-ACC^{ser79}, serine phosphorylated ACC are shown (*C*–*E*). Typical chromatographic run (*C*) depicting the ATP, ADP, and AMP fractions in control (black line) and HPD (dotted line) rats, as mean ATP content (*D*) and as AMP-to-ATP ratio ($n = 6$) (*E*), is represented. *$P < 0.05$, HPD vs. control.

HPD modulates AMPK and mTOR in the same specific neuronal subset and modulates hypothalamic neuropeptides. To investigate coexpression of AMPK with mTOR, we carried out double-staining confocal microscopy. Using this technique, most neurons expressing AMPK in arcuate and paraventricular nuclei were shown to possess mTOR (Fig. 4*A*). Consistent with results to

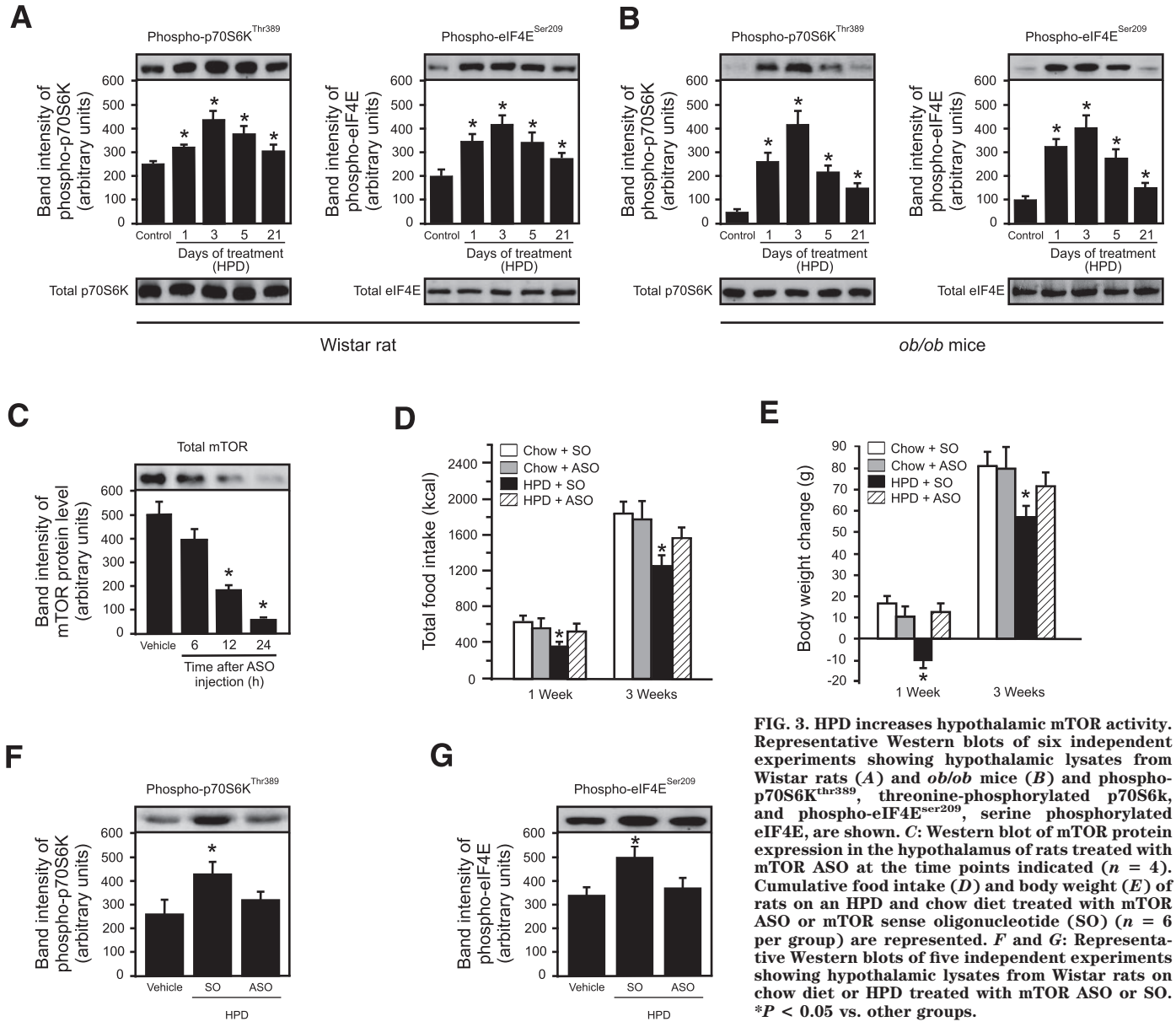

FIG. 3. HPD increases hypothalamic mTOR activity. Representative Western blots of six independent experiments showing hypothalamic lysates from Wistar rats (*A*) and *ob/ob* mice (*B*) and phospho-p70S6K^{thr389}, threonine-phosphorylated p70S6k, and phospho-eIF4E^{ser209}, serine phosphorylated eIF4E, are shown. *C*: Western blot of mTOR protein expression in the hypothalamus of rats treated with mTOR ASO at the time points indicated (n = 4). Cumulative food intake (*D*) and body weight (*E*) of rats on an HPD and chow diet treated with mTOR ASO or mTOR sense oligonucleotide (SO) (n = 6 per group) are represented. *F* and *G*: Representative Western blots of five independent experiments showing hypothalamic lysates from Wistar rats on chow diet or HPD treated with mTOR ASO or SO. *P < 0.05 vs. other groups.

detect AMPK, we found that hypothalamic phosphorylated ACC (pACC) immunoreactivity was highly localized in neurons of the arcuate and paraventricular nuclei in fasted rats (Fig. 4*B*). After 3 days of HPD in rats, low-intensity pACC immunofluorescence was detected in cells of arcuate and paraventricular nuclei of rats (Fig. 4*D*). Conversely, high-intensity pp70S6K immunofluorescence was detected in cells of arcuate and paraventricular nuclei of rats after HPD treatment (Fig. 4*D*). Similar results were observed in lateral nucleus (data not shown). The HPD-induced pp70S6K immunoreactivity was not increased in surrounding hypothalamic areas, including the ventromedial hypothalamic nucleus and zona incerta area (Fig. 4*C* and *E*).

To explore the mechanism(s) by which HPD regulates food intake, we examined the expression of hypothalamic neuropeptides involved in the control of energy homeostasis in Wistar rats. Under ad libitum fed and 12 h fasting, HPD decreased NPY mRNA levels to a greater extent than in controls (Fig. 4*D*, *left panel*). Consistent with these findings, HPD increased POMC mRNA levels to a greater extent than in controls (Fig. 4*D*, *right panel*). Similar results were observed in *ob/ob* mice (Fig. 4*E*).

Leucine reduces food intake and body weight in rodents. To determine whether a major component of HPD is responsible for its effect in the control of food intake and body weight, we tested the possibility of a direct activation of this kinase by leucine. We measured plasma and CSF leucine levels after 1 week of treatment; leucine supplementation increased plasma and CSF leucine concentrations to a similar extent to HPD, compared with standard rodent chow (Fig. 5*A*). To determine whether leucine reduces food intake and body weight, we chronically administered leucine in Wistar rats and in two models of obese mice (*ob*/*ob* and *db*/*db*). The addition of leucine, in place of an equivalent amount of casein used in the HPD, to the diet of Wistar rats during 3 weeks led to a large decrease in food intake and body weight (Fig. 5*B* and *C*). Weight gain and expansion of fat mass were significantly attenuated in leucine-supplemented rats without changes in total water and lean body mass (Fig. 5*D*). To evaluate the possibility that the anorectic effects of leucine

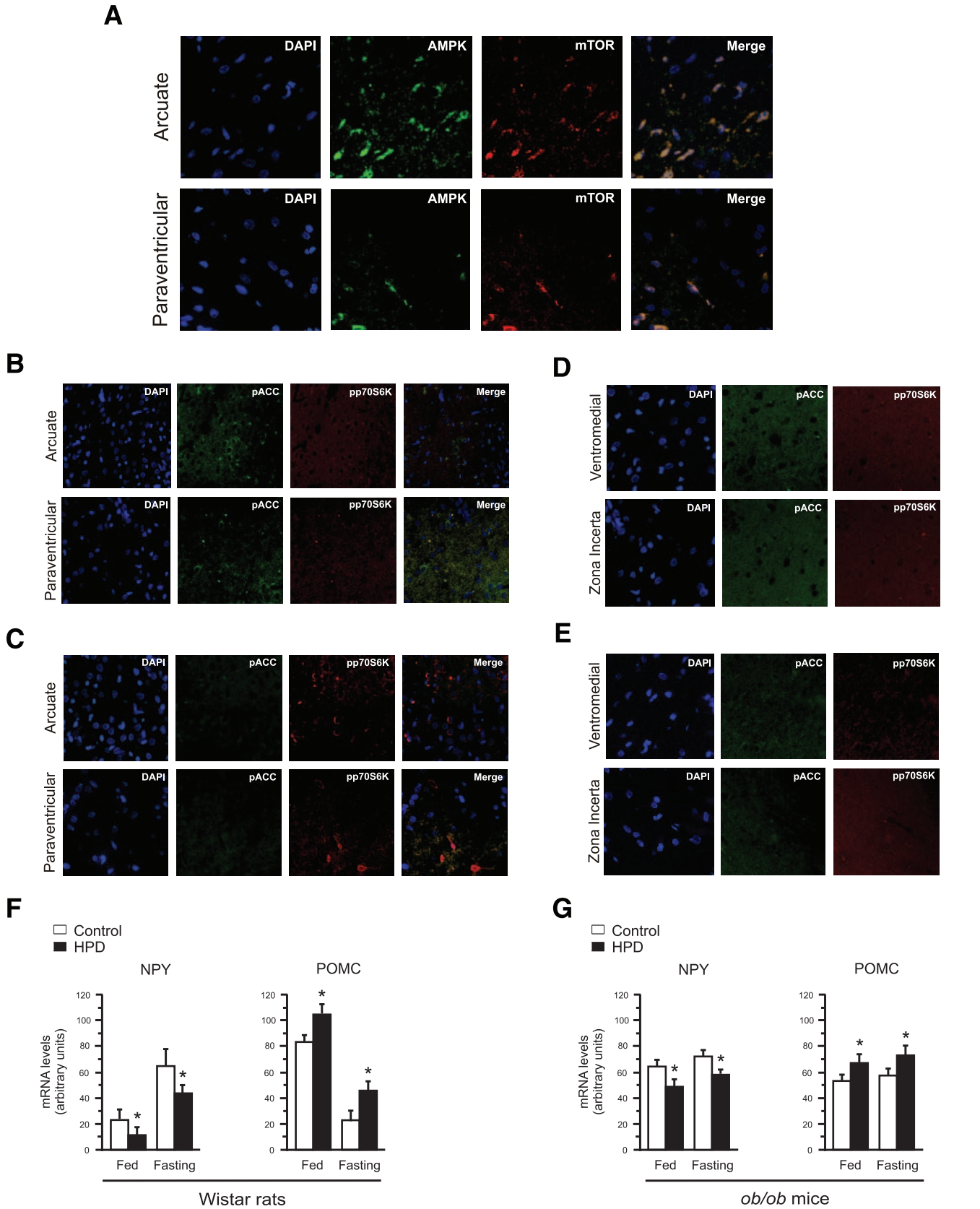

FIG. 4. HPD enhances phosphorylated p70S6k (pp70S6K) immunoreactivity primarily in AMPK-expressing arcuate and paraventricular nuclei and modulates hypothalamic neuropetides. *A*: Confocal microscopy of AMPK and mTOR in the arcuate and paraventricular nucleus of Wistar rat. pACC and pp70S6K in the arcuate and paraventricular nucleus (*B*) and in ventromedial nucleus and zona incerta (*C*) of 12-h fasted rats is shown. Also represented is pACC and pp70S6K in the arcuate and paraventricular nucleus (*D*) and in ventromedial nucleus and zona incerta (*E*) of HPD-fed rats. Rats were submitted to chow diet, 12 h of fasting, or 3 days of HPD; sections (×200 magnification) are shown of arcuate, paraventricular, and ventromedial nucleus and zona incerta immunostained for 4′,6-diamidine-2-phenylindole (DAPI, blue), AMPK (green), mTOR (red), phospho-ACC (green), and phospho-p70S6K (red). HPD modulates mRNA levels of NPY and POMC in the ad libitum fed and fasting state in Wistar rats (*F*) and *ob/ob* mice (*G*) ($n = 5$ per group). *$P < 0.05$ HPD vs. chow diet. IB, immunoblotted; IP, immunoprecipitated; PY, phosphotyrosine.

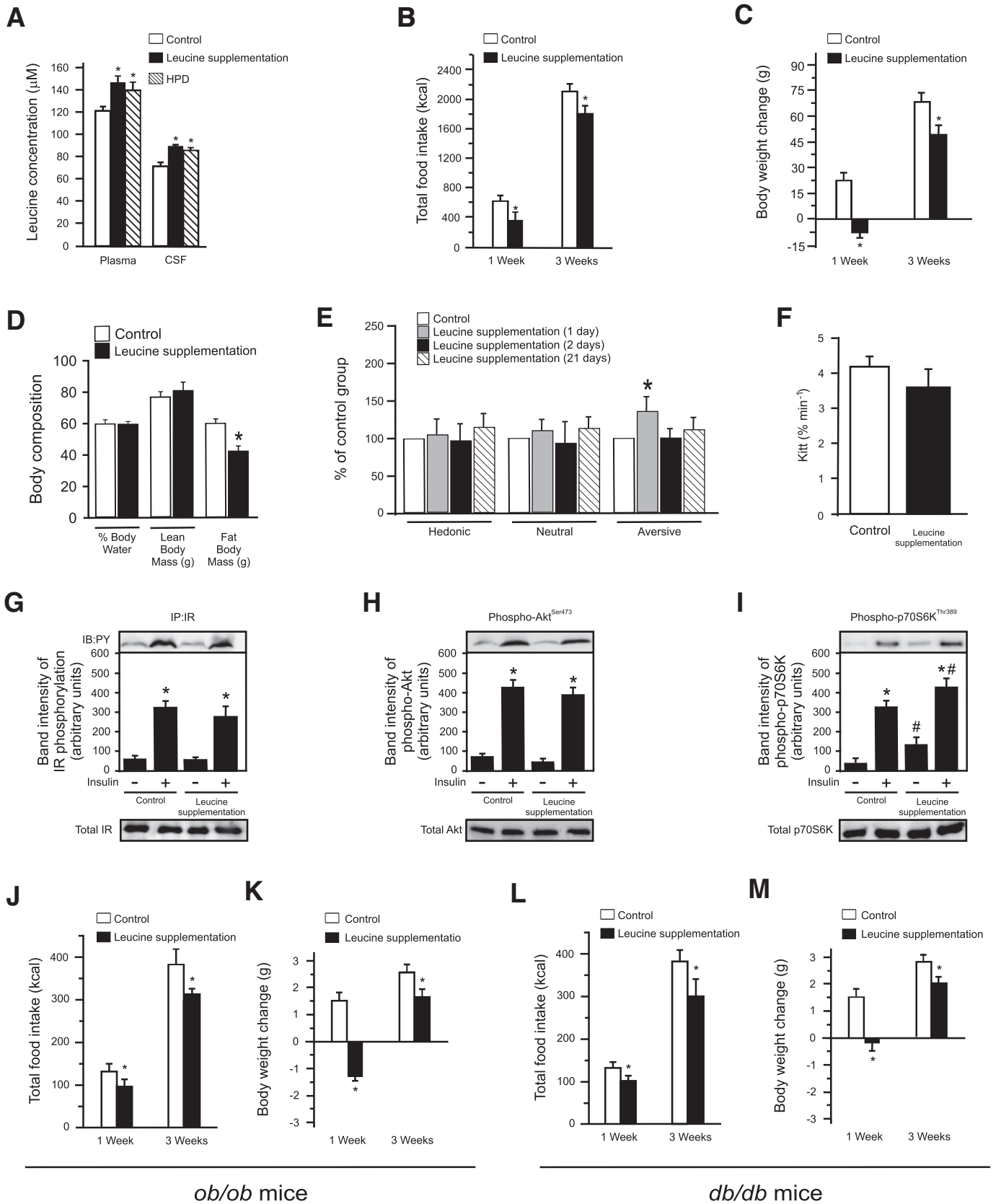

FIG. 5. Leucine supplementation causes anorexia and weight loss. *A*: Leucine levels in the plasma and CSF of standard chow–fed, leucine-supplemented, or HFD-fed rats ($n = 6$). Cumulative food intake (*B*) and body weight (*C*) of rats on a leucine-supplemented and chow diet ($n = 6$) is shown. *D*: Body composition of standard chow– and leucine supplementation–fed rats ($n = 8$). *E*: Taste reactivity test ($n = 8$). *$P < 0.05$ vs. control group. *F*: Insulin tolerance test ($n = 8$). Western blot analysis of insulin receptor (IR) tyrosine phosphorylation (*G*), phospho-Akt^{Ser473}, serine-phosphorylated Akt (*H*), and phospho-p70S6K^{thr389}, threonine-phosphorylated p70S6K (*I*) ($n = 6$) is shown. *$P < 0.05$ vs. vehicle-injected rats; #$P < 0.05$ vs. the respective control group. Cumulative food intake (*J*) and body weight (*K*) of *ob/ob* mice on a leucine-supplemented and chow diet ($n = 5$). Cumulative food intake (*L*) and body weight (*M*) of *db/db* mice on a leucine-supplemented and chow diet ($n = 5$) are shown. *$P < 0.05$ vs. control. IB, immunoblotted; IP, immunoprecipitated; PY, phosphotyrosine.

supplementation were caused by diet taste aversion, we carried out a taste reactivity test. As shown in Fig. 5*E*, the total numbers of hedonic and neutral reactions during the 15-min recording period remained the same; the aversive reactions were increased on the first day of HPD and returned to control levels thereafter. We also did not observe changes in insulin tolerance test (Fig. 5*F*) and on insulin receptor (Fig. 5*G*) and Akt (Fig. 5*H*) phosphorylation in Wistar rats. The phosphorylated p70S6K was increased in leucine-supplemented rats at both basal and after insulin stimulation (Fig. 5*I*). To explore the anorectic effects of leucine-supplemented diet in obese model animals, we gave this diet to *ob*/*ob* and *db*/*db* mice. Leucine supplementation promoted a reduction in cumulative food intake and induced weight loss in *ob/ob* (Fig. 5*J* and *K*) and *db/db* (Fig. 5*L* and *M*) mice.

Leucine decreases hypothalamic AMPK and activates mTOR signaling. To determine whether leucine modulates hypothalamic AMPK/ACC signaling, we injected leucine into the third ventricle of rats and evaluated food intake and AMPK signaling. Leucine caused a significant reduction in food intake (Fig. 6*A*) and suppressed hypothalamic AMPK and ACC phosphorylation in a dose-dependent manner (Fig. 6*B* and *C*). We next investigated whether the microinfusion of leucine modulates the hypothalamic ATP concentration. Figure 6*D* shows that leucine (4.0 mmol/l) changed ATP, ADP, and AMP concentrations in the hypothalamus of rats, whereas 40 min after leucine injection, the ATP content increased by ~32% (Fig. 6*E*) and reduced the AMP-to-ATP ratio by ~55% in Wistar rats (Fig. 6*F*).

Interestingly, the activation of the AMPK/ACC pathway is inhibited by intracerebroventricular leucine in vivo; thus, we evaluated the effect of intraperitoneal 2-DG on the activities of these enzymes in male Wistar rats. We showed that the activation of AMPK results in an increase in food intake (Fig. 6*G*) and body weight gain (Fig. 6*H*); however, pretreatment with intracerebroventricular leucine with a dose that did not alter food intake (0.5 mmol/l) reversed the effects of 2-DG. In parallel, intraperitoneal injection of 2-DG induced hypothalamic AMPK (Fig. 6*I*) and ACC (Fig. 6*J*) phosphorylation, and these effects were blocked by leucine.

Consistent with previous work (13), leucine increased p70S6K and peIF4E phosphorylation in a dose-dependent manner (Fig. 6*K* and *L*). To determine whether the effects of leucine on food intake are mTOR dependent, we first identified a dose of rapamycin that did not alter food intake (15 μg) when administered at the onset of the dark cycle. We then evaluated the effect of intracerebroventricular pretreatment with this dose of the inhibitor, or its vehicle, on the anorectic response to intracerebroventricular leucine (4 mmol/l), and we observed that the anorectic response to intracerebroventricular leucine was reversed by rapamycin (Fig. 6*M*).

Leucine modulates AMPK and mTOR in the same specific neuronal subset and modulates hypothalamic neuropetides. After the administration of leucine intracerebroventricularly into rat hypothalamus, low intensity of pACC immunofluorescence was detected in cells of arcuate and paraventricular nuclei of rats. Conversely, high intensity of pp70S6K immunofluorescence was detected in cells of arcuate and paraventricular nuclei of rats (Fig. 7*A*). Similar results were observed in the lateral nucleus (data not shown). The leucine-induced pp70S6K immunoreactivity was not increased in surrounding hypothalamic areas, including the ventromedial hypothalamic nucleus and zona incerta area (not shown).

To explore the mechanism(s) by which leucine regulates food intake, we examined the expression of hypothalamic neuropeptides involved in the control of energy homeostasis in Wistar rats. Under ad libitum fed and 12 h fasting, HPD decreased NPY mRNA levels to a greater extent than in controls (Fig. 7*B*). Consistent with these findings, leucine increased POMC mRNA levels to a greater extent than in controls (Fig. 7*C*), and rapamycin blocked the decrease in NPY and the increase in POMC caused by leucine (Fig. 7*B* and *C*).

DISCUSSION

The results of this study show that an HPD markedly reduces food intake and body weight in both normal rats and *ob*/*ob* mice. Our data indicate that an HPD, signaling through AMPK and mTOR, inhibits NPY and increases POMC expression in the hypothalamus. The intracerebroventricular administration of leucine, but not other amino acids (data not shown), reduced food intake in a dose-dependent manner, and the magnitude of weight loss and reduction of food intake in leucine-supplemented diet is similar to that achieved by an HPD in normal rats and in *ob*/*ob* mice, suggesting that leucine is a major component of the effects of HPD.

Another possibility that should be mentioned as a cause of the reduced food intake is that an HPD may induce conditioned taste aversion (36). Conversely, another study has shown that the behavioral effect of HPD is not caused by conditioned taste aversion, but is probably due to a lower initial palatability of HPD and its enhanced satiety effect (26). We cannot exclude the influence of the adverse reaction to the HPD or leucine-supplemented diet to reduce food intake, since our results showed an increased aversiveness to these diets on the first day.

Although leucine, when administered to rat brains, suppresses feeding and weight gain (13), it is critical to determine whether physiological changes in amino acid concentration act on the hypothalamus to influence energy balance. Our results show that, after 3 weeks of HPD, the body weights of rats and *ob*/*ob* mice fed on an HPD were much lower than these of rats fed on a standard diet. Subcutaneous fat pad measurements and expansion of fat mass revealed remarkable differences between the two groups. These results are in agreement with others (37,38) and can be explained, to some extent, by the reduction in caloric intake, but we also observed increased UCP-1 levels that may reflect an increase in energy expenditure.

Changes in hypothalamic AMPK activity regulates food intake; orexigenic factors (e.g., ghrelin) activate hypothalamic AMPK, whereas anorexigenic agents (e.g., leptin) suppresses AMPK activity in the hypothalamus. To gain further insight into the mechanism by which HPD produces weight loss, we examined the role of AMPK. Our results demonstrate that after HPD, hypothalamic ATP level was increased and the AMP-to-ATP ratio was reduced. In parallel, we observed a decrease in AMPK and ACC phosphorylation in rats submitted to HPD.

The mTOR, central to integrating similar signals to control food intake, has now emerged as a detector of hormonal and nutritional signals in the hypothalamus (13). In this study, we investigated whether HPD activates mTOR. HPD increased mTOR activity; moreover, knockdown of central mTOR reverses the anorectic effect of

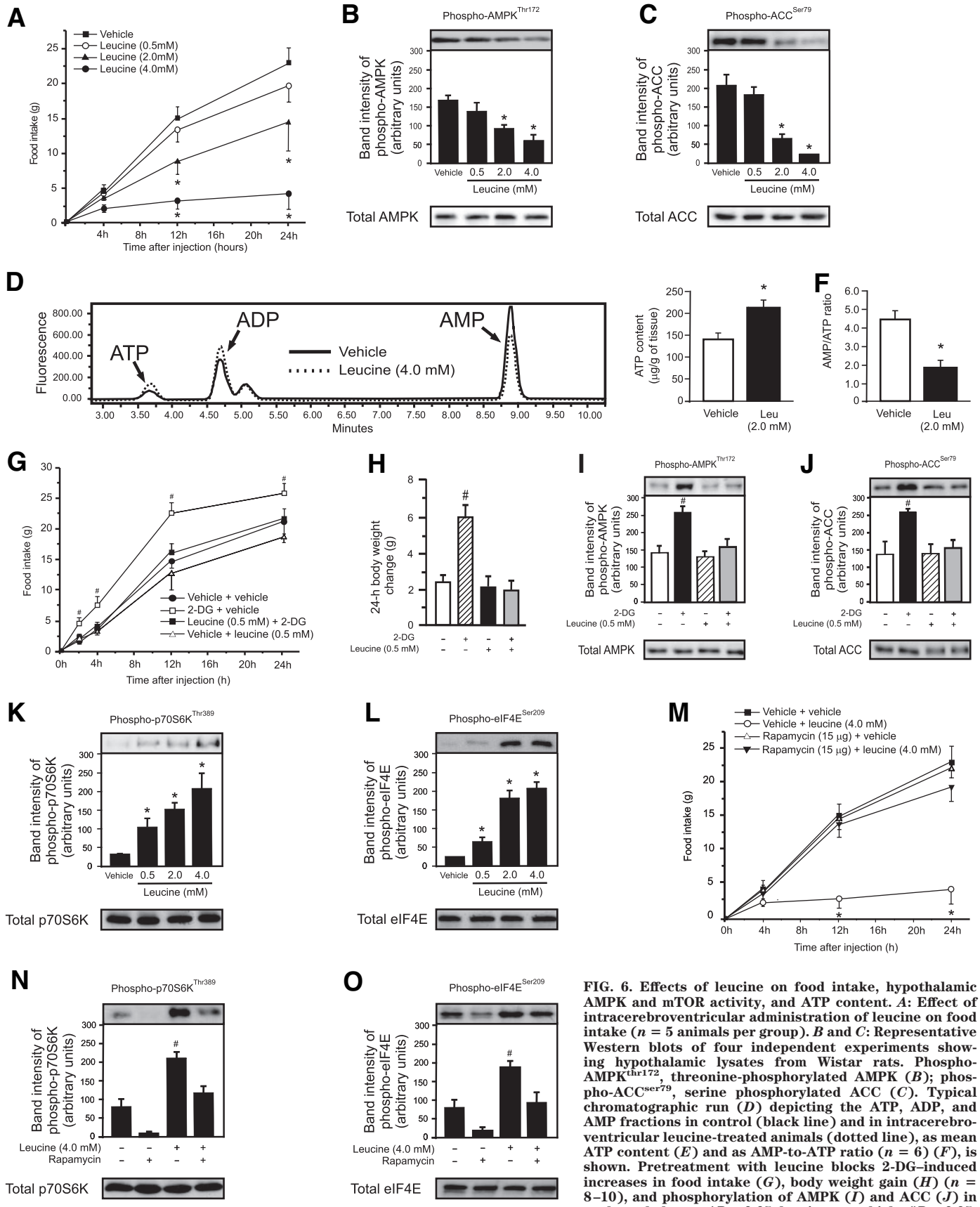

FIG. 6. Effects of leucine on food intake, hypothalamic AMPK and mTOR activity, and ATP content. *A*: Effect of intracerebroventricular administration of leucine on food intake ($n = 5$ animals per group). *B* and *C*: Representative Western blots of four independent experiments showing hypothalamic lysates from Wistar rats. Phospho-AMPK^{thr172}, threonine-phosphorylated AMPK (*B*); phospho-ACC^{ser79}, serine phosphorylated ACC (*C*). Typical chromatographic run (*D*) depicting the ATP, ADP, and AMP fractions in control (black line) and in intracerebroventricular leucine-treated animals (dotted line), as mean ATP content (*E*) and as AMP-to-ATP ratio ($n = 6$) (*F*), is shown. Pretreatment with leucine blocks 2-DG–induced increases in food intake (*G*), body weight gain (*H*) ($n = 8$–10), and phosphorylation of AMPK (*I*) and ACC (*J*) in rat hypothalamus. *$P < 0.05$, leucine vs. vehicle; #$P < 0.05$, 2-DG vs. other groups. Representative Western blots of four independent experiments showing hypothalamic lysates from Wistar rats are shown. *K*: Phospho-p70S6K^{thr389}, threonine-phosphorylated p70S6K. *L*: Phospho-eIF4E^{ser209}, serine- phosphorylated eIF4E. Pretreatment with rapamycin blocks leucine-induced anorexia (*M*) ($n = 5$ animals per group). Representative Western blots of five independent experiments showing hypothalamic lysates from Wistar rats are shown. Phospho-p70S6K^{thr389}, threonine-phosphorylated p70S6k; *$P < 0.05$ vs. vehicle-injected rats.

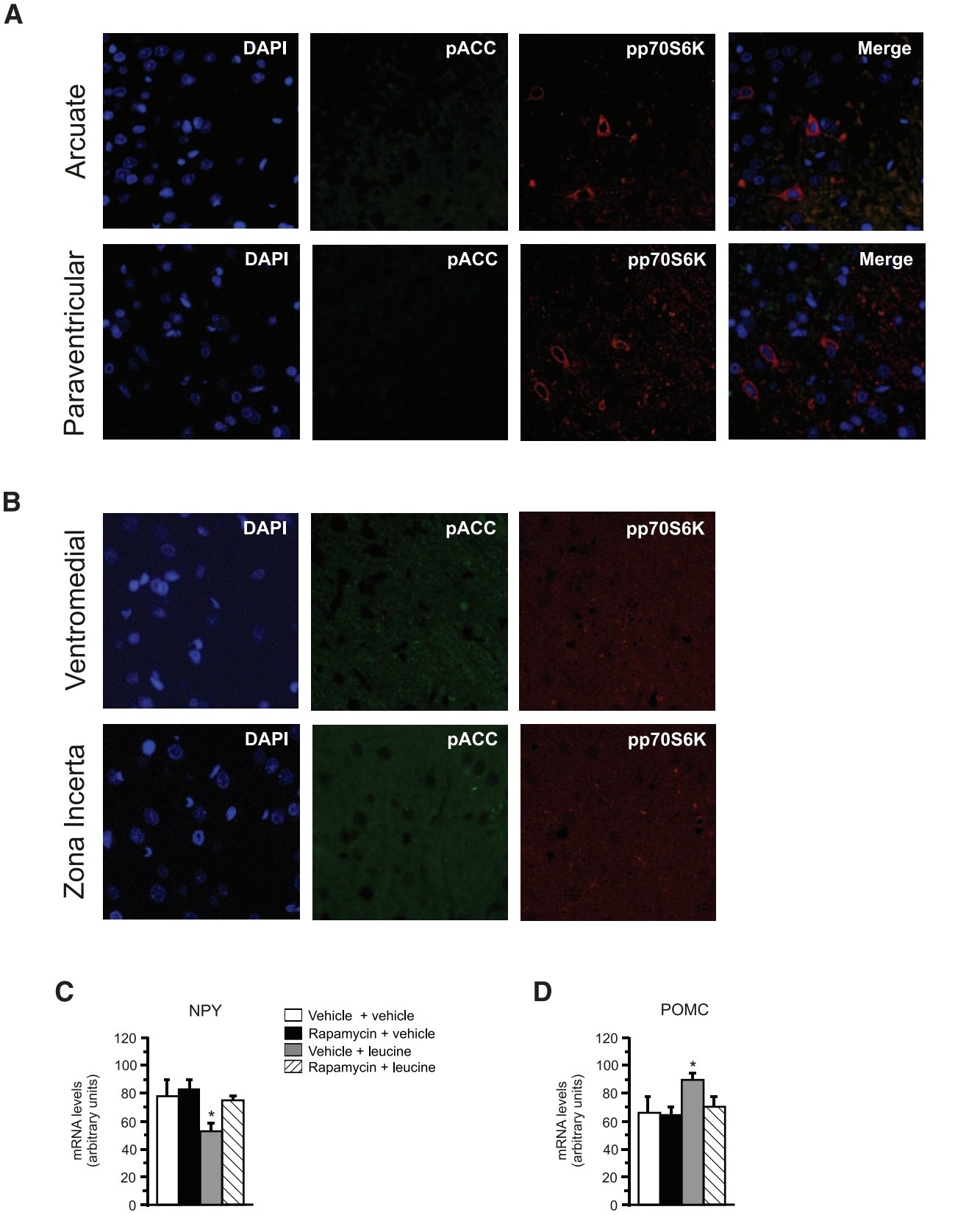

FIG. 7. Leucine enhances phosphorylated p70S6k (pp70S6K) immunoreactivity primarily in arcuate and paraventricular nuclei and modulates hypothalamic neuropetides. pACC and pp70S6K in the arcuate and paraventricular nucleus (*A*) of the Wistar rat are shown. The animals were submitted to leucine-supplemented diet during 3 days, and the sections (×200 magnification) are shown of arcuate and paraventricular immunostained for 4′,6-diamidine-2-phenylindole (DAPI, blue), phospho-ACC (green), and phospho-p70S6K (red) with images merged. Rapamycin blocks leucine modulation of NPY (*B*) and POMC (*C*) mRNA levels in Wistar rats ($n = 5$ per group). *$P < 0.05$ vs. other groups.

HPD. Consistent with a cross-regulation between AMPK and mTOR to control food intake, our data show that the activation of these enzymes occurs in the same specific neuronal subtypes.

Several factors make leucine an ideal direct nutrient signal to the brain. First, in contrast to plasma glucose and triglyceride concentrations, which do not change appreciably with feeding, leucine concentrations increased severalfold in circulation during a meal (39). Second, leucine regulates the mTOR-signaling pathway in neurons, in vivo (40). Third, leucine is more efficacious than other amino acids as a modulator of mTOR signaling. Indeed, in accordance with Cota et al. (13), we did not observe the other amino acids to be regulators of mTOR signaling in hypothalamus. Lastly, leucine is the most abundant amino acid in many dietary proteins. To further explore the potential nutrient regulation of food intake by leucine, we examined the effect of leucine supplementation on food intake. Animals eating the rat food supplemented with leucine had lower food intake and weight gain than the control animals.

Consistent with the hypothesis that leucine is a major regulator of the mTOR-sensitive response of food intake to HPD, HPD caused a similar reduction in food intake, fat mass, and increased CSF leucine compared with when leucine was supplemented in the diet. Furthermore, mTOR knockdown causes a similar change in the HPD-associated rise in food intake, compared with when leucine was supplemented in the diet. Similarly to an HPD, leucine enhances POMC and diminishes NPY expression in the hypothalamus in an AMPK- and mTOR-dependent manner; on the other hand, we could not detect alterations in food intake with other amino acids. However, the ability of HPD to effect contrasting changes in NPY and POMC neurons deserves further investigation.

How leucine activates mTOR in neurons is unknown. In other cells, it has been suggested that amino acids may activate the mTOR/Raptor/G-protein–β-subunit–like protein complex by promoting phosphorylation of the tumor suppressor complex and inhibition of the small Ras homolog enriched in brain GTPase (41,42). Recently, it has been shown that intracerebroventricular administration of leucine or leptin increases hypothalamic mTOR signaling and decreases food intake (13). Our data extend these findings by implicating AMPK in the anorectic actions of leucine and suggest an intricate relationship between these enzymes.

Nevertheless, this study shows that an HPD is associated with decreased AMPK and increased mTOR activity that results in a reduction in food intake and weight loss in rats and in *ob*/*ob* and *db*/*db* mice and suggests leucine to be the principal modulator of the AMPK and mTOR pathway present in HPD. These findings provide support for the hypothesis that AMPK and mTOR interact in the hypothalamus to regulate feeding during HPD in a leucine-dependent manner.

ACKNOWLEDGMENTS

These studies were supported by grants from Fundacão de Amparo à Pesquisa do Estado de São Paulo (FAPESP) and Conselho Nacional de desenvolvimento científico e tecnológico (CNPq).

We thank Dr. Nicola Conran for English language editing.

REFERENCES

1. Freedman MR, King J, Kennedy E: Popular diets: a scientific review. *Obes Res* 9 (Suppl. 1):1S–40S, 2001
2. Atkins RC: *Dr. Atkins' New Diet Revolution.* New York, Avon Books, 1998
3. Eades MR, Eades MD: *Protein Power: The Metabolic Breakthrough.* New York, Bantam Books, 1996
4. Dansinger ML, Gleason JA, Griffith JL, Selker HP, Schaefer EJ: Comparison of the Atkins, Ornish, Weight Watchers, and Zone diets for weight loss and heart disease risk reduction: a randomized trial. *JAMA* 293:43–53, 2005
5. Foster GD, Wyatt HR, Hill JO, McGuckin BG, Brill C, Mohammed BS, Szapary PO, Rader DJ, Edman JS, Klein S: A randomized trial of a low-carbohydrate diet for obesity. *N Engl J Med* 348:2082–2090, 2003
6. Samaha FF, Iqbal N, Seshadri P, Chicano KL, Daily DA, McGrory J, Williams T, Williams M, Gracely EJ, Stern L: A low-carbohydrate as compared with a low-fat diet in severe obesity. *N Engl J Med* 348:2074–2081, 2003
7. Gardner CD, Kiazand A, Alhassan S, Kim S, Stafford RS, Balise RR, Kraemer HC, King AC: Comparison of the Atkins, Zone, Ornish, and LEARN diets for change in weight and related risk factors among overweight premenopausal women: the A TO Z Weight Loss Study: a randomized trial. *JAMA* 297:969–977, 2007
8. Halton TL, Hu FB: The effects of high protein diets on thermogenesis, satiety and weight loss: a critical review. *J Am Coll Nutr* 23:373–385, 2004
9. Andersson U, Filipsson K, Abbott CR, Woods A, Smith K, Bloom SR, Carling D, Small CJ: AMP-activated protein kinase plays a role in the control of food intake. *J Biol Chem* 279:12005–12008, 2004
10. Minokoshi Y, Alquier T, Furukawa N, Kim YB, Lee A, Xue B, Mu J, Foufelle F, Ferre P, Birnbaum MJ, Stuck BJ, Kahn BB: AMP-kinase regulates food intake by responding to hormonal and nutrient signals in the hypothalamus. *Nature* 428:569–574, 2004
11. Ropelle ER, Pauli JR, Zecchin KG, Ueno M, de Souza CT, Morari J, Faria MC, Velloso LA, Saad MJ, Carvalheira JB: A central role for neuronal adenosine 5′-monophosphate-activated protein kinase in cancer-induced anorexia. *Endocrinology* 148:5220–5229, 2007
12. Kahn BB, Alquier T, Carling D, Hardie DG: AMP-activated protein kinase: ancient energy gauge provides clues to modern understanding of metabolism. *Cell Metab* 1:15–25, 2005
13. Cota D, Proulx K, Smith KA, Kozma SC, Thomas G, Woods SC, Seeley RJ: Hypothalamic mTOR signaling regulates food intake. *Science* 312:927–930, 2006
14. Brunn GJ, Hudson CC, Sekulic A, Williams JM, Hosoi H, Houghton PJ, Lawrence JC Jr, Abraham RT: Phosphorylation of the translational repressor PHAS-I by the mammalian target of rapamycin. *Science* 277:99–101, 1997
15. Shamji AF, Nghiem P, Schreiber SL: Integration of growth factor and nutrient signaling: implications for cancer biology. *Mol Cell* 12:271–280, 2003
16. Dennis PB, Jaeschke A, Saitoh M, Fowler B, Kozma SC, Thomas G: Mammalian TOR: a homeostatic ATP sensor. *Science* 294:1102–1105, 2001
17. Inoki K, Li Y, Zhu T, Wu J, Guan KL: TSC2 is phosphorylated and inhibited by Akt and suppresses mTOR signalling. *Nat Cell Biol* 4:648–657, 2002
18. Kimura N, Tokunaga C, Dalal S, Richardson C, Yoshino K, Hara K, Kemp BE, Witters LA, Mimura O, Yonezawa K: A possible linkage between AMP-activated protein kinase (AMPK) and mammalian target of rapamycin (mTOR) signalling pathway. *Genes Cells* 8:65–79, 2003
19. Shaw RJ, Bardeesy N, Manning BD, Lopez L, Kosmatka M, DePinho RA, Cantley LC: The LKB1 tumor suppressor negatively regulates mTOR signaling. *Cancer Cell* 6:91–99, 2004
20. Shigemitsu K, Tsujishita Y, Miyake H, Hidayat S, Tanaka N, Hara K, Yonezawa K: Structural requirement of leucine for activation of p70 S6 kinase. *FEBS Lett* 447:303–306, 1999
21. Kimball SR, Jefferson LS: Molecular mechanisms through which amino acids mediate signaling through the mammalian target of rapamycin. *Curr Opin Clin Nutr Metab Care* 7:39–44, 2004
22. Xu G, Kwon G, Cruz WS, Marshall CA, McDaniel ML: Metabolic regulation by leucine of translation initiation through the mTOR-signaling pathway by pancreatic beta-cells. *Diabetes* 50:353–360, 2001
23. Ropelle ER, Pauli JR, Prada PO, de Souza CT, Picardi PK, Faria MC, Cintra DE, Fernandes MF, Flores MB, Velloso LA, Saad MJ, Carvalheira JB: Reversal of diet-induced insulin resistance with a single bout of exercise in the rat: the role of PTP1B and IRS-1 serine phosphorylation. *J Physiol* 577:997–1007, 2006
24. Scott AM, Atwater I, Rojas E: A method for the simultaneous measurement of insulin release and B cell membrane potential in single mouse islets of Langerhans. *Diabetologia* 21:470–475, 1981

25. Rosen H: A modified ninhydrin colorimetric analysis for amino acids. *Arch Biochem Biophys* 67:10–15, 1957
26. Bensaid A, Tome D, L'Heureux-Bourdon D, Even P, Gietzen D, Morens C, Gaudichon C, Larue-Achagiotis C, Fromentin G: A high-protein diet enhances satiety without conditioned taste aversion in the rat. *Physiol Behav* 78:311–320, 2003
27. Carvalheira JB, Siloto RM, Ignacchitti I, Brenelli SL, Carvalho CR, Leite A, Velloso LA, Gontijo JA, Saad MJ: Insulin modulates leptin-induced STAT3 activation in rat hypothalamus. *FEBS Lett* 500:119–124, 2001
28. Lebedev SV, Blinov DV, Petrov SV: Spatial characteristics of cisterna magna in rats and novel technique for puncture with a stereotactic manipulator. *Bull Exp Biol Med* 137:635–638, 2004
29. Carvalheira JB, Ribeiro EB, Araujo EP, Guimaraes RB, Telles MM, Torsoni M, Gontijo JA, Velloso LA, Saad MJ: Selective impairment of insulin signalling in the hypothalamus of obese Zucker rats. *Diabetologia* 46:1629–1640, 2003
30. Amaral ME, Barbuio R, Milanski M, Romanatto T, Barbosa HC, Nadruz W, Bertolo MB, Boschero AC, Saad MJ, Franchini KG, Velloso LA: Tumor necrosis factor-alpha activates signal transduction in hypothalamus and modulates the expression of pro-inflammatory proteins and orexigenic/anorexigenic neurotransmitters. *J Neurochem* 98:203–212, 2006
31. Marin RM, Franchini KG, Rocco SA: Analysis of adenosine by RP-HPLC method and its application to the study of adenosine kinase kinetics. *J Sep Sci* 30:2473–2479, 2007
32. Tsukumo DM, Carvalho-Filho MA, Carvalheira JB, Prada PO, Hirabara SM, Schenka AA, Araujo EP, Vassallo J, Curi R, Velloso LA, Saad MJ: Loss-of-function mutation in Toll-like receptor 4 prevents diet-induced obesity and insulin resistance. *Diabetes* 56:1986–1998, 2007
33. Araujo EP, Amaral ME, Souza CT, Bordin S, Ferreira F, Saad MJ, Boschero AC, Magalhaes EC, Velloso LA: Blockade of IRS1 in isolated rat pancreatic islets improves glucose-induced insulin secretion. *FEBS Lett* 531:437–442, 2002
34. Mai JK, Assheuer J, Paxinos G: *Atlas of the Human Brain.* San Diego, CA, Academic, 1997
35. Dalgaard LT, Pedersen O: Uncoupling proteins: functional characteristics and role in the pathogenesis of obesity and type II diabetes. *Diabetologia* 44:946–965, 2001
36. Tews JK, Repa JJ, Harper AE: Protein selection by rats adapted to high or moderately low levels of dietary protein. *Physiol Behav* 51:699–712, 1992
37. Jean C, Rome S, Mathe V, Huneau JF, Aattouri N, Fromentin G, Achagiotis CL, Tome D: Metabolic evidence for adaptation to a high protein diet in rats. *J Nutr* 131:91–98, 2001
38. Morens C, Gaudichon C, Fromentin G, Marsset-Baglieri A, Bensaid A, Larue-Achagiotis C, Luengo C, Tome D: Daily delivery of dietary nitrogen to the periphery is stable in rats adapted to increased protein intake. *Am J Physiol Endocrinol Metab* 281:E826–E836, 2001
39. Lynch CJ, Gern B, Lloyd C, Hutson SM, Eicher R, Vary TC: Leucine in food mediates some of the postprandial rise in plasma leptin concentrations. *Am J Physiol Endocrinol Metab* 291:E621–E630, 2006
40. Lynch CJ, Fox HL, Vary TC, Jefferson LS, Kimball SR: Regulation of amino acid-sensitive TOR signaling by leucine analogues in adipocytes. *J Cell Biochem* 77:234–251, 2000
41. Nobukuni T, Joaquin M, Roccio M, Dann SG, Kim SY, Gulati P, Byfield MP, Backer JM, Natt F, Bos JL, Zwartkruis FJ, Thomas G: Amino acids mediate mTOR/raptor signaling through activation of class 3 phosphatidylinositol 3OH-kinase. *Proc Natl Acad Sci U S A* 102:14238–14243, 2005
42. Roccio M, Bos JL, Zwartkruis FJ: Regulation of the small GTPase Rheb by amino acids. *Oncogene* 25:657–664, 2006

APÊNDICE *III*

OPEN ACCESS Freely available online

PLoS one

Central Exercise Action Increases the AMPK and mTOR Response to Leptin

Eduardo R. Ropelle[9], Maria Fernanda A. Fernandes[9], Marcelo B. S. Flores, Mirian Ueno, Silvana Rocco, Rodrigo Marin, Dennys E. Cintra, Lício A. Velloso, Kleber G. Franchini, Mario J. A. Saad, José B. C. Carvalheira*

Department of Internal Medicine, FCM, State University of Campinas (UNICAMP), Campinas, São Paulo, Brazil

Abstract

AMP-activated protein kinase (AMPK) and mammalian Target of Rapamycin (mTOR) are key regulators of cellular energy balance and of the effects of leptin on food intake. Acute exercise is associated with increased sensitivity to the effects of leptin on food intake in an IL-6-dependent manner. To determine whether exercise ameliorates the AMPK and mTOR response to leptin in the hypothalamus in an IL-6-dependent manner, rats performed two 3-h exercise bouts, separated by one 45-min rest period. Intracerebroventricular IL-6 infusion reduced food intake and pretreatment with AMPK activators and mTOR inhibitor prevented IL-6-induced anorexia. Activators of AMPK and fasting increased food intake in control rats to a greater extent than that observed in exercised ones, whereas inhibitor of AMPK had the opposite effect. Furthermore, the reduction of AMPK and ACC phosphorylation and increase in phosphorylation of proteins involved in mTOR signal transduction, observed in the hypothalamus after leptin infusion, were more pronounced in both lean and diet-induced obesity rats after acute exercise. Treatment with leptin reduced food intake in exercised rats that were pretreated with vehicle, although no increase in responsiveness to leptin-induced anorexia after pretreatment with anti-IL6 antibody, AICAR or Rapamycin was detected. Thus, the effects of leptin on the AMPK/mTOR pathway, potentiated by acute exercise, may contribute to appetite suppressive actions in the hypothalamus.

Citation: Ropelle ER, Fernandes MFA, Flores MBS, Ueno M, Rocco S, et al. (2008) Central Exercise Action Increases the AMPK and mTOR Response to Leptin. PLoS ONE 3(12): e3856. doi:10.1371/journal.pone.0003856

Editor: Jose A. L. Calbet, University of Las Palmas de Gran Canaria, Spain

Received August 7, 2008; **Accepted** November 6, 2008; **Published** December 4, 2008

Funding: These studies were supported by grants from Fundacão de Amparo à Pesquisa do Estado de São Paulo (FAPESP), Coordenação de Aperfeiçoamento de Pessoal de Nível Superior (CAPES) and Conselho Nacional de desenvolvimento científico e tecnológico (CNPq).

Competing Interests: The authors have declared that no competing interests exist.

* E-mail: carvalheirajbc@uol.com.br

[9] These authors contributed equally to this work.

Introduction

Prolonged exercise of medium to high intensity is known to profoundly affect energy balance [1–3]. Studies of individuals who have maintained significant weight loss for >1 year have demonstrated that dieters who achieve long-term success are often those who engage in regular and extensive exercise programs [4]. Although the energy expenditure aspects of such exercise may contribute to the effects of weight maintenance, it has been suggested that exercise may also contribute to the energy balance by altering food intake [5,6]. Rodents submitted to exercise have increased sensitivity to leptin, conversely animals with diet-induced obesity and most obese humans are resistant to leptin [5,7,8]. Thus, the mechanism for leptin increased responsiveness in exercise is of great interest and understanding this mechanism could lead to new approaches to prevent or treat obesity.

The hypothalamus plays a central role in integrating hormonal (leptin and insulin) and nutritional signals from the periphery and modulating food intake, energy expenditure, and peripheral metabolism [9]. Multiple factors control food intake, including hormones, fuels and behaviour. AMPK is the downstream component of a kinase cascade that acts as a sensor of cellular energy charge, being activated by rising AMP coupled with falling ATP. Once activated, AMPK phosphorylates acetyl-CoA carboxylase (ACC) and switches on energy-producing pathways at the expense of energy-depleting processes [10–12]. Another target molecule for the control of food intake and energy homeostasis is represented by the phosphoprotein mammalian target of rapamycin, mTOR, in which the PI(3)K/Akt pathway has been suggested to affect the mTOR phosphorylation state and catalytic activity [13]. Activated signaling through mTOR phosphorylates the serine/threonine kinase p70S6K and the translational repressor eukaryotic initiation factor (eIF) 4E binding protein (4EBP1) [14,15]. mTOR signaling is inhibited under conditions of low nutrients, such as glucose and amino acids and low intracellular ATP levels [16]. While mTOR was presumed to serve as the direct cellular sensor for ATP levels [17], mounting evidence has implicated AMPK in the regulation of mTOR activity [15,18–20].

The level of circulating interleukin-6 (IL-6) increases dramatically in response to exercise [21], with IL-6 being produced by working muscle [22,23] and adipose tissue [24,25] and its concentration correlates temporally with increases in AMPK in multiple tissues [26]. In addition, AMPK activity is diminished in IL-6 deficient mice at rest and the absolute increases in AMPK activity in these tissues caused by exercise is diminished compared with control mice [27]. It also appears that centrally-acting IL-6 plays a role in the regulation of appetite, energy expenditure, and body composition [5,28]. The signaling mechanism of IL-6 in the

hypothalamus is, however, not fully understood. In cells, binding IL-6 to the α subunit of its receptor triggers the recruitment of gp130, subsequently leading to the activation of the gp130-associated JAK [29–31]. JAK links cytokine receptor to the STAT3 and MAP kinase pathway [29,30,32]. In addition to JAK/STAT and MAP kinase pathways, IL-6 also activates the PI(3)K/Akt pathway [33].

In this study, we sought to determine whether the improved response of the AMPK and mTOR pathways to leptin could contribute to the increased molecular response of leptin in rats submitted to exercise in an IL-6-dependent manner. We therefore, examined hypothalamic modulation of AMPK/ACC and mTOR signaling pathways, induced by IL-6, as well as the role of IL-6 in those signaling pathways induced by leptin in rats after acute exercise.

Results

IL-6 decreases hypothalamic AMPK and increases mTOR signaling

To determine whether IL-6 modulates hypothalamic AMPK/ACC signaling, we injected IL-6 into the third ventricle of rats and evaluated food intake and AMPK signaling. IL-6 caused a significant reduction in food intake (Figure 1a). We next investigated whether the microinfusion of IL-6 modulates the hypothalamic ATP concentration. Figure 1b shows that IL-6 (200 ng) changed ATP, ADP and AMP concentrations in the hypothalamus of rats, whereas, sixty minutes after IL-6 injection, the ATP content increased by ~88% (Figure 1c) and decreased AMP:ATP ratio by ~54% in Wistar rats (Figure 1d). Consistent with the modulation of the AMP:ATP ratio, we observed reduced hypothalamic AMPK and ACC phosphorylation induced by IL-6 (Figures 1e and f); whilst IL-6 increases p70S6K and 4EBP1 phosphorylation (Figures 1g and h). The αAMPK, ACC, p70S6K and 4EBP1 protein levels were not different between the groups (Figures 1e–h, lower panels).

If the effect of IL-6 on food intake is mediated by AMPK inhibition, AICAR infusion at doses that do not change food intake, but still increase AMPK and ACC phosphorylation, could be sufficient to block the effects of IL-6. Thus, to determine whether the effects of IL-6 on food intake are AMPK-dependent, we first identified a dose of AICAR that did not alter food intake (0.5 mM) when administered at the onset of the dark cycle. We then evaluated the effect of i.c.v. pretreatment with this dose of AICAR, or its vehicle, on the anorectic response to i.c.v. IL-6 (200 ng) and we observed that the anorectic response to i.c.v. IL-6 was reversed by AICAR at the time points studied (figure 1a). These findings indicate that inactivation of neuronal AMPK is necessary for some of the effects of IL-6 on food intake.

Immunohistochemistry with anti-Interleukin-6 Receptor (IL-6R)-specific antibody showed that IL-6R is expressed in a majority of neurons in the arcuate nucleus (Figure 1i). Double-staining confocal microscopy showed the positive immunoreactivity of IL-6R and AMPK in the hypothalamic arcuate nucleus of rats 60 minutes after i.c.v. saline or IL-6 (200 ng) infusion. The immunoreactivity of IL-6R and pp70S6K was not detected in the hypothalamic arcuate nucleus of rats after i.c.v. saline infusion. However, we observed the positive double-staining of IL-6R and pp70S6K 60 minutes after i.c.v. IL-6 (200 ng) infusion (Figure 1j).

IL-6 induction of hypothalamic mTOR does not require changes in PI(3)K signaling

If the effect of IL-6 on food intake is mediated by mTOR activation, Rapamycin infusion at doses that do not change food intake, but still decrease p70S6K and 4EBP1 phosphorylations could be sufficient to block the effects of IL-6. Thus to determine whether IL-6 modulates hypothalamic mTOR signaling, we injected IL-6 (200 ng) into the third ventricle of rats and evaluated food intake and mTOR signaling. IL-6 caused a significant reduction in food intake (Figure 2a) and induced hypothalamic p70S6K and 4EBP1 phosphorylation (Figures 2b and c). The p70S6K and 4EBP1 protein levels were not different between the groups (Figures 2b and c, lower panels). To determine whether the effects of IL-6 on food intake are mTOR-dependent, we first identified a dose of Rapamycin that did not alter food intake (25 μg) when administered at the onset of the dark cycle. We then evaluated the effect of i.c.v. pretreatment with this dose of Rapamycin or its vehicle, on the anorectic response to i.c.v. IL-6 and we observed that IL-6 reduction of food intake was reversed by Rapamycin.

We next examined whether PI(3)K signaling is required for the IL-6-dependent reduction of food intake, by IL-6 administration in LY294002 pretreated (i.c.v.) animals. Pretreatment with LY294002 at a dose that did not alter food intake (1 nmol) had no effect on anorectic response to i.c.v. IL-6 (Figure 2d). Consistent with these data, we observed that a single IL-6 i.c.v. injection did not change Akt phosphorylation status in the hypothalamus (Figure 2e). The Akt protein levels were not different between the groups (Figure 2e, lower panel). These findings indicates that activation of neuronal mTOR is necessary for some of the effects of IL-6 on food intake and that these effects of IL-6 do not require any change in PI(3)K signaling.

We also injected IL-6 (200 ng) into the third ventricle of rats and evaluated food intake and JAK2/STAT3 signaling. IL-6 caused a significant reduction in food intake (Figure 2f) and induced hypothalamic JAK2 and STAT3 phosphorylation (Figures 2g and h). The JAK2 and STAT3 protein levels were not different between the groups (Figures 2g and h, lower panels). To determine whether the effects of IL-6 on food intake are also JAK2/STAT3-dependent, we first identified a dose of AG490 that did not alter food intake when administered at the onset of the dark cycle. We then evaluated the effect of i.c.v. pretreatment with this dose of AG490 or its vehicle, on the anorectic response to i.c.v. IL-6 and we observed that IL-6 reduction of food intake was reversed by AG490 (Figure 2f).

Physiological parameters measured in basal conditions after exercise protocol

The plasma glucose level was lower in the exercised group compared to the control group (3.6±0.8 *vs* 4.6±0.5 mmol/L; n = 5; $p<0.05$) and the insulin levels were also lower (88±12 *vs* 193±17 pmol/L, n = 5; $p<0.05$). Exercise did not, however, reduce plasma leptin (2.6±0.5 *vs* 2.3±0.7 ng/ml). Insulinemia and leptinemia were not altered by third ventricle microinjection of leptin (data not shown).

Exercise partially reverses the effects of AMPK agonists and fasting on food intake through modulation of the AMPK-mTOR signaling pathway in the hypothalamus

To test the role of a single session of exercise on AICAR-increased food intake, AICAR (2 mM) or its vehicle were administered (i.c.v.) to control and exercised animals. 12-hour total food intake was measured after exercise. In exercised rats, AICAR (2 mM) did not cause any acute change in food intake but, in the control group, AICAR (2 mM) increased food intake by 32% (Figure 3a), suggesting that AICAR is not effective in exercised rats. Comparing AICAR-treated groups (control *vs.*

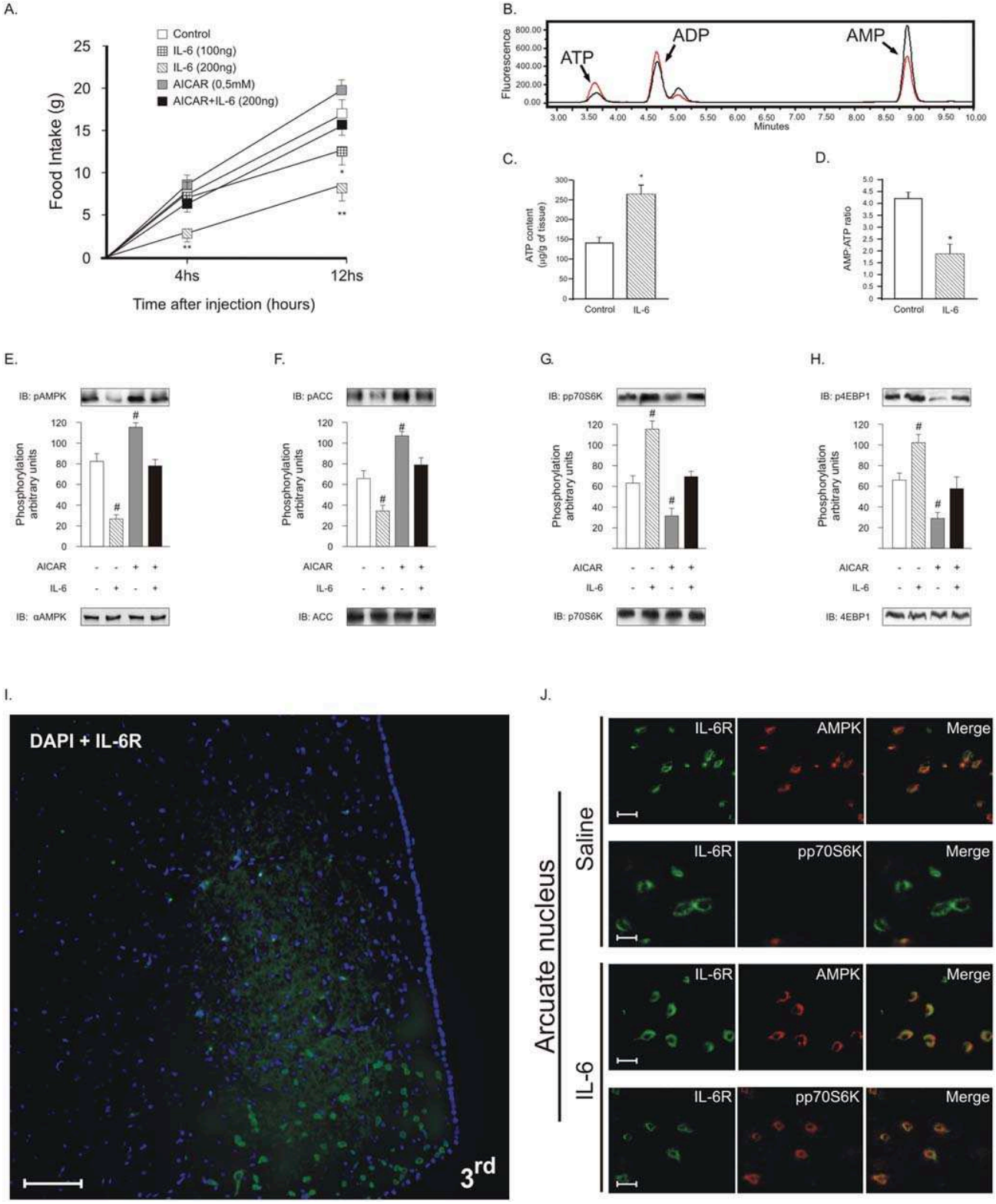

Figure 1. Effects of IL-6 on food intake, hypothalamic AMPK/mTOR activity and ATP content. (a) Effect of i.c.v. administration of IL-6 on food intake; pretreatment with AICAR blocks IL-6-induced anorexia ($n = 12–15$ animals per group). (b, c, d) Typical chromatographic run (b) depicting the ATP, ADP, and AMP fractions in control (black line) and in i.c.v. IL-6 treated animals (red line), as mean ATP content and as AMP:ATP ratio (c, d). (e, f, g, h) Representative Western blots of four independent experiments showing hypothalamic lysates from Wistar rats. Phospho-AMPK^{thr172}, threonine-phosphorylated AMPK and total AMPK (e); phospho-ACC^{ser79}, serine phosphorylated ACC and total ACC (f); phospho-p70S6Kinase^{thr389}, threonine phosphorylated p70S6Kinase and total p70S6K (g); phospho-4EBP1^{thr70}, threonine phosphorylated 4EBP1 and total 4EBP1 (h). Confocal

microscopy was performed using IL-6 receptor (IL-6R)-specific antibody (green) and DAPI (blue), with 50× magnification (i). Co-localization of IL-6R (green) and AMPK (red) and IL-6R (green) and phospho-p70S6K (red) 60 minutes after i.c.v. saline or IL-6 infusion in the arcuate nuclei of rats, with 200× magnification (j). Data are the means±SEM. *$p<0.05$, *vs.* control group; **$p<0.01$, *vs.* control group; # $p<0.05$, *vs.* other groups.
doi:10.1371/journal.pone.0003856.g001

exercise), exercised animals showed a 33% reduction in 12-hour total food intake (Figure 3a).

Consistent with food intake, AICAR increased AMPK threonine and ACC serine phosphorylation levels in the hypothalami of control rats, whilst in exercised animals, AICAR did not change AMPK/ACC phosphorylation status (Figures 3b and c). Comparing AICAR treated groups (control *vs.* exercise), exercised animals showed reductions in AMPK threonine and ACC serine phosphorylation of 52% and 31%, respectively. AICAR reduced p70S6K and 4EBP1 threonine phosphorylation levels in the hypothalamus of control and exercised rats. However, comparing AICAR treated groups (control *vs.* exercise), exercised animals showed increases in p70S6K and 4EBP1 threonine phosphorylation of 230% and 310%, respectively (Figures 3d and e). The αAMPK, ACC, p70S6K and 4EBP1 protein levels were not different between the groups (Figures 3b–e, lower panels). Similar results were observed after intraperitoneal treatment with 2-DG, another pharmacological activator of AMPK (Figure 3f–j).

To be sure that the experiments represent a physiological condition we measured food intake in control and exercised animals after fasting. In the control animals, prolonged fasting (48 hours) increased ~35% of food intake during 12-hours of refeeding period compared to control group. However, in the fasted rats, acute exercise session prevented fasting-induced hyperphagic response (Figure 3k). Comparing fasting treated groups (control *vs.* exercise), exercised animals showed reductions in AMPK threonine and ACC serine phosphorylation of 65% and 41%, respectively (Figures 3l and m). Comparing fasting groups (control *vs.* exercise), exercised animals showed increases in p70S6K and 4EBP1 threonine phosphorylation of 261% and 240%, respectively (Figures 3n and o). The αAMPK, ACC, p70S6K and 4EBP1 protein levels were not different between the groups (Figures 3l–o, lower panels).

Intracerebroventricular α-LA reduces food intake by modulating AMPK-mTOR hypothalamic phosphorylation levels to a greater extent in exercised animals

α-LA is an essential cofactor of mitochondrial respiratory enzymes and exerts potent anti-obesity effects by suppressing hypothalamic AMPK activity [34]. The effects of α-LA (3 μg) intracerebroventricular administration, or its vehicle, on food intake control were studied by measuring the 12-hour total food intake after an acute exercise bout. In exercised rats, α-LA (3 μg) reduced food intake by 86% while control group showed a reduction of 58%. Comparing α-LA treated groups (control *vs.* exercise), exercised animals showed a 64% reduction in 12-hour total food intake (Figure 4a).

To determine the effects of exercise on the AMPK-mTOR signaling pathway, α-LA was i.c.v. administered and AMPK, ACC, p70S6K and 4EBP1 phosphorylation levels were assessed in the hypothalamus of all rats. α-LA reduced AMPK and ACC phosphorylation levels, in the hypothalami of control and exercised rats. Comparing α-LA treated groups (control *vs.* exercise), in exercised animals α-LA reduced both AMPK threonine phosphorylation and ACC serine phosphorylation of 39% and 57%, respectively (Figures 4b and c).

α-LA induced p70S6K and 4EBP1 threonine phosphorylation in the hypothalami of control and exercised rats. Comparing α-LA treated groups (control *vs.* exercise), in exercised animals, α-LA increased p70S6K and 4EBP1 threonine phosphorylation of 19% and 11%, respectively (Figures 4d and e). α-LA did not change αAMPK, ACC, p70S6K and 4EBP1 protein expression (Figures 4b–e, lower panels).

Intracerebroventricular leptin reduces food intake by modulating AMPK-mTOR hypothalamic phosphorylation levels to a greater extent in exercised animals

The effects of leptin (10^{-6} M) i.c.v. administration or its vehicle on food intake control were studied by measuring the 12-hour total food intake after an acute exercise bout. In exercised rats, leptin (10^{-6} M) reduced food intake by 43%, when compared with exercised plus vehicle treated group, while the control group showed a reduction of 25%, when compared with vehicle treated group. Comparing leptin-treated groups (control *vs.* exercise), exercised animals showed a 31% reduction in 12-hour total food intake (Figure 5a).

To determine the effects of exercise on AMPK-mTOR signaling pathway, leptin was i.c.v. administered and AMPK, ACC, p70S6K and 4EBP1 phosphorylation levels were assessed in the hypothalamus of all rats. Leptin reduced AMPK and ACC phosphorylation levels in the hypothalami of control and exercised rats. Comparing leptin-treated groups (control *vs.* exercise), in exercised animals, leptin reduced both AMPK threonine phosphorylation and ACC serine phosphorylation of 57% and 45%, respectively (Figures 5b and c). Leptin induced p70S6K and 4EBP1 threonine phosphorylation in the hypothalamus of control and exercised rats. Comparing leptin treated groups (control *vs.* exercise), in exercised animals, leptin increased both p70S6K and 4EBP1 threonine phosphorylation of 30% and 40% respectively (Figures 5d and e). The αAMPK, ACC, p70S6K and 4EBP1 protein levels were not different between the groups (Figures 5b–e, lower panels).

Role of IL-6 in anorectic response to leptin

Hypothalamic IL-6 expression was detected in control animals; however, a 420% increase was observed in the exercised group (Figure 6a). We tested whether the inhibitory effects of leptin on food intake depends on IL-6, by i.c.v. infusion of anti–IL-6 antibody into exercised rats. Treatment with leptin (10^{-6} M) markedly reduced 12-h food intake in exercised rats pretreated with vehicle, although pretreatment with anti–IL-6 antibody blocked exercise-induced leptin responsiveness in a concentration-dependent manner (Figure 6b).

Both AMPK and ACC phosphorylation levels, reduced by exercise, were reversed by anti–IL-6 antibody (Figure 6c and d). We also observed that the increased phosphorylations of p70S6K and 4EBP1, induced by exercise, were also reversed by anti–IL-6 infusion (Figures 6e and f). The αAMPK, ACC, p70S6K and 4EBP1 protein levels were not different between the groups (Figures 6c–f, lower panels).

The role of IL-6 on leptin responsiveness in the hypothalamus of diet-induced obesity (DIO) rats

We next investigated the effect of IL-6 on leptin responsiveness in the hypothalamus of diet-induced obesity (DIO) rats after acute exercise. Hypothalamic IL-6 expression was detected in the

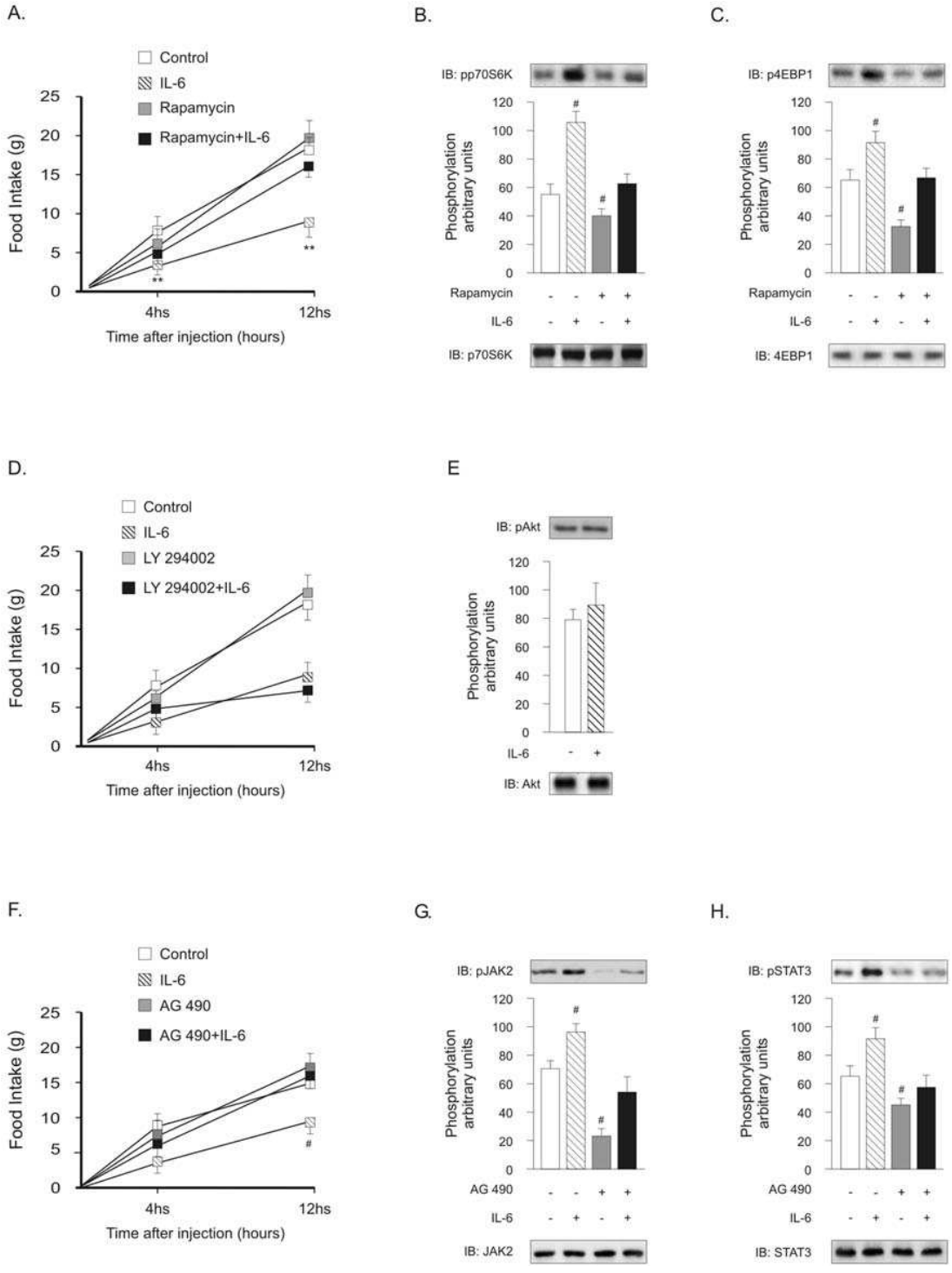

Figure 2. Effects of IL-6 on food intake and hypothalamic PI(3)K/mTOR and JAK/STAT activity. (a) Pretreatment with Rapamycin blocks IL-6-induced anorexia ($n = 10–12$ animals per group). (b, c) Representative Western blots of four independent experiments showing hypothalamic lysates from Wistar rats. Phospho-p70S6Kinase^{thr389}, threonine phosphorylated p70S6Kinase and total p70S6K (b); phospho-4EBP1^{thr70}, threonine phosphorylated 4EBP1 and total 4EBP1 (c). (d) Pretreatment with LY294002 had no effect on anorectic response to IL-6 ($n = 10–12$). (e) Representative western blot of four independent experiments showing hypothalamic lysates from Wistar rats. Phospho-Akt^{ser473}, serine phosphorylated Akt and total Akt. (f) Pretreatment with AG490 blocks IL-6-induced anorexia ($n = 10–12$ animals per group). (g, h) Representative Western blots of four independent experiments showing hypothalamic lysates from Wistar rats. Phospho-JAK2, tyrosine phosphorylated JAK2 and total JAK2 (g); phospho-STAT3, Tyrosine phosphorylated STAT3 and total STAT3 (h). Data are the means±SEM. $^{**}p<0.01$, *vs.* control group; # $p<0.05$, *vs.* other groups.
doi:10.1371/journal.pone.0003856.g002

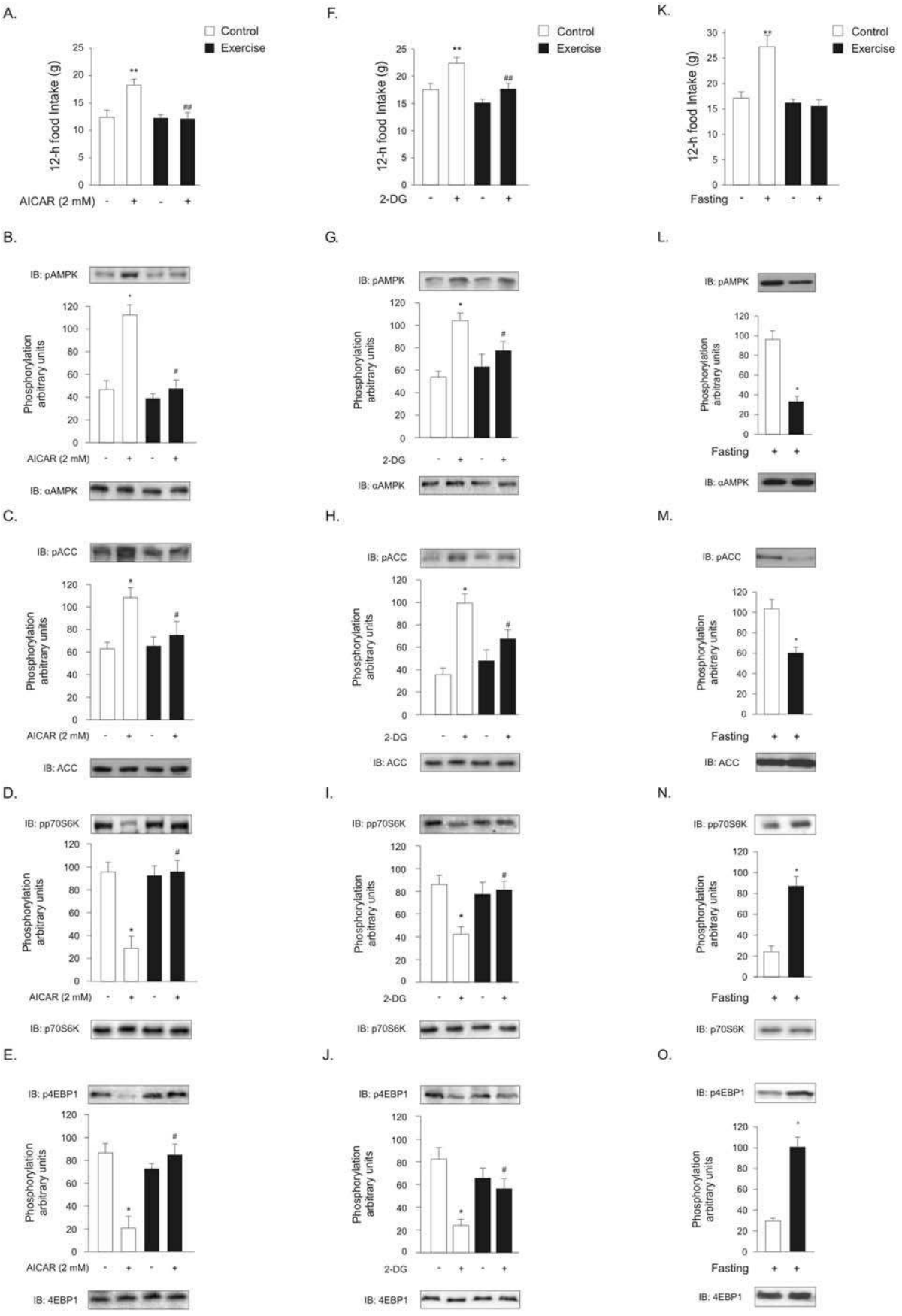
A.
Control
Exercise
12-h food Intake (g)
AICAR (2 mM)
F.
2-DG
K.
Fasting
B.
IB: pAMPK
Phosphorylation arbitrary units
IB: αAMPK
G.
L.
C.
IB: pACC
IB: ACC
H.
M.
D.
IB: pp70S6K
IB: p70S6K
I.
N.
E.
IB: p4EBP1
IB: 4EBP1
J.
O.

Figure 3. AICAR, 2-DG and fasting effects on 12-h cumulative food intake and AMPK/mTOR signaling, in the hypothalami of control and exercised rats. (a) AICAR (2 mM) was administered in control and exercised rats. Animals were immediately exposed to food for a 12-hour period ($n = 12–15$ animals per group). (b, c, d, e) Representative Western blots of five independent experiments showing hypothalamic lysates from Wistar rats. (f) 2-DG (500 mg/Kg) was administered in control and exercised rats. Animals were immediately exposed to food for a 12-hour period ($n = 12–15$ animals per group). (g, h, i, j) Representative Western blots of five independent experiments showing hypothalamic lysates from Wistar rats. (k) Exercise decreases food intake in the fasting state (48 h fasting). Animals were immediately exposed to food for a 12-hour period ($n = 12–15$ animals per group). (l, m, n, o) Representative Western blots of five independent experiments showing hypothalamic lysates from Wistar rats. Phospho-AMPK^{thr172}, threonine-phosphorylated AMPK and total AMPK; phospho-ACC^{ser79}, serine phosphorylated ACC and total ACC; phospho-p70S6Kinase^{thr389}, threonine phosphorylated p70S6Kinase and total p70S6K; phospho-4EBP1^{thr70}, threonine phosphorylated 4EBP1 and total 4EBP1. Data are the means±SEM. * $p<0.05$, ** $p<0.01$, *vs.* control group; # $p<0.05$, ## $p<0.001$ *vs.* AICAR- or 2-DG-stimulated control group.
doi:10.1371/journal.pone.0003856.g003

hypothalamus of diet-induced obesity (DIO) rats; however, a 156% increase was observed in the DIO rats after acute exercise (Figure 7a). The effects of leptin (10^{-6} M) i.c.v. administration on energy intake control were studied by measuring the 12-hour total food intake after an acute exercise bout in DIO rats. Comparing leptin-treated rats (control vs. DIO), the energy intake was 28% higher in DIO rats after leptin infusion. However, the i.c.v. infusion of leptin was able to reduce the energy intake by about 31% in DIO rats after the exercise protocol, compared to DIO rats at rest (Figure 7b). Interestingly, the i.c.v. pretreatment with anti-IL-6 antibody (25 ng) blunted the anorexigenic effects of leptin in exercised DIO rats.

To determine the effects of exercise on the AMPK-mTOR signaling pathway in the hypothalamus of DIO rats, leptin was i.c.v. administered and AMPK, ACC, p70S6K and 4EBP1 phosphorylation levels were assessed in the hypothalamus. The suppressive effects of i.c.v. infusion of leptin on AMPK and ACC phosphorylation were impaired in the hypothalamus of DIO rats by about 58 and 54%, respectively, when compared to the control group (Figure 7c and d). In exercised DIO rats, leptin reduced the phosphorylation of AMPK by 65% and ACC by 37%, compared to DIO rats at rest and the i.c.v. pretreatment with anti-IL6 antibody before the exercise protocol, reversed the suppressive effects of leptin on AMPK/ACC pathway in the hypothalamus of exercised DIO rats (Figures 7c and d). The AMPK and ACC protein levels did not differ between the groups (Figures 7c and d, lower panels).

In addition, p70S6K and 4EBP1 phosphorylation in the hypothalamus of DIO rats after i.c.v. leptin infusion was reduced by about 46% and 45%, respectively, when compared to the control group. In exercised DIO animals, leptin increased the phosphorylation of p70S6K by 62% and 4EBP1 by 59%, compared to DIO rats at rest. I.c.v. pretreatment with anti-IL6 antibody before the exercise protocol blocked these effects in the hypothalamus of exercised DIO rats (Figures 7e and f). The p70S6K and 4EBP1 protein levels were not different between the groups (Figures 7e and f, lower panels).

Blocking effects of AICAR and Rapamycin on leptin-induced anorexia

We tested whether the i.c.v. administration of AICAR or Rapamycin, 60 minutes before the administration of leptin (10^{-6} M), prevents the anorexigenic effects of leptin. Leptin (10^{-6} M) treatment markedly reduced 12-h food intake in both control and exercised groups, although leptin was much more effective in exercised rats. AICAR (0.5 mM) or Rapamycin (25 μg), at doses that do not alter ingestion, completely blocked the suppression of food intake induced by an i.c.v. injection of leptin (10^{-6} M) (Figure 8a). The i.c.v. administration of leptin (10^{-6} M) to exercised rats pretreated with vehicle reduced AMPK and ACC phosphorylation in the hypothalamus by 63% and 60% respectively, compared with the control group. The administration of AICAR increased AMPK threonine and ACC serine phosphorylation, although at this dose, AICAR was not sufficient to induce significant an increase in food intake in exercised animals (data not shown). Comparing exercised animals, i.c.v. administration of leptin (10^{-6} M) to rats pretreated with AICAR increased both AMPK and ACC phosphorylation levels in the hypothalamus (Figures 8b and c).

The i.c.v. administration of leptin (10^{-6} M) to exercised rats pretreated with vehicle induced p70S6K and 4EBP1 phosphorylation in the hypothalamus of 60% and 70%, respectively, compared with the control group. Comparing exercised animals, i.c.v. administration of leptin (10^{-6} M) to rats pretreated with AICAR reduced both p70S6K and 4EBP1 phosphorylation levels in the hypothalamus. Exercised animals pretreated with Rapamycin also reduced hypothalamic p70S6K and 4EBP1 phosphorylation (Figures 8d and e). The αAMPK, ACC, p70S6K and 4EBP1 protein levels were not different between the groups (Figures 8b–e, lower panels).

Discussion

During the last decade, a substantial number of studies have investigated the role of physical activity in the control of energy intake in rodents [5,6,35] and in humans [36–38]. However, the molecular mechanisms by which exercise controls food intake are still unsolved. Several experimental studies have demonstrated that neither acute [5,36] nor chronic [6,39] exercise per se change food intake, on the other hand, accumulating evidence shows that both acute and chronic exercise potentiate the anorexigenic effects of leptin in the hypothalamus. Our data indicate that IL-6 signaling through AMPK and mTOR reduces food intake in a dose-dependent manner. Leptin, as well as α-LA infusion, reduced food intake in exercised rats to a greater extent than that observed in control animals. Conversely, AICAR, 2-DG and fasting increased food intake in exercised rats to a lower extent than that observed in control animals. Exercise was associated with the effects of leptin on the AMPK/mTOR pathway activity in the hypothalamus. In addition, we investigated the regulatory role of IL-6 in mediating the increase in leptin responsiveness in the hypothalamus. Treatment with leptin markedly reduced food intake, AMPK activity and increased mTOR activity in exercised rats that were pretreated with vehicle, although no increase in response to leptin-induced anorexia and modulation of AMPK/mTOR pathway were detected after i.c.v. pretreatment with anti-IL-6 antibody. Taken together, these results suggest that IL-6 is a major component of the effects of exercise on the control of food intake.

Increasing evidence shows that leptin and IL-6 activates AMPK in the peripheral tissues, such as skeletal muscle and adipose tissue, increasing fatty acid oxidation and glucose uptake in these tissues [40–42], however, leptin has an opposing effect in hypothalamic tissue, reducing neuronal AMPK activity [12,43]. As well as in response to leptin, in the present study, we demonstrated that IL-6 alone reduced AMPK phosphorylation in the hypothalamus of rats. We also show that, IL-6 increased ATP levels and decreased

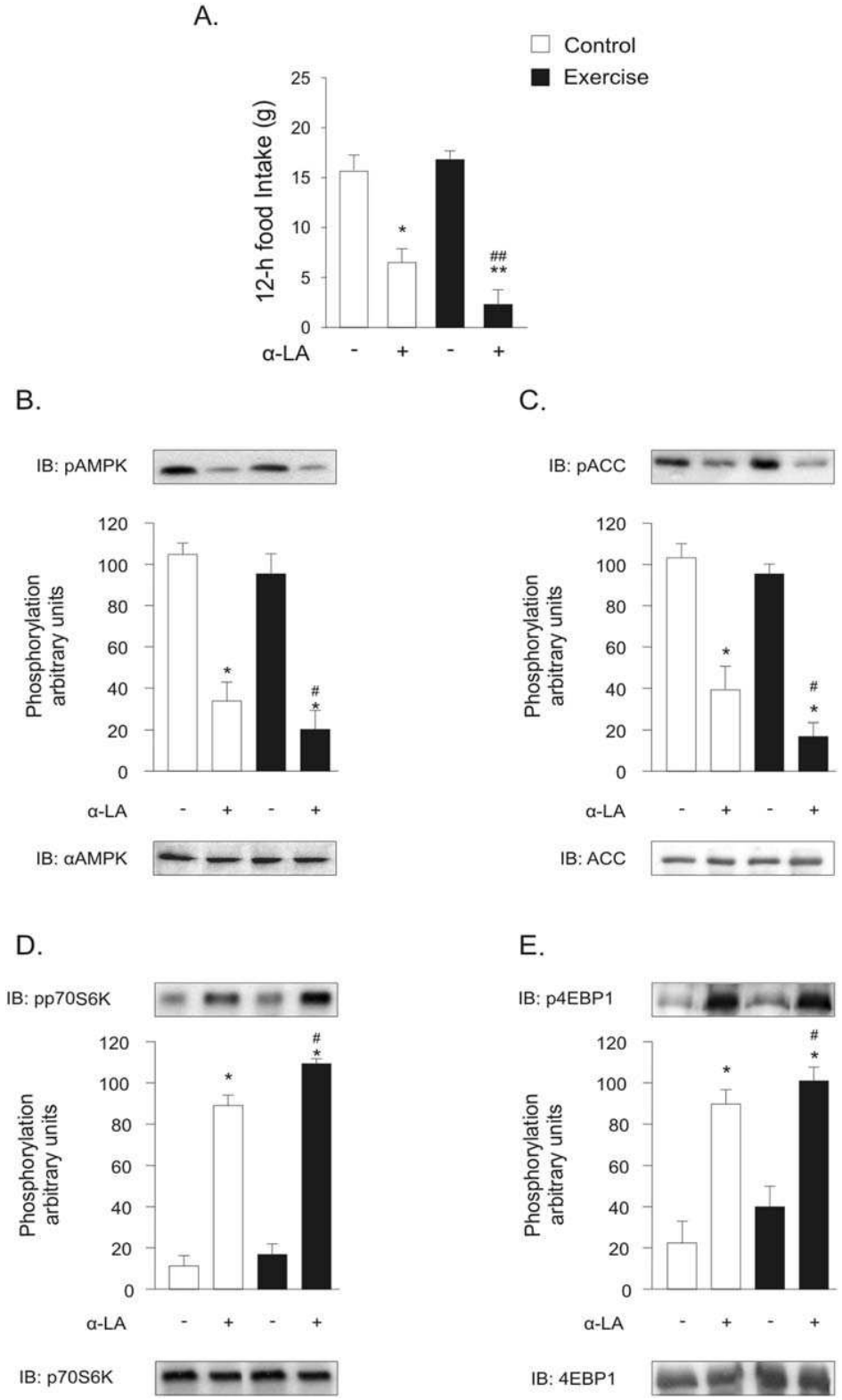

Figure 4. α-LA effects on 12-h cumulative food intake and AMPK/mTOR signaling, in the hypothalami of control and exercised rats. (a) α-LA (3 µg) was administered in control and exercised rats. Animals were immediately exposed to food for a 12-hour period ($n = 8–10$ animals per group). (b, c, d, e) Representative Western blots of four independent experiments showing hypothalamic lysates from Wistar rats. Phospho-AMPK^{thr172}, threonine-phosphorylated AMPK and total AMPK (b); phospho-ACC^{ser79}, serine phosphorylated ACC and total ACC (c); phospho-p70S6Kinase^{thr389}, threonine phosphorylated p70S6Kinase and total p70S6K (d); phospho-4EBP1^{thr70}, threonine phosphorylated 4EBP1 and total 4EBP1 (e). Data are the means±SEM. * $p<0.05$, *vs.* control group; # $p<0.05$, *vs.* exercised non-stimulated group.
doi:10.1371/journal.pone.0003856.g004

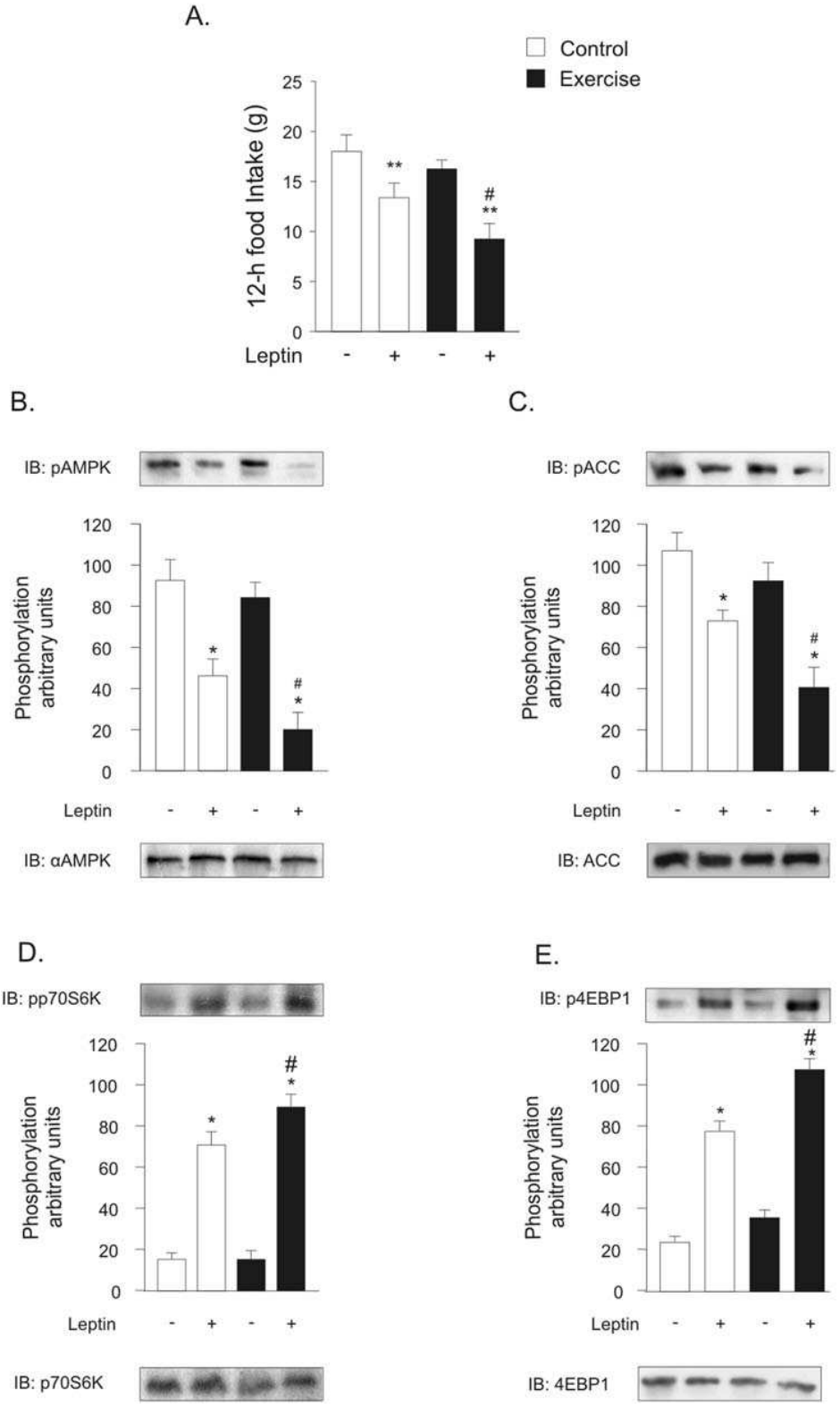

Figure 5. Leptin effects on 12-h cumulative food intake and AMPK/mTOR signaling, in the hypothalami of control and exercised rats. (a) Leptin (10^{-6} M) was administered in control and exercised rats. Animals were immediately exposed to food for a 12-hour period ($n = 12–15$ animals per group). (b, c, d, e) Representative Western blots of five independent experiments showing hypothalamic lysates from Wistar rats. Phospho-AMPK^{thr172}, threonine-phosphorylated AMPK and total AMPK (b); phospho-ACC^{ser79}, serine phosphorylated ACC and total ACC (c); phospho-p70S6Kinase^{thr389}, threonine phosphorylated p70S6Kinase and total p70S6K (d); phospho-4EBP1^{thr70}, threonine phosphorylated 4EBP1 and total 4EBP1 (e). Data are the means±SEM. * $p<0.05$, ** $p<0.01$, *vs.* control group; # $p<0.05$, ## $p<0.01$ *vs.* leptin-stimulated control group.
doi:10.1371/journal.pone.0003856.g005

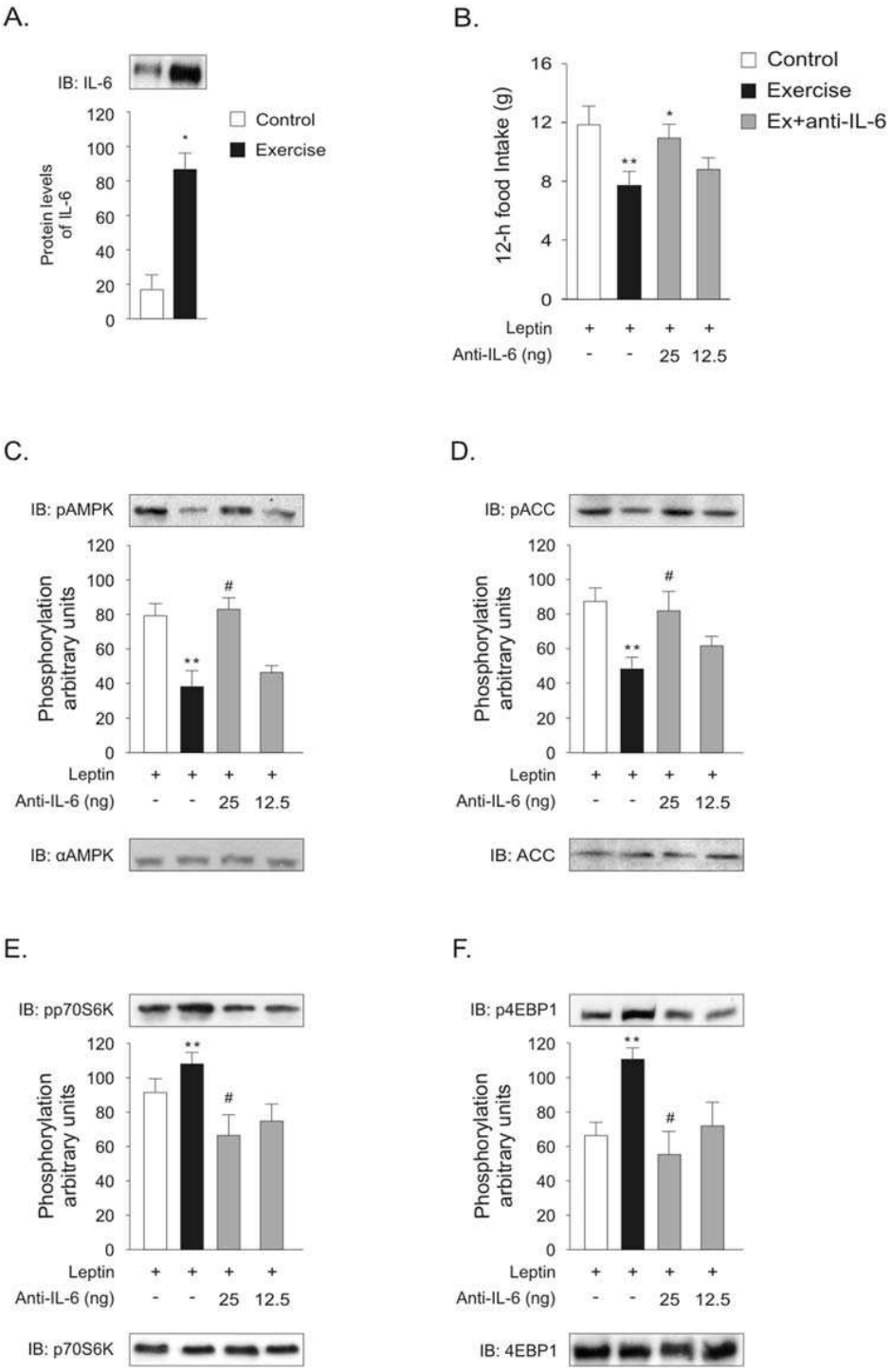

Figure 6. Blockade of leptin induced inhibition of food intake by anti–IL-6 antibody. Hypothalami from rats were prepared as described in *Research Design and Methods*. (a) Tissue extracts from control and exercised rats were immunoblotted with anti–IL-6 antibody. (b) Leptin was injected intracerebroventricularly in control rats, exercised rats and exercised rats pretreated with anti–IL-6 at the doses indicated, and the animals were immediately exposed to food for a 12-hour period ($n = 10$–12 animals per group). (c, d, e, f) Representative Western blots of four independent experiments showing hypothalamic lysates from Wistar rats. Phospho-AMPK^{thr172}, threonine-phosphorylated AMPK and total AMPK (c); phospho-ACC^{ser79}, serine phosphorylated ACC and total ACC (d); phospho-p70S6Kinase^{thr389}, threonine phosphorylated p70S6Kinase and total p70S6K (e); phospho-4EBP1^{thr70}, threonine phosphorylated 4EBP1 and total 4EBP1 (f). Data are the means±SEM. *$p<0.05$, vs. control, **$p<0.05$, vs. control plus leptin, #$p<0.05$, *vs.* exercise plus leptin.
doi:10.1371/journal.pone.0003856.g006

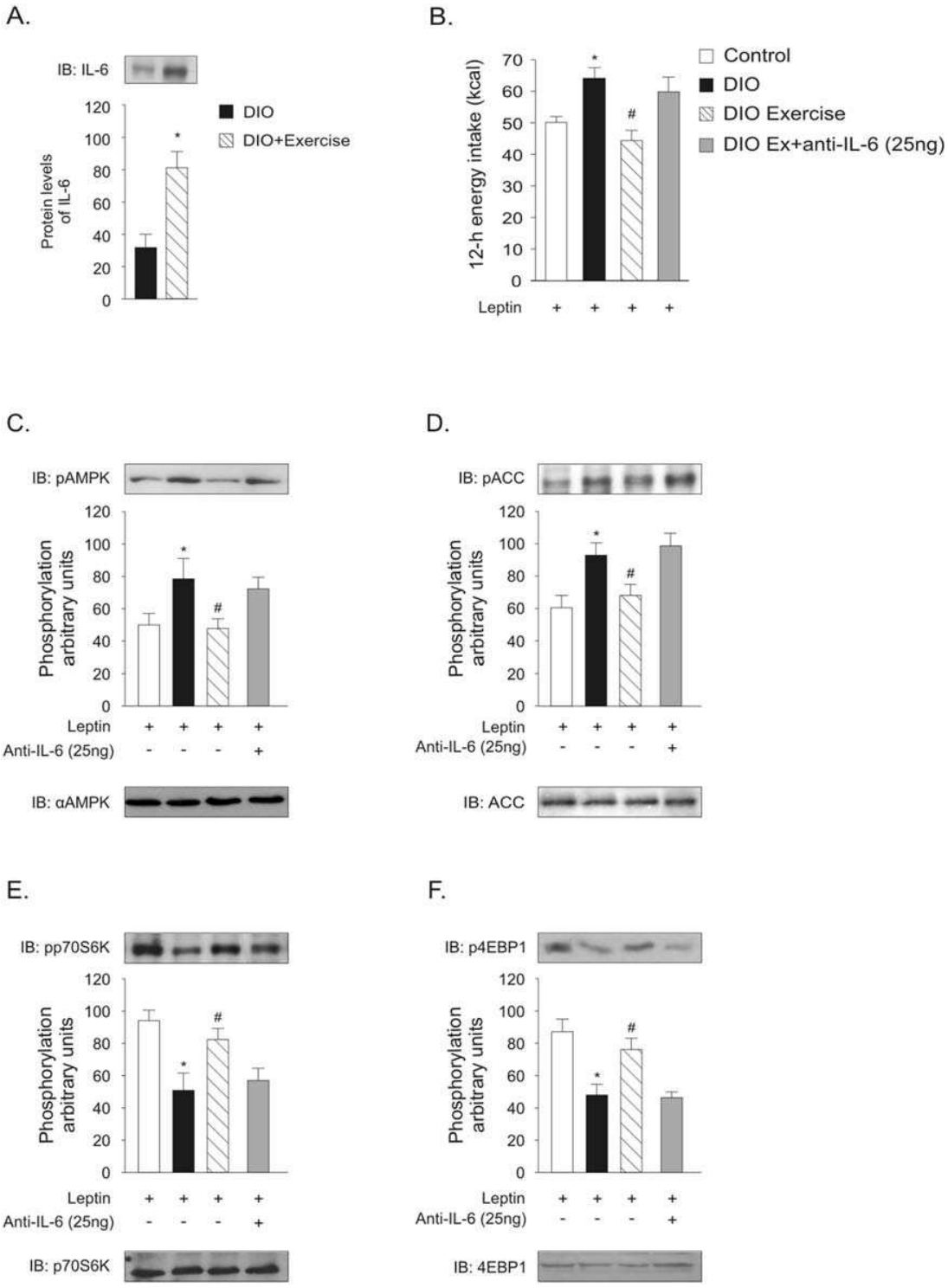

Figure 7. Leptin effects on 12-h cumulative food intake and AMPK/mTOR signaling in the hypothalami of control, DIO and exercised DIO rats. (a) Representative Western blots of five independent experiments showing hypothalamic IL-6 expression in DIO Wistar rats at rest and immediately after acute exercise. (b) Leptin (10^{-6} M) was administered in control, DIO and exercised DIO rats. Animals were immediately exposed to food for a 12-hour period ($n = 12–15$ animals per group). (c, d, e and f) Representative Western blots of five independent experiments showing hypothalamic lysates from Wistar rats. Phospho-AMPK^{thr172}, threonine-phosphorylated AMPK and total AMPK (c); phospho-ACC^{ser79}, serine phosphorylated ACC and total ACC (d); phospho-p70S6Kinase^{thr389}, threonine phosphorylated p70S6Kinase and total p70S6K (e); phospho-4EBP1^{thr70}, threonine phosphorylated 4EBP1 and total 4EBP1 (f). Data are the means±SEM. * $p<0.05$, *vs.* control group, # $p<0.05$, *vs.* DIO group.
doi:10.1371/journal.pone.0003856.g007

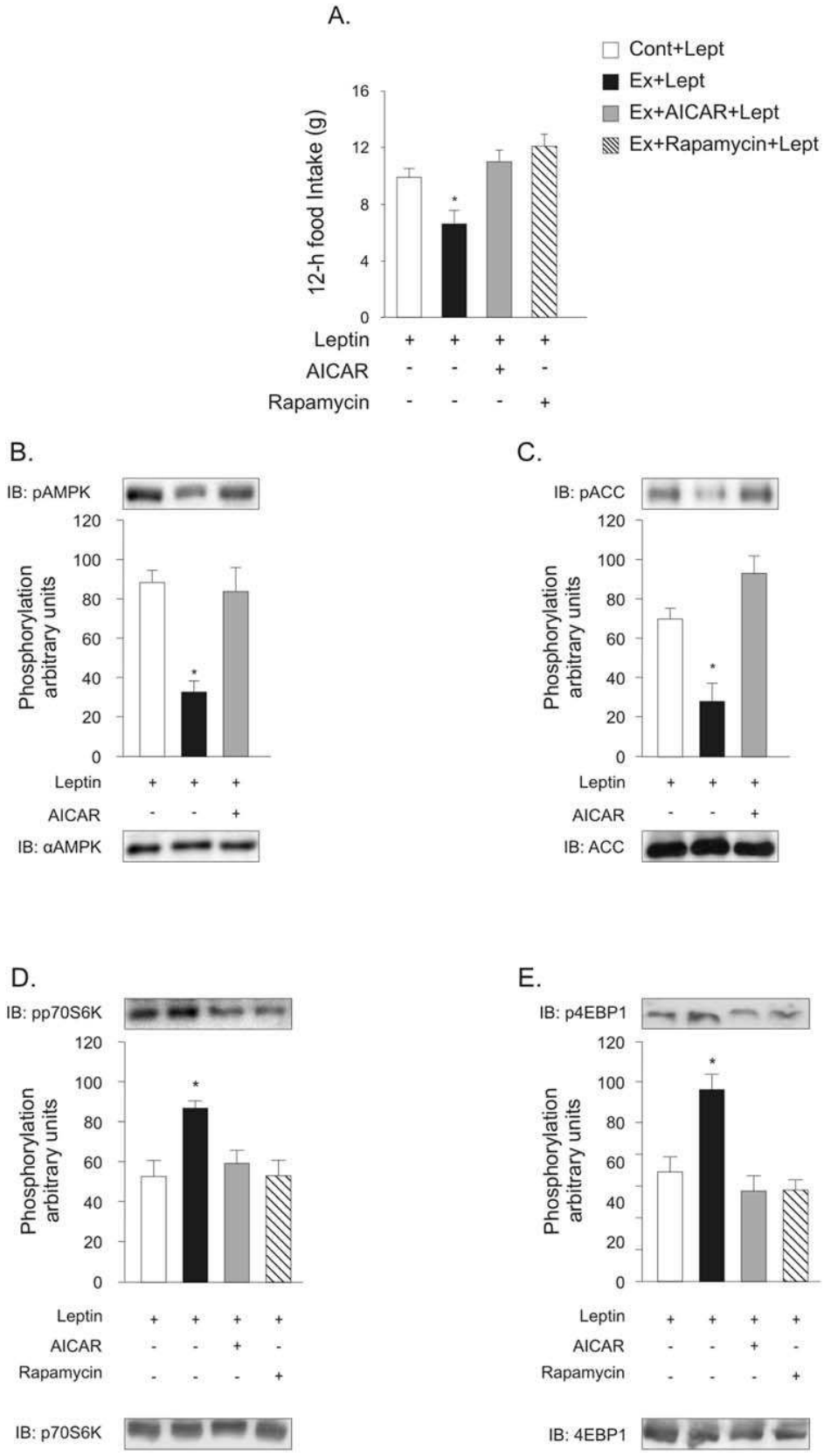
A.
Cont+Lept
Ex+Lept
Ex+AICAR+Lept
Ex+Rapamycin+Lept
12-h food Intake (g)
16
12
8
4
0
*
Leptin + + + +
AICAR - - + -
Rapamycin - - - +
B.
IB: pAMPK
Phosphorylation arbitrary units
120
100
80
60
40
20
0
*
Leptin + + +
AICAR - - +
IB: αAMPK
C.
IB: pACC
Phosphorylation arbitrary units
120
100
80
60
40
20
0
*
Leptin + + +
AICAR - - +
IB: ACC
D.
IB: pp70S6K
Phosphorylation arbitrary units
120
100
80
60
40
20
0
*
Leptin + + + +
AICAR - - + -
Rapamycin - - - +
IB: p70S6K
E.
IB: p4EBP1
Phosphorylation arbitrary units
120
100
80
60
40
20
0
*
Leptin + + + +
AICAR - - + -
Rapamycin - - - +
IB: 4EBP1

Figure 8. Blocking effects of AICAR and Rapamycin on leptin-induced anorexia. (a) Effect of i.c.v. administration of leptin on exercised rats; pretreatment with AICAR or Rapamycin ($n = 8$–10 animals per group). (b, c, d, e) Representative Western blots of five independent experiments showing hypothalamic lysates from Wistar rats. Phospho-AMPK^{thr172}, threonine-phosphorylated AMPK and total AMPK (b); phospho-ACC^{ser79}, serine phosphorylated ACC and total ACC (c); phospho-p70S6Kinase^{thr389}, threonine phosphorylated p70S6Kinase and total p70S6K (d); phospho-4EBP1^{thr70}, threonine phosphorylated 4EBP1 and total 4EBP1 (e). Data are the means±SEM. *$p<0.05$, *vs.* other groups.
doi:10.1371/journal.pone.0003856.g008

the AMP/ATP ratio in the hypothalamus (figures 1b–d), but the mechanisms by which IL-6 modulates the ATP levels require further investigations.

A number of recent studies have shown that AMPK plays a key role in regulating both energy intake and expenditure [12,34,44,45]. In peripheral tissues, such as skeletal muscle, activation of AMPK switches on energy producing pathways and switches off energy consuming pathways. In the hypothalamus, activation of AMPK leads to increased feeding, thereby increasing energy intake. Conversely, inhibition of AMPK in the hypothalamus reduces food intake. These dual functions of AMPK suggest that it may act to coordinate energy expenditure with energy intake. There is already some evidence that this may be the case in one situation. More recently, Gao and colleagues [10] demonstrated that the hypothalamic ACC activation makes an important contribution to the anorexigenic effects of leptin that are mediated by AMPK. The aim of this study was to investigate whether IL-6 could affect AMPK activity in the hypothalamus, thereby providing a potential mechanism for the coordination of energy expenditure and energy intake during, or following exercise. Beyond STAT3 activation, we detected changes in the hypothalamic AMPK activity in rats after i.c.v. infusion of IL-6; we show that, IL-6 markedly decreased phospho-AMPK abundance (an index of activity) in the hypothalamus. In accordance with the reduction in AMPK^{thr172} phosphorylation, we observed that, after IL-6 administration, hypothalamic AMP:ATP ratio was decreased.

Wallenius et al [28] elegantly showed that long-term peripheral IL-6 treatment to Il6$^{-/-}$ mice caused a decrease in body weight. In addition to increasing energy expenditure, IL-6 may prevent obesity by inhibiting feeding as obese IL-6$^{-/-}$ mice had increased absolute food intake. However, central IL-6 treatment at the same dose that we used does not influence food intake in mice. In concordance with our results another study of the same group showed a reduced daily food intake over a two-week ICV treatment period with IL-6 in rats indicating a different pattern of response between rats and mice [46].

The mTOR, an evolutionary conserved serine-threonine kinase, central to integrating similar signals to control food intake, has now emerged as a detector of hormonal and nutritional signals in the hypothalamus [13,15]. In this study, we investigated whether IL-6 activates mTOR. IL-6 increased mTOR activity; moreover inhibition of central mTOR reversed the anorectic effect of IL-6. In addition, the anorexigenic effect of IL-6 was absent in AICAR- and Rapamycin-pretreated rats, however, pretreatment with LY294002 - a PI(3)K inhibitor - had no effect on IL-6 induced anorexia, indicating that, in the hypothalamus, the effect of IL-6 is independent of the PI(3)K pathway. Signaling through gp130 commonly results in activation of PI(3)K, and IL-6 can activate PI(3)K [47] and its downstream target Akt [48–51], but it should be noted that this effect has not been observed in all studies [52], suggesting a tissue-dependent effect.

Next, we investigated whether the increased sensitivity of the leptin action on food intake induced by exercise, could be due to the modulation of AMPK activity. As previously shown [43], exercise, per se, does not alter AMPK activity in the hypothalamus; however, we observed that the normal inhibition of AMPK phosphorylation and activity in the hypothalamus, induced by leptin administration, was improved in both lean and diet-induced obesity rats after acute protocol of exercise.

In addition, we did not observe any normal stimulation of AMPK activity by AICAR in the hypothalamus of exercised rats, indicating that AMPK pathway is disrupted. This observation agrees with data from aging studies in which acute stimulation with AICAR was blunted in skeletal muscle of old rats [53]. Furthermore, fasting and the use of another activator of AMPK (2-DG) in exercising rats resulted in a lower activation of AMPK when compared to the control animals. In contrast, the pharmacological inhibition of AMPK by α-LA results in a greater inhibition of AMPK activity, compared to control animals.

The mechanism by which exercise inhibits AMPK-induced food intake in the hypothalamus is not clear. Several lines of evidence point to a possible link between inhibited AMPK-induced food intake in the hypothalamus and IL-6 signaling through the AMPK/mTOR pathway. Firstly, we found that the leptin-inhibited food intake enhanced by exercise was blunted by anti-IL-6 antibody. Secondly, exercise induced increased response of leptin-inhibited AMPK signaling was reverted by AICAR. Finally, exercise induced increased responsiveness of leptin stimulated mTOR signaling was reverted by rapamycin.

Our data are in accordance with earlier studies demonstrating that IL-6 treatment enhances energy expenditure in both rodents and humans [28,54–56]. In exercising rats, hypothalamic leptin and insulin responsiveness are increased in an IL-6-dependent manner [5,6]. It has been previously shown that IL-6 treatment stimulates energy expenditure at the level of the brain in rodents [28,55,57], and it might be assumed that endogenous IL-6 also acts on the brain during exercise. The IL-6 exerting this effect during exercise could be produced by the brain itself, which has been shown to have increased IL-6 production during exercise [58]. Alternatively, the large quantities of endocrine IL-6 produced from working skeletal muscle [58] might reach appropriate sites in the brain [21,59,60].

Interestingly, we did not observe any difference in food intake over a 12-h period, although the levels of hypothalamic IL-6 dramatically increased after exercise. At first glance, these data appear to be contradictory. However, a large decrease in insulin level was observed after exercise, and we have previously shown a synergic effect of IL-6 on the insulin and leptin signaling pathway, in the rat hypothalamus [5]. Since we did not observe modifications in the phosphorylation of JAK2 and the downstream targets of mTOR after exercise, these data suggest that the cross-talk between insulin, IL-6 and leptin have an essential role in controlling food intake after exercise. In this case, it is possible that increases in IL-6 levels were counterbalanced by the reduction in insulin levels.

However, the present study has certain limitations. Exercise per se did not evoke any meaningful effect in terms of food intake; rather, it seemed to enhance the anorectic effect of exogenous leptin. Thus, the data presented herein may suggest but do not establish the mechanism by which long term exercise decreases leptin levels; whilst increases the response to leptin, contributing to its food-suppressive actions. Furthermore, settings of activation of AMPK or inactivation of mTOR were selected to induce changes in target protein phosphorylation, but not food intake. Such dissociation does not preclude a pharmacological rather than physiological effect of our data.

Increased responsiveness of leptin action in the hypothalamus, through modulation of the AMPK-mediated pathway by exercise, could be pathophysiologically important in the prevention of obesity. Recent studies have shown that modulation of leptin signaling through the AMPK pathway could be involved in the development of obesity [61]. Taken together, these data indicate that the anti-obesity actions, induced by leptin, could be increased due to the more pronounced inhibition of the AMPK pathway observed after leptin infusion in the hypothalamus of both lean and diet-induced obesity rats after acute exercise. If the mechanism used by IL-6 to reduce food intake is AMPK-dependent, as our results suggest, the defective activation of AMPK in the hypothalamic neurons induced by exercise may increase the ability of leptin to reduce food intake.

In conclusion, exercise improved the AMPK and mTOR responses to leptin administration and contributed to appetite-suppressive actions. This increased dynamic responsiveness of the AMPK/mTOR pathway to leptin could provide information regarding the molecular mechanism underlying the biological sensitivity to leptin in exercise. Furthermore, these findings provide support to the hypothesis that AMPK and mTOR interact in the hypothalamus to control feeding in exercised rats, in an IL-6-dependent manner.

Methods

Antibodies and Chemicals

Reagents for SDS-polyacrylamide gel electrophoresis and immunoblotting were from Bio-Rad (Richmond, CA, USA). Tris[hydroxymethyl]amino-methane (Tris), aprotinin, ATP, dithiothreitol, phenylmethylsulfonyl fluoride, Triton X-100, Tween 20, glycerol, and bovine serum albumin (fraction V) were from Sigma Aldrich (St. Louis, MO, USA). Protein A-Sepharose 6 MB and Nitrocellulose paper (Hybond ECL, 0.45 μm) from Amersham Pharmacia Biotech United Kingdom Ltd. (Buckinghamshire, United Kingdom). Ketamin was from Parke-Davis (São Paulo, SP, Brazil) and diazepam and thiopethal were from Cristália (Itapira, SP, Brazil). Anti-phospho-[Ser^{79}] ACC (rabbit polyclonal, #07-184) and anti-phospho- [$Tyr^{1007/1008}$] JAK2 (rabbit polyclonal, AB3805) antibodies were from Upstate Biotechnology (Charlottesville, VA, USA). Anti-ACC (goat polyclonal, sc-26816), anti-JAK2 (rabbit polyclonal, sc 278), anti-STAT3 (rabbit polyclonal, sc 483) and anti-IL-6 (rabbit polyclonal, sc-7920) antibodies were from Santa Cruz Biotechnology, Inc. Anti-phospho-[Thr^{172}] AMPKα (rabbit polyclonal, #2531), anti-AMPKα (rabbit polyclonal, #2532), anti-phospho- [tyr705] STAT3 (rabbit polyclonal, #9135), anti-phospho- [Thr389] p70S6K (rabbit polyclonal, #9205), anti-p70S6K (rabbit polyclonal, #9202), anti-phospho- [Thr70]4EBP1 (rabbit polyclonal, #9455), anti-4EBP1 (rabbit polyclonal, #9452), anti-phospho-[Ser 473]Akt (rabbit polyclonal, #9271), and anti-Akt (rabbit polyclonal, #9272) were from Cell Signalling Technology (Beverly, MA, USA). Leptin, LY294002, and Interleukin-6 were from Calbiochem (San Diego, CA, USA); 5-Aminoimidazole-4-carboxamide 1-β-D-ribofuranoside (AICAR), 2-Deoxy-D-glucose and α-lipoic acid were from Sigma Chemical Co. (St. Louis, MO). Rapamycin was from LC Laboratories (Woburn, MA, USA). Routine reagents were purchased from Sigma Chemical Co. (St. Louis, MO) unless otherwise specified.

Serum insulin and leptin quantification

Plasma was separated by centrifugation (1100 *g*) for 15 minutes at 4°C and stored at −80°C until assayed. RIA was employed to measure serum insulin, according to a previous description [62]. Leptin concentrations were determined using a commercially available Enzyme Linked Immuno Sorbent Assay (ELISA) kit (Crystal Chem Inc, Chicago, IL).

Experimental Animals

Male Wistar rats (8 weeks old/250–300 g) obtained from the University of Campinas Animal Breeding Center were used in the experiments. The investigation was approved by the ethics committee and followed the University guidelines for the use of animals in experimental studies and conforms to the *Guide for the Care and Use of Laboratory Animals*, published by the US National Institutes of Health (NIH publication no. 85-23 revised 1996). The animals were maintained on 12h:12h artificial light–dark cycles and housed in individual cages.

Diet induced obesity (DIO)

Male 4-wk-old Wistar rats from the University of Campinas Breeding Center were randomly divided into two groups, control, fed standard rodent chow (3948 $kcal.Kg^{-1}$) and DIO, fed a fat-rich chow (5358 $kcal.Kg^{-1}$) *ad libitum* for 3 months and then submitted to the different experimental protocols. This diet composition has been previously used [63].

Intracerebroventricular (i.c.v.) cannulation

The animals were stereotaxically instrumented under intraperitoneal injection of a mix of ketamin (10 mg) and diazepam (0.07 mg) (0.2 ml/100 g body weight) with a chronic 26-gauge stainless steel indwelling guide cannula, aseptically placed into the third ventricle (0.5 mm posterior and 8.5 mm ventral to bregma), as previously described [64]. After a 1-wk recovery period, cannula placement was confirmed by a positive drinking response after administration of Angiotensin II (40 ng/2 μL); animals that did not drink 5 mL of water within 15 minutes after treatment were not included in the experiment.

Exercise Protocol

Rats were acclimated to swimming for 2 days (10 min per day). On the day of the experiment, animals swam in groups of four, in plastic barrels of 45 cm in diameter, filled to a depth of 50 cm. Water temperature was maintained at 34–35°C. They performed two 3-h exercise bouts, separated by one 45-min rest period, as previously described [65]. After the last exercise bout, some rats were injected into the cannula and food intake was determined over the next 4 and/or 12 h; the other rats were injected into the cannula and then anesthetized with intraperitoneal injection of sodium thiopethal (5 mg/100 g body weight) and hypothalamus was removed.

Treatments

For acute treatments, rats were deprived of food for 6 h with free access to water and i.p. injected (200 μl bolus injection) with either vehicle or 2-DG (500 mg/kg) or i.c.v. injected (3 μl bolus injection) with either vehicle, IL-6 (100 ng or 200 ng), AICAR (0.5 or 2.0 mM), Rapamycin (25 μg), α-LA (3 μg), leptin (10^{-6} M), LY294002 (50 μM) or anti-IL-6 antibody. Similar studies were carried out in rats that were initially pre-treated with i.c.v. microinjection of vehicle, AICAR, Rapamycin, anti-IL-6 antibody or LY294002, and after 60 min with i.c.v. microinjection of IL-6 or leptin. Thereafter, standard chow was given and food intake was determined by measuring the difference between the weight of chow given and the weight of chow at the end of 4 and/or 12-h periods. All acute treatments were performed at 5:00 and 6:00 p.m.

Western Blot Analysis

After exercise and i.c.v. treatments, rats were anaesthetized with intraperitoneal injection of a mix of ketamin (10 mg) and diazepam (0.07 mg) (0.2 ml/100 g body weight), and used as soon as anesthesia was assured by the loss of pedal and corneal reflexes. The rats were killed, and hypothalamus was quickly removed, minced coarsely and homogenized immediately in a freshly prepared ice-cold buffer (1% Triton X-100, 100 mmol/l Tris pH 7.4, 100 mmol/l sodium pyrophosphate, 100 mmol/l sodium fluoride, 10 mmol/l EDTA, 10 mmol/l sodium vanadate, 2 mmol/l phenyl methylsulphonyl fluoride and 0.1 mg aprotinin) suitable for preserving phosphorylation states of enzymes and Western blot was performed, as previously described [66]. Insoluble material was removed by centrifugation (50 000 g) for 25 minutes at 4°C. Total extracts of hypothalamus were prepared and 0.25 mg total proteins were separed by SDS-PAGE. After SDS-PAGE (15% resolving gels for phospho-4EBP1 and 4EBP1; 12% resolving gels for phospho-AMPK, AMPKα2; phospho-p70S6K, p70S6K, phospho-Akt, Akt, phospho-STAT3 and STAT3; 8% resolving gels for phosphor-JAK2 and JAK2; 6.5% resolving gels for ACC and phospho-ACC), proteins were transferred from gel to nitrocellulose membrane. Membranes were blocked in 5% nonfat dried milk in PBST (139 mM NaCl, 2.7 mM KH_2PO_4, 9.9 mM Na_2HPO_4, and 0.1% Tween 20) for 2 hours and then incubated overnight with specific antibodies. After incubation with the relative second antibody, immune complexes were detected using the ECL method. Results were visualized by autoradiography using preflashed Kodak XAR film (Eastman Kodak, Rochester, N.Y., USA) with Cronex Lightning Plus intensifying screens at −80°C for 12–48 h. (Mass., USA). Band intensities were quantified by optical densitometry of developed autoradiographs (Scion Image software - *Scion Corporation*, Frederick, Md., USA).

Confocal microscopy

Paraformaldehyde-fixed hypothalami were sectioned (5 µm). The sections were obtained from hypothalamus of six rats per group in the same localization (antero-posterior = −1.78 from bregma) and used in regular single- or double-immunofluorescence staining using DAPI, anti-IL6 receptor (IL6R), anti-AMPK, anti-phospho-p70S6K (1:200; Santa Cruz Biotechnology), antibodies, according to a previously described protocol [67]. Analysis and photodocumentation of results were performed using a LSM 510 laser confocal microscope (Zeiss, Jena, Germany). The anatomical correlations were made according to the landmarks given in a stereotaxic atlas [68].

Chromatography

After exercise, i.c.v. infusion of IL-6 or vehicle, rats were anaesthetized, and used as soon as anesthesia was assured by the loss of pedal and corneal reflexes. The animals were killed and, within 40 seconds, the cranium was opened, the brain was removed and the hypothalamus was quickly dissected and frozen in liquid N_2 for chromatographic analyses.

Chromatographic analyses were carried out on a Waters Alliance equipment series 2695 (Milford, MA, USA) equipped with a quaternary pump, an autosampler, a degasser, and a Waters 2475 fluorescence detector model. The fluorescence of derivatized compounds (ATP, ADP, AMP, and ADO) was monitored with excitation and emission wavelengths set at 280 and 420 nm, respectively. Chromatographic separations of the compounds were achieved at room temperature, using a reversed-phase Cosmosil 5C18-MS column (150×4.6 mm i.d.; 5 µm particle size) with a Cosmosil guard column (5C18-MS 10×4.6 mm) purchased from Phenomenex (Torrance, CA, USA). The mobile phase composition was 50 mmol/L KH_2PO_4, 25 mmol/L citric acid (pH 4.5), and methanol (90:10, v/v), which was prepared immediately before use and filtered through a 0.45 µm filter (Millipore, Milford, MA, USA). The column was equilibrated and eluted under isocratic conditions using a flow rate of 1.0 ml/min. The chromatographic run time for each analysis was 20 min. Aliquots of 25 µl were injected into the HPLC system. System control, data acquisition, and processing were performed with a PC-Pentium IV Processor personal computer from Dell, operated with Microsoft Windows XP version 2003 and Waters Empower 2002 chromatography software. A validation chromatographic run included a set of calibration samples assayed in duplicate and quality control samples at four levels in triplicate. The standard calibration curves for known amounts of ATP, ranging from 0.025 to 10.0 µmol/L, were linear ($R>0.999$) and could be described by the linear regression equation: $y = 0.4992*x - 0.0463$ ($n = 4$, $P<0.0001$, $r = 0.9997$), in which y is the ATP concentration in micromoles and x is the chromatogram peak area.

Statistical Analysis

All numeric results are expressed as the means±SEM of the indicated number of experiments. The results of blots are presented as direct comparisons of bands or spots in autoradiographs and quantified by optical densitometry (Scion Image). Statistical analysis was performed by employing the ANOVA test with *Bonferroni post test*. Significance was established at the $p<0.05$ level.

Acknowledgments

We thank Dr Nicola Conran for English language editing.

Author Contributions

Conceived and designed the experiments: ERR MFAF MBF MJS JBC. Performed the experiments: ERR MFAF MBF MU SR RM DEC. Analyzed the data: ERR MFAF LAV MJS JBC. Contributed reagents/materials/analysis tools: SR RM DEC LAV KGF MJS. Wrote the paper: ERR MFAF JBC.

References

1. Richard D, Lachance P, Deshaies Y (1989) Effects of exercise-rest cycles on energy balance in rats. Am J Physiol 256: R886–891.
2. Richard D, Rivest S (1989) The role of exercise in thermogenesis and energy balance. Can J Physiol Pharmacol 67: 402–409.
3. Rivest S, Richard D (1990) Involvement of corticotropin-releasing factor in the anorexia induced by exercise. Brain Res Bull 25: 169–172.
4. Wing RR, Hill JO (2001) Successful weight loss maintenance. Annu Rev Nutr 21: 323–341.
5. Flores MB, Fernandes MF, Ropelle ER, Faria MC, Ueno M, et al. (2006) Exercise improves insulin and leptin sensitivity in hypothalamus of Wistar rats. Diabetes 55: 2554–2561.
6. Shapiro A, Matheny M, Zhang Y, Tumer N, Cheng KY, et al. (2008) Synergy between leptin therapy and a seemingly negligible amount of voluntary wheel running prevents progression of dietary obesity in leptin-resistant rats. Diabetes 57: 614–622.
7. Heymsfield SB, Greenberg AS, Fujioka K, Dixon RM, Kushner R, et al. (1999) Recombinant leptin for weight loss in obese and lean adults: a randomized, controlled, dose-escalation trial. Jama 282: 1568–1575.
8. Van Heek M, Compton DS, France CF, Tedesco RP, Fawzi AB, et al. (1997) Diet-induced obese mice develop peripheral, but not central, resistance to leptin. J Clin Invest 99: 385–390.
9. Schwartz MW, Woods SC, Porte D Jr, Seeley RJ, Baskin DG (2000) Central nervous system control of food intake. Nature 404: 661–671.
10. Gao S, Kinzig KP, Aja S, Scott KA, Keung W, et al. (2007) Leptin activates hypothalamic acetyl-CoA carboxylase to inhibit food intake. Proc Natl Acad Sci U S A 104: 17358–17363.

11. Kahn BB, Alquier T, Carling D, Hardie DG (2005) AMP-activated protein kinase: ancient energy gauge provides clues to modern understanding of metabolism. Cell Metab 1: 15–25.
12. Minokoshi Y, Alquier T, Furukawa N, Kim YB, Lee A, et al. (2004) AMP-kinase regulates food intake by responding to hormonal and nutrient signals in the hypothalamus. Nature 428: 569–574.
13. Cota D, Proulx K, Smith KA, Kozma SC, Thomas G, et al. (2006) Hypothalamic mTOR signaling regulates food intake. Science 312: 927–930.
14. Brunn GJ, Hudson CC, Sekulic A, Williams JM, Hosoi H, et al. (1997) Phosphorylation of the translational repressor PHAS-I by the mammalian target of rapamycin. Science 277: 99–101.
15. Ropelle ER, Pauli JR, Fernandes MF, Rocco SA, Marin RM, et al. (2008) A central role for neuronal AMP-activated protein kinase (AMPK) and mammalian target of rapamycin (mTOR) in high-protein diet-induced weight loss. Diabetes 57: 594–605.
16. Shamji AF, Nghiem P, Schreiber SL (2003) Integration of growth factor and nutrient signaling: implications for cancer biology. Mol Cell 12: 271–280.
17. Dennis PB, Jaeschke A, Saitoh M, Fowler B, Kozma SC, et al. (2001) Mammalian TOR: a homeostatic ATP sensor. Science 294: 1102–1105.
18. Inoki K, Li Y, Zhu T, Wu J, Guan KL (2002) TSC2 is phosphorylated and inhibited by Akt and suppresses mTOR signalling. Nat Cell Biol 4: 648–657.
19. Kimura N, Tokunaga C, Dalal S, Richardson C, Yoshino K, et al. (2003) A possible linkage between AMP-activated protein kinase (AMPK) and mammalian target of rapamycin (mTOR) signalling pathway. Genes Cells 8: 65–79.
20. Gleason CE, Lu D, Witters LA, Newgard CB, Birnbaum MJ (2007) The role of AMPK and mTOR in nutrient sensing in pancreatic beta-cells. J Biol Chem 282: 10341–10351.
21. Pedersen BK, Steensberg A, Fischer C, Keller C, Keller P, et al. (2003) Searching for the exercise factor: is IL-6 a candidate? J Muscle Res Cell Motil 24: 113–119.
22. Penkowa M, Keller C, Keller P, Jauffred S, Pedersen BK (2003) Immunohistochemical detection of interleukin-6 in human skeletal muscle fibers following exercise. Faseb J 17: 2166–2168.
23. Steensberg A, van Hall G, Osada T, Sacchetti M, Saltin B, et al. (2000) Production of interleukin-6 in contracting human skeletal muscles can account for the exercise-induced increase in plasma interleukin-6. J Physiol 529 Pt 1: 237–242.
24. Keller C, Keller P, Marshal S, Pedersen BK (2003) IL-6 gene expression in human adipose tissue in response to exercise–effect of carbohydrate ingestion. J Physiol 550: 927–931.
25. Lyngso D, Simonsen L, Bulow J (2002) Metabolic effects of interleukin-6 in human splanchnic and adipose tissue. J Physiol 543: 379–386.
26. Ruderman NB, Keller C, Richard AM, Saha AK, Luo Z, et al. (2006) Interleukin-6 Regulation of AMP-Activated Protein Kinase: Potential Role in the Systemic Response to Exercise and Prevention of the Metabolic Syndrome. Diabetes 55 Suppl 2: S48–54.
27. Kelly M, Keller C, Avilucea PR, Keller P, Luo Z, et al. (2004) AMPK activity is diminished in tissues of IL-6 knockout mice: the effect of exercise. Biochem Biophys Res Commun 320: 449–454.
28. Wallenius V, Wallenius K, Ahren B, Rudling M, Carlsten H, et al. (2002) Interleukin-6-deficient mice develop mature-onset obesity. Nat Med 8: 75–79.
29. Lutticken C, Wegenka UM, Yuan J, Buschmann J, Schindler C, et al. (1994) Association of transcription factor APRF and protein kinase Jak1 with the interleukin-6 signal transducer gp130. Science 263: 89–92.
30. Murakami M, Hibi M, Nakagawa N, Nakagawa T, Yasukawa K, et al. (1993) IL-6-induced homodimerization of gp130 and associated activation of a tyrosine kinase. Science 260: 1808–1810.
31. Narazaki M, Witthuhn BA, Yoshida K, Silvennoinen O, Yasukawa K, et al. (1994) Activation of JAK2 kinase mediated by the interleukin 6 signal transducer gp130. Proc Natl Acad Sci U S A 91: 2285–2289.
32. Sadowski HB, Shuai K, Darnell JE Jr, Gilman MZ (1993) A common nuclear signal transduction pathway activated by growth factor and cytokine receptors. Science 261: 1739–1744.
33. Chen RH, Chang MC, Su YH, Tsai YT, Kuo ML (1999) Interleukin-6 inhibits transforming growth factor-beta-induced apoptosis through the phosphatidylinositol 3-kinase/Akt and signal transducers and activators of transcription 3 pathways. J Biol Chem 274: 23013–23019.
34. Kim EK, Miller I, Aja S, Landree LE, Pinn M, et al. (2004) C75, a fatty acid synthase inhibitor, reduces food intake via hypothalamic AMP-activated protein kinase. J Biol Chem 279: 19970–19976.
35. Bi S, Scott KA, Hyun J, Ladenheim EE, Moran TH (2005) Running wheel activity prevents hyperphagia and obesity in Otsuka long-evans Tokushima Fatty rats: role of hypothalamic signaling. Endocrinology 146: 1676–1685.
36. Bruce CR, Lee JS, Kiens B, Hawley JA (2004) Postexercise muscle triacylglycerol and glycogen metabolism in obese insulin-resistant zucker rats. Obes Res 12: 1158–1165.
37. Martins C, Robertson MD, Morgan LM (2008) Effects of exercise and restrained eating behaviour on appetite control. Proc Nutr Soc 67: 28–41.
38. Martins C, Truby H, Morgan LM (2007) Short-term appetite control in response to a 6-week exercise programme in sedentary volunteers. Br J Nutr 98: 834–842.
39. Santti E, Huupponen R, Rouru J, Hanninen V, Pesonen U, et al. (1994) Potentiation of the anti-obesity effect of the selective beta 3-adrenoceptor agonist BRL 35135 in obese Zucker rats by exercise. Br J Pharmacol 113: 1231–1236.
40. Daval M, Foufelle F, Ferre P (2006) Functions of AMP-activated protein kinase in adipose tissue. J Physiol 574: 55–62.
41. Long YC, Zierath JR (2006) AMP-activated protein kinase signaling in metabolic regulation. J Clin Invest 116: 1776–1783.
42. Minokoshi Y, Kim YB, Peroni OD, Fryer LG, Muller C, et al. (2002) Leptin stimulates fatty-acid oxidation by activating AMP-activated protein kinase. Nature 415: 339–343.
43. Andersson U, Treebak JT, Nielsen JN, Smith KL, Abbott CR, et al. (2005) Exercise in rats does not alter hypothalamic AMP-activated protein kinase activity. Biochem Biophys Res Commun 329: 719–725.
44. Carling D (2004) The AMP-activated protein kinase cascade–a unifying system for energy control. Trends Biochem Sci 29: 18–24.
45. Hardie DG, Scott JW, Pan DA, Hudson ER (2003) Management of cellular energy by the AMP-activated protein kinase system. FEBS Lett 546: 113–120.
46. Wallenius K, Wallenius V, Sunter D, Dickson SL, Jansson JO (2002) Intracerebroventricular interleukin-6 treatment decreases body fat in rats. Biochem Biophys Res Commun 293: 560–565.
47. Boulton TG, Stahl N, Yancopoulos GD (1994) Ciliary neurotrophic factor/leukemia inhibitory factor/interleukin 6/oncostatin M family of cytokines induces tyrosine phosphorylation of a common set of proteins overlapping those induced by other cytokines and growth factors. J Biol Chem 269: 11648–11655.
48. Al-Khalili L, Bouzakri K, Glund S, Lonnqvist F, Koistinen HA, et al. (2006) Signaling specificity of interleukin-6 action on glucose and lipid metabolism in skeletal muscle. Mol Endocrinol 20: 3364–3375.
49. Weigert C, Brodbeck K, Staiger H, Kausch C, Machicao F, et al. (2004) Palmitate, but not unsaturated fatty acids, induces the expression of interleukin-6 in human myotubes through proteasome-dependent activation of nuclear factor-kappaB. J Biol Chem 279: 23942–23952.
50. Weigert C, Hennige AM, Brodbeck K, Haring HU, Schleicher ED (2005) Interleukin-6 acts as insulin sensitizer on glycogen synthesis in human skeletal muscle cells by phosphorylation of Ser473 of Akt. Am J Physiol Endocrinol Metab 289: E251–257.
51. Weigert C, Hennige AM, Lehmann R, Brodbeck K, Baumgartner F, et al. (2006) Direct cross-talk of interleukin-6 and insulin signal transduction via insulin receptor substrate-1 in skeletal muscle cells. J Biol Chem 281: 7060–7067.
52. Carey AL, Steinberg GR, Macaulay SL, Thomas WG, Holmes AG, et al. (2006) Interleukin-6 increases insulin-stimulated glucose disposal in humans and glucose uptake and fatty acid oxidation in vitro via AMP-activated protein kinase. Diabetes 55: 2688–2697.
53. Reznick RM, Zong H, Li J, Morino K, Moore IK, et al. (2007) Aging-associated reductions in AMP-activated protein kinase activity and mitochondrial biogenesis. Cell Metab 5: 151–156.
54. Stouthard JM, Romijn JA, Van der Poll T, Endert E, Klein S, et al. (1995) Endocrinologic and metabolic effects of interleukin-6 in humans. Am J Physiol 268: E813–819.
55. Rothwell NJ, Busbridge NJ, Lefeuvre RA, Hardwick AJ, Gauldie J, et al. (1991) Interleukin-6 is a centrally acting endogenous pyrogen in the rat. Can J Physiol Pharmacol 69: 1465–1469.
56. Tsigos C, Papanicolaou DA, Defensor R, Mitsiadis CS, Kyrou I, et al. (1997) Dose effects of recombinant human interleukin-6 on pituitary hormone secretion and energy expenditure. Neuroendocrinology 66: 54–62.
57. Li G, Klein RL, Matheny M, King MA, Meyer EM, et al. (2002) Induction of uncoupling protein 1 by central interleukin-6 gene delivery is dependent on sympathetic innervation of brown adipose tissue and underlies one mechanism of body weight reduction in rats. Neuroscience 115: 879–889.
58. Nybo L, Nielsen B, Pedersen BK, Moller K, Secher NH (2002) Interleukin-6 release from the human brain during prolonged exercise. J Physiol 542: 991–995.
59. Febbraio MA, Pedersen BK (2002) Muscle-derived interleukin-6: mechanisms for activation and possible biological roles. Faseb J 16: 1335–1347.
60. Pedersen BK, Hoffman-Goetz L (2000) Exercise and the immune system: regulation, integration, and adaptation. Physiol Rev 80: 1055–1081.
61. Martin TL, Alquier T, Asakura K, Furukawa N, Preitner F, et al. (2006) Diet-induced obesity alters AMP kinase activity in hypothalamus and skeletal muscle. J Biol Chem 281: 18933–18941.
62. Scott AM, Atwater I, Rojas E (1981) A method for the simultaneous measurement of insulin release and B cell membrane potential in single mouse islets of Langerhans. Diabetologia 21: 470–475.
63. Pauli JR, Ropelle ER, Cintra DE, Carvalho-Filho MA, Moraes JC, et al. (2008) Acute physical exercise reverses S-nitrosation of the insulin receptor, insulin receptor substrate 1 and protein kinase B/Akt in diet-induced obese Wistar rats. J Physiol 586: 659–671.
64. Carvalheira JB, Siloto RM, Ignacchitti I, Brenelli SL, Carvalho CR, et al. (2001) Insulin modulates leptin-induced STAT3 activation in rat hypothalamus. FEBS Lett 500: 119–124.
65. Ropelle ER, Pauli JR, Prada PO, de Souza CT, Picardi PK, et al. (2006) Reversal of diet-induced insulin resistance with a single bout of exercise in the rat: the role of PTP1B and IRS-1 serine phosphorylation. J Physiol 577: 997–1007.
66. Carvalheira JB, Ribeiro EB, Araujo EP, Guimaraes RB, Telles MM, et al. (2003) Selective impairment of insulin signalling in the hypothalamus of obese Zucker rats. Diabetologia 46: 1629–1640.

67. Araujo EP, Amaral ME, Souza CT, Bordin S, Ferreira F, et al. (2002) Blockade of IRS1 in isolated rat pancreatic islets improves glucose-induced insulin secretion. FEBS Lett 531: 437–442.

68. Mai JK, Assheuer J, Paxinos G (1997) Atlas of the human brain. San Diego; London: Academic. pp viii, 336.

APÊNDICE *IV*

IL-6 Anti-inflammatory Activity Links Exercise to Hypothalamic Insulin and Leptin Sensitivity through IKKβ and ER Stress Inhibition.

Eduardo R. Ropelle, Marcelo B. Flores, Dennys E. Cintra, Guilherme Z. Rocha, José R. Pauli, Joseane Morari, Cláudio T. de Souza, Juliana C. Moraes, Lício A. Velloso, Mario J. A. Saad, José B. C. Carvalheira.

Department of Internal Medicine, FCM, State University of Campinas (UNICAMP), Campinas, São Paulo, Brazil.

Please address correspondence to:

José B. C. Carvalheira, MD.
Department of internal medicine
FCM - State University of Campinas (UNICAMP)
13081-970 - Campinas, SP, Brazil.
Fax: + 55 19 3521-8950
E-mail: carvalheirajbc@uol.com.br

SUMMARY

Overnutrition is associated with hypothalamic insulin and leptin resistance, through IKKβ activation and endoplasmatic reticulum (ER) stress. Here, we show that physical exercise suppresses hyperphagia mediated by overnutrition, reducing hypothalamic IKKβ/NF-κB activation and ER stress, improving insulin and leptin action in an IL-6 dependent-manner. The disruption of hypothalamic-specific IL-6 action blocked the effects of exercise on the re-balance of food intake. This molecular mechanism, mediated by physical activity, involves the anti-inflammatory protein, IL-10, a core inhibitor of IKKβ/NF-κB signaling and ER stress. We report that exercise and recombinant IL-6 requires IL-10 expression to suppress hyperphagia related-obesity. Moreover, in contrast to control, C3H/HeJ mice sustained lower levels of hypothalamic IL-6 and IL-10 after exercise and failed to reverse the pharmacological activation o IKKβ and ER stress. Hence, IL-6 and IL-10 are important physiological contributors to the central action of insulin and leptin, mediated by exercise, linking it to hypothalamic ER stress and inflammation.

INTRODUCTION

Overnutrition and sedentary lifestyle are among the most important factors that lead to an unprecedented increase in the prevalence of obesity. In mammals, food intake and energy expenditure are tightly regulated by specific neurons localized in the hypothalamus. The hypothalamus can gather information on the body's nutritional status by integrating multiple signals, including potent hormonal signals such as insulin and leptin [1,2]. The impairment of hypothalamic insulin and leptin signaling pathways is sufficient to promote hyperphagia, obesity and type 2 diabetes (T2D) in different genetic rodent models with neuronal ablation of insulin and leptin signaling [1,3,4]. We and others have proposed that overnutrition induces the central insulin and leptin resistance through the aberrant hypothalamic activation of proinflammatory molecules, including TLR4 and IKKβ [5,6,7̃].

IKKβ is a key player in controlling both innate and adaptive immunity. Activation of IKKβ by phosphorylation at S177 and S181 induces phosphorylation, ubiquitination and subsequent proteosomal degradation of its substrate IκBα. The degradation of IκBα allows NF-κB proteins to translocate to the nucleus and bind their cognate DNA binding sites to regulate the transcription of a large number of genes, including, stress-response proteins and cytokines [8]. Growing evidence provides an intriguing link between metabolic inflammation and dysfunction of insulin and leptin signaling via activation of IKKβ and endoplasmatic reticulum (ER) stress [9,10,11]. Examination of ER stress markers in different tissues of dietary (high-fat diet-induced) and genetic (*ob/ob*) mouse models of obesity demonstrated increased levels of PERK phosphorylation, eIF2α phosphorylation, and JNK and IKKβ activity [7,10]. Furthermore, a recent study showed that the high-fat diet atypically activates

hypothalamic IKKβ/NF-κB, at least in part, through elevated endoplasmic reticulum stress in the hypothalamus and that these phenomena are associated with central insulin and leptin resistance, hyperphagia and body weight gain in mice [7]. Thus, strategies to reduce the aberrant activation of inflammatory signaling and/or ER stress in hypothalamic neurons are of great interest to improve the central insulin and leptin action and prevent or treat obesity and related diseases.

Physical activity is considered a cornerstone of the treatment for obesity. Exercise has long been reported to reduce body weight and visceral adiposity, increasing the energy expenditure and improving glycaemic control in overweight or T2D patients [12,13]. Since the discovery of interleukin (IL)-6 releases from contracting skeletal muscle, accumulating evidence indicates that exercise induces metabolic changes in other organs, such as the liver, the adipose tissue and hypothalamus, in an IL-6 dependent manner. IL-6 is most often classified as a pro-inflammatory cytokine, although consistent data also demonstrate that IL-6 has an anti-inflammatory effect, and may negatively regulate the inflammation of acute phase response by increasing Interleukin-10 (IL-10), IL-1 receptor antagonist (IL-1ra), and soluble TNF- receptors (sTNF-R) [14]. Moreover, IL-6 appears that to play a central role in the regulation of appetite, energy expenditure, and body composition [15,16]. However, the effects of physical activity in the metabolic regulatory pathways in the central nervous system (CNS) remain unexplored. Thus we hypothesized that exercise could exert its effects in the central nervous system by modulating the specific hypothalamic neurons responsible for the control of food consumption. In the present study, we investigated the effect of the anti-inflammatory response, mediated by IL-6, on hypothalamic IKKβ activation and ER stress, central insulin and leptin sensitivity and food intake in diet-induced rats after physical activity.

RESULTS

Exercise suppresses hyperphagia mediated by overnutrition

It has been demonstrated that physical activity may contribute to the energy balance by increasing energy expenditure. Although the energy expenditure aspects of such exercise may contribute to the effects of weight loss, the effect of exercise on the control of energy intake remains unclear. To evaluate the impact of physical activity on food consumption, we measured the 12-hour total energy intake in lean and diet-induced obese (DIO) rats after acute exercise. Exercise did not change the energy intake in lean animals; however exercise suppressed the hyperphagic response, mediated by chronic overnutrition, restoring the energy intake to the levels of lean animals (Figure 1A). To assess whether the effects of exercise on food intake are dependent on the neuropeptides modulation, we performed a real time-PCR assay to determine the mRNA levels of Neuropeptide-Y (NPY) and Proopiomelanocortin (POMC). After 9 hours of fasting, we found that chronic overnutrition increased NPY mRNA and reduced POMC mRNA levels, whilst physical activity restored the NPY (Figure 1B) and POMC mRNA levels (Figure 1C) in obese animals; on the other hand, exercise did not change the NPY and POMC mRNA levels in lean rats (Figure 1B and C).

Chronic overnutrition increased body weight, epididymal fat and serum insulin and leptin, compared to age-matched controls (Figures 1D-G). No significant variations were found in body weight, epididymal fat and serum leptin between exercised and respective control animals under resting conditions (Figures 1 D, E and G). The insulin levels were lower in both lean and obese rats after exercise (Figure 1 F). These results reinforce the negative relationship between body weight change and the appetite-suppressive actions mediated by exercise.

To extend our hypothesis, we investigated food intake in leptin-deficient mice (*ob/ob*) after physical activity. Acute exercise there was no change in food intake in wild type mice (WT), however the energy intake was restored in *ob/ob* mice to the wild type levels (Figure 1 H). Exercise did not change the total body weight and epididymal fat pad weight in wild type and *ob/ob* mice (Figures 1 I and J) and reduced the insulin levels in wild type and *ob/ob* mice (Figure 1 K). Thus, our data demonstrate that exercise modulates hypothalamic neuropeptides (NPY and POMC) and suppresses food intake in obese, but not in lean, rodents without changing the adipose tissue content.

Exercise restores insulin and leptin sensitivity in the hypothalamus.

To assess whether exercise modulates insulin signaling, we evaluate the distal of protein of insulin signaling, FOXO1, in the hypothalamus. Western blot analysis revealed that FOXO1 phosphorylation was similar between the groups (Figure 2A). Although exercise did not change the FOXO1 phosphorylation, we next performed intrahypothalamic insulin (200 mU) or its vehicle injection to evaluated food intake and insulin sensitivity after the exercise protocol. Overnutrition markedly reduced the ability of intrahypothalamic insulin infusion to reduce food intake, when compared to chow-fed animals; however, exercise restored the central effects of insulin on reduced food intake (Figure 2B). Using Western blotting analysis, we determined the effects of exercise on the insulin sensitivity in hypothalamic tissue. The high-fat diet impaired insulin-induced tyrosine phosphorylation of insulin receptor β (IRβ), insulin receptor substrate-1 (IRS-1) and IRS-2 in the hypothalamus. Similar results were observed for the serine phosphorylation of Akt and FOXO1 (Figure 2C). Physical activity was able to restore insulin-induced hypothalamic IRβ, IRS-1 and IRS-2 tyrosine phosphorylation and insulin-induced hypothalamic Akt and FOXO1 serine phosphorylation in DIO rats

(Figure 2C). There was no difference in basal levels of IR, IRS-1, IRS-2 and Akt phosphorylation between the groups (data not shown). Subcellular fraction of hypothalamic extract was then performed to evaluate the nuclear FOXO1 expression. Intrahypothalamic infusion of insulin reduced the nuclear FOXO1 expression in control rats, but insulin failed to reduce the nuclear FOXO1 expression in rats after overnutrition (Figure 2D). After exercise, insulin reduced the nuclear FOXO1 expression in neuronal cells of obese animals (52%), when compared to DIO at rest (Figure 2D). No difference between the basal levels of FOXO1 nuclear expression was observed (data not shown).

We then explored the effects of exercise on hypothalamic leptin action, monitoring STAT-3 tyrosine phosphorylation. Exercise did not change the STAT-3 phosphorylation in lean animals; however overnutrition reduced STAT-3 phosphorylation when compared to lean animals. Interestingly, physical activity was able to increase the neuronal STAT-3 tyrosine phosphorylation in obese animals (Figure 2E). In addition we investigated the effects of exercise on leptin sensititvity. Intrahypothalamic infusion of leptin markedly reduced the 12-hour total energy intake in control rats; however, the anorexigenic effects of leptin were attenuated in obese rats. In contrast, exercise restored the central effects of leptin on reduced food intake (Figure 2F). We noted that leptin modestly promoted the hypothalamic tyrosine phosphorylation of Janus Kinase-2 (JAK2), IRS-1, IRS-2 and STAT-3 after high-fat diet treatment. Conversely, exercise restored leptin-induced hypothalamic JAK2, IRS-1, IRS-2 and STAT-3 tyrosine phosphorylation in obese animals (Figures 2G). There were no differences in the basal levels of JAK2 and STAT-3 phosphorylation between the groups (data not shown).

We also evaluated nuclear STAT3 expression after intrahypothalamic leptin infusion. After overnutrition, leptin failed to increase the expression of nuclear STAT3 in the hypothalamus. On the other hand, exercise increased the ability of leptin to increase the nuclear expression of STAT3 (48%) in the hypothalamus of obese animals (Figure 2H). No difference between the basal levels of STAT3 nuclear expression was observed (data not shown).

Increasing hypothalamic levels of IL-6 reverses IKKβ and ER stress caused by obesity

Recently, Interleukin-6 (IL-6) was reported as the first myokine that is produced and released by contracting skeletal muscle fibres, exerting its effects on other organs of the body [17], including the hypothalamus [15,18]. Thus, we evaluated the central role of IL-6 in the control of food intake. Firstly, the serum level of IL-6 was observed to be slightly up-regulated after high-fat diet treatment and was dramatically increased immediately after physical activity, as expected (Figure S1). Similar results were found when IL-6 protein expression in the hypothalamic tissue was evaluated (Figures 3A). To investigate whether neuronal cells were producing IL-6 in response to exercise, we performed real time PCR to evaluate IL-6 mRNA levels in the hypothalamic tissue. IL-6 mRNA levels were slightly up-regulated after high-fat diet treatment and were increased by about 40% immediately after physical activity (Figure 3B). Exercise also increased the protein levels and mRNA of IL-6 in the hypothalamus of control animals (data not show). Thus, these data demonstrate that exercise increases the serum and hypothalamic levels of IL-6.

Next, we sought to determine whether exercise requires IL-6 to mediate the anti-hyperphagic response. First we showed that the infusion of recombinant IL-6 into the

third ventricle of obese animals under resting conditions, reduced the food intake in a dose-dependent manner (Figure 3C) and restored the anorexigenic effects of insulin and leptin (Figure S2A and B). We hypothesized that if exercise requires hypothalamic IL-6 activity to reduce food intake, inhibiting the hypothalamic effects of IL-6 should diminish the appetite suppressive action mediated by exercise. To address this hypothesis, we developed an experimental strategy aimed at antagonizing the central action of IL-6 in the presence of a systemic elevation in plasma IL-6 concentration after physical activity. For this, we injected an anti-IL-6 antibody into the third-hypothalamic ventricle in obese animals at fifteen minutes before the exercise protocol. Interestingly, pretreatment with anti-IL-6 antibody blocked the anorexigenic effects of insulin and leptin in exercised DIO rats (Figures 3D and E).

We then explored the mechanism by which IL-6 improves insulin and leptin signaling in the hypothalamus. High-fat diet induced the aberrant activation of the NF-κB pathway components in the hypothalamic tissue, increasing IKKβ serine phosphorylation and the IκBα degradation (Figure 3F and G). In addition we monitored PERK and eIF2α phosphorylation in the hypothalamus to evaluate endoplasmatic reticulum (ER) stress, as previously described [7,10]. High-fat diet also activated ER stress, increasing PERK and eIF2α phosphorylation in the hypothalamus (Figures 3H and I). In addition, high-fat diet increased IRS-1 serine 307 phosphorylation (Figure 3J). Exercise and the intrahypothalamic injection of recombinant IL-6, in obese rats at rest, markedly reduced IKKβ serine phosphorylation (~60%) and prevented IκBα degradation in obese animals (Figures 3F and G). Both recombinant IL-6 and exercise dramatically reduced PERK and eIF2α phosphorylation by about 60% (Figures 3H and I) and IRS-1 serine phosphorylation by about 60% (Figures 3J) in the hypothalamic

tissue. In addition, recombinant IL-6 and exercise restored insulin-induced Akt and leptin-induced and STAT-3 phosphorylation in the hypothalamus of obese animals (Figures S3A and B). Interestingly, our results show that anti-IL-6 antibody attenuated the ability of exercise to reduce the IKKβ/IκBα pathway, ER stress and IRS1 serine phosphorylation in the hypothalamus (Figures 3F-J). The pretreatment with anti-IL6 antibody also blocked insulin-induced Akt and leptin-induced and STAT-3 phosphorylation, mediated by exercise in the hypothalamus of obese animals (Figures S3A and B). There were no differences in the basal levels of Akt and STAT3 phosphorylation between the groups (data not shown).

Immunohistochemistry with an anti-Interleukin-6 Receptor (IL-6R)-specific antibody showed that IL-6R is expressed in a majority of neurons in the arcuate nucleus (Figure 3K). Double-staining confocal microscopy showed that IL-6R is expressed in POMC neurons and that most neurons expressing IL-6R in arcuate nucleus were shown to possess IKKβ, PERK, IRS-1 in obese rats, showing a possible interaction between these molecules (Figure 3L).

Pharmacological activation of IKKβ and ER stress is suppressed by IL-6

To further support data indicating that may IL-6 modulate ER stress, we performed an acute intrahypothalamic injection of an ER stress inducer, thapsigargin (TG) in lean rats. Our results revealed that intrahypothalamic infusion of thapsigargin blocked the anorexigenic effects mediated by insulin and leptin in lean rats, but the injection of recombinant IL-6 and exercise restored the suppressive appetite action of insulin and leptin (Figures 4A and B). However, the infusion of anti-IL6 antibody blocked the improvement in insulin and leptin action mediated by exercise (Figures 4A and B).

Thapsigargin markedly activated the inflammatory signaling and ER stress in lean rats, as reflected by increased levels of hypothalamic IKKβ and PERK phosphorylation, respectively (Figures 4C and D), and induced central insulin and leptin resistance, increasing IRS-1 serine phosphorylation (Figure 4E) and reducing insulin-induced Akt serine phosphorylation and leptin-induced STAT-3 tyrosine phosphorylation (Figures 4F and G). There were no differences in the basal levels of Akt and STAT-3 phosphorylation between the groups (data not shown). Intrahypothalamic infusion of recombinant IL-6 and physical activity were sufficient to reverse all these phenomena (Figures 4C-G). Conversely, the infusion of intrahypothalamic anti-IL6 antibody before exercise protocol blocked these effects mediated by exercise (Figures 4C-G).

Low dose TNF-α has been reported to induce insulin and leptin resistance in the hypothalamus [19]. We injected a low dose of TNF-α into the hypothalamus of lean rats to investigate the effects of IL-6 on low-grade inflammation. TNF-α infusion blocked the anorexigenic actions of insulin and leptin in lean rats (Figure S4A and B). The anorexigenic actions of these hormones were restored with the central infusion of recombinant IL-6 or after exercise in lean rats injected with TNF-α. In addition, the pretreatment with anti-IL6 antibody into the third ventricle blocked the improvement in insulin and leptin action mediated by exercise (Figures S4A and B).

TNF-α also induced IKKβ serine, PERK threonine and IRS-1 serine phosphorylation and reduced insulin-induced Akt serine phosphorylation and leptin-induced STAT-3 tyrosine phosphorylation in the hypothalamus of lean rats (Figure S4C-G). Intrahypothalamic infusion of recombinant IL-6 and physical activity were also sufficient to reverse all these phenomena. On the other hand, the central infusion of anti-

IL6 antibody before the exercise protocol blocked the effects of physical activity (Figures S4C-G). Thus, the forced activation of ER stress or low-grade inflammation in the hypothalamus of lean animals each enhance the other, furthermore, physical exercise is able to reduce ER stress and inflammation and improve insulin and leptin actions in the hypothalamus, in an IL-6-dependent manner.

IL-6 requires IL-10 to reduce IKKβ and ER stress in the hypothalamus.

Next, we sought to determine how IL-6 reduces the inflammatory response and ER stress in the hypothalamus after exercise. Several studies have reported that exercise-induced increases in plasma IL-6 levels are followed by increased circulating levels of well-known anti-inflammatory cytokines such as the Interleukin-1 receptor antagonist (IL-1ra) and IL-10 [20,21]. We found that the IL-1ra protein level was not changed in the hypothalamus after chronic overnutrition or after acute exercise (Figure 5A); however, IL-10 protein expression was slightly increased in the hypothalamus in obese animals and was robustly increased (45%) in the hypothalamus of DIO rats after physical exercise, when compared to DIO rats at rest (Figure 5B). The increase in hypothalamic IL-10 levels mediated by physical activity was confirmed by real time-PCR assay (Figure 5C). Exercise also increased the protein levels and mRNA of IL-10 in the hypothalamus of control animals (data not shown).

We then investigated whether IL-10 reduced the energy intake in rodents. Intrahypothalamic injection of recombinant IL-10 reduced food intake in obese animals in a dose-dependent manner (Figure 5D). To explore whether IL-6 requires IL-10 expression to improve insulin and leptin action in the hypothalamus, we used an IL-10 antisense oligonucleotide (ASO IL-10) in the hypothalamus of obese rats. Three days after ASO IL-10 treatment, IL-10 protein expression was reduced by about 75% in the

hypothalamus of obese animals (Figure 5E). Thereafter, exercise and recombinant IL-6 infusion failed to improve the anorexigenic effects of insulin and leptin in obese animals treated with ASO IL-10 (Figures 5F and G).

IL-10 is a pleiotropic cytokine that controls inflammatory processes by suppressing the production of proinflammatory cytokines and blocking IKK/NF-κB signaling and ER stress [22,23]. Thus, we investigated whether exercise and IL-6 requires IL-10 expression to reduce IKKβ activation and ER stress in the hypothalamus of obese animals. As demonstrated above, recombinant IL-6 infusion and exercise reduced IKKβ, PERK and IRS-1^{Ser307} phosphorylation (Figures 3F-J) and restored insulin and leptin signaling in the hypothalamus of obese animals (Figures S3), but the intrahypothalamic IL-10 ASO treatment abolished all these parameters mediated by recombinant IL-6 and exercise (Figures 5H-L). Conversely, the injection of recombinant IL-10 in the hypothalamus of obese animals at rest markedly reduced IKKβ, PERK and IRS-1^{Ser307} phosphorylation and increased insulin-induced Akt and leptin-induced STAT-3 phosphorylation in the hypothalamic tissue (Figures 5H-L). There were no differences in the basal levels of Akt and STAT-3 phosphorylation between the groups (data not shown).

Attenuating TLR-4-dependent IL-6 and IL-10 production abolishes exercise sensitization of insulin and leptin in the hypothalamus

Several studies showed that Toll-like receptor inactivation results in an attenuation of the secretion of several cytokine. TLR4- and MyD88-deficient mice sustain significantly lower levels of serum cytokines such as IL-1β, IL-6, TNFα and IL-10 after different pro-inflammatory stimuli [24,25,26]. Since TLR4 mediates IL-6 transcriptional responses in skeletal myocytes and in the skeletal muscle of C3H/HeJ

mice [27], we investigated whether exercise restores insulin and leptin signaling in the hypothalamus of TLR4-deficient mice (C3H/HeJ) injected with Thapsigargin (TG). In contrast to wild type mice, TLR4-deficient mice were found to sustain significantly lower hypothalamic levels of IL-6 (Figure 6A) and IL-10 (Figures 6B) after exercise. The food consumption was similar between C3H/HeN and C3H/HeJ under basal conditions and, acutely, Thapsigargin alone did not affect the food intake in these mice (data not shown), furthermore, the intrahypothalamic administration of TG impaired the anorexigenic effects of insulin and leptin in wild type (C3H/HeN) and in TLR4-deficient mice; however, physical activity restored the appetite suppressive actions of insulin and leptin in wild type but not in TLR4-deficient mice (Figures 6C and D). Furthermore, the intrahypothalamic injection of either recombinant IL-6 or IL-10 restored the anorexigenic actions of insulin and leptin in both wild type and TLR4-deficient mice injected with TG (Figures 6C and D). We also observed that the intrahypothalamic infusion of recombinant IL-6 was able to increase the IL-10 protein expression in the hypothalamus of wild type and TLR4-deficient mice (Figure 6E). Moreover, exercise failed to reduce inflammation and ER stress and failed to improve insulin and leptin sensitivity in the hypothalamus of TLR4-deficient mice injected with TG (Figures 6F-J). On the other hand, the intrahypothalamic injection of recombinant IL-6 or IL-10 reduced IKKβ, PERK and IRS-1^{Ser307} phosphorylation and restored insulin and leptin signaling in the hypothalamus of TLR4-deficient mice injected with TG (Figures 6F-J). There were no differences in the basal levels of Akt and STAT-3 phosphorylation between the groups (data not shown). Finally, immunohistochemistry with anti-Interleukin-6 Receptor (IL-6R) and anti-Interleukin-10 Receptor (IL-10R) - specific antibodies revealed that IL-6R and IL-10R are expressed in the same specific neuronal subtypes in the arcuate nucleus (Figure 6K).

DISCUSSION

Exercise as a Potential Target for Countering Hyperphagia and Obesity

Physical activity is a cornerstone in the prevention of obesity and related diseases. Although the energy expenditure aspects of such exercise may contribute to the effects of weight loss, it has been suggested that physical exercise may also contribute to negative energy balance by altering appetite and reducing food intake in rodents [18,28] and humans [29,30]. Our study shows that acute exercise per se did not evoke any meaningful effect, in terms of food intake in lean animals, but interestingly, it was crucial for suppressing hyperphagia mediated by overnutrition, reducing hypothalamic IKKβ/NF-κB activation and ER stress, thus, improving insulin and leptin action in an IL-6-and IL-10-dependent manner (Figure 7).

The central effect of exercise was associated with improvements in the action of insulin and leptin in the hypothalamus of diet-induced obesity rats, in accordance with previous studies [18,28]. Furthermore, we reported that physical activity reduced the hyperphagic response by reducing NPY mRNA and increasing POMC mRNA in the hypothalamus of obese animals. It is important to emphasize that acute exercise did not change the total body weight or epididymal fat pad weight, showing that physical activity can induce the anorexigenic response in the hypothalamus, independently of the body weight change. Thus, we hypothesized that some factor, produced during the exercise session, could be involved in this anorexigenic response.

IL-6 is a Crucial Cytokine for Exercise to Restore Hypothalamic Insulin and Leptin Signaling

Skeletal muscle is an endocrine organ that, upon contraction, stimulates the production and release of cytokines, also called myokines, which can influence metabolism and modify cytokine production in tissue and organs. IL-6 is the first cytokine present in the circulation during exercise [14]. IL-6 can elicit proinflammatory or anti-inflammatory effects, depending on the *in vivo* environmental circumstances. Although, IL-6 has been associated with low-grade inflammation and insulin resistance, it has been demonstrated that acute IL-6 treatment enhances insulin-stimulated glucose disposal in humans [31].

Centrally-acting IL-6 appears to play a role in the regulation of appetite, energy expenditure, and body composition. Wallenius and colleagues elegantly showed that long-term peripheral IL-6 treatment to IL6−/− mice caused a decrease in body weight. In addition to increasing energy expenditure, IL-6 may prevent obesity by inhibiting feeding as obese IL-6−/− mice had increased absolute food intake [32]. Recently we demonstrated that exercise requires IL-6 to increase hypothalamic insulin and leptin sensitivity [15] and increase the effects of leptin on the AMPK/mTOR pathway in the hypothalamus of rodents [18]. As observed in animal models, IL-6 is also released from the brain during prolonged exercise in humans [33]. In the present study, we showed that the increment of IL-6 expression in the hypothalamus was crucial to exercise for reducing the inflammation and ER stress activation induced by overnutrition. Conversely, these effects, promoted by exercise, were not observed when we used an intrahypothalamic infusion of anti-IL-6 antibody before the exercise protocol. In addition, the infusion of recombinant IL-6 into the third hypothalamic ventricle reduced the energy intake in obese animals under resting conditions, in a dose-dependent manner, and reduced hypothalamic IKKβ and ER stress activation. These results are

significant, since IKKβ and ER stress activation were strongly associated with insulin and leptin resistance in the hypothalamic tissue.

Hypothalamic IL-10: A Core Anti-inflammatory Cytokine Induced by IL-6.

Although our findings clearly show that IL-6 diminished hypothalamic IKKβ and ER stress activation and restored the central insulin and leptin action in an animal model of obesity, the question remains as to how IL-6 promotes these events in the hypothalamus. Following exercise, the high circulating levels of IL-6 are followed by an increase in two anti-inflammatory molecules, IL-1ra and IL-10 [21]. Therefore, IL-6 induces an anti-inflammatory environment by inducing the production of IL-1ra and IL-10. In our study, we found that exercise increased the hypothalamic levels of IL-10, but did not change IL-1ra expression in this tissue. Thus, we showed that the anti-inflammatory response mediated by IL-6 involves the increase of IL-10 expression in the hypothalamus.

IL-10 is an important immunoregulatory cytokine with multiple biological effects. In the cytoplasm, it has been demonstrated that IL-10 blocks NF-κB activity at two levels; suppressing IKK activity and NF-κB DNA binding activity [22]. Moreover, IL-10 reduced ER stress in intestinal eptithelial cells, whereas IL-10-/- mice demonstrated that the expression of the ER stress response protein grp-78/BiP was increased in intestinal eptithelial cells under conditions of chronic inflammation [23].

In the central nervous system, the anti-inflammatory role of IL-10 (CNS) has been extensively studied in experimental autoimmune encephalomyelitis, an animal model of human multiple sclerosis. The increase in IL-10 expression in the CNS during

recovery from brain inflammation and the inability of IL-10 null mice to recover from acute CNS inflammation suggests that the presence of IL-10 within this target organ is required for disease remission [34,35]. However, the role of hypothalamic IL-10 in the control of low-grade inflammation generated during obesity was unknown. Here, we discovered that intrahypothalamic infusion of recombinant IL-10 blocked IKK/NF-κB signaling and ER stress and restored Akt and STAT3 phosphorylation, promoting a re-balance in the energy intake in obese animals. On the other hand, the selective decreases in IL-10 expression in discrete hypothalamic nuclei of obese animals mediated by ASO treatment blunted the effects of both, exercise and the intrahypothalamic infusion of recombinant IL-6 in the restoration of central insulin and leptin actions. In addition, we demonstrated that in mice that sustained significantly lower hypothalamic levels of IL-6 and IL-10 after exercise (C3H/HeJ), there was no reduction in pharmacological ER stress activation, in contrast to wild type mice. These data are intriguing as IL-10 represents an important cytokine that may reduce both inflammation and ER stress in the hypothalamus. Thus, the modulation of IL-10 expression constitutes a promising alternative to reduce hypothalamic inflammation and ER stress related to obesity.

Since IKKβ/NF-κB inhibition in the CNS represents a potential target therapy to combat obesity and most anti-inflammatory therapies have limited direct effects on IKKβ/NF-κB and a limited capacity for concentration in the CNS, our study provides substantial evidence that physical activity could help to reorganize the set point of nutritional balance and therefore aid in counteracting the energy imbalance induced by overnutrition through the anti-inflammatory response in hypothalamic neurons. Hence, IL-6 and IL-10 are important physiological contributors to the central insulin and leptin action mediated by physical activity, linking it to hypothalamic ER stress and inflammation.

EXPERIMENTAL PROCEDURES

Antibodies and Chemicals

Protein A-Sepharose 6 MB and Nitrocellulose paper (Hybond ECL, 0.45 μm) were from Amersham Pharmacia Biotech United Kingdom Ltd. (Buckinghamshire, United Kingdom). Ketamin was from Parke-Davis (São Paulo, SP, Brazil) and diazepam and thiopethal were from Cristália (Itapira, SP, Brazil). Anti-phospho- JAK2 (rabbit polyclonal, AB3805) antibody was from Upstate Biotechnology (Charlottesville, VA, USA). Anti-JAK2 (rabbit polyclonal, SC-278), anti-STAT3 (rabbit polyclonal, SC-483), anti-phospho-IRβ (rabbit polyclonal, SC-25103), anti-IRβ (rabbit polyclonal, SC-711), anti-phospho-IRS-1 (rabbit polyclonal, SC-17199), anti-IRS-1 (rabbit polyclonal, SC-559), anti-IRS-2 (rabbit polyclonal, SC-1556), anti-phosphotyrosine (mouse monoclonal, SC-508), anti-Foxo1 (rabbit polyclonal, SC-11350), anti-IL-1β (rabbit polyclonal, SC-7884), anti-IL-1ra (goat polyclonal, SC-8481), anti-TNF-α (rabbit polyclonal, SC-8301), anti- IKKβ (goat polyclonal, SC-34673), anti-PERK, anti-phospho-PERK (rabbit polyclonal, SC-32577), anti-IL-10 (goat polyclonal, SC-1783) and anti-IL-6 (rabbit polyclonal, SC-7920) antibodies were from Santa Cruz Biotechnology, Inc. Anti -phospho- STAT3 (rabbit polyclonal, #9131), anti-phospho-Akt (rabbit polyclonal, #9271), anti-phospho-Foxo1 (rabbit polyclonal, #9461), anti-beta tubulin (rabbit polyclonal, #2146), anti-phospho-IKKα/β (rabbit polyclonal, #2687), anti-phospho-IRS-1 307 (rabbit polyclonal, #2381) and anti-Akt (rabbit polyclonal, #9272) were from Cell Signalling Technology (Beverly, MA, USA). Leptin, Thapsigargin, recombinant Interleukin-6 and 10 were from Calbiochem (San Diego, CA, USA). Routine reagents were purchased from Sigma Chemical Co. (St. Louis, MO) unless otherwise specified.

Serum insulin, leptin and IL-6 quantification.

Blood was collected from the cava vein 15 minutes after the exercise protocols. Plasma was separated by centrifugation (1100 *g*) for 15 minutes at 4°C and stored at –80°C until assay. RIA was employed to measure serum insulin. Leptin and IL-6 concentrations were determined using a commercially available Enzyme Linked Immunosorbent Assay (ELISA) kit (Crystal Chem Inc, Chicago, IL).

Animals

Male 4-wk-old Wistar rats were obtained from the University of Campinas Breeding Center. The investigation was approved by the ethics committee and followed the University guidelines for the use of animals in experimental studies and experiments conform to the *Guide for the Care and Use of Laboratory Animals,* published by the US National Institutes of Health (NIH publication no. 85-23 revised 1996). The animals were maintained on 12h:12h artificial light–dark cycles and housed in individual cages. Rats were randomly divided into two groups, control, fed on standard rodent chow (3948 kcal.Kg^{-1}) and DIO, fed a fat-rich chow (5358 kcal.Kg^{-1}) *ad libitum* for 3 months. This diet composition has been previously used [36].

Male (10-week-old) *ob/ob* mice and their respective controls C57BL/6J background were obtained from The Jackson Laboratory and provided by the University of São Paulo. The mice were bred under specific pathogen-free conditions at the Central Breeding Center of University of Campinas.

Male C3H/HeJ (10-week-old) mice and their respective controls C3H/HeN were obtained from The Jackson Laboratory and provided by the University of São Paulo.

The mice were bred under specific pathogen-free conditions at the Central Breeding Center of the University of Campinas.

Intracerebroventricular cannulation

The animals were stereotaxically instrumented under intraperitoneal injection of a mix of ketamin (10mg) and diazepam (0.07mg) (0.2ml/100g body weight) with a chronic 26-gauge stainless steel indwelling guide cannula, aseptically placed into the third ventricle at the midline coordinates of 0.5 mm posterior to the bregma and 8.5 mm below the surface of the skull of rats and 1.8 mm posterior to the bregma and 5.0 mm below the surface of the skull of mice.

Exercise Protocols

Animals were acclimated to swimming for 2 days (10 min per day). Water temperature was maintained at 34-35°C. Rats performed two 3-h exercise bouts, separated by one 45-min rest period. The rats swam in groups of three in plastic barrels of 45 cm in diameter that were filled to a depth of 50 cm. This protocol was conducted between 11:00am and 6:00pm, as previously described [37] and mice performed four 30-min exercise bouts, separated by one 5-min rest period. The mice swam in groups of four in plastic barrels of 40 cm in diameter that were filled to a depth of 20 cm. This protocol was conducted between 3:00pm and 6:00pm. Both exercise protocols finished at 6:00pm for evaluation of food intake and analysis of hypothalamic tissue.

Intracerebroventricular treatments

Rats or mice were deprived of food for 2 h with free access to water and received 3 μl of bolus injection into the third-ventricle, as follows:

Insulin and leptin treatments: Animals received inthahypothalamic infusion of vehicle, insulin (200mU) or leptin (10^{-6}M) at 6:00pm to evaluate the food intake or insulin and leptin signaling. Food intake was determined by measuring the difference between the weight of chow given and the weight of chow at the end of a 12-h period.

Recombinant IL-6 and IL-10 treatments: Animals received inthahypothalamic infusion of vehicle, or recombinant IL-6 (50, 100 or 200ng) or recombinant IL-10 (0.5, 1.0 or 3.0ng) at 6:00pm to evaluate the food intake. For Western blott analysis, we injected recombinant IL-6 or IL-10 two hours after DMSO or Thapsigargin into the third-ventricle and the hypothalamus was excised 2 hours later.

Thapsigargin treatments: Animals received inthahypothalamic infusion of vehicle, or Thapsigargin (3.0μg). To evaluate the energy intake and for Western blott analysis, Thapsigargin was infused 40 minutes before the exercise protocol and 2 hours before the recombinant IL-6 infusion. Immediately after exercise or 2 hours after IL-6 infusion, animals received intrahypothalamic infusion of insulin (200mU) or leptin (10^{-6}M).

IL-6 neutralizing antibody: Animals were randomly selected for treatment with saline, rabbit pre-immune serum (RPIS) or rabbit antiserum against IL-6 (IL-6 Ab) in different doses. IL-6 Ab was injected into the third-ventricle of the rats 15 minutes before the exercise protocol.

IL-10 antisense oligonucleotide treatments: Phosphorthioate-modified sense and antisense oligonucleotides (produced by Invitrogen Corp., Carlsbad, CA, USA) were diluted to final concentration of 1nmol/μl in dilution buffer containing 10 mmol/l Tris–HCl and 1.0 mmol/l EDTA. The oligonucleotides were designed according to the *Mus*

musculus IL-10 sequence deposited at the NIH-NCBI (http://www.ncbi.nlm.nih.gov/entrez) under the designation NM 010548, and were composed of 5′-GCC AGT CAG TAA GAG CAG-3′ (sense) and 5′-TGA GAT CTG CAA TGC A-3′ (antisense). Obese Wistar rats were injected into the third ventricle with two daily doses of 3 µl of dilution buffer containing, or not, sense (Sense IL-10) or antisense oligonucleotides (ASO IL-10) for 3 days. For Western blotting analysis, after ASO IL-10 treatment, obese animals were submitted to the exercise protocol or intrahypothalamic infusion of recombinant IL-6. In some experiments, the rats also received intrahypothalamic infusion of insulin (200mU) or leptin (10^{-6}M) for the determination of food intake and Akt and STAT3 phosphorylation.

Food intake determination

Intrahypothalamic infusions were performed between 5:00 and 6:00 pm. Thereafter standard chow or high-fat diet was given and food intake was determined by measuring the difference between the weight of chow given and the weight of chow at the end of a 12-h period. Similar studies were carried out in animals after exercise.

Western Blot Analysis

After exercise and/or i.c.v. treatments, the animals were anaesthetized, the hypothalamus was quickly removed, minced coarsely and homogenized immediately in a freshly prepared ice-cold buffer (1% Triton X-100, 100mmol/l Tris pH 7.4, 100mmol/l sodium pyrophosphate, 100mmol/l sodium fluoride, 10mmol/l EDTA, 10mmol/l sodium vanadate, 2mmol/l phenyl methylsulphonyl fluoride and 0.1mg aprotinin) suitable for preserving phosphorylation states of enzymes and Western blot was performed, as previously described [1].

Nuclear extract

Foxo1 and STAT-3 nuclear expression were obtained as described [38]. Fragments of hypothalamic tissue from untreated rats or rats treated with insulin or leptin were obtained 30 minutes after insulin or leptin infusion and were minced and homogenized in 2 vol. of STE buffer (0.32 M sucrose, 20 mM Tris–HCl (pH 7.4), 2 mM EDTA, 1 mM DTT, 100 mM sodium fluoride, 100 mM sodium pyrophosphate, 10 mM sodium orthovanadate, 1 mM PMSF, and 0.1 mg aprotinin/ml] at 4 °C with a Polytron homogenizer. The homogenates were centrifuged (1000 × g, 25 min, 4 °C) to obtain pellets. The pellet was washed once and suspended in STE buffer (nuclear fraction). The nuclear fraction was solubilized in Triton buffer [1% (v/v) Triton X-100/150 mM NaCl/10 mM Tris/HCl (pH 7.4)/1 mM EGTA/1 mM EDTA/0.2 mM sodium orthovanadate/20 μM leupeptin A/0.2 mM PMSF/50 mM NaF/0.4 nM microcystin LR]. The fraction was centrifuged (15000 g, 30 min, 4 °C), and the supernatant (nuclear extract) was stored at -80 °C.

Confocal microscopy

Paraformaldehyde-fixed hypothalami were sectioned (5 μm). The sections were obtained from the hypothalami of six rats per group in the same localization (antero-posterior= -1.78 from bregma) and used in regular single- or double-immunofluorescence staining using DAPI, anti-IL6 receptor alpha (rabbit IgG, SC-13947), anti-IL-10 receptor (rabbit IgG, SC-987), anti- IKKβ (goat IgG, SC-34673), anti-PERK (rabbit IgG, SC-32577), anti-POMC (rabbit IgG, FL-267) and rabbit anti-IRS-1 (rabbit IgG, SC-559) (1:200; Santa Cruz Biotechnology) antibodies. After incubation with the primary antibody, sections were washed and incubated with specific biotinylated anti-rabbit or anti-goat secondary antibodies (1:150 dilution) for 2 hours at

room temperature, followed by incubation with Streptoavidin reagent (containing avidin-conjugated peroxidase) and colour reaction using the DAB substrate kit (Vector Laboratories, Burlingame, Calif., USA), according to recommendations of the manufacturer. Analysis and photodocumentation of results were performed using a LSM 510 laser confocal microscope (Zeiss, Jena, Germany). The anatomical correlations were made according to the landmarks given in a stereotaxic atlas [39].

mRNA isolation and real time-PCR.

Hypothalamic total RNA was extracted using Trizol reagent (Life Technologies, Gaithersburg, MD, USA), according to the manufacturer's recommendations. Total RNA was rendered genomic DNA free by digestion with Rnase-free Dnase (RQ1, Promega, Madison, WI, USA). Rats were deprived of food for 9 h after for real time PCR analysis. Real time-PCR and mRNA isolation were performed using a commercial kit, as follows: IL-6: Rn00561420_m1 IL-10: Rn00563409_m1, POMC: Rn00595020_m1, NPY: Rn00561681_m1, GAPD, #4352338E, for rat and RPS-29 (NCBI: NM012876), sense: 5'-AGGCAAGATGGGTCACCAGC-3', antisense: 5'-AGTCGAATCATCCATTCAGGTCG-3'.

Statistical Analysis

All numeric results are expressed as the means ±SEM of the indicated number of experiments. The results of blots are presented as direct comparisons of bands or spots in autoradiographs and quantified by optical densitometry (Scion Image). Statistical analysis was performed by employing the ANOVA test with *Bonferroni post test*. Significance was established at the $p<0.05$ level.

ACKNOWLEDGMENTS

This study was supported by grants from Fundacão de Amparo à Pesquisa do Estado de São Paulo (FAPESP) and Conselho Nacional de desenvolvimento científico e tecnológico (CNPq).

We thank Mr. Luiz Janeri for the technical assistance and Nicola Conran for the English language editing.

REFERENCES

1. Carvalheira JB, Ribeiro EB, Araujo EP, Guimaraes RB, Telles MM, et al. (2003) Selective impairment of insulin signalling in the hypothalamus of obese Zucker rats. Diabetologia 46: 1629-1640.

2. Niswender KD, Morton GJ, Stearns WH, Rhodes CJ, Myers MG, Jr., et al. (2001) Intracellular signalling. Key enzyme in leptin-induced anorexia. Nature 413: 794-795.

3. Bruning JC, Gautam D, Burks DJ, Gillette J, Schubert M, et al. (2000) Role of brain insulin receptor in control of body weight and reproduction. Science 289: 2122-2125.

4. El-Haschimi K, Pierroz DD, Hileman SM, Bjorbaek C, Flier JS (2000) Two defects contribute to hypothalamic leptin resistance in mice with diet-induced obesity. J Clin Invest 105: 1827-1832.

5. De Souza CT, Araujo EP, Bordin S, Ashimine R, Zollner RL, et al. (2005) Consumption of a fat-rich diet activates a proinflammatory response and induces insulin resistance in the hypothalamus. Endocrinology 146: 4192-4199.

6. Milanski M, Degasperi G, Coope A, Morari J, Denis R, et al. (2009) Saturated fatty acids produce an inflammatory response predominantly through the activation of TLR4 signaling in hypothalamus: implications for the pathogenesis of obesity. J Neurosci 29: 359-370.

7. Zhang X, Zhang G, Zhang H, Karin M, Bai H, et al. (2008) Hypothalamic IKKbeta/NF-kappaB and ER stress link overnutrition to energy imbalance and obesity. Cell 135: 61-73.

8. Hayden MS, Ghosh S (2008) Shared principles in NF-kappaB signaling. Cell 132: 344-362.

9. Ozcan L, Ergin AS, Lu A, Chung J, Sarkar S, et al. (2009) Endoplasmic reticulum stress plays a central role in development of leptin resistance. Cell Metab 9: 35-51.

10. Ozcan U, Cao Q, Yilmaz E, Lee AH, Iwakoshi NN, et al. (2004) Endoplasmic reticulum stress links obesity, insulin action, and type 2 diabetes. Science 306: 457-461.

11. Tsiotra PC, Tsigos C (2006) Stress, the endoplasmic reticulum, and insulin resistance. Ann N Y Acad Sci 1083: 63-76.

12. Misra A, Alappan NK, Vikram NK, Goel K, Gupta N, et al. (2008) Effect of supervised progressive resistance-exercise training protocol on insulin sensitivity, glycemia, lipids, and body composition in Asian Indians with type 2 diabetes. Diabetes Care 31: 1282-1287.

13. Tuomilehto J, Lindstrom J, Eriksson JG, Valle TT, Hamalainen H, et al. (2001) Prevention of type 2 diabetes mellitus by changes in lifestyle among subjects with impaired glucose tolerance. N Engl J Med 344: 1343-1350.

14. Petersen AM, Pedersen BK (2005) The anti-inflammatory effect of exercise. J Appl Physiol 98: 1154-1162.

15. Flores MB, Fernandes MF, Ropelle ER, Faria MC, Ueno M, et al. (2006) Exercise improves insulin and leptin sensitivity in hypothalamus of Wistar rats. Diabetes 55: 2554-2561.

16. Wallenius V, Wallenius K, Ahren B, Rudling M, Carlsten H, et al. (2002) Interleukin-6-deficient mice develop mature-onset obesity. Nat Med 8: 75-79.

17. Pedersen BK, Steensberg A, Schjerling P (2001) Muscle-derived interleukin-6: possible biological effects. J Physiol 536: 329-337.

18. Ropelle ER, Fernandes MF, Flores MB, Ueno M, Rocco S, et al. (2008) Central exercise action increases the AMPK and mTOR response to leptin. PLoS ONE 3: e3856.

19. Moraes JC, Amaral ME, Picardi PK, Calegari VC, Romanatto T, et al. (2006) Inducible-NOS but not neuronal-NOS participate in the acute effect of TNF-alpha on hypothalamic insulin-dependent inhibition of food intake. FEBS Lett 580: 4625-4631.

20. Pedersen BK, Fischer CP (2007) Physiological roles of muscle-derived interleukin-6 in response to exercise. Curr Opin Clin Nutr Metab Care 10: 265-271.

21. Steensberg A, Fischer CP, Keller C, Moller K, Pedersen BK (2003) IL-6 enhances plasma IL-1ra, IL-10, and cortisol in humans. Am J Physiol Endocrinol Metab 285: E433-437.

22. Schottelius AJ, Mayo MW, Sartor RB, Baldwin AS, Jr. (1999) Interleukin-10 signaling blocks inhibitor of kappaB kinase activity and nuclear factor kappaB DNA binding. J Biol Chem 274: 31868-31874.

23. Shkoda A, Ruiz PA, Daniel H, Kim SC, Rogler G, et al. (2007) Interleukin-10 blocked endoplasmic reticulum stress in intestinal epithelial cells: impact on chronic inflammation. Gastroenterology 132: 190-207.

24. Bruns B, Maass D, Barber R, Horton J, Carlson D (2008) Alterations in the cardiac inflammatory response to burn trauma in mice lacking a functional Toll-like receptor 4 gene. Shock 30: 740-746.

25. Kobbe P, Kaczorowski DJ, Vodovotz Y, Tzioupis CH, Mollen KP, et al. (2008) Local exposure of bone components to injured soft tissue induces Toll-like receptor 4-dependent systemic inflammation with acute lung injury. Shock 30: 686-691.

26. Naugler WE, Sakurai T, Kim S, Maeda S, Kim K, et al. (2007) Gender disparity in liver cancer due to sex differences in MyD88-dependent IL-6 production. Science 317: 121-124.

27. Frost RA, Nystrom GJ, Lang CH (2006) Multiple Toll-like receptor ligands induce an IL-6 transcriptional response in skeletal myocytes. Am J Physiol Regul Integr Comp Physiol 290: R773-784.

28. Patterson CM, Bouret SG, Dunn-Meynell AA, Levin BE (2009) Three weeks of postweaning exercise in DIO rats produces prolonged increases in central leptin sensitivity and signaling. Am J Physiol Regul Integr Comp Physiol 296: R537-548.

29. Martins C, Robertson MD, Morgan LM (2008) Effects of exercise and restrained eating behaviour on appetite control. Proc Nutr Soc 67: 28-41.

30. Martins C, Truby H, Morgan LM (2007) Short-term appetite control in response to a 6-week exercise programme in sedentary volunteers. Br J Nutr 98: 834-842.

31. Carey AL, Steinberg GR, Macaulay SL, Thomas WG, Holmes AG, et al. (2006) Interleukin-6 increases insulin-stimulated glucose disposal in humans and glucose uptake and fatty acid oxidation in vitro via AMP-activated protein kinase. Diabetes 55: 2688-2697.

32. Wallenius K, Wallenius V, Sunter D, Dickson SL, Jansson JO (2002) Intracerebroventricular interleukin-6 treatment decreases body fat in rats. Biochem Biophys Res Commun 293: 560-565.

33. Nybo L, Nielsen B, Pedersen BK, Moller K, Secher NH (2002) Interleukin-6 release from the human brain during prolonged exercise. J Physiol 542: 991-995.

34. Kennedy MK, Torrance DS, Picha KS, Mohler KM (1992) Analysis of cytokine mRNA expression in the central nervous system of mice with experimental autoimmune encephalomyelitis reveals that IL-10 mRNA expression correlates with recovery. J Immunol 149: 2496-2505.

35. Samoilova EB, Horton JL, Chen Y (1998) Acceleration of experimental autoimmune encephalomyelitis in interleukin-10-deficient mice: roles of interleukin-10 in disease progression and recovery. Cell Immunol 188: 118-124.

36. Pauli JR, Ropelle ER, Cintra DE, Carvalho-Filho MA, Moraes JC, et al. (2008) Acute physical exercise reverses S-nitrosation of the insulin receptor, insulin receptor substrate 1 and protein kinase B/Akt in diet-induced obese Wistar rats. J Physiol 586: 659-671.

37. Ropelle ER, Pauli JR, Prada PO, de Souza CT, Picardi PK, et al. (2006) Reversal of diet-induced insulin resistance with a single bout of exercise in the rat: the role of PTP1B and IRS-1 serine phosphorylation. J Physiol 577: 997-1007.

38. Ropelle ER, Pauli JR, Prada P, Cintra DE, Rocha GZ, et al. (2009) Inhibition of hypothalamic Foxo1 expression reduced food intake in diet-induced obesity rats. J Physiol 587: 2341-2351.

39. Mai JK, Assheuer J, Paxinos G (1997) Atlas of the human brain. San Diego ; London: Academic. viii, 336 p.

FIGURE LEGENDS

Figure 1. Exercise induces appetite-suppressive actions in different models of obesity. (A) 12-hour of food intake (kcal) in lean and diet-induced obesity (DIO) Wistar rats under resting conditions or after exercise (exe) (n = 20-35 animals per group). Rats were fasted during 9 hours and the hypothalamic levels (B) NPY and (C) POMC mRNA were examined using real time-PCR assay. (D) Body weight, (E) epididymal fat pad weight (F) serum insulin and (G) leptin levels of lean and obese rats at rest or immediately after exercise. (H) 12-hour food intake of leptin-deficient mice ($Lept^{ob/ob}$) and respective wild type group. (I) Body weight, (J) epididymal fat pad weight and (L) serum insulin of wild type and leptin-deficient mice under resting conditions or immediately after exercise (n = 10 animals per group). Data are the means ± SEM. # $p< 0.05$, vs. respective lean group at rest; *$p< 0.05$, vs. respective obese group at rest. Lean animals (white bars) and obese animals (black bars).

Figure 2. Hypothalamic insulin and leptin signaling after exercise. Western blots showing hypothalamic lysates from Wistar rats; (A) Hypothalamic Foxo1 phosphorylation. (B) 12-hour food intake (kcal) after intrahypothalamic infusion of insulin in lean and diet-induced obesity (DIO) Wistar rats under resting conditions or after exercise (n = 6 animals per group). Western blots of five independent experiments showing hypothalamic lysates from Wistar rats; (C) Insulin-induced IRβ, IRS-1, IRS-2, Akt and Foxo1 phosphorylation in the hypothalamus. (D) Subcellular fractionation was performed to evaluate the nuclear Foxo1 expression in the hypothalamus of lean and obese rats at 30 minutes after insulin infusion. (E) Hypothalamic STAT-3 tyrosine phosphorylation. (F) 12-hour food intake (kcal) after intrahypothalamic infusion of leptin (n = 6 animals per group). Western blots showing hypothalamic lysates from

Wistar rats; (G) Leptin-induced Jak2, IRS-1, IRS-2 and STAT3 tyrosine phosphorylation in the hypothalamus. (H) Subcellular fractionation was performed to evaluate the nuclear STAT3 expression in the hypothalamic cells of lean and obese rats 30 minutes after leptin infusion. Data are the means ± SEM. # $p< 0.05$, vs. lean group at rest; *$p< 0.05$, vs. obese group at rest. Lean animals (white bars) and obese animals (black bars).

Figure 3. Anti-hyperphagic response mediated by IL-6. (A) Protein expression of IL-6 and (B) IL-6 mRNA in the hypothalamus of lean or diet-induced obesity (DIO) rats under resting conditions and obese rats immediately after the exercise protocol. (C) 12-h of food intake in obese rats under resting conditions following intrahypothalamic infusion of different doses of recombinant IL-6. Counter regulatory effects of anti-IL-6 antibody on food intake in exercised obese rats after insulin (D) or leptin (E) infusion. Western blots of five independent experiments showing hypothalamic lysates from Wistar rats; (F) IKKβ, (G) IκBα, (H) PERK, (I) eIF2α and (J) IRS-1Ser307 phosphorylation from lean, obese, obese injected with recombinant IL-6, obese after exercise and obese pretreated with anti-IL-6 antibody before the exercise protocol. Data are the means ± SEM. # $p< 0.05$, *vs.* lean group; *$p< 0.05$, *vs.* obese group at rest; **$p< 0.01$, *vs.* stimulated obese group at rest; § $p< 0.05$, *vs.* obese group injected with recombinant IL-6 and exercised obese rats (n=6-8 animals per group). Lean animals (white bars), obese animals (blue bars) and exercised obese plus IL-6 anti-body (yellow bars). (K) Confocal microscopy was performed using IL-6 receptor (IL-6R)-specific antibody (green) and DAPI (blue), with 50x magnification. (L) Co-localization of IL-6R (green) and IKKβ, PERK, IRS-1 and POMC (red) in the arcuate nuclei of obese rats, with 200x magnification (scale bar, 20 μm).

Figure 4- IL-6 reversed pharmacological endoplasmatic reticulum stress induction in the hypothalamus. (A) Anorexigenic effects of insulin in the hypothalamus of lean rats pretreated with Thapsigargin. (B) Anorexigenic effects of leptin in the hypothalamus of lean rats pretreated with Thapsigargin. Western blots showing hypothalamic lysates from Wistar rats; (C) IKKβ, (D) PERK, and (E) IRS-1Ser307 phosphorylation from lean rats pretreated with Thapsigargin. (F) Insulin-induced Akt serine phosphorylation and (G) leptin-induced STAT3 tyrosine phosphorylation in the hypothalamus of lean animals pretreated with Thapsigargin. Data are the means ± SEM. # $p< 0.05$, *vs.* DMSO group; *$p< 0.05$, *vs.* lean plus Thapsigargin; § $p< 0.05$, *vs.* Thapsigargin plus recombinant IL-6 or Thapsigargin plus exercised (n=6-8 animals per group).

Figure 5- Role of hypothalamic IL-10 in the control of energy intake during obesity. Western blots showing hypothalamic lysates from Wistar rats; (A) IL-1ra and (B) IL-10 expression in the hypothalamus. (C) IL-10 mRNA in the hypothalamus was examined using real time-PCR assay. (D) 12-h food intake (kcal) in obese rats under resting conditions after intrahypothalamic infusion of different doses of recombinant IL-10. Western blots showing hypothalamic lysates from Wistar rats; (E) IL-10 expression after ASO IL-10 treatment in obese animals. (F) Intrahypothalamic treatment with ASO IL-10 blocked the anorexigenic response mediated by (F) insulin and (G) leptin in exercised obese animals or obese animals at rest injected with recombinant IL-6. Western blots showing hypothalamic lysates from Wistar rats; (H) IKKβ, (I) PERK, and (J) IRS-1Ser307 phosphorylation after ASO IL-10 treatment of after acute recombinant IL-10 infusion. (F) Insulin-induced Akt serine phosphorylation and (G) leptin-induced STAT3 tyrosine phosphorylation in the hypothalamus after ASO IL-10 treatment of after acute recombinant IL-10 infusion. Data are the means ± SEM. # $p< 0.05$, *vs.* chow

group (sense); *p< 0.05, *vs.* obese (sense); n=6-8 animals per group. Lean animals (white bars), obese animals (black bars) and exercised obese plus recombinant IL-10 (grey bars).

Figure 6- The central anti-inflammatory response mediated by exercise requires augmented of hypothalamic levels of IL-6 and IL-10. Western blots showing hypothalamic lysates from C3H/NeN and C3H/HeJ mice under resting conditions or after physical activity; (A) IL-6 and (B) IL-10 expression. Anorexigenic effects of insulin (C) or leptin (D) in C3H/NeN and C3H/HeJ mice under resting conditions, after Thapsigargin, Thapsigargin plus exercise and Thapsigargin plus recombinant IL-6 or IL-10. Western blots showing hypothalamic lysates from mice; (E) IL-10 expression at 2 hours after intrahypothalamic injection of recombinant IL-6 (200 ng) in C3H/NeN and C3H/HeJ mice under resting conditions. (F) IKKβ, (G) PERK, and (H) IRS-1Ser307 phosphorylation and (I) Insulin-induced Akt serine phosphorylation and (J) leptin-induced STAT3 tyrosine phosphorylation in the hypothalamus of C3H/HeJ mice after intrahypothalamic infusion of DMSO, Thapsigargin, Thapsigargin plus exercise and Thapsigargin plus recombinant IL-6 or IL-10. Data are the means ± SEM. **p< 0.05, *vs.* respective control group at rest; # p< 0.05, *vs.* respective control group non stimulated or stimulated with DMSO; *p< 0.05, *vs.* Thapsigargin; n=5-6 animals per group. C3H/NeN (yellow bars) and C3H/HeJ (blue bars). (K) Co-localization of IL-6R (green) and IL-10R (red) in the arcuate nuclei of lean rats, with 200x magnification (scale bar, 10 μm).

Figure 7- Schematic diagrams of the proposed role of the hypothalamic anti-inflammatory response mediated by exercise. (A) Overnutrition induces hypothalamic IKKβ activation and endoplasmatic reticulum stress, leading to central

insulin and leptin resistance, hyperphagia and obesity. (B) We propose that exercise increases the central anti-inflammatory response, increasing hypothalamic IL-6 and IL-10 expression, this phenomenon is crucial for reducing hypothalamic IKKβ activation and endoplasmatic reticulum stress and turn, restoring insulin and leptin signaling and reorganizing the set point of nutritional balance.

Figure 1

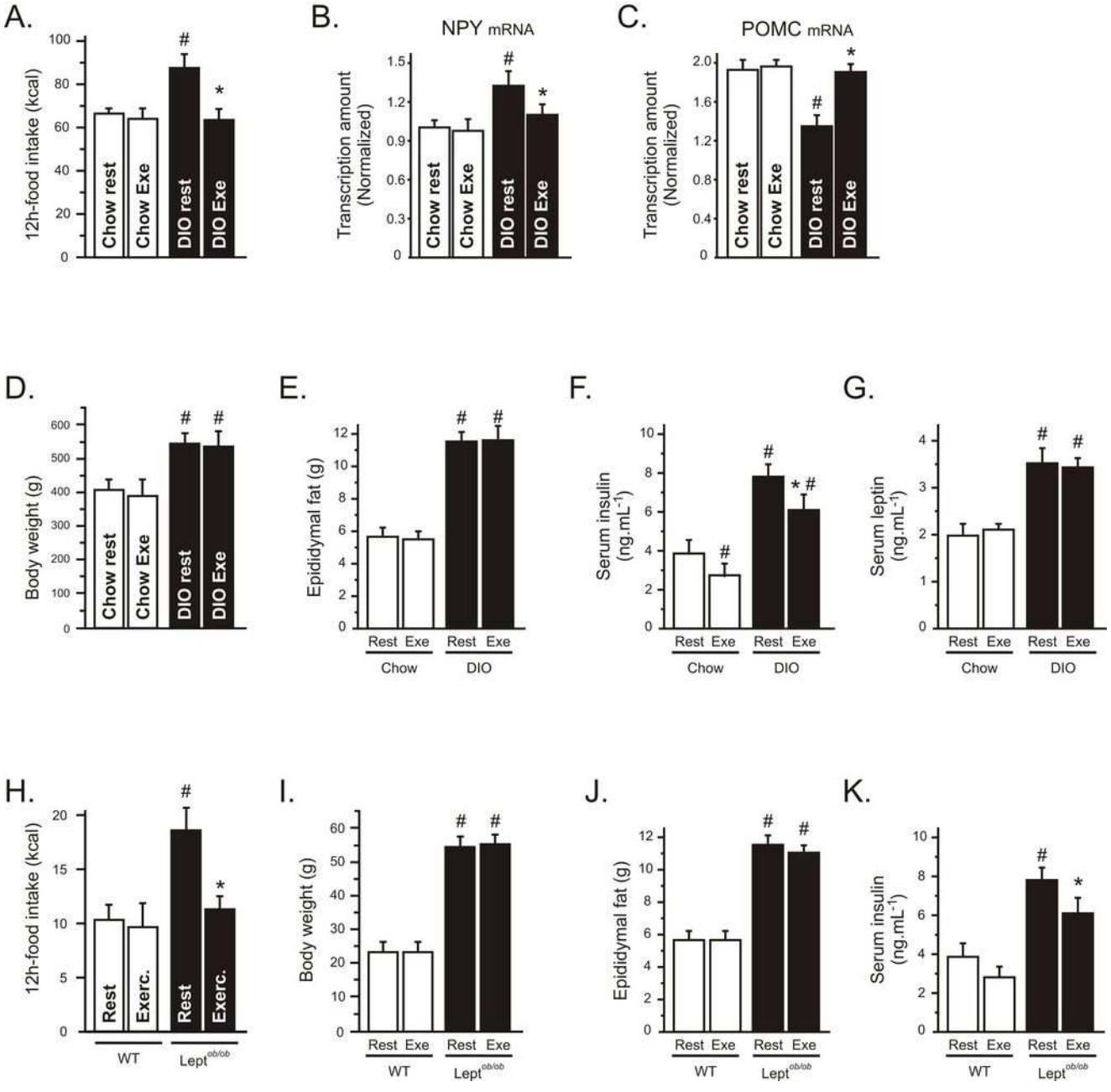
A.
12h-food intake (kcal)
Chow rest
Chow Exe
DIO rest
DIO Exe
B.
NPY mRNA
Transcription amount (Normalized)
C.
POMC mRNA
D.
Body weight (g)
E.
Epididymal fat (g)
Rest Exe Rest Exe
Chow DIO
F.
Serum insulin (ng.mL-1)
G.
Serum leptin (ng.mL-1)
H.
Rest
Exerc.
WT
Lept ob/ob
I.
J.
K.

Figure 2

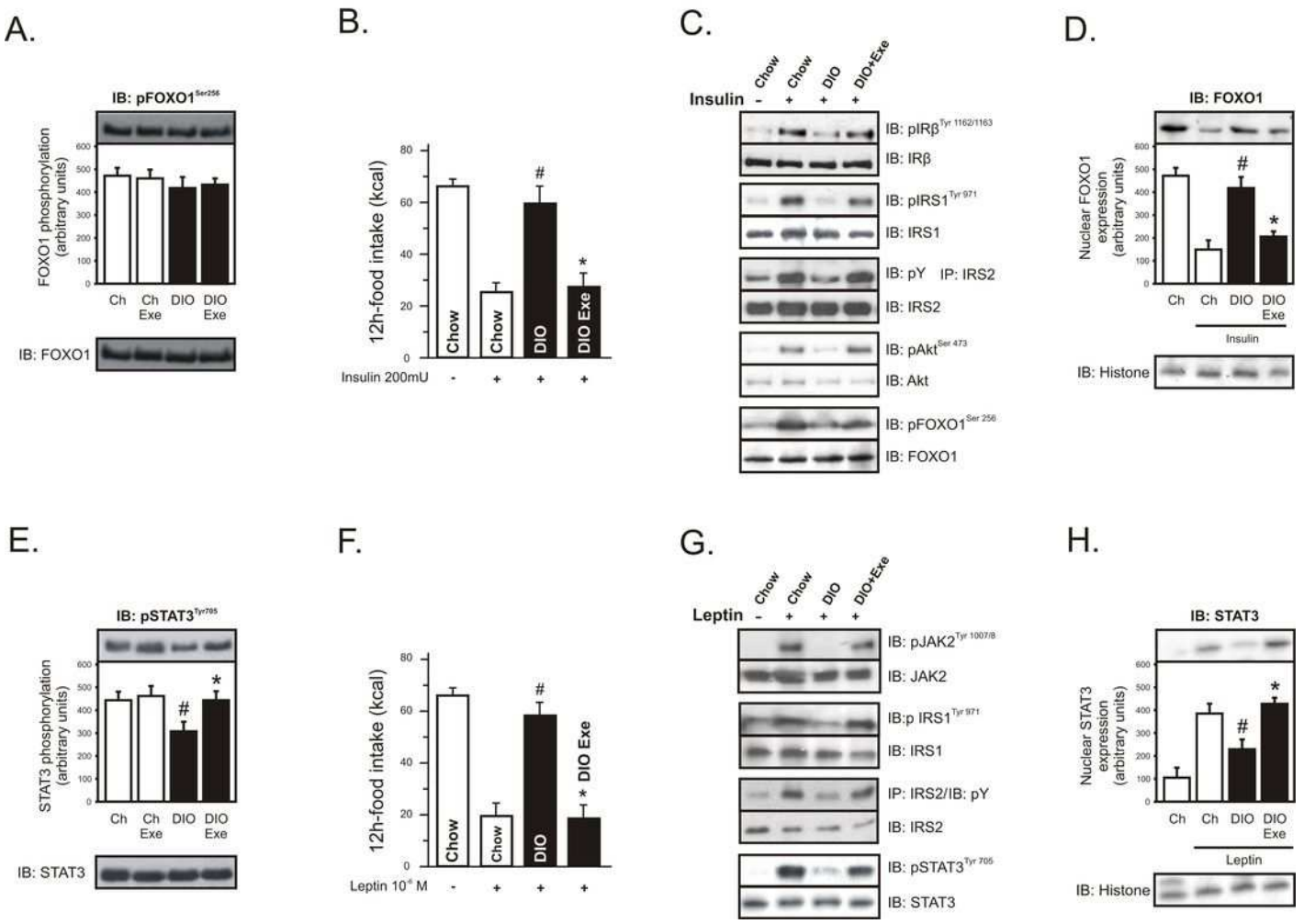
A.
IB: pFOXO1Ser256
FOXO1 phosphorylation (arbitrary units)
Ch
Ch Exe
DIO
DIO Exe
IB: FOXO1
B.
12h-food intake (kcal)
Chow
Chow
DIO
DIO Exe
Insulin 200mU
C.
Chow
Chow
DIO
DIO+Exe
Insulin
IB: pIRβTyr 1162/1163
IB: IRβ
IB: pIRS1Tyr 971
IB: IRS1
IB: pY IP: IRS2
IB: IRS2
IB: pAktSer 473
IB: Akt
IB: pFOXO1Ser 256
IB: FOXO1
D.
IB: FOXO1
Nuclear FOXO1 expression (arbitrary units)
Ch
Ch
DIO
DIO Exe
Insulin
IB: Histone
E.
IB: pSTAT3Tyr705
STAT3 phosphorylation (arbitrary units)
Ch
Ch Exe
DIO
DIO Exe
IB: STAT3
F.
12h-food intake (kcal)
Chow
Chow
DIO
DIO Exe
Leptin 10-6 M
G.
Chow
Chow
DIO
DIO+Exe
Leptin
IB: pJAK2Tyr 1007/8
IB: JAK2
IB:p IRS1Tyr 971
IB: IRS1
IP: IRS2/IB: pY
IB: IRS2
IB: pSTAT3Tyr 705
IB: STAT3
H.
IB: STAT3
Nuclear STAT3 expression (arbitrary units)
Ch
Ch
DIO
DIO Exe
Leptin
IB: Histone

Figure 3

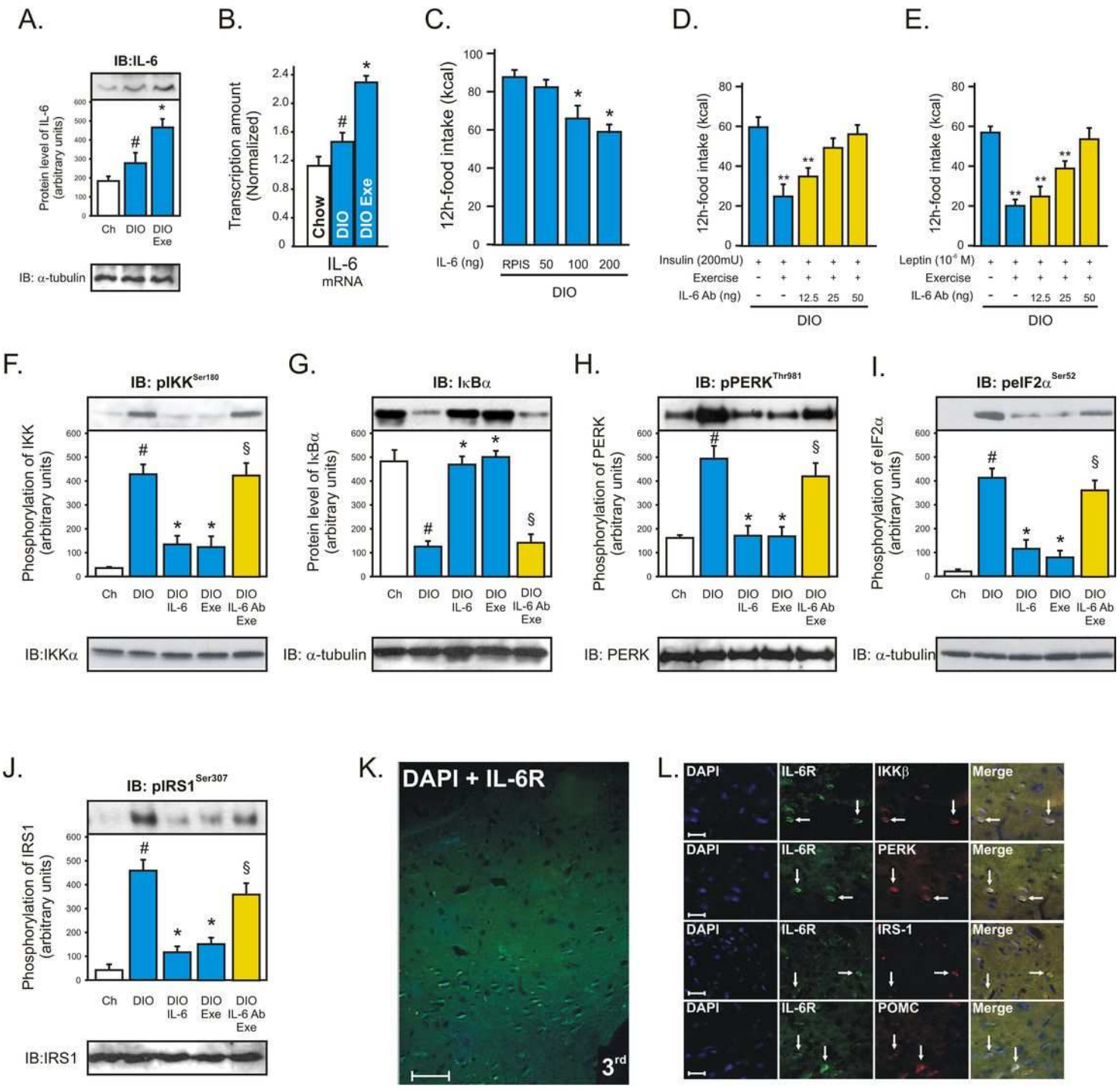
A.
IB:IL-6
Protein level of IL-6 (arbitrary units)
Ch DIO DIO Exe
IB: α-tubulin
B.
Transcription amount (Normalized)
Chow
DIO
DIO Exe
IL-6 mRNA
C.
12h-food intake (kcal)
IL-6 (ng)
RPIS 50 100 200
DIO
D.
12h-food intake (kcal)
Insulin (200mU)
Exercise
IL-6 Ab (ng)
12.5 25 50
DIO
E.
12h-food intake (kcal)
Leptin (10⁻⁶ M)
Exercise
IL-6 Ab (ng)
12.5 25 50
DIO
F.
IB: pIKK Ser180
Phosphorylation of IKK (arbitrary units)
Ch DIO DIO IL-6 DIO Exe DIO IL-6 Ab Exe
IB:IKKα
G.
IB: IκBα
Protein level of IκBα (arbitrary units)
Ch DIO DIO IL-6 DIO Exe DIO IL-6 Ab Exe
IB: α-tubulin
H.
IB: pPERK Thr981
Phosphorylation of PERK (arbitrary units)
Ch DIO DIO IL-6 DIO Exe DIO IL-6 Ab Exe
IB: PERK
I.
IB: peIF2α Ser52
Phosphorylation of eIF2α (arbitrary units)
Ch DIO DIO IL-6 DIO Exe DIO IL-6 Ab Exe
IB: α-tubulin
J.
IB: pIRS1 Ser307
Phosphorylation of IRS1 (arbitrary units)
Ch DIO DIO IL-6 DIO Exe DIO IL-6 Ab Exe
IB:IRS1
K.
DAPI + IL-6R
3rd
L.
DAPI IL-6R IKKβ Merge
DAPI IL-6R PERK Merge
DAPI IL-6R IRS-1 Merge
DAPI IL-6R POMC Merge

Figure 4

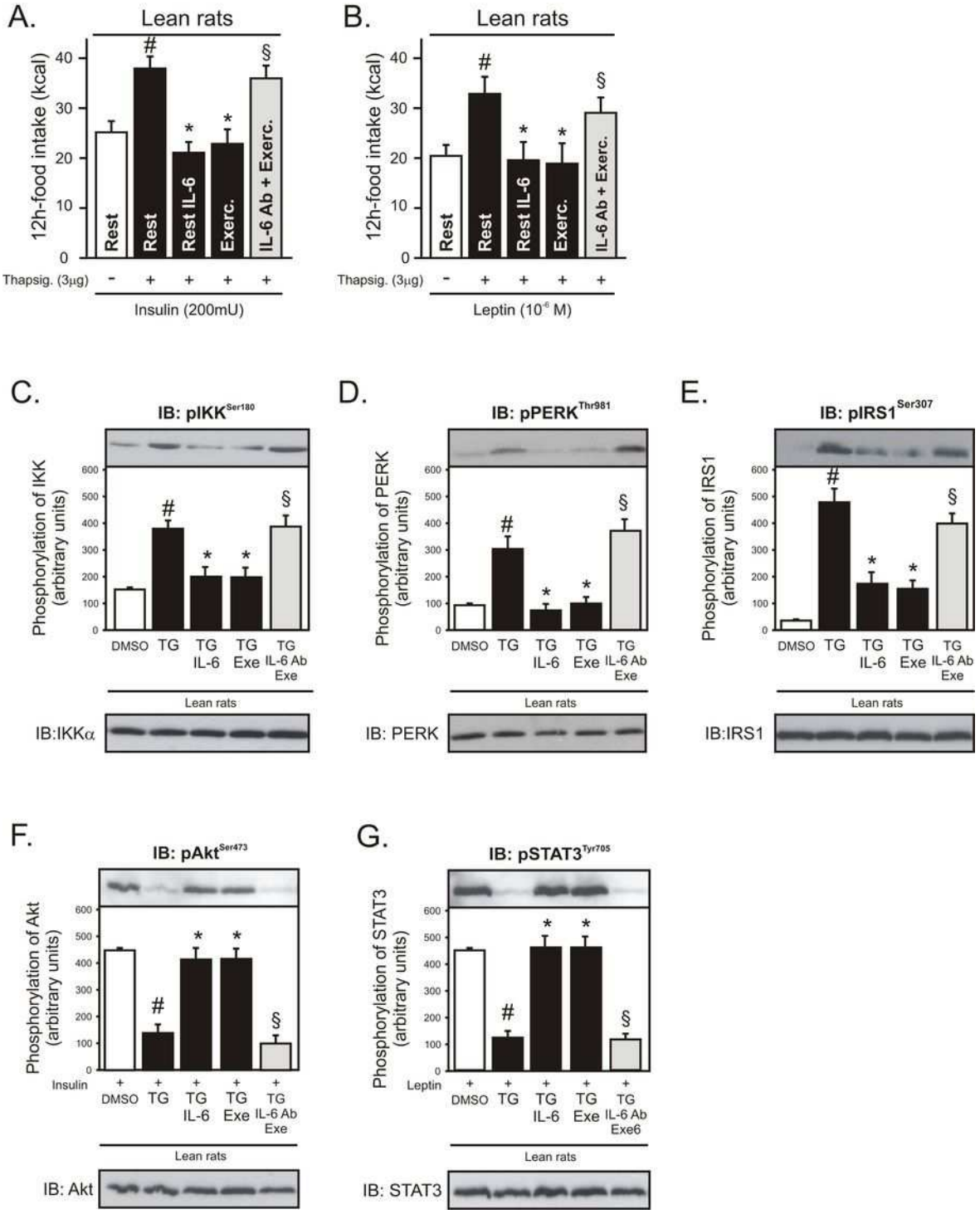
A.
Lean rats
12h-food intake (kcal)
Rest
Rest
Rest IL-6
Exerc.
IL-6 Ab + Exerc.
Thapsig. (3μg)
Insulin (200mU)
B.
Lean rats
12h-food intake (kcal)
Thapsig. (3μg)
Leptin (10-6 M)
C.
IB: pIKKSer180
Phosphorylation of IKK (arbitrary units)
DMSO
TG
TG IL-6
TG Exe
TG IL-6 Ab Exe
Lean rats
IB:IKKα
D.
IB: pPERKThr981
Phosphorylation of PERK (arbitrary units)
IB: PERK
E.
IB: pIRS1Ser307
Phosphorylation of IRS1 (arbitrary units)
IB:IRS1
F.
IB: pAktSer473
Phosphorylation of Akt (arbitrary units)
Insulin
IB: Akt
G.
IB: pSTAT3Tyr705
Phosphorylation of STAT3 (arbitrary units)
Leptin
TG IL-6 Ab Exe6
IB: STAT3

Figure 5

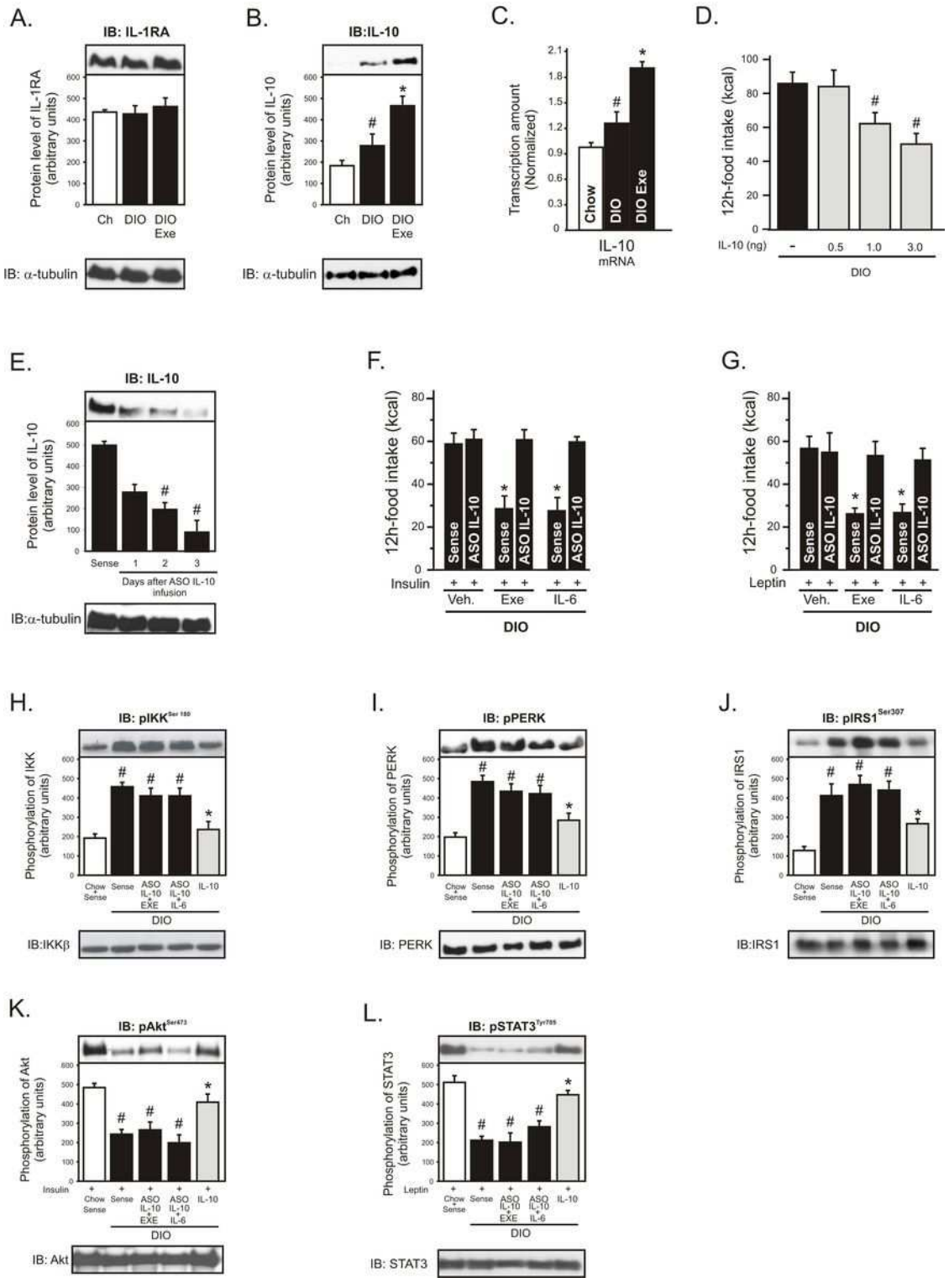
A.
IB: IL-1RA
Protein level of IL-1RA (arbitrary units)
Ch
DIO
DIO Exe
IB: α-tubulin
B.
IB:IL-10
Protein level of IL-10 (arbitrary units)
Ch
DIO
DIO Exe
IB: α-tubulin
C.
Transcription amount (Normalized)
Chow
DIO
DIO Exe
IL-10 mRNA
D.
12h-food intake (kcal)
IL-10 (ng)
-
0.5
1.0
3.0
DIO
E.
IB: IL-10
Protein level of IL-10 (arbitrary units)
Sense
1
2
3
Days after ASO IL-10 infusion
IB:α-tubulin
F.
12h-food intake (kcal)
Sense
ASO IL-10
Insulin
Veh.
Exe
IL-6
DIO
G.
12h-food intake (kcal)
Sense
ASO IL-10
Leptin
Veh.
Exe
IL-6
DIO
H.
IB: pIKKSer 180
Phosphorylation of IKK (arbitrary units)
Chow + Sense
Sense
ASO IL-10 + EXE
ASO IL-10 + IL-6
IL-10
DIO
IB:IKKβ
I.
IB: pPERK
Phosphorylation of PERK (arbitrary units)
Chow + Sense
Sense
ASO IL-10 + EXE
ASO IL-10 + IL-6
IL-10
DIO
IB: PERK
J.
IB: pIRS1Ser307
Phosphorylation of IRS1 (arbitrary units)
Chow + Sense
Sense
ASO IL-10 + EXE
ASO IL-10 + IL-6
IL-10
DIO
IB:IRS1
K.
IB: pAktSer473
Phosphorylation of Akt (arbitrary units)
Insulin
Chow + Sense
Sense
ASO IL-10 + EXE
ASO IL-10 + IL-6
IL-10
DIO
IB: Akt
L.
IB: pSTAT3Tyr705
Phosphorylation of STAT3 (arbitrary units)
Leptin
Chow + Sense
Sense
ASO IL-10 + EXE
ASO IL-10 + IL-6
IL-10
DIO
IB: STAT3

Figure 6

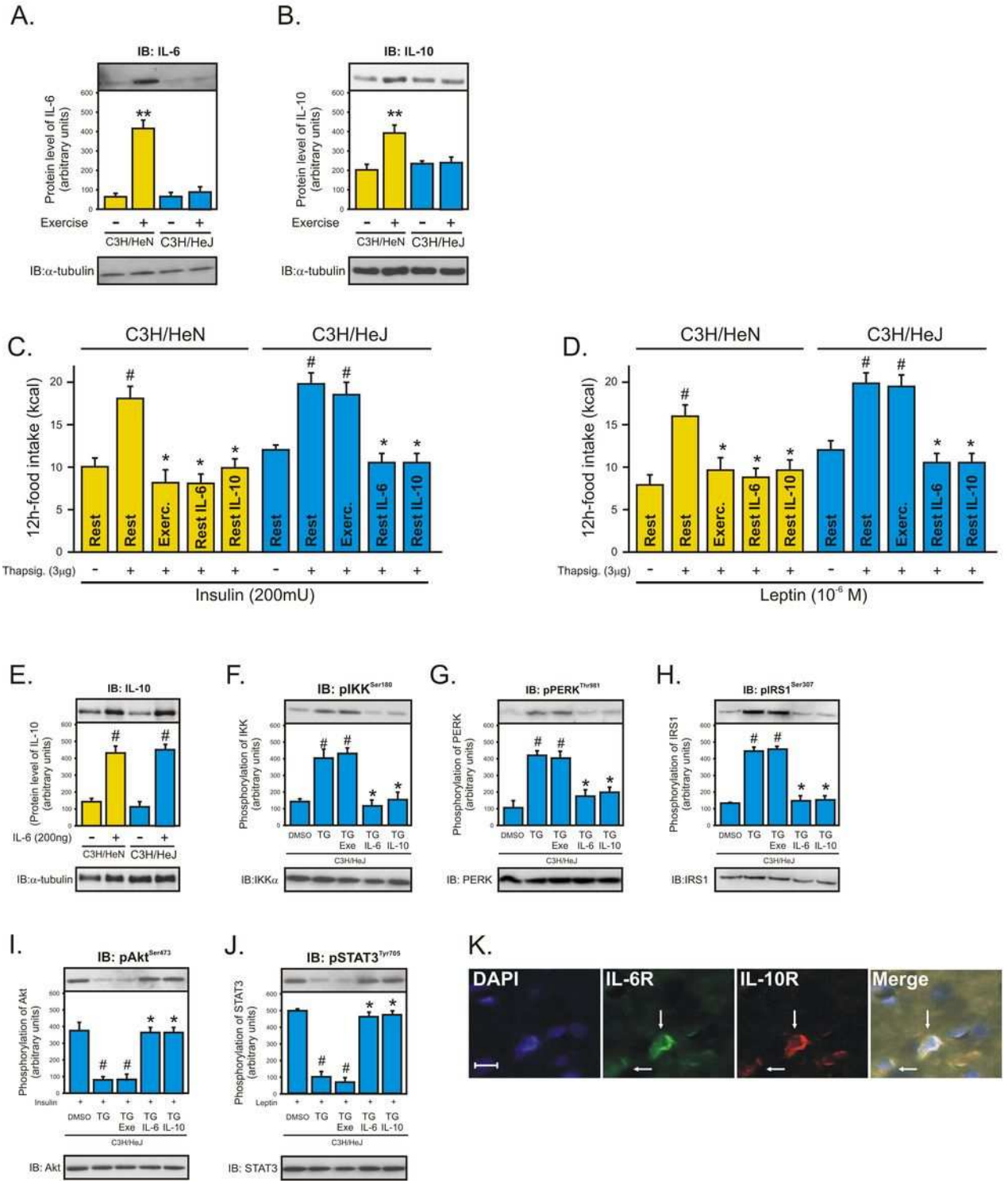
A.
IB: IL-6
Protein level of IL-6 (arbitrary units)
Exercise
C3H/HeN
C3H/HeJ
IB:α-tubulin
B.
IB: IL-10
Protein level of IL-10 (arbitrary units)
C.
D.
12h-food intake (kcal)
Rest
Exerc.
Rest IL-6
Rest IL-10
Thapsig. (3μg)
Insulin (200mU)
Leptin (10-6 M)
E.
IB: IL-10
IL-6 (200ng)
F.
IB: pIKKSer180
Phosphorylation of IKK (arbitrary units)
DMSO
TG
TG Exe
TG IL-6
TG IL-10
IB:IKKα
G.
IB: pPERKThr981
Phosphorylation of PERK (arbitrary units)
IB: PERK
H.
IB: pIRS1Ser307
Phosphorylation of IRS1 (arbitrary units)
IB:IRS1
I.
IB: pAktSer473
Phosphorylation of Akt (arbitrary units)
Insulin
IB: Akt
J.
IB: pSTAT3Tyr705
Phosphorylation of STAT3 (arbitrary units)
Leptin
IB: STAT3
K.
DAPI
IL-6R
IL-10R
Merge

Figure 7

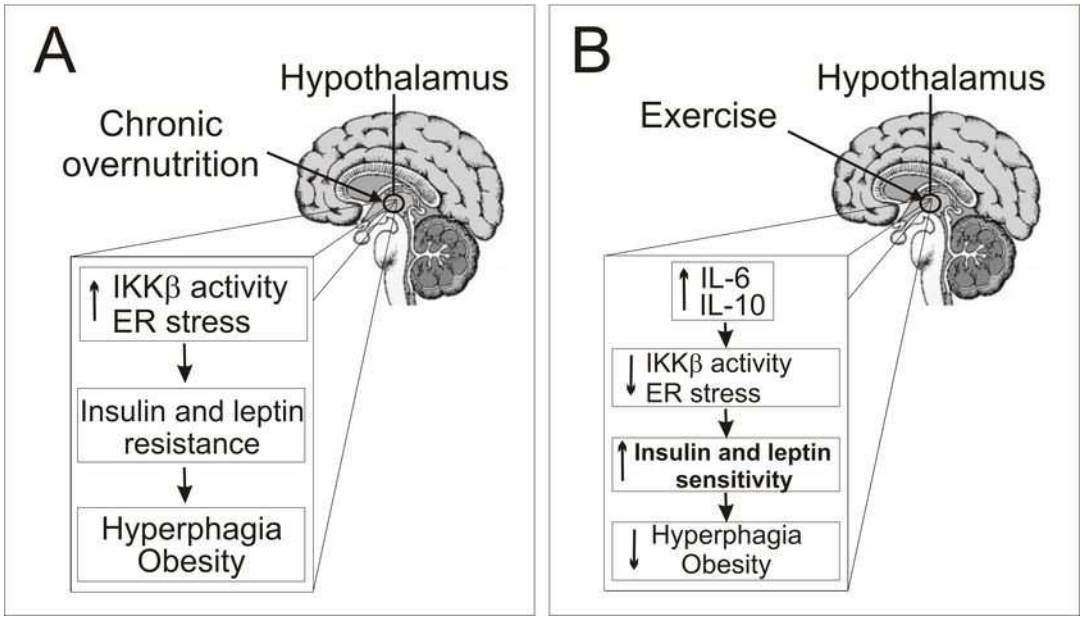
A
Hypothalamus
Chronic overnutrition
↑ IKKβ activity ER stress
Insulin and leptin resistance
Hyperphagia Obesity
B
Hypothalamus
Exercise
↑ IL-6 IL-10
↓ IKKβ activity ER stress
↑ Insulin and leptin sensitivity
↓ Hyperphagia Obesity

APÊNDICE *V*

Regulación central de la ingestión alimentaria y el gasto energético: acciones moleculares de la insulina, la leptina y el ejercicio físico

D.E. Cintra, E.R. Ropelle, J.R. Pauli

REGULACIÓN CENTRAL DE LA INGESTIÓN ALIMENTARIA Y EL GASTO ENERGÉTICO: ACCIONES MOLECULARES DE LA INSULINA, LA LEPTINA Y EL EJERCICIO FÍSICO

Resumen. Introducción. *La condición de sobrepeso y obesidad representa una preocupación significativa de la sanidad pública, ya que se asocia a varias enfermedades crónicas degenerativas. En los últimos diez años, desde que se descubrió la hormona leptina, se han conseguido avances considerables en la caracterización de los mecanismos hipotalámicos del control de la ingestión alimentaria y de la termogénesis.* Desarrollo. *Esta revisión muestra los avances más recientes en esta área, fijándose especialmente en la acción de la leptina y de la insulina en el hipotálamo e investigando la hipótesis de que la resistencia a la acción de estas hormonas puede desempeñar un papel clave en el desarrollo de la obesidad. La actividad física es un componente importante en el control de peso a largo plazo. El ejercicio aumenta la fosforilación y la actividad de diversas proteínas implicadas en la transducción de la señal de la insulina y la leptina en el hipotálamo. Recientemente, en nuestro laboratorio, se ha demostrado que el efecto anorético de la actividad física se produce en virtud del aumento de la sensibilidad hipotalámica de la insulina y la leptina tras el incremento de la producción de interleucina-6.* Conclusiones. *Estos descubrimientos apoyan la hipótesis de que el efecto supresor del ejercicio sobre el apetito puede ser mediado por el hipotálamo. [REV NEUROL 2007; 45: 672-82]*

Palabras clave. *Ejercicio físico. Hipotálamo. Insulina. Interleucina-6. Leptina. Obesidad.*

INTRODUCCIÓN

A lo largo de la existencia humana, la búsqueda de la mejor calidad de vida –considerando, entre otros fines, el conseguir una mayor longevidad– ha estimulado la realización de innumerables proyectos científicos y tecnológicos. A pesar de este escenario de crecimiento y desarrollo, muchos problemas parecen asociarse a las propias modificaciones de las condiciones de vida y a la adquisición de nuevos hábitos impuestos por la modernidad, como la obesidad y la hiperlipidemia [1].

La obesidad representa un complejo fenotipo multifactorial, influido tanto por factores genéticos como no genéticos (nutricionales, metabólicos, moleculares, de gasto energético, psicológicos y sociales), los cuales pueden interaccionar de diferentes maneras, dificultando la identificación exacta de la etiología o tratamiento de este problema.

Sin embargo, el creciente número de personas obesas en el mundo y la preocupación de asegurar la salud, manteniendo unos niveles séricos e histológicos normales de grasa, han estimulado las investigaciones en las que se evalúan, entre otros aspectos, los mecanismos fisiológicos y moleculares implicados en el control de la ingestión alimentaria y el gasto energético. No obstante, a pesar de los avances conseguidos en esta área, el problema de la obesidad aún no se ha esclarecido por completo.

En ese contexto, investigaciones recientes demuestran que el hipotálamo ejerce un papel central, integrando señales hormonales y nutricionales de la periferia y modulando la ingestión alimentaria, el gasto energético y el metabolismo periférico [2,3]. Esta revisión presenta los avances más recientes en esta área, centrándose especialmente en la acción hipotalámica de la insulina y la leptina e investigando la hipótesis de que la resistencia a la acción central de estas hormonas puede ser el eslabón entre la obesidad y otras condiciones clínicas en las que la resistencia a la insulina desempeñe un papel patogénico prominente. Al influir en ese sistema de control central del hambre, se señalan los posibles efectos favorables de la actividad física que conducen a una supresión del apetito, lo cual contribuye al retraso del acúmulo energético bajo la forma de tejido adiposo y la consecuente prevención de la obesidad.

CONTROL CENTRAL DEL HAMBRE

Hace 50 años se consideró por primera vez el hipotálamo como responsable de la estabilidad del aumento de masa corporal. Investigaciones realizadas lesionando o estimulando el núcleo hipotalámico determinaron al principio que el núcleo ventromedial constituía el 'centro de saciedad', y el núcleo hipotalámico lateral, un 'centro del hambre' [4]. Mientras tanto, más que considerar los núcleos hipotalámicos específicos como responsables del control de la homeostasis energética, se piensa que la regulación se produce en los circuitos neuronales, que utilizan neuropéptidos específicos. Se sugiere la existencia de dos grandes grupos de neuropéptidos implicados en los procesos: orexígenos y anorexígenos [2]. Las neuronas que expresan esos neuropéptidos interaccionan con las otras y con cada una de las señales que llegan con posterioridad de la periferia (insulina, leptina, grelina...), actuando en la regulación del control y del gasto energético [3]. Entre los neuropéptidos orexígenos se encuentran el neuropéptido Y (NPY) y el neuropéptido agouti (AgRP), mientras que entre los neuropéptidos anorexígenos se halla la proopiomelanocortina, que es la principal precursora del α-melanocito estimulador (αMSH) y el transcrito relacionado con la cocaína y la anfetamina (CART) [5]. Estos nuevos descubrimientos han hecho posible avanzar en la caracterización de los mecanismos hipotalámicos del con-

Aceptado tras revisión externa: 05.09.07.

Departamento de Clínica Médica. FCM. Universidade Estadual de Campinas (UNICAMP). Campinas, São Paulo, Brasil.

Correspondencia: Prof. Dr. José Rodrigo Pauli. Rua XV de Novembro, 1701, Centro. Piracicaba, SP, Brasil. CEP 13400370. Fax: (19) 34347717. E-mail: rodrigosere@yahoo.com.br

FAPESP, CNPq y CAPES otorgaron apoyo financiero en forma de proyectos y becas.

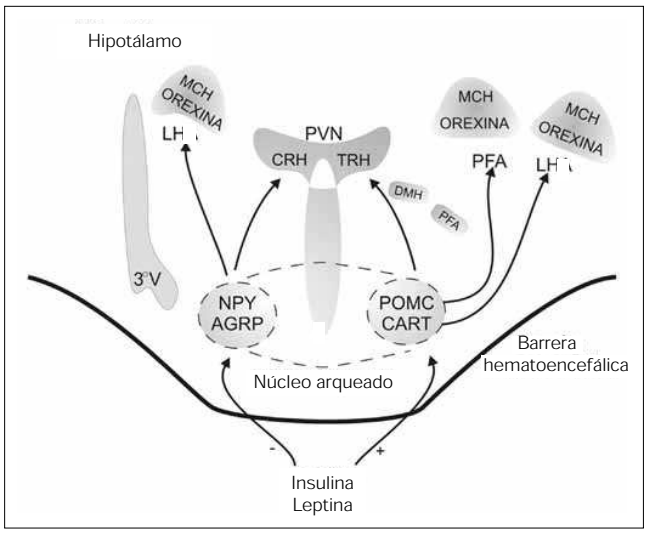

Figura 1. Centros hipotalámicos implicados en el control del hambre. Las neuronas NPY/AgRP y POMC/CART en el núcleo arqueado, adyacente al tercer ventrículo (3ºV), son neuronas de primer orden de la respuesta hipotalámica de las señales circulantes de adiposidad (leptina e insulina). Poblaciones de neuronas de primer orden localizadas en el núcleo arqueado, NPY/AgRP (orexigénicas) y POMC/CART (anorexigénicas), interactúan entre sí y con señales que llegan de la periferia (leptina e insulina); las señales anorexigénicas se proyectan desde esta región a otras –núcleo paraventricular (PVN), hipotálamo lateral (LH) y área perifornical (PFA)–, donde se localizan neuropéptidos hipotalámicos de segundo orden implicados en la regulación de la ingestión alimentaria y la homeostasis energética.

trol del hambre y de la homeostasis energética, que se tratan en esta revisión.

CENTROS HIPOTALÁMICOS EN EL CONTROL DE LA SACIEDAD

La localización de los receptores neuronales para cada señal orexigénica y anorexigénica no se conoce con precisión. Sin embargo, se sabe que los receptores para estas señales están presentes en el núcleo arqueado (ARC) y núcleo paraventricular (PVN) hipotalámicos, pero no están restringidos a estas áreas [6]. Se piensa que el núcleo ARC, en particular, es el lugar donde se produce la interacción de las señales implicadas en la regulación del apetito. El ARC es accesible a las señales del balance energético procedente de la circulación, transportadas a través de la barrera hematoencefálica y los órganos periventriculares del cerebro [7].

Sin embargo, los núcleos hipotalámicos como el PVN, hipotálamo dorsomedial (DMH), hipotálamo lateral (LH) y el área perifornical (PFA) reciben NPY/AgRP y POMC/CART de las proyecciones neuronales del ARC [6]. Esos núcleos contienen neuronas secundarias que procesan informaciones relacionadas con la homeostasis energética (Fig. 1). Se ha demostrado que ciertas moléculas de señalización que se expresan en estas regiones están fisiológicamente implicadas en el balance energético. Las hormonas leptina e insulina actúan modulando neuropéptidos centrales en el control de la ingestión alimentaria y por ese motivo constituyen el centro de estudio de diversos investigadores [8-10]. En este contexto, sin duda alguna, el ejercicio físico ha sido una herramienta importante en los programas de reeducación alimentaria y adelgazamiento. Además del aumento del gasto energético diario, la actividad física se considera importante en el control central del hambre. Estos nuevos descubrimientos científicos ayudan a una mejor comprensión de los centros hipotalámicos implicados en el control central del hambre y los mecanismos involucrados en la acción supresora del ejercicio físico sobre el apetito.

TRANSMISIÓN DE LA SEÑAL DE LA LEPTINA AL HIPOTÁLAMO

La leptina es una hormona peptídica producida principalmente en el tejido adiposo blanco y está implicada en el control de la ingestión alimentaria y en el gasto energético, actuando en células neuronales del hipotálamo, en el sistema nervioso central (SNC). Además, estudios recientes muestran que la leptina regula diferentes vías endocrinas con acciones centrales y periféricas. Se sintetiza en el epitelio gástrico, la glándula mamaria y la placenta [10], posee una estructura semejante a la de las citocinas y tiene su pico de liberación durante la noche y las primeras horas de la mañana [11], y una vida media plasmática de 30 min [12]. Se han descrito seis formas proteicas diferentes de este receptor, que se denominan Ob-Ra a Ob-Rf [13,14]. Ob-R se produce alternativamente en diferentes formas de *splice*, denominadas Ob-Ra, Ob-Rb, Ob-Rc, Ob-Rd, Ob-Re y Ob-Rf [15,16], que tienen en común un dominio extracelular de 800 aminoácidos, un dominio transmembrana de 34 aminoácidos y un dominio variable intracelular, característico para cada isoforma. Estas isoformas puede dividirse en tres clases: cortas, largas y secretadas [17].

La forma Ob-Rb es la que se expresa predominantemente en las neuronas del ARC y, de acuerdo con la mayoría de los estudios realizados, es la principal responsable de la transducción de la señal de la leptina en esta región anatómica [13]. Como otros miembros de la familia de receptores de la clase I de citocinas, el Ob-Rb (así como el resto de Ob-R) no posee una actividad catalítica intrínseca y está constitutivamente ligada a una proteína citosólica con actividad tirosincinasa, denominada Janus cinasa 2 (JAK-2) [18].

Ob-Ra y Ob-Rc se expresan ampliamente en el plexo coroideo y en los microvasos, donde actúan en la captación de la leptina o en la efusión del líquido cefalorraquídeo, así como en el transporte de la leptina a través de la barrera hematoencefálica [19,20]. La isoforma Ob-Re, que carece de dominio intracelular y puede codificar un receptor soluble, se representa mediante un producto de *splice* o de clivaje proteolítico [15]. En ratones se ha descrito que cuando la Ob-Re se produce en grandes cantidades, actúa como un sistema tampón, captando la leptina que está libre en la circulación [21]. Se ha demostrado que la Ob-R soluble es el principal conector de la leptina en actividad en la sangre humana [22] y que este hecho puede estar determinado por el sexo, la adiposidad y la administración de leptina [23]. En principio, las acciones directas de la leptina se describieron sólo en el SNC. Sin embargo, recientemente se ha observado que la distribución de Ob-Ra y Ob-Rb se reflejan en la multiplicidad de efectos biológicos en tejidos extraneuronales, lo que sugiere evidencias sobre las diferentes funciones pleiotrópicas de la leptina [17].

La conexión de la leptina con su receptor promueve la captación de otra unidad de receptor que se encuentre adyacente, formando así una estructura transitoriamente dimérica (Fig. 2a) [24]. La modificación conformacional inducida por la unión de la leptina y por la dimerización de los receptores induce la actividad catalítica de la enzima JAK-2 asociada, que se autofosforila en varios residuos de tirosina, volviéndose activa, y así, a continuación, fosforilar y activar otra molécula de JAK-2 ligada a un segundo receptor [13]. En consecuencia, las JAK-2 activas catalizan la fosfo-

rilación de los receptores Ob-Rb en las tirosinas 985 y 1138 [25]. De esta manera se crean tres sitios activos que darán continuidad a la señal de la leptina (Fig. 2b). El primer sitio promueve el reclutamiento y la fosforilación de la familia de sustratos del receptor de la insulina (IRS) [26]. Los IRS (principalmente, el IRS-2) fosforilados son los responsables de la activación de la enzima PI3K, que desempeña un papel relevante en la transducción de la señal de la leptina en relación con el control del ritmo de disparos neuronales, lo que, en última instancia, regula la liberación de neurotransmisores relacionados con el control del hambre y la termogénesis en los terminales sinápticos [27]. El segundo lugar se encuentra próximo al residuo tirosina 985 fosforilado en la Ob-Rb. No obstante, este sitio es responsable de la captación y activación de la enzima SHP-2, que actúa como intermediaria en la activación de p21ras y de la vía MAP cinasa, culminando con la activación de los ERK, que desempeñan un papel aún desconocido en el control de la expresión génica neuronal controlada por la leptina [28]. Por último, el tercer sitio se encuentra en las proximidades de la tirosina 1138 de la Ob-Rb fosforilada. Este sitio promueve el reclutamiento de moléculas de la familia de transductores de señal y activadores de la transcripción (STAT) –fundamentalmente, STAT-3–, responsables de conducir la señal generada por la leptina al núcleo, donde coordinará la transcripción de los genes neurotransmisores que se encargan de la señal hormonal [19].

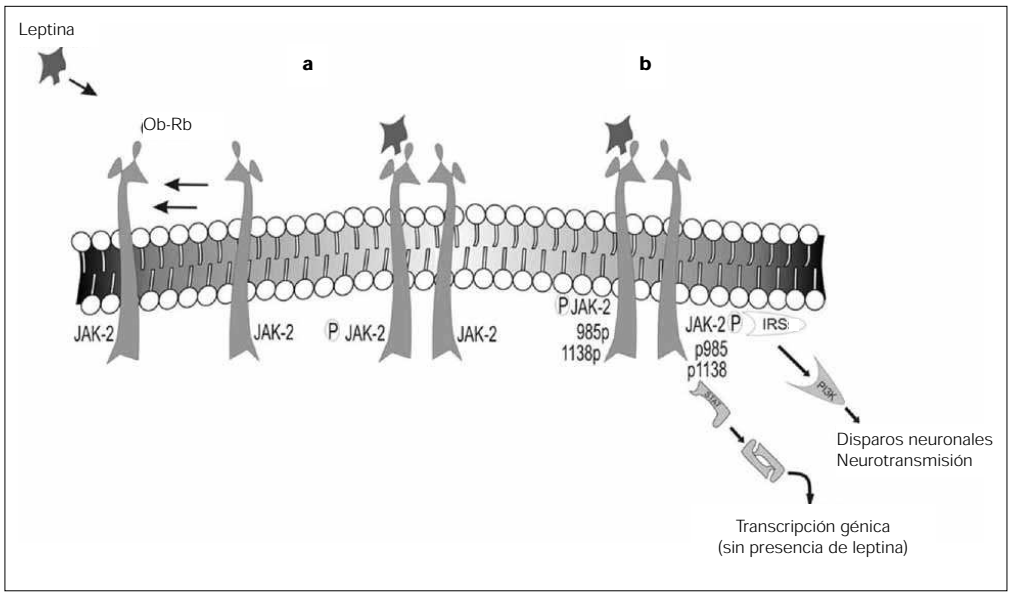

Figura 2. Señalización de la leptina en el hipotálamo. La leptina se une a su receptor (Ob-Rb), que se encuentra constitutivamente asociado a una molécula de JAK-2. La unión de la hormona promueve la dimerización de Ob-Rb. Una vez producida la dimerización, tiene lugar la fosforilación en tirosina de las moléculas de JAK-2 (a), que por fin catalizan la fosforilación de los Ob-Rb en los residuos tirosina 985 y 1138 (b). Los residuos tirosina fosforilados en las moléculas JAK-2 reclutan y fosforilan proteínas de la familia IRS (particularmente IRS-2), que dan continuidad a la señal de la leptina al activar la enzima fosfatidilinositol-3-cinasa (PI3K). Una vez se activa la PI3K, controla el ritmo de disparos neuronales y la liberación de neurotransmisores en las sinapsis. El residuo tirosina 1138 fosforilado en el Ob-Rb reúne y activa (a través de la acción catalítica de la JAK-2) proteínas de la familia STAT (particularmente STAT-3). Una vez fosforiladas, las proteínas STAT-3 se dimerizan y emigran al núcleo, donde actúan como factores de transcripción controlando la expresión de genes de neurotransmisores y otras proteínas que responden al estímulo de la leptina.

La comprensión del mecanismo molecular de la acción de la leptina en el hipotálamo proporcionó grandes avances en ese campo, pero, más tarde, las investigaciones realizadas en nuestro laboratorio demostraron que la transducción de la señal de esta hormona sufre un control importante mediante vías paralelas de señalización celular, resultando que, hasta el momento, la insulina destaca como la principal moduladora de la señal de la leptina [29-31]. Así pues, la comprensión de los efectos de la leptina sobre el control hipotalámico del hambre y la termogénesis requiere también el entendimiento de las acciones de la insulina en este lugar anatómico.

TRANSMISIÓN DE LA SEÑAL DE LA INSULINA EN EL HIPOTÁLAMO

La insulina se produce en el páncreas, en la células β de las islas pancreáticas y, al igual que la leptina, sus niveles plasmáticos son proporcionales a los cambios en la adiposidad [32], aumentando en los momentos de balance energético positivo y disminuyendo en los negativos.

El papel de la acción de la insulina en el SNC se describió hace dos décadas en un modelo primate que presentaba una disminución en la ingestión de alimentos cuando se infundía una baja dosis de insulina por vía intracerebroventricular [33]. Investigaciones recientes con animales de laboratorio demostraron que la insulina ejerce una función primordial en el SNC para incitar la saciedad, aumentar el gasto energético y regular la acción de la leptina [9]. Este descubrimiento despertó el interés de muchos investigadores, que pretenden encontrar respuestas que puedan explicar la acción de esta hormona en el control central de la saciedad.

Al contrario de lo que sucede con la leptina, las acciones moleculares de la insulina constituyen el centro de los estudios desde los años ochenta, cuando ya se caracterizaba la actividad tirosincinasa de su receptor (IR) [34]. El objetivo de la mayoría de los estudios realizados era entender el mecanismo molecular de esa hormona en los tejidos periféricos. Hay que señalar que tan sólo en los últimos diez años se han conseguido avances importantes en el conocimiento de su acción central o, más específicamente, de su acción hipotalámica.

No existen diferencias estructurales entre el IR expresado en tejidos periféricos (músculo, hígado, tejido adiposo...) y en el SNC [35]. Así, la insulina, tras unirse al IR (subunidad α) presente en el hipotálamo, promueve, a través de la modificación conformacional, la activación de un lugar catalítico en la región que comprende las tirosinas de la subunidad β del receptor (Fig. 3a) [36].

Una vez activo, este sitio conduce a la autofosforilación del receptor, que lo convierte en apto para dar continuidad a la transducción de la señal [36]. En el hipotálamo, la insulina promueve la activación de por lo menos dos vías distintas de seña-

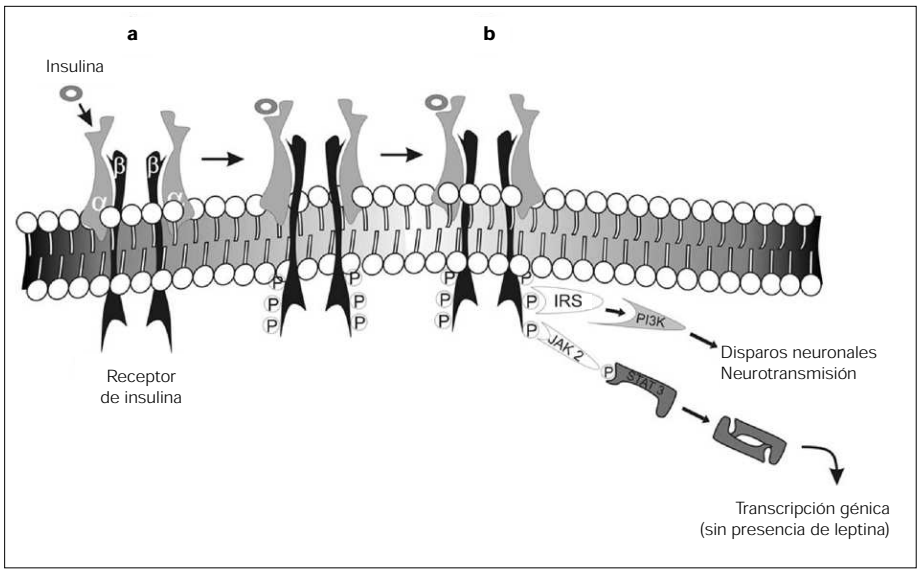

Figura 3. Señalización de la insulina en el hipotálamo. La insulina se une a su receptor heterotetramérico transmembrana (IR, de subunidades α y β), promoviendo la activación de su parte catalítica. Una vez activo, el IR cataliza su autofosforilación, la cual lo convierte en apto para reunir sustratos intracelulares que darán continuidad a la señal (a). Los residuos tirosina fosforilados captan y fosforilan las proteínas de la familia IRS (especialmente IRS-2), que transmiten la señal de la insulina y activan la enzima fosfatilinositol-3-cinasa (PI3K). Una vez activa, la PI3K controla el ritmo de disparos neuronales y la liberación de neurotransmisores en las sinapsis. El IR es capaz incluso de captar y activar la proteína JAK-2. Una vez fosforilada, la JAK-2 capta y fosforila proteínas de la familia STAT (particularmente STAT-3). Una vez fosforiladas, las proteínas STAT-3 se dimerizan y emigran hacia el núcleo, donde actúan como factores de transcripción controlando la expresión de genes de neurotransmisores y otras proteínas que responden al estímulo de la insulina, siempre que exista un coestímulo por parte de la leptina.

lización. La primera vía molecular depende de la captación y fosforilación en tirosina del IR y de los IRS [29,37]. Aquí, el IRS-2, de manera análoga al caso de la leptina, parece desempeñar un papel predominante, lo que se puede explicar en parte por la expresión preferencial en regiones que poseen un mayor número de neuronas que portadoras del IR [36]. La fosforilación del IRS promueve la unión y activación del enzima PI3K [28,37], el cual, como en el caso de la leptina, conecta la señal de la insulina al control del ritmo de los disparos neuronales [27], lo que es condicionado por la activación de los canales de potasio ATP-dependientes [39]. Mediante el control del ritmo de los disparos neuronales, la insulina modula, paralelamente a la leptina, la liberación de neurotransmisores en las sinapsis efectoras [40]. La segunda vía depende de la activación de la enzima JAK-2. A pesar de poseer actividad tirosincinasa intrínseca, el IR es capaz de interactuar y activar el JAK-2 en varios tejidos, incluso el hipotálamo [29,30]. Tras fosforilarse y activarse, la enzima JAK-2 recluta y fosforila STAT-3, que conecta la señal de la insulina al control de transcripción de los genes de neurotransmisores implicados en el control del hambre y la termogénesis (Fig. 3b) [29]. Cabe señalar que la activación de la transcripción génica de la insulina a través de la STAT-3 sólo es posible en presencia de la leptina [29].

La comprensión de los mecanismos intracelulares de actuación de la insulina y la leptina en el hipotálamo conducen a la interpretación de que las acciones hormonales se producen en vías celulares similares. Por tanto, ambas hormonas controlan de manera recíproca los efectos generados por la otra. A este fenómeno de comunicación entre vías de señalización y modulación de los sucesos celulares se le denomina *cross-talk* molecular. Todo indica que el *cross-talk* entre las vías de señalización de la leptina y la insulina ejerce un importante papel regulador sobre los efectos fisiológicos finales de cada una de estas hormonas.

EL *CROSS-TALK* ENTRE LAS VÍAS DE SEÑALIZACIÓN DE LA LEPTINA Y LA INSULINA EN EL HIPOTÁLAMO

La confirmación de la existencia de un *cross-talk* entre las vías de señalización de la leptina y la insulina fue presentada por primera vez por un grupo de investigadores que observó que el tratamiento periférico con leptina era capaz de mejorar la hiperglucemia en los ratones ob/ob (obeso e hiperglucémico por deficiencia en leptina), independientemente de la reducción de la masa corporal [41]. El progreso en esa línea de investigación y la interpretación de los resultados conseguidos en referencia a la acción de la insulina en el hipotálamo hicieron que se creyera que también en el hipotálamo la leptina y la insulina podrían interactuar y producir efectos complementarios. Estudios posteriores realizados en nuestro laboratorio confirmaron la sospecha y revelaron que este *cross-talk* se produce en al menos dos vías distintas, produciendo resultados funcionales también diferentes [29]. La primera vía es la JAK-2/STAT-3. Como se ha mencionado anteriormente, tanto la leptina como la insulina son capaces de inducir la activación de la JAK-2 y la fosforilación de la STAT-3. Sin embargo, sólo la leptina, cuando actúa de manera aislada, es capaz de inducir la transcripción génica mediada por STAT-3. Cuando la fosforilación de la STAT-3 se produce mediante la insulina, la transcripción observada con la leptina no se produce. Sin embargo, cuando actúan en conjunto, se pone en evidencia que la insulina potencia la actividad transcripcional de STAT-3 inducida por la leptina (Fig. 4). Así, se concluye que en el hipotálamo, la vía JAK-2/STAT-3 es controlada en primer lugar por la leptina, sufriendo una modulación incrementada por la insulina [29].

La segunda vía que participa del *cross-talk* entre esas hormonas es la vía IRS/PI3K. Los estudios muestran que, en este caso, el efecto de la insulina predomina sobre el de la leptina, lo cual provoca una mayor activación de la PI3K y, en consecuencia, un mayor ritmo de los disparos neuronales porque entonces la leptina desempeña un papel potenciador [4,38] (Fig. 4).

De este modo, tanto la leptina como la insulina desempeñan acciones clave en la modulación de la saciedad. No obstante, nuevos descubrimientos han puesto de manifiesto que las proteínas que actúan tras la PI3K también tienen acciones importantes en el control central del hambre. La PI3K activa la Akt (una proteína que actúa tras la PI3K) y promueve la fosforilación del factor de transcripción de la família *forkhead BOX O* (FOXO1) [42]. La fosforilación de la FOXO1 conduce a la exclusión nuclear y a la degradación proteosómica, y gracias a eso reduce su acción. Se sabe que la FOXO1 modula las accio-

nes de la insulina, incluyendo la gluconeogénesis, la oferta de glucosa al músculo esquelético, la diferenciación de los adipocitos y el crecimiento de las células β pancreáticas [43,44]. Sin embargo, además de los efectos periféricos, la FOXO1 regula la señalización de la insulina en el hipotálamo y la grasa corporal, controlando ambos circuitos. En un estudio reciente [42], un grupo de investigadores demostró que la activación de la FOXO1 en el ARC del hipotálamo aumenta la ingestión alimentaria y disminuye el gasto energético. Ambos cambios conducen al aumento de la masa corporal. Por el contrario, la inhibición central de la FOXO1 reduce la ingestión alimentaria y la masa corporal. De manera notable, los efectos anorexigénicos de la insulina y la leptina disminuían significativamente cuando se activaba la FOXO1 hipotalámica.

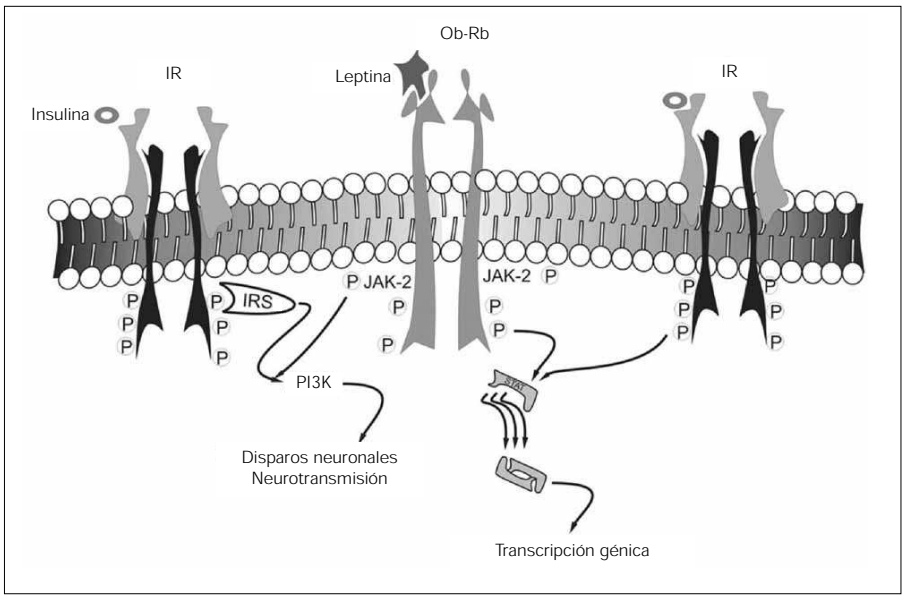

Figura 4. *Cross-talk* entre las vías de señalización de la leptina y la insulina en el hipotálamo. La unión de la insulina y la leptina a sus respectivos receptores (IR y Ob-Rb), promueve la activación de las vías intracelulares, que pueden comunicarse por lo menos en dos niveles distintos. El primer nivel (a la izquierda de la figura) cuenta con la enzima fosfatidilinositol-3-cinasa (PI3K), que se comporta como un centro preferencial de las proteínas de la familia IRS (especialmente IRS-2) activadas a través del IR. En presencia de una señal de leptina simultánea, se produce una acentuación de la señal de la insulina a través de esta vía. El segundo nivel (a la derecha de la figura) cuenta con las proteínas de la familia STAT (particularmente STAT-3). Una vez activos primordialmente a través de Ob-Rb, la señal mediante STAT-3 puede intensificarse en presencia de una señal concomitante de insulina.

La FOXO1 promueve tales modificaciones fisiológicas porque estimula la transcripción de los neuropéptidos orexígenos –NPY y AgRP– a través de la vía de señalización de la PI3K, pero suprime la transcripción anorexigénica de la POMC por la acción antagonista y la actividad de la señal de la STAT-3 [42]. Estos datos sugieren que la supresión de la actividad de la FOXO1 hipotalámica es necesaria para la inducción de la anorexia de la leptina y la insulina, estableciendo una nueva vía de señalización mediante la cual la insulina y la leptina actúan en neuronas hipotalámicas para controlar la ingestión alimentaria.

Por tanto, es evidente que existe un complejo mecanismo del control central de la saciedad, y todo indica que ese control va más allá de las proteínas iniciales de la cascada de señalización de la insulina y la leptina, lo cual sugiere que las vías distales también desempeñan un papel clave en la modulación del apetito. A continuación veremos los resultados funcionales de la acción de la leptina y de la insulina en el hipotálamo. Los efectos predominantes de estas hormonas en vías distintas tienen implicaciones importantes en el patrón temporal de control de la regulación de la ingestión alimentaria. La insulina, que actúa fundamentalmente sobre ritmos de disparos, ejerce control sobre fenómenos más inmediatos, mientras que la leptina, al controlar la transcripción génica, se encarga de fenómenos más duraderos.

PAPEL FUNCIONAL DE LA INSULINA Y LA LEPTINA EN EL CONTROL HIPOTALÁMICO DE LA SACIEDAD Y LA TERMOGÉNESIS

Como se refirió al principio, la expresión de los receptores Ob-Rb e IR en el SNC se identificó en diversas regiones del cerebro; sin embargo, varios investigadores demostraron que están situados en el hipotálamo y, más específicamente, en el ARC [14,37,45,46]. La mayoría de estudios sugiere que ambos, Ob-Rb e IR, están igualmente presentes en las dos subpoblaciones de neuronas, es decir, tanto en las que expresan los neurotransmisores NPY y AgRP, como en las que expresan los neurotransmisores anorexigénicos α-MSH (clivado a partir de POMC y CART) [4,19,25,27]. Sin embargo, en una investigación reciente, Xu et al [27] presentaron evidencias de que sólo las neuronas α-MSH/CARTérgicas expresan Ob-Rb e IR, y que las neuronas NPY/AgRPérgicas poseen tan sólo el IR [27]. A pesar de que, desde el punto de vista funcional, tal controversia se centre en pocas diferencias, cuando se discute la viabilidad de utilizar tratamientos neuromoduladores como método farmacoterapéutico para la obesidad, esa información pasa a tener un valor determinante, tal y como se discute más adelante.

Las neuronas α-MSH/CARTérgicas del ARC poseen conexiones inhibidoras cortas con las neuronas NPY/AgRPérgicas y conexiones inhibidoras largas con neuronas localizadas en el (LH), además de poseer largas conexiones excitadoras con neuronas del PVN [2]. Las características de las conexiones de las neuronas NPY/AgRPérgicas son más controvertidas. Desde el punto de vista tradicional –que postula que tanto las neuronas NPY/AgRPérgicas como las α-MSH/CARTérgicas expresan Ob-Rb e IR–, estas neuronas apenas poseen conexiones inhibidoras largas con el PVN y excitadoras largas con el LH [2]. Sin embargo, de acuerdo con la visión más reciente del sistema –que postula que tan sólo las neuronas α-MSH/CARTérgicas expresan Ob-Rb e IR, mientras que las neuronas NPY/AgRPérgicas expresan sólo el IR–, además de poseer conexiones inhibidoras largas con el PVN y excitadoras largas con el LH, las neuronas NPY/AgRPérgicas poseen también conexiones inhibidoras cortas con las neuronas α-MSH/CARTérgicas [27]. Las conexiones de ambos tipos de neuronas se efectúan con dos subpoblaciones distintas tanto en el PVN como en el LH. En el PVN existen neuronas que expresan los neurotransmisores CRH

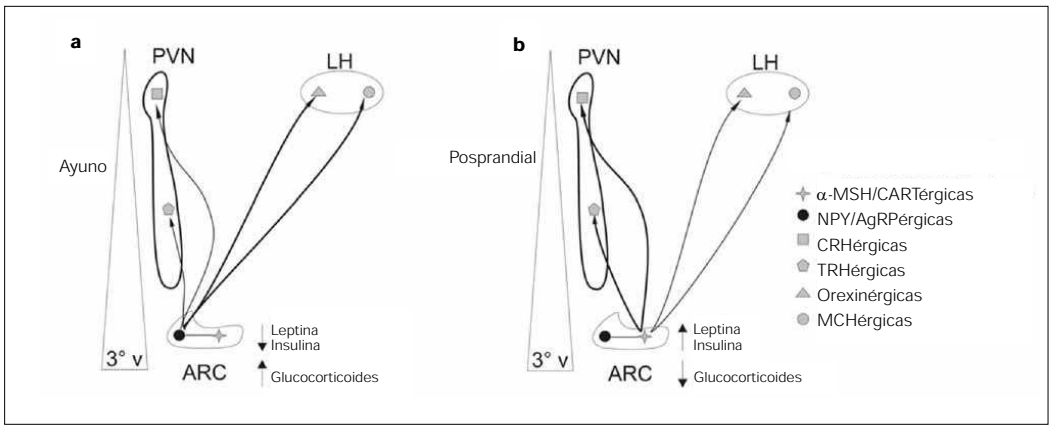

Figura 5. Regulación funcional de las neuronas hipotalámicas en respuesta a la leptina e insulina. Los receptores de la insulina y la leptina se distribuyen de manera predominante en dos subpoblaciones de neuronas del núcleo arqueado (ARC). Durante el ayuno (a), los bajos niveles de leptina e insulina llevan a la reducción de la producción de α-MSH/CART y al aumento de la producción de NPY/AgRP en el ARC. Las neuronas NPY/AgRPérgicas inhiben la producción de CRH y TRH por parte de las neuronas del núcleo paraventricular (PVN) y estimulan la producción de orexina y MCH por parte de las neuronas del hipotálamo lateral (LH), promoviendo un aumento del hambre y una reducción de la termogénesis. En períodos posprandiales (b), los niveles elevados de leptina e insulina inhiben la producción de NPY/AgRP y estimulan la producción de α-MSH/CART por las neuronas del ARC. Las neuronas α-MSH/CART inhiben la producción de orexina y MCH por el LH y estimulan la producción de CRH y TRH por el PVN, llevando a la saciedad y al aumento de la termogénesis. Además, otras señales endocrinas, como el aumento de la concentración de glucocorticoides (en el ayuno) y la reducción de la concentración de esos esteroides (posprandial), pueden regular las neuronas hipotalámicas del control del hambre.

y TRH [2]. Ambos neurotransmisores tienen funciones anorexigénicas y protermogénicas, ya que la TRH desempeña de manera predominante la función protermogénica, mientras que la CRH ejerce fundamentalmente una función anorexigénica [42, 45]. Por otro lado, en el LH también se han caracterizado dos subpoblaciones distintas, una de ellas que expresa la orexina, con un papel fundamentalmente orexigénico, y la otra que expresa el MCH, con un papel sobre todo –aunque no exclusivamente– antitermogénico [2,3,47].

En situaciones donde predominan los bajos niveles de leptina e insulina, como por ejemplo durante un ayuno prolongado y en individuos con un bajo porcentaje de grasa corporal, la mayor parte de los receptores Ob-Rb e IR del ARC están desocupados. En esta situación predominan las señales y conexiones excitadoras para las neuronas NPY/AgRpérgicas y las señales de conexiones inhibidoras para las α-MSH/CARTérgicas [3] (Fig. 5a). Como resultado, se produce un aumento de la expresión de la orexina y de MCH en el LH, acompañado de una reducción de la expresión de TRH y CRH en el PVN [3]. Por otro lado, tras una comida –que es principalmente el momento en que aumentan los niveles de insulina– o cuando se produce un leve aumento de la masa de tejido adiposo –lo que da como resultado un aumento de los niveles de leptina e insulina–, existe una reducción de la expresión de la orexina y MCH en el LH y un aumento de la expresión de TRH y CRH en el PVN (Fig. 5b). Los neurotransmisores expresados en el LH y el PVN no son los efectores finales de este complejo sistema de control del hambre y la homeostasis energética, pero sus participaciones son indispensables para que se produzca un funcionamiento adecuado e integrado de todo el sistema. Sólo a través de la modulación de la expresión de cada uno de estos intermediarios, las señales llevadas desde la periferia por la leptina y la insulina se convertirán en respuestas funcionales adecuadas que, en última instancia, mantendrán un perfecto acoplamiento entre la ingestión alimentaria y la termogénesis, dando como resultado una estabilidad en el peso corporal.

Además, otras señales hormonales, como el aumento de los niveles de glucocorticoides, pueden modular la homeostasis energética. Algunos estudios demuestran que la infusión de glucocorticoides en roedores aumenta el peso corporal y la ingestión alimentaria [48]. Paralelamente a estos sucesos fisiológicos, se pueden observar los aumentos de los niveles de NPY [49]. En este contexto, Ponsalle et al [50] demostraron que la adrenalectomía bloquea el aumento de los niveles de ARNm de la NPY inducida por el ayuno [50]. Por otro lado, otros datos apuntan que los elevados niveles de corticosterona sérica inducida por el ayuno no serían suficientes para aumentar los niveles de ARNm de la NPY en el hipotálamo de las ratas [51]. Tales datos sugieren que diversos factores son responsables del control del hambre y del gasto energético, siendo precipitado señalar un único agente para explicar estos hechos. Se confirma que fallos en algunos de los componentes de este complejo sistema de control de la homeostasis energética pueden desempeñar un importante papel en la génesis de la obesidad.

Esta controversia en los estudios no supone mucha diferencia desde el punto de vista funcional; sin embargo, cuando se discute la viabilidad de planteamientos neuromoduladores como método farmacoterapéutico para la obesidad, esa información puede tener un valor determinante. Así pues, los nuevos estudios deberían centrarse en aclarar esta cuestión.

RESISTENCIA A LA ACCIÓN DE LAS HORMONAS LEPTINA E INSULINA EN EL HIPOTÁLAMO EN LA GÉNESIS DE LA OBESIDAD

Los descubrimientos evidenciaron la acción hipotalámica de la insulina, como en el caso del fenómeno de resistencia a la insulina, clásicamente abordado en los tejidos periféricos, pero que también se podría producir en el hipotálamo. Una de las posibles consecuencias de su manifestación sería la reducción de la actividad anorexigénica y protermogénica ejercida por esta hormona. Además, considerando la acción moduladora positiva de la insulina sobre la actividad hipotalámica de la leptina, sería pertinente acreditar que la propia función adipostática de la leptina pueda estar afectada. Así, la búsqueda de evidencias experimentales y clínicas de que el fenómeno de resistencia hipotalámica a la acción de la insulina y la leptina podría existir y formar parte del cuadro de obesidad pasó a constituir el foco de interés de varios grupos en actividad en esta área del conocimiento.

La creación de un modelo transgénico de ratones con deleción del gen *IR* en neuronas específicas (NIRKO) se llevó a cabo

en el estudio de la acción de la insulina en el cerebro y sus respuestas fisiológicas. Resulta muy interesante que los ratones NIR-KO presentan como características la obesidad, la resistencia a la insulina, los elevados niveles plasmáticos de leptina y la alteración del perfil lipídico [52]. Las alteraciones fisiológicas observadas en esos animales proporcionan pruebas incontestables para afirmar que los defectos en el IR en el SNC conllevan descontrol del hambre y termogénesis, lo cual conduce a la obesidad.

Además del IR, la fosforilación de los IRS es determinante en la propagación de la señal de la insulina y las consiguientes respuestas moleculares de la hormona. Las funciones fisiológicas del IRS-1 e IRS-2 se establecieron recientemente a través de la producción de ratones sin los genes que codifican el IRS-1 o presenta resistencia a la insulina y retraso en el crecimiento, pero no es diabético [53]. Se demostró que el IRS-2 podría compensar parcialmente la ausencia de IRS-1, lo que explicaría el fenotipo de resistencia a la insulina sin hiperglucemia del ratón *knockout* de IRS-1. El ratón que no expresa el IRS-2 se generó posteriormente [54] y mostró un fenotipo diferente del ratón sin IRS-1: hiperglucemia acentuada como resultado de diversas anormalidades en la acción de la insulina en los tejidos periféricos, asociada a falta de actividad secretora de las células β. Esta última alteración es probablemente consecuencia de la reducción significativa de la masa de células β pancreáticas. Por tanto, parece evidente que el IRS-2 desempeña un papel predominante en el hipotálamo.

En cuanto a la actividad funcional de la leptina, se sabe que la expresión de la hormona está influida por diversas sustancias, como la insulina, los glucocorticoides, las endotoxinas y las citocinas proinflamatorias. Los estados infecciosos pueden elevar la concentración plasmática de la leptina. Por contra, la testosterona, la exposición al frío y las catecolaminas reducen la síntesis de esta hormona [55]. En situaciones de estrés, como el ejercicio físico intenso y el ayuno prolongado, se observa un nivel menor de la leptina circulante, lo que muestra la actuación del SNC en la inhibición de la liberación de la leptina por los adipocitos [56].

En animales de experimentación como los ratones ob/ob se ha confirmado que las altas concentraciones de leptina reducen la ingestión de alimentos, mientras que las bajas concentraciones inducen hiperfagia y un aumento de peso excesivo (obesidad) [57]. La leptina producida por el tejido adiposo informa del estado nutricional del individuo a los centros hipotalámicos, que regulan la ingestión alimentaria y el gasto energético. Así, la reducción de la cantidad de tejido adiposo conduce a la disminución de los niveles circulantes de leptina, estimulando la ingestión de alimentos y reduciendo el gasto energético. Por el contrario, el aumento de reservas de tejido adiposo se asocia al incremento de los niveles séricos de la leptina, lo que disminuye la ingestión alimentaria y aumenta el gasto energético. A través de ese mecanismo, el peso del individuo se mantiene estable durante varios años. ¿Por qué entonces algunos individuos desarrollan actividad y otros no? Se cree que la sensibilidad a la leptina puede ser variable y que los individuos obesos deben ser resistentes a la leptina [55,57,58]. Tan sólo una ínfima parte de la población obesa tiene bajos niveles séricos de leptina y desarrolla obesidad de manera semejante al ratón ob/ob [59,60].

Estos datos conflictivos entre animales de laboratorio y seres humanos indican que los mecanismos que controlan el metabolismo y el peso corporal son más complejos de lo que suele imaginarse.

EFECTOS DEL EJERCICIO FÍSICO EN EL CONTROL DEL APETITO: IMPLICACIONES EN EL BALANCE ENERGÉTICO

Hace mucho tiempo que se intenta comprender cómo se realiza la regulación del balance energético y el control del peso; la interrelación entre la actividad física y la ingestión alimentaria es importante porque ambos fenómenos son fundamentales en el control del peso corporal. Aunque los beneficios que el ejercicio proporciona a la salud están bien documentados, el impacto sobre la disminución de la masa adiposa es aún controvertido. Numerosos estudios han investigado los efectos de la actividad física en la ingestión de energía y el balance energético [61-63]. La mayoría de ellos presenta problemas, con una gran variedad de protocolos experimentales (ejercicios intermitentes o continuos, aerobios o anaerobios, etc.) utilizados en los estudios, o bien no cuentan con un grupo control ni incluyen información sobre la alimentación diaria [64,65]. Así pues, la interpretación de los datos aportados por las investigaciones es difícil. Con el fin de observar los resultados más concluyentes respecto a los efectos del ejercicio físico en el control alimentario, los investigadores llevan algunos años trabajando con animales de experimentación con el fin de descubrir los mecanismos moleculares mediante los cuales la actividad física desempeña un papel modulador sobre la ingestión alimentaria y la termogénesis. Más específicamente, en esta revisión presentamos algunas vías de señalización que el ejercicio físico puede modular en el SNC, y la posibilidad de que se aplique en la prevención y tratamiento del acúmulo excesivo de peso corporal.

EJERCICIO Y TRANSMISIÓN DE LA SEÑAL DE LA INSULINA

Trabajos realizados durante las últimas décadas demuestran claramente que el ejercicio físico aumenta la captación de glucosa en el músculo [66,67]. Además, recientemente se ha demostrado que la reducción de peso corporal asociada al aumento de la actividad física en individuos con un riesgo mayor de desarrollar diabetes, disminuye en un 58% la incidencia de esa enfermedad [68].

La insulina y el ejercicio físico son los estimuladores fisiológicos más relevantes en el transporte de la glucosa en el músculo esquelético [69]. Aunque el ejercicio físico no sea capaz de aumentar la fosforilación en tirosina del IR ni aumentar la fosforilación en tirosina del IRS-1 estimulada por la insulina [70], se observa que el ejercicio potencia el efecto de la insulina en la fosforilación del IRS-2 como consecuencia del aumento de la actividad de la PI3K [71]. Además, también se produce una mayor fosforilación en serina de la Akt, proteína fundamental para iniciar la translocación del GLUT4 a la membrana citoplasmática [72]. Los resultados publicados en nuestro laboratorio mostraron que el ejercicio de endurecimiento mejora la sensibilidad a la insulina, aumentando la fosforilación del IRS-1 y IRS-2 ,y la asociación de esas proteínas con la PI3K [66].

Todos esos datos confirman la importancia de la actividad física para mejorar la captación de la glucosa con mediación de la insulina en la periferia. A continuación veremos si el ejercicio físico puede proporcionar efectos favorable en el SNC.

EJERCICIO FÍSICO Y SNC

La importancia del ejercicio físico en el éxito de programas para perder y controlar el peso se ha reconocido desde hace varios

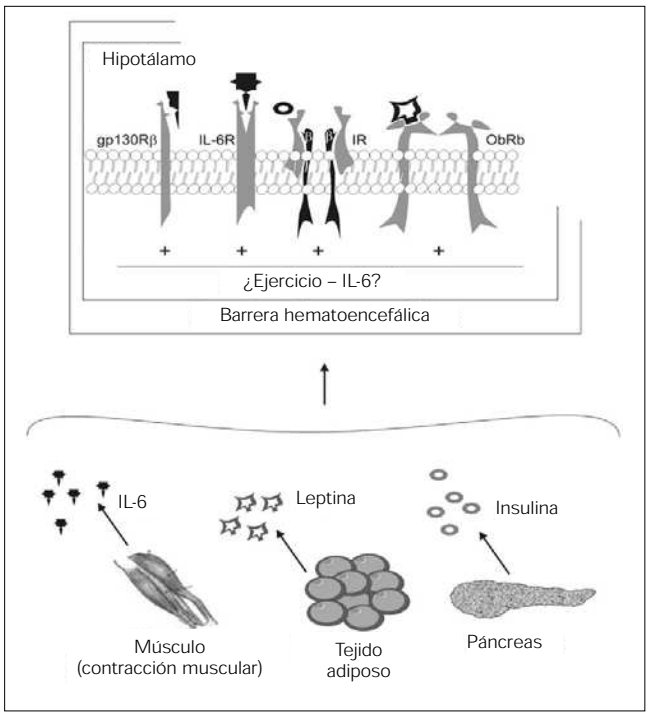

Figura 6. Ejercicio físico en la modulación de las vías intracelulares de control del hambre en el hipotálamo. El ejercicio físico aumenta la acción de la leptina y la insulina en el hipotálamo y eso favorece la reducción de la ingestión alimentaria. Posiblemente, este efecto supresor sobre el apetito se lleve a cabo por la producción de interleucina-6 (IL-6) por parte del músculo en actividad y tras su propia síntesis en el cerebro durante el ejercicio. La señalización a través del receptor gp130Rβ es similar a la de Ob-Rb. La señalización de la IL-6, al unirse a su receptor (IL-6Ra/gpP130Rβ), da como resultado la señalización de JAK/STAT e IRS/PI3K. La señal positiva (+) representa el aumento de la acción de la insulina, leptina e IL-6 gracias al ejercicio.

años [73,74]. El ejercicio físico aumenta el gasto energético a corto plazo y cuando se combina con la dieta es uno de los mejores predictores de la pérdida de peso a largo plazo [74]. Sin embargo, el efecto del ejercicio sobre las vías neuronales de control de la ingestión alimentaria y el gasto energético no está claro. Hasta el momento, pocos estudios inciden en la explicación de la relación entre el ejercicio y las vías hipotalámicas que regulan la homeostasis energética [75-77]. Por otro lado, numerosos estudios demuestran los efectos del ejercicio sobre otras funciones cerebrales que también utilizan neurotransmisores y factores tróficos para controlar la homeostasis energética. Éstos incluyen el factor liberador de la corticotropina (CRF) [78], la norepinefrina, la serotonina, el ácido γ-aminobutírico (GABA) [79] y el factor neurotrófico derivado del cerebro (BDNF) [80]. En el hipotálamo, la norepinefrina tiene efectos anabólicos [81], mientras que el CRF, la serotonina [82] y el BDNF [83] tienen efectos catabólicos.

En un trabajo reciente, Bi et al [84] confirmaron que los animales obesos sometidos a sesiones de ejercicios aerobios reducían de manera notable su adiposidad y la recuperación del peso se retrasaba. A pesar de haberse verificado concentraciones plasmáticas reducidas de leptina, no se observó un aumento de la ingestión alimentaria como medida compensatoria a la pérdida de peso. Ese efecto fue secundario a la acción directa del ejercicio en los núcleos dorsomediales del hipotálamo, regulando la expresión de los neuropéptidos CRF y NPY. Además, se ha demostrado que el ejercicio reduce la expresión de NPY en el hipotálamo de ratas diabéticas, lo cual sugiere que el ejercicio puede ser capaz de modular la ingestión alimentaria y el gasto energético a través de los circuitos neuronales [85].

Por tanto, de hecho, el ejercicio produce señales metabólicas, hormonales y neuronales que llegan hasta el cerebro, informándolo de que el cuerpo se está ejercitando. Entre esos factores, la interleucina-6 (IL-6) es particularmente interesante por el hecho de que es liberada por el músculo en contracción y puede, junto a la señalización de la melanocortina, aumentar la expresión de CRF en el PVN [79] y posiblemente en el núcleo dorsomedial. El estudio de Bi et al [84] apunta hacia un nuevo estado de algunas proteínas hipotalámicas responsables de la homeostasis energética, que tras interaccionar con moléculas liberadas por el músculo en contracción, responden a nuevos patrones energéticos en las ratas ejercitadas, como disminución de la ingestión alimentaria y menor acúmulo adipocitario.

EFECTOS DEL EJERCICIO FÍSICO EN LA MODULACIÓN DE LAS VÍAS INTRACELULARES DEL CONTROL DEL HAMBRE EN EL HIPOTÁLAMO

Se sabe que la actividad física de intensidad moderada y alta altera de manera acentuada el balance energético en ratas. En estudios anteriores, con animales, los programas de ejercicios de moderados a intensos contribuyen a la reducción de peso corporal y así retrasan el acúmulo energético en forma de tejido adiposo [73,74,78]. Mientras, no se conocen por completo las causas exactas que llevan a la supresión del apetito, mediadas por el ejercicio. Se sospecha que el ejercicio puede actuar en diversas regiones del cerebro y en diferentes neuropéptidos. Kotz [77] menciona que el estímulo o lesión de la LH provoca alteraciones en el comportamiento alimentario y en la actividad física diaria voluntaria, lo que conduce al entendimiento de una posible integración de estos dos sistemas comportamentales.

A continuación discutiremos las investigaciones científicas realizadas en nuestro laboratorio, presentando una discusión actual sobre el papel del ejercicio físico en el control central del hambre. Como ya se ha mencionado, la insulina y la leptina tienen efectos inductores de anorexia a través de la vía de la PI3K. En una reciente investigación evaluamos si el ejercicio altera la expresión y/o la actividad de las proteínas implicadas en la transducción de la señal de la insulina en el hipotálamo, tras ser estimuladas con la leptina y la insulina en ratas sometidas a una sesión intensa de natación. Las infusiones intracerebroventriculares de leptina e insulina redujeron de manera más acentuada la ingestión alimentaria en ratas que practicaron ejercicio que en animales sedentarios. La leptina y la insulina estimularon la fosforilación de las proteínas IRS-1 e IRS-2, así como las asociaciones de estos sustratos con la PI3K. También se observó que la fosforilación hipotalámica de la Akt es menor en animales sedentarios que en animales que practican ejercicio [86]. Esta tentativa de análisis e interpretación de los resultados conseguidos en ese estudio comprueba los datos irrefutables acerca de la señalización hipotalámica de la insulina y demuestra un aumento de la sensibilidad del hipotálamo para la acción tanto de la leptina como de la insulina en animales sometidos a ejercicio físico. Esos datos apoyan la hipótesis de que el ejercicio puede tener acciones supresoras del apetito a través de la vía hipotalámica de la PI3K.

Además, las evidencias científicas documentan que la IL-6 producida durante el ejercicio es capaz de actuar como un sensor de demanda energética en el músculo y, posiblemente, también

puede actuar en vías de señalización del cerebro implicadas en la homeostasis energética [87]. Así pues, investigamos la hipótesis de si la producción de IL-6 en el ejercicio aumenta la sensibilidad hipotalámica a la leptina y a la insulina. Cuando pretratamos los animales con el anticuerpo anti-IL-6, no se detectaron los efectos anorexigénicos de la insulina y la leptina administrada por vía intercerebroventricular [86]. Estos resultados corroboran estudios anteriores que demostraron que el tratamiento con IL-6 aumenta el gasto energético tanto en humanos como en animales [37,46,52]. Es posible que los efectos supresores del apetito ejercidos por la IL-6 pueden ser el resultado de su propia síntesis en el cerebro durante el ejercicio [54]. Por otro lado, la cantidad de IL-6 endocrina secretada por el trabajo muscular durante el ejercicio [55] puede alcanzar de manera apropiada el cerebro [30] e inducir su efecto supresor. De esta manera, parece evidente que el ejercicio físico aumenta la sensibilidad a la leptina y a la insulina en el hipotálamo y eso posiblemente deba ocurrir, como mínimo en parte, por la producción de IL-6 (Fig. 6).

Algunos estudios previos demostraron que diversas respuestas biológicas en diferentes tipos de células son inducidas por la IL-6, que activa STAT-3 vía JAK [88,89]. Como ya se discutió anteriormente, la leptina se une a un receptor homodimérico (LRb) que resulta de autofosforilar y activar la JAK, activando posteriormente la vía de señalización de la insulina IRS-1/PI3K (Fig. 4). La unión de la IL-6 al receptor IL-6R/gp130Rβ es el resultado de la activación de la señalización JAK/STAT e IRS-1/PI3K (Fig. 6) [90]. Los receptores gp130Rβ, LRb e IL-6R son homólogos al formar parte de la superfamilia de las citocinas y activan la vía de señalización JAK/STAT [91]. Reforzando esa idea, tales receptores son capaces de activar JAK/STAT y, a continuación, vías de transducción de las señales importantes del balance energético, como la vía de la PI3K [92,93] y de la mTOR [88]. Así pues, se sugiere que la IL-6 producida durante el ejercicio activa la vía de señalización de la JAK/STAT, y por ese motivo está implicada en la activación de las señales mediante los receptores de la insulina y la leptina, en el hipotálamo de las ratas (Fig. 6). Además, las moléculas que se unen al gp130R pueden actuar en el SNC a través de la presencia de este receptor en neuronas POMC (anorexigénico) y con ello reducir la ingestión alimentaria [89] (Fig. 6). En este contexto, el aumento de la producción de IL-6 por el ejercicio puede actuar de manera importante en el control alimentario y explica, al menos en parte, la acción molecular del ejercicio en el SNC.

A pesar de ser un asunto muy reciente, parece que no hay dudas respecto a los efectos del ejercicio físico en la supresión del apetito y su contribución al gasto energético. Cabe ahora investigar qué tipo de ejercicio, duración e intensidad provocan las mejores adaptaciones, y así la actividad física podrá utilizarse con mayor precisión en la prevención y lucha contra la obesidad.

CONCLUSIONES

La caracterización de la resistencia a la acción de la insulina y la leptina en el hipotálamo de humanos y animales obesos abre nuevas perspectivas de objetivos terapéuticos en el tratamiento de esa enfermedad. Particularmente, todo indica que el ejercicio físico puede ser una estrategia terapéutica para restaurar la acción de la insulina y la leptina en la transducción de la señal del hipotálamo de individuos obesos. Este aumento de sensibilidad del hipotálamo a la acción de esas hormonas puede ser mediada por la interacción de la IL-6, que aumenta en situación de práctica de ejercicio. Esos datos apoyan la hipótesis de que el ejercicio puede tener acciones supresoras del apetito mediadas por el hipotálamo.

BIBLIOGRAFÍA

1. Booth FW, Chakravarthy MV, Spangenburg EE. Exercise and gene expression: physiological regulation of the human genome through activity. J Physiol 2002; 543: 399-411.
2. Schwartz MW, Woods SC, Porte D Jr, Seeley RJ, Baskin DG. Central nervous system control of food intake. Nature 2000; 404: 661-71.
3. Flier JS. Obesity wars: molecular progress confronts an expanding epidemic. Cell 2004; 116: 337-50.
4. Stellar E. The physiology of motivation. Physiol Rev 1994; 101: 301-11.
5. Broberger C. Brain regulation of food intake and appetite: molecules and networks. J Intern Med 2005; 258: 301-27.
6. Wynne K, Stanley S, McGowan B, Bloom S. Appetite control. J Endocrinol 2005; 184: 291-318.
7. Broadwell RD, Brightman MW. Entry peroxidase into neurons of the central and peripheral nervous systems from extracerebral and cerebral blood. J Comp Neurol 1976; 166: 257-83.
8. Niswender KD, Baskin DG, Schwartz MW. Insulin and its evolving partnership with leptin in the hypothalamic control of energy homeostasis. Trends Endocrinol Metab 2004; 15: 362-8.
9. Baskin DG, Lattemann DF, Seeley RJ, Woods SC, Porte D Jr, Schwartz MW. Insulin and leptin: dual adiposity signals to the brain for the regulation of food intake and body weight. Brain Res 1999; 848: 114-23.
10. Friedman JM, Halaas JL. Leptin and the regulation of body weight in mammals. Nature 1998; 395: 763-70.
11. Sinha MK, Sturis J, Ohannesian J, Magosin S, Stephens T, Heiman M, et al. Ultradian oscillations of leptin secretion in humans. Biochem Biophys Res Commun 1996; 228: 733-8.
12. Maurigeri D, Bonanno MR, Speciale S, Santangelo A, Lentinia A, Russo MS, et al. The leptin, a new hormone of adipose tissue: clinical findings and perspectives in geriatrics. Arch Gerontol Geriatr 2002; 34: 47-54.
13. Tartaglia LA. The leptin receptor. J Biol Chem 1997; 272: 6093-6.
14. Chua SC Jr, Chung WK, Wu-Peng XS, Zhang Y, Liu SM, Tartaglia L, et al. Phenotypes of mouse diabetes and rat fatty due mutations in the OB (leptin) receptor. Science 1996; 271: 994-6.
15. Lee GH, Proenca R, Montez JM, Carroll KM, Darvishzadeh JG, Lee JI, et al. Abnormal splicing of the leptin receptor in diabetic mice. Nature 1996; 379: 632-5.
16. Wang MY, Zhou YT, Newgard CB, Unger RH. A novel leptin receptor isoform in rat. FEBS Lett 1998; 392: 87-90.
17. Fruhbeck G. Intracellular signaling pathways activated by leptin. Biochem J 2006; 393 (Pt 1): 7-20.
18. Bjorbaek C, Uotani S, Da Silva B, Flier JS. Divergent signaling capacities of the long and short isoforms of the leptin receptor. J Biol Chem 1997; 272: 32686-95.
19. Bjorbaek C, Kahn BB. Leptin signaling in the central nervous system and the periphery. Rec Prog Horm Res 2004; 59: 305-31.
20. Hileman SM, Pierroz DD, Masuzaki H, Bjorbaek C, El-Haschimi K, Banks WA, et al. Characterization of short isoforms of the leptin receptor in rat cerebral microvessels and of brain uptake of leptin in mouse models of obesity Endocrinology 2002; 143: 775-83.
21. Löllmann B, Gruninger S, Stricker-Krongrad A, Chiesi M. Detection and quantification of the leptin receptor splice variants Ob-Ra, b, and e in different mouse tissues. Biochem Biophys Res Commun 1997; 238: 648-52.
22. Lammert A, Kiess W, Bottner A, Glasow A, Kratzsch J. Soluble leptin receptor represents the main leptin binding activity in human blood. Biochem Biophys Res Commun 2001; 283: 982-8.
23. Chan JL, Bluher S, Yiannakouris N, Suchard MA, Kratzsch J, Mantzoros CS. Regulation of circulating soluble leptin receptor levels by gender, adiposity, sex steroids, and leptin: observational and interventional studies in humans. Diabetes 2002; 51: 2105-12.
24. Zabeau L, Lavens D, Peelman F, Eyckerman S, Vandekerckhove J, Tavernier J. The ins and outs of leptin receptor activation. FEBS Lett 2003; 546; 45-50.
25. Munzberg H, Myers MG. Molecular and anatomical determinants of central leptin resistance. Nat Neurosci 2005; 8: 566-70.
26. Kelerrer M, Koch M, Metzinger E, Mushack J, Capp E, Haring HU. Leptin activates PI3 kinase in C2C12 myotubes via janus kinase-2

(JAK-2) and insulin receptor substrate-2 (IRS-2) dependent pathways. Diabetologia 1997; 40: 1358-62.
27. Xu AW, Kaelin CB, Takeda K, Akira S, Schwartz MW, Barsh GS. PI3K integrates the action of insulin and leptin on hypothalamic neurons. J Clin Invest 2005; 115: 951-8.
28. Bjorbaek C, Buchholz RM, Davis SM, Bates SH, Pierroz DD. Divergent roles of SHP-2 in ERK activation by leptin receptors. J Biol Chem 2001; 276: 4747-55.
29. Carvalheira JB, Siloto RM, Ignacchitti I, Brenelli SL, Carvalho CR. Insulin modulates leptin-induced STAT3 activation in rat hypothalamus. FEBS Lett 2001; 500: 119-24.
30. Carvalheira JB, Ribeiro EB, Folli F, Velloso LA, Saad MJ. Interaction between leptin and insulin signaling pathways differentially affects JAK-STAT and PI3-kinase-mediated signaling in rat liver. Biol Chem 2003; 384: 151-9.
31. Carvalheira JB, Torsoni MA, Ueno M, Amaral ME, Araujo EP, Velloso LA, et al. Cross-talk between the insulin and leptin signaling systems in rat hypothalamus. Obes Res 2005; 13: 48-57.
32. Kahn BB, Flier JS. Obesity and insulin resistance. J Clin Invest 2000; 106: 473-81.
33. Woods SC, Lotter EC, McKay LD, Porte D Jr. Chronic intracerebroventricular infusion of insulin reduces food intake and body weight of baboons. Nature 1979; 282: 503-5.
34. Kasuga M, Karisson FA, Kahn CR. Insulin stimulates the phosphorilation of the 95,000-dalton subunit of its own receptor. Science 1982; 215: 185-7.
35. Saltiel AR, Kahn CR. Insulin signaling and the regulation of glucose and lipid metabolism. Nature 2001; 414: 799-806.
36. White MF. The insulin signaling system and the IRS proteins. Diabetologia 1997; 40: S2-17.
37. Torsoni MA, Carvalheira JB, Pereira-Da Silva M, De Carvalho-Filho MA, Saad MJ, Velloso LA. Molecular and functional resistance to insulin in hypothalamus of rats exposed to cold. Am J Physiol Endocrinol Metab 2003; 285: E216-23.
38. Carvalheira JB, Ribeiro EB, Araujo EP, Guimaraes RB, Telles MM. Selective impairment of insulin signaling in the hypothalamus of obese Zucker rats. Diabetologia 2003; 46: 1629-40.
39. Plum L, Schubert M, Bruning JC. The role of insulin receptor signaling in the brain. Trends Endocrinol Metab 2005; 16: 59-65.
40. Saad MJ, Carvalho CR, Thirone AC, Velloso LA. Insulin reduces tyrosine phosphorylation of JAK2 in insulin-sensitive tissues of the intact rat. J Biol Chem 1996; 271: 22100-4.
41. Sivitz WI, Walsh SA, Morgan DA, Thomas MJ, Haynes WG. Effects of leptin on insulin sensitivity in normal rats. Endocrinology 1997; 138: 3395-401.
42. Kim MS, Pak YK, Jang PG, Namkoong C, Choi YS, Won JC, et al. Role of hypothalamic Foxo1 in the regulation of food intake and energy homeostasis. Nat Neurosci 2006; 9: 1-6.
43. Puigserver P, Rhee J, Donovan J, Walkey CJ, Yoon JC, Oriente F, et al. Insulin-regulated hepatic gluconeogenesis through FOXO1–PGC-1alpha interaction. Nature 2003; 423: 550-5.
44. Kitamura T. Nakae J, Kitamura Y, Kido Y, Biggs WH III, Wright CV, et al. The forkhead transcription factor Foxo1 links insulin signaling to Pdx1 regulation of pancreatic beta cell growth. J Clin Invest 2002; 110: 1839-47.
45. Folli F, Bonfanti L, Renard E, Kahn CR, Merighi A. Insulin receptor substrate-1 (IRS1) distribution in the rat central nervous system. J Neurosci 1994; 14: 6412-22.
46. De L.A. Fernandes ML, Saad MJ, Velloso LA. Insulin induces tyrosine phosphorylation of the insulin receptor and SHC, and SHC/GRB2 association in cerebellum but not in forebrain cortex of rats. Brain Res 1999; 826: 74-82.
47. Pereira-Da Silva M, Torsoni MA, Nourani HV, Augusto VD, Souza CT, Gasparetti AL, et al. Hypothalamic melanin-concentrating hormone is induced by cold exposure and participates in the control of energy expenditure in rats. Endocrinology 2003; 144: 4831-40.
48. Michel C, Cabanac M. Effects of dexamethasone on the body weight set point of rats. Physiol Behav 1999, 68: 145-50.
49. Zakrzewska KE, Cusin I, Stricker-Krongrad A, Boss O, Ricquier D, Jeanrenaud B, et al. Induction of obesity and hyperleptinemia by central glucocorticoid infusion in the rat. Diabetes 1999; 48: 365-70.
50. Ponsalle P, Srivistava LS, Uht RM, White JD. Glucocorticoids are required for food-deprivation-induced increases in hypothalamic neuropeptide Y expression. Neuroendocrinology 1993, 4: 585-91.
51. Hanson ES, Levin N, Dallman MF. Elevated corticosterone is not required for the rapid induction of neuropeptide Y gene expression by an overnight fast. Endocrinology 1997; 138: 1041-7.
52. Bruning JC, Gautam D, Burks DJ, Gillete J, Schubert M, Orban PC, et al. Role of brain insulin receptor in control of body weight and reproduction. Science 2000; 289: 2122-5.
53. Araki E, Lipes MA, Patti ME, Bruning JC, Haag B, Johnson RS. Alternative pathway of insulin signalling in mice with targeted disruption of the IRS-1 gene. Nature 1994; 372: 186-90.
54. Withers DJ, Gutiérrez JS, Towery H, Burks DJ, Ren JM, Previs S. Disruption of IRS-2 causes type 2 diabetes in mice. Nature 1998; 391: 900-4.
55. Friedman JM, Halaas JL. Leptin and the regulation of body weight in mammals. Nature 1998; 395: 763-70.
56. Sandoval DA, Davis SN. Leptin: metabolic control and regulation. J Diabetes Complications 2003; 2: 108-13.
57. Wilding JP. Leptin and the control of obesity. Curr Opin Pharmacol 2001; 6: 656-61.
58. Considine RV, Sinha MK, Heiman ML, Kriauciunas A, Stephens TW, Nyce MR. Serum immunoreactive-leptin concentrations in normal-weight and obese humans. N Engl J Med 1996: 334: 292-5.
59. Farooqi IS, Keogh JM, Kamath S, Jones S, Gibson WT, Trussell R, et al. Partial leptin deficiency and human adiposity. Nature 2001; 414: 34-5.
60. Montague CT, Farooqi IS, Whitehead JP, Soos MA, Rau H Wareham NJ, et al. Congenital leptin deficiency is associated with severe early-onset obesity in humans. Nature 1997; 387: 903-8.
61. Jakicic JM, Otto AM. Physical activity considerations for the treatment and prevention of obesity. Am J Clin Nutr 2005; 82: S226-9.
62. Kretschmer BD, Schelling P, Norbert B, Liebscher C, Treutel S, Kruger N, et al. Modulatory role of food, feeding regime and physical exercise on body weight and insulin resistance. Life Sci 2005; 76: 1553-73.
63. Long SJ, Hart K, Morgan M. The ability of habitual exercise to influence appetite and food intake in response to high- and low-energy preloads in man. Br J Nutr 2002; 87: 517-23.
64. Melzer K, Kayser B, Saris WHM, Pichard C. Effects of physical activity on food intake. Clin Nutr 2005; 8: 2-11.
65. Donnely JE, Smith B, Jacobsen DJ, Kirk E, Du Bose K, Hyder M, et al. The role of exercise for weight loss and maintenance. Bets Pract Res Clin Gastroenterol 2004; 18: 1009-29.
66. Luciano E, Carneiro EM, Carvalho CR, Carvalheira JB, Peres SB, Reis MA, et al. Endurance training improves responsiveness to insulin and modulates insulin signal transduction through the phosphatidylinositol 3-kinase/Akt-1 pathway. Eur J Endocrinol 2002; 147: 149-57.
67. Kennedy JW, Hirshman MF, Gervino EV, Ocel JV, Forse RA, Hoenig SJ, et al. Acute exercise induces GLUT4 translocation in skeletal muscle of normal human subjects and subjects with type 2 diabetes. Diabetes 1999; 48: 1192-7.
68. Knowler WC, Barrett-Connor E, Fowler SE, Hamman RF, Lachin JM, Walker EA, et al. Reduction in the incidence of type 2 diabetes with lifestyle intervention or metformin. N Engl J Med 2002; 346: 393-403.
69. Goodyear LJ, Kahn BB. Exercise, glucose transport, and insulin sensitivity. Annu Rev Med 1998; 49: 235-61.
70. Henriksen EJ. Invited review: effects of acute exercise and exercise training on insulin resistance. J Appl Physiol 2002; 93: 788-96.
71. Howlett KF, Sakamoto K, Hirshman MF, Aschenbach WG, Dow M, White MF, et al. Insulin signaling after exercise in insulin receptor substrate-2-deficient mice. Diabetes 2002; 51: 479-83.
72. Wojtaszewski JF, Higaki Y, Hirshman MF, Michael MD, Dufresne SD, Kahn CR, et al. Exercise modulates postreceptor insulin signaling and glucose transport in muscle-specific insulin receptor knockout mice. J Clin Invest 1999; 104: 1257-64.
73. Miller WC, Koceja DM, Hamilton EJA. Meta-analysis of the past 25 years of weight loss research using diet, exercise or diet plus exercise intervention. Int J Obes Relat Metab Disord 1997; 21: 941-7.
74. Pronk NP, Wing RR, Hamilton EJ. Physical activity and long-term maintenance of weight loss. Obes Res 1994; 2: 587-91.
75. Bovetto S, Richard D. Lesion of central nucleus of amygdala promotes fat gain without preventing effect of exercise on energy balance. Am J Physiol 1995; 269: R781-6.
76. Rivest S, Richard D. Involvement of corticotropin-releasing factor in the anorexia induced by exercise. Brain Res Bull 1990; 25: 169-72.
77. Kotz CM. Integration of feeding and spontaneous physical activity: role for orexin. Physiol Behav 2006; 88: 294-301.
78. Pauli JR, Gomes RJ, Luciano E. Eje hipotálamo-pituitario: efectos del entrenamiento físico en ratas Wistar con administración de dexametasona. Rev Neurol 2006; 42: 325-31.
79. Dishman RK. Brain monoamines, exercise, and behavioral stress: animal models. Med Sci Sports Exerc 1997; 29: 63-74.
80. Neeper SA, Gómez-Pinilla F, Choi J, Cotman CW. Physical activity increases mRNA for brain-derived neurotrophic factor and nerve growth factor in rat brain. Brain Res 1996; 726: 49-56.
81. Leibowitz SF, Roossin P, Rosenn M. Chronic norepinephrine injection

into the hypothalamic paraventricular nucleus produces hyperphagia and increased body weight in the rat. Pharmacol Biochem Behav 1984; 21: 801-8.
82. Waldbillig RJ, Bartness TJ, Stanley BG. Increased food intake, body weight, and adiposity in rats after regional neurochemical depletion of serotonin. J Comp Physiol Psychol 1981; 95: 391-405.
83. Lyons WE, Mamounas LA, Ricaurte GA, Coppola V, Reid SW, Bora SH, et al. Brain-derived neurotrophic factor-deficient mice develop aggressiveness and hyperphagia in conjunction with brain serotonergic abnormalities. Proc Natl Acad Sci U S A 1999; 96: 15239-44.
84. Bi S, Scott KA, Hyun J, Ladenheim EE, Moran TH. Running wheel activity prevents hyperphagia and obesity in Otsuka long-evans Tokushima fatty rats: role of hypothalamic signaling. Endocrinology 2005; 146: 1676-85.
85. Shin MS, Kim H, Chang HK, Lee TH, Jang MH, Shin MC, et al. Treadmill exercise suppresses diabetes-induced increment of neuropeptide Y expression in the hypothalamus of rats. Neurosci Lett 2003; 346: 157-60.
86. Flores MB, Fernandes MF, Ropelle ER, Faria MC, Ueno M, Velloso LA, et al. Exercise improves insulin and leptin sensitivity in hypothalamus of Wistar rats. Diabetes 2006; 55: 2554-61.
87. Pedersen BK, Steenberg A, Fischer C, Keller C, Keller P, Plomgaard P, et al. The metabolic role of IL-6 produced during exercise: is IL-6 an exercise factor? Proc Nutr Soc 2004; 63: 263-7.
88. Cota D, Proulx K, Smith KA, Kozma SC, Thomas G, Woods SC, et al. Hypothalamic mTOR signaling regulates food intake. Science 2006; 312: 927-30.
89. Febbraio MA. gp130 receptor ligands as potential therapeutic targets for obesity. J Clin Invest 2007; 117: 841-9.
90. Janoschek R, Plum L, Koch L, Munzberg H, Diano S, Bruning JC. gp130 signaling in proopiomelanocortin neurons mediates the acute anorectic response to centrally applied ciliary neurotrophic factor. Proc Natl Acad Sci U S A 2006; 103: 10707-12.
91. Ernst M, Jenkins BJ. Acquiring signaling specificity from the receptor gp130. Trends Genet 2004; 20: 23-32.
92. Cohen B, Novick D, Rubinstein M. Modulation of insulin activities by leptin. Science 1996; 274: 1185-8.
93. Boulton TG, Stahl N, Yancopoulos GD. Ciliary neurotrophic factor/leukemia inhibitory factor/interleukin 6/oncostatin M family of cytokines induces tyrosine phosphorylation of a common set of proteins overlapping those induced by other cytokines and growth factors. J Biol Chem 1994; 269: 11648-55.

BRAIN REGULATION OF FOOD INTAKE AND EXPENDITURE ENERGY: MOLECULAR ACTION OF INSULIN, LEPTIN AND PHYSICAL EXERCISE

Summary. Introduction. *Overweight and obesity present significant public health concerns because of the link with numerous chronic health conditions. During the last ten years, since the discovery of leptin, great advances were obtained in the characterization oh the hypothalamic mechanisms involved in the control of food intake and thermogenesis.* Development. *This review will present some the most recent findings in this field. It will be focused on the actions of leptin and insulin in the hypothalamus and will explore the hypothesis that hypothalamic resistance to the action of these hormones may play a key role in the development of obesity. The physical activity is an important component on long-term weight control. The exercise markedly increased phosphorylation activity of several proteins involved in leptin and insulin signal transduction in the hypothalamus. Recently our laboratory showed that physical activity increase in sensitivity to leptin- and insulin-induced anorexia after enhances interleukin-6 production.* Conclusions. *These findings provide support for the hypothesis that the appetite-suppressive actions of exercise may be mediated by the hypothalamus. [REV NEUROL 2007; 45: 672-82]*
Key words. *Hypothalamus. Insulin. Interleukin-6. Leptin. Obesity. Physical exercise.*

APÊNDICE *VI*

J Physiol 587.9 (2009) pp 2069–2076

The Journal of Physiology

Acute exercise modulates the Foxo1/PGC-1α pathway in the liver of diet-induced obesity rats

Eduardo R. Ropelle[1], José R. Pauli[2], Dennys E. Cintra[1], Marisa J. S. Frederico[3], Ricardo A. de Pinho[3], Lício A. Velloso[1] and Cláudio T. De Souza[3]

[1]*Departamento de Clínica Médica, FCM, Universidade Estadual de Campinas (UNICAMP), Campinas, SP, Brazil*
[2]*Curso de Educação Física – Modalidade Saúde, Departamento de Biociências, UNIFESP, Santos, SP, Brazil*
[3]*Laboratório de Fisiologia e Bioquímica do Exercício, Programa de Pós-graduação em Ciências da Saúde, Universidade do Extremo Sul Catarinense, SC, Brazil*

PGC-1α expression is a tissue-specific regulatory feature that is extremely relevant to diabetes. Several studies have shown that PGC-1α activity is atypically activated in the liver of diabetic rodents and contributes to hepatic glucose production. PGC-1α and Foxo1 can physically interact with one another and represent an important signal transduction pathway that governs the synthesis of glucose in the liver. However, the effect of physical activity on PGC-1α/Foxo1 association is unknown. Here we investigate the expression of PGC-1α and the association of PGC-1α/Foxo1 in the liver of diet-induced obese rats after acute exercise. Wistar rats swam for two 3 h-long bouts, separated by a 45 min rest period. Eight hours after the acute exercise protocol, the rats were submitted to an insulin tolerance test (ITT) and biochemical and molecular analysis. Results demonstrate that acute exercise improved insulin signalling, increasing insulin-stimulated Akt and Foxo1 phosphorylation and decreasing PGC-1α expression and PGC-1α/Foxo1 interaction in the liver of diet-induced obesity rats under fasting conditions. These phenomena are accompanied by a reduction in the expression of gluconeogenesis genes, such as phosphoenolpyruvate carboxykinase (PEPCK) and glucose-6-phosphate (G6Pase). Thus, these results provide new insights into the mechanism by which exercise could improve fasting hyperglycaemia.

(Received 30 September 2008; accepted after revision 4 March 2009; first published online 9 March 2009)
Corresponding author Claudio Teodoro de Souza: Exercise Biochemistry and Physiology Laboratory. Postgraduate Program in Health Sciences. Health Sciences Unit. University of Southern Santa Catarina, Criciúma, SC, Brazil. Email: ctsouza@unesc.net

Abbreviations AMPK, AMP-activated protein kinase; BAT, brown adipose tissue; DTT, dithiothreitol; EDTA, ethylenediamine tetraacetic acid; G6Pase, glucose-6-phosphatase; GLUT4, glucose transporter-4; IRE, insulin response elements; ITT, insulin tolerance test; Kitt, rate constant for plasma glucose disappearance; PEPCK, phosphoenolpyruvate carboxykinase; PGC-1α, peroxisome proliferator-activated receptor-γ coactivator 1α; PI3K, phosphoinositide 3-kinase; PMSF, phenylmethanesulphonylfluoride; PPARγ, peroxisome proliferator-activated receptor-γ; RIA, radioimmunoassay; SDS-PAGE, sodium dodecyl sulfate-polyacrylamide gel electrophoresis; Tris, tris(hydroxymethyl)aminomethane.

In both type 1 and type 2 diabetes, excessive hepatic glucose production is a major contributor to both fasting and postprandial hyperglycaemia. Regulation of gluconeogenesis is crucial for the maintenance of glucose homeostasis. Phosphoenolpyruvate carboxykinase (PEPCK) and glucose-6-phosphatase (G6Pase) are nutritionally regulated in the liver at the transcriptional level, are highly activated during fasting or starvation, and are suppressed in the fed state. The regulation of both PEPCK and G6Pase genes at the transcriptional level involves a 'crosstalk' between a network of transcription factors. The PEPCK promoter has been extensively studied and is known to be induced by transcription factors such as Foxo1 and peroxisome proliferator-actived receptor-γ coativator-1α (PGC-1α) (for a review, see Postic *et al.* 2004). PGC-1α was identified through its functional interaction with the nuclear receptor peroxisome proliferator-activated receptor-γ (PPARγ) in brown adipose tissue (BAT), a mitochondria-rich tissue that is specialized in thermogenesis (Puigserver *et al.* 1998). However, PGC-1α expression is one of the tissue-specific regulatory features relevant to diabetes. Recent studies in animal models and humans link altered PGC-1α signalling to glucose intolerance, insulin

DOI: 10.1113/jphysiol.2008.164202

Table 1. Components of high fat and chow diet

Ingredients	Standard chow		High fat diet	
	(g kg^{-1})	(kcal kg^{-1})	(g kg^{-1})	(kcal kg^{-1})
Cornstarch (QSP)	397.5	1590	115.5	462
Casein	200	800	200	800
Sucrose	100	400	100	400
Dextrinated starch	132	528	132	528
Lard	—	—	312	2808
Soybean oil	70	630	40	360
Cellulose	50	—	50	—
Mineral mix	35	—	35	—
Vitamin Mix	10	—	10	—
L-Cystine	3	—	3	—
Choline	2.5	—	2.5	—
Total	1000	3948	1000	5358

resistance and diabetes. PGC-1α activity is as robustly activated in diabetic liver as it is in the fasted state (Herzig *et al.* 2001; Yoon *et al.* 2001; Puigserver *et al.* 2003; Rhee *et al.* 2003), potentially increasing hepatic glucose production, which in turn contributes to circulating hyperglycaemia. Adenovirus-mediated overexpression of PGC-1α in the rat liver causes an increase in hepatic glucose production, through the activation of all the key enzymes of gluconeogenesis, the transcriptional pathway implying that PGC-1α plays a crucial role in the transcriptional regulation of PEPCK and G6Pase genes. Indeed, PGC-1α affects gluconeogenic enzyme regulation by directly binding to transcription factors, such as Foxo1 (Puigserver *et al.* 2003). This factor plays an important role in the suppression of hepatic gluconeogenesis by insulin. *In vitro* studies have shown that Foxo1 regulates both PEPCK and G6Pase genes through an interaction with their consensus insulin response elements (IRE) present in their promoters (Daitoku *et al.* 2003). Therefore, insulin signalling through Akt can attenuate the effects of increased levels of PGC-1α in fasting and other conditions by promoting the dissociation of PGC-1α from Foxo1. Taken together, these results indicate that the complex formed by PGC-1α and Foxo1 is of crucial importance for the regulation of gluconeogenesis.

Exercise is widely perceived to be beneficial for glycaemic control in patients with type 2 diabetes. Increased physical exercise has been linked to improved glucose homeostasis and enhanced insulin sensitivity. After an acute bout of exercise, the insulin sensitivity is enhanced in insulin-sensitive tissues, such as skeletal muscle, adipose, liver and hypothalamus (Luciano *et al.* 2002; Aoi *et al.* 2004; Flores *et al.* 2006; Peres *et al.* 2005; Ropelle *et al.* 2006; Pauli *et al.* 2008). It is well established that exercise training, even acute training, can improve insulin sensitivity in the muscle of obese rats (Betts *et al.* 1993; Bruce *et al.* 2001). The molecular mechanism for enhanced insulin-mediated glucose uptake with exercise training may be partly related to increased expression and activity of key proteins known to regulate glucose metabolism in skeletal muscle and liver (Chibalin *et al.* 2000; Aoi *et al.* 2004; Ropelle *et al.* 2006). However, the molecular mechanisms involved in this improvement in insulin signalling in liver are poorly studied.

Insulin is a dominant suppressor of gluconeogenesis and several animal models of insulin signalling deficiency show a rise in hepatic PGC-1α expression (Yoon *et al.* 2001), since insulin (via foxo1) may control PGC-1α expression *in vivo* either through a direct action on hepatocytes. In the present study, we further investigate the PGC-1α/Foxo1 complex, hypothesizing that it may be a potential target for reduced hepatic glucose production in acute exercise.

Methods

Animals and diet

Male Wistar rats from the University of Campinas Central Animal Breeding Center were used in the experiments. All experiments were approved by the Ethics Committee of the State University of Campinas (UNICAMP). The 4-week-old Wistar rats were divided into three groups: control rats (CTL) fed standard rodent chow; obese rats, fed on a high fat diet for 3 months (DIO) (Table 1) and a third group which also received a high fat diet, but were submitted to acute exercise (DIO+EXE).

Exercise protocol

Rats were adapted to swimming for 10 min for 2 days. The animals swam in groups of three in plastic barrels of 45 cm in diameter that were filled to a depth of 60 cm, for two 3 h-long bouts, separated by a 45 min rest period and the water temperature was maintained at ~32°C.

Table 2. Physiological and metabolic parameters

Groups ($n = 9$)	Body weight (g)	Epididymal fat (g)	Fasting insulin (ng ml^{-1})	Fasting glucose (mg dl^{-1})
DIO	530.9 ± 31.11*	11.2 ± 2.23*	7.7 ± 2.64*	85.5 ± 8.17
DIO+EXE	515.6 ± 22.01*	11.9 ± 2.82*	7.2 ± 3.02*	82.5 ± 6.26
Control	394.5 ± 15.22	5.1 ± 1.09	2.8 ± 0.69	78.3 ± 4.14

*$P < 0.05$, diet-induced obese rat at rest and exercised *versus* control.

This exercise protocol was adapted from a previously published procedure (Chibalin *et al.* 2000). Eight hours after the exercise protocol, the rats were anaesthetized with an intraperitoneal (I.P.) injection of sodium thiopental (40 mg (kg body weight)$^{-1}$). Following the experimental procedures, the rats were killed under anaesthesia (thiopental 200 mg kg^{-1}) following the recommendations of the NIH publication no. 85–23.

Fasting glucose, insulin tolerance test (ITT), serum insulin quantification and glycogen content

After the exercise protocol, the rats were submitted to an insulin tolerance test (ITT; 1.5 U (kg body weight)$^{-1}$ of insulin) after 6 h of fasting. Briefly, 1.5 IU kg^{-1} of human recombinant insulin (Humulin R; from Eli Lilly, Indianapolis, IN, USA) was infused intraperitoneally into anaesthetized rats and blood samples were collected at 0, 5, 10, 15, 20, 25 and 30 min from the tail for serum glucose determination. The rate constant for plasma glucose disappearance (Kitt) was calculated using the formula, 0.693/biological half life ($t_{1/2}$). The plasma glucose $t_{1/2}$ was calculated from the slope of the last square analysis of the plasma glucose concentration during the linear phase of decline (Bonora *et al.* 1989). Plasma glucose was determined using a glucose meter (Advantage, Boehringer Mannheim, USA). Plasma was separated by centrifugation (1100 *g*) for 15 min at 4°C and stored at −80°C until assay. RIA was employed to measure serum insulin, according to a previous description (Scott *et al.* 1981). Glycogen content liver fragments were measured, according to a previously described method (Ropelle *et al.* 2006).

Protein analysis by immunoblotting

As soon as anaesthesia was assured by the loss of pedal and corneal reflexes, the abdominal cavity was opened, the cava vein exposed, and 0.2 ml of normal saline or insulin (10^{-6} mol l^{-1}) was injected. After insulin injection, hepatic tissue fragments were excised. The tissues were pooled, minced coarsely and homogenized immediately in extraction buffer (mM) (1% Triton X-100, 100 Tris, pH 7.4, containing 100 sodium pyrophosphate, 100 sodium fluoride, 10 EDTA, 10 sodium vanadate, 2 PMSF and 0.1 mg of aprotinin ml^{-1}) at 4°C with a Polytron PTA 20S generator (Brinkmann Instruments model PT 10/35) operated at maximum speed for 30 s. The extracts were centrifuged at 9,000 *g*. and 4°C in a Beckman 70.1 Ti rotor (Beckman, Palo Alto, CA, USA) for 40 min to remove insoluble material, and the supernatants of these tissues were used for protein quantification, using the Bradford method (Bradford, 1976). Proteins were denatured by boiling in Laemmli (Laemmli, 1970) sample buffer containing 100 mM DTT, run on SDS-PAGE and transferred to nitrocellulose membranes. Membranes were blocked, probed and developed as described previously (De Souza *et al.* 2005). The Akt and Foxo1 were immunoblotted from rats' liver with or without previous insulin infusion in the cava vein. Antibodies used for immunoblotting were anti-phospho-Akt, anti-PEPCK, anti-phospho-Foxo1, anti-Foxo1 (Cell Signaling Technology, Inc., Beverly, MA, USA), anti-Akt, and anti-G6Pase (Santa Cruz Biotechnology, Inc., Santa Cruz, CA, USA), and anti-PGC-1α (Immuny Biotechnology, SP, Brazil). Blots were exposed to preflashed Kodak XAR film with Cronex Lightning Plus intensifying screens at −80°C for 12–48 h. Band intensities were quantitated by optical densitometry (Scion Image software, ScionCorp, Frederick, MD, USA) of the developed autoradiographs.

Statistical analysis

The results were expressed as means ± S.E.M. Differences between the Control group and DIO rats at rest and after the exercise protocol were evaluated using one-way analysis of variance (ANOVA). When the ANOVA indicated significance, Bonferroni's *post hoc* test was performed.

Results

Physiological and metabolic parameters

Table 2 shows comparative data regarding control, diet-induced obesity (DIO) rats and DIO rats submitted to exercise protocol (DIO+EXE). The DIO rat had a greater body weight, epididymal fat and fasting serum insulin, but not fasting glucose, than age matched controls. No significant variations were found in body weight,

epididymal fat, fasting serum insulin and fasting glucose of DIO rats after acute exercise when compared to the DIO rested animals.

Acute exercise improves insulin signalling in the liver of obese rats

The effects of *in vivo* I.V. insulin injection on Akt and Foxo1 serine phosphorylation were examined in the liver of CTL, DIO and DIO rats submitted to the exercise protocol (DIO+EXE). Insulin induced 4.7-fold increases in Akt serine phosphorylation in the liver of CTL rats when compared to saline injection (Fig. 1*A*). In DIO rats at rest, Akt serine phosphorylation was reduced after insulin injection by 2.3-fold, when compared with control (Fig. 1*A*). In the liver of the DIO+EXE group Akt serine phosphorylation increased by 1.6-fold compared to the DIO group at rest (Fig. 1*A*). There was no difference in basal levels of Akt serine phosphorylation in the groups (data not shown). The protein expression of Akt in the hepatic tissue was quantified by immunoblotting with anti-Akt antibody. The Akt protein levels were not different in the groups (Fig. 1*A*, lower panels).

Insulin induced a 4.9-fold increase in Foxo1 phosphorylation in the liver of control rats, when compared to saline injection (Fig. 1*B*). In the DIO group at rest, Foxo1 phosphorylation was reduced by 2.5-fold after insulin injection, when compared with the control group (Fig. 1*B*). In the liver of the DIO+EXE group, Foxo1 increased by 1.8-fold, compared with the DIO at rest group (Fig. 1*B*). There was no difference in basal levels of Foxo1 phosphorylation between the groups (data not shown). The protein expression of Foxo1 in the hepatic tissue was quantified by immunoblotting with anti-Foxo1 antibody. The Foxo1 protein levels did not differ between the groups (Fig. 1*B*, lower panels).

Acute exercise reduces PGC-1α expression, Foxo1–PGC-1α association, and PEPCK and G6Pase expression in hepatic tissue of DIO rats

Liver-specific overexpression strategies indicate that PGC1α, when activated, drives hepatic glucose production, a potential contributor to the development of obesity-related diabetes. Thus, we evaluated the effect of diet-induced obesity on PGC-1α expression. Diet-induced obesity increased PGC1α expression in the liver of control rats by 4.4-fold, when compared with the control group (Fig. 2*A*); it also increased the association with Foxo1 by 2.3-fold (Fig. 2*B*). In the liver of the DIO+EXE group, PGC-1α was reduced by 1.8-fold, compared with that of the liver of DIO rats at rest (Fig. 2*A*). Exercise also reduced the Foxo1–PGC-1α association by 2.0-fold (Fig. 2*B*).

We next observed the expressions of PEPCK and G6Pase in the livers of the CTL, DIO and DIO+EXE groups under fasting conditions. In the hepatic tissue of DIO rats at rest, the PEPCK and G6Pase expressions were increased by 2.2- and 3.9-fold, respectively, when compared with control rats (Fig. 2*B* and *C*, respectively). Interestingly, 8 h after acute exercise, the PEPCK and G6Pase protein level

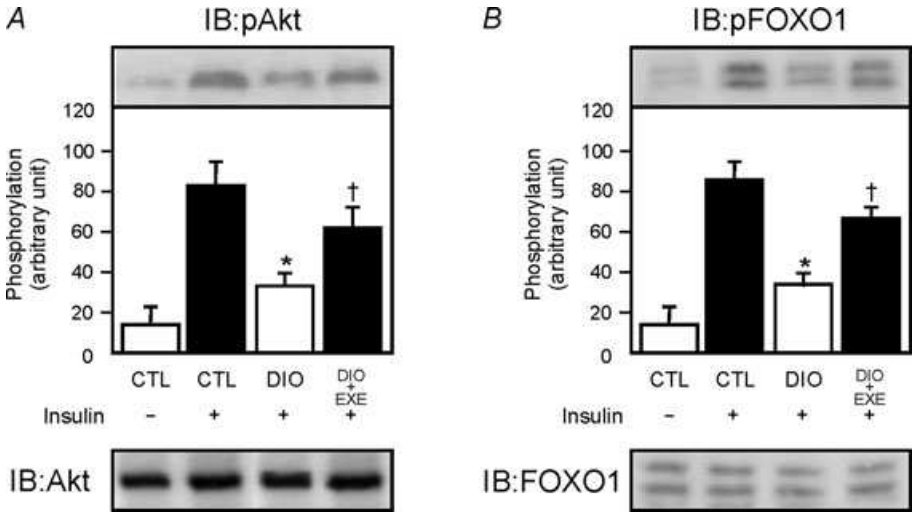

Figure 1. Insulin signalling in the liver of lean (CTL), obese (DIO) and obese–acute exercise (DIO+EXE) rats

Liver extracts from rats injected with saline (–) or insulin (+) were prepared, as described in Methods. *A*, liver extracts were immunoblotted (IB) with anti-phospho-Akt or anti-Akt antibody (upper and lower panels, respectively). *B*, liver extracts were immunoblotted with anti-phospho-Foxo1 or anti-Foxo1 antibody (upper and lower panels, respectively). The results of scanning densitometry are expressed as arbitrary units. Bars represent means ± S.E.M. of $n = 6$ rats. *$P < 0.05$, DIO rats at rest *versus* CTL; †$P < 0.05$, DIO+EXE group *versus* DIO group at rest.

was decreased by 1.7- and 1.6-fold, respectively, in the DIO+EXE group when compared with the DIO group at rest (Fig. 2*B* and *C*, respectively).

Acute exercise increases glycogen content and insulin sensitivity

Liver glucose uptake is independent of insulin action; however, the pancreatic hormone tightly regulates hepatic gluconeogenesis. Since acute exercise leads to high glucose turnover in spite of low basal and stimulated insulin levels, we decided to evaluate glycogen contents. In DIO rats at rest, glycogen content was reduced by 1.9-fold, when compared with lean rats (Fig. 3*A*). In the liver of the DIO+EXE group, glycogen content increased by 1.7-fold, compared with the respective group at rest (Fig. 3*A*).

Finally, we observed an increased insulin sensitivity in the DIO+EXE group. We found a significant impairment (49%) in the glucose disappearance rate (K_{ITT}) in DIO rats at rest when compared with controls; furthermore, exercise improved (41%) the glucose disappearance rate in diet-induced obesity rats (Fig. 3*B*).

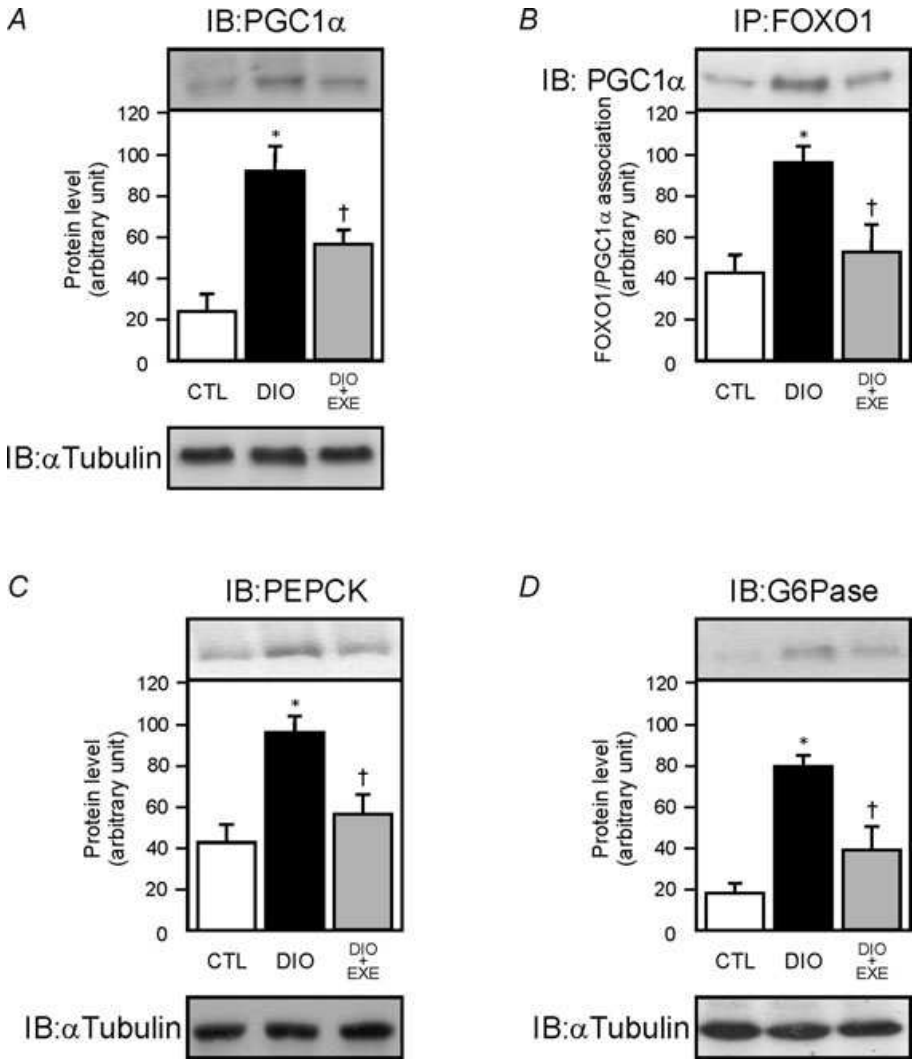

Figure 2. Protein level of co-activator, co-activator association with transcription factor and hepatic production glucose implicated enzymes in the liver of CTL, DIO and DIO+EXE groups
Liver extract rats were submitted to immunobloting for PGC-1α, PEPCK and G6Pase expression, as described in Methods. *A*, samples were blotted (IB) with anti-PGC-1α antibody. *B*, tissue extracts were immunoprecipitated (IP) with anti-Foxo1 antibody and blotted (IB) with anti-PGC-1α antibody (Foxo1–PGC-1α association), as described in Methods. *C*, tissue extracts were blotted (IB) with anti-PEPCK antibody. *D*, tissue extracts were blotted (IB) with anti-G6Pase antibody. Immunoblot was performed employing anti-α-tubulin antibody as the loaded protein (lower panels in *A*, *C* and *D*). The results of scanning densitometry are expressed as arbitrary units. Bars represent means ± S.E.M. of $n = 6$ rats. *$P < 0.05$, DIO rats at rest *versus* CTL; †$P < 0.05$, DIO+EXE group *versus* DIO group at rest.

Discussion

In patients with type 2 diabetes, the rate of hepatic gluconeogenesis is considerably increased, compared with that of control subjects, thereby contributing significantly to fasting hyperglycaemia in diabetes (Saltiel, 2001). In addition, mice with an organ-specific insulin receptor knockout in the liver show severely impaired glucose tolerance and an increased hepatic glucose production with elevated G6Pase and PEPCK expression levels in the liver (Michael *et al.* 2000). In the present study, we demonstrate that acute exercise improves fasting glucose in insulin-resistance rats through a diminished association of Foxo1 with PGC-1α, which controls PEPCK and G6Pase in the liver of DIO rats.

PGC-1α interacts with several transcription factors and is an important regulator of mitochondrial biogenesis, respiration, thermogenesis and hepatic gluconeogenesis (Lin *et al.* 2005; Finck & Kelly, 2006). Some studies have demonstrated a role for this coactivator family in the control of organ-specific biological responses to physiological and pathophysiological milieux (for review see Finck & Kelly, 2006). Given the versatile and pleiotropic nature of the PGC-1α family regulatory circuit, it is suggested that environmental alterations can increase or decrease PGC-1α expression in a tissue-specific manner. In a previous study, we showed that cold induces hyper-expression of PGC-1α and participates in the control of skeletal muscle glucose uptake through a mechanism that controls GLUT4 expression in Wistar rats (Oliveira *et al.* 2004).

The biological roles of PGC-1α in skeletal muscle have been elucidated largely through murine gain and loss of function studies. Mice with skeletal muscle-specific overexpression of PGC-1α demonstrate an increased proportion of oxidative or type I muscle fibres coincident with an increased expression of mitochondrial markers (Lin *et al.* 2002). A bout of exercise or stimulation of muscle contractions induces increases in PGC-1α mRNA and protein in skeletal muscle (Goto *et al.* 2000; Baar *et al.* 2002; Terada *et al.* 2002; Pilegaard *et al.* 2003; Russell *et al.* 2003). In addition, exercise capacity, as measured on a motorized treadmill, and fatigue resistance index in electrically stimulated muscle are significantly reduced in the *Pgc1α*$^{-/-}$ mice (Leone *et al.* 2005). However, study exercise and PGC-1α expression in hepatic tissue are unknown.

Under normal, *ad libitum*-fed conditions, the expression of PGC-1α is relatively low in liver compared with other tissues that rely on aerobic metabolism for ATP production (Puigserver *et al.* 1998). The tissue-specific actions of PGC-1α on systemic glucose metabolism and insulin sensibility have been studied. Systemic glucose tolerance and insulin sensibility have been characterized in PGC-1α-deficient mice; indeed, liver-specific overexpression and knockdown strategies indicate that PGC-1α, when activated, drives hepatic glucose production (Yoon *et al.* 2001). It is possible that reduction of hepatic glucose production via the gluconeogenic pathway contributes to the enhanced glucose tolerance of PGC-1α deficient mice. In the present study, 8 h after an exercise session, PGC-1α expression was suppressed in the liver of DIO rats.

As described above, PGC-1α is induced in liver during fasting and is elevated in several models of diabetes or deficiency in signalling insulin. Notably, PGC-1α expression at physiological levels turns on the entire programme of gluconeogenesis (Herzig *et al.* 2001; Yoon *et al.* 2001). In an elegant study, Puigserver and colleagues showed that Foxo1 and PGC-1α can physically interact with one another and that the combined action of PGC-1α and Foxo1 in various liver cell types results in a synergistic induction of endogenous G6Pase gene expression (Puigserver *et al.* 2003). Thus, PGC-1α stimulates G6Pase gene expression, in part, through a direct interaction with Foxo1 bound to the G6Pase promoter. Our results show that acute exercise can increase Foxo1 phosphorylation and reduce PGC-1α expression and markedly reduce the PGC-1α–Foxo1 association.

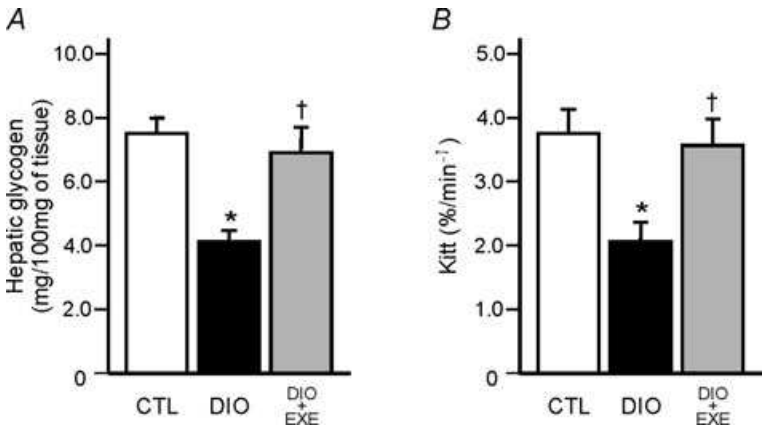

Figure 3. Glycogen content and insulin sensitivity under fasting conditions in the hepatic tissue of CTL, DIO and DIO+EXE rats
Liver extracts from rats were prepared as described in Methods. *A*, hepatic glycogen content expressed as mg (100 mg tissue)$^{-1}$. *B*, the rate constant for glucose disappearance during an insulin tolerance test (K_{ITT}) (% min^{-1}). Bars represent means ± S.E.M. of $n = 9$ rats. *$P < 0.05$, DIO rats at rest *versus* CTL; †$P < 0.05$, DIO+EXE group *versus* DIO group at rest.

In vitro studies have shown that Foxo1 regulates both PEPCK and G6Pase genes through an interaction with their consensus insulin response elements (IRE) present in their promoters (Vander Kooi *et al.* 2003; Hall *et al.* 2000). Insulin repression of these genes occurs through a PI3K/Akt-mediated phosphorylation of the Foxo1 protein, resulting in its translocation out of the nucleus (Biggs *et al.* 1999; Kops *et al.* 1999). Interestingly, the association of Foxo1 with PGC-1α is also abrogated by Akt-mediated phosphorylation (Puigserver *et al.* 2003). Therefore, insulin signalling through Akt can attenuate the effects of increased levels of PGC-1α in fasting and other conditions by promoting the dissociation of PGC-1α from Foxo1. In addition, glycogen levels were increased as compared with those of obese rats, but were similar to lean controls. This fact reinforces that the insulin action in the liver is indeed improved, as also confirmed at the molecular level by the finding that Akt and Foxo1 activations are significantly increased. At least part of this effect may be related to the reduced levels of G6Pase, since in this situation there is less glycogenolysis, resulting in increased glycogen levels. Although this is an indirect evaluation we believe it supports our hypothesis about reduced glyconeogenesis in trained rats.

Liver-specific overexpression and knockdown strategies indicate that PGC-1α is crucial in the control of hepatic glucose production. Although we did not evaluate the hepatic glucose production in the present study, in previous investigations, we and others have shown that the reduction of PGC-1α expression using different approaches diminished hepatic glucose production, as evaluated by hyperinsulinaemic-euglycaemic clamp procedures (Herzig *et al.* 2001; Yoon *et al.* 2001; Puigserver *et al.* 2003; Rhee *et al.* 2003; De Souza *et al.* 2005).

Our results show that exercise induced a decrease in Foxo1–PGC-1α association via Akt phosphorylation and plays an important role in the suppression of hepatic gluconeogenesis. However, although this was not the focus of this work, we cannot exclude a role for insulin-independent mechanisms in the effects described; for example, activation of AMPK in muscle by exercise. It will be important to investigate possible connections between non-insulin-dependent mechanisms (for example, reactive oxygen species) and the inactivation of Foxo1.

In conclusion, our data demonstrate that exercise improves insulin sensitivity in the liver. The effect of exercise on insulin action is further supported by our findings that exercised rats show a reduction in both coactivator and transcription factor expression, a mechanism by which exercise may diminish the expressions of the glyconeogenic enzymes, PEPCK and G6Pase, and consequently hepatic glucose production. Thus, these results provide insights into the mechanism by which exercise may improve fasting hyperglycaemia.

References

Aoi W, Ichiishi E, Sakamoto N, Tsujimoto A, Tokuda H & Yoshikawa T (2004). Effect of exercise on hepatic gene expression in rats: a micro array analysis. *Life Sci* **75**, 3117–3128.

Baar K, Wende AR, Jones TE, Marison M, Nolte LA, Chen M, Kelly DP & Holloszy JO (2002). Adaptations of skeletal muscle to exercise: rapid increase in the transcriptional co activator PGC-1. *FASEB J* **16**, 1879–1886.

Betts JJ, Sherman WM, Reed MJ & Gao JP (1993). Duration of improved muscle glucose uptake after acute exercise in obese Zucker rats. *Obes Res* **1**, 295–302.

Biggs WH 3rd, Meisenhelder J, Hunter T, Cavenee WK & Arden KC (1999). Protein kinase B/Akt-mediated phosphorylation promotes nuclear exclusion of the winged helix transcription factor FKHR1. *Proc Natl Acad Sci U S A* **96**, 7421–7426.

Bonora E, Moghetti P, Zancanaro C, Cigolini M, Querena M, Cacciatori V, Corgnati A & Muggeo M (1989). Estimates of in vivo insulin action in man: comparison of insulin tolerance tests with euglycemic and hyperglycemic glucose clamp studies. *J Clin Endocrinol Metab* **68**, 374–378.

Bradford MM (1976). A rapid and sensitive method for the quantitation of microgram quantities of protein utilizing the principle of protein-dye binding. *Anal Biochem* **72**, 248–254.

Bruce CR, Lee JS & Hawley JA (2001). Postexercise muscle glycogen resynthesis in obese insulin-resistant Zucker rats. *J Appl Physiol* **91**, 1512–1519.

Chibalin AV, Yu M, Ryder JW, Song XM, Galuska D, Krook A, Wallberg-Henriksson H & Zierath JR (2000). **97**, 38–43.

Daitoku H, Yamagata K, Matsuzaki H, Hatta M & Fukamizu A (2003). Regulation of PGC-1 promoter activity by protein kinase B and the forkhead transcription factor FKHR. *Diabetes* **52**, 642–649.

De Souza CT, Araujo EP, Bordin S, Ashimine R, Zollner RL, Boschero AC, Saad MJ & Velloso LA (2005). *Endocrinology* **146**, 4189–4191.

Finck BN & Kelly DP (2006). PGC-1 coactivators: inducible regulators of energy metabolism in health and disease. *J Clin Invest* **116**, 615–622.

Flores MB, Fernandes MF, Ropelle ER, Faria MC, Ueno M, Velloso LA, Saad MJ & Carvalheira JB (2006). Exercise improves insulin and leptin sensitivity in hypothalamus of Wistar rats. *Diabetes* **55**, 2554–2561.

Goto M, Terada S, Kato M, Katoh M, Yokozeki T, Tabata I & Shimokawa T (2000). cDNA cloning and mRNA analysis of PGC-1 in epitrochlearis muscle in swimming-exercised rats. *Biochem Biophys Res Commun* **274**, 350–354.

Hall RK, Yamasaki T, Kucera T, Waltner-Law M, O'Brien R & Granner DK (2000). Regulation of phosphoenolpyruvate carboxykinase and insulin-like growth factor-binding protein-1 gene expression by insulin. The role of winged helix/forkhead proteins. *J Biol Chem* **275**, 30169–30175.

Herzig S, Long F, Jhala US, Hedrick S, Quinn R, Bauer A, Rudolph D, Schutz G, Yoon C, Puigserver P, Spiegelman B & Montminy M (2001). CREB regulates hepatic gluconeogenesis through the coactivator PGC-1. *Nature* **413**, 179–183.

Kops GJ, de Ruiter ND, De Vries-Smits AM, Powell DR, Bos JL & Burgering BM (1999). Direct control of the Forkhead transcription factor AFX by protein kinase B. *Nature* **398**, 630–634.

Laemmli, UK (1970). Cleavage of structural proteins during the assembly of the head of bacteriophage T4. *Nature* **227**, 680–685.

Leone TC, Lehman JJ, Finck BN, Schaeffer PJ, Wende AR, Boudina S, Courtois M, Wozniak DF, Sambandam N, Bernal-Mizrachi C, Chen Z, Holloszy JO, Medeiros DM, Schmidt RE, Saffitz JE, Abel ED, Semenkovich CF & Kelly DP (2005). PGC-1α deficiency causes multi-system energy metabolic derangements: muscle dysfunction, abnormal weight control and hepatic steatosis. *PLoS Biol* **3**, e101.

Lin J, Handschin C & Spiegelman BM (2005). Metabolic control through the PGC-1 family of transcription coactivators. *Cell Metab* **1**, 361–370.

Lin J, Wu H, Tarr PT, Zhang CY, Wu Z, Boss O, Michael LF, Puigserver P, Isotani E, Olson EN, Lowell BB, Bassel-Duby R & Spiegelman BM (2002). Transcriptional co-activator PGC-1α drives the formation of slow-twitch muscle fibers. *Nature* **418**, 797–801.

Luciano E, Carneiro EM, Carvalho CR, Cavalheira JB, Peres SB, Reis MA, Saad MJ, Boschero AC & Velloso LA (2002). Endurance training improves responsiveness to insulin and modulates insulin signal transduction through the phosphatidylinositol 3-kinase/Akt-1 pathway. *Eur J Endocrinol* **147**, 149–157.

Michael MD, Kulkarni RN, Postic C, Previs SF, Shulman GI, Magnuson MA & Kahn CR (2000). Loss of insulin signaling in hepatocytes leads to severe insulin resistance and progressive hepatic dysfunction. *Mol Cell* **6**, 87–97.

Oliveira RL, Ueno M, De Souza CT, Pereira-da-Silva M, Gasparetti AL, Bezerra RM, Alberici LC, Vercesi AE, Saad MJ & Velloso LA (2004). Cold-induced PGC-1α expression modulates muscle glucose uptake through an insulin receptor/AKT-independent, AMPK-dependent pathway. *Am J Physiol Endocrinol Metab* **287**, E686–695.

Pauli JR, Ropelle ER, Cintra DE, Carvalho-Filho MA, Moraes JC, De Souza CT, Velloso LA, Carvalheira JB & Saad MJ (2008). Acute physical exercise reverses S-nitrosation of the insulin receptor, insulin receptor substrate 1 and protein kinase B/Akt in diet-induced obese Wistar rats. *J Physiol* **586**, 659–671.

Peres SB, de Moraes SM, Costa CE, Brito LC, Takada J, Andreotti S, Machado MA, Alonso-Vale MI, Borges-Silva CN & Lima FB (2005). Endurance exercise training increases insulin responsiveness in isolated adipocytes through IRS/PI3-kinase/Akt pathway. *J Appl Physiol* **98**, 1037–1043.

Pilegaard H, Saltin B & Neufer PD (2003). Exercise induces transient transcriptional activation of the PGC-1α gene in human skeletal muscle. *J Physiol* **546**, 851–858.

Postic C, Dentin R & Girard J (2004). Role of the liver in the control of carbohydrate and lipid homeostasis. *Diabetes Metab* **30**, 398–408.

Puigserver P, Wu Z, Park CW, Graves R, Wright W & Spiegelman BM (1998). A cold-inducible coactivator of nuclear receptors linked to adaptive thermogenesis. *Cell* **92**, 829–839.

Puigserver P, Rhee J, Donovan J, Walkey CJ, Yoon JC, Oriente F, Kitamura Y, Altomonte J, Dong H, Accili D & Spiegelman BM (2003). Insulin-regulated hepatic gluconeogenesis through FOXO1-PGC-1α interaction. *Nature* **423**, 550–555.

Rhee J, Inoue Y, Yoon JC, Puigserver P, Fan M, Gonzalez FJ & Spiegelman BM (2003). Regulation of hepatic fasting response by PPARγ coactivator-1α (PGC-1): requirement for hepatocyte nuclear factor 4α in gluconeogenesis. *Proc Natl Acad Sci U S A* **100**, 4012–4017.

Ropelle ER, Pauli JR, Prada PO, de Souza CT, Picardi PK, Faria MC, Cintra DE, Fernandes MF, Flores MB, Velloso LA, Saad MJ & Carvalheira JB (2006). Reversal of diet-induced insulin resistance with a single bout of exercise in the rat: the role of PTP1B and IRS-1 serine phosphorylation. *J Physiol* **577**, 997–1007.

Russell AP, Feilchenfeldt J, Schreiber S, Praz M, Crettenand A, Gobelet C, Meier CA, Bell DR, Kralli A, Giacobino JP & Dériaz O (2003). Endurance training in humans leads to fiber type-specific increases in levels of peroxisome proliferator-activated receptor-γ coactivator-1 and peroxisome proliferator-activated receptor-α in skeletal muscle. *Diabetes* **52**, 2874–2881.

Saltiel AR (2001). New perspectives into the molecular pathogenesis and treatment of type 2 diabetes. *Cell* **104**, 517–529.

Scott AM, Atwater I & Rojas E (1981). A method for the simultaneous measurement of insulin release and B cell membrane potential in single mouse islets of Langerhans. *Diabetologia* **21**, 470–475.

Vander Kooi BT, Streeper RS, Svitek CA, Oeser JK, Powell DR & O'Brien RM (2003). The three insulin response sequences in the glucose-6-phosphatase catalytic subunit gene promoter are functionally distinct. *J Biol Chem* **278**, 11782–11793.

Terada S, Goto M, Kato M, Kawanaka K, Shimokawa T & Tabata I (2002). Effects of low-intensity prolonged exercise on PGC-1 mRNA expression in rat epitrochlearis muscle. *Biochem Biophys Res Commun* **296**, 350–354.

Yoon JC, Puigserver P, Chen G, Donovan J, Wu Z & Rhee J (2001). Control of hepatic gluconeogenesis through the transcriptional coactivator PGC-1. *Nature* **413**, 131–138.

Author contributions

E.R.R.: conception, design, analysis and interpretation of data; J.R.P.: conception, design, analysis and interpretation of data; D.E.C.: conception and design; M.J.S.F.: conception and design; R.A.P.: conception and design; L.A.V.: drafting the article and revising it critically for important intellectual content; C.T.D.S.: conception, design, analysis and interpretation of data, drafting the article and revising it critically for important intellectual content.

Acknowledgements

The authors thank Mrs Gerson Ferraz and Márcio A. da Cruz for technical assistance. This study was supported by grants from Conselho Nacional de Desenvolvimento Científico e Tecnológico (CNPq). We thank Dr Nicola Conran for English language editing.

APÊNDICE *VII*

EGFR Tyrosine Kinase Inhibitor (PD153035) Improves Glucose Tolerance and Insulin Action in High-Fat Diet–Fed Mice

Patricia O. Prada,[1] Eduardo R. Ropelle,[1] Rosa H. Mourão,[1] Claudio T. de Souza,[1] Jose R. Pauli,[1] Dennys E. Cintra,[1] André Schenka,[2] Silvana A. Rocco,[3] Roberto Rittner,[3] Kleber G. Franchini,[1] José Vassallo,[2] Lício A. Velloso,[1] José B. Carvalheira,[1] and Mario J.A. Saad[1]

OBJECTIVE—In obesity, an increased macrophage infiltration in adipose tissue occurs, contributing to low-grade inflammation and insulin resistance. Epidermal growth factor receptor (EGFR) mediates both chemotaxis and proliferation in monocytes and macrophages. However, the role of EGFR inhibitors in this subclinical inflammation has not yet been investigated. We investigated, herein, in vivo efficacy and associated molecular mechanisms by which PD153035, an EGFR tyrosine kinase inhibitor, improved diabetes control and insulin action.

RESEARCH DESIGN AND METHODS—The effect of PD153035 was investigated on insulin sensitivity, insulin signaling, and c-Jun NH_2-terminal kinase (JNK) and nuclear factor (NF)-κB activity in tissues of high-fat diet (HFD)-fed mice and also on infiltration and the activation state of adipose tissue macrophages (ATMs) in these mice.

RESULTS—PD153035 treatment for 1 day decreased the protein expression of inducible nitric oxide synthase, tumor necrosis factor (TNF)-α, and interleukin (IL)-6 in the stroma vascular fraction, suggesting that this drug reduces the M1 proinflammatory state in ATMs, as an initial effect, in turn reducing the circulating levels of TNF-α and IL-6, and initiating an improvement in insulin signaling and sensitivity. After 14 days of drug administration, there was a marked improvement in glucose tolerance; a reduction in insulin resistance; a reduction in macrophage infiltration in adipose tissue and in TNF-α, IL-6, and free fatty acids; accompanied by an improvement in insulin signaling in liver, muscle, and adipose tissue; and also a decrease in insulin receptor substrate-1 Ser^{307} phosphorylation in JNK and inhibitor of NF-κB kinase (IKKβ) activation in these tissues.

CONCLUSIONS—Treatment with PD153035 improves glucose tolerance, insulin sensitivity, and signaling and reduces subclinical inflammation in HFD-fed mice. ***Diabetes*** **58:2910–2919, 2009**

From the [1]Department of Internal Medicine, State University of Campinas, Campinas, Brazil; the [2]Chemistry Institute, State University of Campinas, Campinas, Brazil; and the [3]Department of Pathology, State University of Campinas, Campinas, Brazil.

Corresponding author: Mario J.A. Saad, msaad@fcm.unicamp.br.

Received 16 April 2008 and accepted 5 August 2009. Published ahead of print at http://diabetes.diabetesjournals.org on 20 August 2009. DOI: 10.2337/db08-0506.

P.O.P. and E.R.R. contributed equally to this article.

Epidermal growth factor receptor (EGFR) tyrosine kinase inhibitors are used in the clinic to treat malignancies (1). It has recently been observed that a modest number of patients, suffering from both malignancies and type 2 diabetes, were successfully treated not only for their malignancies but also for diabetes when given some tyrosine kinase inhibitors (2–5). However, the molecular mechanisms that account for the effect of these drugs on insulin action and glucose metabolism are unknown.

Insulin stimulates a signaling network composed of a number of molecules, initiating the activation of insulin receptor tyrosine kinase and phosphorylation of insulin receptor substrates, including insulin receptor substrate (IRS)-1 and IRS-2 (6–8). Following tyrosine phosphorylation, IRS-1/IRS-2 bind and activate the enzyme phosphatidylinositol 3-kinase (PI3-K). The activation of PI3-K increases serine phosphorylation of Akt, which is responsible for most of the metabolic actions of insulin, such as glucose transport, lipogenesis, and glycogen synthesis (7,8).

In the most prevalent forms of insulin resistance, diet-induced obesity, and type 2 diabetes, there is a downregulation in this signaling pathway in insulin-sensitive tissues, parallel to a state of chronic low-grade inflammation (6). Several serine/threonine kinases are activated by inflammatory or stressful stimuli and contribute to inhibition of insulin signaling, including c-Jun NH_2-terminal kinase (JNK) (9–13) and inhibitor of nuclear factor (NF)-κB kinase (IKKβ) (12,14). In obesity, an increased macrophage infiltration in adipose tissue occurs, contributing to this low-grade inflammation (15–17), which has an important role in the increased tissue production of proinflammatory molecules and acute-phase proteins associated with obesity (13,14). EGFR has been described in monocytes and in macrophages and mediates both chemotaxis and proliferation in macrophages (18–20). However, the role of EGFR inhibitors on this subclinical inflammation of obesity was not yet investigated.

PD153035 has been shown to possess highly potent and selectively inhibitory activity against EGFR tyrosine kinase and rapidly suppresses autophosphorylation of EGFR at low nanomolar concentrations in fibroblasts and human epidermoid carcinoma cells, as well as selectively blocking EGF-mediated cellular processes, including mitogenesis and early gene expression (21–23). In addition, PD153035 has been shown to reduce JNK and IKK/IκB/NF-κB pathways (24,25). Moreover, EGFR and other ty-

rosine kinase inhibitors have also been shown to inhibit the growth of monocyte/macrophages, suggesting possible mechanisms to improve insulin action (26–29).

Herein, we investigated the in vivo efficacy and associated molecular mechanisms by which PD153035, an EGFR tyrosine kinase inhibitor, improved diabetes control and insulin action. We studied the effect of acute (1 day) or chronic (14 days) administration of PD153035 on insulin sensitivity, insulin signaling, and JNK and NF-κB activity in liver, muscle, and adipose tissue of high-fat diet (HFD)-fed mice and also on the infiltration and activation state of adipose tissue macrophages (ATMs) in these mice.

RESEARCH DESIGN AND METHODS

Male Swiss mice were obtained from the University of Campinas, São Paulo. The mice were bred under specific pathogen-free conditions at the Central Breeding Center of the University of Campinas. Antiphosphotyrosine (α-PY), anti-IRβ (α-IR), anti–IRS-1, anti-Akt1/2, anti–p-JNK, anti–inducible nitric oxide synthase (iNOS), anti–tumor necrosis factor (TNF)-α, anti–interleukin (IL)-6, anti-EGFR, anti-caveolin, anti-actin, anti-IKKβ, anti-pIKKβ, anti–p-c-Jun, and anti-IκBα antibodies were from Santa Cruz Technology (Santa Cruz, CA). Anti-pAkt was from Cell Signaling Technology (Beverly, MA). Anti–phospho-IRS-1^{ser307} was obtained from Upstate Biotechnology (Lake Placid, NY). Human recombinant insulin was from Eli Lilly and Company (Indianapolis, IN). Routine reagents were purchased from Sigma Chemical (St. Louis, MO), unless specified elsewhere.

Compound PD153035 [4-*N*-(3′-bromo-phenyl)amino-6,7-dimethoxyquinazoline hydrochloride] was synthesized, as previously described (30). The compound was >99% pure, as determined by elemental analysis, high-performance liquid chromatography, mass spectrometry, and ^{1}H and ^{13}C nuclear magnetic resonance (30).

Animal care and experimental procedures. All experiments were approved by the ethics committee of the State University of Campinas. Eight-week-old male Swiss mice were divided into four groups with similar body weights and assigned to receive the following diet and/or treatment: control group received a standard rodent diet and water ad libitum; HFD group received an HFD consisting of 55% calories from fat, 29% from carbohydrate, and 16% from protein for 8 weeks; and HFD with PD153035 for 14 days (HFPD14days) received the same HFD for 8 weeks, but in the last 2 weeks these animals also received PD153035 (30 mg/kg) by gavage once a day. A group of HFD animals also received the same dose of PD153035 at 24 and 2 h before the experiments, and this group was called HFPD1day. Body weight and food intake were measured weekly. Glucose tolerance tests and insulin tolerance tests were performed on these mice after 8 weeks on the diets, as previously described (31,32).

Assays. Insulin, leptin, and adiponectin concentrations were determined by enzyme-linked immunosorbent assay (ELISA) (Linco). Serum free fatty acid (FFA) levels were analyzed using the NEFA-kit-U (Wako Chemical, Neuss, Germany), with oleic acid as a standard. Glucose values were measured from whole venous blood with a glucose monitor (Glucometer; Bayer). Serum concentrations of IL-6 and TNF-α were determined using mouse IL-6 ELISA and mouse TNF-α ELISA (Pierce Endogen, Rockford, IL). Monocyte chemoattractant protein (MCP)-1, MCP-2, and MCP-3 ELISA kits were purchased from Antigenix America (Huntington Station, NY).

Light microscopy and morphometry. Mice were fasted for 12 h and killed with an overdose of anesthetic (sodium thiopental). Epididymal, retroperitoneal, and mesenteric adipose tissues were dissected and assessed by light microscopy and morphometry. Tissue sections were observed with a Zeiss Axiophot light microscope using a ×40 objective, and digital images were captured with a Canon PowerShot G5. Crown-like structure (CLS) density (average CLS within 10 high-power fields, per animal) and mean adipocyte surface area (average surface area of 30 randomly sorted adipocytes, per animal) were determined using the Imagelab Analysis software (version 2.4), as previously described (33).

Tissue extraction, immunoprecipitation, and immunoblotting. Mice were anesthetized by intraperitoneal injection of sodium thiopental and were used 10–15 min later (i.e., as soon as anesthesia was assured by the loss of pedal and corneal reflexes). Five minutes after the insulin injection (3.8 units/kg i.p.) liver, muscle, and adipose tissue were removed, minced coarsely, and homogenized immediately in extraction buffer, as described elsewhere (34). Extracts were used for immunoprecipitation with α-IR, α-IRS-1, α-EGFR, and protein A-sepharose 6MB (Pharmacia, Uppsala, Sweden). The precipitated proteins and/or whole tissue extracts were subjected to SDS-PAGE and immunoblotting as previously described (6,31).

Determination of NFκB activation. NFκB p50 activation was determined in nuclear extracts from liver, muscle, and adipose tissue by ELISA (89858; Pierce Biotechnology), according to the recommendations of the manufacturer.

Isolation of the stroma vascular fraction and adipocyte fraction of adipose tissue. Epididymal, retroperitoneal, or mesenteric fat pads were excised, and isolation of the stroma vascular fraction and adipocyte fraction of adipose tissue were performed, as previously described (33). A summary of the method is presented in the online appendix (available at http://diabetes.diabetesjournals.org/cgi/content/full/db08-0506/DC1).

Arginase assay. Arginase activity assays were performed, as previously described (35). A summary of the method is presented in the online appendix.

Statistical analysis. Data are expressed as means ± SE, and the number of independent experiments is indicated. For statistical analysis, the groups were compared using a two-way ANOVA with the Bonferroni test for post hoc comparisons. The level of significance adopted was $P < 0.05$.

RESULTS

Effect of PD153035 on EGFR tyrosine phosphorylation in liver, muscle, and adipose tissue of mice. The drug PD153035 was developed in 1994 as a specific tyrosine kinase inhibitor of the EGFR (20). To investigate the effect of PD153035 administration on EGFR phosphorylation, we immunoprecipitated liver, muscle, and adipose tissue extracts of controls, HFD-fed animals, and HFD-fed animals treated with PD153035 for 1 or 14 days with anti-EGFR antibody and performed immunoblotting with anti-phosphotyrosine antibody. The results showed that PD153035 administration was able to reduce EGFR tyrosine phosphorylation in the three tissues by 70–90% in a similar fashion after 1 or 14 days (Fig. 1*A–C*). HFD did not change the tissue levels of EGFR in liver, muscle, and epidydimal fat pad; however, there was an increase in EGFR expression (Fig. 1*C*) and in tyrosine phosphorylation in the mesenteric and retroperitoneal fat pads. The reduction in EGFR tyrosine phosphorylation, induced by PD153035, was greater in the mesenteric and retroperitoneal fat pads compared with the epididymal fat pad (Fig. 1*C*). PD153035 treatment reduced EGFR tyrosine phosphorylation in a dose-dependent manner in liver, muscle, and retroperitoneal tissues (online appendix Fig. S1).

Effect of PD153035 on body weight and fat pads in HFD-fed mice. Eight-week-old male Swiss mice were placed on HFD and then supplemented, or not, with PD153035 on the last day (HFPD1) or during 14 days (HFPD14) before the experiments. Weight gain after 8 weeks was similar in HFD or HFPD groups and was higher in these groups than in the control group that received standard rodent diet (Fig. 1*D*). There is a slight reduction in body weight after 14 days of PD153035 compared with HFD or HFDPD1, which is not statistically significant. Daily food intake was similar in HFD or HFPD, and 8-week cumulative food intake was higher for both groups on HFD (data not shown). As expected, the epididymal, retroperitoneal, and mesenteric fat pad weights were higher in the HFD group, and PD153035 treatment for 1 day did not change these fat pad weights, but after 14 days there was a significant reduction in retroperitoneal and mesenteric fat pad weights (Fig. 1*E–G*).

Effect of PD153035 on metabolic parameters in HFD-fed mice. The fasting plasma glucose levels were higher in HFD and in HFPD1 than in the other groups (Figs. 1*H*). PD153035 treatment reduced fasting plasma glucose levels in a dose-dependent manner (Fig. S2). During the glucose tolerance test, the plasma glucose and serum insulin levels were significantly higher in HFD and HFPD1 mice compared with controls, and PD153035 administration for 14 days improved glucose tolerance and reduced insulin

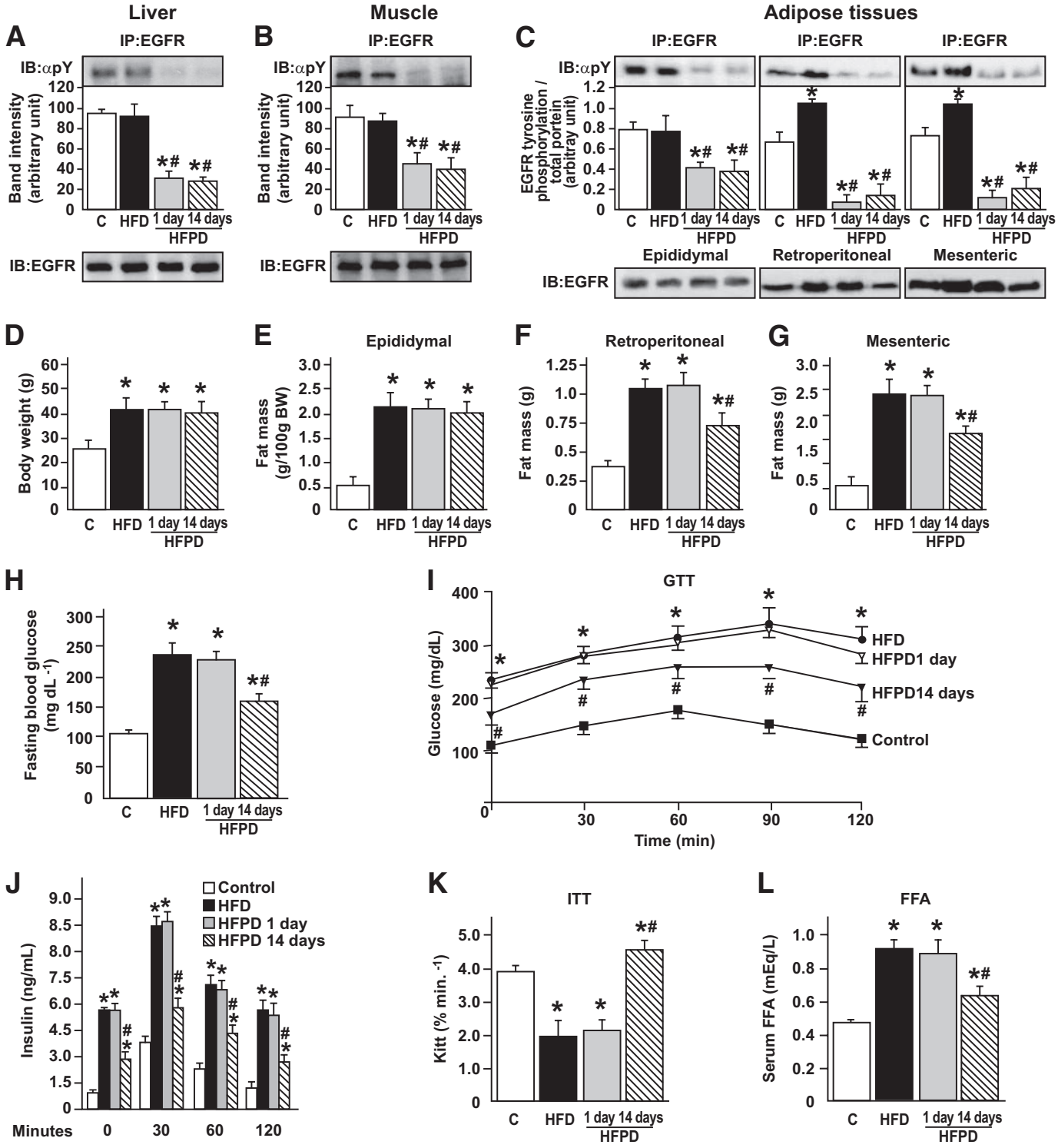

FIG. 1. Effects of acute or chronic PD153035 administration in fed mice. (*A–C*, *upper panels*). Representative blots show the tyrosine phosphorylation of EGFR of control mice, HFD mice, and HFDPD 1 and 14 days in liver (*A*), muscle (*B*), and adipose (*C*). Total protein expression of EGFR (*A–C*, *lower panels*). *D*: Body weight. *E*: Epididymal fat pad weight. *F*: Retroperitoneal fat pad weight. *G*: Mesenteric fat pad weight. *H*: Fasting plasma glucose. *I*: Glucose tolerance test. *J*: Serum insulin during glucose tolerance test. *K*: Glucose disappearance rate. *L*: Serum FFAs. Data are presented as means ± S.E.M from six to eight mice per group. *$P < 0.05$ vs. control group; #$P < 0.01$ vs. HFD. IB, immunoblot; IP, immunoprecipitate.

levels at all time points studied (Fig. 1*I* and *J*). The glucose disappearance rate was lower in HFD and in HFPD1 groups, and PD153035 administration for 14 days (HFPD14) reversed these alterations (Fig. 1*K*). Taken together, the lower insulin levels during the glucose tolerance test and the increase in glucose disappearance rate during the insulin tolerance test after PD153035 treatment for 14 days suggest that this drug improves insulin sensitivity. FFA levels were significantly higher in HFD and HFPD1 and returned to levels close to those of the control group after 14 days of PD153035 administration (Fig. 1*L*).

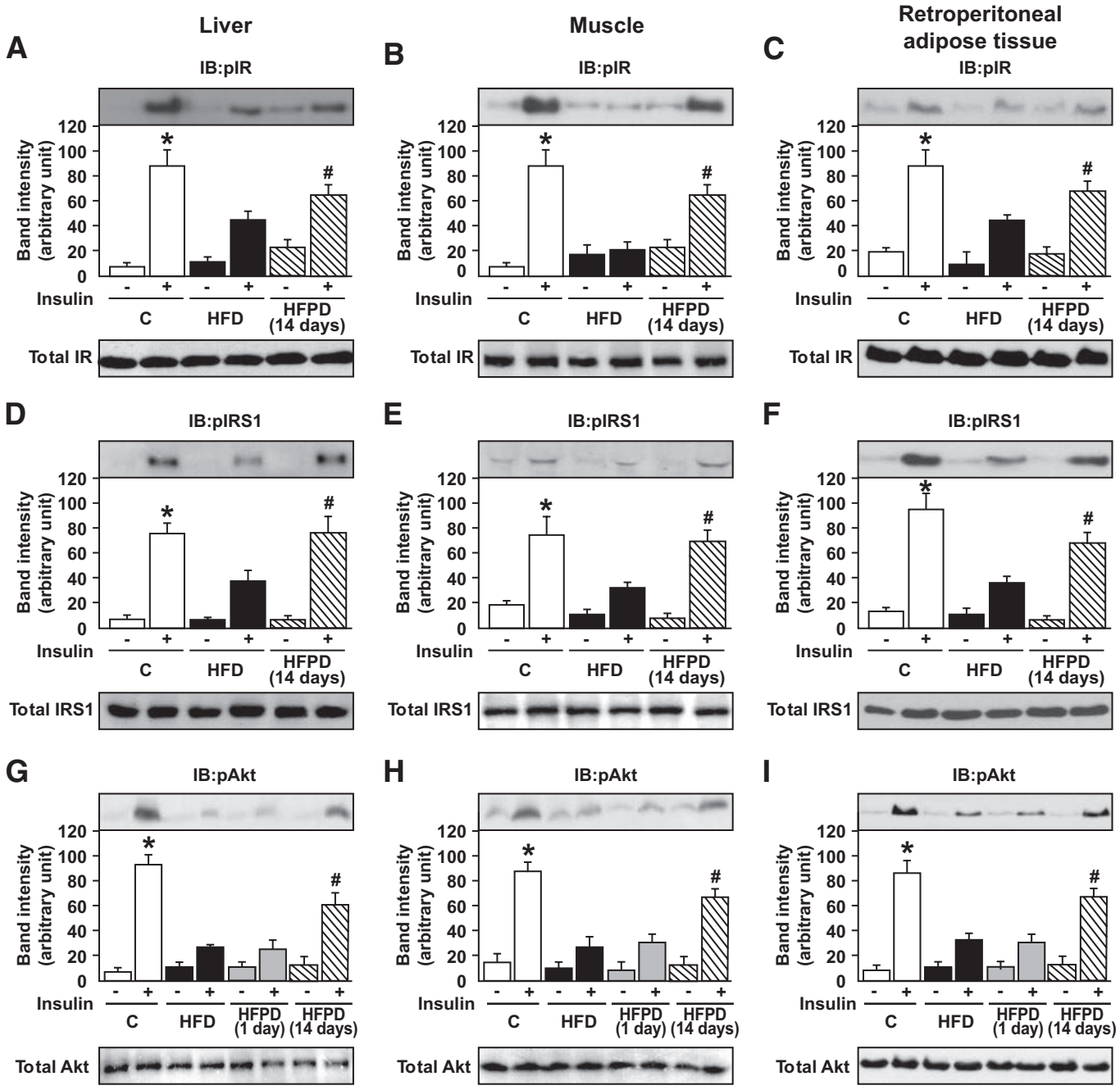

FIG. 2. Effects of PD153035 administration on insulin signaling in fed mice. Representative blots show tyrosine phosphorylation of IRβ in liver (*A*), muscle (*B*), and adipose (*C*) of control mice, HFD mice, and HFDPD during 14 days (*upper panels*). Total protein expression of IRβ (*A–C*, *lower panels*). Tyrosine phosphorylation of IRS-1 in liver (*D*), muscle (*E*), and retroperitoneal (*F*) of control mice, HFD mice, and HFDPD 14 days (*upper panels*). Total protein expression of IRS1 (*D–F*, *lower panels*). Serine phosphorylation of Akt in liver (*G*), muscle (*H*), and adipose (*I*) of control mice, HFD mice, and HFDPD 1 and 14 days (*upper panels*). Total protein expression of Akt (*G–I*, *lower panels*). Data are presented as means ± SE from six to eight mice per group. **P* < 0.05 control vs. HFD group; #*P* < 0.05 HFPD 14 days vs. HFD. IB, immunoblot.

Effect of PD153035 on insulin signaling in liver, muscle, and retroperitoneal adipose tissue of HFD-fed mice. In liver, muscle, and retroperitoneal adipose tissues, insulin-induced IRβ (Fig. 2*A–C*) and IRS-1 tyrosine phosphorylation (Fig. 2*D–F*) and Akt serine phosphorylation (Fig. 2*G–I*) were reduced by 50–70% in mice fed on an HFD compared with controls. The treatment with PD153035 for 1 day did not change the insulin-induced tyrosine phosphorylation levels of IR and IRS-1 (data not shown) and also did not improve Akt serine phosphorylation levels in liver muscle and adipose tissues (Fig. 2*G–I* and online appendix Fig. S3). However, 14 days of treatment reversed these reductions in the three tissues studied (Fig. 2*A–I*). The protein concentration of IR, IRS-1, and Akt in liver, muscle, and retroperitoneal adipose did not change between the groups.

The effect of PD153035 improving Akt phosphorylation in HFD-fed mice was dose dependent (online appendix Fig. S3). In control animals, PD153035 did not change insulin-induced Akt phosphorylation in liver, muscle, or epididymal adipose tissue or glucose uptake in isolated muscle (online appendix Fig. S4).

Ser^{307} phosphorylation of IRS-1 and activation of JNK and IKKβ in liver, muscle, and retroperitoneal tissue of HFD-fed mice treated with PD153035. IKKβ activity was monitored using IKKβ phosphorylation and IκBα protein abundance, as previously described (12). IKKβ phosphorylation was increased and IκBα protein levels were reduced in liver, muscle, and retroperitoneal adipose tissue of mice fed an HFD or HFPD1 diet but not in these tissues of HFPD14 mice (Fig. 3*A–F*). We also measured the nuclear NF-κB subunit p50 activation and found an increase in the DNA binding of nuclear p50 in liver, muscle, and retroperitoneal of mice on an HFD and HFPD1, but there was a clear decrease in the three tissues in HFPD14 (Fig. 3*G–I*). JNK activation was determined by monitoring phosphorylation of JNK (Thr183 and Tyr185) and the protein levels of p-c-Jun. JNK phosphorylation and p-c-Jun were increased in liver, muscle, and white adipose tissue (WAT) of mice fed on an HFD and HFPD1, and this increase was reversed by 14 days of PD153035 treatment (Fig. 3*J–O*). We tested Ser^{307} phosphorylation of IRS-1 in liver, muscle, and WAT in the four groups of mice. Ser^{307} phosphorylation was induced by an HFD in the three tissues of mice, and the treatment with PD153035 for 14 days reversed this alteration (Fig. 3*P–R*).

Effect of PD153035 on retroperitoneal adipose tissue morphology and ultrastructural features in HFD-fed mice. Morphometric analysis revealed that in retroperitoneal fat pad, adipocytes from HFPD14 were consistently smaller than adipocytes from control mice fed on an HFD or HFPD1, with an average 40% decrease in size (Fig. 4*A* and *B*). In mesenteric and epididymal depots, the reduction in adipocytes in HFPD14 was 30–40% average decrease in size (online appendix Fig. S5). In addition, the frequency and distribution of mature macrophages in fixed WAT differed between the groups. As previously described (15), macrophages were aggregated in CLSs, which contained up to 15 macrophages surrounding what appeared to be individual adipocytes. CLS formation was a rare event in control mice (24 ± 9) but was increased >200-fold (489 ± 58) in control mice on HFD or on HFPD1 (506 ± 66) and only ~8-fold (150 ± 23) in HFPD14, indicating a much lower macrophage infiltration in the WAT of the latter group. To analyze if PD153035 was able to reduce macrophage infiltration in retroperitoneal adipose tissue, immunohistochemical staining using specific macrophage marker F4/80+ was performed. As shown in Fig. 4*C* and *D*, HFD increased F4/80+ staining, and PD153035 treatment for 14 days reduced this staining, suggesting less macrophage were present (Fig. 4*C* and *D*). In epididymal and mesenteric fat pads (online appendix Figs. S5 and S6) the results were very similar to the retroperitoneal. As shown in Fig. 4*E*, treatment with PD153035 significantly impaired the migration of human monocytic leukemia cell line (THP1) in a dose-response manner (online appendix).

Effect of PD153035 on tissue protein levels of TNF-α, IL-6, and iNOS and arginase activity in adipocytes and stroma vascular fraction. In retroperitoneal adipose tissue, separation of the stroma vascular fraction (SVF) from adipocytes of lean, HFD, HFPD1, and HFPD14 animals indicated that there was a modest increase in TNF-α protein expression in adipocytes from HFD animals compared with controls and that PD153035 reduced the expression of this cytokine only after 14 days of treatment (Fig. 5*A*). In adipocytes, the expressions of IL-6 and iNOS were higher in mice that received the HFD; these expressions were not significantly affected by PD153035 treatment for 1day. However, after 14 days of PD153035 administration, there was a clear decrease in the expression of these proteins in adipose tissue (Fig. 5*B* and *C*). Similar results were observed in liver and muscle (online appendix Fig. S7). Treatment with PD153035 for 1 or 14 days reduced EGFR tyrosine phosphorylation in adipoctyes (Fig. 5*D*) In SVF, the expressions of TNF-α, IL-6, and iNOS were also higher in HFD animals compared with controls. Different from adipocytes, PD153035 administration for just 1 day was able to reduce the SVF expressions of TNF-α, IL-6, and iNOS, which were normalized after 14 days administration of this drug (Fig. 5*F–H*). There was a significant increase in EGFR tyrosine phosphorylation in SVF of HFD group, and the treatment with PD153035 for 1 or 14 days induced a marked reduction in EGFR tyrosine phosphorylation levels in SVF (Fig. 5*I*). Similar results were observed in adipocytes and SVF from epididymal (online appendix Fig. S8) and mesenteric (data not shown) fat depots.

An important characteristic of the alternative macrophage activation state is the increased arginase activity (35). Arginase activity was measured in adipocytes and SVF samples from controls, HFD, and HFD rats treated with PD153035 for 1 or 14 days. Results showed that the activity of this enzyme did not differ between the isolated adipocytes from the four groups of animals (Fig. 5*K*). However, arginase activity was significantly reduced in the SVF of rats on an HFD, and a significant increase was observed after just 1 day of PD153035 administration. After 14 days of treatment, arginase activity was similar to that of control animals (Fig. 5*K*).

Adiponectin levels were reduced in control mice on an HFD and HFPD1 but increased significantly after 14 days of PD153035 administration. (Fig. 5*L*). Serum leptin levels were higher in the HFD group, and PD153035 administration did not change these levels (Fig. 5*N*). Serum TNF-α and IL-6 levels were higher in mice on an HFD; interestingly, PD153035 administration for 1 day reduced the levels of these cytokines. After 2 weeks of PD153035 treatment, TNF-α and IL-6 returned to normal levels (Fig. 5*M* and *O*).

The protein levels of MCP-1 and MCP-3 were significantly increased in adipose tissue of HFD mice, and treatment with PD153035 for 14 days significantly reduced these chemokines. MCP-2 protein levels were not influenced by high fat as previously described (36) or PD153035 (Fig. 5*P–R*).

DISCUSSION

Our results show that the use of PD153035 (EGFR tyrosine kinase inhibitor) in HFD-fed mice for 14 days induced a marked improvement in glucose tolerance; a reduction in insulin resistance; a reduction in macrophage infiltration in adipocytes and in low-grade inflammation, accompanied by an improvement in insulin signaling in liver, muscle, and adipose tissue; and also an increase in serum adiponectin levels.

It is important to emphasize that administration of PD153035 for 1 day did not change insulin sensitivity/signaling or macrophage infiltration in adipose tissue but reduced the circulating levels of IL-6 and TNF-α, probably as a consequence of reduced activation of macrophage, as shown by a reduction in the expression of these cytokines in the SVF. These data suggest that the first effect observed

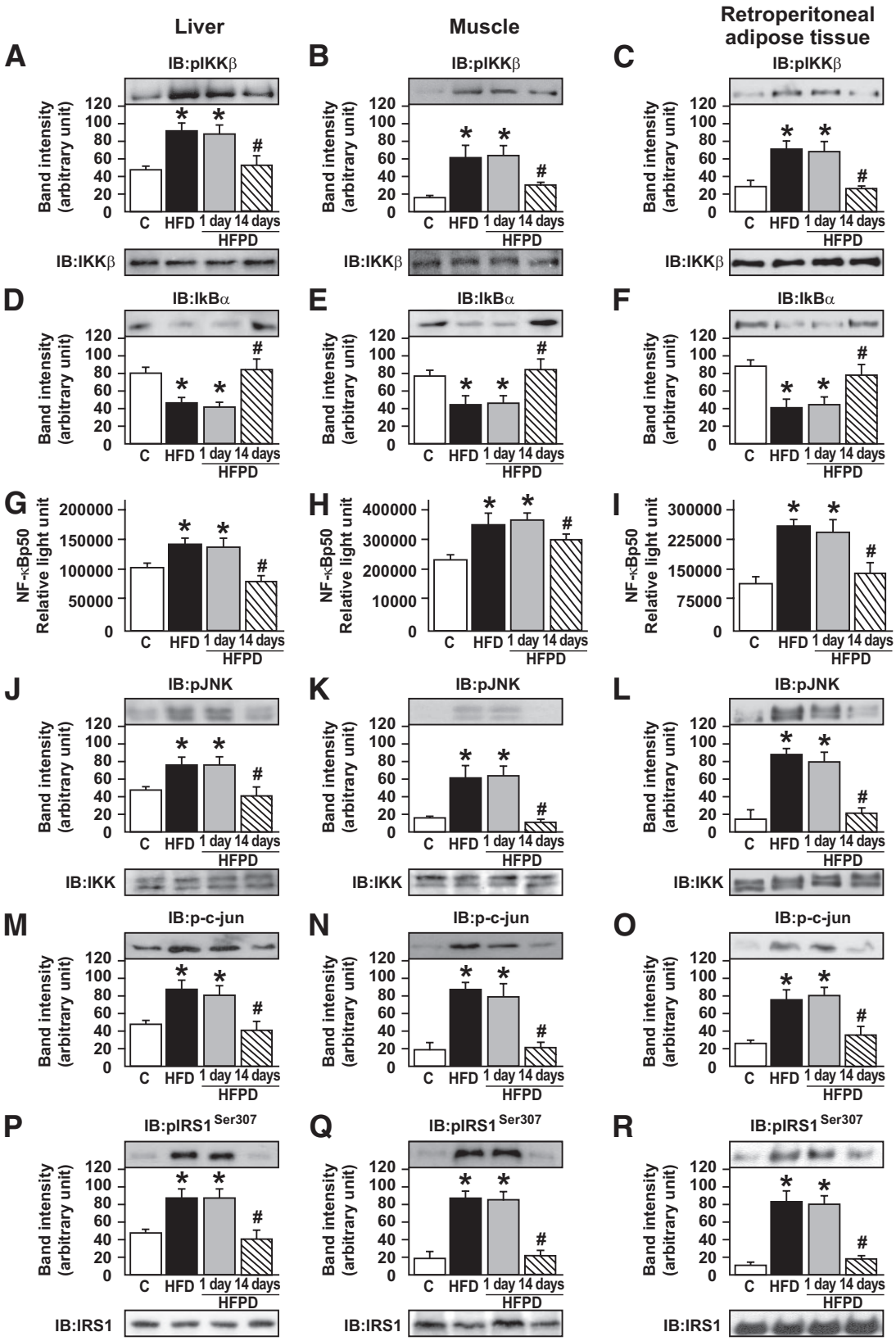

FIG. 3. Effects of PD153035 administration on modulators of insulin signaling. Representative blots show the expression of IKKβ phosphorylation in liver (*A*), muscle (*B*), and retroperitoneal (*C*) of control mice, HFD mice, and HFDPD 1 and 14 days (*upper panels*). Total protein expression of IKKβ (*A–C*, *lower panels*). IκBα in liver (*D*), muscle (*E*), and adipose (*F*) of control mice, HFD mice, and HFDPD 1 and 14 days. NFκB p50 activation was determined in nuclear extracts from liver (*G*), muscle (*H*), and adipose (*I*) tissue by ELISA. JNK phosphorylation in liver (*J*), muscle (*K*), and adipose (*L*) of control mice, HFD mice, and HFDPD 1 and 14 days (*upper panels*). Total protein expression of JNK (*J–L*, *lower panels*). c-Jun phosphorylation in liver (*M*), muscle (*N*), and adipose (*O*) of control mice, HFD mice, and HFDPD 1 and 14 days. IRS1 serine 307 phosphorylation in liver (*P*), muscle (*Q*), and adipose (*R*) of control mice, HFD mice, and HFPD 1 and 14 days (*upper panels*). Total protein expression of IRS-1 (*P–R*, *lower panels*). Data are presented as means ± SE from six mice per group, *$P < 0.05$ vs. control group and #$P < 0.05$ vs. HFD. IB, immunoblot.

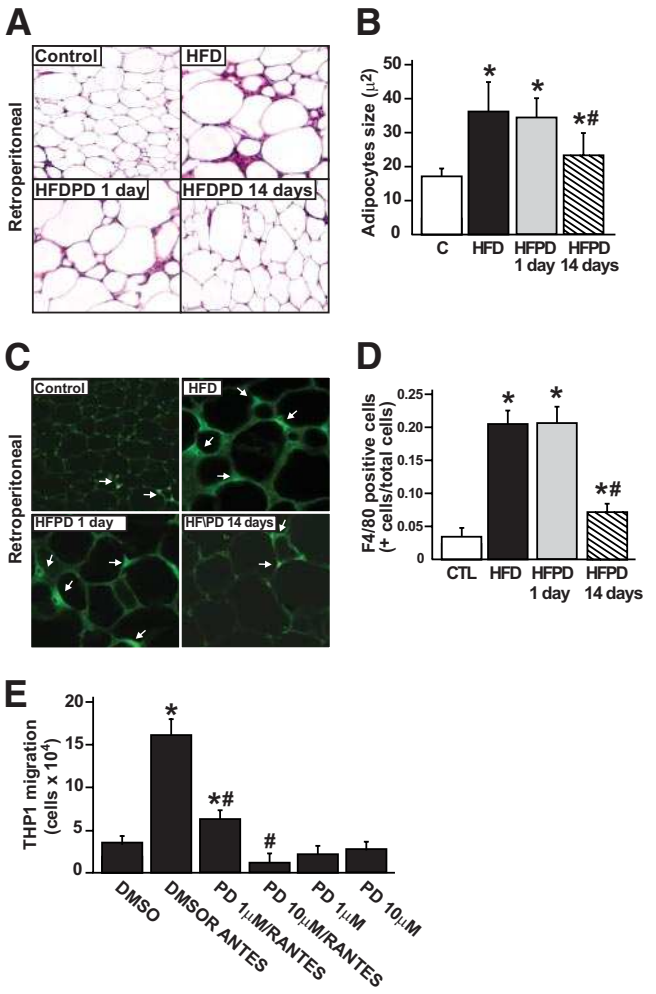

FIG. 4. Effects of PD153035 on adipocyte morphology and activation and migration of macrophages in adipocyte tissue. *A*: Histological sections of retroperitoneal fat pads from control, HFD, and HFDPD after 1 or 14 days, 50-μm scale bar for all pictures. *B*: Quantification of adipocyte size. About 100 cells were measured in each group, and the average adipocyte was calculated. *C*: Representative immunohistochemical staining of WAT using the specific macrophage marker F4/80+. *D*: F4/80-positive cells (+cells/total cells) of all above groups. Data are presented as means ± SE from six mice per group, *$P < 0.05$ vs. control group and #$P < 0.05$ vs. HFD. *E*: Bar graph indicates the number of THP1 cells that migrate from the top to the bottom level of the Boyden blindwell chamber stimulated or not with chemotatic agent RANTES. *$P < 0.05$ vs. DMSO alone; #$P < 0.05$ vs. DMSO/RANTES. Values represent the average of five different assays. (A high-quality color digital representation of this figure is available in the online issue.)

with this drug is a change in macrophage activation. Macrophage activation has been defined across two separate polarization states, M1 and M2 (35,37,38). M1 or "classically activated" macrophages are induced by proinflammatory mediators, such as lipopolysaccharide and interferon-γ, and have enhanced cytokine production (IL-6 and TNF-α) and generate reactive oxygen species such as NO via activation of iNOS. M2 or "alternatively activated" macrophages have low proinflammatory cytokine expression and, instead, generate high levels of the anti-inflammatory cytokines IL-10 and IL-1 decoy receptor. In addition, in these macrophages, arginase production (an enzyme that blocks iNOS activity) is increased (39). In summary, M2 macrophages are believed to participate in the blockade of inflammatory responses and in the promotion of tissue repair (37). Our data show that PD153035 treatment for just 1 day reduced the expression of IL-6, TNF-α, and iNOS in the SVF and, in parallel, induced an increase in arginase activity, suggesting that PD153035 may lead to a shift in the activation state of ATMs, reducing the M1 proinflammatory state that contributes to insulin resistance. Since EGFR tyrosine phosphorylation was increased in the SVF of HFD mice, it is possible that the primary action of PD153035 is on ATMs, but a direct relation between EGFR and macrophage activation deserves further investigation.

In mice treated with PD153035 for 14 days, the HFD induced a less marked macrophage infiltration in adipose tissue, accompanied by an attenuated increase in TNF-α, IL-6, and FFAs. This decrease in macrophage infiltration may be a direct effect of EGFR tyrosine kinase inhibition. In agreement, our data show that PD153035 reduces monocyte migration. Recent studies (21–23) demonstrated that EGFR and/or other tyrosine kinase inhibitors inhibit the growth and/or activation of some nonmalignant hematopoietic cells, including monocyte/macrophages. Interestingly, another study (40) has shown that a reduction in macrophage infiltration and/or resident alternatively activated macrophages can decrease local inflammation in WAT. In accordance with this, our data show that in the adipose tissue of HFD-fed mice treated with PD153035 for 14 days, in parallel with a reduction in macrophage infiltration, there were lower expressions of TNF-α, IL-6, and iNOS, indicating that this drug decreases local inflammation in WAT of HFD mice. In addition, in HFD mice treated with PD153035 for 14 days there was also a decrease in MCP-1 and MCP-3 in adipose tissue, which may have a role in the reduced macrophage infiltration. These results lead us to suggest that this decrease in inflammation in WAT may have an important role in the effect of PD153035, improving insulin resistance and glucose tolerance in HFD mice.

The improvement in insulin action induced after 14 days of PD153035 administration was also demonstrated at the tissue level in the insulin signaling pathway. The blunted insulin-stimulated IR tyrosine phosphorylation and phosphorylation of Akt and the increase of IRS-1 Ser^{307} in liver, muscle, and WAT of HFD mice was prevented by treatment with PD153035, providing a biochemical correlate for the increase in in vivo insulin sensitivity. Ser^{307} is reported to be a phosphoacceptor of JNK and IKKβ (10,41); as previously described (42–45), our results also show that these kinases are activated in tissues of HFD mice. Our data demonstrated that PD 153035 administration for 14 days prevents the activation of IKKβ and JNK in liver, muscle, and WAT, which may be a consequence of the reduction in inflammation in WAT and in the circulating levels of FFAs, TNF-α, and IL-6. However, we cannot exclude the possibility of a direct effect of PD153035 on JNK and IKKβ/NFκB pathways as previously described in cell culture (24,25), although our data show that acute administration of PD153035 did not have this effect.

It is unlikely that PD153035 improved insulin action by a direct effect on glucose transport in muscle because the administration of this drug to isolated muscle did not increase insulin-induced glucose uptake. Another mechanism that may have contributed to the effect of PD153035 on glucose homeostasis is the reversal of the decreased adiponectin levels observed in HFD mice. It is possible that the reduced inflammatory state in adipose tissue and smaller adipocytes in HFPD14 may have allowed the restoration or even an increase in adiponectin secretion.

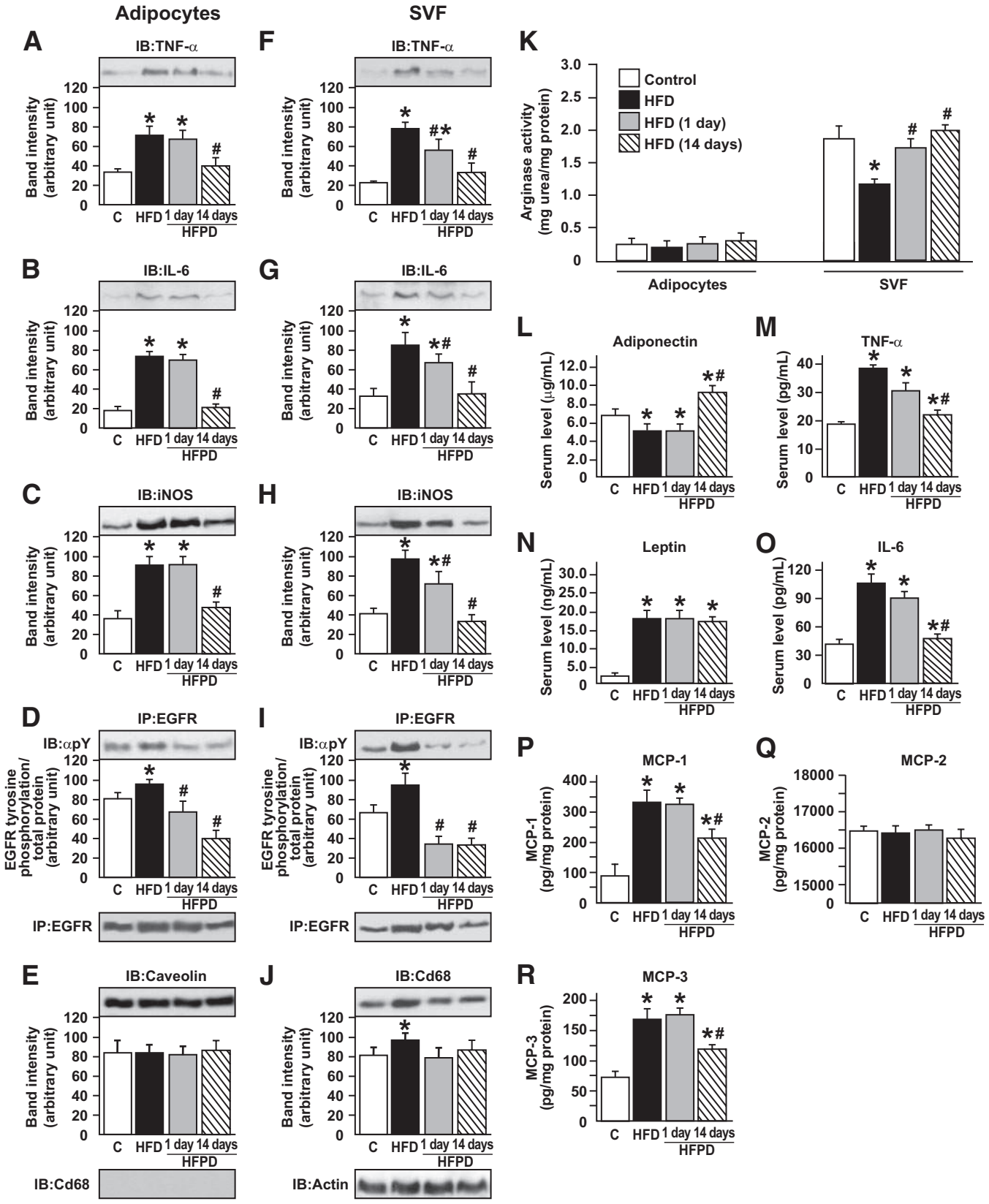

FIG. 5. Effect of PD153035 on tissue protein levels of TNF-α, IL-6, and iNOS and arginase activity in adipocytes and SVF from retroperitoneal adipose tissue. Representative blots show the tissue levels of TNF-α, IL-6, iNOS, EGRF tyrosine phosphorylation, EGRF, Caveolin, and Cd68 protein expression in adipocytes (*A–D*) and TNF-α, IL-6, iNOS, EGRF tyrosine phosphorylation, EGRF, Cd68, and actin protein expression in the SVF (*F–J*). *K*: Arginase activity of adipocytes and SVF from control mice, HFD mice, and HFDPD 1 and 14 days. Serum levels of adiponectin (*L*), TNF-α (*M*), leptin (*N*), and IL-6 (*O*) and MCP-1 (*P*), MCP-2 (*Q*), and MCP-3 (*R*) protein expression were obtained using ELISA assay. Data are presented as means ± SE of six to eight mice per group. *$P < 0.05$ vs. control group; #$P < 0.05$ vs. HFD group.

The distribution of body fat appears to be even more important than the total amount of fat. The adverse metabolic impact of visceral fat has been attributed to distinct biological properties of adipocytes in this depot, including variations in the metabolic activity of fat cells and in the expression of cytokines, hormones, and polypeptides (46,47). Our data showed that HFD increased EGFR expression and basal tyrosine phosphorylation in mesenteric and retroperitoneal (internal fat depot) but not in epididymal fat pads, suggesting a role of this receptor in the development of central obesity and/or its metabolic consequences. Moreover, the more marked decrease in EGFR tyrosine phosphorylation after PD153035 treatment in the internal fat depots accompanied the significant reduction in the weight of these fat depots. It is possible that the decrease in fat depots may contribute to the improvement in glucose tolerance and insulin sensitivity in animals treated with PD153035 for 14 days. In this regard, the regulation of EGFR in macrophages and in mesenteric and retroperitoneal fat pads in HFD suggests that this receptor and/or signaling pathway may have a role in the insulin resistance of obesity and diabetes and deserves further exploration.

In summary, our results show that the use of PD153035 for just 1 day was able to reduce the protein expressions of iNOS, TNF-α, and IL-6 in SVF. We can thus suggest that PD153035 inhibits EGFR tyrosine kinase activity in ATMs, reducing the M1 proinflammatory state as an initial effect. This reduces the circulating levels of TNF-α and IL-6, initiating an improvement in insulin signaling and sensitivity. After 14 days of the drug administration, there was a marked improvement in glucose tolerance; a reduction in insulin resistance; a reduction in macrophage infiltration in adipocytes and in TNF-α, IL-6, and FFAs; accompanied by an improvement in insulin signaling in liver muscle and adipose tissue. We, therefore, suggest that PD153035 presents an attractive opportunity for the treatment of insulin resistance and type 2 diabetes.

ACKNOWLEDGMENTS

This study was supported by grants from Fundação de Amparo à Pesquisa do Estado de São Paulo and Conselho Nacional de Pesquisa.

No potential conflicts of interest relevant to this article were reported.

The authors thank Luiz Janeri, Jósimo Pinheiro, and Márcio A. da Cruz for technical assistance.

REFERENCES

1. Gusterson BA, Hunter KD. Should we be surprised at the paucity of response to EGFR inhibitors? Lancet Oncol 2009;10:522–527
2. Breccia M, Muscaritoli M, Aversa Z, Mandelli F, Alimena G. Imatinib mesylate may improve fasting blood glucose in diabetic Ph+ chronic myelogenous leukemia patients responsive to treatment. J Clin Oncol 2004;22:4653–4655
3. Costa DB, Huberman MS. Improvement of type 2 diabetes in a lung cancer patient treated with Erlotinib. Diabetes Care 2006;29:1711
4. Templeton A, Brandle M, Cerny T, Gillessen S. Remission of diabetes while on sunitinib treatment for renal cell carcinoma. Ann Oncol 2008;19:824–825
5. Veneri D, Franchini M, Bonora E. Imatinib and regression of type 2 diabetes. N Engl J Med 2005;352:1049–1050
6. Prada PO, Zecchin HG, Gasparetti AL, Torsoni MA, Ueno M, Hirata AE, Corezola do Amaral ME, Hoer NF, Boschero AC, Saad MJ. Western diet modulates insulin signaling, c-Jun N-terminal kinase activity, and insulin receptor substrate-1ser307 phosphorylation in a tissue-specific fashion. Endocrinology 2005;146:1576–1587
7. Saltiel AR, Pessin JE. Insulin signaling pathways in time and space. Trends Cell Biol 2002;12:65–71
8. Taniguchi CM, Emanuelli B, Kahn CR. Critical nodes in signalling pathways: insights into insulin action. Nat Rev Mol Cell Biol 2006;7:85–96
9. Aguirre V, Uchida T, Yenush L, Davis R, White MF. The c-Jun NH(2)-terminal kinase promotes insulin resistance during association with insulin receptor substrate-1 and phosphorylation of Ser(307). J Biol Chem 2000; 275:9047–9054
10. Aguirre V, Werner ED, Giraud J, Lee YH, Shoelson SE, White MF. Phosphorylation of Ser307 in insulin receptor substrate-1 blocks interactions with the insulin receptor and inhibits insulin action. J Biol Chem 2002;277:1531–1537
11. Dandona P, Aljada A, Bandyopadhyay A. Inflammation: the link between insulin resistance, obesity and diabetes. Trends Immunol 2004;25:4–7
12. Gao Z, Zuberi A, Quon MJ, Dong Z, Ye J. Aspirin inhibits serine phosphorylation of insulin receptor substrate 1 in tumor necrosis factor-treated cells through targeting multiple serine kinases. J Biol Chem 2003;278:24944–24950
13. Pickup JC. Inflammation and activated innate immunity in the pathogenesis of type 2 diabetes. Diabetes Care 2004;27:813–823
14. Shoelson SE, Lee J, Goldfine AB. Inflammation and insulin resistance. J Clin Invest 2006;116:1793–1801
15. Cinti S, Mitchell G, Barbatelli G, Murano I, Ceresi E, Faloia E, Wang S, Fortier M, Greenberg AS, Obin MS. Adipocyte death defines macrophage localization and function in adipose tissue of obese mice and humans. J Lipid Res 2005;46:2347–2355
16. Weisberg SP, McCann D, Desai M, Rosenbaum M, Leibel RL, Ferrante AW Jr: Obesity is associated with macrophage accumulation in adipose tissue. J Clin Invest 2003;112:1796–1808
17. Xu H, Barnes GT, Yang Q, Tan G, Yang D, Chou CJ, Sole J, Nichols A, Ross JS, Tartaglia LA, Chen H. Chronic inflammation in fat plays a crucial role in the development of obesity-related insulin resistance. J Clin Invest 2003;112:1821–1830
18. Eales-Reynolds LJ, Laver H, Modjtahedi H. Evidence for the expression of the EGF receptor on human monocytic cells. Cytokine 2001;16:169–172
19. Lamb DJ, Modjtahedi H, Plant NJ, Ferns GA. EGF mediates monocyte chemotaxis and macrophage proliferation and EGF receptor is expressed in atherosclerotic plaques. Atherosclerosis 2004;176:21–26
20. Scholes AG, Hagan S, Hiscott P, Damato BE, Grierson I. Overexpression of epidermal growth factor receptor restricted to macrophages in uveal melanoma. Arch Ophthalmol 2001;119:373–377
21. Bos M, Mendelsohn J, Kim YM, Albanell J, Fry DW, Baselga J. PD153035, a tyrosine kinase inhibitor, prevents epidermal growth factor receptor activation and inhibits growth of cancer cells in a receptor number-dependent manner. Clin Cancer Res 1997;3:2099–2106
22. Fry DW, Kraker AJ, McMichael A, Ambroso LA, Nelson JM, Leopold WR, Connors RW, Bridges AJ. A specific inhibitor of the epidermal growth factor receptor tyrosine kinase. Science 1994;265:1093–1095
23. Rae JM, Lippman ME. Evaluation of novel epidermal growth factor receptor tyrosine kinase inhibitors. Breast Cancer Res Treat 2004;83:99–107
24. Wan YS, Wang ZQ, Voorhees J, Fisher G. EGF receptor crosstalks with cytokine receptors leading to the activation of c-Jun kinase in response to UV irradiation in human keratinocytes. Cell Signal 2001;13:139–144
25. Wu W, Jaspers I, Zhang W, Graves LM, Samet JM. Role of Ras in metal-induced EGF receptor signaling and NF-kappaB activation in human airway epithelial cells. Am J Physiol Lung Cell Mol Physiol 2002;282: L1040–L1048
26. Bartolovic K, Balabanov S, Hartmann U, Komor M, Boehmler AM, Buhring HJ, Mohle R, Hoelzer D, Kanz L, Hofmann WK, Brummendorf TH. Inhibitory effect of imatinib on normal progenitor cells in vitro. Blood 2004;103:523–529
27. Cheon H, Woo YS, Lee JY, Kim HS, Kim HJ, Cho S, Won NH, Sohn J. Signaling pathway for 2,3,7,8-tetrachlorodibenzo-p-dioxin-induced TNF-alpha production in differentiated THP-1 human macrophages. Exp Mol Med 2007;39:524–534
28. Dewar AL, Domaschenz RM, Doherty KV, Hughes TP, Lyons AB. Imatinib inhibits the in vitro development of the monocyte/macrophage lineage from normal human bone marrow progenitors. Leukemia 2003;17:1713–1721
29. Normanno N, De Luca A, Aldinucci D, Maiello MR, Mancino M, D'Antonio A, De Filippi R, Pinto A. Gefitinib inhibits the ability of human bone marrow stromal cells to induce osteoclast differentiation: implications for the pathogenesis and treatment of bone metastasis. Endocr Relat Cancer 2005;12:471–482
30. Rocco SA, Velho JA, Marin RM, de Arruda Rolim Filho L, Vercesi AE, Rittner R, Franchini KG. High performance liquid chromatography analysis of a 4-anilinoquinazoline derivative (PD153035), a specific inhibitor of the

epidermal growth factor receptor tyrosine kinase, in rat plasma. J Chromatogr B Analyt Technol Biomed Life Sci 2005;817:297–302
31. Carvalho-Filho MA, Ueno M, Hirabara SM, Seabra AB, Carvalheira JB, de Oliveira MG, Velloso LA, Curi R, Saad MJ. S-nitrosation of the insulin receptor, insulin receptor substrate 1, and protein kinase B/Akt: a novel mechanism of insulin resistance. Diabetes 2005;54:959–967
32. De Souza CT, Araujo EP, Stoppiglia LF, Pauli JR, Ropelle E, Rocco SA, Marin RM, Franchini KG, Carvalheira JB, Saad MJ, Boschero AC, Carneiro EM, Velloso LA. Inhibition of UCP2 expression reverses diet-induced diabetes mellitus by effects on both insulin secretion and action. Faseb J 2007;21:1153–1163
33. Tsukumo DM, Carvalho-Filho MA, Carvalheira JB, Prada PO, Hirabara SM, Schenka AA, Araujo EP, Vassallo J, Curi R, Velloso LA, Saad MJ. Loss-of-function mutation in Toll-like receptor 4 prevents diet-induced obesity and insulin resistance. Diabetes 2007;56:1986–1998
34. Thirone AC, Carvalheira JB, Hirata AE, Velloso LA, Saad MJ. Regulation of Cbl-associated protein/Cbl pathway in muscle and adipose tissues of two animal models of insulin resistance. Endocrinology 2004;145:281–293
35. Lumeng CN, Bodzin JL, Saltiel AR. Obesity induces a phenotypic switch in adipose tissue macrophage polarization. J Clin Invest 2007;117:175–184
36. Jiao P, Chen Q, Shah S, Du J, Tao B, Tzameli I, Yan W, Xu H. Obesity-related upregulation of monocyte chemotactic factors in adipocytes: involvement of nuclear factor-κB and c-Jun NH_2-terminal kinase pathways. Diabetes, 2009;58:104–115
37. Gordon S, Taylor PR. Monocyte and macrophage heterogeneity. Nat Rev Immunol 2005;5:953–964
38. Mantovani A, Sica A, Sozzani S, Allavena P, Vecchi A, Locati M. The chemokine system in diverse forms of macrophage activation and polarization. Trends Immunol 2004;25:677–686
39. Bronte V, Zanovello P. Regulation of immune responses by L-arginine metabolism. Nat Rev Immunol 2005;5:641–654
40. Furuhashi M, Tuncman G, Gorgun CZ, Makowski L, Atsumi G, Vaillancourt E, Kono K, Babaev VR, Fazio S, Linton MF, Sulsky R, Robl JA, Parker RA, Hotamisligil GS. Treatment of diabetes and atherosclerosis by inhibiting fatty-acid-binding protein aP2. Nature 2007;447:959–965
41. Gao Z, Hwang D, Bataille F, Lefevre M, York D, Quon MJ, Ye J. Serine phosphorylation of insulin receptor substrate 1 by inhibitor kappa B kinase complex. J Biol Chem 2002;277:48115–48121
42. Hirosumi J, Tuncman G, Chang L, Gorgun CZ, Uysal KT, Maeda K, Karin M, Hotamisligil GS. A central role for JNK in obesity and insulin resistance. Nature 2002;420:333–336
43. Lee YH, Giraud J, Davis RJ, White MF. c-Jun N-terminal kinase (JNK) mediates feedback inhibition of the insulin signaling cascade. J Biol Chem 2003;278:2896–2902
44. Ropelle ER, Pauli JR, Prada PO, de Souza CT, Picardi PK, Faria MC, Cintra DE, Fernandes MF, Flores MB, Velloso LA, Saad MJ, Carvalheira JB. Reversal of diet-induced insulin resistance with a single bout of exercise in the rat: the role of PTP1B and IRS-1 serine phosphorylation. J Physiol 2006;577:997–1007
45. Yuan M, Konstantopoulos N, Lee J, Hansen L, Li ZW, Karin M, Shoelson SE. Reversal of obesity- and diet-induced insulin resistance with salicylates or targeted disruption of Ikkbeta. Science 2001;293:1673–1677
46. Giorgino F, Laviola L, Eriksson JW. Regional differences of insulin action in adipose tissue: insights from in vivo and in vitro studies. Acta Physiol Scand 2005;183:13–30
47. Montague CT, O'Rahilly S. The perils of portliness: causes and consequences of visceral adiposity. Diabetes 2000;49:883–888

APÊNDICE *VIII*

Hypothalamic Actions of Tumor Necrosis Factor α Provide the Thermogenic Core for the Wastage Syndrome in Cachexia

Ana Paula Arruda, Marciane Milanski, Talita Romanatto, Carina Solon, Andressa Coope, Luciane C. Alberici, William T. Festuccia, Sandro M. Hirabara, Eduardo Ropelle, Rui Curi, José B. Carvalheira, Aníbal E. Vercesi, and Licio A. Velloso

Laboratory of Cell Signaling (A.P.A., M.M., T.R., C.S., A.C., W.T.F., L.A.V.) and Departments of Internal Medicine (E.R., J.B.C., L.A.V.) and Clinical Pathology (L.C.A., A.E.V.), University of Campinas, 13084-960 Campinas, Brazil; and Department of Physiology and Biophysics (S.M.H., R.C.), University of Sao Paulo, 05508-090 Sao Paulo, Brazil

TNFα is an important mediator of catabolism in cachexia. Most of its effects have been characterized in peripheral tissues, such as skeletal muscle and fat. However, by acting directly in the hypothalamus, TNFα can activate thermogenesis and modulate food intake. Here we show that high concentration TNFα in the hypothalamus leads to increased O_2 consumption/CO_2 production, increased body temperature, and reduced caloric intake, resulting in loss of body mass. Most of the thermogenic response is produced by β3-adrenergic signaling to the brown adipose tissue (BAT), leading to increased BAT relative mass, reduction in BAT lipid quantity, and increased BAT mitochondria density. The expression of proteins involved in BAT thermogenesis, such as β3-adrenergic receptor, peroxisomal proliferator-activated receptor-γ coactivator-1α, and uncoupling protein-1, are increased. In the hypothalamus, TNFα produces reductions in neuropeptide Y, agouti gene-related peptide, proopiomelanocortin, and melanin-concentrating hormone, and increases CRH and TRH. The activity of the AMP-activated protein kinase signaling pathway is also decreased in the hypothalamus of TNFα-treated rats. Upon intracerebroventricular infliximab treatment, tumor-bearing and septic rats present a significantly increased survival. In addition, the systemic inhibition of β3-adrenergic signaling results in a reduced body mass loss and increased survival in septic rats. These data suggest hypothalamic TNFα action to be important mediator of the wastage syndrome in cachexia. **(*Endocrinology* 151: 683–694, 2010)**

In severely ill patients with cancer or infectious diseases, the development of cachexia is one of the main determinants of rapid progression to failure of multiple organs, with a direct impact on mortality (1). Hampering the installation and progression of cachexia significantly improves quality of life and delays death. However, anticachexia approaches used to date lack specificity because little is known about the mechanisms leading to each component of the wastage syndrome (2, 3).

Increased proteolysis and thermogenesis, accompanied by anorexia, are the main consumptive components of cachexia. All these phenomena are highly dependent on the actions of inflammatory cytokines, in which TNFα is the most important (4–6). Although the effects of TNFα on muscle proteolysis and adipocyte metabolism can be partially attributed to the action of this cytokine directly on target tissues (7, 8), recent studies demonstrated that much of the anorexigenic and prothermogenic effects of

ISSN Print 0013-7227 ISSN Online 1945-7170
Printed in U.S.A.

doi: 10.1210/en.2009-0865 Received July 23, 2009. Accepted November 6, 2009.
First Published Online December 8, 2009

Abbreviations: ACC, Acetyl-coenzyme A carboxylase; AgRP, agouti gene-related peptide; AMPK, AMP-activated protein kinase; BAT, brown adipose tissue; CART, cocaine- and amphetamine-induced transcript; Dio2, D2 deiodinase; GAPD, glyceraldehyde-3-phosphate dehydrogenase; ICV, intracerebroventricular; MCH, melanin-concentrating hormone; NPY, neuropeptide Y; pACC, phospho-ACC; pAMPK, phospho-AMPK; PGC1, peroxisomal proliferator-activated receptor-γ coactivator 1; POMC, proopiomelanocortin; UCP, uncoupling protein.

TNFα result from its actions in the central nervous system, particularly in the hypothalamus (9, 10).

The hypothalamus harbors a complex network of neurons that coordinate the energy homeostasis in the body. TNFα, acting in the hypothalamus, can modulate energy expenditure by directly controlling neurotransmitter expression or modifying the adipostatic signals delivered by leptin and insulin (9–11). In addition, a previous study has shown that TNFα action in the hypothalamus leads to increased thermogenesis and O_2 consumption (12). However, the paths connecting the central actions of TNFα with peripheral thermogenic organs and the molecular mechanisms driving this response have not been fully evaluated.

Here we show that TNFα, acting in the hypothalamus, increases body temperature and whole-body oxygen consumption, leading to the loss of body mass by a mechanism dependent on the sympathetic activation of the brown adipose tissue (BAT) thermogenesis. These mechanisms are paralleled by the direct modulation of neurotransmitter expression and AMP-activated protein kinase (AMPK) signaling in the hypothalamus. Inhibiting hypothalamic TNFα action by intracerebroventricular (ICV) infliximab increases life span and improves morbidity in cachexia induced by cancer and sepsis. In addition, inhibiting β3-adrenergic activity significantly reduces morbidity and mortality in sepsis.

Materials and Methods

Antibodies and chemicals

Antibodies against uncoupling protein (UCP)-1 (sc-6529, goat polyclonal), and β3-adrenergic receptor (sc-1473, goat polyclonal) were from Santa Cruz Biotechnology (Santa Cruz, CA). Antibodies against peroxisomal proliferator-activated receptor-γ coactivator 1 (PGC1)-α (no. 2178, rabbit monoclonal), phospho-AMPK (pAMPK, no. 2535s, rabbit monoclonal), AMPK (no. 2532, rabbit monoclonal), phospho-acetyl-coenzyme A carboxylase (ACC; pACC, no. 3661s, rabbit monoclonal), and ACC (no. 3662, rabbit monoclonal) were from Cell Signaling Technology (Beverly, MA). Antibody against cytochrome C (no. 7H8.2C12, mouse monoclonal) was from BD Biosciences (Franklin Lakes, NJ). Antibody against β-actin (ab6276, mouse monoclonal) was from Abcam (Cambridge, MA). All the reagents for SDS-PAGE and immunoblotting were from Bio-Rad (Hercules, CA). HEPES, phenylmethylsulfonyl fluoride, aprotinin, dithiothreitol, Triton X-100, Tween 20, glycerol, BSA fatty acid free (A-6003), SR59230A, and angiotensin II were from Sigma-Aldrich (St. Louis, MO). Mouse recombinant TNFα was from Calbiochem (La Jolla, CA). Sodium thiopental, ketamine, and diazepam were from Cristalia (Itapira, Brazil). All the chemicals and primers used in real-time PCR were from Applied Biosystems (Foster City, CA). Infliximab was from Centocor (Horsham, PA).

ICV cannulation

For ICV cannulation, 8-wk-old male Wistar rats (*Rattus norvegicus*) with a body mass of 250–300 g were used. The animals were obtained from the University of Campinas Central Animal Breeding Center. The rats were allowed access to standard rodent chow and water *ad libitum* and were maintained on a 12-h light, 12-h dark cycle. All experiments were conducted in accordance with the principles and procedures described by the National Institutes of Health Guidelines for the Care and Use of Experimental Animals and were approved by the University of Campinas Ethical Committee. The rats were stereotaxically instrumented using a Stoelting stereotaxic apparatus, according to a previously described method (10). Cannula efficiency was tested 1 wk after cannulation by the evaluation of the drinking response elicited by ICV angiotensin II (13). Stereotaxic coordinates were anteroposterior, 0.2 mm/lateral, 1.5 mm/depth, 4.0 mm. ICV-cannulated rats were treated for 4 d, once a day, with TNFα (2.0 μl, 10^{-8} M, corresponding to a solution containing 170 ng/ml, which provides a final tissue concentration of 50–100 pg/ml, ED_{50} 20–50 pg/ml; controls were treated with similar volume saline). The TNFα dose used in this study was based on previous studies (9, 10) and is regarded as a high dose of the cytokine. In some experiments the rats were treated with the β3-antagonist SR59230A (0.1 mg/kg in 200 μl, ip) twice a day.

Denervation of BAT

Under anesthesia, five branches of the right only (monolateral denervation) or right and left (bilateral denervation) intercostal nerve bundles that contain sympathetic fibers entering the right and left sides of the interscapular BAT were isolated, and a fragment of 5.0 mm was removed from each one. Surgical denervation was performed 6 d before the experiments and was performed according to a previously published method (14).

Indirect calorimetry and body temperature

O_2 consumption, CO_2 release, and respiratory exchange ratio were measured in fed animals through an indirect open circuit calorimeter (Oxymax deluxe system; Columbus Instruments, Columbus, OH), as described previously (15). Rectal temperature was measured with a digital thermometer, and the values presented represent the mean of two daily determinations or the means of all measures obtained during the experimental period.

Blood gas analysis

Blood pO_2, pCO_2, and pH were determined in a venous blood sample and analyzed automatically in an ABL 800 FLEX radiometer blood gas analyzer (Radiometer, Copenhagen, Denmark).

Light and transmission electron microscopy

BAT depots were dissected and assessed by light microscopy and transmission electron microscopy. For light microscopy, BAT depots were fixed by immersion in 4% formaldehyde in 0.1 mM phosphate buffer (pH 7.4), dehydrated, cleared, and then embedded in paraffin. Serial sections (5.0 μm thick) were obtained and then stained by hematoxylin and eosin to assess the morphology. For electron microscopy, BAT was prefixed in 2.5% glutaraldehyde and 2% paraformaldehyde in 0.05 M (pH 7.2) cacodylate buffer plus 0.001 M $CaCl_2$ for 2 h, postfixed in 1% osmium tetroxide in the same buffer for 1 h, and then stained

with 0.5% aqueous uranyl acetate overnight. The samples were dehydrated in acetone and embedded in Spurr's or Epon low-viscosity embedding medium. Blocks were sectioned in an Ultracut UCT ultramicrotome (Leica, Wetzlar, Germany), stained with 3% aqueous uranyl acetate and Reynold's lead citrate, and examined under an EM 900 transmission electron microscope (Zeiss, Jena, Germany) (16). The number of mitochondria and the area of adipose tissue depots in histological specimens were determined by the Imagelab Analysis software (Imagelab, Modena, Italy).

Real-time PCR

The expressions of UCP1, PGC1α, D2 deiodinase (Dio2), UCP3, neuropeptide Y (NPY), agouti gene-related peptide (AgRP), TRH, CRH, proopiomelanocortin (POMC), melanin-concentrating hormone (MCH), and cocaine- and amphetamine-induced transcript (CART) mRNAs were measured in samples (BAT, soleus muscle gastrocnemius muscle, or hypothalamus) obtained from rats treated ICV with saline (control) or TNFα 10^{-8} M. Intron-skipping primers were obtained from Applied Biosystems. Glyceraldehyde-3-phosphate dehydrogenase (GAPD) primers were used as control, and normalization experiments are shown in supplemental Fig. S1, published as supplemental data on The Endocrine Society's Journals Online web site at http://endo.endojournals.org. The endogenous control for normalization of GAPD was hypoxanthine-guanine phosphoribosyl transferase. No significant change in GAPD expression was detected in the different experimental conditions. Real-time PCR analysis of gene expression was performed in an ABI Prism 7700 sequence detection system (Applied Biosystems). The optimal concentration of cDNA and primers, as well as the maximum efficiency of amplification, was obtained through five-point, 2-fold dilution curve analysis for each gene. Each PCR contained 3.0 ng of reverse-transcribed RNA, 200 nM of each specific primer, TaqMan (Applied Biosystems), and ribonuclease-free water to a final volume of 20 μl. Real-time data were analyzed using the Sequence Detector System 1.7 (Applied Biosystems).

Immunoblotting

For evaluation of protein expression in the hypothalami, BAT, soleus, and gastrocnemius muscles, the specimens were excised and immediately homogenized in solubilization buffer [1% Triton X-100, 100 mM Tris-HCl (pH 7.4), 100 mM sodium pyrophosphate, 100 mM sodium fluoride, 10 mM EDTA, 10 mM sodium orthovanadate, 2.0 mM phenylmethylsulfonyl fluoride and 0.1 mg aprotinin per milliliter] at 4 C with a Polytron PTA 20S generator (model PT 10/35; Brinkmann Instruments, Westbury, NY). Insoluble material was removed by centrifugation for 15 min at 9000 × *g*. The protein concentration of the supernatants was determined by the Bradford dye binding method. Samples containing 0.05–0.2 mg of protein extracts were separated by SDS-PAGE, transferred to nitrocellulose membranes, and blotted with anti-UCP1, anti-PGC1α, anticytochrome C, anti-β3-adrenergic receptor, anti-pAMPK or anti-pACC antibodies. For evaluation of protein loading, membranes were stripped and reblotted with anti-β-actin, anti-AMPK or anti-ACC antibodies, as appropriate. Specific bands were detected by chemiluminescence and visualization/capture was performed by exposure of the membranes to RX films.

Skeletal muscle oxygen consumption and citrate synthase activity

Fragments (1.0–3.0 mg) of the soleus muscle were placed in a petri dish on ice with 1 ml of relaxing solution containing Ca^{2+}/EGTA buffer (10 mM), free calcium (0.1 μM), imidazole (20 mM), K^+/4-morpholinoethanesulfonic acid (50 mM), dithiothreitol (0.5 mM), $MgCl_2$ (6.56 mM), ATP (5.77 mM), and phosphocreatine (15 mM) (pH 7.1), and individual fiber bundles were separated with a sharp forceps. The fiber bundles were permeabilized for 30 min in an ice-cold relaxing solution containing saponin (50 μg/ml). The fibers were washed twice for 10 min each. The muscle bundles were then immediately transferred into a Oroboros respirometer (Innsbruck, Austria) containing an air-saturated respiration medium at 37 C. Oxygen consumption was measured in the respiration medium, MiR05, containing potassium lactobionate (60 mM), EGTA (0.5 mM), $MgCl_2 \cdot 6H_2O$ (3.0 mM), taurine (20 mM), KH_2PO_4 (10 mM), HEPES (20 mM), sucrose (110 mM), and BSA (2.0 mg/ml) (pH 7.1), in the presence of pyruvate (7.0 mM) and malate (4.0 mM). The respiration rate in state III was measured after addition of ADP (2.0 mM) and the state IV in the presence of oligomycin (1.0 μg/ml). The Oxygraph-2k (Oroborus, Innsbruk, Austria) is a two-chamber titration-injection respirometer with a limit of oxygen flux detection of 1.0 pmol/$sec^{-1} \cdot ml^{-1}$. Citrate synthase activity was determined in soleus and gastrocnemius muscles by spectrophotometry, as previously described (17).

Cecal ligation and perforation

ICV-cannulated rats were anesthetized with ketamine (80 mg/kg) and diazepam (30 mg/kg) diluted in sterile saline and administered ip. Laparotomy was performed with a 2-cm midline incision through the linea alba; the cecum was exposed and totally or partially obstructed with sterile 3-0 silk below the ileocecal junction. The cecum was punctured once (in the group with partially obstructed cecum) or 12 times (in the group with totally obstructed cecum) with an 18-gauge needle and was then gently squeezed to empty its content through the puncture. The cecum was then returned to the peritoneal cavity, and the abdominal muscle and skin incisions were closed in layers using a 3-0 nylon suture line (18). After recovery, the animals were divided into two groups; one group received saline (2.0 μl) and the other group received infliximab (0.3 μg in 2.0 μl) ICV, twice a day, for 4 d or while alive. For the experiments using the β3-adrenergic antagonist, SR59230A, the animals were treated ip (0.1 mg/kg in 200 μl) twice a day (19).

Tumor xenograft model

The Walker-256 tumor cell line (originally obtained from the Christ Hospital Line, National Cancer Institute Bank, Cambridge, UK) is currently maintained frozen in liquid nitrogen. Walker-256 tumor cells were obtained from the ascitic fluid of the peritoneal cavity of Wistar rats, 5 d after the ip injection of 2.0×10^7 cells. After cell harvesting, the percentage of viable cells was determined using 1% Trypan blue solution in a Neubauer chamber. Tumor cells (2.0×10^6 cells in 1.0 ml saline solution) were injected in the right flank after the surgical implantation of the ICV cannula. The experiments were performed 1 wk after complete recovery from the stereotaxic surgery. Each animal's individual baseline 24-h food intake was defined as the average daily food intake over a period of 3 consecutive days. In tumor-bearing animals, cancer anorexia was defined as a single

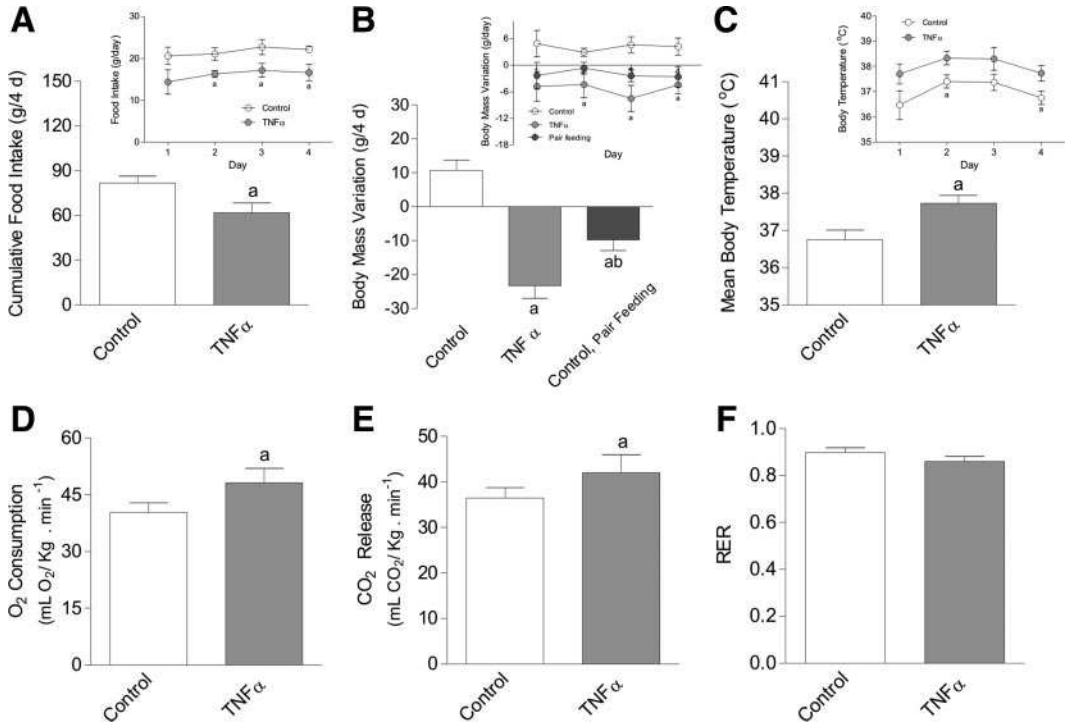

FIG. 1. Metabolic parameters of rats treated with TNFα. ICV-cannulated rats were treated with 2.0 μl saline (control) or TNFα (10^{-8} M) once a day for 4 d. A, Cumulative food intake during 4 d and daily food intake (*inset*). B, Total body mass variation (final-initial) during 4 d and daily body mass variation (*inset*); control pair feeding represents rats treated with saline ICV and fed 15.2 g chow per day. C, Mean body temperature, and daily temperature (*inset*). D, O_2 consumption (VO_2). E, CO_2 production (VCO_2). F, Respiratory quotient (VCO_2/VO_2). Data are means ± SEM; a, $P < 0.05$ *vs.* control. In all experiments n = 6–8 animals. RER, Respiratory exchange ratio.

value of less than 70% baseline, occurring after a steady decline of at least 3 d duration. When criteria for anorexia had been met, tumor-bearing animals were daily treated with inflixmab (0.3 μg in 2.0 μl, ICV, twice a day) or saline for 4 d or while alive. Chronic treatment was conducted for survival curve determination. Water intake was not altered by these treatments, compared with the respective control group (data not shown).

Statistical analysis

Mean values ± SEM obtained from densitometry scans and real-time PCR, body mass determination, and food intake were compared using Tukey-Kramer test (ANOVA) or Student's *t* test, as appropriate; $P < 0.05$ was accepted as statistically significant. The survival curves were estimated using Kaplan-Meier's estimates, and curves were compared using the log-rank test and the level of significance was set at $P < 0.001$. In all experiments, n refers to the number of animal in each experimental group.

Results

ICV TNFα affects energy homeostasis by modulating food intake and thermogenesis

To determine the effects of hypothalamic TNFα on whole-body energy homeostasis, ICV-cannulated rats were treated for 4 d with a high dose of TNFα (9, 10). The treatment led to a reduction in caloric intake (Fig. 1A) and an expressive decrease in body mass, in contrast to the body mass gain presented by control rats (Fig. 1B). The effect on body mass was not due only to reduction on food intake because pair-fed rats lost significantly less body mass than TNFα-treated rats (Fig. 1B). Most body mass change was due to reduction on white adipose tissue mass (Table 1). These outcomes were accompanied by increased body temperature (Fig. 1C), increased oxygen consump-

TABLE 1. Body mass and tissue-specific mass variation in TNFα-treated rats

	Control	TNFα
Initial body mass	265.78 ± 7.70	275.78 ± 5.78
Final body mass	270.06 ± 7.23	241.02 ± 5.70[a]
BAT mass	0.202 ± 0.016	0.235 ± 0.018
BAT/body mass	0.738 ± 0.044	1.022 ± 0.092[a]
Epididimal fat mass	3.04 ± 0.252	2.46 ± 0.107[a]
Epididimal fat/body mass	11.06 ± 0.916	10.61 ± 0.821
Retroperitonial fat	2.91 ± 0.69	1,87 ± 0.283[a]
Retroperitonial fat/ body mass	10.47 ± 2.250	7.99 ± 1.083[a]
Soleus muscle mass	0.10 ± 0.003	0.08 ± 0.007[a]
Soleus muscle/body mass	0.37 ± 0.007	0.35 ± 0.030
Gastrocnemius muscle mass	1.64 ± 0.043	1.72 ± 0.223
Gastrocnemius muscle/ body mass	5.96 ± 0.183	6.26 ± 0.259

[a] In all conditions, $P < 0.05$ (n = 5).

TABLE 2. Venous blood gas analysis

	Control	TNFα
pCO_2	51.96 ± 1.106	42.65 ± 1.54[a]
pO_2	34.28 ± 7.416	33.06 ± 7.96
pH	7.38 ± 0.008	7.46 ± 0.04

[a] In all conditions, $P < 0.05$ (n = 3).

tion (Fig. 1D), and carbon dioxide production (Fig. 1E), without significantly affecting respiratory exchange ratio (Fig. 1F). On blood gas analysis, only the pCO_2 levels were significantly reduced in TNFα-treated rats (Table 2).

ICV TNFα induces the activation of BAT thermogenesis

The macroscopic characteristics of BAT were clearly modified by ICV TNFα treatment. Its reddish color was more intense (Fig. 2A) and its relative mass was significantly increased (Fig. 2B). Under light microscopy examination, the fat droplets were reduced and nuclei were more densely distributed, suggesting a reduction in mean cell size (Fig. 2C). Upon morphometric analysis, the BAT from TNFα-treated rats had a significantly reduced fat area (66 ± 4 *vs.* 32 ± 3% for control and TNFα-treated rats, respectively, $P < 0.05$, n = 5). The expression of UCP1, a key protein involved in BAT thermogenesis, was increased in BAT obtained from animals treated with TNFα (Fig. 2, D and E). In addition, there was an increase in the expression of PGC1α and cytochrome C, suggesting an increment of mitochondria number (Fig. 2, D and E). The increase in mitochondria number (Fig. 2F) (17.1 ± 2.2 *vs.* 44.0 ± 3.5 mitochondria per 12 μm^2 for control and TNFα-treated rats, respectively, $P < 0.05$, n = 5; graph is depicted as supplemental Fig. S2) was further confirmed by transmission electronic microscopy that also showed a clear reduction in fat droplet area (Fig. 2F) (63 ± 4 *vs.* 38 ± 2% for control and TNFα-treated rats, respectively, $P < 0.05$, n = 5).

No activation of skeletal muscle thermogenesis by ICV TNFα

The treatment of rats with TNFα ICV resulted in no modification of mitochondria biogenesis markers, such as cytochrome C expression (Fig. 2G) and citrate synthase activity (Fig. 2H) in both soleus and gastrocnemius skeletal muscle. In addition, ICV TNFα produced no significant effect on the soleus and gastrocnemius muscle expression of UCP3 (Fig. 2I). All these negative findings were accompanied by no modulation of coupled (state III) and uncoupled (state IV) soleus muscle mitochondria respiration (Fig. 2J).

ICV TNFα-induced BAT thermogenesis is mediated by sympathetic neural activation

ICV TNFα induces a significant increase in BAT β3-adrenergic receptor expression (Fig. 3A). To evaluate whether sympathetic neural transmission may play a role in TNFα-induced BAT thermogenesis, Wistar rats were submitted to monolateral sympathetic denervation and then treated ICV with TNFα. As depicted in Fig. 3B, in the denervated side, ICV-TNFα produced no modification of the steady-state characteristics of BAT, which maintained with a milder reddish color, as compared with the innervated side. Light microscopy demonstrated that the denervated side displayed large fat droplets and a dispersed distribution of nuclei that was clearly different from the innervated side (Fig. 3C) and resembled the histological characteristics of steady-state BAT (as seen in Fig. 2). Upon morphometric analysis the innervated side had a significantly reduced fat area (73 ± 3 *vs.* 31 ± 4%, for denervated and innervated sides, respectively, $P < 0.05$, n = 5) compared with the denervated side.

The TNFα stimulation of BAT produced an increase in Dio2 mRNA expression (Fig. 3D), an enzyme able to convert thyroid hormone T_4 into T_3 in the intracellular compartment. This increase was completely restored by BAT denervation but not by β3-adrenergic inhibition (Fig. 3D). Conversely, both denervation and β3-adrenergic inhibition reverted ICV TNFα-induced expression of UCP1 (Fig. 3, D–F) and PGC1α (Fig. 3, E and F).

To assess the effects of BAT denervation and β3-adrenergic inhibition on ICV TNFα-induced hyperthermia and changes in food intake and body mass, rats were submitted to a complete (bilateral) sympathetic denervation or treated with the β3-adrenergic receptor antagonist, SR59230A, and then treated ICV with TNFα. As depicted in Fig. 3G, BAT denervation and β3-adrenergic antagonism reverted TNFα-induced inhibition of food intake. In addition, both BAT denervation and β3-adrenergic antagonism produced significant inhibition of ICV TNFα-induced body mass loss (Fig. 3H) and hyperthermia (Fig. 3I).

TNFα modulates hypothalamic neurotransmitter expression

To determine the hypothalamic mechanisms involved in TNFα-induced modulation of thermogenesis, we measured the mRNA levels of the most relevant hypothalamic neurotransmitters involved in the control of whole-body energy homeostasis. As depicted in Fig. 4A, ICV TNFα resulted in significant reductions in NPY, AgRP, POMC, and MCH and significant increases in TRH and CRH. No significant modulation of CART was detected. The effects of ICV TNFα on the control of neurotransmitter expression was paralleled by the control of important proteins

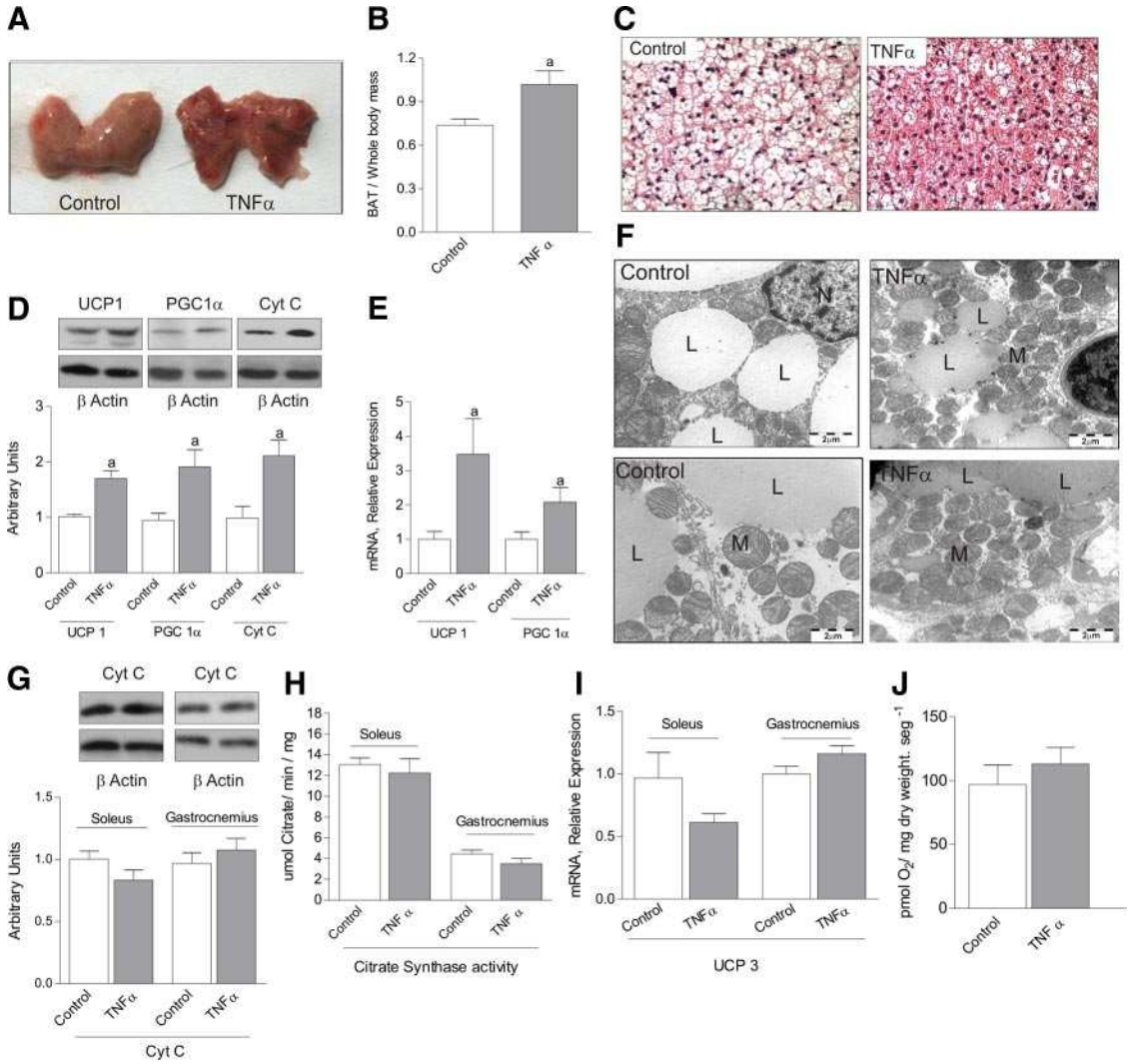

FIG. 2. Effect of ICV TNFα on BAT activation and mitochondria biogenesis in BAT and skeletal muscle. ICV-cannulated rats were treated with 2.0 μl saline (control) or TNFα (10^{-8} M) once a day for 4 d. A, Typical BAT macroscopic features, representative of five independent experiments. B, BAT mass/whole-body mass (n = 4). C, Histological analysis of BAT stained with hematoxylin and eosin, representative of five independent experiments. D, UCP1 (n = 13), PGC1α (n = 8), and cytochrome-C (Cyt C) (n = 4) protein levels in BAT assessed by immunoblotting. E, UCP1 and PGC1α mRNA levels in BAT assessed by real-time PCR (n = 5 for both genes). F, Transmission electron microscopy images of typical BAT from control and TNFα-treated rats, representative of five independent experiments. L, Lipid droplet. G, Cyt C protein levels in soleus and gastrocnemius skeletal muscle assessed by immunoblotting (n = 16). H, Citrate synthase activity measured in total homogenates from the soleus and gastrocnemius skeletal muscle (n = 8). I, UCP3 mRNA levels in samples obtained from the soleus and gastrocnemius skeletal muscle, assessed by real-time PCR (n = 6). J, O_2 flux in permeabilized soleus skeletal muscle fibers. The fibers derived from control and TNFα-treated rats were permeabilized with saponin (50 μg/ml), and the oxygen consumption was measured with a high-resolution oxygraph (Oxygraph-2k; Oroboros). The respiration in state III was measured in the presence of pyruvate (7.0 mM) + malate (4.0 mM) and ADP (2.0 mM) (pH 7.2) at 37 C. The respiration in state IV was measured in the presence of 1.0 μg/ml oligomycin (n = 6). Data are means ± SEM; a, $P < 0.05$ *vs.* control. In D and G, membranes were reblotted with β-actin antibody. In E and I, the gene used as constitutive endogenous control was GAPD (normalization presented in supplemental Fig. S1).

involved in the hypothalamic response to metabolic inputs such as AMPK and ACC, which were less phosphorylated in the hypothalamus of TNFα-treated rats, suggesting a role for this cytokine in the inactivation of AMPK and activation of ACC (Fig. 4B).

ICV TNFα plays a major role in sepsis- and cancer-induced energy wastage

To determine the clinical relevance of hypothalamic TNFα actions, we evaluated the outcomes of TNFα inhibition in the hypothalamus and also the systemic inhibition of β3-adrenergic signaling in two animal models of high TNFα production, sepsis and cancer. First, we induced mild and nonlethal sepsis by performing a single perforation of the cecum and a loose tying of the ascendant colon. Using this approach, the rats could present a serious infection, accompanied by a reduction in food intake and body mass, followed by complete recovery after 7–10 d. Under this condition the body temperature rose, which was accompanied by increased BAT expression of UCP1. The treatment of these

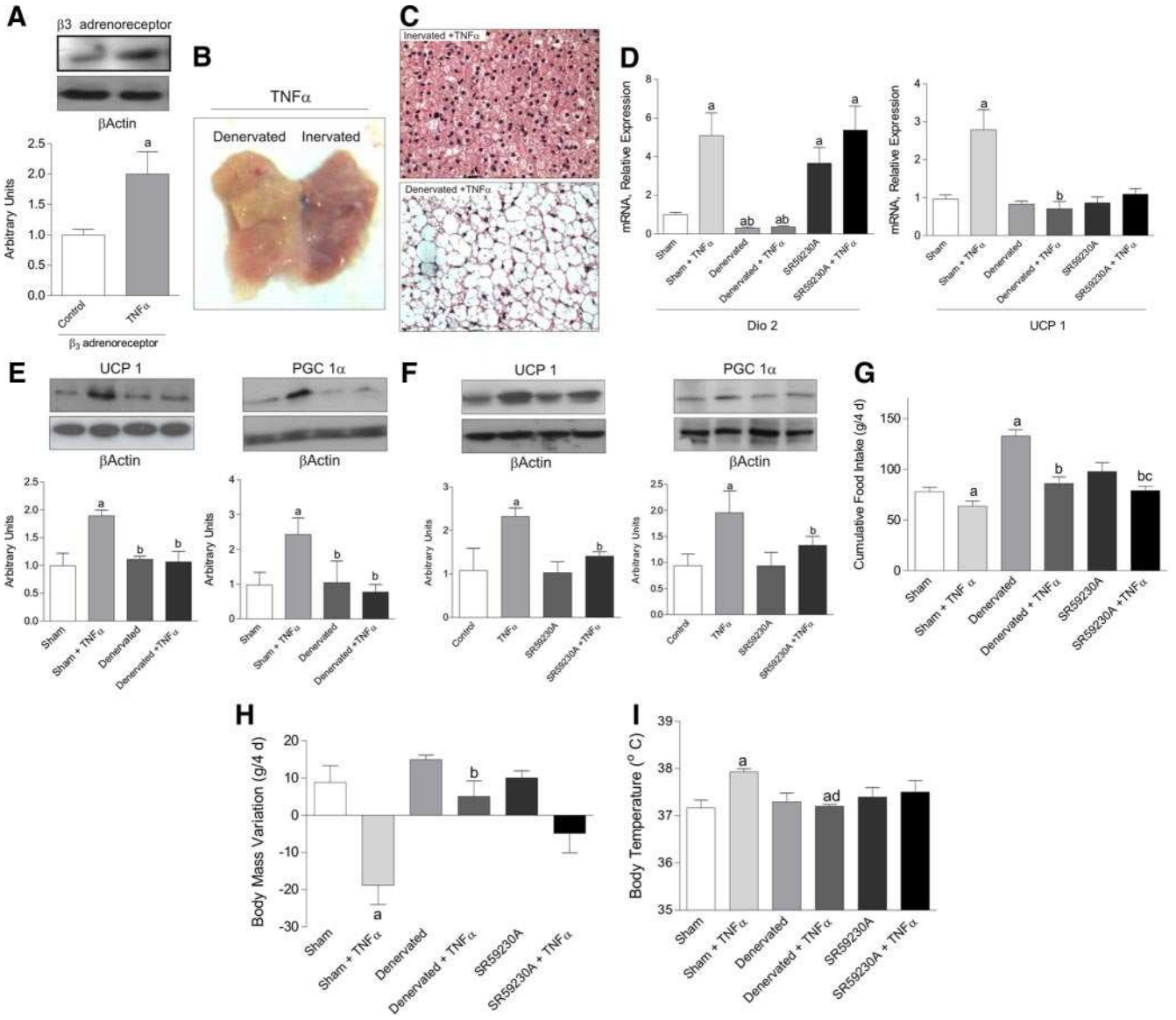

FIG. 3. Effect of ICV TNFα on BAT adrenergic stimulation. A–C, Interscapular BAT samples were obtained from ICV-cannulated rats submitted or not to sympathetic denervation; the animals were treated with 2.0 μl saline (control) or TNFα (10^{-8} M) once a day for 4 d. A, β3-Adrenergic receptor protein levels in innervated BAT assessed by immunoblotting (n = 5). B, Gross morphological features of monolateral sympathetic denervated BAT of rats treated with TNFα (10^{-8} M), representative of five independent experiments. C, Histological analysis of innervated and sympathetically denervated BAT of rats treated with TNFα (10^{-8} M), stained with hematoxilin and eosin, representative of five independent experiments. D–I, Interscapular BAT samples were obtained from ICV cannulated rats submitted or not (sham) to sympathetic denervation; the animals were treated with 2.0 μl saline or TNFα (10^{-8} M) once a day for 4 d; some rats were treated ip with SR59230A (0.1 mg/kg in 200 μl) twice a day for 4 d. D, Dio2 and UCP1 mRNA levels in samples obtained from BAT assessed by real-time PCR (n = 5). E and F, UCP1 and PGC1α protein levels in BAT assessed by immunoblotting (n = 4). G, Cumulative food intake during 4 d (n = 5). H, Total body mass variation (final-initial) during 4 d (n = 5). I, Mean body temperature (n = 5). a, $P < 0.05$ *vs.* control (or sham); in D–F, b, $P < 0.05$ *vs.* TNFα (or sham+TNFα); in G-H, b, $P < 0.05$ *vs.* denervated; in G, c, $P < 0.05$ *vs.* SR59230A; in I, d, $P < 0.05$ *vs.* TNFα. In A, E, and F, membranes were reblotted with β-actin antibody. In D, the gene used as constitutive endogenous control was GAPD (normalization presented in supplemental Fig. S1).

rats with ICV infliximab resulted in no modification of food intake (Fig. 5A); however, body mass variation (Fig. 5B) and mean body temperature (Fig. 5C) were at least partially restored. These effects were accompanied by significant reduction of BAT UCP1 expression (Fig. 5, D and E). The treatment of mildly septic rats with systemic SR59230A resulted in a significant increase of food intake (Fig. 5A), a significant inhibition of body mass loss (Fig. 5B), and a partial recovery of hyperthermia (Fig. 5C). As for the infliximab treatment, SR59230A also produced a significant decrease of BAT UCP1 expression (Fig. 5D). Most interestingly, in severely septic rats (obtained by performing several perforations of the cecum followed by a tight tying of the ascendant colon), the systemic treatment with either infliximab or SR59230A resulted in significant extension of life (Fig. 5F). Finally in tumor-bearing rats, ICV infliximab also promoted a signif-

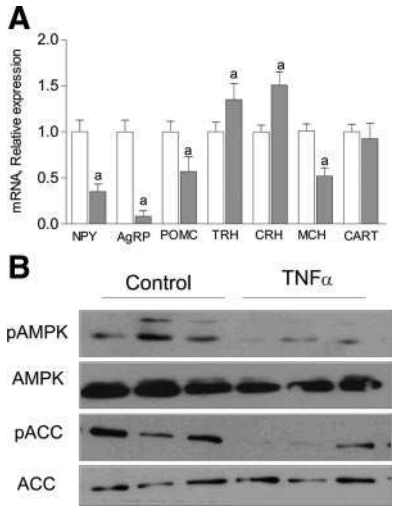

FIG. 4. Effect of ICV TNFα on the expression of hypothalamic neuropeptides and AMPK signaling in rats. ICV-cannulated rats were treated with 2.0 μl saline (*white bars*, control) or TNFα (10^{-8} M) (*gray bars*) once a day for 4 d. A, NPY (n = 9), AgRP (n = 3), POMC, (n = 8), TRH (n = 8), CRH (n = 8), MCH (n = 7), and CART (n = 8) mRNA levels in samples obtained from hypothalami assessed by real-time PCR. The gene used as a constitutive endogenous control was GAPD (normalization presented in supplemental Fig. S1); a, $P < 0.05$ *vs.* respective control. B, pAMPK, AMPK, pACC and ACC protein levels in hypothalami assessed by immunoblotting (n = 3).

icant increase of food intake (Fig. 5G) and an extension of life (Fig. 5H).

Discussion

Infectious and neoplastic diseases are frequently complicated by the installation of a wastage syndrome that increases morbidity and accelerates mortality (1). TNFα is one of the main mediators of this syndrome and the full characterization of the mechanisms by which this cytokine acts in cachexia may open new therapeutic opportunities for the most diverse forms of wastage syndromes (6).

Here we explored the hypothesis that the hypothalamic actions of TNFα play a major role in the increased thermogenesis, which is a hallmark of cachexia. The basis for this hypothesis came from a number of previous studies showing the primary role played by hypothalamic neurons in the general control of thermogenesis (20, 21). Several distinct factors ranging from hormones, nutrients, neurotransmitters, and cytokines act on specific subpopulations of hypothalamic neurons to control caloric intake and energy expenditure, therefore providing an optimal balance for energy flow in the body (22–25). In cachexia, both the reduction in caloric intake and the increase in energy expenditure, mostly due to increased thermogenesis, act in synergy to accelerate body mass depletion (26). In recent studies, we and others have evaluated the role of cachexia and hypothalamic TNFα in the control of food intake (10, 26). Two mechanisms operate in parallel to promote anorexia. The first is the direct effect of TNFα to induce and enhance the activity of the Janus kinase JAK2-signal transducer and activator of transcription-3 signaling pathway in the hypothalamus (10). This pathway is involved in leptin anorexigenic signaling and leads to the control of neurotransmitter expression (22). The second mechanism was observed in tumor-bearing rats and controls the AMPK signaling pathway; rats with cachexia had a significantly reduced activation of AMPK, and treating the rats with pharmacological compounds capable of inducing the activation of AMPK produced an increase in food intake and prolonged survival (27).

Depending on its local concentrations, TNFα differently affects the signaling systems involved in the control of energy homeostasis in the central nervous system (9, 10). To mimic the effects observed in severe infection and cancer, we used a high dose of TNFα, which has been previously evaluated and is known to produce anorexia and acutely modulate O_2 consumption/CO_2 production (10). With this dose, we were able to produce a phenotype of anorexia and massive body mass loss. First indications of increased thermogenesis came from the evaluations of body temperature, which was significantly increased, and respirometry that demonstrated significant increases in O_2 consumption and CO_2 production. In rodents and also in humans, thermogenesis can be induced in BAT and skeletal muscle (28, 29). To evaluate the sites involved in peripheral thermogenesis in response to hypothalamic TNFα, we determined the expressions of proteins involved in thermogenesis and also mitochondria activity in BAT and skeletal muscle. In BAT, we found morphological, molecular, and functional indications of increased thermogenesis. The proteins UCP1 and PGC1α were increased and the macro- and microscopic aspects of BAT were suggestive of its increased thermogenic activity. Of special interest, the transmission electron microscopic analysis revealed a reduced number and volume of lipid droplets, paralleled by an increased number of mitochondria, as seen in other prothermogenic conditions (30, 31). However, in samples containing fast and slow-twitch skeletal muscle we found no molecular and functional indications of increased thermogenesis. Therefore, we then concentrated efforts on characterizing the mechanisms involved in the induction of BAT thermogenesis.

Increased sympathetic tonus is regarded as one of the main mechanisms involved in the induction of BAT thermogenic activity (32). After ICV TNFα treatment, we observed a significant increase in β3-adrenergic receptor expression. The sympathetic denervation of BAT or the systemic antagonism of β3-adrenergic receptor reversed TNFα-induced changes in morphology and/or the expression of proteins involved in BAT thermogenesis. In addi-

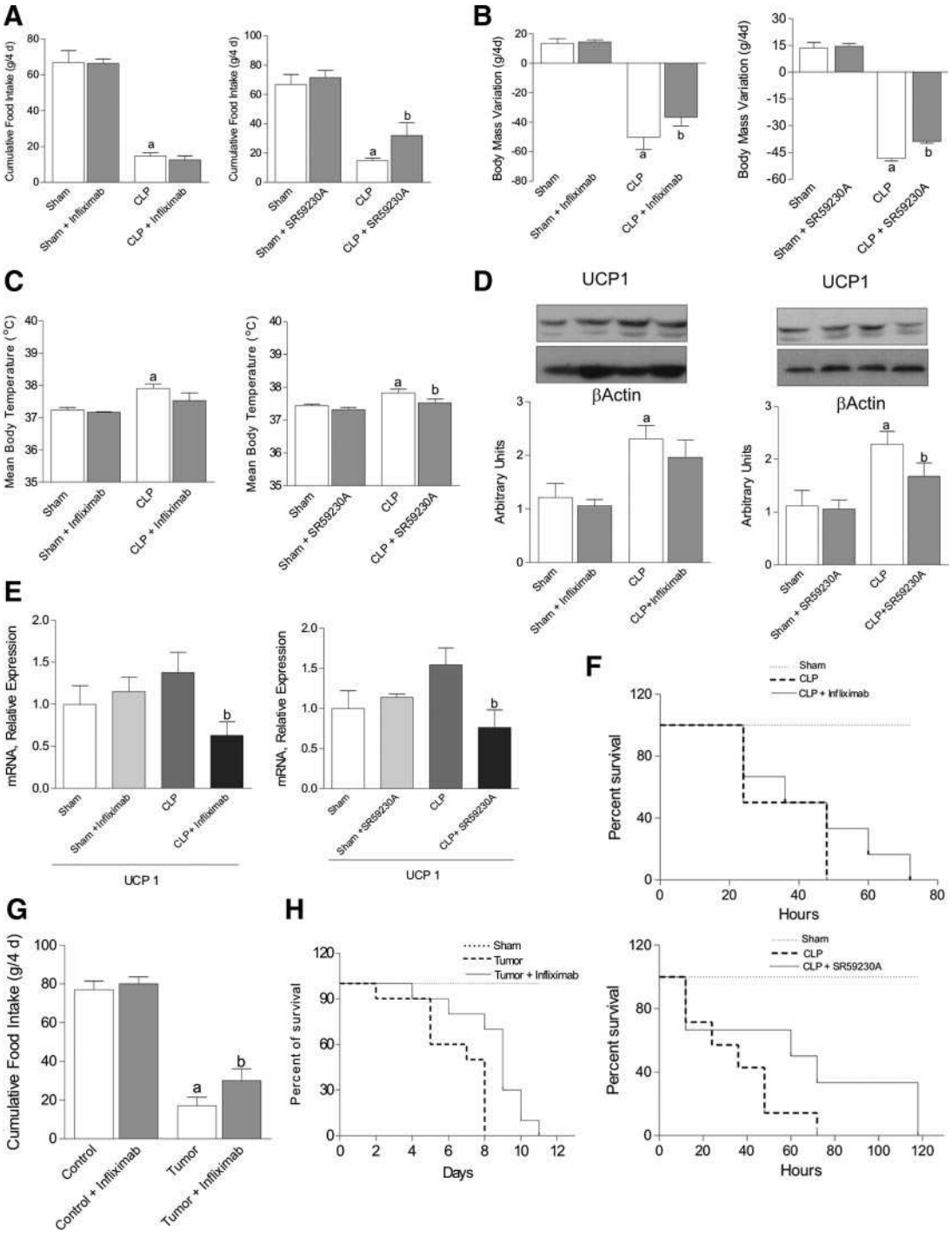

FIG. 5. Effect of infliximab and SR59230A on septic and tumor-bearing rats. A–F, Rats were submitted (CLP) or not (sham) to moderate, nonlethal (A–E) or severe, lethal (F) sepsis induced by cecal ligation and perforation; some rats were treated with infliximab (0.3 μg in 2.0 μl, ICV, twice a day) or SR59230A (0.2 mg/kg in 200 μl, ip, twice a day). A, Cumulative food intake in 4 d (n = 5). B, Body mass variation (final-initial) in 4 d (n = 5). C, Mean body temperature in 4 d (n = 5). D, UCP1 protein levels in BAT assessed by immunoblotting (n = 5). E, UCP1 mRNA levels in samples obtained from BAT assessed by real-time PCR (n = 5). F, Survival time of rats with severe sepsis (n = 10). G and H, Control and tumor-bearing rats were treated or not with infliximab (0.3 μg in 2.0 μl, ICV, twice a day). G, Cumulative food intake in 4 d (n = 10). H, Survival time of tumor-bearing rats (n = 10). a, $P < 0.05$ *vs.* sham (or control); b, $P < 0.05$ *vs.* CLP (or tumor). D, Membranes were reblotted with β-actin antibody. E, The gene used as constitutive endogenous control was GAPD (normalization presented in supplemental Fig. S1).

tion, the complete denervation of BAT almost completely inhibited TNFα-induced hyperthermia, suggesting that most of the thermogenetic activity was indeed due to BAT activation.

As previously shown, hyperthermia induced by peripherally injected lipopolysaccharide can be partially inhibited by the use of β-adrenergic antagonists and also by BAT denervation (33). Interestingly, the hyperthermic re-

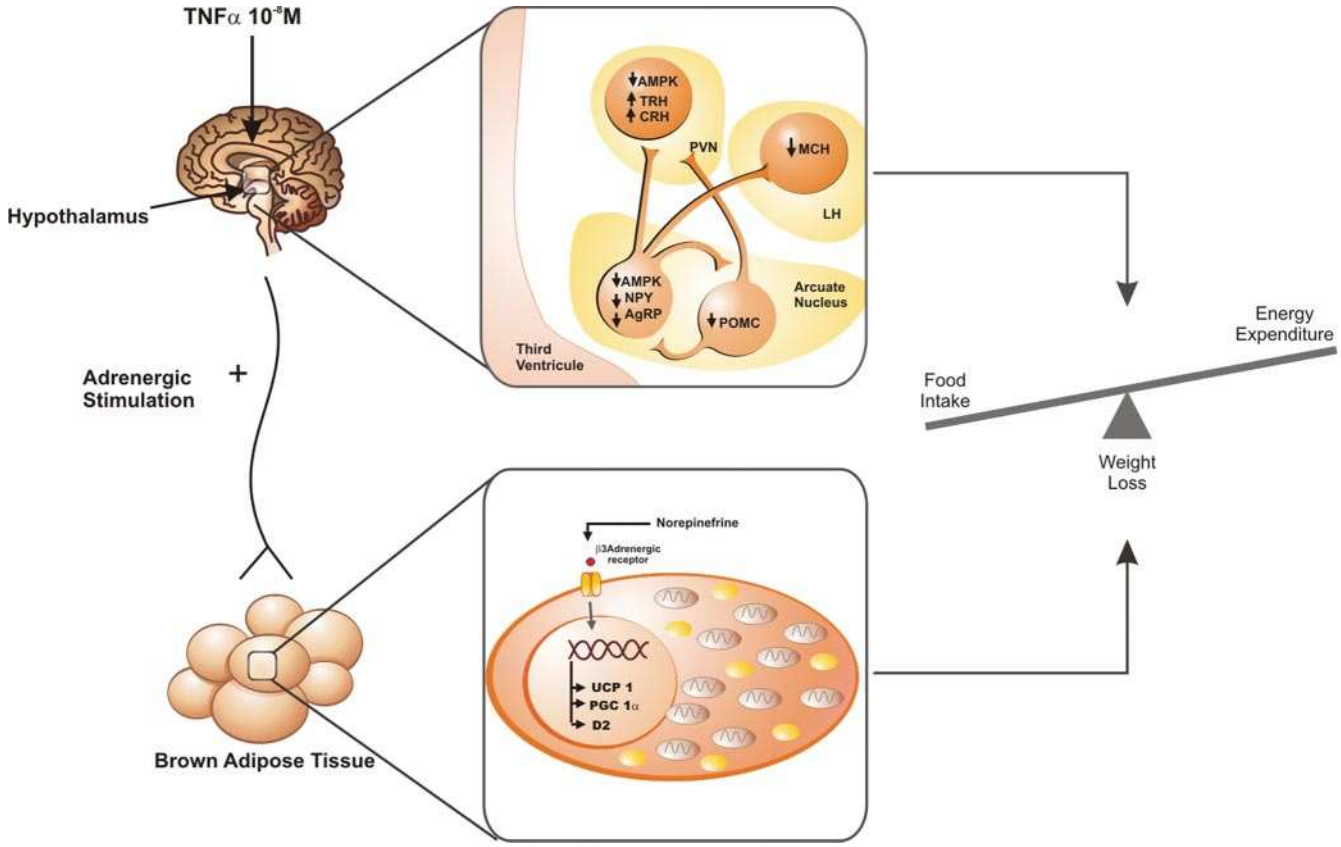

FIG. 6. Proposed scheme for the action of high concentration of TNFα in the hypothalamus. TNFα acts in the hypothalamus-modulating neurotransmitter expression and signal transduction pathways, such as the AMPK system. This results in increased sympathetic tonus, which acts mostly in the BAT, activating PGC1α, inducing mitochondrial biogenesis and UCP1 expression. The result is increased body temperature, increased oxygen consumption/carbon dioxide production, and energy expenditure.

sponse to lipopolysaccharide can also be modulated by different types of diet, suggesting an integration of feeding and pyretic responses (33). Taking these data together with ours, it may be suggested that in endotoxemia, TNFα, acting predominantly in the hypothalamus, plays a central role in the modulation of both thermogenic and anorexigenic responses.

Because previous studies showed an effect of TNFα in modulating neurotransmitter expression and signaling pathways in hypothalamic neurons (9, 10), we next determined the levels of the main neurotransmitters involved in energy homeostasis, and also we determined the effects of TNFα on the AMPK signaling pathway. As expected, the levels of the orexigenic neurotransmitters, NPY and AgRP, were drastically reduced in the TNFα-treated rats. In nonpathological conditions, reductions in the expressions of NPY and AgRP occur in fed states and lead to not only satiety but also thermogenesis (34). Here, even in the fasting state, the levels of these neurotransmitters were low, indicating that they are important targets for TNFα action in the hypothalamus. However, POMC, which is usually repressed in fasting state and possesses a potent anorexigenic effect, was also low and therefore not modulated in response to TNFα. Most interesting were the increased levels of the neurotransmitters of the paraventricular nucleus, TRH, and CRH, which were stimulated by TNFα. These neurotransmitters are known to play an important role in thermogenesis (35, 36), and as for the results shown herein, they seem to be important intermediaries in the thermogenic response to TNFα.

With regard to TRH, a thermogenic response to this neurotransmitter can be produced by neural and/or hormonal mechanisms (35). To evaluate the participation of a hormonal mechanism, we determined the blood level of T_3, which was similar between control and TNFα-treated rats (not shown). However, the expression of Dio2 in BAT was increased and, although this may indicate an increased activity of T_3 in this tissue, it most probably results from the sympathetic activation of BAT because cAMP is the most important inducer of Dio2 expression (37). It is important to notice that adrenergic tonus acting not only through β3 receptor, but also through other receptor types, can activate Dio2 (37), which may explain why an increase of Dio2 expression occurred after β3-adrenergic antagonism, whereas a complete inhibition was obtained with denervation.

Because we have previously shown that hypothalamic TNFα modulates signal transduction through the Janus kinase-2-signal transducer and activator of transcription-3 signaling pathway (10), we herein determined the effect of TNFα on another important intracellular signaling pathway involved in the hypothalamic control of feeding and thermogenesis, the AMPK signaling pathway. This pathway, which is most active in NPY/AgRP and TRH/CRH neurons, is known to play an important role in connecting hormonal and nutrient inputs that control feeding and thermogenesis. By demonstrating that TNFα can directly modulate this signaling system, we unveil yet another mechanism of control of hypothalamic signaling pathways involved in the control of energy homeostasis.

In the final part of the study, we evaluated the effects of the inhibition of TNFα in the brain and the systemic inhibition of β3-adrenergic signaling in two animal models of cachexia. Infliximab was capable of significantly retarding mortality in tumor-bearing rats and reducing body mass loss in mildly septic rats, whereas β3-adrenergic inhibition significantly reduced body mass loss in mildly septic rats and retarded mortality in severely septic rats. The effects of hypothalamic TNFα inhibition and systemic β3-adrenergic antagonism on the clinical parameters of septic rats were accompanied by reduction of expression of markers of thermogenesis, suggesting that excessive thermogenesis induced under this pathological condition play a role in energy depletion and rapid progression to death. These data provide the clinical basis to support the concept that TNFα, produced under critical clinical conditions, such as cancer and septicemia, act predominantly in the hypothalamus to induce thermogenesis in BAT through the activation of a sympathetic response.

Although some previous studies explored the role of TNFα on the activation of thermogenesis (5, 12, 33), one of the main advances of this work is the demonstration of the potentiality of inhibition of β3-adrenergic signaling as a therapeutic approach for severe cachexia. In addition, it is important to emphasize that, until recently, BAT was thought to play an important physiological and pathological role only in small mammals and infants, with negligible relevance in adult humans. However, the recent detection of multiple depots of BAT in the cervical region of adult humans has reinvigorated the interest in the study of this tissue in humans (29, 38, 39). A hypothetical scheme with the proposed mechanisms involved in the hypothalamic response to high concentrations of TNFα and its connections with BAT is presented in Fig. 6. The present study places the hypothalamic actions of TNFα and the activation of BAT thermogenesis in a central position in the pathogenesis of cachexia and provides new candidate targets for the therapeutic approaches of wastage syndromes.

Acknowledgments

The Laboratory of Cell Signaling is a member of the Instituto Nacional de Ciência e Tecnologia de Obesidade e Diabetes and also a member of the Gastrocentro-University of Campinas. We thank Dr. N. Conran for English grammar review and Mr. G. Ferraz for technical assistance. We also thank Dr. Eliot Kitajima (head of the Núcleo de Apoio à Pesquisa/Microscopia Eletrônica em Pesquisa Agropecuária from the Escola Superior de Agronomia Luiz de Queiroz-University of São Paulo) for assistance with the eletron microscopy.

Address all correspondence and requests for reprints to: Licio A. Velloso, DCM-FCM, University of Campinas, 13084-960 Campinas SP, Brazil. E-mail: lavelloso@fcm.unicamp.br.

This work was supported by Fundação de Amparo à Pesquisa do Estado de Sao Paulo and Conselho Nacional de Desenvolvimento Científico e Tecnológico.

Disclosure Summary: The authors have nothing to declare.

References

1. **Tisdale MJ** 2009 Mechanisms of cancer cachexia. Physiol Rev 89: 381–410
2. **Laviano A, Meguid MM, Inui A, Muscaritoli M, Rossi-Fanelli F** 2005 Therapy insight: cancer anorexia-cachexia syndrome—when all you can eat is yourself. Nat Clin Pract Oncol 2:158–165
3. **Deboer MD, Marks DL** 2006 Cachexia: lessons from melanocortin antagonism. Trends Endocrinol Metab 17:199–204
4. **Tracey KJ, Cerami A** 1993 Tumor necrosis factor, other cytokines and disease. Annu Rev Cell Biol 9:317–343
5. **Argilés JM, López-Soriano J, Busquets S, López-Soriano FJ** 1997 Journey from cachexia to obesity by TNF. FASEB J 11:743–751
6. **Tisdale MJ** 2008 Catabolic mediators of cancer cachexia. Curr Opin Support Palliat Care 2:256–261
7. **Jackman RW, Kandarian SC** 2004 The molecular basis of skeletal muscle atrophy. Am J Physiol Cell Physiol 287:C834–C843
8. **Cawthorn WP, Sethi JK** 2008 TNF-α and adipocyte biology. FEBS Lett 582:117–131
9. **Amaral ME, Barbuio R, Milanski M, Romanatto T, Barbosa HC, Nadruz W, Bertolo MB, Boschero AC, Saad MJ, Franchini KG, Velloso LA** 2006 Tumor necrosis factor-α activates signal transduction in hypothalamus and modulates the expression of pro-inflammatory proteins and orexigenic/anorexigenic neurotransmitters. J Neurochem 98:203–212
10. **Romanatto T, Cesquini M, Amaral ME, Roman EA, Moraes JC, Torsoni MA, Cruz-Neto AP, Velloso LA** 2007 TNF-α acts in the hypothalamus inhibiting food intake and increasing the respiratory quotient—effects on leptin and insulin signaling pathways. Peptides 28:1050–1058
11. **Velloso LA, Araújo EP, de Souza CT** 2008 Diet-induced inflammation of the hypothalamus in obesity. Neuroimmunomodulation 15: 189–193
12. **Rothwell NJ** 1988 Central effects of TNFα on thermogenesis and fever in the rat. Biosci Rep 8:345–352
13. **Johnson AK, Epstein AN** 1975 The cerebral ventricles as the avenue

for the dipsogenic action of intracranial angiotensin. Brain Res 86: 399–418
14. **Festuccia WT, Kawashita NH, Garofalo MA, Moura MA, Brito SR, Kettelhut IC, Migliorini RH** 2003 Control of glyceroneogenic activity in rat brown adipose tissue. Am J Physiol Regul Integr Comp Physiol 285:R177–R182
15. **Tsukumo DM, Carvalho-Filho MA, Carvalheira JB, Prada PO, Hirabara SM, Schenka AA, Araújo EP, Vassallo J, Curi R, Velloso LA, Saad MJ** 2007 Loss-of-function mutation in Toll-like receptor 4 prevents diet-induced obesity and insulin resistance. Diabetes 56: 1986–1998
16. **Kitajima EW, Groot TV, Novelli VM, Freitas-Astúa J, Alberti G, de Moraes GJ** 2007 *In situ* observation of the Cardinium symbionts of Brevipalpus (Acari: Tenuipalpidae) by electron microscopy. Exp Appl Acarol 42:263–271
17. **Arruda AP, Ketzer LA, Nigro M, Galina A, Carvalho DP, de Meis L** 2008 Cold tolerance in hypothyroid rabbits: role of skeletal muscle mitochondria and sarcoplasmic reticulum Ca^{2+} ATPase isoform 1 heat production. Endocrinology 149:6262–6271
18. **d'Avila JC, Santiago AP, Amâncio RT, Galina A, Oliveira MF, Bozza FA** 2008 Sepsis induces brain mitochondrial dysfunction. Crit Care Med 36:1925–1932
19. **Cesquini M, Stoppa GR, Prada PO, Torsoni AS, Romanatto T, Souza A, Saad MJ, Velloso LA, Torsoni MA** 2008 Citrate diminishes hypothalamic acetyl-CoA carboxylase phosphorylation and modulates satiety signals and hepatic mechanisms involved in glucose homeostasis in rats. Life Sci 82:1262–1271
20. **Elmquist JK, Maratos-Flier E, Saper CB, Flier JS** 1998 Unraveling the central nervous system pathways underlying responses to leptin. Nat Neurosci 1:445–450
21. **Gao Q, Horvath TL** 2007 Neurobiology of feeding and energy expenditure. Annu Rev Neurosci 30:367–398
22. **Myers MG, Cowley MA, Münzberg H** 2008 Mechanisms of leptin action and leptin resistance. Annu Rev Physiol 70:537–556
23. **Murphy KG, Bloom SR** 2006 Gut hormones and the regulation of energy homeostasis. Nature 444:854–859
24. **Xue B, Kahn BB** 2006 AMPK integrates nutrient and hormonal signals to regulate food intake and energy balance through effects in the hypothalamus and peripheral tissues. J Physiol 574:73–83
25. **Inui A, Asakawa A, Bowers CY, Mantovani G, Laviano A, Meguid MM, Fujimiya M** 2004 Ghrelin, appetite, and gastric motility: the emerging role of the stomach as an endocrine organ. FASEB J 18: 439–456
26. **Laviano A, Inui A, Marks DL, Meguid MM, Pichard C, Rossi Fanelli F, Seelaender M** 2008 Neural control of the anorexia-cachexia syndrome. Am J Physiol Endocrinol Metab 295:E1000–E1008
27. **Ropelle ER, Pauli JR, Zecchin KG, Ueno M, de Souza CT, Morari J, Faria MC, Velloso LA, Saad MJ, Carvalheira JB** 2007 A central role for neuronal adenosine 5′-monophosphate-activated protein kinase in cancer-induced anorexia. Endocrinology 148:5220–5229
28. **Silva JE** 2006 Thermogenic mechanisms and their hormonal regulation. Physiol Rev 86:435–464
29. **Cypess AM, Lehman S, Williams G, Tal I, Rodman D, Goldfine AB, Kuo FC, Palmer EL, Tseng YH, Doria A, Kolodny GM, Kahn CR** 2009 Identification and importance of brown adipose tissue in adult humans. N Engl J Med 360:1509–1517
30. **Valerio A, Cardile A, Cozzi V, Bracale R, Tedesco L, Pisconti A, Palomba L, Cantoni O, Clementi E, Moncada S, Carruba MO, Nisoli E** 2006 TNF-α downregulates eNOS expression and mitochondrial biogenesis in fat and muscle of obese rodents. J Clin Invest 116:2791–2798
31. **Dali-Youcef N, Mataki C, Coste A, Messaddeq N, Giroud S, Blanc S, Koehl C, Champy MF, Chambon P, Fajas L, Metzger D, Schoonjans K, Auwerx J** 2007 Adipose tissue-specific inactivation of the retinoblastoma protein protects against diabesity because of increased energy expenditure. Proc Natl Acad Sci USA 104:10703–10708
32. **Lowell BB, Bachman ES** 2003 β-Adrenergic receptors, diet-induced thermogenesis, and obesity. J Biol Chem 278:29385–29388
33. **Jepson MM, Millward DJ, Rothwell NJ, Stock MJ** 1988 Involvement of sympathetic nervous system and brown fat in endotoxin-induced fever in rats. Am J Physiol 255:E617–E620
34. **van den Pol AN** 2003 Weighing the role of hypothalamic feeding neurotransmitters. Neuron 40:1059–1061
35. **Lechan RM, Fekete C** 2006 The TRH neuron: a hypothalamic integrator of energy metabolism. Prog Brain Res 153:209–235
36. **Richard D, Huang Q, Timofeeva E** 2000 The corticotropin-releasing hormone system in the regulation of energy balance in obesity. Int J Obes Relat Metab Disord 24(Suppl 2):S36–S39
37. **Bianco AC, Kim BW** 2006 Deiodinases: implications of the local control of thyroid hormone action. J Clin Invest 116:2571–2579
38. **Virtanen KA, Lidell ME, Orava J, Heglind M, Westergren R, Niemi T, Taittonen M, Laine J, Savisto NJ, Enerbäck S, Nuutila P** 2009 Functional brown adipose tissue in healthy adults. N Engl J Med 360:1518–1525
39. **van Marken Lichtenbelt WD, Vanhommerig JW, Smulders NM, Drossaerts JM, Kemerink GJ, Bouvy ND, Schrauwen P, Teule GJ** 2009 Cold-activated brown adipose tissue in healthy men. N Engl J Med 360:1500–1508

APÊNDICE *IX*

Diabetologia (2009) 52:2425–2434
DOI 10.1007/s00125-009-1498-1

ARTICLE

Aspirin attenuates insulin resistance in muscle of diet-induced obese rats by inhibiting inducible nitric oxide synthase production and *S*-nitrosylation of IRβ/IRS-1 and Akt

M. A. Carvalho-Filho · E. R. Ropelle · R. J. Pauli · D. E. Cintra · D. M. L. Tsukumo · L. R. Silveira · R. Curi · J. B. C. Carvalheira · L. A. Velloso · M. J. A. Saad

Received: 1 April 2009 / Accepted: 15 July 2009 / Published online: 3 September 2009

Abstract
Aim/hypothesis High-dose aspirin treatment improves fasting and postprandial hyperglycaemia in patients with type 2 diabetes, as well as in animal models of insulin resistance associated with obesity and sepsis. In this study, we investigated the effects of aspirin treatment on inducible nitric oxide synthase (iNOS)-mediated insulin resistance and on *S*-nitrosylation of insulin receptor (IR)-β, IRS-1 and protein kinase B (Akt) in the muscle of diet-induced obese rats and also in *iNos* (also known as *Nos2*)$^{-/-}$ mice on high fat diet.
Methods Aspirin (120 mg kg^{-1} day^{-1} for 2 days) or iNOS inhibitor (L-NIL; 80 mg/kg body weight) were administered to diet-induced obese rats or mice and iNOS production and insulin signalling were investigated. *S*-nitrosylation of IRβ/IRS-1 and Akt was investigated using the biotin switch method.
Results iNOS protein levels increased in the muscle of diet-induced obese rats, associated with an increase in *S*-nitrosylation of IRβ, IRS-1 and Akt. These alterations were reversed by aspirin treatment, in parallel with an improvement in insulin signalling and sensitivity, as measured by insulin tolerance test and glucose clamp. Conversely, while aspirin reversed the increased phosphorylation of IκB kinase β and c-Jun amino-terminal kinase, as well as IRS-1 serine phosphorylation in diet-induced obese rats and *iNos*$^{-/-}$ mice on high-fat diet, these alterations were not associated with the improvement of insulin action induced by this drug.
Conclusions/interpretation Our data demonstrate that aspirin treatment not only reduces iNOS protein levels, but also *S*-nitrosylation of IRβ, IRS-1 and Akt. These changes are associated with improved insulin resistance and signalling, suggesting a novel mechanism of insulin sensitisation evoked by aspirin treatment.

Keywords Aspirin · iNOS · Insulin resistance · Muscle · *S*-Nitrosylation

Abreviations

Akt	Protein kinase B
HENS	HEPES, EDTA, neocuproine and SDS
IKKβ	IκB kinase β
iNOS	Inducible nitric oxide synthase
IR	Insulin receptor
JNK	c-Jun amino-terminal kinase
L-NAME	N^{ω}-nitro-L-arginine methyl ester
NFκB	Nuclear factor kappa B
L-NIL	L-N^6-(1-iminoethyl)lysine
PPAR	Peroxisome proliferator-activated receptor

M. A. Carvalho-Filho · E. R. Ropelle · R. J. Pauli · D. E. Cintra · D. M. L. Tsukumo · L. R. Silveira · R. Curi · J. B. C. Carvalheira · L. A. Velloso · M. J. A. Saad (✉)
FCM-UNICAMP,
Rua Tessália Vieira de Camargo, 126,
Cidade Universitária Zeferino Vaz,
Campinas, São Paulo 13083-887, Brazil
e-mail: msaad@fcm.unicamp.br

Introduction

Diet-induced obesity is an experimental model of obesity and insulin resistance that is associated with a chronic inflammatory response and characterised by abnormal cytokine production, increased acute-phase reactants and

other stress-induced molecules [1]. It is now well established that this inflammatory response is associated with the activation of intra-cellular inflammatory pathways that can negatively modulate insulin signalling, such as the IκB kinase β (IKK-β)/nuclear factor kappa B (NFκB), c-Jun amino-terminal kinase (JNK) and inducible nitric oxide synthase (iNOS) pathways [2–4].

High-dose aspirin treatment improved fasting and postprandial hyperglycaemia in patients with type 2 diabetes, as well as in animal models of insulin resistance associated with obesity and sepsis [5–7]. This improved insulin signalling was postulated to be secondary to blockage of the IKK-β/NFκB and JNK pathways, which prevent serine phosphorylation of IRS-1, a well-established mechanism of insulin resistance [8].

Recently, we and others reported that enhanced iNOS production is associated with obesity and inflammatory responses and can negatively modulate insulin signalling through *S*-nitrosylation of proteins involved in early steps of insulin signalling, such as insulin receptor (IR)-β, IRS-1 and protein kinase B (Akt) [3, 9]. Furthermore, pharmacological or genetic blockage of iNOS production/activity ameliorates insulin resistance associated with obesity or lipopolysaccharide treatment by inhibiting *S*-nitrosylation of these proteins [9, 10]. Interestingly, aspirin treatment can also decrease iNOS production and activity in several cell lines [11–13], but its effects on iNOS-induced insulin resistance in the muscle of obese rats has not yet been investigated.

In this study, we investigated the effects of aspirin treatment on iNOS-mediated insulin resistance and on *S*-nitrosylation of IR-β, IRS-1 and Akt in the muscle of diet-induced obese rats and also in *iNos* (also known as *Nos2*)$^{-/-}$ mice on a high-fat diet.

Methods

Materials Antiphosphotyrosine, anti-IRβ, anti-IRS-1, anti-iNOS, anti-Akt, anti-pser307-IRS-1 and anti-phospho-JNK antibodies were from Santa Cruz Biotechnology (Santa Cruz, CA, USA). Anti-p[ser^{473}]Akt antibody was from Cell Signaling Technology (Beverly, MA, USA). Human recombinant insulin (Humulin R) was purchased from Eli Lilly (Indianapolis, IN, USA). Routinely used reagents were purchased from Sigma (St. Louis, MO), unless otherwise specified.

Animals Male Wistar rats and C57BL/6 mice were obtained from the UNICAMP Central Animal Breeding Center (Campinas, São Paulo, Brazil). The *iNos*-knockout mice used were C57BL/6-backcrossed *iNos*$^{-/-}$ mice (C57BL/6-Nos2^{tm1Lau} colony; Jackson Laboratory, Bar Harbor, ME, USA). Animals were allowed free access to standard rodent chow and water. Diet-induced obese animals were obtained by high-fat diet administration to one group of Wistar rats, to one group of C57BL/6 mice and to one group of *iNos*$^{-/-}$ mice. High-fat diet was initiated at 8 weeks of age and administered for 4 weeks; control animals were of the same age. The high-fat diet consisted of 55% energy derived from fat, 29% from carbohydrate and 16% from protein. Food was withdrawn 6 h before the experiments. The Ethics Committee of the University of Campinas approved all experiments involving animals.

Aspirin treatment Aspirin (120 mg kg^{-1} day^{-1}) or saline in equal volumes were given by oral gavage to diet-induced obese rats or mice for 2 days.

iNOS inhibitor treatment Diet-induced obese rats received an intraperitoneal injection of the iNOS inhibitor L-N^6-(1-iminoethyl)lysine (L-NIL; 80 mg/kg body weight) or saline twice daily (every 12 h) for 2 days. This treatment protocol with L-NIL was adapted from a previously published procedure [14].

Insulin tolerance test Rats were fasted for 6 h and submitted to a 30 min insulin tolerance test. Briefly, 1.5 IU/kg insulin was infused intraperitoneally in rats and glucose was measured at 0 (basal), 5, 10, 15, 20, 25 and 30 min thereafter. The glucose disappearance rate (K_{itt}) was calculated from the formula $0.693/t_{1/2}$, where $t_{1/2}$ stands for time for glucose to reach 50% of the basal value. Glucose $t_{1/2}$ was calculated from the slope of the least square analysis of blood glucose concentration during the linear phase of decline [15].

Euglycaemic–hyperinsulinaemic clamp studies After 5 h of fasting, animals were anaesthetised i.p. with sodium pentobarbital (50 mg/kg body weight) and catheters were inserted into the left jugular vein (for tracer infusions) and carotid artery (for blood sampling), as previously described [16]. Each animal was monitored for food intake and weight gain for 5 days after surgery to ensure complete recovery. Food was removed for 12 h before the beginning of in vivo studies. A 120 min euglycaemic–hyperinsulinaemic clamp procedure was conducted in conscious, unrestrained, catheterised rats, as shown previously [16], with a prime continuous infusion of human insulin at a rate of 3.6 mU (kg body weight)$^{-1}$ min^{-1} to raise the plasma insulin concentration to approximately 800–900 pmol/l. Blood samples (20 μl) were collected at 5 min intervals for the immediate measurement of plasma glucose concentration; 10% (vol./vol.) unlabelled glucose was infused at variable rates to maintain plasma glucose at fasting levels

IRβ, IRS-1 and iNOS immunoprecipitation Anaesthetised mice were injected intraperitoneally either with saline or insulin (3.8 U/kg); 90 s later soleus muscles were removed and homogenised, as described below. Muscle lysates were incubated with anti-IRβ (0.3 mg/ml), anti-IRS-1 (1:1,000) or anti-iNOS (1:1,000) antibodies for 2 h and then incubated with protein A sepharose for a further 2 h. Beads were then washed with TRIS containing 1% (vol./vol.) Triton X-100 and phosphatase inhibitors, boiled for 5 min in Laemmli buffer and subjected to western blotting analysis [17, 18].

Western blot analysis Muscle extracts, immunoprecipitates or biotinylated nitrosocysteines were subjected to sodium dodecyl sulphate polyacrylamide electrophoresis and immunoblotting was performed as described [17]. Immunoreactive bands were detected by the enhanced chemiluminescense method (RPN 2108; Amersham Biosciences - Sweden).

Detection of S-nitrosated proteins by biotin switch method The biotin switch assay was performed essentially as previously described [19, 20]. Muscle tissue was extracted and homogenised in extraction buffer (250 mmol/l HEPES, pH 7.7, 1 mmol/l EDTA, 0.1 mmol/l neocuproine). After centrifugation at 9,000×*g* for 20 min, insoluble material was removed, extracts were adjusted to a concentration of 0.5 mg/ml protein and equal amounts were blocked with four volumes of blocking buffer (225 mmol/l HEPES, pH 7.7, 0.9 mmol/l neocuproine, 2.5% (vol./vol.) SDS and 20 mmol/l methyl-methanethiosulfonate [MMTS]) at 50°C for 30 min while being agitated. After blocking, extracts were precipitated with two volumes of cold acetone (−20°C), chilled at −20°C for 10 min, centrifuged at 2,000×*g* and 4°C for 5 min, washed with acetone, dried and finally resuspended in 0.1 ml HENS buffer (250 mmol/l HEPES, pH 7.7, 1 mmol/l EDTA, 0.1 mmol/l neocuproine and 1% (vol./vol.) SDS) per mg of protein. Until this point, all operations were carried out in the dark. A one-third volume of *N*-(6-(ciotinamido)hexyl)-3′-(2′-pyridyldithio)-propionamide (biotin-HPDP) 4 mmol/l and 2.5 mmol/l ascorbic acid was added, followed by incubation for 1 h at room temperature. Proteins were acetone-precipitated again and re-suspended in the same volume of HENS buffer.

For purification of biotinylated proteins, samples from the biotin switch assay were diluted with two volumes of neutralisation buffer (20 mmol/l HEPES, pH 7.7, 100 mmol/l NaCl, 1 mmol/l EDTA and 0.5% (vol./vol.) Triton X-100) and 15 μl of neutravidin–agarose/mg of protein in the initial extract were added, followed by incubation for 1 h at room temperature while being agitated. Beads were washed five times with washing buffer (20 mmol/l HEPES, pH 7.7, 600 mmol/l NaCl, 1 mmol/l EDTA and 0.5% Triton X-100) and incubated for 20 min at 37°C with elution buffer (20 mmol/l HEPES, pH 7.7, 100 mmol/l NaCl, 1 mmol/l EDTA and 100 mmol/l 2-mercaptoethanol) with gentle stirring. Supernatant fractions were collected, Laemmli buffer was added and proteins were separated by SDS-PAGE. Immunoblotting was performed as described above [19, 20].

Primary rat skeletal muscle cell isolation and culture Male Wistar rats (90 g) were killed by cervical dislocation. The hindlimbs were quickly removed and used to prepare muscle cell culture, as described, previously [21]. The cells were cultured for the first 2 days in primary growth medium containing DMEM with 20% (vol./vol.) fetal calf serum and, thereafter, in fusion medium containing DMEM with 10% (vol./vol.) horse serum.

Salicylate treatment The skeletal muscle cell cultures were divided in two different groups: control and salicylate (5 mmol/l). The cells were then incubated in DMEM containing all of the treatment substances described above.

Nitric oxide synthase activity assay After 24 h, the cells were scraped off and homogenised in TRIS buffer (50 mmol/l, pH 7.4) containing l-citrulline (1 mmol/l), EDTA (0.1 mmol/l), dithiothreitol (1 mmol/l), leupeptin (10 μg/ml), soyabean trypsin inhibitor (10 μg/ml), aprotinin (2 μg/ml) and phenyl methyl sulfonyl fluoride (1 mmol/l). Homogenates were centrifuged (1,000×*g*) for 10 min and the supernatant fractions were passed over an ionic form, hydrogen, dry mesh column (Dowex 50WX8-200, 100–200; Dow Chemical, St Louis, MO, USA) to remove endogenous arginine. The samples (50 μl) were incubated in a modified TRIS buffer (50 mmol/l, pH 7.4) containing EGTA (1 mmol/l), flavin adenine dinucleotide (10 μmol/l), NADPH (1 mmol/l), BH4 (100 μmol/l) and 10 μmol/l l-arginine containing 100,000 cpm of L-[2,3,4,5-^{3}H]arginine monohydrochloride (Amersham), previously equilibrated for 5 min at 37°C in a final volume of 100 μl. Pharmacological controls of enzymatic activity were performed in parallel and consisted of N^{ω}-nitro-L-arginine methyl ester (L-NAME) addition (1 mmol/l) to the incubation medium. After 15 min, the reaction was stopped by adding 1 ml ice-cold buffer (pH 5.4) containing HEPES (20 mmol/l) and EDTA (1 mmol/l), followed by vortex mixing. The samples were then applied to a 0.6 ml Dowex 50WX8-200, pre-equilibrated with the stopping buffer. L-[2,3,4,5-^{3}H]Citrulline was eluted and washed with 1 ml stopping buffer and radioactivity was determined by liquid scintillation counting. All measurements were made in duplicate. Protein concentrations were determined according to the method of Bradford [22] and the activity was expressed as pmol L-citrulline (mg protein)$^{-1}$ min^{-1}. The values were corrected

for the amount of L-[2,3,4,5-^{3}H]-citrulline found in the presence of L-NAME (1 mmol/l), which was added exogenously [23].

Statistical analysis The results of blots are presented as direct comparisons of bands or dots in autoradiographs and were quantified by densitometry using Scion Image software (ScionCorp, Fredrick, MD, USA). Data were analysed by two-tailed unpaired Student's *t* test or by repeated measures ANOVA (one- or two-way ANOVA), followed by post hoc analysis of significance (Bonferroni's test) when appropriate, comparing experimental and control groups. The level of significance was set at $p<0.05$.

Results

Effect of aspirin on insulin sensitivity and signalling and cytokine production The animals receiving the high-fat diet (diet-induced obese rats) had higher food intake, a pattern not affected by administration of aspirin or L-NIL (Fig. 1a). As expected, these animals had an increase in body weight; however, treatment with aspirin or aspirin with L-NIL for 2 days did not change body weight compared with respective controls (Fig. 1b). Fasting insulin levels were higher in animals on the high-fat diet and were not changed by treatment with aspirin or aspirin plus L-NIL (Fig. 1c). Plasma glucose did not change significantly in any group of animals (Fig. 1d); however, insulin sensitivity, as determined by the glucose disappearance rate (Fig. 1e) or glucose clamp (Fig. 1f), was decreased in high-fat fed rats and showed an improvement after aspirin treatment.

Effect of aspirin on insulin signalling in diet-induced obese rats An 80% reduction was observed in insulin-induced tyrosine phosphorylation of IRβ, as well as a 70% reduction in IRS-1 tyrosine phosphorylation, a 70% reduction in IRS-1 protein levels and an 80% reduction in Akt serine phosphorylation in muscle of diet-induced obese rats. These reductions were all reversed by aspirin treatment (Fig. 2a–d).

Effect of aspirin treatment on iNOS production/activity and S-nitrosylation of IRβ/IRS-1 and Akt in muscle of diet-induced obese rats Inducible nitric oxide protein levels increased in the muscle of diet-induced obese rats, but the increase was blunted following aspirin treatment in the same animal group (Fig. 3a). We also investigated whether salicylate was able to modulate iNOS activity in cultured muscle cells of control rats. Results showed that salicylate treatment for 2 h reduced iNOS activity by ~50% (Fig. 3b).

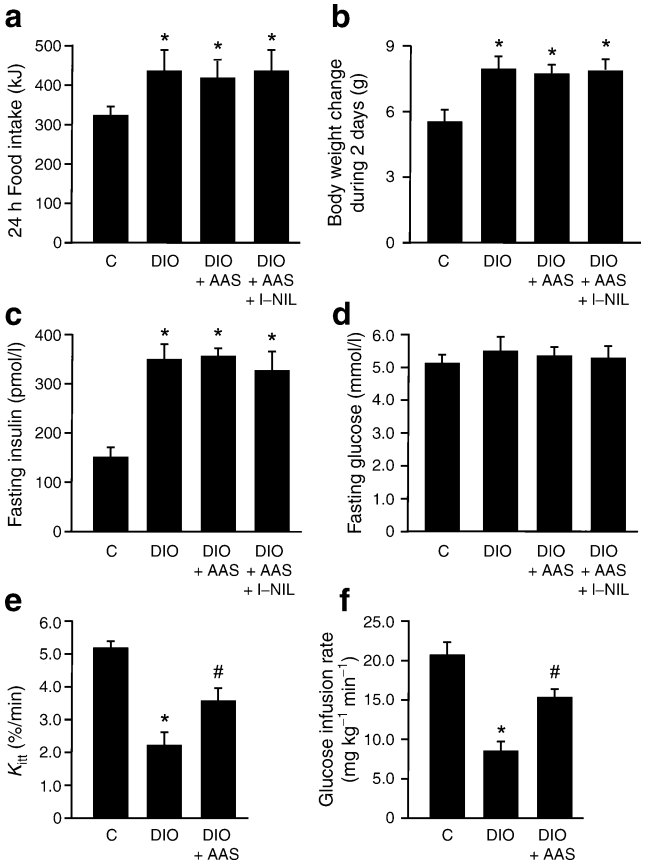

Fig. 1 Effect of aspirin on metabolic variables in diet-induced obese (DIO) rats. **a** Food intake (per 24 h), (**b**) body weight change, (**c**) fasting insulin and (**d**) fasting glucose during 2 days after aspirin (AAS) and/or L-NIL administration. Insulin sensitivity, as determined by (**e**) glucose disappearance rate (K_{itt}) or (**f**) euglycaemic–hyperinsulinaemic clamp. Bars represent mean ± SEM from six to eight rats. *$p<0.05$ vs control group; †$p<0.05$ vs diet-induced obesity rats. C, control

The enhanced iNOS production in high-fat fed rats was associated with an increase in *S*-nitrosylation of IRβ, IRS-1 and Akt. These increases were also reversed by aspirin treatment (Fig. 3c–e).

Effect of aspirin treatment on serine phosphorylaton of IRS-1 and JNK in the muscle of diet-induced obese rats Increased JNK and IKKβ phosphorylation was observed in the muscle of diet-induced obese rats, accompanied by an increase in IRS-1 serine phosphorylation. After aspirin treatment there was a reduction in JNK and IKKβ phosphorylation, as well as in IRS-1 serine phosphorylation (Fig. 4a–c).

Effect of aspirin and L-NIL on Akt phosphorylation and on S-nitrosylation of IRS-1 and Akt in muscle of diet-induced obese rats To show that aspirin attenuates insulin resistance in the muscle of diet-induced obese rats through the inhibition of *S*-nitrosylation of early steps of insulin action,

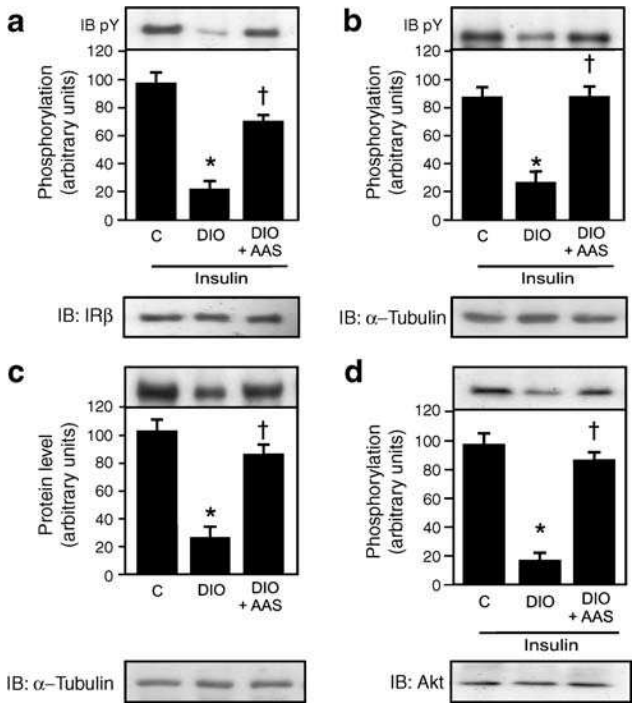

Fig. 2 Effect of aspirin treatment on insulin signalling. Insulin-induced tyrosine phosphorylation (immunoblotting pY) of (**a**) immunoprecipitated IRβ and (**b**) IRS-1 in the muscle of control (C), diet-induced obese (DIO) and DIO rats after aspirin (AAS) treatment. **c** Protein levels in immunoblots (IB) of IRS-1 and (**d**) insulin-induced serine phosphorylation of Akt in the muscle of control, DIO and DIO rats after AAS treatment. Representative blots (**a**–**d**) are from experiments that were repeated independently, with similar results. α-Tubulin was used in immunoblotting as protein control. Bars represent quantification of blots as mean ± SEM from six to eight rats. *$p<0.05$ vs control group; †$p<0.05$ vs DIO rats

we also investigated the effect of the iNOS inhibitor, L-NIL, either alone or in combination with aspirin, on insulin sensitivity, insulin signalling and *S*-nitrosylation of IRS-1 and Akt. Administration of L-NIL for 2 days resulted in improved insulin sensitivity, as demonstrated by an increase in glucose disappearance rate during the insulin tolerance test and also by an increase in glucose infusion rate during the glucose clamp. When L-NIL was added to aspirin, no further increase in insulin sensitivity was detected by either test (Fig. 5a, b). Insulin-induced Akt phosphorylation, which was decreased in diet-induced obese rats, showed a similar improvement after treatment with aspirin or L-NIL, both of which did not show any additional effect (Fig. 5c). *S*-nitrosylation of IRS-1 and Akt, which were increased in diet-induced obese rats, was similarly decreased after aspirin and/or L-NIL treatment (Fig. 5d, e).

Effect of aspirin treatment on Akt phosphorylation and S-nitrosylation of IRS-1 and Akt in muscle of iNos$^{-/-}$ mice on high-fat diet To investigate whether the effects of aspirin, associated with an inhibitor of iNOS, would also be reproduced in an *iNos* knockout animal, we investigated the effect of aspirin on insulin sensitivity and insulin signalling in muscle of *iNos*$^{-/-}$ mice on a high-fat diet.

Insulin sensitivity was determined using the glucose disappearance rate, which shows a good correlation with the gold standard glucose clamp, as previously described [15] and as also confirmed in this study with rats. As expected, control mice on a high-fat diet showed reduced insulin sensitivity (Fig. 6a). Interestingly, *iNos*$^{-/-}$ mice had higher insulin sensitivity than controls. When these animals were fed a high-fat diet for 2 months, they had a mild, but significant decrease in insulin sensitivity, as demonstrated by reduced glucose disappearance rate, when compared with control *iNos*$^{-/-}$ mice, but not when compared with wild-type mice on standard rodent chow. The treatment with aspirin showed no improvement in insulin sensitivity in *iNos*$^{-/-}$ mice on a high-fat diet (Fig. 6a).

Insulin-induced Akt activation was moderately decreased in control animals, but only mildly decreased in *iNos*$^{-/-}$ mice on a high-fat diet; these alterations were reversed with aspirin treatment (Fig. 6b). As expected, there was an increase in *S*-nitrosylation of IRS-1 and Akt in the muscle of control mice on a high-fat diet, the increase being reversed by aspirin. However, we did not observe *S*-nitrosylation of IRS-1 or Akt in the muscle of *iNos*$^{-/-}$ mice on a high-fat diet (Fig. 6c, d).

As demonstrated in the muscle of rats on a high-fat diet, JNK and IKKβ phosphorylation increased in the muscle of control mice on a high-fat diet, accompanied by an increase in IRS-1 serine phosphorylation that was reversed by aspirin treatment (Fig. 6e–g). JNK and IKKβ phosphorylation were slightly increased, in parallel with an increase in IRS-1 serine phosphorylation, in the muscle of *iNos*$^{-/-}$ mice on a high-fat diet; these alterations were reversed by aspirin treatment (Fig. 6e–g).

Discussion

The glucose-lowering effects of aspirin, observed decades ago in patients with diabetes, are complex, possibly tissue-specific and probably not related to the inhibition by aspirin of cyclo-oxygenase enzymes [8]. Recently, new effects of aspirin have been described. Thus aspirin can directly inhibit IKKβ, downregulating inflammatory signalling through NF-κB in this pathway, which is implicated in developing insulin resistance [7]. Gene- and diet-induced obesity are associated with enhanced IKKβ activity in liver, which may induce serine phosphorylation of IRS-1, preventing its tyrosine phosphorylation by insulin [8, 24]. However, in muscle, data on the importance of IKKβ activation in the development of insulin resistance remain

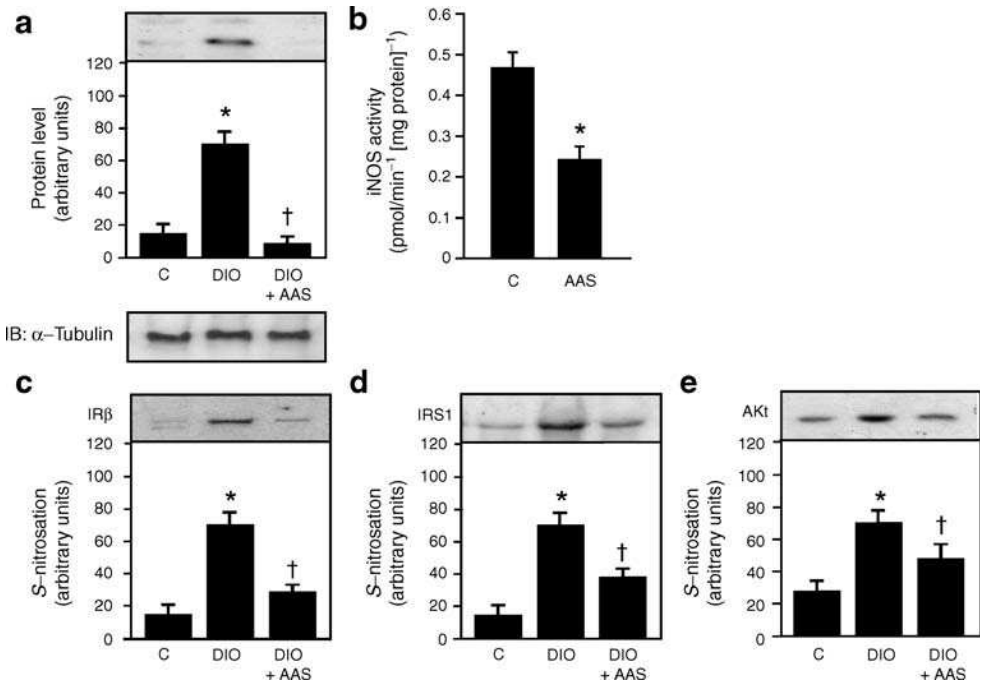

Fig. 3 Effects of aspirin on iNOS content/activity and *S*-nitrosylation of IRβ/IRS-1 and Akt in the muscle of diet-induced obesity (DIO) rats. **a** iNOS protein levels in immunoblots of gastrocnemius muscle of control (C), DIO and DIO rats after aspirin (AAS) administration. **b** iNOS activity was measured in control cultured muscle cells treated or not with salicylate (5 mmol/l), as described in Methods. **c** The biotin switch method was performed to detect S-nitrosylation of IRβ, (**d**) IRS-1 and (**e**) Akt in the muscle of control, DIO and DIO+AAS. Representative blots (**a**, **c**–**e**) are from experiments that were repeated independently, with similar results. α-Tubulin was used in immunoblotting as protein control. Bars represent quantification of blots as mean ± SEM of six to eight rats. *$p<0.05$ vs control group; †$p<0.05$ vs DIO rats

conflicting [25]. Another mechanism by which aspirin could prevent insulin resistance induced by obesity is through inhibition of JNK, another serine kinase associated with serine-phosphorylation of IRS-1 and therefore with insulin resistance. This mechanism has been described in HEK293 cells and observed in the muscle of septic and growth hormone-treated rats [5, 26, 27].

Our data show that, in the muscle of diet-induced obese rats and mice, aspirin was able to reduce IKKβ and JNK phosphorylation, and also IRS-1 serine phosphorylation. However, two results from our study suggest that these alterations were not crucial to the improvement in insulin action induced by aspirin. First, in diet-induced obese rats the effect of L-NIL, an inhibitor of iNOS, on insulin

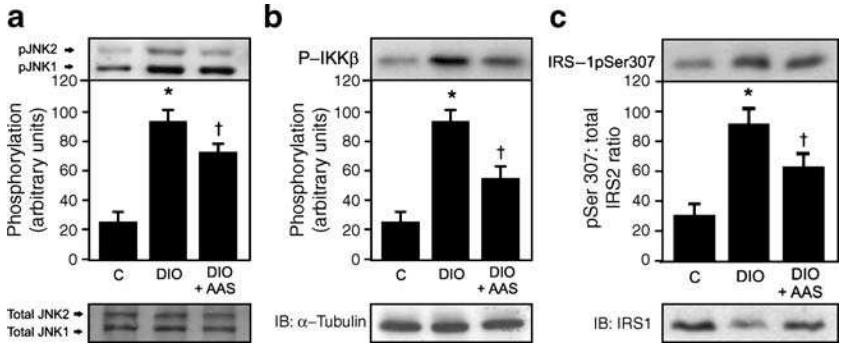

Fig. 4 Effect of aspirin on JNK, IKK and IRS-1 serine phosphorylaton in the muscle of diet-induced obesity (DIO) rats. Representative immunoblots blots show (**a**) JNK and (**b**) IKKβ serine phosphorylation. **c** Ratio of IRS-1 serine phosphorylation/IRS-1 protein content ratio in the muscle of control (C), DIO and DIO rats after aspirin (AAS) administration, as shown by immunoblots and quantified in bar graph. Representative blots (**a**–**c**) are from experiments that were repeated independently, with similar results. α-Tubulin was used in immunoblotting as protein control. Bars represent quantification of blots as mean ± SEM of six to eight rats. *$p<0.05$ vs control group; †$p<0.05$ vs DIO rats

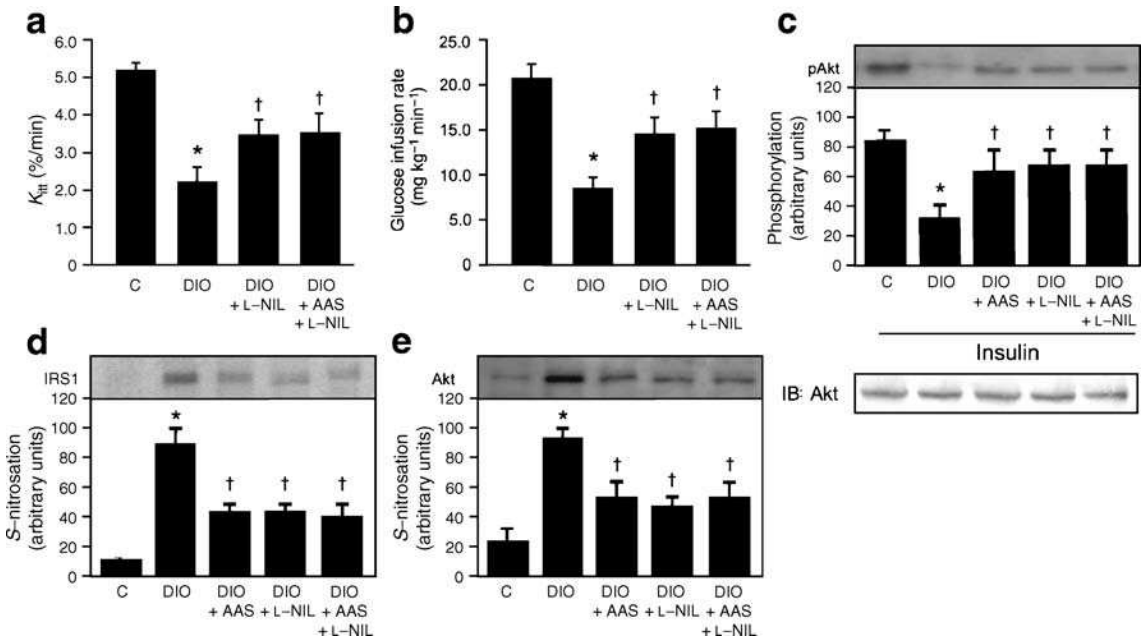

Fig. 5 Effects of aspirin and/or L-NIL treatment on Akt phosphorylation and S-nitrosylation of IRS-1 and Akt in muscle of diet-induced obesity (DIO) rats. **a** Glucose disappearance rate and (**b**) euglycaemic–hyperinsulinaemic clamp were determined 2 days after L-NIL and L-NIL plus aspirin (AAS) administration in DIO rats. **c** Representative immunoblots and quantification by bar graph of insulin-induced Akt serine phosphorylation in the muscle of controls (C), DIO rats and DIO rats 2 days after AAS, L-NIL or AAS plus L-NIL. **d** *S*-nitrosylation of IRS-1 and (**e**) Akt in the muscle after treatment as above (**c**). Representative blots (**c**–**e**) are from experiments that were repeated independently, with similar results. Bars represent quantification of blots as mean ± SEM of six to eight rats. *$p<0.05$ vs control group; $^{\dagger}p<0.05$ vs DIO rats

sensitivity was not synergised by aspirin treatment. Second, in *iNos*$^{-/-}$ mice on a high-fat diet, we saw an increase in IKKβ and JNK phosphorylation, as well as in IRS-1 serine phosphorylation. These increases were associated with only a mild reduction in insulin sensitivity, which was not reversed by aspirin treatment. These data suggest that, although aspirin reverses the increased IKKβ and JNK phosphorylation, as well as increased IRS-1 serine phosphorylation observed in diet-induced obese rats or in *iNos*$^{-/-}$ mice on a high-fat diet, these alterations have no parallel with the improvement in insulin action induced by this drug in muscle.

Insulin sensitivity was increased in *iNos*$^{-/-}$ mice, in parallel to an increase in insulin-induced Akt phosphorylation, suggesting that mechanisms related to iNOS may have a role in the control of physiological insulin sensitivity and not only in situations related to insulin resistance. When these mice were fed a high-fat diet for 2 months, they had a mild reduction in insulin sensitivity; however, the glucose disappearance rate under this diet was similar to that of wild-type mice on control rodent chow. As described above, in *iNos*$^{-/-}$ mice on a high-fat diet, aspirin did not improve insulin sensitivity, despite its improvement of insulin-induced Akt phosphorylation. These data suggest that minor changes in insulin signalling may have no influence on insulin sensitivity.

Although we did not investigate whether aspirin could attenuate insulin resistance in the liver of these obese animals, a previous report [28] has shown that iNOS content was enhanced in the liver of *ob/ob* mice, an enhancement associated with reduced protein levels of IRS-1 and IRS-2, which was prevented by iNOS blockage with L-NIL. This finding demonstrates that iNOS plays a role in fasting hyperglycaemia and contributes to hepatic insulin resistance in *ob/ob* mice. The effect of high-fat diet on fasting glucose levels was only modest in our model, and probably the importance of hepatic insulin resistance was only mild. In more prolonged high-fat diet treatment these effects of iNOS on hepatic insulin resistance would probably be more evident [28].

Several reports have shown that salicylates or aspirin inhibit the production of iNOS induced by cytokines in different cell types and suggest that one of the therapeutic actions of these drugs could be mediated by a reduction in iNOS content and nitric oxide production [11, 13]. This reduction in iNOS protein levels may be secondary to a decrease in NFκB activation [29]; however, a limitation of our study was that we did not directly measure NFκB activity in these experiments. Aspirin can also directly inhibit iNOS enzymatic activity, although some questions remain as to whether this occurs at therapeutic concentrations [12]. Our data show that aspirin reduced iNOS

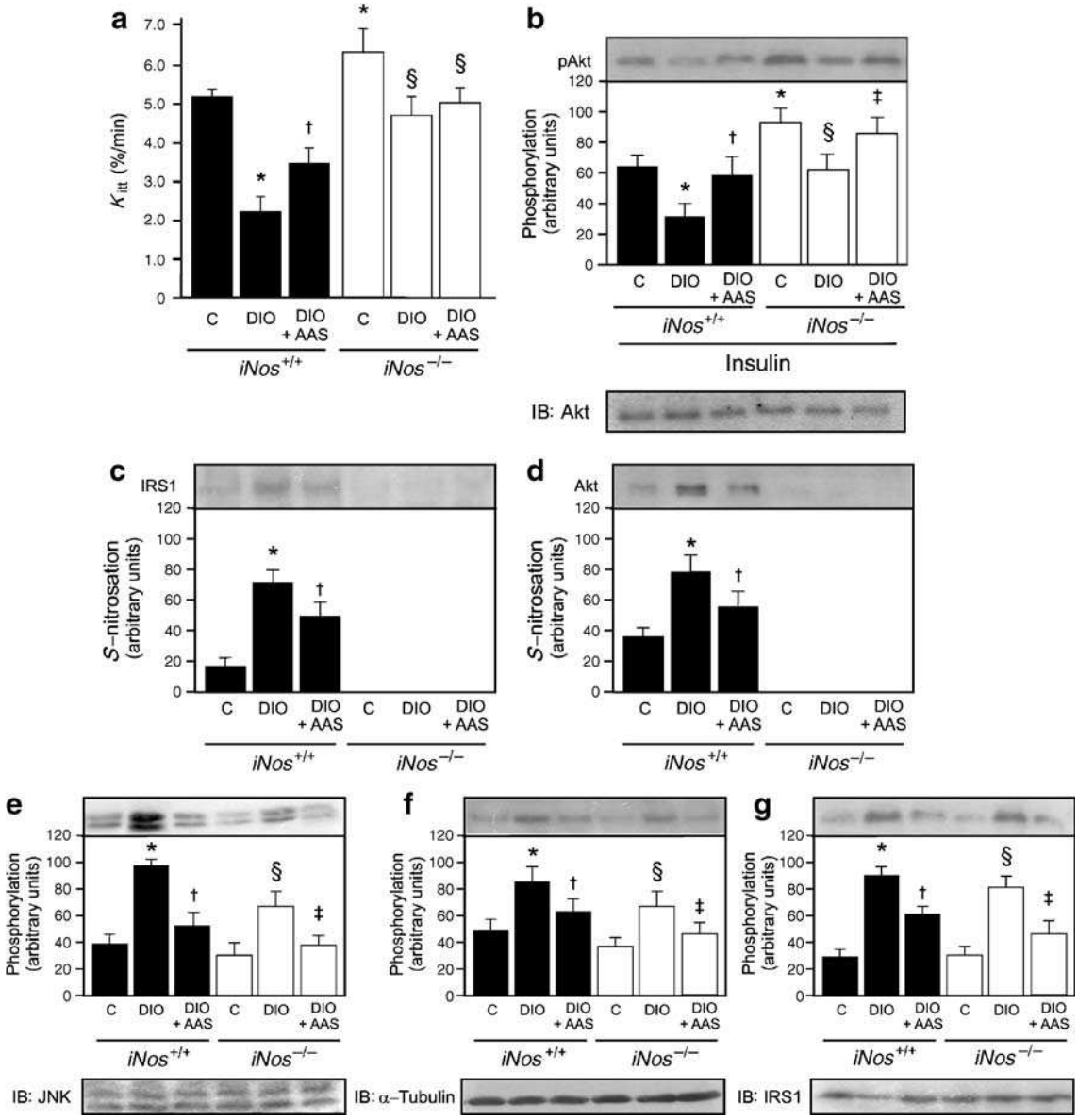

Fig. 6 Effect of aspirin on insulin sensitivity, Akt phosphorylation and *S*-nitrosylation of IRS-1 and Akt in muscle of *iNos*$^{-/-}$ mice on a high-fat diet. **a** Glucose disappearance rate in control and *iNos* knockout mice at 2 days after aspirin (AAS) administration. **b** Representative immunoblots blots, quantified as bar graphs, of insulin-induced Akt serine phosphorylation and (**c**, **d**) of *S*-nitrosylation of IRS-1 and Akt respectively in the muscle of control (C) and iNOS knockout mice 2 days after AAS administration. **e** JNK, (**f**) IKKβ and (**g**) IRS-1 serine phosphorylation in the muscle of animals treated as above (**c**, **d**) Representative blots (**b**–**g**) are from experiments that were repeated independently, with similar results. Bars represent quantification of blots as mean ± SEM of six to eight mice. *$p<0.05$ vs control mice; $^{\dagger}p<0.05$ vs DIO mice; $^{\ddagger}p<0.05$ vs DIO *iNos*$^{-/-}$; $^{\S}p<0.05$ vs control *iNos*$^{-/-}$

activity in cultured muscle cells and also reduced iNOS content in muscle of diet-induced obese rats. These data suggest that aspirin has a direct effect on muscle, reducing iNOS activity.

Recently, we demonstrated that iNOS induction in the muscle of diet-induced obese rats, *ob/ob* mice and lipopolysaccharide-treated mice is associated with enhanced nitric oxide production and enhanced *S*-nitrosylation of IRβ, IRS-1 and Akt [9, 10]. *S*-nitrosylation of IRβ and Akt was associated with reductions in their kinase activities, leading to downregulation of the IRβ/IRS-1/PI 3-kinase/Akt pathway [9, 30]. Mutated Akt1(C224S), in which cysteine 224 is substituted by serine, is resistant to nitric oxide donor-induced *S*-nitrosylation and inactivation, indicating that cysteine 224 is a major *S*-nitrosylation acceptor site. In vitro denitrosylation with reducing agent reactivated cellular Akt from nitric oxide donor-treated cells. In combination, these data demonstrated that *S*-

nitrosylation of Akt is a specific post-translational modification that regulates its activity [30]. *S*-nitrosylation of IRS-1 is associated with its reduced protein levels in muscle, which may be secondary to degradation via the ubiquitin–proteasome system [9, 14]. Since the IRβ/IRS-1/Akt pathway plays a central role in metabolic actions of insulin in muscle, including stimulation of glucose uptake and glycogen synthesis, downregulation of this pathway in muscle by *S*-nitrosylation may be an important mechanism of iNOS-induced insulin resistance. The results of the present study reinforce the above data and show that, in *iNos*$^{-/-}$ mice on a high-fat diet, only a mild alteration in insulin sensitivity is observed. In addition, in these mice, while aspirin reduced IKKβ, JNK and IRS-1 serine phosphorylation, it did not improve insulin sensitivity. Similar results were observed in diet-induced obese rats treated with an iNOS inhibitor and aspirin. These data suggest that iNOS-induced insulin resistance is an important mechanism that modulates insulin sensitivity and that probably the beneficial effect of aspirin in insulin resistance is related to a reduction of iNOS protein levels and *S*-nitrosylation of IRβ, IRS-1 and Akt.

Insulin resistance is certainly a metabolic situation related to several mechanisms that act in parallel to downregulate insulin signalling. Our data reinforce the hypothesis that: (1) multiple mechanisms are involved in insulin resistance in diet-induced obese rats and mice; but that (2) iNOS-induced insulin resistance is an important mechanism modulating insulin signalling and insulin sensitivity in parallel; and (3) aspirin is able to improve this mechanism.

Recently, Dallaire and colleagues investigated whether targeted disruption of iNOS modulates the metabolic effect of rosiglitazone in obese mice [31]. Their results demonstrated that the iNOS/nitric oxide pathway is a critical modulator of peroxisome proliferator-activated receptor (PPAR)-γ activation and that invalidation of this pathway improves the efficacy of PPAR-γ agonism in an animal model of obesity and insulin resistance.

Taken together, our data show that aspirin treatment not only reduced iNOS protein levels, but also *S*-nitrosylation of IRβ, IRS-1 and Akt, which was related to improvements in insulin-induced tyrosine phosphorylation of IRβ and IRS-1, and serine phosphorylation of Akt. This suggests a novel mechanism of insulin sensitisation, evoked by aspirin treatment. These findings also suggest that inhibition of iNOS might be a major mediator of the insulin-sensitising effects of IKKβ inhibition.

Recently, in a double-masked, placebo-controlled trial, 20 obese non-diabetic adults were evaluated at baseline and after 1 month of salsalate treatment, a non-acetylated salicylate but with a lower bleeding risk. This proof-of-principle study demonstrates that salsalate reduces glycaemia and may improve inflammatory cardiovascular risk indexes in overweight individuals [32]. In addition, aspirin treatment improved glycaemic control of diabetic patients, in parallel with reductions in inflammatory response, including reduced levels of serum nitrite, which at least in part may be secondary to reduced iNOS activation [33]. These new concepts are important for an understanding of how anti-inflammatory drugs attenuate insulin resistance, since direct therapeutic targets may be identified.

Acknowledgements This work was supported by grants from Fundação de Amparo à Pesquisa do Estado de São Paulo (FAPESP) and Conselho Nacional de Desenvolvimento Científico e Tecnológico (CNPq).

Duality of interest The authors declare that there is no duality of interest associated with this manuscript.

References

1. Sethi JK, Hotamisligil GS (1999) The role of TNF alpha in adipocyte metabolism. Semin Cell Dev Biol 10:19–29
2. Hirosumi J, Tuncman G, Chang L et al (2002) A central role for JNK in obesity and insulin resistance. Nature 420:333–336
3. Perreault M, Marette A (2001) Targeted disruption of inducible nitric oxide synthase protects against obesity-linked insulin resistance in muscle. Nat Med 7:1138–1143
4. Yuan M, Konstantopoulos N, Lee J et al (2001) Reversal of obesity- and diet-induced insulin resistance with salicylates or targeted disruption of Ikkbeta. Science 293:1673–1677
5. Barreiro GC, Prattali RR, Caliseo CT et al (2004) Aspirin inhibits serine phosphorylation of IRS-1 in muscle and adipose tissue of septic rats. Biochem Biophys Res Commun 320:992–997
6. Hundal RS, Petersen KF, Mayerson AB et al (2002) Mechanism by which high-dose aspirin improves glucose metabolism in type 2 diabetes. J Clin Invest 109:1321–1326
7. Kim JK, Kim YJ, Fillmore JJ et al (2001) Prevention of fat-induced insulin resistance by salicylate. J Clin Invest 108:437–446
8. Gao Z, Zuberi A, Quon MJ, Dong Z, Ye J (2003) Aspirin inhibits serine phosphorylation of insulin receptor substrate 1 in tumor necrosis factor-treated cells through targeting multiple serine kinases. J Biol Chem 278:24944–24950
9. Carvalho-Filho MA, Ueno M, Hirabara SM et al (2005) S-nitrosylation of the insulin receptor, insulin receptor substrate 1, and protein kinase B/Akt: a novel mechanism of insulin resistance. Diabetes 54:959–967
10. Carvalho-Filho MA, Ueno M, Carvalheira JB, Velloso LA, Saad MJ (2006) Targeted disruption of iNOS prevents LPS-induced S-nitrosylation of IRbeta/IRS-1 and Akt and insulin resistance in muscle of mice. Am J Physiol Endocrinol Metab 291:E476–E482
11. Cieslik K, Zhu Y, Wu KK (2002) Salicylate suppresses macrophage nitric-oxide synthase-2 and cyclo-oxygenase-2 expression by inhibiting CCAAT/enhancer-binding protein-beta binding via a common signaling pathway. J Biol Chem 277:49304–49310
12. Katsuyama K, Shichiri M, Kato H, Imai T, Marumo F, Hirata Y (1999) Differential inhibitory actions by glucocorticoid and aspirin on cytokine-induced nitric oxide production in vascular smooth muscle cells. Endocrinology 140:2183–2190
13. Wang Z, Brecher P (1999) Salicylate inhibition of extracellular signal-regulated kinases and inducible nitric oxide synthase. Hypertension 34:1259–1264

14. Sugita H, Fujimoto M, Yasukawa T et al (2005) Inducible nitric-oxide synthase and NO donor induce insulin receptor substrate-1 degradation in skeletal muscle cells. J Biol Chem 280:14203–14211
15. Bonora E, Moghetti P, Zancanaro C et al (1989) Estimates of in vivo insulin action in man: comparison of insulin tolerance tests with euglycemic and hyperglycemic glucose clamp studies. J Clin Endocrinol Metab 68:374–378
16. Prada PO, Zecchin HG, Gasparetti AL et al (2005) Western diet modulates insulin signaling, c-Jun N-terminal kinase activity, and insulin receptor substrate-1ser307 phosphorylation in a tissue-specific fashion. Endocrinology 146:1576–1587
17. Saad MJ, Araki E, Miralpeix M, Rothenberg PL, White MF, Kahn CR (1992) Regulation of insulin receptor substrate-1 in liver and muscle of animal models of insulin resistance. J Clin Invest 90:1839–1849
18. Tremblay F, Lavigne C, Jacques H, Marette A (2001) Defective insulin-induced GLUT4 translocation in skeletal muscle of high fat-fed rats is associated with alterations in both Akt/protein kinase B and atypical protein kinase C (zeta/lambda) activities. Diabetes 50:1901–1910
19. Jaffrey SR, Snyder SH (2001) The biotin switch method for the detection of S-nitrosylated proteins. Sci STKE 2001: PL1
20. Martinez-Ruiz A, Lamas S (2004) Detection and proteomic identification of S-nitrosylated proteins in endothelial cells. Arch Biochem Biophys 423:192–199
21. Lynge J, Juel C, Hellsten Y (2001) Extracellular formation and uptake of adenosine during skeletal muscle contraction in the rat: role of adenosine transporters. J Physiol 537:597–605
22. Bradford MM (1976) A rapid and sensitive method for the quantitation of microgram quantities of protein utilizing the principle of protein-dye binding. Anal Biochem 72:248–254
23. Pollock JS, Forstermann U, Mitchell JA et al (1991) Purification and characterization of particulate endothelium-derived relaxing factor synthase from cultured and native bovine aortic endothelial cells. Proc Natl Acad Sci U S A 88:10480–10484
24. Cai D, Yuan M, Frantz DF et al (2005) Local and systemic insulin resistance resulting from hepatic activation of IKK-beta and NF-kappaB. Nat Med 11:183–190
25. Rohl M, Pasparakis M, Baudler S et al (2004) Conditional disruption of IkappaB kinase 2 fails to prevent obesity-induced insulin resistance. J Clin Invest 113:474–481
26. Jiang G, Dallas-Yang Q, Liu F, Moller DE, Zhang BB (2003) Salicylic acid reverses phorbol 12-myristate-13-acetate (PMA)- and tumor necrosis factor alpha (TNFalpha)-induced insulin receptor substrate 1 (IRS1) serine 307 phosphorylation and insulin resistance in human embryonic kidney 293 (HEK293) cells. J Biol Chem 278:180–186
27. Prattali RR, Barreiro GC, Caliseo CT et al (2005) Aspirin inhibits serine phosphorylation of insulin receptor substrate 1 in growth hormone treated animals. FEBS Lett 579:3152–3158
28. Fujimoto M, Shimizu N, Kunii K, Martyn JA, Ueki K, Kaneki M (2005) A role for iNOS in fasting hyperglycemia and impaired insulin signaling in the liver of obese diabetic mice. Diabetes 54:1340–1348
29. Taylor BS, Geller DA (2000) Molecular regulation of the human inducible nitric oxide synthase (iNOS) gene. Shock 13:413–424
30. Yasukawa T, Tokunaga E, Ota H, Sugita H, Martyn JA, Kaneki M (2005) S-nitrosylation-dependent inactivation of Akt/protein kinase B in insulin resistance. J Biol Chem 280:7511–7518
31. Dallaire P, Bellmann K, Laplante M et al (2008) Obese mice lacking inducible nitric oxide synthase are sensitized to the metabolic actions of peroxisome proliferator-activated receptor-gamma agonism. Diabetes 57:1999–2011
32. Fleischman A, Shoelson SE, Bernier R, Goldfine AB (2008) Salsalate improves glycemia and inflammatory parameters in obese young adults. Diabetes Care 31:289–294
33. Goldfine AB, Silver R, Aldhahi W et al (2008) Use of salsalate to target inflammation in the treatment of insulin resistance and type 2 diabetes. Clin Transl Sci 1:36–43

APÊNDICE *X*

Acta Physiologica

Acta Physiol 2010, **198**, 61–69

Acute exercise reverses TRB3 expression in the skeletal muscle and ameliorates whole body insulin sensitivity in diabetic mice

A. Matos,[1] E. R. Ropelle,[2] J. R. Pauli,[3] M. J. S. Frederico,[4] R. A. de Pinho,[4] L. A. Velloso[2] and C. T. De Souza[1,4]

1 *Universidade Cruzeiro do Sul, Unicsul, São Paulo, SP, Brazil*

2 *Departamento de Clínica Médica, FCM, Universidade Estadual de Campinas (UNICAMP), Campinas, SP, Brazil*

3 *Curso de Educação Física – Modalidade Saúde, Departamento de Biociências, UNIFESP, Santos, SP, Brazil*

4 *Exercise Biochemistry and Physiology Laboratory, Postgraduate Program in Health Sciences, Health Sciences Unit, University of Southern Santa Catarina, Criciúma, SC, Brazil*

Received 25 September 2008, revision requested 4 January 2009, final revision received 5 June 2008, accepted 24 July 2009
Correspondence: C. T. de Souza, Laboratório de Fisiologia e Bioquímica do Exercício, Programa de Pós-Graduação em Ciências da Saúde, Universidade do Extremo Sul Catarinense, 88806-000 Criciúma, SC, Brazil.
E-mail: ctsouza@unesc.net

Abstract

Aim: TRB3 became of major interest in diabetes research when it was shown to interact with and inhibit the activity of Akt. Conversely, physical exercise has been linked to improved glucose homeostasis. Thus, the current study was designed to investigate the effects of acute exercise on TRB3 expression and whole body insulin sensitivity in obese diabetic mice.

Methods: Male leptin-deficient (ob/ob) mice swam for two 3-h-long bouts, separated by a 45-min rest period. After the second bout of exercise, food was withdrawn 6 h before antibody analysis. Eight hours after the exercise protocol, the mice were submitted to an insulin tolerance test (ITT). Gastrocnemius muscle samples were evaluated for insulin receptor (IR) and IRS-1 tyrosine phosphorylation, Akt serine phosphorylation, TRB3/Akt association and membrane GLUT4 expression.

Results: Western blot analysis showed that TRB3 expression was reduced in the gastrocnemius of leptin-deficient (ob/ob) mice submitted to exercise when compared with respective ob/ob mice at rest. In parallel, there was an increase in the insulin-signalling pathway in skeletal muscle from leptin-deficient mice after exercise. Furthermore, the GLUT4 membrane expression was increased in the muscle after the exercise protocol. Finally, a single session of exercise improved the glucose disappearance (K_{ITT}) rate in ob/ob mice.

Conclusion: Our results demonstrate that acute exercise reverses TRB3 expression and insulin signalling restoration in muscle. Thus, these results provide new insights into the mechanism by which physical activity ameliorates whole body insulin sensitivity in type 2 diabetes.

Keywords exercise, GLUT4 translocation, insulin, insulin sensitivity, muscle, TRB3 expression.

Physical exercise is known to be essential in the treatment of type 2 diabetes. Both the acute and persistent effects of exercise on glucose uptake and disposal have important implications for individuals with diabetes in terms of chronic metabolic control and acute regulation of glucose homeostasis. The finding that rates of glucose uptake in hindquarter skeletal muscle are elevated for several hours after exercise in the presence, but not in the absence of insulin, supports this hypothesis (Garetto *et al.* 1984). Although some

 doi: 10.1111/j.1748-1716.2009.02031.x

studies suggest that the persistent increase in glucose uptake post-exercise requires the presence of insulin (Young *et al.* 1987, Wallberg-Henriksson *et al.* 1988), the molecular signalling pathways that lead to the stimulation of glucose uptake in skeletal muscle or other cell types have not been completely elucidated.

Insulin receptor (IR) is a protein with endogenous tyrosine kinase activity that, following activation by insulin, undergoes rapid autophosphorylation and subsequently phosphorylates intracellular protein substrates, including IRS-1 and IRS-2 (Cheathan & Kahn 1995). IRS proteins act as messenger molecule-activated receptors to signalling by Src homology 2 domains, which are important steps in insulin action. After stimulation by insulin, IRS-1 and -2 associate with several proteins, including phosphatidylinositol 3-kinase (PI 3-K) (Folli *et al.* 1992, Saad *et al.* 1993, White & Kahn 1994). Downstream to PI 3-K, the serine threonine kinase, Akt, is activated and plays a pivotal role in the regulation of various biological processes, including apoptosis, proliferation, differentiation and intermediary metabolism (Downward 1998, Chen *et al.* 2001). The protein kinase Akt functions both in the control of cell proliferation and as a critical node in insulin signalling, appearing to mediate most of the metabolic effects of insulin (Tanaguchi *et al.* 2006). Akt is activated by phosphorylation of Thr^{308} within the T loop of the catalytic domain and Ser^{473}, located in a C-terminal, non-catalytic region of the enzyme (Alessi *et al.* 1996).

TRB3, a mammalian homolog of *Drosophila tribbles*, has been proposed to be a suppressor of Akt activity, predominantly in conditions of fasting and diabetes (Du *et al.* 2003). This protein is emerging as an important player in the regulation of insulin signalling, as it can bind directly to Ser/Thr protein kinase Akt, the major downstream kinase of insulin signalling. TRB3 binds the kinase domain of Akt in the activation loop and inhibits phosphorylation of Akt at, Thr^{308} and Ser^{473}, the critical events for Akt activation, induced by growth factors and insulin (Du *et al.* 2003). In addition, overexpression of TRB3 decreases, and knockdown of TRB3 expression increases Akt activation by insulin in the liver and muscle (Koo *et al.* 2004, Matsushima *et al.* 2006, Hegedus *et al.* 2007). Correspondingly, knockdown of TRB3 expression by shRNA in mouse diabetic liver increases insulin sensitivity. Conversely, increased TRB3 expression via adenoviral transfer in the normal liver leads to decreased insulin sensitivity and glucose intolerance. Furthermore, overexpression of TRB3 in C2C12 myoblasts results in blunted insulin-stimulated Akt phosphorylation, demonstrating that TRB3 inhibits insulin-stimulated Akt phosphorylation in skeletal muscle cells. In skeletal muscle, the phosphorylation of Akt-induced insulin-increased glucose transport is mediated by translocation of glucose transporter isoform 4 (GLUT4) from an intracellular pool to the plasma membrane.

The molecular mechanism for enhanced insulin sensitivity following exercise training may be partly related to the increased expression and activity of key proteins known to regulate glucose metabolism in skeletal muscle (Chibalin *et al.* 2000, Aoi *et al.* 2004, Ropelle *et al.* 2006). However, the molecular basis underlying the effects of exercise on muscle TRB3 expression remains unclear. Thus, the current study was designed to investigate the effects of acute exercise on TRB3 expression and whole body insulin sensitivity in obese diabetic mice.

Methods

Animals

Male leptin-deficient (ob/ob) and lean control mice, originally imported from the Jackson Laboratories (Bar Harbor, ME, USA), were used in all of the experiments, in accordance with the guidelines of the Brazilian College for Animal Experimentation (COBEA). The ethics committee of the State University of Campinas approved the experiments. Room temperature was maintained stable (28 ± 1 °C) and mice were housed in individual cages, subjected to a standard light-dark cycle (06:00 hours to 18:00 hours/06:00 hours to 18:00 hours), and provided with standard rodent chow and water *ad libitum*. Six mice ($n = 7$) were used per group: lean group (control group), sedentary leptin-deficient mice (ob/ob group), and exercised ob/ob mice (Exer group).

Exercise protocol

The swimming protocol was employed as described previously (Ryder *et al.* 1999), with minor modifications. Adult mice were acclimatized to swimming for 10 min for 2 days. Seven animals swam together in plastic containers measuring 45 cm in diameter. Water temperature was maintained at 32–33 °C. Mice swam for four 30-min periods, with 5-min rest periods for a total swimming time of 2 h. After acute exercise, mice were fed *ad libitum* and food was withdrawn 6 h before tissue extraction. With the exception of swimming, leptin-deficient mice (ob/ob group) were submitted to the same procedures. Eight hours after the exercise protocol or rest, the mice were anaesthetized with an intraperitoneal (i.p.) injection of sodium thiopental (40 mg kg^{-1} body weight) and gastrocnemius muscle collected. Following the experimental procedures, the mice were killed under anaesthesia (thiopental

Journal compilation © 2009 Scandinavian Physiological Society, doi: 10.1111/j.1748-1716.2009.02031.x

200 mg kg^{-1}) following the recommendations of the NIH publication no. 85-23.

Fasting glucose, insulin tolerance test (ITT), serum insulin quantification and glycogen content

After the exercise protocol, the mice were submitted to an ITT (1.5 U kg^{-1} body weight of insulin) after 6 h of fasting. Briefly, 1.5 IU kg^{-1} of human recombinant insulin (Humulin R) from Eli Lilly (Indianapolis, IN, USA) was infused intraperitoneally to anaesthetized mice; the blood samples were collected at 0, 5, 10, 15, 20, 25 and 30 min from the tail for serum glucose determination. The rate constant for plasma glucose disappearance (K_{ITT}) was calculated using the formula 0.693/biological half-life ($t_{1/2}$). The plasma glucose $t_{1/2}$ was calculated from the slope of the last square analysis of the plasma glucose concentration during the linear phase of decline (Bonora *et al.* 1989). Plasma glucose was determined using a glucosemeter (Advantage; Boehringer Mannheim, Irvine, CA, USA). Plasma was separated by centrifugation (1100 ***g***) for 15 min at 4 °C and stored at −80 °C until assay. Radioimmunoassay (RIA) was employed to measure serum insulin, according to a previous description (Scott *et al.* 1981). Glycogen content in gastrocnemius was measured according to a previously described method (Pimenta *et al.* 1989).

Protein analysis by immunoblotting

As soon as anaesthesia was assured by the loss of pedal and corneal reflexes, the abdominal cavity was opened, the cava vein exposed, and 0.2 mL of normal saline (−) or insulin (10^{-6} mol L^{-1}) (+) were injected. After insulin injection, portions of gastrocnemius were excised. The tissues were pooled, minced coarsely and homogenized immediately in extraction buffer (mM) (1% Triton-X 100, 100 Tris, pH 7.4, containing 100 sodium pyrophosphate, 100 sodium fluoride, 10 EDTA, 10 sodium vanadate, 2 PMSF and 0.1 mg of aprotinin mL^{-1}) at 4 °C with a Polytron PTA 20S generator (model PT 10/35; Brinkmann Instruments, Westbury, NY, USA) operated at maximum speed for 30 s. The extracts were centrifuged at 9000 ***g*** and 4 °C in a Beckman 70.1 Ti rotor (Palo Alto, CA, USA) for 40 min to remove insoluble material, and the supernatants of these tissues were used for protein quantification, using the Bradford method (Bradford 1976). Proteins were denatured by boiling in Laemmli (Laemmli 1970) sample buffer containing 100 mM DTT, run on SDS-PAGE and transferred to nitrocellulose membranes. Membranes were blocked, probed and developed, as described previously (De Souza *et al.* 2008). The IRβ and IRS-1 were immunoprecipitated from mice muscle with or without previous insulin infusion in the cava vein. Antibodies used for immunoblotting were anti-phosphotyrosine, anti-IR, anti-IRS-1 (Upstate Biotechnology, Lake Placid, NY, USA), anti-phospho-Akt Ser[473], anti-Akt, anti GLUT4, anti-β-actin and anti-TRB3 (Santa Cruz Biotechnology, Santa Cruz, CA, USA). Chemiluminescent detection was performed with horseradish peroxidase-conjugated secondary antibodies. Band intensities were quantified by optical desitometry (Scion Image software; ScionCorp, Frederick, MD, USA) of the developed autoradiographs.

Plasma membrane GLUT4 determination

To characterize the plasma membrane, a GLUT4 expression protocol was employed, as described previously by others (Klip *et al.* 1987, Douen *et al.* 1989, Lavoie *et al.* 1996). Gastrocnemius muscle from mice injected with saline (−) or with insulin (+) (0.2 mL, 10^{-6} M, tissue obtained 15 min after insulin injection, cava vein). The muscles (25 g) were then minced and homogenized for 5 s with a Polytron in buffer A (10 mM NaHCO3, 0.25 M sucrose, 5 mM NaN_3, pH 7.0) at 4 °C. The homogenate was then centrifuged at 1200 ***g*** for 10 min at 4 °C. The supernatant was saved, and the pellet was resuspended, homogenized and centrifuged again at 1200 ***g*** for 10 min. The two supernatants were then combined and centrifuged at 9000 ***g*** for 10 min at 4 °C and the resulting supernatant was centrifuged at 190 000 ***g*** for 60 min at 4 °C. The pellet (crude membranes) was then resuspended in 7 mL of 38% sucrose (w/v) and 5 mL each of 25%, 30% and 35% sucrose solutions were layered over the top. The 30% sucrose layer was adjusted to 7 mL in order to minimize plasma membrane contamination with intracellular membranes. The gradient was centrifuged at 150 000 ***g*** for 16 h. Membranes from the gradient were then collected (on 25% sucrose plasma membranes), diluted with homogenization buffer and centrifuged again at 190 000 ***g*** for 60 min. The resulting pellets were resuspended in the extraction buffer (as described above in immunoblotting methods), and total membrane protein content was determined by Bradford methods; aliquots (100 μg of protein) were subjected to SDS-PAGE and Western blotting with anti-GLUT4 antibodies.

Statistics

The results were expressed as means ± SEM. Differences between the lean groups and ob/ob mice at rest and after the exercise protocol were evaluated using one-way analysis of variance (ANOVA). When ANOVA indicated significance, a *Bonferroni post hoc* test was performed.

 doi: 10.1111/j.1748-1716.2009.02031.x

Results

Physiological and metabolic parameters

Table 1 shows comparative data regarding lean controls, leptin-deficient (ob/ob) mice at rest and after acute exercise (Exer group). The ob/ob mice at rest have a greater body weight, epididymal fat, fasting serum insulin and fasting glucose than age-matched controls (lean). No significant variations were found in body weight, epididymal fat and fasting serum insulin of ob/ob mice after acute exercise when compared with those of diabetic mice at rest. However, fasting glucose was reduced (66%) in ob/ob mice at 8 h after the exercise protocol (Exer group). Although the acute exercise protocol used has been established previously (Ryder *et al.* 1999, Yang *et al.* 2002, Lima *et al.* 2009), we evaluated the AMP-activated protein kinase (AMPK) and acetyl-CoA carboxylase (ACC) phosphorylation for certification of its efficiency. AMPK and ACC phosphorylation was found to be increased in mice ob/ob submitted to acute exercise ($46 \pm 5\%$, $P < 0.05$ and $62 \pm 7\%$, $P < 0.01$ respectively) when compared with mice at rest.

Acute exercise improves insulin signalling in the muscle of ob/ob mice.

The effects of *in vivo* i.v. insulin injection on IR and IRS-1 tyrosine phosphorylation and Akt serine phosphorylation were examined in the muscle of lean, ob/ob and Exer animals. The muscle protein was immunoprecipitated with anti-IR antibody and then blotted with anti-phosphotyrosine antibody. Insulin induced a 3.3-fold increase in IR tyrosine phosphorylation in the muscle of lean mice when compared with saline injection (Fig. 1a). In ob/ob mice at rest, IR tyrosine phosphorylation was reduced after insulin injection by 2.3-fold when compared with respective lean mice (Fig. 1a). In the muscle of Exer group mice, IR phosphorylation increased by 1.9-fold, compared with the respective ob/ob group at rest (Fig. 1a). There was no difference in basal levels of IR tyrosine phosphorylation between the groups (data not shown). The protein expression of IR in the muscle of lean, ob/ob at rest and Exer groups was quantified by immunoblotting with the anti-IR antibody. The IR protein levels did not differ between the groups (Fig. 1a – lower panels). No difference was observed in the non–insulin-injected groups (saline).

Insulin induced a 5.2-fold increase in IRS-1 tyrosine phosphorylation in the muscle of lean controls when compared with saline injection (Fig. 1b). In obese mice at rest, IRS-1 tyrosine phosphorylation was reduced after insulin injection by 3.1-fold when compared with respective lean mice (Fig. 1b). In the muscle of the Exer group, IRS-1 tyrosine phosphorylation increased by 2.1-fold compared with the respective ob/ob group at rest (Fig. 1b). There was no difference in basal levels of IRS-1 tyrosine phosphorylation between the groups (data not shown). The protein expression of IRS-1 in the muscle of lean, ob/ob at rest and Exer groups was quantified by immunoblotting with the anti-IRS-1 antibody. The IRS-1 protein levels were not different between the groups (Fig. 1b – lower panels). No difference in the saline (−) groups was observed.

Insulin induced a 3.4-fold increase in Akt serine phosphorylation in the muscle of lean mice when compared with saline injection (Fig. 1c). In ob/ob at rest, Akt serine phosphorylation was reduced after insulin injection by 2.2-fold when compared with lean mice (Fig. 1c). In the muscle of the Exer group, Akt serine increased by 1.9-fold compared with that of diabetic mice at rest (Fig. 1c). There was no difference in basal levels of Akt serine phosphorylation between the groups (data not shown). The protein expression of Akt in the muscle of lean, ob/ob at rest and Exer mice was quantified by immunoblotting with the anti-Akt antibody. The Akt protein levels were not different between the groups (Fig. 1c – lower panels). Akt phosphorylation did not differ in the non–insulin-injected (−) groups.

Acute exercise suppressed TRB3 expression and Akt/TRB3 association in the muscle of ob/ob mice

TRB3, a mammalian homologue of *Drosophila tribbles*, functions as a negative modulator of Akt. TRB3

Table 1 Physiological and metabolic parameters

Groups ($n = 7$)	Body weight (g)	Epididymal fat (g)	Fasting insulin (ng mL^{-1})	Fasting glucose (mg dL^{-1})
Lean	27.8 ± 1.53*	0.82 ± 0.12*	1.93 ± 0.69*	89.3 ± 9.14*
Obese	51.8 ± 3.91	4.09 ± 0.73	11.3 ± 2.84	272.8 ± 15.17
Exer	50.4 ± 3.41	4.55 ± 0.82	10.1 ± 3.19	122.9 ± 12.26†

*$P < 0.05$, lean vs. obese mice at rest.
†$P < 0.05$, Exer vs. respective obese mice at rest.

Journal compilation © 2009 Scandinavian Physiological Society, doi: 10.1111/j.1748-1716.2009.02031.x

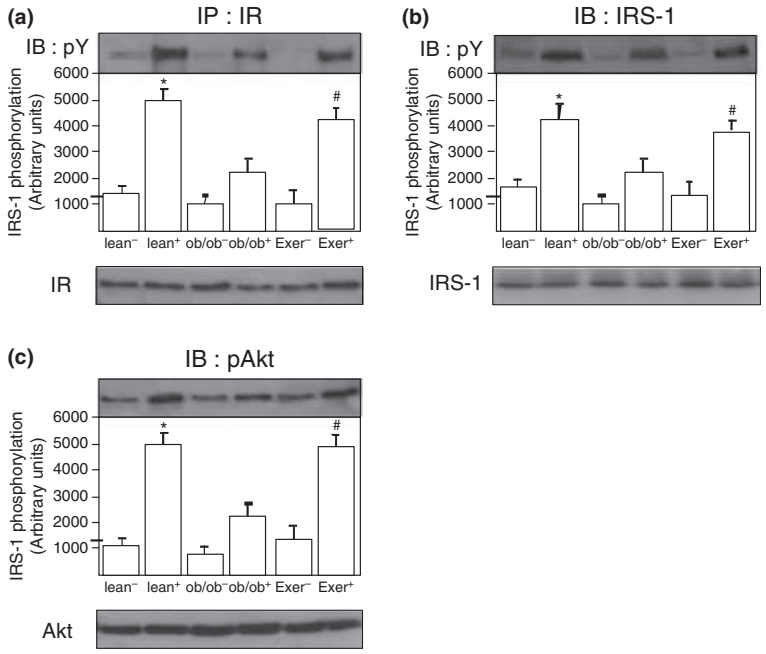

Figure 1 Insulin signalling in the muscle of lean (controls), obese (ob/ob) and Exer (obese acute exercise) mice. Gastrocnemius extracts from mice injected with saline (−) or insulin (+) were prepared as described in Methods. (a) Tissue extracts were immunoprecipitated (IP) with anti-IRβ antibody and blotted (IB) with anti-PY antibody (upper panels) or anti-IRβ antibody (lower panels). (b) Tissue extracts were IP with anti-IRS-1 antibody and IB with antibodies anti-PY (upper panels) or anti-IRS-2 (lower panels). (c) Muscle extracts were IB with anti-phospho Akt or anti-Akt antibody (upper and lower panels respectively). The results of scanning densitometry are expressed as arbitrary units. Bars represent means ± SEM of $n = 7$ mice. *$P < 0.05$, lean vs. ob/ob mice at rest; $P < 0.05$, Exer group vs. ob/ob mice at rest. #$P < 0.05$, Exer group vs. ob/ob mice at rest.

expression is induced in muscle under fasting conditions, and TRB3 disrupts insulin signalling by binding directly to Akt and blocking activation of the kinase. TRB3 activity was then determined in the gastrocnemius of lean controls, ob/ob and Exer group mice. The muscles were blotted with anti-TRB3. In the muscle of ob/ob mice at rest, TRB3 expression was increased by 2.4-fold when compared with lean controls. However, 8 h after a single bout of exercise, the TRB3 activity was reduced by 1.7-fold in the muscle of Exer when compared with the ob/ob group at rest (Fig. 2a).

The muscle protein was immunoprecipitated with anti-TRB3 antibody and then blotted with the anti-Akt antibody. The association of TRB3/Akt increased by 2.5-fold in the muscle of the ob/ob group when compared with the lean group (Fig. 2b). Conversely, in the muscle of exercised diabetic mice, the TRB3/Akt association decreased by 2.1-fold compared with ob/ob mice at rest (Fig. 2b). In addition, no difference in TRB3 expression and association was observed in the non–insulin-injected groups.

Exercise increases membrane GLUT4 expression, glycogen content in skeletal muscle and ameliorates whole body insulin sensitivity in diabetic mice

The improvement in the early steps of the insulin pathway in the muscle of ob/ob mice submitted to the exercise protocol was accompanied by a significant increase in plasma membrane GLUT4 expression in whole gastrocnemius protein extracts (2.6-fold) of the lean group compared with a 1.4-fold increase in the muscle from the ob/ob group and a 2.1-fold increased GLUT4 of the Exer group (representing an increase of 1.3-fold compared with the ob/ob group) (Fig. 3a). As acute exercise increases glucose uptake, we decided to evaluate glycogen contents. In diabetic mice (ob/ob) at rest, glycogen content was reduced by 2.3-fold when compared with lean mice (Fig. 3c). In the muscle of the Exer group, glycogen content increased by 1.7-fold compared with ob/ob mice at rest (Fig. 3c).

Finally, we observed increased insulin sensitivity in the Exer group. A significant impairment (64%) in the glucose disappearance rate (K_{ITT}) was found in ob/ob mice at rest when compared with lean controls and a single session of exercise improved (41%) the glucose disappearance rate in ob/ob mice (Fig. 3b).

Discussion

The prevalence of diabetes is increasing dramatically worldwide, with this disorder now being considered as possibly epidemic by some health organizations and researchers. Although the rate of diabetes is increasing, it has long been recognized that exercise has important health benefits for people with type 2 diabetes. Physical exercise can positively moderate glucose homeostasis in people with type 2 diabetes, due to enhanced glucose transport and insulin action in the working skeletal muscles, which are the major tissues responsible for total body glucose disposal (DeFronzo *et al.* 1981). The molecular mechanism for enhanced insulin sensitivity with exercise training may be related to increased expression and/or activation of key proteins that regulate glucose metabolism (Houm-

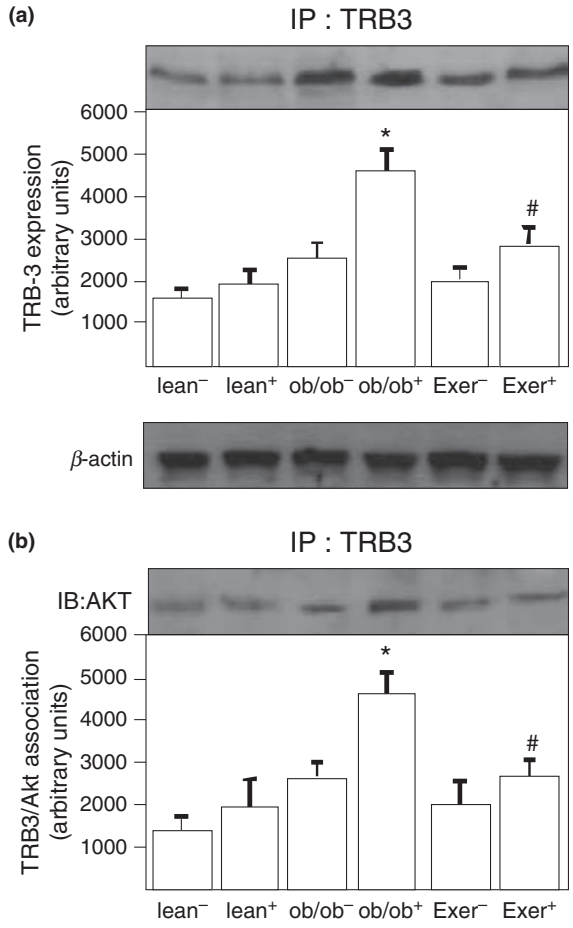

Figure 2 Expression of TRB3 and TRB3/Akt association in the muscle of lean controls, ob/ob and Exer mice. Gastrocnemius extracts from mice injected with saline or insulin were submitted to immunoblotting (TRB3 expression) or immunoprecipitated (TRB3/Akt association) as described in Methods. (a) Samples were blotted (IB) with anti-TRB3 antibody. (b) Tissue extracts were immunoprecipitated (IP) with anti-TRB3 antibody and blotted (IB) with anti-Akt antibody. The results of scanning densitometry are expressed as arbitrary units. Bars represent means ± SEM of $n = 7$ mice. *$P < 0.05$, lean vs. ob/ob mice at rest; $P < 0.05$, Exer group vs. ob/ob mice at rest. #$P < 0.05$, Exer group vs. ob/ob mice at rest.

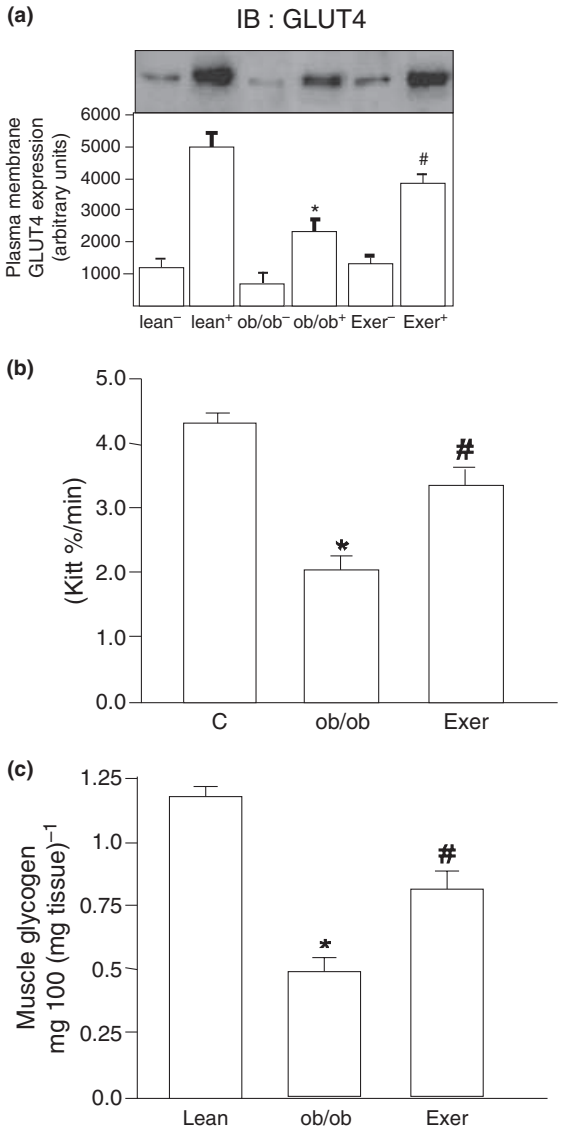

Figure 3 Plasma membrane GLUT4 expression and insulin sensitivity under fasting conditions in the gastrocnemius muscle of lean (control), ob/ob (obese) and Exer mice. Gastrocnemius extracts from mice were prepared as described in Methods. (a) Samples were blotted (IB) with anti-GLUT4 antibody in the plasma membrane, the results of scanning densitometry are expressed as arbitrary units. (b) The rate constant for glucose disappearance during an insulin tolerance test (K_{ITT}) was expressed as percentage per minute. (c) Glycogen contents are expressed as mg 100 mg^{-1} of wet tissue. Bars represent means ± SEM of $n = 7$ mice. *$P < 0.05$, lean vs. ob/ob mice at rest; #$P < 0.05$, Exer group vs. ob/ob mice at rest.

ard *et al.* 1999, Chibalin *et al.* 2000, Ropelle *et al.* 2006). As the IR/PI 3-K/Akt pathway is involved in glucose uptake in the skeletal muscle (Holman & Kasuga 1997), we may suggest that physical activity, by acting on this pathway, partially reverses insulin resistance of diabetic mice following a single session of exercise. In the present study, we demonstrate that acute exercise reduces TRB3/Akt association in diabetic mice. Eight hours after an exercise session, the TRB3 expression is suppressed in gastrocnemius muscle from leptin-deficient mice. This phenomenon is accompanied by an increase in insulin signalling in the muscle, resulting in increased whole body insulin sensitivity in fasted mice.

One of the molecular mechanisms mediating insulin resistance may involve increased TRB-3 expression. Initially cloned as an inducible gene in neuronal PC-3

cells following NGF withdrawal (termed NIPK) (Mayumi-Matsuda *et al.* 1999), TRB3 is emerging as an important player in the regulation of insulin signalling. TRB3 became of major interest in diabetes research when it was shown to interact with and inhibit the activity of Akt. The use of transgenic and knockout mouse models is beginning to make an impact on the understanding of the role of TRB3 in insulin signalling. TRB3 overexpression in the liver resulted in hyperglycaemia and inactivation of Akt, and its knockdown increased phosphorylation of Akt and its substrates (Koh *et al.* 2006). The protein kinase Akt functions both in the control of cell proliferation and as a critical node in insulin signalling, appearing to mediate most of the metabolic effects of insulin (Tanaguchi *et al.*2006). Akt is activated by phosphorylation of Thr308 within the T loop of the catalytic domain and Ser473, located in a C-terminal, non-catalytic region of the enzyme (Alessi *et al.* 1996). To support the role of TRB3 in the development of insulin resistance, in humans, the Q84R polymorphism of TRB3, which has a higher capacity of inhibiting Akt activation, is found to be associated with insulin resistance and related cardiovascular risk (Prudente *et al.* 2005).

In the present study, we found that TRB3 expression was diminished in the muscle of mice, 8 h after the exercise protocol, when compared with diabetic mice at rest. TRB was expressed in most human tissues with the highest levels in skeletal muscle, thyroid gland, pancreas, peripheral blood leucocytes and bone marrow (Kiss-Toth *et al.* 2004). However, the effect of exercise on TRB3 expression remains totally unknown.

Glucose transport into muscle is a key element in maintaining glucose homeostasis. Insulin increases glucose transport mediated by translocation of GLUT4 in the skeletal muscle (Lund *et al.* 1995, Thorell *et al.* 1999, Sakamoto & Goodyear 2002, Chang *et al.* 2004). Acute exercise induces glucose transport through GLUT4 translocation in an additive manner to insulin action in skeletal muscle (Garetto *et al.* 1984, Nesher *et al.* 1985, Zorzano *et al.* 1986, Wallberg-Henriksson *et al.* 1988, Lund *et al.* 1995).

Stimulation of glucose transport in contracting muscles involves a plasma membrane- and T-tubule-directed mobilization of GLUT4-containing vesicles from exercise-sensitive intracellular storage sites (Douen *et al.* 1989, Marette *et al.* 1992, Coderre *et al.* 1995, Dohm & Dudek 1998, Ploug *et al.* 1998). Proximal signalling, leading to contraction-induced muscle glucose uptake, is at the moment under intense investigation by many research groups. Our results show that at 8 h after a single session of exercise, GLUT4 expression in the membrane fraction is increased in the gastrocnemius muscle of ob/ob mice. Up to 2 h after exercise, glucose uptake is in part elevated due to insulin-independent mechanisms, probably involving a contraction-induced increase in the amount of GLUT4, associated with the plasma membrane and T-tubules (for a review, see Borghouts & Keizer 2000). However, a single bout of exercise can increase insulin sensitivity for at least 16 h post exercise in healthy and in NIDDM subjects. Recent studies have accordingly shown that acute exercise also enhances insulin-stimulated GLUT4 content (O'Gorman *et al.* 2006).

Increases in muscle GLUT4 protein content contribute to this effect and it has also been hypothesized that the depletion of muscle glycogen stores with exercise plays a role in this effect. In the present study, we show an increased glycogen content in ob/ob exercised mice. In the period after prolonged and heavy physical activity, glycogen synthesis is of high priority for previously exercised muscles. In accordance with this, muscle glycogen synthase activity and glucose transport are increased following exercise. In addition, an enhanced metabolic action of insulin in skeletal muscle (glucose transport, glycogen synthase activity and glycogen synthesis) is usually also observed after exercise (Mikines *et al.* 1988, Richter *et al.* 1989, Perseghin *et al.* 1996). The duration of this period with enhanced insulin sensitivity may last up to 48 h (Mikines *et al.* 1988), probably depending upon the rate of muscle glycogen repletion. Enhanced insulin sensitivity in skeletal muscle contributes to the restoration, or even super-compensation, of the glycogen stores. Thus, our results demonstrate that acute exercise improves fasting glucose metabolism in diabetic mice by increasing insulin signalling in skeletal muscle. The effect of exercise on insulin action is further supported by our findings that exercised mice present a reduction in TRB3 expression, a mechanism by which acute exercise may increase glucose uptake in the muscle. Thus, these results provide new insights into the mechanism by which physical exercise improves insulin resistance in type 2 diabetes patients.

Conflict of interest

There is no conflict of interest.

This study was supported by grants from Conselho Nacional de Desenvolvimento Científico e Tecnológico (CNPq). We thank Dr Nicola Conran for English language editing.

References

Alessi, D.R., Andjelkovic, M., Caudwell, B., Cron, P., Morrice, N., Cohen, P. & Hemmings, B.A. 1996. Mechanism of activation of protein kinase B by insulin and IGF-1. *EMBO J* **15**, 6541–6551.

Aoi, W., Ichiishi, E., Sakamoto, N., Tsujimoto, A., Tokuda, H. & Yoshikawa, T. 2004. Effect of exercise on hepatic

 doi: 10.1111/j.1748-1716.2009.02031.x

gene expression in rats: a microarray analysis. *Life Sci* **75**, 3117–3128.

Bonora, E., Moghetti, P., Zancanaro, C., Cigolini, M., Querena, M., Cacciatori, V., Corgnati, A. & Muggeo, M. 1989. Estimates of in vivo insulin action in man: comparison of insulin tolerance tests with euglycemic and hyperglycemic glucose clamp studies. *J Clin Endocrinol Metab* **68**, 374–378.

Borghouts, L.B. & Keizer, H.A. 2000. Exercise and insulin sensitivity: a review. *Int J Sports Med* **21**, 1–12.

Bradford, M.M. 1976. A rapid and sensitive method for the quantitation of microgram quantities of protein utilizing the principle of protein-dye binding. *Anal Biochem* **72**, 248–254.

Chang, L., Chiang, S.H. & Saltiel, A.R. 2004. Insulin signaling and the regulation of glucose transport. *Mol Med* **10**, 65–71.

Cheathan, B. & Kahn, C.R. 1995. Insulin action and the insulin signaling network. *Endocr Res* **16**, 117–142.

Chen, Y.A., Scales, S.J., Duvvuri, V., Murthy, M., Patel, S.M., Schulman, H. & Scheller, R.H. 2001. Calcium regulation of exocytosis PC12 cells. *J Biol Chem* **276**, 266–287.

Chibalin, A.V., Yu, M., Ryder, J.W., Song, X.M., Galuska, D., Krook, A., Wallberg-Henriksson, H. & Zierath, J.R. 2000. Exercise-induced changes in expression and activity of proteins involved in insulin signal transduction in skeletal muscle: differential effects on insulin-receptor substrates 1 and 2. *Proc Natl Acad Sci USA* **97**, 38–43.

Coderre, L., Kandror, K.V., Vallega, G. & Pilch, P.F. 1995. Identification and characterization of NA exercise-sensitive pool of glucose transporters in skeletal muscle. *J Biol Chem* **270**, 27584–27588.

De Souza, C.T., Araujo, E.P., Bordin, S., Ashimine, R., Zollner, R.L., Boschero, A.C., Saad, M.J. & Velloso, L.A. 2008. Consumption of a fat-rich diet activates a proinflammatory response and induces insulin resistance in the hypothalamus. *Endocrinology* **146**, 4192–4199.

DeFronzo, R.A., Jacot, E., Jequier, E., Maeder, E., Wahren, J. & Felber, J.P. 1981. The effect of insulin on the disposal of intravenous glucose. Results from indirect calorimetry and hepatic and femoral venous catheterization. *Diabetes* **30**, 1000–1007.

Dohm, G.L. & Dudek, R.W. 1998. Role of transverse tubules (T-tubules) in muscle glucose transport. *Adv Exp Med Biol* **441**, 27–34.

Douen, A.G., Ramlal, T., Klip, A., Young, D.A., Cartee, G.D. & Holloszy, J.O. 1989. Exercise-induced increase in glucose transporters in plasma membranes of rat skeletal muscle. *Endocrinology* **124**, 449–454.

Downward, J. 1998. Mechanism and consequences of PKB/Akt activation. *Curr Opin Cell Biol* **10**, 262–267.

Du, K., Herzig, S., Kulkami, R.N. & Montminy, M. 2003. TRB3: a tribbles homolog that inhibits Akt/PKB activation by insulin in liver. *Science* **300**, 1574–1577.

Folli, F., Saad, M.J., Backer, J.M. & Kahn, C.R. 1992. Insulin stimulation of phosphatidylinositiol 3-kinase activity and association with receptor substrate 1 in liver and muscle of the intact rat. *J Biol Chem* **267**, 22171–22177.

Garetto, L.P., Richter, E.A., Goodman, M.N. & Ruderman, N.B. 1984. Enhanced muscle glucose metabolism after exercise in the rat: the two phases. *Am J Physiol* **246**, E471–E475.

Hegedus, Z., Czibula, A. & Kiss-Toth, E. 2007. Tribbles: a family of kinase-likeproteins with potent signalling regulatory function. *Cell Signal* **19**, 238–250.

Holman, G.D. & Kasuga, M. 1997. From receptor to transporter: insulin signalling to glucose transport. *Diabetologia* **40**, 991–1003.

Houmard, J.A., Shaw, C.D., Hickey, M.S. & Tanner, C.J. 1999. Effect of short-term exercise training on insulin-stimulated PI 3-kinase activity in human skeletal muscle. *Am J Physiol* **277**, E1055–E1060.

Kiss-Toth, E., Bagstaff, S.M., Sung, H.Y., Jozsa, V., Dempsey, C., Caunt, J.C., Oxley, K.M., Wyllie, D.H., Polgar, T., Harte, M., O'neill, L.A., Qwarnstrom, E.E. & Dower, S.K. 2004. Humas tribbles, a protein family controlling mitogen-activited protein kinase cascades. *J Biol Chem* **279**, 42703–42708.

Klip, A., Ramlal, T., Young, D.A. & Holloszy, J.O. 1987. Insulin-induced decrease in 5′-nucleotidase activity in skeletal muscle membranes. *FEBS Lett* **224**, 224–230.

Koh, H.J., Arnolds, D.E., Fujii, N., Tran, T.T., Rogers, M.J., Jessen, N., Li, Y., Liew, C.W., Ho, R.C., Hirshman, M.F., Kulkarni, R.N., Kahn, C.R. & Goodyear, L.J. 2006. Skeletal muscle-selective knockout of LKB1 increases insulin sensitivity, improves glucose homeostasis, and decreases TRB3. *Mol Cell Biol* **26**, 8217–8227.

Koo, S.H., Satoh, H., Herzig, S., Lee, C.H., Hedrick, S., Kulkarni, R., Evans, R.M., Olefsky, J. & Montminy, M. 2004. PGC-1 promotes insulin resistance in liver through PPAR-alpha-dependent induction of TRB3. *Nat Med* **7**, 755.

Laemmli, U.K. 1970. Cleavage of structural proteins during the assembly of the head of bacteriophage T4. *Nature* **227**, 680–685.

Lavoie, L., Roy, D., Ramlal, T., Dombrowski, L., Martín-Vasallo, P. & Marette, A. 1996. Insulin-induced translocation of Na+-K+-ATPase subunits to the plasma membrane is muscle fiber type specific. *Am J Physiol* **270**, C1421–C1429.

Lima, A.F., Ropelle, E.R., Pauli, J.R., Cintra, D.E., Frederico, M.J., Pinho, R.A., Velloso, L.A. & De Souza, C.T. 2009. Acute exercise reduces insulin resistance-induced TRB3 expression and amelioration of the hepatic production of glucose in the liver of diabetic mice. *J Cell Physiol* **221**, 92–97.

Lund, S., Holman, G.D., Schmitz, O. & Pedersen, O. 1995. Contraction stimulates translocation of glucose transporter GLUT4 in skeletal muscle through a mechanism distinct from that of insulin. *Proc Natl Acad Sci USA* **92**, 5817–5821.

Marette, A., Burdett, E., Douen, A., Vranic, M. & Klip, A. 1992. Insulin induces the translocation of GLUT4 from a unique intracellular organelle to transverse tubules in rat skeletal muscle. *Diabetes* **41**, 1562–1569.

Matsushima, R., Harada, N., Webster, N.J., Tsutsumi, Y.M. & Nakaya, Y. 2006. Effect of TRB3 on insulin and nutrient-stimulated hepatic p70 S6 kinase activity. *J Biol Chem* **281**, 29719–29729.

Mayumi-Matsuda, K., Kojima, S., Siziki, H. & Sakata, T. 1999. Identification of a novel kinase-like gene induced

Journal compilation © 2009 Scandinavian Physiological Society, doi: 10.1111/j.1748-1716.2009.02031.x

during neuronal cell death. *Biochem Biophys Res Commun* **258**, 260–264.

Mikines, K.J., Sonne, B., Farrell, P.A., Tronier, B. & Galbo, H. 1988. Effect of physical exercise on sensitivity and responsiveness to insulin in humans. *Am J Physiol* **254**, E248–E259.

Nesher, R., Karl, I.E. & Kipnis, D.M. 1985. Dissociation of effects of insulin and contraction on glucose transport in rat epitrochlearis muscle. *Am J Physiol* **249**, C226–C232.

O'Gorman, D.J., Karlsson, H.K., McQuaid, S., Yousif, O., Rahman, Y., Gasparro, D., Glund, S., Chibalin, A.V., Zierath, J.R. & Nolan, J.J. 2006. Exercise training increases insulin-stimulated glucose disposal and GLUT4 (SLC2A4) protein content in patients with type 2 diabetes. *Diabetologia* **49**, 2983–2992.

Perseghin, G., Price, T.B., Petersen, K.F., Roden, M., Cline, G.W., Gerow, K., Rothman, D.L. & Shulman, G.I. 1996. Increased glucose transport-phosphorylation and muscle glycogen synthesis after exercise training in insulin-resistant subjects. *N Engl J Med* **335**, 1357–1362.

Pimenta, W.P., Saad, M.J., Paccola, G.M., Piccinato, C.E. & Foss, M.C. 1989. Effect of oral glucose on peripheral muscle fuel metabolism in fasted men. *Braz J Med Biol Res* **22**, 465–476.

Ploug, T., van Deurs, B., Ai, H., Cushman, S.W. & Ralston, E. 1998. Analysis of GLUT4 distribution in whole skeletal muscle fibers: identification of distinct storage compartments that are recruited by insulin and muscle contractions. *J Cell Biol* **142**, 1429–1446.

Prudente, S., Hribal, M.L., Flex, E., Turchi, F., Morini, E., De Cosmo, S., Bacci, S., Tassi, V., Cardellini, M., Lauro, R., Sesti, G., Dallapiccola, B. & Trischitta, V. 2005. The functional Q84R polymorphism of mammalian Tribbles homolog TRB3 is associated with insulin resistance and related cardiovascular risk in Caucasians from Italy. *Diabetes* **54**, 2807–2811.

Richter, E.A., Mikines, K.J., Galbo, H. & Kiens, B. 1989. Effect of exercise on insulin action in muscle. *J Appl Physiol* **66**, 876–885.

Ropelle, E.R., Pauli, J.R., Prada, P.O., de Souza, C.T., Picardi, P.K., Faria, M.C., Cintra, D.E., Fernandes, M.F., Flores, M.B., Velloso, L.A., Saad, M.J. & Carvalheira, J.B. 2006. Reversal of diet-induced insulin resistance with a single bout of exercise in the rat: the role of PTP1B and IRS-1 serine phosphorylation. *J Physiol* **577**, 997–1007.

Ryder, J.W., Kawano, Y., Galuska, D., Fahlman, R., Wallberg-Henriksson, H., Charron, M.J. & Zierath, J.R. 1999. Post-exercise glucose uptake and glycogen synthesis in skeletal muscle from GLUT4-deficient mice. *FASEB J* **13**, 2246–2256.

Saad, M.J., Folli, F., Backer, J.M. & Kahn, C.R. 1993. Regulation of phophatidylinositol 3 -kinase activity in liver and muscle of animal models of insulin-resistant and insulin-deficient diabetes mellitus. *J Clin Invest* **92**, 1787–1794.

Sakamoto, K. & Goodyear, L.J. 2002. Invited review: intracellular signaling in contracting skeletal muscle. *J Appl Physiol* **93**, 369–383.

Scott, A.M., Atwater, I. & Rojas, E. 1981. A method for the simultaneous measurement of insulin release and B cell membrane potential in single mouse islets of Langerhans. *Diabetologia* **21**, 470–475.

Tanaguchi, C.M., Emanuelli, B. & Kahn, C.R. 2006. Critical nodes in signalling pathways: insights into insulin action. *Nat Rev Mol Cell Biol* **7**, 85–96.

Thorell, A., Hirshman, M.F., Nygren, J., Jorfeldt, L., Wojtaszewski, J.F., Dufresne, S.D., Horton, E.S., Ljungqvist, O. & Goodyear, L.J. 1999. Exercise and insulin cause GLUT-4 translocation in human skeletal muscle. *Am J Physiol* **277**, E733–E741.

Wallberg-Henriksson, H., Constable, S.H., Young, D.A. & Holloszy, J.O. 1988. Glucose transport into rat skeletal muscle: interaction between exercise and insulin. *J Appl Physiol* **65**, 909–913.

White, M.F. & Kahn, C.R. 1994. The insulin signaling system. *J Biol Chem* **269**, 1–4.

Yang, H.T., Ren, J., Laughlin, M.H. & Terjung, R.L. 2002. Prior exercise training produces NO-dependent increases in collateral blood flow after acute arterial occlusion. *Am J Physiol* **282**, 301–310.

Young, D.A., Wallberg-Henriksson, H., Sleeper, M.D. & Holloszy, J.O. 1987. Reversal of the exercise-induced increase in muscle permeability to glucose. *Am J Physiol* **253**, E331–E335.

Zorzano, A., Balon, T.W., Jakubowski, J.A., Goodman, M.N., Deykin, D. & Ruderman, N.B. 1986. Effects of insulin and prior exercise on prostaglandin release from perfused red muscle. Evidence that prostaglandins do not mediate changes in glucose uptake. *Biochem J* **240**, 437–443.

APÊNDICE *XI*

Novos mecanismos pelos quais o exercício físico melhora a resistência à insulina no músculo esquelético

New mechanisms by which physical exercise improves insulin resistance in the skeletal muscle

José Rodrigo Pauli[1,2], Dennys Esper Cintra[2], Claudio Teodoro de Souza[3], Eduardo Rochette Ropelle[2]

RESUMO

O prejuízo no transporte de glicose estimulada por insulina no músculo constitui um defeito crucial para o estabelecimento da intolerância à glicose e do diabetes tipo 2. Por outro lado, é notório o conhecimento de que tanto o exercício aeróbio agudo quanto o crônico podem ter efeitos benéficos na ação da insulina em estados de resistência à insulina. No entanto, pouco se sabe sobre os efeitos moleculares pós-exercício sobre a sinalização da insulina no músculo esquelético. Assim, esta revisão apresenta novos entendimentos sobre os mecanismos por meio dos quais o exercício agudo restaura a sensibilidade à insulina, com destaque ao importante papel que proteínas inflamatórias e a S-nitrosação possuem sobre a regulação de proteínas da via de sinalização da insulina no músculo esquelético. Arq Bras Endocrinol Metab. 2009;53(4):399-408.

Descritores

Exercício; resistência à insulina; inflamação; músculo esquelético

ABSTRACT

Insulin resistance of skeletal muscle glucose transport is a key-defect for the development of impaired glucose tolerance and type 2 diabetes. However, it is known that both an acute bout of exercise and chronic endurance exercise training can bring beneficial effects on insulin action in insulin-resistant states. However, little is currently known about the molecular effects of acute exercise on muscle insulin signaling in the post-exercise state in insulin-resistant organisms. This review provides new insight into the mechanism through which acute exercise restores insulin sensitivity, highlighting an important role for inflammatory proteins and S-nitrosation in the regulation of insulin signaling proteins in skeletal muscle. Arq Bras Endocrinol Metab. 2009;53(4):399-408.

Keywords

Exercise; insulin resistance; inflammation; skeletal muscle

[1] Departamento de Biociências, Faculdade de Educação Física, modalidade Saúde, Universidade Federal de São Paulo (Unifesp), Santos, SP, Brasil
[2] Departamento de Clínica Médica, Faculdade de Ciências Médicas, Universidade Estadual de Campinas (Unicamp), Campinas, SP, Brasil
[3] Laboratório de Fisiologia e Bioquímica do Exercício, Programa de Pós-graduação em Ciências da Saúde, Universidade do Extremo Sul Catarinense (Unesc), Criciúma, SC, Brasil

Correspondência para:
José Rodrigo Pauli
Departamento de Biociências, Curso de Educação Física – Modalidade Saúde
Av. Dona Ana Costa, 95 – Vila Mathias
11060-001 – Santos, SP, Brasil
rodrigosere@yahoo.com.br

Recebido em 18/Mar/2009
Aceito em 6/Mai/2009

INTRODUÇÃO

O músculo esquelético representa aproximadamente 40% da massa corporal total e exerce papel primordial no metabolismo da glicose (1). Esse tecido é responsável por aproximadamente 30% do consumo energético, além de ser um dos principais tecidos responsáveis pela captação, liberação e estocagem de glicose (2). Trabalhos realizados nas últimas décadas demonstraram claramente que o exercício físico aumenta a captação de glicose pelo músculo esquelético (3-6). Além disso, recentemente, foi demonstrado que a redução de peso corporal associada ao aumento da atividade física em indivíduos com risco aumentado para desenvolver diabetes reduz em 58% a incidência dessa doença (7). Assim, atualmente, o exercício físico é considerado uma das pedras angulares tanto da prevenção como do tratamento do diabetes tipo 2. Os mecanismos moleculares envolvidos no aumento da captação de glicose muscular vêm sendo intensamente pesquisados. Nesta revisão, serão abordados alguns aspectos dessa fascinante área que está se desenvolvendo rapidamente.

EXERCÍCIO FÍSICO E SINALIZAÇÃO DA INSULINA: PERSPECTIVA HISTÓRICA

As primeiras evidências do efeito favorável do processo de contração muscular na captação de glicose surgiram em 1887, quando Chauveau e Kaufamann reportaram redução da quantidade de glicose proveniente da musculatura do masseter de cavalos enquanto eles mastigavam o feno (8). Quatro décadas depois, foi demonstrado que a insulina tem o mesmo efeito do exercício na indução da captação de glicose pelos músculos (9). Tais pesquisas deram origem a uma série de investigações que buscaram elucidar a possível interação entre insulina e o exercício na regulação da captação de glicose. Em 1972, Bjorntorp e cols. demonstraram melhora da tolerância à glicose e níveis de insulina menores em homens que participavam regularmente de esportes competitivos em comparação aos controles. O mesmo grupo de pesquisadores evidenciou que mulheres hiperinsulinêmicas e obesas apresentaram os níveis de insulina plasmático diminuídos após seis semanas de treinamento físico (10-11). Tais descobertas hipotetizaram que o exercício regular poderia aumentar a sensibilidade à insulina no músculo e em outros tecidos, ideia confirmada apenas na década de 1980 por Carl Mondon e cols. mediante experimento com roedores (12).

Com a confirmação do papel favorável do exercício físico na ação metabólica da insulina, inúmeros estudos buscaram desvendar os mecanismos moleculares por meio dos quais o exercício atua como estimulador fisiologicamente relevante ao transporte de glicose em diferentes tecidos. Cientistas têm evidenciado, nos últimos anos, que o exercício tem efeito importante nos mecanismos moleculares de captação de glicose no músculo esquelético tanto em indivíduos saudáveis como nos portadores de resistência à insulina. No entanto, para que sejam compreendidos os mecanismos moleculares por meio dos quais o exercício físico contribui para melhorar a captação de glicose e prevenir e tratar o diabetes tipo 2, é necessário, inicialmente, descrever como a insulina transmite seu sinal celular desde o receptor até os efetores finais.

VIA DE TRANSMISSÃO DO SINAL DE INSULINA

A insulina é um hormônio polipeptídico anabólico produzido pelas células-beta do pâncreas, cuja síntese é ativada pelo aumento dos níveis circulantes de glicose e aminoácidos após as refeições. Sua ação ocorre em vários tecidos periféricos, incluindo fígado, músculo esquelético e tecido adiposo. Seus efeitos metabólicos imediatos incluem: aumento da captação de glicose, principalmente em tecido muscular e adiposo, aumento da síntese de proteínas, ácidos graxos e glicogênio, bem como bloqueio da produção hepática de glicose, lipólise e proteólise, entre outros.

A sinalização intracelular da insulina começa com sua ligação a um receptor específico de membrana, uma proteína heterotetramérica com atividade quinase intrínseca, composta por duas subunidades alfa e duas subunidades beta, denominado receptor de insulina (IR) (13). A ativação do IR resulta em fosforilação em tirosina de diversos substratos, incluindo substratos do receptor de insulina 1 e 2 (IRS-1 e IRS-2) (14-15). A fosforilação das proteínas IRS cria sítios de ligação para outra proteína citosólica, denominada fosfatidilinositol 3-quinase (PI3q), promovendo sua ativação (16). A PI3q é importante na regulação da mitogênese, na diferenciação celular e no transporte de glicose estimulada pela insulina. A ativação da PI3q aumenta a fosforilação em serina da proteína quinase B (Akt) e isso permite o transporte de glicose no músculo e no tecido adiposo, através da translocação da proteína Glut-4 para a membrana celular (17). Portanto, a ativação da Akt resulta na translocação do Glut-4 para a membrana, permitindo a entrada de glicose por difusão facilitada. Os Glut-4 são os principais responsáveis pela captação da glicose circulante nos humanos. Atividades físicas praticadas regularmente estimulam a translocação dos Glut-4 e promovem captação de glicose e redução da sua concentração sanguínea. Além disso, o sinal transmitido pela PI3q ativa a síntese de glicogênio no fígado e no músculo, e da lipogênese no tecido adiposo (14,18). Portanto, a via PI3q/Akt tem um importante papel nos efeitos metabólicos da insulina. O esquema resumido das etapas de sinalização da insulina envolvida na captação de glicose encontra-se apresentado na figura 1.

BASES MOLECULARES DO EXERCÍCIO FÍSICO E A HOMEOSTASE DA GLICOSE

O exercício físico aumenta a captação de glicose no músculo esquelético por diferentes mecanismos moleculares. Evidências experimentais demonstraram que a contração muscular não necessariamente estimula a fosforilação do IR e dos seus substratos (IRS-1 e IRS-2) em resíduos de tirosina, ou da enzima chave da via a PI3q. Tal confirmação foi estabelecida por experimentos *in vitro*, nos quais o bloqueio farmacológico da

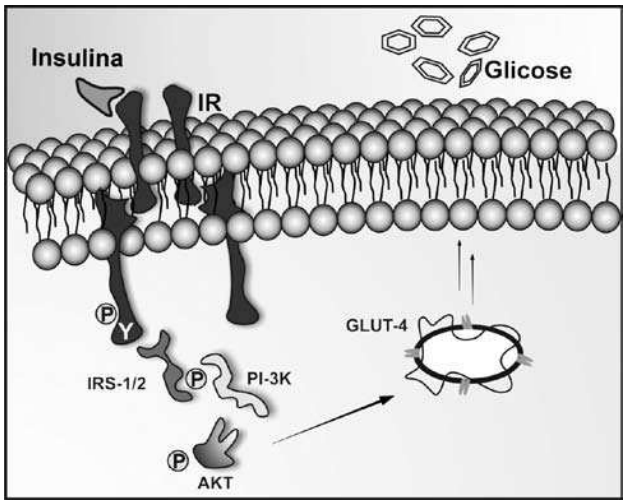

Figura 1. Via de sinalização da insulina na captação de glicose. A insulina, ao se ligar ao seu receptor de membrana, promove a autofosforilação da subunidade beta em resíduos de tirosina e desencadeia uma cascata de sinalizações que convergem para as vesículas que contêm GLUT-4, promovendo o seu transporte para a membrana celular.

PI3q através do *wortmannin* não bloqueou o transporte de glicose estimulada por contração do músculo esquelético (19). Portanto, existem diferentes formas de condução do sinal para que ocorra o transporte de glicose mediada pela insulina ou pelo exercício no músculo esquelético. Foi então que houve a descoberta de uma enzima chave de resposta à contração muscular denominada AMPK (proteína quinase ativada por AMP), que também estimula o transporte de glicose no músculo esquelético, mas por meio de um mecanismo independente de insulina.

A ativação da AMPK é resultado do decréscimo do estado energético celular. Na situação em que a relação AMP:ATP aumenta, ocorre uma mudança conformacional na molécula, deixando-a suscetível à fosforilação e ativação pela AMPK quinase (AMPKK) (20). A AMPK fosforilada ativa vias que geram o aumento de ATP, tais como a oxidação de ácidos graxos, ao mesmo tempo que desativa as vias anabólicas que consomem o ATP, como a síntese de ácidos graxos. Esse aumento da atividade da AMPK em resposta a uma necessidade em gerar ATP durante o exercício físico promove a translocação das vesículas contendo Glut-4, facilitando o transporte de glicose para o músculo de maneira semelhante à da insulina, embora isso ocorra por vias de sinalização diferentes e independentes. Nessa situação, a redução da malonil-CoA permite o aumento da ação da carnitina acil transferase 1, que aumenta a eficiência do transporte de ácidos graxos para as mitocôndrias e consequente oxidação (21).

No entanto, o mecanismo de transporte de glicose através da via de sinalização da AMPK não parece ser o único mecanismo responsável por esse processo metabólico. De maneira semelhante, existem inúmeras outras moléculas envolvidas nesse mecanismo de sinalização durante o exercício. O aumento na concentração do íon cálcio no interior da célula, a atividade da óxido nítrico sintase (NOS) e a síntese por ela de óxido nítrico (NO), o aumento na concentração de bradicinina ou até mesmo a hipóxia podem estimular a captação de glicose através do aumento da translocação do Glut-4 para a membrana durante a contração muscular (22-25).

Além disso, novas evidências científicas mostram que o exercício físico pode, além dos efeitos positivos sobre a via de sinalização dependente de insulina (IR/IRSs/PI3-q/Akt) e/ou independente de insulina (via AMPK e/ou outras biomoléculas), também beneficiar o indivíduo obeso com resistência à insulina por diminuir a expressão e/ou atividade de proteínas inflamatórias de efeito negativo à ação da insulina (26-28).

OBESIDADE E RESISTÊNCIA À INSULINA

O preciso mecanismo envolvido na causa da resistência à insulina ainda não é totalmente conhecido. Contudo, muitos estudos têm demonstrado que alterações moleculares na via de sinalização da insulina, principal responsável pela ativação da translocação do transportador de glicose (Glut's) à membrana plasmática, são determinantes no estado de resistência à insulina em tecidos periféricos, como o músculo esquelético e o tecido adiposo (29-32). No entanto, deve-se levar em consideração que a relevância de mecanismos relacionados ao prejuízo da translocação de vesículas ricas em Glut's é específica para tecidos cuja forma Glut-4 é expressa de maneira relevante.

O Glut-4 é o transportador de insulina-dependente mais abundante nas membranas celulares do músculo esquelético, cardíaco e tecido adiposo. Sem o estímulo hormonal, a concentração de Glut-4 na membrana é muito baixa, estando armazenadas em vesículas citoplasmáticas. Após a estimulação pela insulina, esses transportadores são translocados para a membrana e o transporte de glicose é aumentado. No entanto, em algumas células, como os hepatócitos, os neurônios e as hemácias, a glicose é capaz de se difundir para o interior da célula na ausência de insulina e, portanto, os mecanismos moleculares relacionados ao prejuízo no sinal da insulina e, consequentemente, na captação de glicose não se aplicam (33-34).

Por outro lado, na obesidade ocorrem alterações em diversos pontos da via de transdução do sinal da insulina, com redução na concentração e atividade quinase do IR, na concentração e fosforilação do IRS-1 e IRS-2, na atividade da PI3q, na translocação dos Glut's e na atividade das enzimas intracelulares. Isso atenua consequentemente a captação de glicose nos tecidos insulino-dependentes, como músculo esquelético e tecido adiposo. O impacto negativo do aumento da quantidade de tecido adiposo nos organismos sobre a sensibilidade à insulina pode ser claramente demonstrado na maioria dos indivíduos, assim como o aumento da sensibilidade à insulina observada com a redução do peso corporal e com exercício físico (35-37).

Inicialmente, os ácidos graxos livres (AGLs) foram implicados nesse processo. A presença de elevados níveis de AGLs circulantes está associada a uma menor fosforilação em sítios específicos e à menor ativação de proteínas-chave da via da insulina (IRSs/PI3q). Evidências científicas apontam uma relação direta entre AGLs e resistência à insulina, que pode ser decorrente do acúmulo de triglicerídeos e metabólitos derivados de ácidos graxos (diacilglicerol, acetil-CoA e ceramidas) no músculo e no fígado (38-39). O aumento desses metabólitos provenientes da oxidação das gorduras no músculo é capaz de provocar a ativação da PKC e/ou da kinase IkB, e também de causar fosforilação em serina do IR e de seus substratos, sendo estes importantes mecanismos que explicam a relação entre acúmulo de gordura tecidual e resistência à insulina (38).

Contudo, nos últimos anos, vários fatores regulatórios produzidos por adipócitos (adipocinas) foram descritos, bem como o papel que desempenham no desenvolvimento de resistência à insulina. A seguir, será apresentado como alguns desses fatores regulam negativamente a ação da insulina, agindo tanto no receptor de insulina quanto em moléculas pós-receptor, para posterior compreensão dos efeitos do exercício físico na atenuação desse processo.

INFLAMAÇÃO E RESISTÊNCIA À INSULINA

A hipótese de que a inflamação em tecidos metabólicos pode contribuir para o desenvolvimento de resistência à insulina teve origem em 1993, quando se deu a descoberta de que também o tecido adiposo era capaz de produzir TNF-α, uma citocina inflamatória que prejudica a via de sinalização da insulina. Posteriormente, desvendou-se que outras citocinas inflamatórias subjacentes ao TNF-α provocariam resistência à insulina induzida por obesidade (40).

Recentes estudos evidenciam que a origem dessas citocinas inflamatórias na obesidade decorre da migração de macrófagos para os adipócitos (30,32); em paralelo, ácidos graxos provenientes da dieta, principalmente os de origem animal, são capazes de ativar proteínas de membrana celulares denominadas TLR-4, um dos tipos de *toll like receptors* que funciona como mediador da via inflamatória com consequências negativas para ações da insulina em tecidos metabólicos.

Recém-descritos, os receptores da família TLR (*toll like receptors*) desempenham uma conexão importante entre o sistema imune inato e o sistema metabólico (41). Evolutivamente preservados, esses receptores sensíveis a patógenos desempenham importante atividade pró-inflamatória, como esperado. Entretanto, esses mesmos receptores, principalmente os TLR-4, são sensíveis também a nutrientes, como os ácidos graxos. A ingestão elevada de gordura na dieta pode ativar esses receptores, ativando também, mesmo na ausência de patógenos, uma resposta inflamatória capaz de interferir nos sinais mediados pelos hormônios controladores da fome e gasto energético, resultando em obesidade (42).

Tal tentativa de interpretação e analogia pode ser reforçada por experimentos com roedores, nos quais camundongos com mutação genética dessa proteína utilizam melhor a glicose, apresentam menor depósito de gordura e não desenvolvem resistência à insulina mesmo quando submetidos a uma dieta rica em gordura. Portanto, ao se ligarem a esse receptor de membrana celular, alguns ácidos graxos acionam proteínas de resposta inflamatória, incluindo a JNK (*c-jun N-terminal kinase)* e IκK (*Ikappa kinase)*, que bloqueiam a ação da insulina (Figura 2). Esses resultados permitem considerar que os TLR-4 sejam justamente a conexão que faltava entre ingestão de dietas ricas em gordura saturada e o desenvolvimento de resistência à insulina (30-32).

A ativação dos substratos intermediários da via de sinalização do TNF-α, como a serina quinase JNK, pode interferir na funcionalidade dos substratos do receptor de insulina, o IRS-1 e IRS-2. Uma vez fosforilados em serina pela JNK, a possibilidade de serem fosforilados em tirosina pelo receptor de insulina fica comprometida, o que contribui para a resistência à transdução do sinal da insulina através dessa via. Outra via pró-inflamatória que pode levar à fosforilação em serina de substratos do receptor de insulina é a via IκK/IκB/NF-κB. Essa via pode ser ativada pelo TNF-α, mas também por

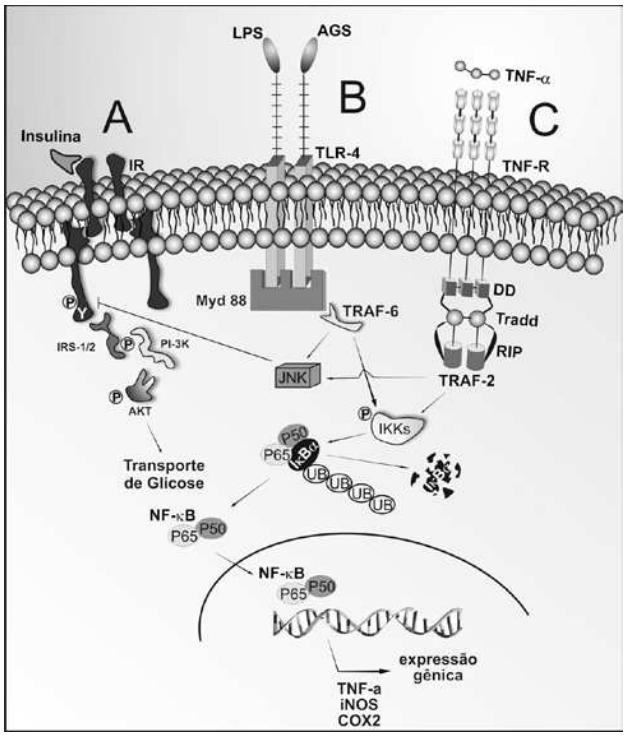

Figura 2. Inflamação e resistência à insulina. A ativação de quinases na obesidade, especialmente *IKappaB Kinase* (IkK) e *c-jun aminoterminal kinase* (JNK), ressalta a sobreposição das vias metabólicas e inflamatórias: essas são as mesmas quinases ativadas na resposta imune inata pelo TLR (*toll-like receptor*) em resposta ao LPS e aos ácidos graxos (AGS). A IkKβ pode interferir na sinalização de insulina através de pelo menos duas vias: primeiro, ela pode fosforilar diretamente os substratos do receptor de insulina (IRS-1 e IRS-2) em resíduos de serina; segundo, ela pode ativar indiretamente o NFkB, um fator de transcrição que, entre outros alvos, pode estimular a produção de vários mediadores inflamatórios, incluindo o TNF-α, iNOS e COX2. A JNK ativada tanto pela via do TLR-4 como pelo TNF-α também pode interferir negativamente na sinalização da insulina, fosforilando o IRS-1 e o IRS-2 em serina. (A) via de sinalização da insulina; (B) via de sinalização do TLR-4; e (C) via de sinalização do TNF-α.

outras citocinas pró-inflamatórias como IL-1β (interleucina 1β). A ativação do IκK promove a dissociação do complexo IκB/NF-κB, mas também pode induzir a fosforilação em serina dos IRS, que compromete a transdução do sinal da insulina através dessa cascata. Em animais com obesidade induzida por dieta rica em gordura, o bloqueio da atividade da IκKβ através da administração de altas doses de salicilatos resultou na melhora da sensibilidade à insulina (43-44).

Estudo recente de Carvalho-Filho e cols. descreveu outro mecanismo por meio do qual se instaura a disfunção celular e o prejuízo na ação da insulina quando animais saudáveis são submetidos a uma dieta rica em gordura, ganham peso excessivamente e tornam-se obesos (45). Recentemente, demonstrou-se que o óxido nítrico (NO) produzido pela proteína óxido nítrico sintase (NOS) é um importante sinalizador intracelular capaz de modificar a função proteica por diversos mecanismos em etapas pós-transcripcionais, incluindo nitrosilação, nitração e S-nitrosação. A S-nitrosação ocorre pela adição de um grupamento NO ao radical tiol (S-H) de um resíduo de cisteína, formando um nitrosotiol (S-NO). Nesse estudo, foi demonstrado que drogas doadoras de NO, nitrosoglutationa (GSNO) ou nitrosocisteína (CISNO) e a própria indução da iNOS seriam capazes de provocar S-nitrosação e com isso modificar a função de proteínas envolvidas na via de sinalização da insulina (45).

Nos últimos dez anos demonstrou-se que, além de suas ações vasodilatadoras, o NO tem também papel fundamental como sinalizador intracelular, controlando várias funções da célula e modulando inclusive a apoptose (46). As NO-sintases (NOS) são as principais fontes intracelulares de NO e dividem-se em três subtipos. A NO sintase neuronal (nNOS ou NOS 1) e a NO sintase endotelial (eNOS ou NOS 3) são cálcio dependentes e exercem funções biológicas importantes em seus respectivos tecidos, como regulação da apoptose neuronal, no caso da nNOS, e vasodilatação, no caso da eNOS. A NO sintase induzível (iNOS ou NOS 2) já foi descrita em detalhe, não é cálcio dependente e pode ter sua expressão induzida a partir do estímulo com interleucinas ou lipopolissacarídeo (LPS) (47). Uma vez produzido, o NO pode modificar a função proteica por meio de processos químicos diferentes, que dependem principalmente da disponibilidade de espécies oxidantes e da concentração de NO liberado (45).

Carvalho-filho e cols. observaram, ainda, indução de iNOS em dois modelos de resistência à insulina, na obesidade induzida por dieta hiperlipídica e no camundongo diabético ob/ob (obesidade induzida por deficiência em leptina) (48). Nesses dois modelos, a sinalização da insulina pela via IR/IRS-1/Akt estava diminuída, e os níveis de S-nitrosação dessas proteínas encontravam-se aumentados no músculo esquelético. Determinou-se, assim, que a S-nitrosação de proteínas envolvidas na transmissão do sinal da insulina seria um novo mecanismo molecular de resistência à insulina associado à indução da iNOS. Ao descobrir tais conexões, imaginou-se uma estratégia de ação: reduzir a resistência à insulina bloqueando a ação da iNOS, caminho que se mostrou promissor em estudos preliminares feitos em laboratório (48).

Portanto, a ativação dessas proteínas na obesidade, especialmente IκK, JNK e iNOS, ressalta a sobreposição das vias metabólicas e inflamatórias: essas são as mesmas moléculas que são ativadas na resposta imune inata pelo TLR-4 em resposta aos LPS e outros pro-

dutos microbianos. Fortalecendo essa hipótese, experimentos com oligonucleotídeo antisense contra TLR-4 mostraram que, ao desativar esse receptor das células de camundongos diabéticos, ocorreu a redução de um tipo de célula de defesa do sangue (macrófagos) (32). Essa é uma possível conexão entre a obesidade e uma inflamação de baixa intensidade em todo o organismo e, geralmente, é observada em indivíduos que estão acima do peso considerado saudável.

Além disso, existem outros reguladores negativos da via de transdução do sinal de insulina que estão estreitamente relacionados ao aumento do programa pró-inflamatório, incluindo a mTOR (*mammalian Target Of Rapamycin*) que é capaz de fosforilar o IRS-1 em serina. A SOCS (*Suppressors Of Cytokine Signaling*), cujos genes são alvos das vias da JNK e IKK, também está implicada na resistência à insulina promovida pelo TNF-α. Isso mostra que diversas proteínas pró-inflamatórias estão elevadas na obesidade e trazem como consequência a resistência à ação da insulina e outras alterações metabólicas (26, 29, 45).

Portanto, fica evidente que diversos fatores, atuando conjuntamente ou de forma independente, podem regular negativamente a ação da insulina, agindo tanto no receptor quanto em moléculas pós-receptor. Em síntese, inúmeras moléculas bioquímicas provenientes dos adipócitos ou dos macrófagos na condição de obesidade podem provocar a ativação de serina-quinases e/ou outras moléculas, especialmente a IκK, JNK e iNOS, capazes de fosforilar moléculas em resíduos de serina ou causar nitrosilação em proteínas como o IRS-1 e IRS-2, inibindo a sinalização da insulina. Vejamos, a seguir, como o exercício físico pode exercer modulação sobre algumas dessas proteínas, confirmando seu papel positivo na prevenção e no tratamento do DM2.

EFEITOS ANTI-INFLAMATÓRIOS DO EXERCÍCIO NA OBESIDADE E RESISTÊNCIA À INSULINA

Diferentes estudos apontam uma forte associação entre a prática de atividade física e a redução do processo inflamatório decorrente da obesidade (28-49). O aumento do tecido adiposo desempenha papel determinante no quadro de resistência à insulina, aumentando de duas a três vezes os níveis séricos de citocinas pró-inflamatórias como, por exemplo, o TNF-α. Nesse contexto, parece lógico entender que o exercício passa a desempenhar um papel anti-inflamatório por reduzir a gordura corporal e, consequentemente, a produção de citocinas pró-inflamatórias. No entanto, estudos em roedores e em seres humanos revelaram que o exercício físico pode reduzir os níveis de citocinas pró-inflamatórias sem que haja alteração do peso corporal. Pedersen e cols. estudaram os efeitos anti-inflamatórios do exercício agudo em indivíduos saudáveis. Os autores relataram que indivíduos que receberam baixas doses de uma endotoxina (*Escherichia coli*) apresentaram um grau de inflamação sistêmica similar ao observado em indivíduos obesos. No entanto, em um grupo de indivíduos previamente exercitados, a endotoxina foi incapaz de gerar processo inflamatório observado no grupo não exercitado (49). Além disso, estudos em voluntários obesos também mostraram que uma única sessão de exercício é capaz de reduzir os níveis séricos de TNF-α e de proteína-C reativa sem alteração do peso corporal total (50).

Apesar de a ação anti-inflamatória do exercício físico estar bem documentada, pouco se sabe como são produzidas, no interior das células, as respostas anti-inflamatórias mediadas pela atividade física. Evidências experimentais e alguns trabalhos com humanos sugerem que a resposta anti-inflamatória observada no músculo esquelético após sessão aguda de exercício ocorra por meio de mecanismos distintos (26-27). Em ratos obesos induzidos por dieta rica em gordura, uma única sessão de natação reduziu a fosforilação da JNK, bloqueou a via IκK/NFκB, reduziu a fosforilação do IRS-1 em serina e atividade da PTP-1B no músculo gastrocnêmio e restabeleceu a sensibilidade à insulina 16 horas após o término do exercício (26). A PTP-1B é uma das tirosina-fosfatases mais estudadas, exerce efeitos negativos sobre a sinalização da insulina, efeitos mediados pela desfosforilação do IR e do IRS-1. De maneira concordante, a inibição farmacológica ou o tratamento com oligonucleotídeo antisense da PTP-1B resultaram em aumento na fosforilação do IR e do IRS-1 (51-52). O camundongo geneticamente modificado que não expressa PTP1B apresenta maior sensibilidade à insulina do que seu controle quando submetido a tratamento com dieta hiperlipídica (53).

Tal tentativa de interpretação e analogia pode ser reforçada por experimentos com humanos, em que a sessão aguda de exercício físico se mostrou eficiente na redução da fosforilação da JNK e no bloqueio da via IκK/NFκB após perfusão de ácidos graxos. O bloqueio da via IκK/NFκB também foi observado no músculo de pacientes diabéticos, e esse bloqueio ocorreu pela menor taxa de degradação do IκBα e do IκBβ, impedindo que o fator de transcrição κB (NF-κB) iniciasse a transcrição

de proteínas pró-inflamatórias. Dessa forma, o bloqueio dessa via inflamatória através do exercício físico foi responsável por diminuir os níveis séricos de TNF-α nesses pacientes (54). Outro efeito positivo acontece por meio da redução da expressão de iNOS e S-nitrosação de proteínas da via de sinalização da insulina.

EXERCÍCIO FÍSICO E A S-NITROSAÇÃO

Em recente pesquisa, ficou demonstrado que o exercício físico pode melhorar agudamente a sensibilidade à insulina em ratos submetidos a uma dieta rica em gordura. Tal fato se deve, no mínimo em parte, à reversão da S-nitrosação de proteínas-chave na sinalização da insulina no músculo esquelético através de uma sessão de exercício de natação (27). Ratos Wistar obesos-induzidos por dieta rica em gordura exibiram menor sensibilidade à insulina, constada pela menor taxa de desaparecimento da glicose durante o teste de tolerância à insulina em relação aos controles. Além disso, houve uma significativa redução na fosforilação do IR, IRS-1 e Akt no músculo gastrocnêmio desses animais. Por conseguinte, quando esses animais foram submetidos a um protocolo de exercício de duas sessões de três horas de natação separadas por um intervalo de 45 minutos de recuperação, resultados satisfatórios em relação à captação de glicose foram evidenciados. O aumento na taxa de desaparecimento da glicose ao final do teste de tolerância à glicose e o significativo aumento na fosforilação das proteínas IR, IRS-1 e Akt estimulada por insulina revelaram a ação favorável da sessão aguda de exercício que perdurou por 16 horas.

A S-nitrosação do IR, IRS-1 e Akt se mostrou inversamente relacionada à fosforilação e à ativação, sendo significativamente aumentada nos animais que se alimentaram com dieta rica em gordura e diminuída nos animais que foram submetidos ao exercício agudo de natação. No entanto, isso foi mais substancialmente pronunciado duas horas após o término do esforço, quando a restauração da sinalização da insulina foi maior (27).

Para confirmação de tais fatos, uma série de experimentos adicionais foi realizada em laboratório. Ratos Wistar que receberam dieta rica em gordura foram tratados com doador de NO (*S-nitrosoglutatione*, GSNO) ou com inibidor da iNOS (*l-N^6-(l-iminoethyl)lysine (L-nil)*) previamente ao exercício de natação. Duas horas após o exercício, a sensibilidade à insulina nos animais obesos induzidos por dieta hiperlipídica tratados com GSNO teve redução similar aos animais obesos que não foram submetidos ao protocolo de exercício. Essa redução na sensibilidade à insulina foi associada à redução na fosforilação e aumento na S-nitrosação do IR, IRS-1 e Akt. Por outro lado, a inibição da atividade da iNOS (mas não a expressão proteica) com $_L$-NIL restaurou a sensibilidade à insulina de maneira similar à verificada nos animais exercitados, ocorrendo também aumento da fosforilação e diminuição da S-nitrosação das proteínas da sinalização da insulina. Além disso, não houve efeito aditivo da inibição da iNOS pelo fármaco com o exercício físico. Coletivamente, esses resultados sugerem que alterações na S-nitrosação são fatores importantes envolvidos na mudança da sinalização e sensibilidade à insulina induzidos por dieta e exercício físico (27).

Investigações subsequentes foram realizadas para descobrir o possível mecanismo por meio do qual o exercício físico reduz a expressão de iNOS. Uma hipótese possível envolve a ativação da AMPK. Dados da literatura indicam que a ativação da AMPK reduz a produção de NO mediada pela iNOS (55). Como o exercício físico é capaz de ativar a AMPK (56-57), isso explicaria a melhora da sensibilidade à insulina entre os animais obesos exercitados.

Ao avaliar a via de sinalização da AMPK, verificou-se redução na ativação da AMPK em ratos alimentados com dieta hiperlipídica, a qual foi restaurada a níveis controles com a realização do exercício físico (27). Uma vez que a AMPK pode suprimir a expressão de iNOS, esses resultados sugerem que, em adição ao papel de aumentar a oxidação de ácidos graxos e a captação de glicose, o aumento na atividade da AMPK por meio do exercício pode contribuir potencialmente para o aumento na sensibilidade à insulina pela redução indireta na S-nitrosação de proteínas da via de sinalização da insulina. Para a confirmação dessa hipótese, experimentos foram realizados de maneira tempo-dependente, nos quais se avaliaram a ativação da AMPK e a expressão da iNOS após o término do exercício físico. Demonstrou-se, então, que a redução nos níveis de AMPK fosforilada é acompanhada por decréscimo na captação de insulina e aumento na expressão de iNOS. Os resultados desse experimento devem ser encarados como mais uma evidência da hipótese de que a ativação da AMPK após a sessão aguda de exercício é importante para a supressão da indução de iNOS em ratos obesos. Curiosamente, ratos obesos induzidos por dieta apresentam menor expressão de AMPK (57). Por outro lado, ratos obesos exercitados regularmente tiveram seus níveis de AMPK normalizados aos seus pares controles (57). Tal fato

confirma o efeito do exercício em estimular a expressão e a atividade da AMPK no músculo esquelético.

É fundamental enfatizar, no entanto, que o exercício induz a síntese das isoformas neuronal e endotelial da enzima óxido nítrico sintase (nNOS e eNOS), e não somente da iNOS. Contudo, é preciso compreender que o efeito do NO na sensibilidade à insulina é dose-dependente e depende também da enzima geradora de NO, que é expressa em diferentes sítios (58-59). Por exemplo, o aumento da síntese de NO pela eNOS em ratos saudáveis pelo exercício físico aumenta a captação de glicose (58). No entanto, em nosso experimento, avaliou-se uma condição de obesidade induzida por dieta rica em gordura saturada na qual a síntese de NO pela iNOS é pronunciada e se associa à resistência à insulina.

Além disso, uma limitação em nosso estudo, na teoria proposta de sensibilização à insulina pela prática do exercício físico, é que a iNOS normalmente não é expressa no músculo esquelético (59) e somente é induzida em condição de resistência à insulina, como na obesidade induzida por dieta rica em gordura saturada. No entanto, o exercício pode prover melhoras na ação da insulina em músculos saudáveis. Por essa razão, essa teoria pode não suprir uma explicação universal e, por isso, é provável que esse seja apenas um dos diversos fatores envolvidos na melhora da sensibilidade à insulina induzida pelo exercício na obesidade induzida por dieta.

CONSIDERAÇÕES FINAIS

Essas novas descobertas demonstraram que o exercício físico pode atuar por diferentes mecanismos intracelulares, sendo uma ferramenta importante na melhora da sinalização da insulina em organismos saudáveis ou com resistência à insulina. Na condição de resistência à insulina associada à obesidade induzida por dieta rica em gordura, pesquisas revelam que o exercício físico é capaz de modular proteínas inflamatórias de efeito negativo no sinal de insulina. A atenuação na atividade da JNK, IκK e iNOS são alguns novos mecanismos moleculares possíveis por intermédio dos quais o exercício melhora o sinal da insulina e a captação de glicose (Figura 3). No entanto, os resultados encontrados pelos diversos estudos carecem de investigações continuadas, uma vez que a duração e a magnitude dos efeitos na sinalização da insulina são variáveis, dependendo do tipo, da duração e da intensidade de exercício e do modelo de obesidade induzida, sem se descartar a possibilidade de os efeitos serem decorrentes de outros fatores e envolverem outras vias moleculares. Uma das possibilidades talvez esteja associada a mudanças hemodinâmicas induzidas pelo exercício. É conhecido que uma única sessão de exercício diminui a atividade simpática e aumenta o fluxo sanguíneo muscular no período após o exercício. É interessante notar que, durante a hiperinsulinemia perante uma única sessão de exercício, a atividade simpática é menor e a vasodilatação muscular, maior. Essas e outras mudanças hemodinâmicas podem, também, contribuir para a reversão da resistência à insulina (60). Apesar da necessidade de se definirem muitas outras etapas da ação do exercício em vias de sinalização intracelular, todas essas descobertas abrem novas perspectivas para a compreensão do efeito do exercício sobre a captação de glicose.

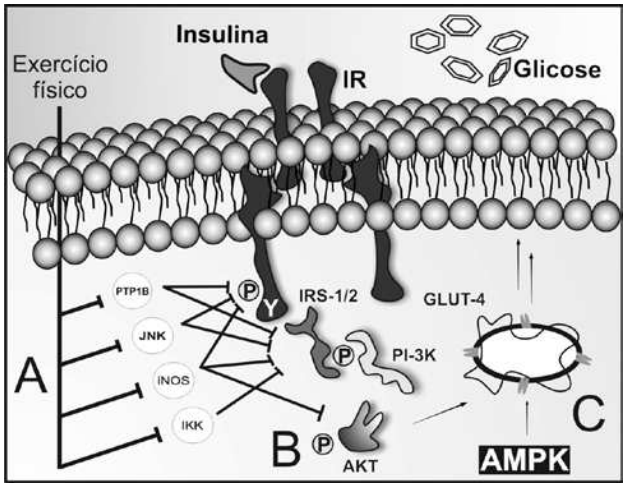

Figura 3. Novos mecanismos de ação do exercício na resistência à insulina induzida por obesidade. O exercício físico reduz a expressão e/ou atividade de proteínas intracelulares de efeito negativo sobre a via de sinalização da insulina, por exemplo, PTP1B, JNK, IKK e iNOS, e com isso aumenta a sensibilidade à insulina e melhora a captação de glicose na obesidade (A). A melhora no metabolismo da glicose em indivíduos exercitados deve-se ainda ao efeito do exercício de aumentar a translocação do Glut-4 por vias moleculares distintas, mediado por insulina (via IR/IRSs/PI3q/Akt) (B) e/ou via AMPK (C) para a membrana do músculo esquelético, independente da perda de peso corporal.

Declaração: os autores declaram não haver conflitos de interesse científico neste estudo.

REFERÊNCIAS

1. Smith AG, Muscat GE. Skeletal muscle and nuclear hormone receptors: implications for cardiovascular and metabolic disease. Int J Biochem Cell Biol. 2005;37(10):2047-63.
2. Nuutila P, Koivisto VA, Knuuti J, Ruotsalainen U, Teras M, Haaparanta M, et al. Glucose-free fatty acid cycle operates in human heart and skeletal muscle in vivo. The J Clin Invest. 1992;89(6):1767-74.
3. James DE, Burleigh KM, Kraegen EW, Chisholm DJ. Effect of acute exercise and prolonged training on insulin response to intravenous glucose in vivo in rat. J Appl Physiol. 1983;55(6):1660-4.

4. Eriksson J, Tuominen J, Valle T, Sundberg S, Sovijarvi A, Lindholm H, et al. Aerobic endurance exercise or circuit-type resistance training for individuals with impaired glucose tolerance? Horm Metab Res. 1998;30(1):37-41.
5. Kennedy JW, Hirshman MF, Gervino EV, Ocel JV, Forse RA, Hoenig SJ, et al. Acute exercise induces GLUT4 translocation in skeletal muscle of normal human subjects and subjects with type 2 diabetes. Diabetes. 1999;48(5):1192-7.
6. Luciano E, Carneiro EM, Carvalho CR, Carvalheira JB, Peres SB, Reis MA, et al. Endurance training improves responsiveness to insulin and modulates insulin signal transduction through the phosphatidylinositol 3-kinase/Akt-1 pathway. Eur J Endocrinol. 2002;147(1):149-57
7. Knowler WC, Barret-Connor E, Fowler SE, Hamman RF, Lachin JM, Walker EA, et al. Reduction in the incidence of type 2 diabetes with lifestyle intervention or metformin. N Engl J Med. 2002;346(6):393-403.
8. Chauveau A, Kaufamann M. Expériences pour la determination du coefficient de l'activité nutritive et respiratoire des muscles en respos et en travail. C R Hebd Seances Acad Sci. 1887;104(1):1126-32.
9. Burn JH, Dale HH. On the location of action of insulin. J Physiol. 1924;59(6):164-92.
10. Bjorntorp P, De Jounge K, Sjostrom L, Sullivan L. The effect of physical training on insulin production in obesity. Metabolism. 1970;19(8):631-8.
11. Bjorntorp P, Fahlen M, Grimby G, Gustafson A, Holm J, Renstrom P, et al. Carbohydrate and lipid metabolism in middle-aged, physically well-trained men. Metabolism. 1972;21(11):1037-44.
12. Mondon CE, Dolkas CB, Reaven GM. Site of enhanced insulin sensitivity in exercise-trained rats at rest. Am J Physiol. 1980;239(3):E169-77.
13. Patti ME, Kahn CR. The insulin receptor: a critical link in glucose homeostasis and insulin action. J Basic Clin Physiol Pharmacol. 1998;9(2-4):89-109.
14. Pessin JE, Saltiel AR. Signaling pathways in insulin action: molecular targets of insulin resistance. J Clin Invest. 2000;106(2)165-9.
15. White MF. The IRS-signalling system: a network of docking proteins that mediate insulin action. Molecular Cell Biochemistry. 1998;182:3-11.
16. Backer JM, Myers MG Jr, Shoelson SE, Chin DJ, Sun XJ, Miralpeix M, et al. Phosphatidylinositol 3'-kinase is activated by association with IRS-1 during insulin stimulation. EMBO J. 1992;11(9):3469-79.
17. Czech MP, Corvera S. Signaling mechanisms that regulate glucose transport. J Biol Chem. 1999;274(4):1865-8.
18. Shephard PR, Nave BT, Siddle K. Insulin stimulation of glycogen synthesis and glycogen synthase activity is blocked by wortmannin and rapamycin in 3T3-L1 adipocytes: evidence for the involvement of phosphoinositide 3-kinase and p70 ribosomal protein-S6 kinase. Biochem J. 1995;305(pt.1):25-8.
19. Hayashi T, Wojtaszewski JF, Goodyear LJ. Exercise regulation of glucose transport in skeletal muscle. Am J Physiol. 1997;273(6):E1039-51.
20. Hardie DG, Carling D. The AMP-activated protein kinase: fuel gauge of the mammalian cell? Eur J Biochem. 1997;246(2):259-73.
21. Simoneau JA, Veerkamp JH, Turcotte LP, Kelley DE. Markers of capacity to utilize fatty acids in human skeletal muscle: relation to insulin resistance and obesity and effects of weight loss. FASEB. 1999;13(14):2051-60.
22. Wicklmayr M, Rett K, Fink E, Tschollar W, Dietze G, Mehnert H. Local liberation oh kinins by working skeletal muscle tissue in man. Hormone Metabolism Research. 1988;20(8):535.
23. Youn JH, Gulve EA, Holloszy JO. Calcium stimulates glucose transport in skeletal muscle by a pathway independent of contraction. Am J Cell Physiol. 1991;260(3 Pt 1):C555-61.
24. Holloszy JO, Hansen PA. Regulation of glucose transport into skeletal muscle. Rev Physiol Biochem Pharmacol. 1996;128:99-103.
25. Roberts CK, Barnard RJ, Jasman A, Balon TW. Acute exercise increases nitric oxide synthase activity in skeletal muscle. Am J physiol Endocrinol Metab. 1999;277(2 Pt 1):E390-4.
26. Ropelle ER, Pauli JR, Prada PO, De Souza CT, Picardi PK, Cintra DE, et al. Reversal of diet-induced insulin resistance with single bout of exercise in the rat the role of PTP1B and IRS-1 serine phosphorylation. J Physiol. 2007;577:997-1007.
27. Pauli JR, Ropelle ER, Cintra DE, Carvalho-filho MA, Moraes, De Souza CT, et al. Acute physical exercise reverses S-nitrosation of the insulin receptor, insulin receptor substrate 1, and protein kinase B/Akt in dietary induce obese Wistar rats. J Physiol. 2008;586:659-71.
28. Handschin C, Spiegelman BM. The role of exercise and PGC-1 in inflammation and chronic disease. Nature. 2008;454:463-9.
29. Hotamisligil GS, Peraldi P, Budavari A, Ellis R, White MF, Spiegelman BM. IRS-1 mediated inhibition of insulin receptor tyrosine kinase activity in TNF-alpha and obesity-induced insulin resistance. Science. 1996;271(5249):665-8.
30. Dandona P, Aljada A, Bandyopadhyay A. Inflammation: the link between insulin resistance, obesity and diabetes. Trends immunology. 2004;25(1):4-7.
31. Waki H, Tontonoz P. Endocrine functions of adipose tissue. Annu Rev Pathol Mech Dis. 2007;2:31-56.
32. Tsukumo DM, Carvalho-Filho MA, Carvalheira JB, Prada PO, Hirabara SM, Schenka AA. Loss-of-function mutation in toll-like receptor 4 prevents diet-induced and insulin resistance. Diabetes. 2007;56(8):1986-8.
33. Foster LJ, Klip A. Mechanism and regulation of GLUT-4 vesicle fusion in muscle and fat cells. Am J Cell Physiol. 2000;279(4):C877-90.
34. Olson AL, Pessin JE. Structure, function, and regulation of the mammalian facilitative glucose transporter gene family. Annu Rev Nutr. 1996;16:235-56.
35. Knowler WC, Barret Connor E, Fowler SE. Reduction in the incidence of type 2 diabetes with lifestyle intervention or metformin. N Engl J Med. 2002;346(6):393-403.
36. McPherson R, Jones PH. The metabolic syndrome and type 2 diabetes: role of the adipocyte. Curr Opin Lipidol. 2003;14(6):549-53.
37. Tuomilehto J, Lindstrom J, Eriksson JG, Valle TT, Hämäläinen H, Ilanne-Parikka P, et al. Prevention of type 2 diabetes mellitus by changes in lifestyle among subjects with impaired glucose tolerance. N Engl J Med. 2001;344:1343-50.
38. Shulman GI. Unraveling the cellular mechanism of insulin resistance in humans: new insights from magnetic resonance spectroscopy. Physiology. 2004;19:183-90.
39. Savage DB, Petersen KF, Shulman GI. Disordered lipid metabolism and the pathogenesis of insulin resistance. Physiol Rev. 2007;87(2):507-20.
40. Waki H, Tontonoz P. Endocrine functions of adipose tissue. Annu Rev Pathol. 2007;2:31-56.
41. Kim JK. Fat uses a TOLL-road to connect inflammation and diabetes. Cell Metab. 2006;4(6):417-9.
42. Milanski M, Degasperi G, Coope A, Morari J, Denis R, Cintra DE. Saturated fatty acids produce an inflammatory response predominantly through the activation of TLR4 signaling in hypothalamus: implications for the pathogenesis of obesity. J Neurosci. 2009;29(2):359-70.
43. Shoelson SE, Lee J, Yuan M. Inflammation and the IKK beta/I kappa N/NF-kappa B axis in obesity- and diet-induced insulin resistance. J Clin Invest. 2003;106:171-6.
44. Hotamisligil GS. Inflammatory pathways and insulin action. Int J Obes Relat Metab Disord. 2003;27:S53-55.
45. Carvalho-Filho MA, Ueno M, Hirabara SM, Seabra AB, Carvalheira JB, de Oliveira MG, et al. S-nitrosation of the insulin receptor,

insulin receptor substrate 1, and protein kinase B/Akt: a novel mechanism of insulin resistance. Diabetes. 2005;54(4):959-67.
46. Gross SS, Wolin MS. Nitric oxide: pathophysiological mechanisms. Annu Rev Physiol. 1995;57:737-69.
47. Sugita H, Kaneki M, Tokunaga E, Sugita M, Koike C, Yasuhara S, et al. Inducible nitric oxide synthase plays a role in LPS-induced hyperglycemia and insulin resistance. Am J Physiol Endocrinol Metab. 2002;282:E386-94.
48. Carvalho-Filho MA, Ueno M, Carvalheira JB, Velloso LA, Saad MJ. Targeted disruption of iNOS prevents LPS-induced S-nitrosation of IRbeta/IRS-1 and Akt and insulin resistance in muscle of mice. Am J Physiol Endocrinol Metab. 2006;291(3):E476-82.
49. Petersen AM, Pedersen BK. The anti-inflammatory effect of exercise. J Appl Physiol. 2005;98(4):1154-62.
50. Fischer CP, Berntsen A, Perstrup LB, Eskildsen P, Pedersen BK. Plasma levels of interleukin-6 and C-reactive protein are associated with physical inactivity independent of obesity. Scand J Med Sci Sports. 2007;17(5):580-7.
51. Xie L, Lee SY, Andersen JN, Waters S, Shen K, Guo XL, et al. Cellular effects of small molecule PTP-1B inhibitors on insulin signaling. Biochemistry. 2003;42(44):3074-84.
52. Gum RJ, Gaede LL, Koterski SL, Heindel M, Clampit JE, Zinker BA. Reduction of protein tyrosine phosphatase 1B increases insulin-dependent signaling in ob/ob mice. Diabetes. 2003;52(1):21-8.
53. Elchebly M, Payette P, Michaliszyn E, Cromlish W, Collins S, Loy AL, et al. Increased insulin sensitivity and obesity resistance in mice lacking the protein tyrosine phosphatase-1B gene. Science. 1999;283(5407):1544-8.
54. Sriwijitkamol A, Coletta DK, Wajcberg E, Balbontin GB, Reyna SM, Barrientes J, et al. Effect of acute exercise on AMPK signaling in skeletal muscle of subjects with type 2 diabetes: a time-course and dose-response study. Diabetes. 2007;56(3):836-48.
55. Pilon G, Dallaire P, Marette A. Inhibition of inducible nitric-oxide synthase by activators of AMP-activated protein kinase: a new mechanism of action of insulin-sensitizing drugs. J Biol Chem. 2004; 279(20): 20767-74.
56. Musi N, Fujii N, Hirshman MF, Ekberg I, Fröberg O, Ljungqvist O, et al. AMP-activated protein kinase (AMPK) is activated in muscle of subjects with type 2 diabetes during exercise. Diabetes. 2001;50(5):921-7.
57. Pauli JR, Ropelle ER, Cintra DE, De Souza CT. Efeitos do exercício físico na expressão e atividade da AMPK em ratos obesos induzidos por dieta rica em gordura. Rev Bras Med Esporte. 2009;15(2):99-104.
58. Balon TW, Nadler JL. Evidence that nitric oxide increases glucose transport in skeletal muscle. J Appl Physiol. 1997;82(1):359-63.
59. Kapur S, Marcotte B, Marette A. Mechanism of adipose tissue iNOS induction in endotoxemia. Am J Physiol Endocrinol Metab. 1999;276(4 Pt 1):E635-41.
60. Bisquolo VA, Cardoso CG Jr, Ortega KC, Gusmao JL, Tinucci T, Negrao CE, et al. Previous exercise attenuates muscle sympathetic activity and increases blood flow during acute euglycemic hyperinsulinemia. J Appl Physiol. 2005;98(3):866-71.

APÊNDICE *XII*

Journal of Cellular Physiology

Acute Exercise Reduces Insulin Resistance-Induced TRB3 Expression and Amelioration of the Hepatic Production of Glucose in the Liver of Diabetic Mice

ATHOS F. LIMA,[1] EDUARDO R. ROPELLE,[2] JOSÉ R. PAULI,[3] DENNYS E. CINTRA,[2] MARISA J.S. FREDERICO,[4] RICARDO A. PINHO,[4] LÍCIO A. VELLOSO,[2] AND CLÁUDIO T. DE SOUZA[4]*

[1] *Universidade Cruzeiro do Sul, Unicsul, São Paulo, SP, Brazil*

[2] *Departamento de Clínica Médica, FCM, Universidade Estadual de Campinas (UNICAMP), Campinas, SP, Brazil*

[3] *Curso de Educação Física—Modalidade Saúde, Departamento de Biociências, UNIFESP, Santos, SP, Brazil*

[4] *Exercise Biochemistry and Physiology Laboratory, Postgraduate Program in Health Sciences, Health Sciences Unit, University of Southern Santa Catarina, Criciúma, SC, Brazil*

TRB3 (a mammalian homolog of *Drosophila*) is emerging as an important player in the regulation of insulin signaling. TRB3 can directly bind to Ser/Thr protein kinase Akt, the major downstream kinase of insulin signaling. Conversely, physical exercise has been linked to improved glucose homeostasis and enhanced insulin sensitivity; however, the molecular mechanisms by which exercise improves glucose homeostasis, particularly in the hepatic tissue, are only partially known. Here, we demonstrate that acute exercise reduces fasting glucose in two models diabetic mice. Western blot analysis showed that 8 h after a swimming protocol, TRB3 expression was reduced in the hepatic tissue from diet-induced obesity (Swiss) and leptin-deficient (ob/ob) mice, when compared with respective control groups at rest. In parallel, there was an increase in insulin responsiveness in the canonical insulin-signaling pathway in hepatic tissue from DIO and ob/ob mice after exercise. In addition, the PEPCK expression was reduced in the liver after the exercise protocol, suggesting that acute exercise diminished hepatic glucose production through insulin-signaling restoration. Thus, these results provide new insights into the mechanism by which physical activity improves glucose homeostasis in type 2 diabetes.

J. Cell. Physiol. 221: 92–97, 2009.

Type 2 diabetes results from a complex interplay between genetic and environmental conditions. It is associated with impaired glucose clearance by the liver in the postprandial state, and with elevated glucose production in the postabsorptive state. Thus, insulin has a potent inhibitory effect on hepatic glucose production by direct actions on hepatic receptors. The insulin receptor (IR) is a protein with intrinsic tyrosine kinase activity that, following activation by insulin, undergoes rapid autophosphorylation and, subsequently, phosphorylates intracellular protein substrates, including IRS-1 and IRS-2 (Cheatham and Kahn, 1995). IRS proteins act as messenger molecule-activated receptors to signaling with Src homology 2 domains, which are important steps in insulin action. After stimulation by insulin, IRS-1 and -2 associate with several proteins, including phosphatidylinositol 3-kinase (PI 3-K) (Folli et al., 1992; Saad et al., 1993; Williamson et al., 2003). Downstream to PI 3-K the serine/threonine kinase, Akt is activated and plays a pivotal role in the regulation of various biological processes, including apoptosis, proliferation, differentiation, and intermediary metabolism (Downward, 1998; Chen et al., 2001).

TRB3, a mammalian homolog of *Drosophila tribbles*, was proposed as a suppressor of Akt activity, predominantly in conditions of fasting and diabetes (Du et al., 2003). TRB3 is emerging as an important player in the regulation of insulin signaling through directly bind to Ser/Thr protein kinase Akt, the major downstream kinase of insulin signaling. In addition, knockdown of TRB3 expression by shRNA in mouse diabetic liver increases insulin sensitivity. Conversely, increased TRB3 expression via adenoviral transfer in the normal liver leads to decreased insulin sensitivity and glucose intolerance.

Insulin modulates nuclear forkhead box O1 (Foxo1) activity in an Akt-dependent manner (Barthel et al., 2001). In loss- and gain-of-function experiments in mice, Foxo1 has been shown to promote hepatic glucose production (Pagliassotti et al., 2002; Puigserver et al., 2003). Previous studies show that a negative modulation of insulin signal transduction through insulin PI 3-K/Akt/Foxo1is involved in gluconeogenesis (Barthel et al., 2001; Cintra et al., 2008). Insulin signaling plays an important role in controlling gluconeogenic gene expression, including that of phosphoenolpyruvate carboxykinase (PEPCK), which catalyzes the rate-limiting step of hepatic gluconeogenesis (Sutherland et al., 1996). A number of observations indicate that the

*Correspondence to: Cláudio T. De Souza, Laboratório de Fisiologia e Bioquímica do Exercício, Programa de Pós-Graduação em Ciências da Saúde, Universidade do Extremo Sul Catarinense, 88806-000 Criciúma, SC, Brazil. E-mail: ctsouza@unesc.net

Received 6 February 2009; Accepted 16 April 2009

Published online in Wiley InterScience (www.interscience.wiley.com.), 2 June 2009.
DOI: 10.1002/jcp.21833

activation of PI 3-K/Akt is a major pathway through which insulin modulates hepatic genes. Thus, blocking insulin-induced PI 3-K activation with wortaminnin and LY-294002 prevents the inhibitory effect of insulin on PEPCK expression (Band and Posner, 1997). Expression of a dominant negative mutant of PI 3-K induces the expression of PEPCK (Miyake et al., 2002).

Increased physical exercise has been linked to improved glucose homeostasis and enhanced insulin sensitivity. After an acute bout of exercise, the insulin sensitivity is enhanced in insulin-sensitive tissues, such as, skeletal muscle, liver, and hypothalamus (Luciano et al., 2002; Flores et al., 2006; Ropelle et al., 2006; Pauli et al., 2008). The molecular mechanism for enhanced insulin-mediated glucose uptake with exercise training may be partly related to increased expression and activity of key proteins known to regulate glucose metabolism in skeletal muscle (Chibalin et al., 2000; Aoi et al., 2004; Ropelle et al., 2006). However, the molecular basis underlying the beneficial effects of exercise on hepatic production glucose in type 2 diabetes remains unclear. The current study was designed to investigate the effects of an acute bout of exercise on TRB3 expression in the insulin-signaling hepatic tissue and, consequently, hepatic production glucose in obese diabetic mice.

Materials and Methods

Experimental animals

Male Swiss mice from the University of Campinas Central Animal Breeding Center were used in the experiments. The 4-week-old Swiss mice were divided into three groups; control mice (lean) fed standard rodent chow; obese mice, fed on an high fat diet (carbohydrate: 45%; protein: 20%; fat 35%, total 5.7 kcal/g) for 2 months (DIO), and a third group, which also received an high fat diet, but was submitted to acute exercise (DIO + EXE). Also, male leptin-deficient (*ob*/*ob*) and lean control mice (*ob*/?), originally imported from the Jackson Laboratories (Bar Harbor, ME), were used in the experiments. All experiments were approved by the Ethics Committee of the State University of Campinas (UNICAMP). Room temperature was maintained stable (28 ± 1°C), and mice were housed in individual cages, subjected to a standard light–dark cycle (6:00 a.m. to 6:00 p.m./6:00 p.m. to 6:00 a.m.), and provided with standard rodent chow and water ad libitum.

Exercise protocol

The swimming protocol employed was described previously (Ryder et al., 1999), with minor modifications. Adult mice were acclimated to swimming for 10 min for 2 days. Eight animals swam together in plastic containers measuring 45 cm in diameter. Water temperature was maintained at 32–33°C. Mice swam for four 30-min periods, with 5-min rest periods for a total swimming time of 2 h. After the acute exercise protocol (DIO + EXE—Swiss *or AE* group—ob/ob), animals were fed ad libitum for 2 h and food was withdrawn 6 h before the tissue extractions. Eight hours after the exercise protocol, the mice were anesthetized with intraperitoneal (i.p.) injection of sodium thiopental (40 mg/kg body weight). Following the experimental procedures, the mice were killed under anesthesia (thiopental 200 mg/kg) following recommendations of the NIH publication no. 85–23.

Fasting glucose, insulin tolerance test (ITT), serum insulin quantification, and glycogen content

After the exercise protocol, the mice were submitted to an insulin tolerance test (ITT; 1.5 U/kg body weight of insulin) after 6 h fasting. Briefly, 1.5 IU/kg of human recombinant insulin (Humulin R) from Eli Lilly (Indianapolis, IN) was infused intraperitoneally to anesthetized mice, the blood samples were collected at 0, 5, 10, 15, 20, 25, and 30 min from the tail for serum glucose determination. The rate constant for plasma glucose disappearance (K_{ITT}) was calculated using the formula 0.693/biological half-life ($t_{1/2}$). The plasma glucose $t_{1/2}$ was calculated from the slope of the last square analysis of the plasma glucose concentration during the linear phase of decline (Bonora et al., 1989). Plasma glucose was determined using a glucose meter (Advantage, Boehringer Mannheim, Irveine, CA). Plasma was separated by centrifugation (1500*g*) for 15 min at 4°C and stored at −80°C until assay. RIA was employed to measure serum insulin, according to a previous description (Scott et al., 1981). Glycogen content in liver fragments was measured according to a previously described method (Pimenta et al., 1989).

Protein analysis by immunoblotting

As soon as anesthesia was assured by the loss of pedal and corneal reflexes, the abdominal cavity was opened, the cava vein exposed, and 0.1 ml of normal saline or insulin (10^{-6} mol/L to 0.1 ml) was injected. After insulin injection, hepatic tissue was excised. The tissue was pooled, minced coarsely, and homogenized immediately in extraction buffer (mM) (1% Triton-X-100, 100 Tris, pH 7.4, containing 100 sodium pyrophosphate, 100 sodium fluoride, 10 EDTA, 10 sodium vanadate, 2 PMSF, and 0.1 mg of aprotinin/ml) at 4°C with a Polytron PTA 20S generator (Brinkmann Instruments, Westbury, NY, model PT 10/35) operated at maximum speed for 30 sec. The extract was centrifuged at 11,000 rpm and 4°C in a Beckman 70.1 Ti rotor (Palo Alto, CA) for 40 min to remove insoluble material, and the supernatant was used for protein quantification, using the Bradford method (Bradford, 1976). Proteins were denatured by boiling in Laemmli (1970) sample buffer containing 100 mM DTT, run on SDS–PAGE, and transferred to nitrocellulose membranes. Membranes were blocked, probed, and developed, as described previously (De Souza et al., 2005). Antibodies used for immunoblotting were anti-phospho-Akt, anti-PEPCK, anti-phospho-Foxo1 (Cell Signaling Technology, Beverly, MA), anti-Akt, anti-Foxo1, anti-TRB3, and anti-β-actin (Santa Cruz Biotecnology, Inc., Santa Cruz, CA). Band intensities were quantitated by optical densitometry (Scion Image software, ScionCorp, Frederick, MD) of the developed autoradiographs. The quantified phospho data were expressed relative to total.

Statistical analysis

The results were expressed as the means ± SEM. Differences between the lean groups and mice at rest (ob/ob or Swiss) and after exercise protocol were evaluated using one-way analysis of

TABLE 1. Physiological and metabolic parameters

Groups (n = 7)	Body weight (g)	Epididymal fat (g)	Fasting insulin (ng ml^{-1})	Fasting glucose (mg dl^{-1})
Control (lean)	25.9 ± 1.22*	0.77 ± 0.09*	1.43 ± 0.69*	90.3 ± 5.14*
ob/ob	47.7 ± 3.11	3.99 ± 0.53	8.3 ± 2.84	248.5 ± 12.17
AE	48.4 ± 2.71	3.55 ± 0.62	9.1 ± 3.19	112.5 ± 5.26#

*$P < 0.05$, lean versus obese mice at rest.
#$P < 0.05$, AE versus respective obese mice at rest.

variance (ANOVA). When the ANOVA indicated significance, a *Bonferroni* post hoc test was performed.

Results

Physiological and metabolic parameters

Two diabetic models were evaluated in present study, deficient leptin (ob/ob) and diet-induced obesity (DIO). Table 1 shows comparative data regarding lean controls, leptin-deficient (ob/ob) mice at rest and after acute exercise. The ob/ob mice at rest have a greater body weight, epididymal fat, fasting serum insulin, and fasting glucose than age-matched controls (lean). No significant variations were found in body weight, epididymal fat, and fasting serum insulin of *ob*/*ob* mice after acute exercise, when compared diabetic mice at rest. However, the fasting glucose was reduced (65%) in *ob*/*ob* mice at 8 h after the exercise protocol (AE group).

Table 2 shows comparative data regarding control, DIO mice, and DIO mice submitted to exercise protocol (DIO + EXE). The DIO mice had a greater body weight, epididymal fat and fasting serum insulin and fasting glucose, than age-matched controls. No significant variations were found in body weight, epididymal fat, and fasting serum insulin of DIO mice after acute exercise; however, acute exercise reverses fasting hyperglycemia of DIO mice.

Acute exercise improves insulin signaling in the liver of ob/ob and DIO mice

Insulin-induced 5.0- (DIO) and 3.2-fold (ob/ob) increases in Akt serine phosphorylation in the liver of lean controls, when compared to saline injection (Fig. 1A,C, respectively). In Swiss and ob/ob mice at rest, Akt serine phosphorylation was reduced after insulin injection by 2.7- and 3.3-fold (respectively), when compared with lean mice (Fig. 1A,C). In the liver of the DIO + EXE and AE group, Akt serine increased by 1.8- and 2.6-fold, respectively, compared with mice at rest (Fig. 1A,C). There was no difference in basal levels of Akt serine phosphorylation in the groups (data not shown). The Akt protein levels were not different between the groups (Figs. 1A,C, lower parts).

Insulin-induced a 4.5- (DIO) and 10.3-fold (ob/ob) increase in Foxo1 phosphorylation in the liver of lean mice, when compared to saline injection (Fig. 1B,D, respectively). In Swiss and ob/ob mice at rest, Foxo1 phosphorylation was reduced after insulin injection by 2.2- and 4.2-fold, respectively, when compared with the lean group (Fig. 1B,D). In the liver DIO + EXE and AE group, Foxo1 increased by 1.5- and 3.1-fold, compared with mice at rest (Fig. 1B,D, respectively). There was no difference in basal levels of Foxo1 phosphorylation between the groups (data not shown). The Foxo1 protein levels were not different between the groups (Fig. 1B,D, lower parts).

Acute exercise suppressed TRB3 expression in the hepatic tissue of *ob*/*ob* mice

TRB3 expression was determined in the hepatic tissue of two animal models. The livers were blotted with anti-TRB3. TRB3 expression was increased by 1.5- and 3.8-fold in the liver of DIO and ob/ob mice at rest (respectively), when compared with lean

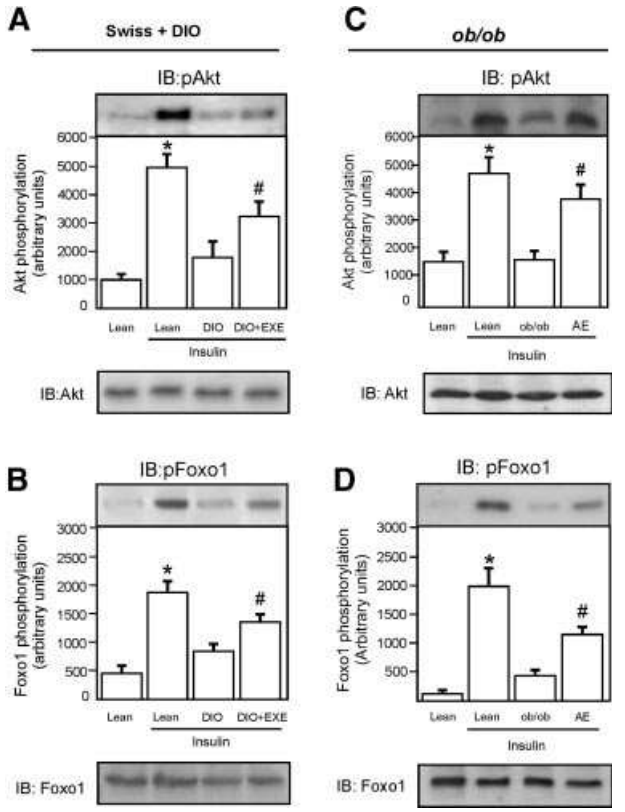

Fig. 1. Insulin signaling in the liver of diet-induced obesity and ob/ob mice. Liver extracts from mice injected with saline (−) or insulin (+) were prepared, as described in Materials and Methods Section. A: Tissue extracts of the Swiss mice were blotted (IB) with anti-phospho Akt antibody or anti-Akt antibody (upper and lower parts, respectively). B: Tissue extracts of the Swiss mice were with IB antibodies anti-phosphoFoxo1 or anti-Foxo1 antibody (upper and lower parts, respectively). C: Liver extracts of the ob/ob mice were IB with anti-phospho Aktor anti-Akt antibody (upper and lower parts, respectively). D: liver extracts of the ob/ob mice were IB with anti-phospho Foxo1 or anti-Foxo1 antibody (upper and lower parts, respectively). The results of scanning densitometry are expressed as arbitrary units (expressed as relative to total). Bars represent means ± SEM of n = 8 mice. *$P < 0.05$, DIO mice at rest versus lean (Swiss) and ob/ob mice at rest versus lean and #$P < 0.05$, DIO + EXE versus DIO mice at rest and AE group versus ob/ob mice at rest.

controls. However, 8 h after a single bout of exercise, the TRB3 expression was reduced by 1.5- and 2.0-fold in the liver of DIO + EXE and AE groups when compared with the DIO and ob/ob groups at rest (Fig. 2A,C, respectively). No significant variations were found in TRB3 expression in ob/ob and Swiss lean (control) after acute exercise with or without injection insulin (data not shown).

The liver was immunoprecipitated with anti-Akt antibody and then blotted with anti-TRB3 antibody. A 2.4- and 2.5-fold increase in Akt/TRB3 association was observed in the liver of

TABLE 2. Physiological and metabolic parameters

Groups (n = 9)	Body weight (g)	Epididymal fat (g)	Fasting insulin (ng ml^{-1})	Fasting glucose (mg dl^{-1})
Lean	24–3 ± 2.22*	0.5 ± 0.10*	1.8 ± 0.59*	97.3 ± 4.14*
DIO	37.9 ± 3.11	2.6 ± 0.43	9.7 ± 2.64	285.5 ± 8.17
DIO + EXE	38.6 ± 3.01	2.9 ± 0.52	9.2 ± 3.02	122.5 ± 6.26#

*$P < 0.05$, lean (control) versus DIO.
#$P < 0.05$ exercised (DIO + EXE) versus DIO mice.

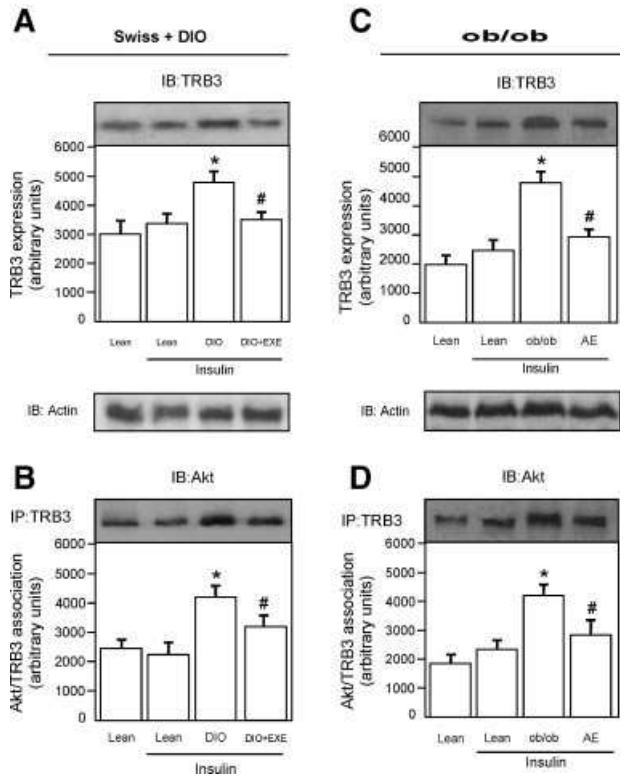

Fig. 2. Expression of TRB3 and TRB3/Akt association. Liver extracts from the Swiss and ob/ob mice injected with saline or insulin were submitted to immunoblotting (TRB3 expression) or immunoprecipitated (TRB3/Akt association), as described in the Materials and Methods Section. A: Samples were blotted (IB) with anti-TRB3 antibody in liver of diet-induced obesity mice. B: Tissue extracts were immunoprecipitated (IP) with anti-TRB3 antibody and blotted (IB) with anti-Akt antibody in liver of diet-induced obesity mice. C: Samples were blotted (IB) with anti-TRB3 antibody in liver of ob/ob mice. D: Tissue extracts were immunoprecipitated (IP) with anti-TRB3 antibody and blotted (IB) with anti-Akt antibody in liver of ob/ob mice. Bars represent means ± SEM of n = 8 mice. *$P < 0.05$, DIO mice at rest versus lean (Swiss) and ob/ob mice at rest versus lean and #$P < 0.05$, DIO + EXE versus DIO mice at rest and AE group versus ob/ob mice at rest.

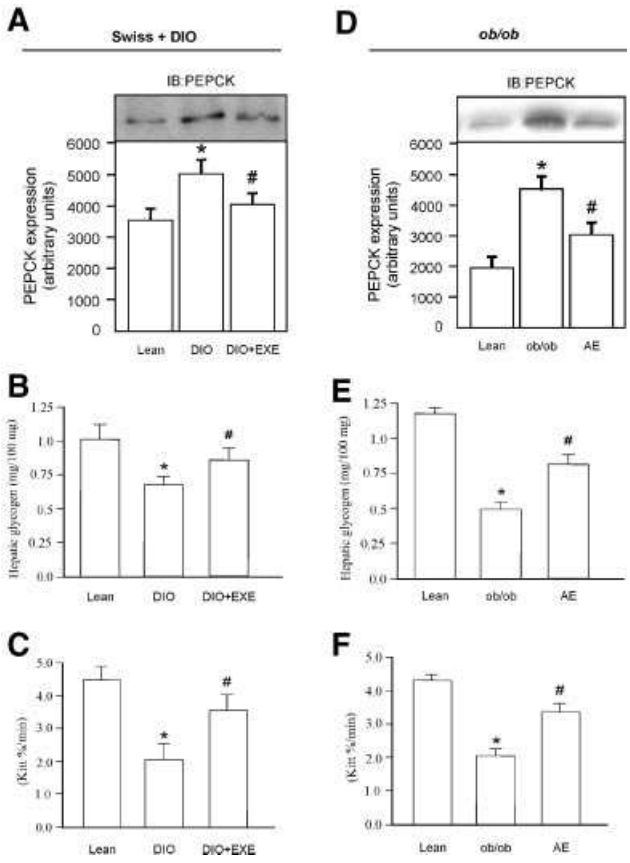

Fig. 3. PEPCK expression, glycogen content, and insulin sensitivity under fasting conditions in the hepatic tissue and of lean (control), ob/ob (obese) and AE mice. Liver extracts from mice were prepared as described in Materials and Methods Section. A: Tissue extracts were blotted (IB) with anti-PEPCK antibody in Swiss mice. B: Hepatic glycogen content in Swiss mice is expressed as mg (100 g tissue)$^{-1}$. C: The rate constant for glucose disappearance during an insulin tolerance test (K_{ITT}) in Swiss mice. D: tissue extracts were blotted (IB) with anti-PEPCK antibody in ob/ob mice. E: Hepatic glycogen content in ob/ob mice is expressed as mg (100 g tissue)$^{-1}$. F: The rate constant for glucose disappearance during an insulin tolerance test (K_{ITT}) in ob/ob mice. The results of scanning densitometry are expressed as arbitrary units. In PEPCK expression, bars represent means ± SEM of n = 8 mice. *$P < 0.05$, DIO mice at rest versus lean (Swiss) and ob/ob mice at rest versus lean and #$P < 0.05$, DIO + EXE versus DIO mice at rest and AE group versus ob/ob mice at rest.

the DIO and ob/ob groups, respectively, when compared with the lean group (Fig. 2B,D). Conversely, in the liver of DIO + EXE and AE groups, the Akt/TRB3 association decreased by 1.1- and 1.6-fold, respectively, compared to DIO and ob/ob mice at rest (Fig. 2B,D). The Akt protein levels were not different between the groups (Fig. 2B,D, lower parts).

Acute exercise reduces PEPCK expression in the hepatic tissue of DIO and *ob/ob* mice

We next observed the expression of PEPCK in the liver of two models, under fasting conditions. The hepatic tissue extracts were blotted with anti-PEPCK antibody. In the hepatic tissue of DIO and ob/ob mice at rest, the PEPCK expression was increased by 1.4- and 2.3-fold in DIO and ob/ob, respectively, when compared with lean groups. Interestingly, 8 h after acute exercise, the PEPCK protein level was decreased by 1.1- and 1.6-fold in the DIO + EXE and AE groups, when compared with diabetic mice at rest (Fig. 3A,D, respectively).

Liver glucose uptake is independent of insulin action; however, the pancreatic hormone tightly regulates hepatic gluconeogenesis. Since acute exercise leads to high glucose turnover in spite of low basal and stimulated insulin levels, we decided to evaluate glycogen contents. In DIO and ob/ob mice at rest glycogen content was reduced by 1.5- and 2.3-fold, respectively, when compared with respective lean groups (Fig. 1B,E). In the liver of the DIO + EXE and AE groups, glycogen content increased by 1.3- and 1.7-fold, compared with DIO and ob/ob mice at rest (Fig. 3B,E, respectively).

Finally, we observed increased insulin sensitivity in the AE group and DIO + EXE. We found a significant impairment (65 and 55%) in the glucose disappearance rate (K_{ITT}) in ob/ob and Swiss mice at rest when compared with lean controls (respectively) and acute exercise improved (39 and 42%) the glucose disappearance rate in ob/ob and Swiss mice, respectively (Fig. 3C,F).

Discussion

Over the past years, components of the insulin-signaling pathways have been validated in an effort to assign the

physiological role for these targets in the regulation of glucose homeostasis. The molecular mechanism for enhanced insulin sensitivity with exercise training may be related to increased expression and/or activation of key proteins that regulate glucose metabolism (Houmard et al., 1999; Chibalin et al., 2000; Ropelle et al., 2006; Pauli et al., 2008). Since the IR/IRS-2/PI 3-K pathway is involved in hepatic glucose production (Kim et al., 2001), we may suggest that physical activity partially reverses insulin resistance of diabetic mice by acting on this pathway, following acute exercise. In the present study, we demonstrate that acute exercise improves fasting glucose in diabetic mice. Eight hours after an exercise session, the TRB3 expression is suppressed in liver from leptin-deficient mice. This phenomenon is accompanied by an increase in insulin sensitivity in the liver, resulting in a reduction in glucose hepatic production in fasted mice.

One molecular mechanism mediating insulin resistance may involve the reduced activity AKT-induced TRB3 expression. The role of TRB3 on Akt activation has been studied in different contents. In both mouse muscle and liver, increased TRB3 expression is associated with impaired Akt activation (Du et al., 2003; Koh et al., 2006; Matsushima et al., 2006); a similar association has also been observed in primary hepatocytes (Matsushima et al., 2006). TRB3, a mammalian homolog of *Drosophila* tribbles, functions as a negative modulator of Akt. TRB3 expression is induced in liver under fasting conditions, and TRB3 disrupts insulin signaling by binding directly to Akt and blocking activation of the kinase. Amounts of TRB3 RNA and protein were increased in livers of db/db diabetic mice compared with those in wild-type mice (Du et al., 2003). Hepatic overexpression of TRB3 in amounts comparable to those in db/db mice promoted hyperglycemia and glucose intolerance (Du et al., 2003). Some authors have suggested that, by interfering with Akt activation, TRB3 contributes to insulin resistance in individuals with susceptibility to type 2 diabetes. In our studies, we found that expression of TRB3 is increased in the liver of leptin-deficient mice. In the present study, we observe that a single bout of exercise inhibits TRB3 expression in the liver of diabetic mice, and this inhibition is accompanied by an increase in the IR/PI 3-K/Akt pathway. Though, recently, we reported that one bout of exercise reduced protein tyrosine phosphatase 1B (PTP1B) activity and IRS-1 serine phosphorylation (two molecular mechanisms mediating insulin resistance), leading to restored insulin sensitivity in the gastrocnemius muscle of DIO rats (Ropelle et al., 2006), the role of acute exercise on PTP1B activity and IRS1 serine phosphorylation in the hepatic tissue was not investigated and could be involved in the improvement on insulin signaling but these mechanisms remain uncertain and deserve further investigations. In the hepatic tissue, insulin resistance is related as reduced insulin stimulation of tyrosine phosphorylation of the IR and its major substrates (Michael et al., 2000; Pagliassotti et al., 2002) and as an increase in gluconeogenesis and hepatic glucose output (Boden et al., 2001), as a result of the inability of PI 3-K to inhibit the activation of glucose-6-phosphatase (G6Pase) and PEPCK (Kotani et al., 1999; Chi et al., 2007). Exercise has been shown to improve insulin action in the liver (Gao et al., 1994); physical exercise ameliorated the insulin-signaling response in diabetes-prone *Psammomys obesus* and inhibited PEPCK activity (Heled et al., 2004). In addition, acute exercise increased responsiveness of whole body glucose disposal and insulin suppress ability of hepatic glucose production in obese SHHF/Mcc-facp rats (Gao et al., 1994). Downstream of PI 3-K, Foxo1 is an important regulator that modulates the expression of gluconeogenic genes in the nucleus, and this is mediated by Akt phosphorylation (Aoyama et al., 2006). Once phosphorylated, Foxo1 translocates to the cytoplasm in response to insulin and reduces gluconeogenic gene transcription. We observed high levels of PECK in the liver of ob/ob and Swiss mice fed on high-fat diet, these data are in accordance with several studies in mice with severe insulin resistance (Michael et al., 2000; Xu et al., 2003), however, some evidences showed that rats fed on high-fat diet had a reduction on PEPCK content in liver (Lessard et al., 2007). Our data provide evidence that acute exercise improves insulin signaling and increases Foxo1 phosphorylation in the liver, leading to reduced hepatic PEPCK expression in ob/ob mice. Thus, since the PI 3-K pathway is involved in glucose output in the liver, we suggest that acute exercise partially reverses the insulin resistance of diabetic animals by acting on this pathway.

Collectively, our results demonstrate that a single bout of exercise improves fasting glucose metabolism in diabetic mice by reversing insulin resistance in hepatic tissue. The effect of exercise on insulin action is further supported by our findings that exercised mice show a reduction in TRB3 expression, a mechanism by which a single bout of exercise may decrease glucose production in the liver. Thus, these results provide new insights into the mechanism by which physical activity improves glucose homeostasis in type 2 diabetes, mainly fasting hyperglycemia.

Acknowledgments

The authors thank Mr. Gerson Ferraz and Márcio A. da Cruz for technical assistance. This study was supported by grants from Conselho Nacional de Desenvolvimento Científico e Tecnológico (CNPq). We thank Dr. Nicola Conran for English language editing.

Literature Cited

Aoi W, Ichiishi E, Sakamoto N, Tsujimoto A, Tokuda H, Yoshikawa T. 2004. Effect of exercise on hepatic gene expression in rats: A microarray analysis. Life Sci 75:3117–3128.
Aoyama H, Daitoku H, Fukamizu A. 2006. Nutrient control of phosphorylation and translocation of Foxo1 in C57BL/6 and db/db mice. Int J Mol Med 18:433–439.
Band CJ, Posner BI. 1997. Phosphatidylinositol 3'-kinase and p70s6k are required for insulin but not bisperoxovanadium 1,10-phenanthroline (bpV(phen)) inhibition of insulin-like growth factor binding protein gene expression. Evidence for MEK-independent activation of mitogen-activated protein kinase by bpV(phen). J Biol Chem 272:138–145.
Barthel A, Schmoll D, Krüger KD, Bahrenberg G, Walther R, Roth RA, Joost HG. 2001. Differential regulation of endogenous glucose-6-phosphatase and phosphoenol pyruvate carboxykinase gene expression by the forkhead transcription factor FKHR in H4IIE-hepatoma cells. Biochem Biophys Res Commun 285:897–902.
Boden G, Chen X, Stein TP. 2001. Gluconeogenesis in moderately and severely hyperglycemic patients with type 2 diabetes mellitus. Am J Physiol Endocrinol Metab 280:E23–E30.
Bonora E, Moghetti P, Zancanaro C, Cigolini M, Querena M, Cacciatori V, Corgnati A, Muggeo M. 1989. Estimates of in vivo insulin action in man: Comparison of insulin tolerance tests with euglycemic and hyperglycemic glucose clamp studies. J Clin Endocrinol Metab 68:374–378.
Bradford MM. 1976. A rapid and sensitive method for the quantitation of microgram quantities of protein utilizing the principle of protein-dye binding. Anal Biochem 72:248–254.
Cheatham B, Kahn CR. 1995. Insulin action and the insulin signaling network. Endocr Rev 16:117–142.
Chen R, Kim O, Yang J, Sato K, Eisenmann KM, McCarthy J, Chen H, Qiu Y. 2001. Regulation of Akt/PKB activation by tyrosine phosphorylation. J Biol Chem 276:31858–31862.
Chi TC, Chen WP, Chi TL, Kuo TF, Lee SS, Cheng JT, Su MJ. 2007. Phosphatidylinositol-3-kinase is involved in the antihyperglycemic effect induced by resveratrol in streptozotocin-induced diabetic rats. Life Sci 80:1713–1720.
Chibalin AV, Yu M, Ryder JW, Song XM, Galuska D, Krook A, Wallberg-Henriksson H, Zierath JR. 2000. Exercise-induced changes in expression and activity of proteins involved in insulin signal transduction in skeletal muscle: Differential effects on insulin-receptor substrates 1 and 2. Proc Natl Acad Sci USA 97:38–43.
Cintra DE, Pauli JR, Araújo EP, Moraes JC, de Souza CT, Milanski M, Morari J, Gambero A, Saad MJ, Velloso LA. 2008. Interleukin-10 is a protective factor against diet-induced insulin resistance in liver. J Hepatol 48:628–637.
De Souza CT, Araujo EP, Bordin S, Ashimine R, Zollner RL, Boschero AC, Saad MJ, Velloso LA. 2005. Consumption of a fat-rich diet activates a proinflammatory response and induces insulin resistance in the hypothalamus. Endocrinology 146:4189–4191.
Downward J. 1998. Mechanisms and consequences of activation of protein kinase B/Akt.1998. Curr Opin Cell Biol 10:262–267.
Du K, Herzig S, Kulkarni RN, Montminy M. 2003. TRB3: A tribbles homolog that inhibits Akt/PKB activation by insulin in liver. Science 300:1574–1577.
Flores MB, Fernandes MF, Ropelle ER, Faria MC, Ueno M, Velloso LA, Saad MJ, Carvalheira JB. 2006. Exercise improves insulin and leptin sensitivity in hypothalamus of Wistar rats. Diabetes 55:2554–2561.
Folli F, Saad MJ, Backer JM, Kahn CR. 1992. Insulin stimulation of phosphatidylinositol 3-kinase activity and association with insulin receptor substrate 1 in liver and muscle of the intact rat. J Biol Chem 267:22171–22177.
Gao J, Sherman WM, McCune SA, Osei K. 1994. Effects of acute running exercise on whole body insulin action in obese male SHHF/Mcc-facp rats. J Appl Physiol 77:534–541.
Heled Y, Shapiro Y, Shani Y, Moran DS, Langzam L, Barash V, Sampson SR, Meyerovitch J. 2004. Physical exercise enhances hepatic insulin signaling and inhibits

phosphoenolpyruvate carboxykinase activity in diabetes-prone Psammomys obesus. Metabolism 53:836–841.
Houmard JA, Shaw CD, Hickey MS, Tanner CJ. 1999. Effect of short-term exercise training on insulin-stimulated PI 3-kinase activity in human skeletal muscle. Am J Physiol 277:E1055–E1060.
Kim JK, Zisman A, Fillmore JJ, Peroni OD, Kotani K, Perret P, Zong H, Dong J, Kahn CR, Kahn BB, Shulman GI. 2001. Glucose toxicity and the development of diabetes in mice with muscle-specific inactivation of GLUT4. J Clin Invest 108:153–160.
Koh HJ, Arnolds DE, Fujii N, Tran TT, Rogers MJ, Jessen N, Li Y, Liew CW, Ho RC, Hirshman MF, Kulkarni RN, Kahn CR, Goodyear LJ. 2006. Skeletal muscle-selective knockout of LKB1 increases insulin sensitivity, improves glucose homeostasis, and decreases TRB3. Mol Cell Biol 26:8217–8227.
Kotani K, Ogawa W, Hino Y, Kitamura T, Ueno H, Sano W, Sutherland C, Granner DK, Kasuga M. 1999. Dominant negative forms of Akt (protein kinase B) and atypical protein kinase Clambda do not prevent insulin inhibition of phosphoenolpyruvate carboxykinase gene transcription. J Biol Chem 274:21305–21312.
Laemmli UK. 1970. Cleavage of structural proteins during the assembly of the head of bacteriophage T4. Nature 227:680–685.
Lessard SJ, Rivas DA, Chen ZP, Bonen A, Febbraio MA, Reeder DW, Kemp BE, Yaspelkis BB III, Hawley JA. 2007. Tissue-specific effects of rosiglitazone and exercise in the treatment of lipid-induced insulin resistance. Diabetes 56:1856–1864.
Luciano E, Carneiro EM, Carvalho CR, Carvalheira JB, Peres SB, Reis MA, Saad MJ, Boschero AC, Velloso LA. 2002. Endurance training improves responsiveness to insulin and modulates insulin signal transduction through the phosphatidylinositol 3-kinase/Akt-1 pathway. Eur J Endocrinol 147:149–157.
Matsushima R, Harada N, Webster NJ, Tsutsumi YM, Nakaya Y. 2006. Effect of TRB3 on insulin and nutrient-stimulated hepatic p70 S6 kinase activity. J Biol Chem 281:29719–29729.
Michael LF, Asahara H, Shulman AI, Kraus WL, Montminy M. 2000. The phosphorylation status of a cyclic AMP-responsive activator is modulated via a chromatin-dependent mechanism. Mol Cell Biol 20:1596–1603.
Miyake K, Ogawa W, Matsumoto M, Nakamura T, Sakaue H, Kasuga M. 2002. Hyperinsulinemia, glucose intolerance, and dyslipidemia induced by acute inhibition of phosphoinositide 3-kinase signaling in the liver. J Clin Invest 110:1483–1491.
Pagliassotti MJ, Kang J, Thresher JS, Sung CK, Bizeau ME. 2002. Elevated basal PI 3-kinase activity and reduced insulin signaling in sucrose-induced hepatic insulin resistance. Am J Physiol Endocrinol Metab 282:E170–E176.
Pauli JR, Ropelle ER, Cintra DE, Carvalho-Filho MA, Moraes JC, De Souza CT, Velloso LA, Carvalheira JB, Saad MJ. 2008. Acute physical exercise reverses S-nitrosation of the insulin receptor, insulin receptor substrate 1 and protein kinase B/Akt in diet-induced obese Wistar rats. J Physiol 586:659–671.
Pimenta WP, Saad MJ, Paccola GM, Piccinato CE, Foss MC. 1989. Effect of oral glucose on peripheral muscle fuel metabolism in fasted men. Braz J Med Biol Res 22:465–476.
Puigserver P, Rhee J, Donovan J, Walkey CJ, Yoon JC, Oriente F, Kitamura Y, Altomonte J, Dong H, Accili D, Spiegelman BM. 2003. Insulin-regulated hepatic gluconeogenesis through FOXO1-PGC-1alpha interaction. Nature 423:550–555.
Ropelle ER, Pauli JR, Prada PO, de Souza CT, Picardi PK, Faria MC, Cintra DE, Fernandes MF, Flores MB, Velloso LA, Saad MJ, Carvalheira JB. 2006. Reversal of diet-induced insulin resistance with a single bout of exercise in the rat: The role of PTP1B and IRS-1 serine phosphorylation. J Physiol 577:997–1007.
Ryder JW, Kawano Y, Galuska D, Fahlman R, Wallberg-Henriksson H, Charron MJ, Zierath JR. 1999. Postexercise glucose uptake and glycogen synthesis in skeletal muscle from GLUT4-deficient mice. FASEB J 13:2246–2256.
Saad MJ, Folli F, Kahn JA, Kahn CR. 1993. Modulation of insulin receptor, insulin receptor substrate-1, and phosphatidylinositol 3-kinase in liver and muscle of dexamethasone-treated rats. J Clin Invest 92:2065–2072.
Scott AM, Atwater I, Rojas E. 1981. A method for the simultaneous measurement of insulin release and B cell membrane potential in single mouse islets of Langerhans. Diabetologia 21:470–475.
Sutherland C, O'Brien RM, Granner DK. 1996. New connections in the regulation of PEPCK gene expression by insulin. Philos Trans R Soc Lond B Biol Sci 351:191–199.
Williamson D, Gallagher P, Harber M, Hollon C, Trappe S. 2003. Mitogen-activated protein kinase (MAPK) pathway activation: Effects of age and acute exercise on human skeletal muscle. J Physiol 547:977–987.
Xu H, Dembski M, Yang Q, Yang D, Moriarty A, Tayber O, Chen H, Kapeller R, Tartaglia LA. 2003. Dual specificity mitogen-activated protein (MAP) kinase phosphatase-4 plays a potential role in insulin resistance. J Biol Chem 278:30187–30192.

APÊNDICE *XIII*

J Cancer Res Clin Oncol (2008) 134:833–839
DOI 10.1007/s00432-008-0359-5

ORIGINAL PAPER

Antineoplastic effect of rapamycin is potentiated by inhibition of IRS-1 signaling in prostate cancer cells xenografts

Josenilson C. Oliveira · Kellen K. Souza · Marília M. Dias · Marcel C. Faria · Eduardo R. Ropelle · Marcelo B. S. Flores · Mirian Ueno · Lício A. Velloso · Sara T. Saad · Mario J. A. Saad · José B. C. Carvalheira

Received: 30 May 2007 / Accepted: 8 January 2008 / Published online: 9 February 2008

Abstract Proper activation of phosphoinositide 3-kinase-Akt pathway is critical for the prevention of tumorigenesis. Recent data have characterized a negative feedback loop, wherein mammalian target of rapamycin (mTOR) blocks additional activation of the Akt/mTOR pathway through inhibition insulin receptor substrate 1 (IRS-1) function. However, the potential of IRS-1 inhibition during rapamycin treatment has not been examined. Herein, we show that IRS-1 antisense oligonucleotide and rapamycin synergistically antagonize the activation of mTOR in vivo and induced tumor suppression, through inhibition of proliferation and induction of apoptosis, in prostate cancer cell xenografts. These data demonstrate that the addition of agents that blocks IRS-1 potentiate the effect of mTOR inhibition in the growth of prostate cancer cell xenografts.

Keywords Protein kinases · Phosphatidylinositol 3-kinase · Insulin receptor substrate 1 · Rapamycin · Prostate neoplasms

Introduction

Prostate cancer is a major health problem in the world, and the available treatment options have proven to be inadequate in controlling the mortality and morbidity associated with this disease (Jemal et al. 2007; Petrylak et al. 2004; Tannock et al. 2004). Research efforts in the last decade have shown that molecular targeted-therapy is a promising approach that could expand the arsenal against prostate cancer.

The mammalian target of rapamycin (mTOR) pathway is a key regulator of cell growth and proliferation, and increasing evidence suggests that its deregulation is associated with human diseases, including cancer and diabetes (Sabatini 2006; Ueno et al. 2005). The mTOR pathway integrates signals from nutrients, energy status and growth factors to regulate many processes, including autophagy, ribosome biogenesis and metabolism (Dennis et al. 2001; Sabatini 2006). Thus, rapamycin and several analogs, such as CCI-779 and RAD001, are currently undergoing clinical evaluation as anticancer agents (Huang and Houghton 2002; Majumder et al. 2004).

The insulin and IGF-1 receptors are tyrosine kinases, which phosphorylates the insulin receptor substrate (IRS) upon ligand binding. Phosphorylated IRS, in turn, acts as a protein scaffold that activates the phosphatidylinositol (PI) 3-kinase/Akt cascade (Yenush and White 1997). The production of phosphatidylinositol 3,4,5-triphosphate (PIP3) by PI 3-kinase recruits the serine/threonine kinases PDK1 and Akt to the plasma membrane, by binding to its N-terminal pleckstrin homology (PH) domain. At the membrane, Akt is phosphorylated by PDK1-mediated phosphorylation (Lawlor and Alessi 2001). Akt phosphorylates many proteins with important physiological roles, including TSC2, inhibiting its GTPase activating protein effect towards the small G-protein Rheb (Inoki et al. 2003). The accumulation of the GTP-bound Rheb leads to the activation of mTOR through an as yet unknown mechanism.

Inactivation of the tumor-suppressor gene, PTEN, occurs in glioblastoma multiforme, endometrial cancer and prostate

Josenilson C. Oliveira and Kellen K. Souza contributed equally to this paper.

J. C. Oliveira · K. K. Souza · M. M. Dias · M. C. Faria · E. R. Ropelle · M. B. S. Flores · M. Ueno · L. A. Velloso · S. T. Saad · M. J. A. Saad · J. B. C. Carvalheira (✉)
Departament of Internal Medicine, FCM-UNICAMP, Cidade Universitária Zeferino Vaz, Campinas, SP 13081-970, Brazil
e-mail: carvalheirajbc@uol.com.br

cancer, among others (Sansal and Sellers 2004). The suppressor-tumor function of PTEN is linked to its lipid phosphatase activity; loss of this activity leads to accumulation of its substrate, PIP3, and activation of the PI 3-kinase signaling pathway (Maehama and Dixon 1998). One consequence of PTEN loss is hyper-phosphorylation downstream Akt substrates (Cross et al. 1995; del Peso et al. 1997; Kops et al. 1999; Nakamura et al. 2000). Phosphorylation of these proteins can lead to enhanced cell survival, increased cell proliferation and altered cellular metabolism.

Recent studies have shown that many kinases, including rapamycin-sensitive enzymes, promote serine/threonine phosphorylation of IRS-1 that inhibits their function and promotes their degradation (Mothe and Van Obberghen 1996; Rui et al. 2001). Insulin- or IGF-stimulated Akt phosphorylation could be rescued by rapamycin treatment, coincident with restored IRS protein levels. The rapamycin-mediated rescue is blunted by reducing IRS-1 expression with specific siRNAs, and rendered unnecessary by overexpression of IRS-1. Thus, chronic hyperactivation of mTOR by inactivation of TSC1–TSC2 stimulates components of the protein synthesis pathway, while inhibiting the IRS branch of the insulin/IGF-1 signaling cascade (Harrington et al. 2004; Shah et al. 2004; Ueno et al. 2005).

To clarify the role of mTOR *feedback* in prostate cancer, we studied the potential of the IRS-1 antisense oligodeoxinucleotide (ASO) as an inhibitor of proliferation during rapamycin treatment, using the PC-3 cell line, which is reported to be PTEN-negative.

Materials and methods

Antibodies, chemicals and buffers

The reagents and apparatus for sodium dodecyl sulfate-polyacrylamide gel electrophoresis (SDS-PAGE) and immunoblotting were obtained from Bio-Rad (Richmond, CA). Tris-[hydroxymethyl]amino-methane (Tris), phenylmethylsulfonylfluoride (PMSF), dithiothreitol (DTT), Triton X-100, Tween 20 and glycerol were obtained from Sigma Chemical (St Louis, MO, USA). Dimethyl sulfoxide (DMSO) was obtained from Calbiochem (La Jolla, CA, USA). Aprotinin was obtained from Bayer (São Paulo, SP, Brazil). Ketamin was obtained from Parke-Davis (São Paulo, SP, Brazil); diazepam and sodium thiopental were obtained from Cristália (Itapira, SP, Brazil). Protein A-Sepharose 6 MB, nitrocellulose membrane (Hybond ECL, 0.45 μm) and ^{125}I-Protein A were obtained from Amersham (Buckinghamshire, UK). Anti-IRS-1 and anti-IRS-1 phosphoserine 307-specific antibodies were from Santa Cruz Biotechnology (Santa Cruz, CA, USA). Anti-phospho-Akt (Ser473) and anti-phospho-p70 S6K (Thr421/Ser424) antibodies were obtained from New England Biolabs (Beverly, MA, USA). Rapamycin was obtained from LC Laboratories (Woburn, MA, USA).

Phosphorothioate-modified oligonucleotides

Sense and antisense phosphorothioate oligonucleotides specific for IRS-1 (sense (SO), 5′-ACC CAC TCC TAT CCC G-3′ and antisense (ASO), 5′-CGG GAT AGG AGT GGG T-3′) were produced by Invitrogen (Carlsbad, CA). The antisense oligonucleotide sequences were submitted to BLAST analyses (http://www.ncbi.nlm.nih.gov) and matched only for the human IRS-1 coding sequence.

Cell culture

The human prostate cancer cell line PC-3 was obtained from ATCC, Philadelphia, PA, USA. Cells were cultured in RPMI containing 10% fetal bovine serum and glutamine without addition of antibiotics or fungicides; they were maintained at 37°C, 5% CO_2.

Human tumor xenograft models

SCID mice were provided by the State University of Campinas–Central Breeding Center (Campinas, SP, Brazil). SCID mice, 5–6 weeks old and weighing approximately 20–25 g, were implanted with 1.0×10^6 PC-3 cells into the dorsal subcutis of male mice. Mice were weighed twice weekly, and tumor measurements were taken by calipers daily starting on day 0. These tumor measurements were converted to tumor volume (V) using the formula ($V = W^2 \times L \times 0.52$), where W and L are the smaller and larger diameters, respectively, and plotted against time. When the tumors were between 50 and 100 mm^3, the animals were pair-matched into treatment and control groups. Each group contained eight mice, each of which was ear tagged and followed individually throughout the experiment. Initial doses were given on the day of pair matching (day 0). Rapamycin and IRS-1 ASO were administered via i.p. injection daily at the doses indicated. On termination, the mice were weighed and killed, and their tumors were excised. Treatment-related toxicity was evaluated by means of serial weight measurements. All experiments were approved by the Ethics Committee of the State University of Campinas.

Tumor extracts

Mice were anesthetized with sodium amobarbital (15 mg/kg body weight, i.p.), and were used 10–15 min later, i.e. as soon as anesthesia was assured by the loss of pedal and corneal reflexes. Tumors were removed, minced coarsely and

homogenized immediately in extraction buffer (1% Triton-X 100, 100 mM Tris, pH 7.4, containing 100 mM sodium pyrophosphate, 100 mM sodium fluoride, 10 mM EDTA, 10 mM sodium vanadate, 2 mM PMSF and 0.1 mg of aprotinin/ml) at 4°C with a Polytron PTA 20S generator (Brinkmann Instruments model PT 10/35) operated at maximum speed for 30 s. The extracts were centrifuged at 15,000 rpm and 4°C in a Beckman 70.1 Ti rotor (Palo Alto, CA) for 45 min to remove insoluble material, and the supernatants of these tissues were used.

Protein analysis by immunoblotting

The whole tissue extract was treated with Laemmli sample buffer (Laemmli 1970) containing 100 mM DTT and heated in a boiling water bath for 4 min after which they were subjected to SDS-PAGE (6% bis-acrylamide) in a Bio-Rad miniature slab gel apparatus (Mini-Protean, Bio-Rad Laboratories, Inc., Richmond, CA, USA). For total extracts, similar sized aliquots (200 μg protein) were subjected to SDS-PAGE.

Electrotransfer of proteins from the gel to nitrocellulose was performed for 90 min at 120 V (constant) in a Bio-Rad miniature transfer apparatus (Mini-Protean), as described by Towbin et al. (1979), except for the addition of 0.02% SDS to the transfer buffer to enhance the elution of high molecular mass proteins. Nonspecific protein binding to the nitrocellulose was reduced by preincubating the filter overnight at 4°C in blocking buffer (5% nonfat dry milk, 10 mM Tris, 150 mM NaCl and 0.02% Tween 20). The nitrocellulose blot was incubated with the indicated antibodies, diluted in blocking buffer (0.3% BSA instead of nonfat dry milk) overnight at 4°C and then washed for 60 min with blocking buffer without milk. The blots were subsequently incubated with 2 μCi of ^{125}I-protein A (30 μCi/μg) in 10 ml of blocking buffer for 2 h at room temperature and then washed again for 30 min as described above. ^{125}I-Protein A bound to the antiphosphotyrosine and antipeptide antibodies was detected by autoradiography using preflashed Kodak XAR film with Cronex Lightning Plus intensifying screens at −80°C for 12–48 h. Band intensities were quantified by optical densitometry of developed autoradiographs (Scion Image software, Scion Corporation, Frederick, MD, USA).

Immunohistochemistry

To detect proliferating cell nuclear antigen (PCNA), microwave post fixation was carried out using a domestic oven (Panasonic Junior, Sao Jose dos Campos, SP, Brazil) at 700 W, which was delivered to slides immersed in 0.01 mol/l citrate buffer, pH 6.0, in twice doses during 7 min separated by a break of 2 min, which allowed for buffer replenishment. The slides were allowed to cool to room temperature before being removed from the oven. Sections were then incubated at room temperature for 1 h with primary antibody PC10 (Dako North America, Inc., Carpinteria, CA, USA) diluted 1:150. Biotinylated horse mouse antihuman (Dako) antibodies for PC10 were applied for 1 h at room temperature. The slides were then incubated with avidin–biotin complex (ABC) reagent (Vector) for 30 min followed by the addition of diaminobenzidine tetrahydrochloride (DAB) (Sigma) as a substrate-chromogen solution. After hematoxylin counterstaining and dehydration, the slides were mounted in Entellan (Merck, Darmstadt, Germany). The experiments were done, at least, in triplicate for each mouse.

A TUNEL apoptosis detection kit (Upstate Biotechnology, Inc., Lake Place, NY, USA) was used for DNA fragmentation fluorescence staining according to the manufacturer's protocol. Following the extraction, the tissue extracts were fixed with 4% paraformaldehyde in 0.1 M NaH_2PO_4, pH 7.4, and incubated with a reaction mix containing biotin-dUTP and terminal deoxynucleotidyl transferase for 60 min. Fluorescein-conjugated avidin was applied to the sample, which was then incubated in the dark for 30 min. Positively stained fluorescein-labeled cells were visualized and photographed by fluorescence microscopy.

Statistical analysis

All groups were studied in parallel. Comparisons between different groups were performed by employing ANOVA, as appropriate. The level of significance adopted was $P < 0.05$.

Results

Effects of treatment with rapamycin and/or IRS-1 ASO, on Akt/mTOR signaling pathway in PC-3 xenografts

To evaluate IRS-1 ASO activity, we performed experiments using samples from PC-3 xenografts, immunoblotted with anti IRS-1 (Fig. 1a). There was an evident decrease in IRS-1 protein levels within 48 h after ASO treatment, which was maximal at 72 h after IRS-1 ASO treatment, representing a reduction in the IRS-1 protein level of ∼75% (Fig. 1a, upper panel). The ASO-mediated IRS-1 inhibition in PC-3 xenografts was dose dependent (Fig. 1b). The inhibition of IRS-1 protein levels was detected after the injection of 0.4 nmol/kg, while inhibition was observed with 0.8 nmol/kg of IRS-1 ASO, representing a reduction in the IRS-1 protein level of ∼70% (Fig. 1b, upper panel). There was no change in IRS-1 protein levels after IRS-1 sense oligonucleotide (SO) treatment (Fig. 1a, b, middle panel).

Immunoblotting experiments were conducted to determine the effects of rapamycin, IRS-1 ASO, and the combination of both on IRS-1 serine phosphorylation in PC-3

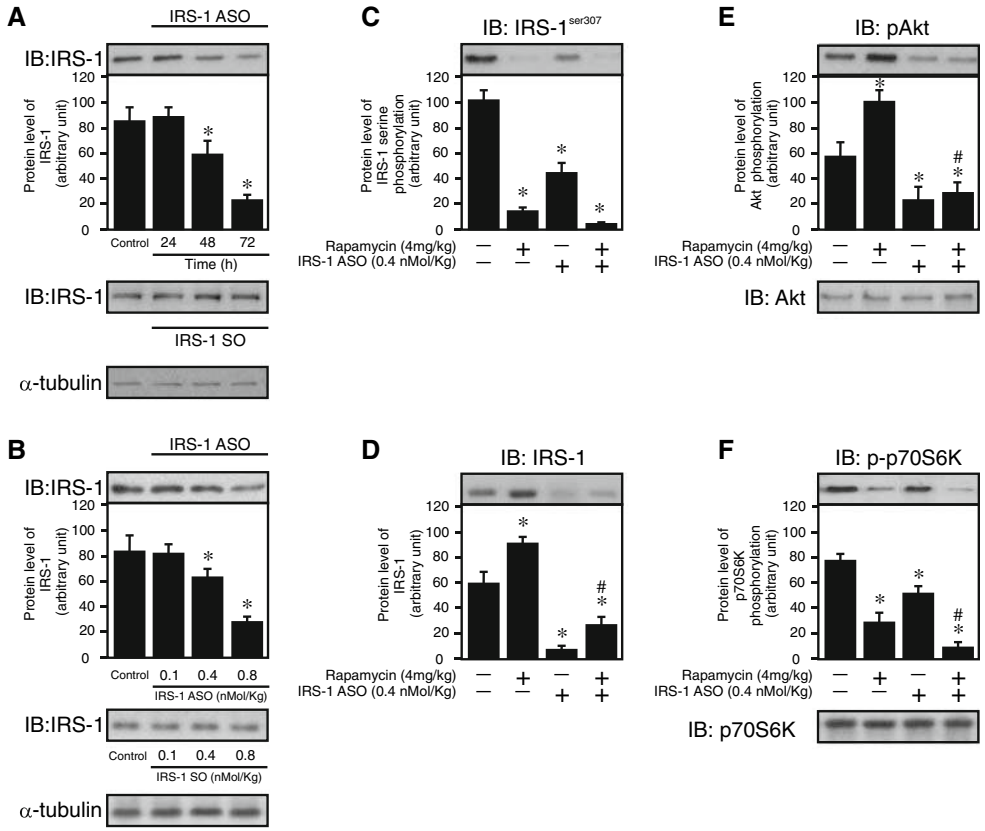

Fig. 1 Phosphorylation status of IRS-1, Akt and p70S6k proteins after treatment with rapamycin and IRS-1 antisense oligonucleotide (IRS-1 ASO) alone, and with the combination of rapamycin and IRS-1 ASO. (**a**, *upper panel*) The time course was performed with SCID mice treated i.p. with 0.4 nmol/kg of IRS-1 ASO, as indicated. At the time-points indicated, after the treatment, they were anesthetized and a fragment from xenograft was removed. Similar treatments were carried out with the IRS-1 SO (**a**, *middle panel*). Loading control with anti-α-tubulin antibodies (**a**, *lower panel*). **b** In a dose response experiment, SCID mice were treated i.p. with varying doses of IRS-1 ASO or with vehicle, as indicated. After 72 h, they were anesthetized, and fragments from xenograft and liver were removed. Similar treatments were carried out with the IRS-1 SO (**b**, *middle panel*). Loading control with anti-α-tubulin antibodies (**b**, *lower panel*). **c–f** Representative Western blots of five independent experiments showing PC-3 lysates. The lysates were immunoblotted (IB) with anti-IRS-1 phospho-serine$^{(307)}$ (**c**), anti-IRS-1 antibodies (**d**), anti-phospho-Akt (pAkt) (**e**, *upper panel*), anti-Akt (**e**, *lower panel*), anti-phospho-p70S6k (p-p70S6k) (**f**, *upper panel*) and anti-p70S6k antibodies (**f**, *lower panel*). *Bars* represent means ± SEM. $^{\#}P < 0.05$ versus rapamycin and $^{*}P < 0.05$ versus control

xenografts (Fig. 1c). Thus, with isolated rapamycin, there was a significant decrease in IRS-1 serine phosphorylation when compared to the control group. The isolated IRS-1 ASO inhibited partially the IRS-1 serine phosphorylation, while the simultaneous treatment with rapamycin and the IRS-1 ASO showed inhibition of IRS-1 serine phosphorylation similar to the treatment with rapamycin alone. There was an increase in IRS-1 protein levels with rapamycin treatment. On the other hand, the isolated administration of IRS-1 ASO strongly decreased IRS-1 protein levels. We observed that IRS-1 ASO blocked the effect of rapamycin on IRS-1 protein expression (Fig. 1d). Isolated rapamycin induced increases in the serine phosphorylation of Akt, compared to the control group. The IRS-1 ASO induced decreases in the phosphorylation of Akt protein; in addition, we observed that IRS-1 ASO blocked the effect of rapamycin on Akt phosphorylation (Fig. 1e). There were no changes in Akt protein levels. Conversely, the isolated treatment with rapamycin induced a great decrease in p70S6k phosphorylation; ASO treatment decreased p70S6k phosphorylation to a small extent compared to rapamycin. The association of both treatments acted synergistically in the reduction of p70S6k phosphorylation, which was significantly lower than each compound alone. There were no changes in p70S6k protein levels.

Effects of treatment with rapamycin and/or IRS-1 ASO on growth of PC-3 xenografts

As shown in Fig. 2, exposure of PC-3 xenografts to isolated IRS-1 ASO resulted in a weak decrease in tumor growth during the experimental period. Rapamycin-treated group showed an important decrease in growth, with a very low velocity of growth. Meanwhile, the combination of rapamycin and IRS-1 ASO enhanced the inhibitory effect on tumor growth, resulting in no important change in tumor

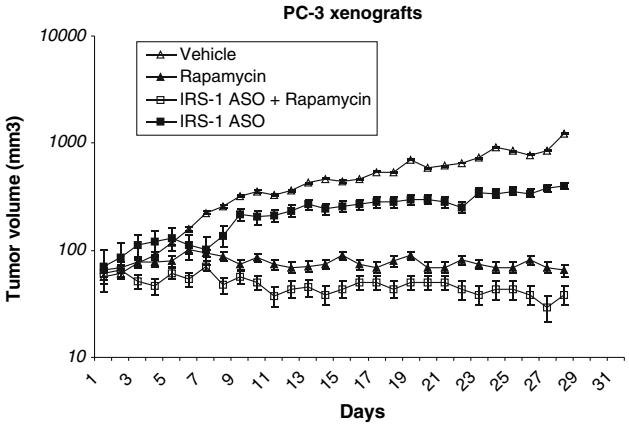

Fig. 2 Growth curves for xenografts derived from PC-3 cells. Rapamycin (4 mg/kg i.p.), IRS-1 ASO (0.4 nmol) or the combination of rapamycin and IRS-1 ASO (4 mg/kg and 0.4 nmol, respectively) were injected daily in mice bearing PC-3 xenografts. Control mice received a similar schedule of the vehicle solution. Points and means for at least eight tumors

volume in the frame shift period of study. No substantial weight loss was observed in any of the groups throughout the 30 days of analysis.

Effects of treatment with rapamycin and/or IRS-1 ASO on proliferation and apoptosis of PC-3 xenografts

We performed immunohistochemistry to detect PCNA, a proliferation index (Fig. 3a). The observed percent of PCNA-positive cells was 45.9 ± 5.2% in the control group. IRS-1 ASO and rapamycin administration significantly reduced the percent of positive cells to 36.6 ± 6.8% and 24.5 ± 4.7%, respectively ($P < 0.05$, for both). The group treated with the combination of rapamycin and IRS-1 ASO was found to be 4.3 ± 3.2% in positive cells. Compared to the control group, the combination of rapamycin- and IRS-1 ASO-treated group showed ±90% of reduction in positive cells ($P < 0.001$). IRS-1 ASO plus rapamycin enhanced the effectiveness of rapamycin by 570%.

To analyze the mechanism responsible for the growth inhibition of PC-3 cells by rapamycin and IRS-1 ASO, the effects of rapamycin and/or IRS-1 ASO on programmed cell death was examined. Thus, DNA fragmentation was measured by TUNEL assay in PC-3 xenografts (Fig. 3b). In relation to the control group, the IRS-1 ASO- and rapamycin-treated groups showed about 4- and 23-fold greater positive cells, respectively ($P < 0.05$, for both). The combination of rapamycin and IRS-1 ASO promoted a 37-fold increase in apoptotic cell number, when compared to the control group ($P < 0.001$), and an up to 2-fold increase compared with that of rapamycin ($P < 0.05$).

Discussion

PTEN alterations have been robustly implicated in human prostate cancer, with PTEN deletions and/or mutations of at least one allele observed in up to 60% of primary prostate cancers, while homozygous PTEN inactivation is more frequently associated with metastatic prostate tissues (Cairns et al. 1997; Gray et al. 1995; Suzuki et al. 1998). In the present study, we show that IRS-1 ASO and rapamycin cooperatively antagonize the activation of mTOR in vivo and act synergistically in tumor suppression in PC-3 prostate cancer xenografts, which do not express PTEN. Our results show that IRS-1 ASO alone reduces the activation of PI 3-kinase pathway, while rapamycin alone reduces the activation of mTOR. Combined treatment with rapamycin

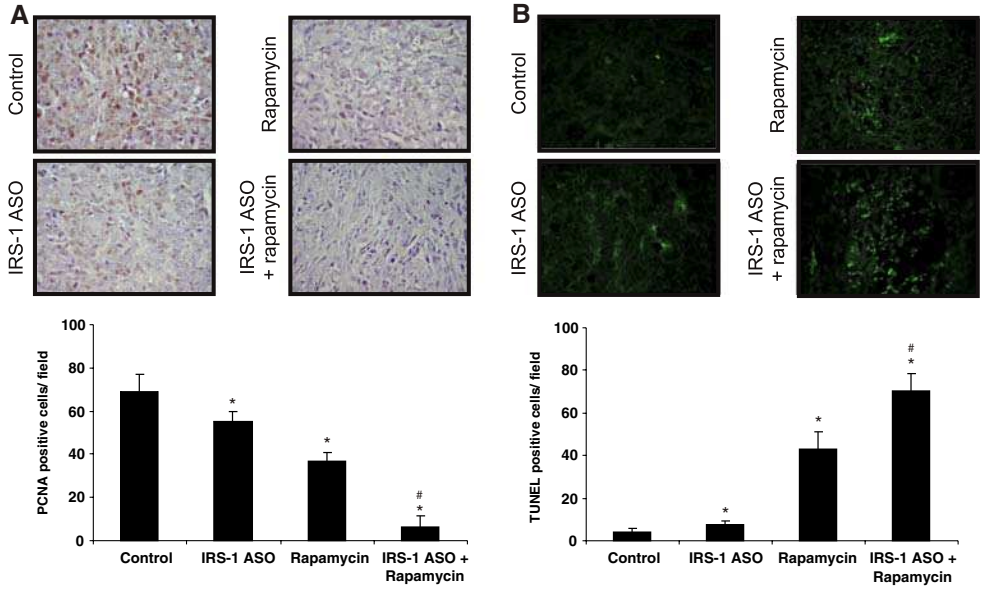

Fig. 3 Effects of vehicle, rapamycin (4 mg/kg i.p.), IRS-1 ASO (0.4 nmol/kg) or the combination of rapamycin and IRS-1 ASO (4 mg/kg and 0.4 nmol, respectively) on cell proliferation (**a**) and on apoptosis (**b**) in PC-3 xenografts. *Bars* represent means ± SEM calculated from PCNA and TUNEL positive cells counted in four fields. $^{\#}P < 0.05$ versus rapamycin and $^{*}P < 0.05$ versus control

and IRS-1 ASO leads to a quantitative inhibition of molecular signaling through the PI 3-kinase pathway. In accordance with these data, the proliferation of PC-3 xenografts after treatment with IRS-1 ASO combined with rapamycin was more pronounced than treatment with each alone.

Tyrosine-phosphorylated IRS-1 proteins are known to bind efficiently a number of SH2 domain-containing proteins involved in activation of downstream signaling pathways, including PI 3-K p85, GRB2, SHP-2, Nck and Crk (for review, see Saltiel and Kahn 2001). There is increasing interest in the potential role of IRS-1 in oncogenesis. Overexpression of IRS-1 in NIH3T3 fibroblasts leads to increased activation of the Ras-MAPK cascade and cell transformation (Ito et al. 1996; Tanaka et al. 1996). IRS-1 overexpression also contributes to the progression of hepatocellular carcinoma, possibly by inhibiting transforming growth factor β1-mediated apoptosis (Tanaka and Wands 1996). Although the LNCaP prostate cancer cell line does not express IRS-1 or IRS-2, introduction of either protein in combination with IGF-IR converts these cells to a more aggressive phenotype (Reiss et al. 2000). A recent study examining endogenous IRS-1 shows that it is constitutively tyrosine-phosphorylated in a wide range of human tumor samples, suggesting that IRS-1 activation may be a common phenomenon in tumors (Chang et al. 2002). Moreover, a relationship between IRS-1 activation and fusion oncoproteins has already been established. TRK-T1 (Miranda et al. 2001) and BCR-ABL (Traina et al. 2003) have both been shown to bind IRS-1 and to be associated with increased IRS-1 tyrosine phosphorylation. Therefore, IRS-1 activation may be a more general mechanism for transformation. We found that inhibition of IRS-1 by IRS-1 ASO can lead to a decrease in the growth of PC-3 xenografts. Our data demonstrate that lowering IRS-1 content leads to a decrease in the number of docking sites for maximal activation of PI 3-kinase-Akt-mTOR cascade, as shown by a reduction of Akt and p70S6k phosphorylation, respectively, further suggesting that IRS-1 is important for PC-3 xenografts growth.

The primary pathway by which most growth factors and cytokines activate mTOR and its downstream targets appears to be the PI 3-kinase/Akt pathway (for review, see Fingar and Blenis 2004). Recent reports have shown that, in absence of TSC2 or in hiperinsulinemic situations, IRS-1 increases its serine phosphorylation in parallel with a reduction in its protein levels. Importantly, all the studies found that long term treatment with rapamycin completely restores IRS-1 protein levels and the insulin/IGF-1 responsiveness of PI 3-kinase Akt pathway (Harrington et al. 2004; Shah et al. 2004; Ueno et al. 2005). In agreement with these studies, our results show an increase in IRS-1 serine phosphorylation as well as a reduction in protein levels in PC-3 xenografts; moreover, the treatment with rapamycin restored IRS-1 levels and activity in the PC-3 xenografts as demonstrated. Furthermore, PC-3 xenografts treated with both IRS-1 ASO and rapamycin exhibit a strong attenuation of the PI 3-kinase pathway. Altogether, these data suggest that loss of PTEN expression in PC-3 xenografts triggers a feedback inhibition of Akt signaling, which is reversed by rapamycin and IRS-1 ASO can overcome.

In addition to the down-regulation of the PI 3-kinase/Akt pathway, continuous treatment with IRS-1 ASO for 4 weeks resulted in significant tumor growth delay, and the treatment with IRS-1 ASO plus rapamycin strongly inhibited cell proliferation and induced apoptosis. The suppression of the PI 3-kinase/Akt pathway in these tumors might potentially result in the reduction of protein synthesis, cell growth and proliferation downstream of mTOR through inactivation of p70S6k and activation of 4E-BP1 (Fingar and Blenis 2004; Fingar et al. 2002; Jefferies et al. 1997).

Based on these results, we propose a model for the synergism between IRS-1 ASO and rapamycin in suppressing growth in PC-3 cells lacking PTEN (Fig. 4a). According to

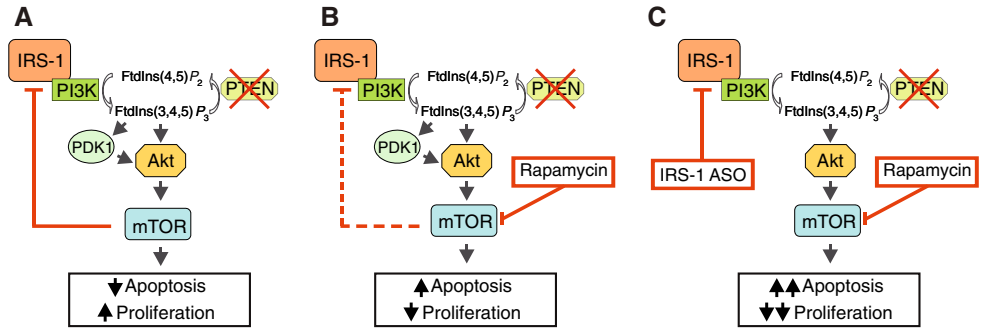

Fig. 4 Model for IRS-1 ASO and rapamycin synergism in PC-3 xenografts. **a** mTOR feedback in PC-3 xenografts. The activated mTOR inhibits IRS-1 signaling towards PI 3-kinase. **b** Rapamycin treatment. Rapamycin inhibits mTOR and activates IRS-1 signaling towards PI 3-kinase. **c** Treatment with combination of IRS-1 ASO and rapamycin. The simultaneous treatment with IRS-1 ASO and rapamycin delivers an additional signal, which leads to enhanced apoptosis and diminished proliferation

this model, rapamycin alone induces mTOR inhibition, which is rapidly followed by IRS-1 activation (Fig. 4b). IRS-1 ASO, in turn, inhibits the expression of IRS-1 and has the same role as mTOR feed back. Thus, the combination of IRS-1 ASO with rapamycin provides an additive signal inhibition, which leads to enhanced apoptosis and diminished proliferation (Fig. 4c).

In conclusion, our data demonstrate that the addition of agents that block IRS-1 potentiate the effect of mTOR inhibition in the growth of PC-3 xenografts.

Acknowledgments These studies were supported by grants from Fundacão de Amparo à Pesquisa do Estado de São Paulo (FAPESP) and Conselho Nacional de desenvolvimento científico e tecnológico (CNPq). We thank Dr. Nicola Conran for English language editing.

References

Cairns P, Okami K, Halachmi S et al (1997) Frequent inactivation of PTEN/MMAC1 in primary prostate cancer. Cancer Res 57:4997–5000

Chang Q, Li Y, White MF, Fletcher JA, Xiao S (2002) Constitutive activation of insulin receptor substrate 1 is a frequent event in human tumors: therapeutic implications. Cancer Res 62:6035–6038

Cross DA, Alessi DR, Cohen P, Andjelkovich M, Hemmings BA (1995) Inhibition of glycogen synthase kinase-3 by insulin mediated by protein kinase B. Nature 378:785–789

del Peso L, Gonzalez-Garcia M, Page C, Herrera R, Nunez G (1997) Interleukin-3-induced phosphorylation of BAD through the protein kinase Akt. Science 278:687–689

Dennis PB, Jaeschke A, Saitoh M, Fowler B, Kozma SC, Thomas G (2001) Mammalian TOR: a homeostatic ATP sensor. Science 294:1102–1105

Fingar DC, Blenis J (2004) Target of rapamycin (TOR): an integrator of nutrient and growth factor signals and coordinator of cell growth and cell cycle progression. Oncogene 23:3151–3171

Fingar DC, Salama S, Tsou C, Harlow E, Blenis J (2002) Mammalian cell size is controlled by mTOR and its downstream targets S6K1 and 4EBP1/eIF4E. Genes Dev 16:1472–1487

Gray IC, Phillips SM, Lee SJ, Neoptolemos JP, Weissenbach J, Spurr NK (1995) Loss of the chromosomal region 10q23–25 in prostate cancer. Cancer Res 55:4800–4803

Harrington LS, Findlay GM, Gray A et al (2004) The TSC1–2 tumor suppressor controls insulin-PI3K signaling via regulation of IRS proteins. J Cell Biol 166:213–223

Huang S, Houghton PJ (2002) Inhibitors of mammalian target of rapamycin as novel antitumor agents: from bench to clinic. Curr Opin Investig Drugs 3:295–304

Inoki K, Li Y, Xu T, Guan KL (2003) Rheb GTPase is a direct target of TSC2 GAP activity and regulates mTOR signaling. Genes Dev 17:1829–1834

Ito T, Sasaki Y, Wands JR (1996) Overexpression of human insulin receptor substrate 1 induces cellular transformation with activation of mitogen-activated protein kinases. Mol Cell Biol 16:943–951

Jefferies HB, Fumagalli S, Dennis PB, Reinhard C, Pearson RB, Thomas G (1997) Rapamycin suppresses 5'TOP mRNA translation through inhibition of p70s6k. EMBO J 16:3693–3704

Jemal A, Siegel R, Ward E, Murray T, Xu J, Thun MJ (2007) Cancer statistics, 2007. CA Cancer J Clin 57:43–66

Kops GJ, de Ruiter ND, De Vries-Smits AM, Powell DR, Bos JL, Burgering BM (1999) Direct control of the Forkhead transcription factor AFX by protein kinase B. Nature 398:630–634

Laemmli UK (1970) Cleavage of structural proteins during the assembly of the head of bacteriophage T4. Nature 227:680–685

Lawlor MA, Alessi DR (2001) PKB/Akt: a key mediator of cell proliferation, survival and insulin responses? J Cell Sci 114:2903–2910

Maehama T, Dixon JE (1998) The tumor suppressor, PTEN/MMAC1, dephosphorylates the lipid second messenger, phosphatidylinositol 3,4,5-trisphosphate. J Biol Chem 273:13375–13378

Majumder PK, Febbo PG, Bikoff R et al (2004) mTOR inhibition reverses Akt-dependent prostate intraepithelial neoplasia through regulation of apoptotic and HIF-1-dependent pathways. Nat Med 10:594–601

Miranda C, Greco A, Miele C, Pierotti MA, Van Obberghen E (2001) IRS-1 and IRS-2 are recruited by TrkA receptor and oncogenic TRK-T1. J Cell Physiol 186:35–46

Mothe I, Van Obberghen E (1996) Phosphorylation of insulin receptor substrate-1 on multiple serine residues, 612, 632, 662, and 731, modulates insulin action. J Biol Chem 271:11222–11227

Nakamura N, Ramaswamy S, Vazquez F, Signoretti S, Loda M, Sellers WR (2000) Forkhead transcription factors are critical effectors of cell death and cell cycle arrest downstream of PTEN. Mol Cell Biol 20:8969–8982

Petrylak DP, Tangen CM, Hussain MH et al (2004) Docetaxel and estramustine compared with mitoxantrone and prednisone for advanced refractory prostate cancer. N Engl J Med 351:1513–1520

Reiss K, Wang JY, Romano G et al (2000) IGF-I receptor signaling in a prostatic cancer cell line with a PTEN mutation. Oncogene 19:2687–2694

Rui L, Fisher TL, Thomas J, White MF (2001) Regulation of insulin/insulin-like growth factor-1 signaling by proteasome-mediated degradation of insulin receptor substrate-2. J Biol Chem 276:40362–40367

Sabatini DM (2006) mTOR and cancer: insights into a complex relationship. Nat Rev Cancer 6:729–734

Saltiel AR, Kahn CR (2001) Insulin signalling and the regulation of glucose and lipid metabolism. Nature 414:799–806

Sansal I, Sellers WR (2004) The biology and clinical relevance of the PTEN tumor suppressor pathway. J Clin Oncol 22:2954–2963

Shah OJ, Wang Z, Hunter T (2004) Inappropriate activation of the TSC/Rheb/mTOR/S6K cassette induces IRS1/2 depletion, insulin resistance, and cell survival deficiencies. Curr Biol 14:1650–1656

Suzuki H, Freije D, Nusskern DR et al (1998) Interfocal heterogeneity of PTEN/MMAC1 gene alterations in multiple metastatic prostate cancer tissues. Cancer Res 58:204–209

Tanaka S, Ito T, Wands JR (1996) Neoplastic transformation induced by insulin receptor substrate-1 overexpression requires an interaction with both Grb2 and Syp signaling molecules. J Biol Chem 271:14610–14616

Tanaka S, Wands JR (1996) Insulin receptor substrate 1 overexpression in human hepatocellular carcinoma cells prevents transforming growth factor beta1-induced apoptosis. Cancer Res 56:3391–3394

Tannock IF, de Wit R, Berry WR et al (2004) Docetaxel plus prednisone or mitoxantrone plus prednisone for advanced prostate cancer. N Engl J Med 351:1502–1512

Towbin H, Staehelin T, Gordon J (1979) Electrophoretic transfer of proteins from polyacrylamide gels to nitrocellulose sheets: procedure and some applications. Proc Natl Acad Sci USA 76:4350–4354

Traina F, Carvalheira JB, Saad MJ, Costa FF, Saad ST (2003) BCR-ABL binds to IRS-1 and IRS-1 phosphorylation is inhibited by imatinib in K562 cells. FEBS Lett 535:17–22

Ueno M, Carvalheira JB, Tambascia RC et al (2005) Regulation of insulin signalling by hyperinsulinaemia: role of IRS-1/2 serine phosphorylation and the mTOR/p70 S6K pathway. Diabetologia 48:506–518

Yenush L, White MF (1997) The IRS-signalling system during insulin and cytokine action. Bioessays 19:491–500

APÊNDICE *XIV*

Available online at www.sciencedirect.com
ScienceDirect
Metabolism Clinical and Experimental 57 (2008) 57 – 65
Metabolism
Clinical and Experimental
www.elsevier.com/locate/metabol

Statin modulates insulin signaling and insulin resistance in liver and muscle of rats fed a high-fat diet

Cristina Alba Lalli, José Rodrigo Pauli, Patrícia Oliveira Prada, Dennys Esper Cintra, Eduardo Rochette Ropelle, Lício Augusto Velloso, Mario José Abdalla Saad*

Departamento de Clínica Médica, FCM, Universidade Estadual de Campinas (UNICAMP) 13081-970 Campinas, SP, Brazil

Received 16 February 2007; accepted 12 July 2007

Abstract

Recent studies have shown that statins might have relevant effects on insulin resistance in animal models and in humans. However, the molecular mechanisms that account for this improvement in insulin sensitivity are not well established. The aim of the present study was to investigate the effect of a statin on insulin sensitivity and insulin signaling in liver and muscle of rats fed on a high-fat diet (HFD) for 4 weeks, treated or not with lovastatin during the last week. Our data show that treatment with lovastatin results in a marked improvement in insulin sensitivity characterized by an increase in glucose disappearance rate during the insulin tolerance test. This increase in insulin sensitivity was associated with an increase in insulin-induced insulin receptor (IR) tyrosine phosphorylation and, in parallel, a decrease in IR serine phosphorylation and association with PTP1B. Our data also show that lovastatin treatment was associated with an increase in insulin-stimulated insulin receptor substrate (IRS) 1/phosphatidylinositol 3-kinase/Akt pathway in the liver and muscle of HFD-fed rats in parallel with a decrease in the inflammatory pathway (c-jun N-terminal kinase and I kappa β kinase (IKKβ)/inhibitor of κB/nuclear factor κB) related to insulin resistance. In summary, statin treatment improves insulin sensitivity in HFD-fed rats by reversing the decrease in the insulin-stimulated IRS-1/phosphatidylinositol 3-kinase/Akt pathway in liver and muscle. The effect of statins on insulin action is further supported by our findings that HFD rats treated with statin show a reduction in IRS-1 serine phosphorylation, I kappa kinase (IKK)/inhibitor of κB/nuclear factor κB pathway, and c-jun N-terminal kinase activity, associated with an improvement in insulin action. Overall, these results provide important new insight into the mechanism of statin action in insulin sensitivity.

1. Introduction

Insulin uses 2 main signaling pathways, the phosphatidylinositol 3-kinase (PI3K)-AKT/protein kinase B (PKB) pathway, which is responsible for most of the metabolic actions of the hormone, and the Ras–mitogen-activated protein kinase pathway, which regulates expression of some genes and cooperates with the PI3K pathway to control cell growth and differentiation [1]. The (PI3K)-AKT pathway initiates when the insulin receptor (IR) undergoes autophosphorylation after insulin binding and phosphorylates a number of intracellular proteins including IR substrate proteins (IRSs; IRS-1 and IRS-2 are the most important) [2]. After tyrosine phosphorylation, IRS-1 and IRS-2 bind and activate the PI3K [2,3]. Downstream to PI3K, activation of a serine/threonine kinase (Akt) occurs, which in turn stimulates glucose transport in the muscle and adipose tissue, stimulates glycogen synthesis in the liver and muscle, and stimulates lipogenesis in the adipose tissue [4]. Therefore, the PI3K/Akt pathway has an important role in the metabolic effects of insulin.

An important mechanism that may contribute to the dysregulation of the insulin-signaling pathway includes serine 307 (Ser^{307}) phosphorylation of IRS proteins by c-jun N-terminal kinase (JNK) [5]. The JNK is a member of the mitogen-activated protein kinase family [6,7] and can be activated by tumor necrosis factor α [8] and interleukin 1β [9,10], both proinflammatory cytokines. Serine 307 is located next to the phosphotyrosine (pY)-binding domain in IRS-1, and its phosphorylation inhibits the interaction of the pY-binding domain with the phosphorylated NPEY motif in the activated IR, causing insulin resistance [11].

* Corresponding author. Department of Internal Medicine, FCM-UNICAMP, 13081-970 Campinas SP, Brazil. Fax: +55 19 3521 8950.
E-mail address: msaad@fcm.unicamp.br (M.J.A. Saad).

0026-0495/$ – see front matter © 2008 Elsevier Inc. All rights reserved.
doi:10.1016/j.metabol.2007.07.021

Furthermore, JNK might serve as a feedback inhibitor during insulin stimulation [5,11].

In rodents and humans, the dietary intake of high amounts of fat has been shown to be associated with increased adiposity and insulin resistance [12]. A recent study has shown that a high-fat diet (HFD) induces a tissue-specific regulation of glucose transport with reduced glucose uptake and insulin signaling in muscle that is accompanied by an increased insulin-stimulated glucose uptake in adipose tissue [13]. In this context, insulin resistance could be tissue specific to the muscle, liver, and hypothalamus, whereas adipose tissue remains sensitive to insulin.

Another mechanism involved in HFD-dependent insulin resistance is the activation of the proinflammatory I kappa β kinase (IKKβ)/inhibitor of κB (IκB)/nuclear factor κB (NFκB) pathway [14-16]. I kappa kinase (IKK) is a serine kinase; and its activation phosphorylates the IκB, a cytoplasmic protein that inhibits nuclear translocation of NFκB, a family of transcription factors that function as homo- or heterodimers in the regulation of the expression of proinflammatory, immunomodulatory, and antiapoptotic genes [17]. After its phosphorylation, IκB is ubiquitinated and degraded in the proteosome, releasing NFκB for translocation to the nucleus and activation of gene expression. It has been proposed that NFκB-increased activation may play an important role in the pathogenesis of insulin resistance [14-17].

Since their discovery in the early 1970s, statins have been used to lower cholesterol, acting as 3-hydroxy-3-methylglutaryl coenzyme A reductase inhibitors [18,19]. However, recent studies have shown that statins might have additional relevant effects on insulin resistance in animal models [20,21] and in humans [22,23]. However, the molecular mechanisms that account for this improvement in insulin sensitivity are not yet well established. The aim of the present study is to investigate the effect of a statin on insulin sensitivity and insulin signaling in the liver and muscle of HFD-fed rats.

2. Materials and methods

2.1. Materials

Male Wistar rats were provided by the State University of Campinas-Central Breeding Center (Campinas, SP, Brazil). Antiphosphotyrosine and anti-IR (αIR) antibodies anti–IRS-1, anti-Akt1/2, and anti-pJNK were from Santa Cruz Technology (Santa Cruz, CA). Anti-pAkt was from Cell Signaling Technology (Beverly, MA). Anti-PI3K and anti–phospho-IRS-1^{ser307} were obtained from Upstate Biotechnology (Lake Placid, NY). Human recombinant insulin (Humulin R) was purchased from Eli Lilly (Indianapolis, IN). Routine reagents were purchased from Sigma Chemical (St Louis, MO) unless otherwise specified. [^{125}I]-Protein A was from Amersham Biosciences Group (Little Chalfont, United Kingdom).

2.2. Animals

Four-week-old male Wistar rats were randomly divided into 3 groups with similar body weights and fed for 4 weeks: control group (C), fed standard rodent chow and water ad libitum (protein, 20 kcal%; carbohydrate, 70 kcal%; lipid, 10 kcal%); HFD group, fed a fat-rich chow and water ad libitum (protein, 20 kcal%; carbohydrate, 35 kcal%; lipid, 45 kcal%, predominantly in the form of lard); and lovastatin group (L), fed a fat-rich chow and water ad libitum and treated daily with lovastatin (6 mg/kg) by oral gavage at night during the last week of the experiment. All experiments were approved by the Ethics Committee of the State University of Campinas.

2.3. Methods

2.3.1. Tissue extraction and immunoprecipitation

Food was withdrawn 12 to 14 hours before the experiments. One hour before the procedure, the animal received the last dose of drug or vehicle. Rats were anesthetized with sodium thiopental (25 mg/kg body weight, intraperitoneally) and were used 10 to 15 minutes later, that is, as soon as anesthesia was ensured by the loss of pedal and corneal reflexes. The abdominal cavity was opened, the cava vein was exposed, and 0.5 mL of isotonic sodium chloride solution or insulin (6 μg) was injected. Fragments of liver and soleus muscle were then collected at 30 and 90 seconds, respectively. The fragments were minced coarsely and homogenized immediately in extraction buffer (1% Triton-X 100, 100 mmol/L Tris [pH 7.4] containing 100 mmol/L sodium pyrophosphate, 100 mmol/L sodium fluoride, 10 mmol/L EDTA, 10 mmol/L sodium vanadate, 2 mmol/L phenylmethylsulfonyl fluoride, and 0.1 mg of aprotinin per milliliter) at 4°C with a Polytron PTA 20S generator (model PT 10/35; Brinkmann Instruments, Littau-Luzern, Switzerland) operated at maximum speed for 30 seconds. The extracts were centrifuged at 15 000 rpm and 4°C in a Beckman 70.1 Ti rotor (Palo Alto, CA) for 45 minutes to remove insoluble material, and aliquots of the resulting supernatants containing 2.0 mg of total protein of these tissues were used for immunoprecipitation with 10 μL of polyclonal antibodies: anti-αIR, αIRS-1, anti-Akt (Cell Signaling Technology), anti–phospho-[Thr183]-JNK, anti–phospho-IRS-1^{ser307}, and anti-IκBα and Protein A Sepharose 6MB or Protein A/G Plus (Pharmacia, Uppsala, Sweden). Tissue extraction and immunoprecipitation overnight were followed by sodium dodecyl sulfate polyacrylamide gel electrophoresis (SDS-PAGE), transfer to nitrocellulose membranes, and blotting with anti-pY, αIR, anti–IRS-1, or anti-p85/PI3 kinase antibodies.

2.3.2. Protein analysis by immunoblotting

The precipitated proteins and/or whole-tissue extracts were treated with Laemmli sample buffer [24] containing 100 mmol/L dithiothreitol and heated in a boiling water bath for 5 minutes, after which they were subjected to SDS-PAGE in a Bio-Rad (Hercules, CA) miniature slab gel apparatus

Table 1
Serum insulin and plasma fasting glucose levels

	C	HFD	L
Plasma glucose (mg/dL)	95 ± 11	118 ± 6	112 ± 11
Serum insulin (ng/mL)	2.22 ± 0.12 *	3.76 ± 0.24 **	2.68 ± 0.08

Serum insulin and plasma glucose levels. Data are expressed as mean ± SEM. Each group was composed of 6 animals.
* $P < .001$: C vs HFD.
** $P < .05$: HFD vs L.

(Mini-Protean). For total extracts, 250 μg of proteins were subjected to SDS-PAGE. Electrotransfer of proteins from the gel to nitrocellulose was performed for 120 minutes at 120 V in a Bio-Rad Mini-Protean transfer apparatus [25]. Nonspecific protein binding to the nitrocellulose was reduced by preincubating the filter for 2 hours in blocking buffer (5% nonfat dry milk, 10 mmol/L Tris, 150 mmol/L NaCl, 0.02% Tween 20). The nitrocellulose blot was incubated with specific antibodies overnight at 4°C and then incubated with 2 mCi FS[^{125}I]-labeled protein A (30μCi/μg). The results were visualized by autoradiography with preflashed Kodak XAR film (Manaus, Amazonas-Brazil). Band intensities were quantified by optical densitometry (model GS300; Hoefer Scientific Instruments, San Francisco, CA).

2.3.3. Insulin tolerance test

All the 3 groups were submitted to an intravenous insulin tolerance test (1 U/kg body weight of insulin, intravenously); and samples for blood glucose measurements were collected at 0 (basal), 4, 8, 12, and 16 minutes after injection. Rats were anesthetized with sodium thiopental (25 mg/kg body weight, intraperitoneally) as described above, 40μL of blood was collected from their tails, and blood glucose concentration was measured by the glucose-oxidase method. Thereafter, the rate constant for plasma glucose disappearance (K_{itt}) was calculated using the formula $0.693/(t_{1/2})$. The plasma glucose $t_{1/2}$ was calculated from the slope of the least squares analysis of the plasma glucose concentrations during the linear phase of decline [26].

2.3.4. Serum insulin analysis

Serum insulin levels were analyzed by radioimmunoassay, as previously described [27].

2.3.5. Statistical analysis

All groups of animals were studied in parallel. Comparisons between different groups were performed by using Student *t* test for unpaired samples and analysis of variance as appropriate. The level of significance adopted was $P < .05$.

3. Results

3.1. Animal characteristics

Body weights were higher in HFD-fed rats than in the control group (HFD: 412 ± 5 g vs C: 347 ± 12 g, $P < .05$) and in the lovastatin group compared with control rats (L: 426 ± 20 g vs C: 347 ± 12 g, $P < .05$). The body weights of HFD-fed rats and the rats of the lovastatin group were not statistically different. The insulin levels in HFD-fed animals were higher than those in the control group (C: 2.22 ± 0.12 ng/mL vs HFD: 3.76 ± 0.24 ng/mL, $P < .001$). The group fed on the diet and treated with lovastatin presented insulin levels that were similar to those of the controls and statistically different from the animals fed the HFD (HFD: 3.76 ± 0.24 ng/mL vs L: 2.68 ± 0.08 ng/mL, $P < .05$). We did not find any difference in fasting plasma glucose concentrations between the 3 groups. Table 1 shows the results of serum insulin and fasting plasma glucose.

The HFD animals were more insulin resistant than the control rats, as expressed by their lower plasma glucose disappearance rates measured by the insulin tolerance test (K_{itt}) (C: 4.3%/min ± 0.6%/min vs HFD: 1.7%/min ± 0.4%/min, $P < .05$). The use of lovastatin increased the insulin sensitivity, as shown by the K_{itt} (L: 3.3%/min ± 0.5%/min), which was different from the HFD group ($P < .05$) (Fig. 1).

3.2. Insulin signaling in liver of controls, HFD-fed rats, and lovastatin-treated rats

There were no differences in IR protein levels between the 3 groups. The insulin-induced IR tyrosine phosphorylation in the liver of HFD rats was decreased when compared with control animals. The animals treated with lovastatin presented insulin-induced IR tyrosine phosphorylation levels that were similar to those of controls (C: 100% ± 4% vs HFD: 48% ± 5%, $P < .001$; HFD vs L: 101% ± 9%, $P < .001$; Fig. 2A and B). The IR serine phosphorylation in the liver of HFD rats was increased when compared with control animals; and after the treatment with lovastatin, the IR serine phosphorylation was similar to that of the control group (C: 100% ± 10% vs HFD: 157% ± 8%, $P < .05$; HFD:

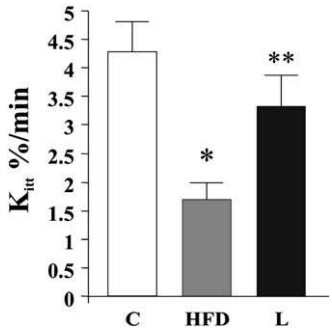

Fig. 1. All 3 groups were submitted to an intravenous insulin tolerance, as described in Materials and methods. Blood samples were collected from the tails of anesthetized rats at 0 (basal), 4, 8, 12, and 16 minutes after injection of 1 U/kg body weight of insulin intravenously; glucose concentration was measured by the glucose-oxidase method; and the rate constant for plasma glucose disappearance (K_{itt}) was calculated. The HFD-fed rats were more resistant than the control rats as shown by K_{itt} (C: 4.3%/min ± 0.6%/min vs HFD: 1.7%/min ± 0.4%/min, $P < .05$), and the use of lovastatin increased the insulin sensitivity (K_{itt} L: 3.3%/min ± 0.5%/min vs HFD: 1.7%/min ± 0.4%/min, $P < .05$).

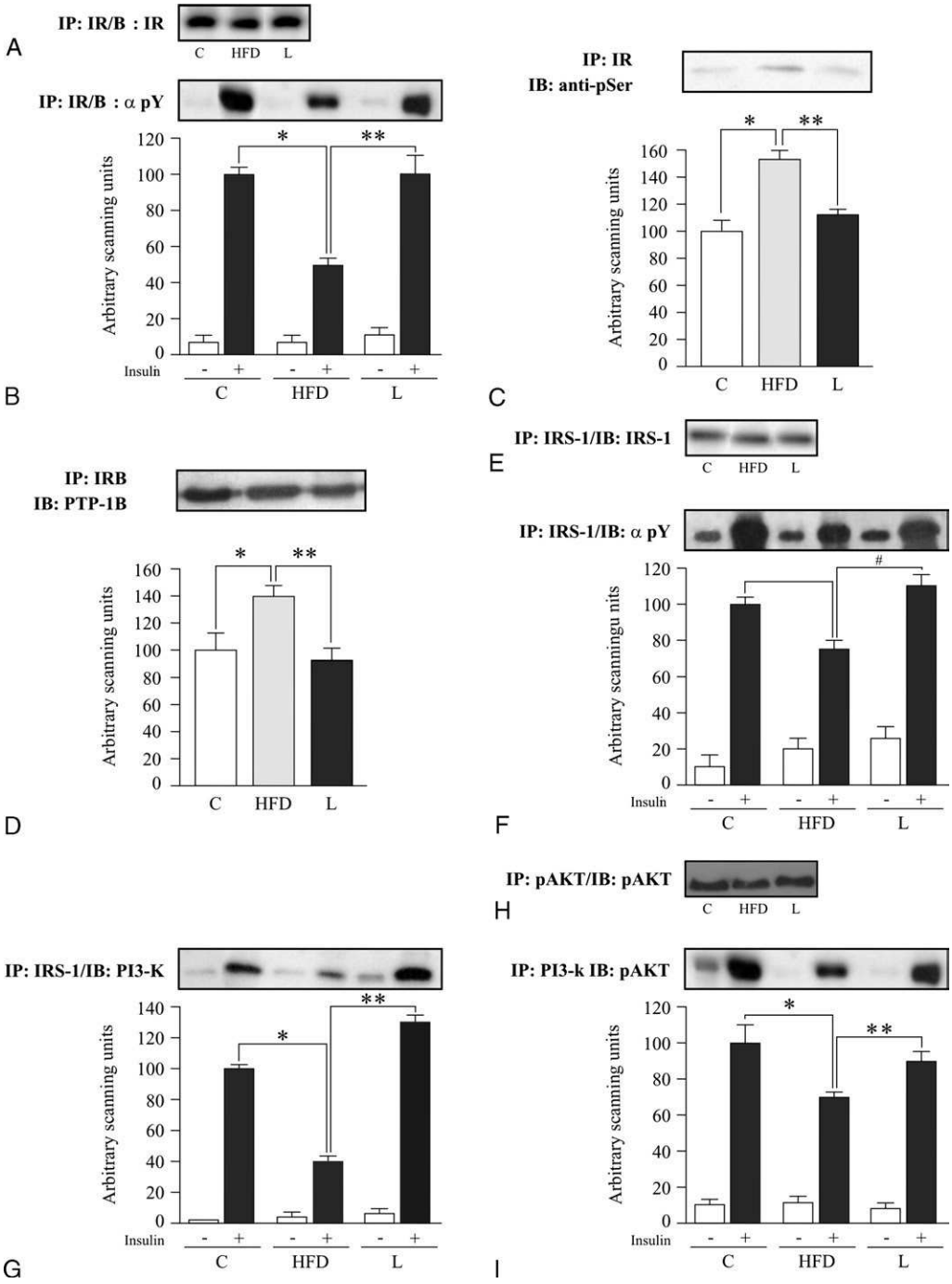

Fig. 2. Insulin signaling in the liver of control animals, animals fed on HFD for 4 weeks, and animals fed on HFD for 4 weeks and treated with lovastatin during the last week. In animals infused with insulin, the samples were extracted at 30 seconds after insulin injection. A, Immunoprecipitation (IP) with αIR and immunoblotting (IB) with α-IR antibodies. B, IP with α-IR and IB with α-PY. C, IP with αIR and IB with antiphosphoserine antibodies. D, IP with αIR and IB with anti-PTP1B antibodies. E, IP with α-IRS-1 and IB with α-IRS-1. F, IP with α-IRS-1 and IB with α-PY. G, IP with α-IRS-1 and IB with PI3K. H, IB with α-AKT1/2 antibodies. I, IB with α-PAKT. Data are mean ± SEM of 10 independent experiments; that is, 10 different cohorts of animals were fed on a control diet, HFD for 4 weeks, or HFD for 4 weeks plus lovastatin treatment during the last week. *HFD vs C, $P < .001$; **HFD vs L, $P < .001$; #L vs HFD, $P < .05$.

157% ± 8% vs L: 112% ± 4%, $P < .05$; Fig. 2C). A similar behavior was seen for the association of IR and PTP1B (C: 100% ± 12% vs HFD: 140% ± 8%, $P < .05$; HFD: 140% ± 8% vs L: 95% ± 10%, $P < 0.05$; Fig. 2D). Despite similar levels of IRS-1 in the liver of the 3 groups, there was a decrease in insulin-stimulated IRS-1 tyrosine phosphorylation in the HFD group with an increase after the use of the drug (C: 100% ± 3%, HFD: 76% ± 7%, and L: 112% ± 14%,

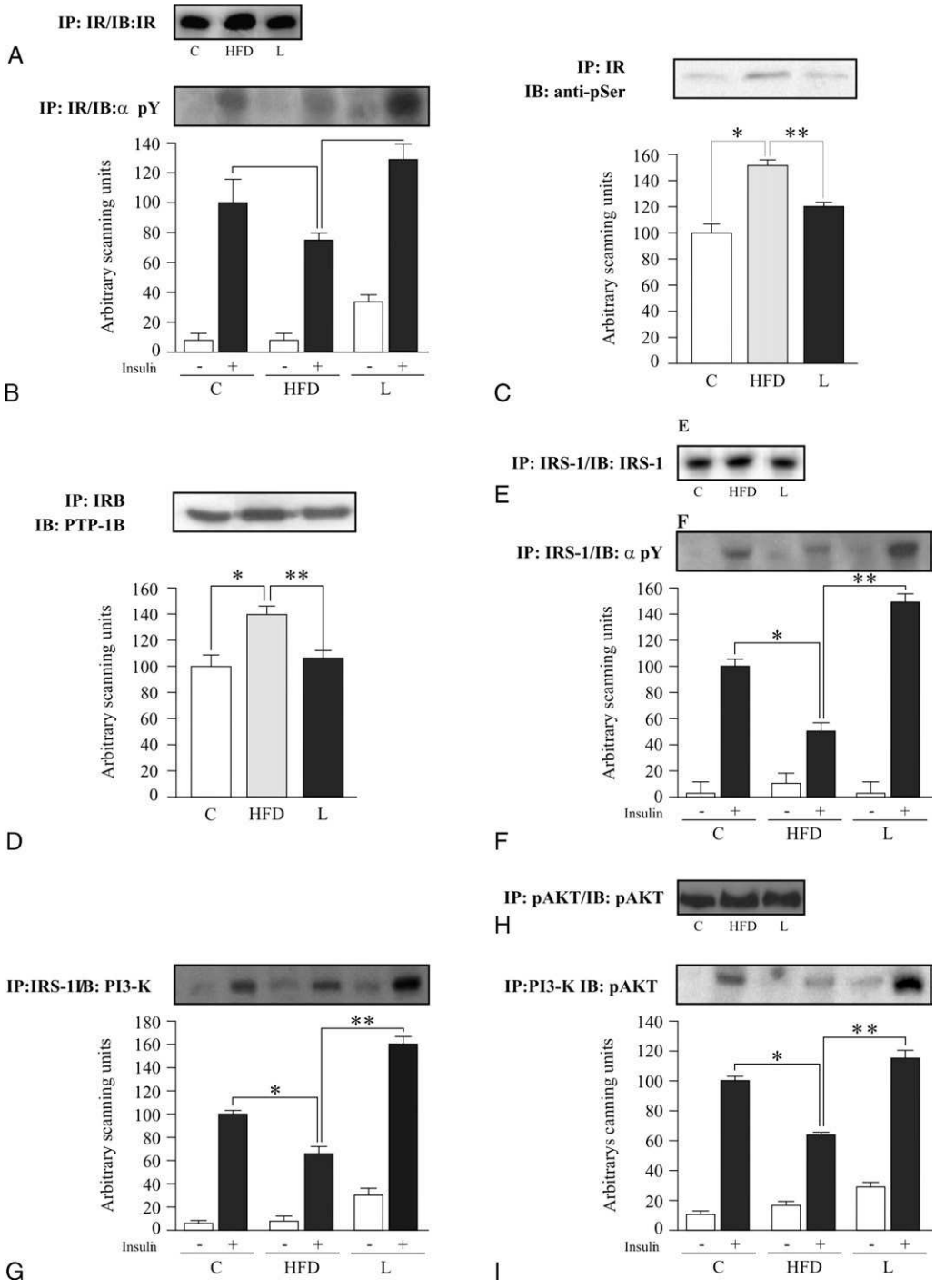

Fig. 3. Insulin signaling in the skeletal muscle of control animals, animals fed on HFD for 4 weeks, and animals fed on HFD for 4 weeks and treated with lovastatin during the last week. In animals infused with insulin, the samples were extracted at 90 seconds after insulin injection. A, IP with α-IR and IB with α-IR antibodies. B, IP with α-IR and IB with α-PY. C, IP with α-IR and IB with antiphosphoserine antibodies. D, IP with αIR and IB with anti-PTP1B antibodies. E, IP with α-IRS-1 and IB with α-IRS-1. F, IP with α-IRS-1 and IB with α-PY. G, IP with α-IRS-1 and IB with PI3K. H, IB with α-AKT1/2 antibodies. I, IB with α-PAKT. Data are mean ± SEM of 10 independent experiments. *HFD vs C, $P < .001$; **HFD vs L, $P < .001$.

$P < .05$ between HFD animals and lovastatin group; Fig. 2E and F). The IRS-1/PI3K association presented a similar behavior (C: 100% ± 0.5% vs HFD: 40% ± 4%, $P < .001$; HFD vs L: 121% ± 4%, $P < .001$; Fig. 2G). There were no differences in Akt protein levels between the groups (Fig. 2H). However, animals fed on the HFD presented a decrease in insulin-induced Akt serine phosphorylation, which was reversed after lovastatin treatment (C: 100% ± 5% vs HFD: 70% ± 2%, $P < .001$; HFD vs L: 95% ± 5%, $P < .001$; C vs L, $P < .05$; Fig. 2I).

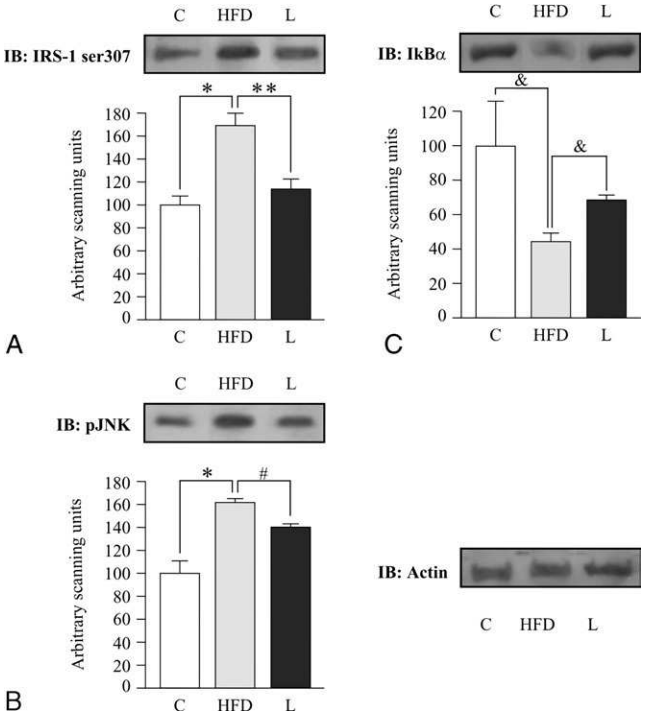

Fig. 4. Insulin signaling in the liver of control animals, animals fed on HFD for 4 weeks, and animals fed on HFD for 4 weeks and treated with lovastatin during the last week. A, IB with α-IRS-1^{ser307} antibodies. B, IB with α-JNK1. C, IB with IκBα. D, IB with antiactin antibodies. Data are mean ± SEM of 10 independent experiments. *HFD vs C, $P < .001$; **HFD vs L, $P < .001$; #HFD vs L, $P < .01$; &C vs HFD and HFD vs L, $P < .05$.

3.3. Insulin signaling in the skeletal muscle of controls, HFD-fed rats, and lovastatin-treated rats

There were no differences in IR protein levels in the skeletal muscle of controls, HFD-fed animals, and lovastatin-treated animals (Fig. 3A). Despite an apparent decrease in insulin-stimulated IR tyrosine phosphorylation in the HFD-fed animals and increase after use of lovastatin, there were no statistical differences between the groups (C: 100% ± 17%, HFD: 76% ± 4%, and L: 129% ± 23%; Fig. 3B). The IR serine phosphorylation in the muscle of HFD rats was increased when compared with control animals (C: 100% ± 8% vs HFD: 155% ± 8%, $P < .05$; Fig. 3C). In the group fed on the HFD and treated with lovastatin, the IR serine phosphorylation was similar to that of the control group (HFD: 155% ± 8% vs L: 116% ± 5%, $P < .05$; Fig. 3C). A similar behavior was seen for the association of IR and PTP1B (C: 100% ± 10% vs HFD: 140% ± 8%, $P < .05$; HFD: 140% ± 8% vs L: 105% ± 8%, $P < .05$; Fig. 3D). However, although no differences were observed in IRS-1 protein levels, the HFD-fed animals presented a significantly reduced insulin-stimulated IRS-1 tyrosine phosphorylation compared with control rats and an increased phosphorylation after the use of the drug (C: 100% ± 5% vs HFD: 51% ± 7%, $P < .001$; HFD vs L: 151% ± 3%, $P < .001$; Fig. 3E and F). The IRS-1/PI3K association presented similar results (C: 100% ± 1% vs HFD: 54% ± 20%, $P < .001$; HFD vs L: 179% ± 11%, $P < .001$; Fig. 3G). There were no differences in Akt protein levels between the groups (Fig. 3H); however, the HFD-fed rats presented a decrease in insulin-induced Akt serine phosphorylation that was reversed by the use of lovastatin (C: 100% ± 2% vs HFD: 64% ± 2%, $P < .001$; HFD vs L: 116% ± 7%, $P < .001$, Fig. 3I).

3.4. Phospho-IRS-1^{ser307}, phospho-JNK, and IκBα in the liver of controls, HFD-fed rats, and lovastatin-treated rats

The consumption of the HFD significantly increased the levels of phospho-IRS-1^{ser307} of the rats in the HFD group compared with those of the control rats, and the treatment with lovastatin decreased it to values similar to those of controls (C: 100% ± 5% vs HFD: 171% ± 20%, $P < .001$; HFD vs L: 113% ± 12%, $P < .001$; Fig. 4A). Similarly, the HFD-fed animals presented a significant increase in the levels of phospho-[Thr183]-JNK compared with controls; and this increase was reversed in the group of animals treated with lovastatin (C: 100% ± 7% vs HFD: 162% ± 3%, $P < .001$; HFD vs L: 141% ± 3%, $P < .01$; Fig. 4B). There was a decrease in IκBα in HFD-fed rats, suggesting an activation of IKKβ, which was reversed in the lovastatin group (C: 100% ± 6%, HFD: 44% ± 4%, and L: 67% ± 2%; Fig. 4C).

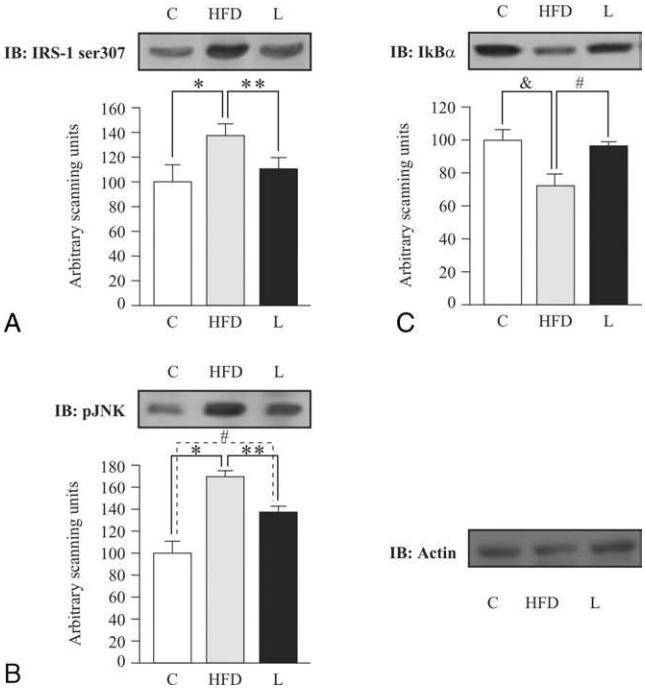

Fig. 5. Insulin signaling in the skeletal muscle of control animals, animals fed on HFD for 4 weeks, and animals fed on HFD for 4 weeks and treated with lovastatin during the last week. A, IB with α-IRS-1^{ser307} antibodies. B, IB with α-JNK1. C, IB with IκBα. D, IB with antiactin antibodies. Data are mean ± SEM of 10 independent experiments. *HFD vs C, $P < .001$; **HFD vs L, $P < .001$; #C vs L, $P < .01$; &C vs HFD and HFD vs L, $P < .05$.

3.4.1. Phospho-IRS-1^{ser307}, phospho-JNK, and IκBα in the skeletal muscle of controls, HFD-fed rats, and lovastatin-treated rats

The levels of phospho-IRS-1^{ser307} increased in the group of animals treated with the HFD compared with the control rats, and this increase was reversed in the lovastatin-treated rats compared with the controls (C: 100% ± 14% vs HFD: 137% ± 7%, $P < .001$; HFD vs L: 110% ± 12%, $P < .05$; Fig. 5A). Increased phospho-[Thr183]-JNK was observed in the HFD-fed rats compared with controls, and a reversal of this increase was also seen in the lovastatin-treated animals (C: 100% ± 6% vs HFD: 172% ± 2%, $P < .001$; HFD vs L: 138% ± 2%, $P < .001$; C vs L, $P < .01$; Fig. 5B). The use of the HFD decreased the IκBα in the HFD group compared with control animals, whereas treatment with lovastatin reversed this decrease to values similar to those of controls rats (C: 100% ± 7% vs HFD: 72% ± 6%, $P < .05$; HFD vs L: 97% ± 3%, $P < .01$; Fig. 5C).

4. Discussion

In the present study, we demonstrated that lovastatin, an 3-hydroxy-3-methylglutaryl coenzyme A reductase inhibitor, has insulin-sensitizing properties in HFD-fed rats. Treatment with lovastatin resulted in a marked improvement in insulin sensitivity characterized by an increase in the glucose disappearance rate during the insulin tolerance test. This increase in insulin sensitivity was associated with an increased insulin-stimulated IRS-1/PI3K/Akt pathway in the liver and muscle of HFD-fed rats in parallel with a decrease in the inflammatory pathway (JNK and IKK/IκB/NFκB) related to insulin resistance.

Our data showing an improvement in insulin sensitivity in statin-treated HFD-fed rats are in agreement with the results of 3 separate studies in humans [28-30]. In these studies, the authors used both simvastatin and cerivastatin and measured insulin action by euglycemic hyperinsulinemic glucose clamp and by homeostatic model assessment. In other studies, the improvement in insulin action by statin was not demonstrated, probably because of the lack of direct assessment of insulin action or inclusion of patients using other drugs that interfered in insulin action [31,32]. A retrospective cohort study using Saskatchewan health databases found that the use of statin was associated with a delay of 10 months in starting insulin treatment in patients with type 2 diabetes mellitus [33]. In Zucker rats, atorvastatin resulted in a dose-dependent increase in insulin sensitivity [21].

In the present study, the increase in insulin sensitivity induced by lovastatin was associated with an increase in insulin-stimulated IR tyrosine phosphorylation in parallel with a reduction in IR serine phosphorylation and also in the IR/PTP1B association in liver and muscle. Previous data showed that an increase in IR serine phosphorylation is associated with impairment in insulin-induced activation of its receptor [34-36]. Another mechanism that controls IR function is the activity of PTP1B, and previous studies have demonstrated an increase in IR/PTP1B association in situations of insulin resistance [36,37]. In this regard, the reversal of increased IR serine phosphorylation and also of IR/PTP1B association induced by lovastatin may have a role in the improved insulin sensitivity induced by this drug. Our data also show that lovastatin treatment was associated with an increase in the insulin-stimulated IRS-1/PI3K/Akt pathway. This finding is consistent with studies demonstrating statin-induced activation of Akt/PKB [38,39]. A previous study suggested that Akt/PKB activation by statin is PI3K dependent [39]. Our data showing an increase in the insulin-induced activation of upstream regulators of Akt/PKB, such as IRS-1 and PI3K, in the liver and muscle of HFD-fed rats reinforce this previous study. This effect of statin may have an important role in the improvement of insulin sensitivity in HFD-fed animals because this pathway has been implicated in glucose transport in muscle and in glycogen synthesis in liver and muscle [40,41].

Serine phosphorylation of IRS proteins is believed to be a major mechanism of suppression of IRS-1 activity that contributes to insulin resistance [40]. One possible kinase that might increase IRS-1 serine phosphorylation in HFD-fed rats is JNK [13]. Our data showing that statin reversed Ser^{307} IRS-1 phosphorylation and blunted JNK activation in liver and muscle provide new insights into the mechanism of statin improvement in insulin action.

Another mechanism involved in HFD-dependent insulin resistance is the activation of the proinflammatory IKK/IκB/NFκB pathway [14,16]. We have also demonstrated a decrease in the level of IκB in the liver and muscle of rats fed on a HFD compared with control animals, suggesting an activation of this pathway. Interestingly, the statin treatment also reversed this activation. Hence, in our study, the use of lovastatin in rats on HFD reversed the deleterious effects of the insulin signaling pathway with regard to JNK activation and IKK/IκB/NFκB pathway.

Clinical and experimental studies strongly support an anti-inflammatory role for statins. Liver is a major site of action of statins, particularly in the inhibition of cholesterol synthesis. However, the hepatocyte is also a source of proinflammatory mediators; and a decrease in the expression of these factors could be an important mechanism of the anti-inflammatory action of these drugs [42]. The cholesterol synthesis is a complex process that generates isoprenoids, such as farnesyl pyrophosphate and geranylgeranyl pyrophosphate, that serve as lipid attachments for a variety of signaling molecules, such as guanosine-3-phosphate (GTP)-binding protein Ras and its related Ras-like proteins, such as Rho, Rac, Rab, Rap, and Ral [43,44]. The translocation of Ras to the membrane is necessary for activity and is dependent on farnesylation. Similarly, attachment of Rho and Rac to the membrane is required for activity; but in contrast to Ras, these factors undergo geranylgeranylation. Ras has been associated with cellular proliferation, Rac with

generation of reactive oxygen species, and Rho with activation of proinflammatory pathways [41,44]. Interestingly, Rho and Rac proteins can induce NFκB activity by a mechanism that induces phosphorylation of IκB and nuclear accumulation of NFκB [45,46]. In the case of NFκB, statins have also been shown to limit NFκB nuclear accumulation and DNA binding, perhaps via an increase in the expression of IκB [47,48]. In addition, statins have been shown to reduce the expression of c-jun [48], indicating a possible effect on JNK activity. Our data showing that statin blunted the activation of IKK/IκB/NFκB and JNK in liver and muscle of HFD-fed rats indicate a possible mechanism for their anti-inflammatory effect on insulin action. In addition to alterations described in this study induced by the HFD, other mechanisms can also induce insulin resistance [49-51]. We cannot exclude the possibility that lovastatin could also be acting through other mechanisms, contributing to its effect of improving insulin action.

In summary, statin treatment improves insulin sensitivity in HFD-fed rats by reversing the decrease in the insulin-stimulated IRS-1/PI3K/Akt pathway in the liver and muscle. The effect of statins on insulin action is further supported by our findings that HFD rats treated with statin demonstrate a reduction in IRS-1 serine phosphorylation, IKK/IκB/NFκB pathway, and JNK activity associated with an improvement in insulin action. Overall, these results provide important new insight into the mechanism of statin action in insulin sensitivity.

References

[1] Avruch J. Insulin signal transduction through protein kinase cascades. Mol Cell Biochem 1998;182:31-48.

[2] Saltiel AR, Pessin JE. Insulin signaling pathway in time and space. Trends Cell Biol 2002;12:65-71.

[3] Saad MJ, Folli F, Kahn JA, Kahn CR. Modulation of insulin receptor, insulin receptor substrate–1, and phosphatidylinositol 3-kinase in liver and muscle of dexamethasone-treated rats. J Clin Invest 1993;92: 2065-72.

[4] Brozinick Jr JT, Birnbaum MJ. Insulin, but not contraction, activates Akt/PKB in isolated rat skeletal muscle. J Biol Chem 1998;273: 14679-82.

[5] Lee YH, Giraud J, Davis RJ, White MF. c-Jun N-terminal kinase (JNK) mediates feedback inhibition of the insulin signaling cascade. J Biol Chem 2003;278:2896-902.

[6] Weston CR, Lambright DG, Davis RJ. Signal transduction: MAP kinase signaling specificity. Science 2002;296:2345-7.

[7] Davis RJ. Signal transduction by the c-Jun N-terminal kinase. Biochem Soc Symp 1999;64:1-12.

[8] Hirosumi J, Tuncman G, Chang L, Gorgun CZ, Uysal KT, Maeda K, et al. A central role for JNK in obesity and insulin resistance. Nature 2002;420:333-6.

[9] Nikulina MA, Sandhu N, Shamim Z, Andersen NA, Oberson A, Dupraz P, et al. The JNK binding domain of islet-brain 1 inhibits IL-1 induced JNK activity and apoptosis but not the transcription of key proapoptotic or protective genes in insulin secreting cell lines. Cytokine 2003;24:13-24.

[10] Ip YT, Davis RJ. Signal transduction by the c-Jun N-terminal kinase (JNK): from inflammation to development. Curr Opin Cell Biol 1998;10:205-19.

[11] Aguirre V, Werner ED, Giraud J, Lee YH, Shoelson SE, White MF. Phosphorylation of Ser307 in insulin receptor substrate–1 blocks interactions with the insulin receptor and inhibits insulin action. J Biol Chem 2002;277:1531-7.

[12] Chopra M, Galbraith S, Darnton-Hill I. A global response to a global problem: the epidemic of overnutrition. Bull World Health Organ 2002;80:952-8.

[13] Prada PO, Zecchin HG, Gasparetti AL, Torsoni MA, Ueno M, Hirata AE, et al. Western diet modulates insulin signaling, JNK activity and IRS-1ser307 phosphorylation in a tissue-specific fashion. Endocrinology 2005;146:1576-87.

[14] Schoelson SE, Lee J, Yuan M. Inflammation and the IKKβ/IκB/NFκB axis in obesity and diet-induced insulin resistance. Int J Obes Relat Metab Disord 2003;27(Suppl 3):S49-S52.

[15] Cai D, Yuan M, Frantz DF, Melandez PA, Hansen L, Lee J, et al. Local and systemic insulin resistance resulting from hepatic activation of IKK-beta and NF-kappaB. Nat Med 2005;11:182-90.

[16] Itaui S, Ruderman NR, Schmieder F, Boden G. Lipid-induced insulin resistance in human muscle is associated with changes in diacylglycerol, protein kinase C and IκB-α. Diabetes 2002;51:2205-11.

[17] Ghosh S, Karin M. Missing pieces in the NF-κB puzzle. Cell 2002; 109:S81-S96.

[18] Endo A, Kuroda M, Tsujita Y. ML-236A, ML-236B and ML-236C, new inhibitors of cholesterogenesis produced by *Penicillium citrinium*. J Antibiot (Tokyo) 1976;29:1346-8.

[19] Istvan ES, Deisenhofer J. Structural mechanism for statin inhibition of HMG-CoA reductase. Science 2001;292:1160-4.

[20] Suzuki M, Kakuta H, Takahashi A, Shimano H, Tada-lida K, Yokoo T, et al. Effects of atorvastatin on glucose metabolism and insulin resistance in KK/Ay mice. J Atheroscler Thromb 2005;12:77-84.

[21] Wong V, Stavar L, Szeto L, Uffelman K, Wang C-H, Fantus G, et al. Atorvastatin induces insulin sensitization in Zucker lean and fatty rats. Atherosclerosis 2006:348-55.

[22] Okada K, Maeda N, Kikuchi K, Tatsukawa M, Sawayama Y, Hayashi J. Pravastatin improves insulin resistance in dyslipidemic patients. J Atheroscler Thromb 2005;12:322-9.

[23] Huptas S, Geiss H-C, Otto C, Parhofer KG. Effect of atorvastatin (10 mg/day) on glucose metabolism in patients with metabolic syndrome. Am J Cardiol 2006;98:66-9.

[24] Laemmli UK. Cleavage of structural proteins during the assembly of head of bacteriophage T4. Nature 1970;227:680-5.

[25] Towbin H, Staehelin T, Gordon J. Electrophoretic transfer of proteins from polyacrylamide gels to nitrocellulose sheets: procedure and some applications. Proc Natl Acad Sci U S A 1979;76:4350-4.

[26] Bonora P, Moghetti C, Zancanaro M, Cigolini M, Querena V, Cacciatori A, et al. Estimates of in vivo insulin action in man: comparison of insulin tolerance tests with euglycemic and hyperglycemic glucose clamp studies. J Clin Endocrinol Metab 1989;68:374-8.

[27] Morgan CR, Lazarow A. Immunoassay of pancreatic and plasma insulin following alloxan injection of rats. Diabetes 1965;14:669-71.

[28] Paolisso G, Barbagallo M, Petrella G, Ragno E, Barbieri M, Giordano M, et al. Effects of simvastatin and atorvastatin administration on insulin resistance and respiratory quotient in aged dyslipidemic non–insulin dependent diabetic patients. Atherosclerosis 2000;150:121-7.

[29] Paolisso G, Sgambato S, De Riu S, Gambardella A, Verza M, Varricchio M, et al. Simvastatin reduces plasma lipid levels and improves insulin action in elderly, non–insulin dependent diabetics. Eur J Clin Pharmacol 1991;40:27-31.

[30] Paniagua JA, Lopez-Miranda J, Escribano A, Berral FJ, Marin C, Bravo D, et al. Cerivastatin improves insulin sensitivity and insulin secretion in early-state obese type 2 diabetes. Diabetes 2002;51:2596-603.

[31] Farrer M, Winocour PH, Evans K, Neil HA, Laker MF, Kesteven P, et al. Simvastatin in non–insulin dependent diabetes mellitus: effect on serum lipids, lipoproteins and haemostatic measures. Diabetes Res Clin Pract 1994;23:111-9.

[32] Ohrvall M, Lithell H, Johansson J, Vessby B. A comparison between the effects of gemfibrozil and simvastatin on insulin sensitivity in

patients with non–insulin-dependent diabetes mellitus and hyperlipoproteinemia. Metabolism 1995;44:212-7.
[33] Yee A, Majumdar SR, Simpson SH, McAlister FA, Tsuyuki RT, Johnson JA. Statin use in type 2 diabetes mellitus is associated with a delay in starting insulin. Diabet Med 2004;9:962-7.
[34] Bollag GE, Roth RA, Beaudoin J, Mochly-Rosen D, Koshl Jr DE. Protein kinase C directly phosphorylates the insulin receptor in vitro and reduces its protein-tyrosine kinase activity. Proc Natl Acad Sci U S A 1986;83:5822-4.
[35] Rosenzweig T, Braiman L, Bak A, Alt A, Kuroki T, Sampson SR. Differential effects of tumor necrosis factor alpha on protein kinase C isoforms and mediate inhibition of insulin receptor signaling. Diabetes 2002;51:1921-30.
[36] Araújo EP, De C, Souza T, Gasparetti AL, Ueno M, Boschero AC, et al. Short-term in vivo inhibition of insulin receptor substrate–1 expression leads to insulin resistance, hyperinsulinemia, and increased adiposity. Endocrinology 2005;146:1428-37.
[37] Hirata AE, Alvarez-Rojas F, Carvalheira JB, Carvalho CR, Dolnikoff MS, Abdalla Saad MJ. Modulation of IR/PTP1B interaction and downstream signaling in insulin sensitive tissues of MSG-rats. Life Sci 2003;73:1369-81.
[38] Contreras JL, Smyth CA, Bilbao G, Young CJ, Thompson JA, Eckhoff DE. Simvastatin induces activation of the serine-threonine protein kinase AKT and increases survival of isolated human pancreatic islets. Transplantation 2002;74:1063-9.
[39] Kureishi Y, Luo Z, Shiojima I, Bialik A, Fulton D, Lefer DJ, et al. The HMG-CoA reductase inhibitor simvastatin activates the protein kinase Akt and promotes angiogenesis in normocholesterolemic animals. Nat Med 2000;6:1004-10.
[40] Saltiel AR, Kahn CR. Insulin signalling and the regulation of glucose and lipid metabolism. Nature 2001;414:799-806.
[41] Cross DA, Alessi DR, Cohen P, Andjelkovich M, Hemmings BA. Inhibition of glycogen synthase kinase–3 by insulin mediated by protein kinase B. Nature 1995;378:785-9.
[42] Arnaud C, Burger F, Steffens S, Veillard NR, Nguyen TH, Trono D, et al. Statins reduce interleukin-6–induced C-reactive protein in human hepatocytes: new evidence for direct antiinflammatory effects of statins. Arterioscler Thromb Vasc Biol 2005;25:1231-6.
[43] Van Aelst L, D'Souza-Schorey C. Rho GTPases and signaling networks. Genes Dev 1997;11:2295-322.
[44] Liao JK, Laufs U. Pleiotropic effects of statins. Annu Rev Pharmacol Toxicol 2005;45:89-118.
[45] Montaner S, Perona R, Saniger L, Lacal JC. Activation of serum response factor by RhoA is mediated by the nuclear factor–κB and C/EBP transcription factors. J Biol Chem 1999;274:8506-15.
[46] Perona R, Lopez-Miranda J, Escribano A, Berral FJ, Marin C, Bravo D, et al. Activation of the nuclear factor–κB by Rho, CDC42, and Rac-1 proteins. Genes Dev 1997;11:463-75.
[47] Wagner AH, Gebauer M, Guldenzoph B, Hecker M. 3-Hydroxy-3-methylglutaryl coenzyme A reductase–independent inhibition of CD40 expression by atorvastatin in human endothelial cells. Arterioscler Thromb Vasc Biol 2002;22:1784-9.
[48] Dichtl W, Dulak J, Erick M, Alber HF, Schwarzacher SP, Ares MP, et al. HMG-CoA reductase inhibitors regulate inflammatory transcription factors in human endothelial and vascular smooth muscle cells. Arterioscler Thromb Vasc Biol 2003;23:58-63.
[49] Maddux BA, Chang YN, Accili D, McGuinness OP, Youngren JF, Goldfine ID. Overexpression of the insulin receptor inhibitor PC-1/ENPP1 induces insulin resistance and hyperglycemia. Am J Physiol Endocrinol Metab 2006;290:E746-9.
[50] Carvalho-Filho MA, Ueno M, Hirabara SM, Seabra AB, Carvalheira JB, de Oliveira MG, et al. S-nitrosation of the insulin receptor, insulin receptor substrate 1, and protein kinase B/Akt: a novel mechanism of insulin resistance. Diabetes 2005;54:959-67.
[51] Pender C, Goldfine ID, Kulp JL, Tanner CJ, Maddux BA, MacDonald KG, et al. Analysis of insulin-stimulated insulin receptor activation and glucose transport in cultured skeletal muscle cells from obese subjects. Metabolism 2005;54:598-603.

APÊNDICE *XV*

Acute physical exercise reverses *S*-nitrosation of the insulin receptor, insulin receptor substrate 1 and protein kinase B/Akt in diet-induced obese Wistar rats

José R. Pauli, Eduardo R. Ropelle, Dennys E. Cintra, Marco A. Carvalho-Filho, Juliana C. Moraes, Cláudio T. De Souza, Lício A. Velloso, José B. C. Carvalheira and Mario J. A. Saad

Departamento de Clínica Médica, FCM, Universidade Estadual de Campinas (UNICAMP), Campinas, SP, Brazil

Early evidence demonstrates that exogenous nitric oxide (NO) and the NO produced by inducible nitric oxide synthase (iNOS) can induce insulin resistance. Here, we investigated whether this insulin resistance, mediated by *S*-nitrosation of proteins involved in early steps of the insulin signal transduction pathway, could be reversed by acute physical exercise. Rats on a high-fat diet were subjected to swimming for two 3 h-long bouts, separated by a 45 min rest period. Two or 16 h after the exercise protocol the rats were killed and proteins from the insulin signalling pathway were analysed by immunoprecipitation and immunoblotting. We demonstrated that a high-fat diet led to an increase in the iNOS protein level and *S*-nitrosation of insulin receptor β (IRβ), insulin receptor substrate 1 (IRS1) and Akt. Interestingly, an acute bout of exercise reduced iNOS expression and *S*-nitrosation of proteins involved in the early steps of insulin action, and improved insulin sensitivity in diet-induced obesity rats. Furthermore, administration of GSNO (NO donor) prevents this improvement in insulin action and the use of an inhibitor of iNOS (L-N^6-(1-iminoethyl)lysine; L-NIL) simulates the effects of exercise on insulin action, insulin signalling and *S*-nitrosation of IRβ, IRS1 and Akt. In summary, a single bout of exercise reverses insulin sensitivity in diet-induced obese rats by improving the insulin signalling pathway, in parallel with a decrease in iNOS expression and in the *S*-nitrosation of IR/IRS1/Akt. The decrease in iNOS protein expression in the muscle of diet-induced obese rats after an acute bout of exercise was accompanied by an increase in AMP-activated protein kinase (AMPK) activity. These results provide new insights into the mechanism by which exercise restores insulin sensitivity.

(Resubmitted 3 August 2007; accepted after revision 30 October 2007; first published online 1 November 2007)
Corresponding author M. J. A. Saad: Departamento de Clínica Médica, FCM-UNICAMP, Cidade Universitária Zeferino Vaz, Campinas, SP, Brasil. Email: msaad@fcm.unicamp.com.br

Nitric oxide (NO) is a free radical and biological signalling molecule produced by the intracellular enzyme, NO synthase (Lane & Gross, 1999). The reactivity of NO towards molecular oxygen, thiols, transition metal centres, and other biological targets enables NO to act as an ubiquitous cell-signalling molecule with diverse physiological and pathophysiological roles (Gross & Wolin, 1995). In this regard, NO can react with cysteine residues in the presence of O_2 to form *S*-nitrosothiol (Stamler *et al.* 1992, 1997), altering the activity of proteins including H-ras (Lander *et al.* 1995), the olfactory cyclic nucleotide-gated channel (Broillet & Firestein, 1996) and glyceraldehyde-3-phosphate dehydrogenase (Molina y Vedia *et al.* 1992). The reversible regulation of protein function by *S*-nitrosation has led to the proposal that *S*-nitrosothiols function as post-translational modifiers, analogous to those created by phosphorylation or acetylation (Stamler *et al.* 1997).

A previous study reported that inducible nitric oxide synthase (iNOS), a cytokine-inducible proinflamatory mediator in several pathological conditions, is over-expressed in the muscle and fat of genetic and dietary models of obesity and type 2 diabetes (Perreault & Marette, 2001), and that this expression is associated with insulin resistance. The iNOS knockout mice are protected from muscle insulin resistance by related diet-induced obesity (Perreault & Marette, 2001). We have recently demonstrated that the insulin resistance induced by increased iNOS in obesity may be related to *S*-nitrosation of insulin signalling proteins, insulin receptor (IR), insulin receptor substrate 1 (IRS1) and protein kinase B (Akt) (Carvalho-Filho *et al.* 2005).

It is well established that exercise training, even acutely, can improve insulin sensitivity in the muscle of obese rats (Betts *et al.* 1993; Bruce *et al.* 2001). However, the molecular mechanisms involved in this improvement

 DOI: 10.1113/jphysiol.2007.142414

Table 1. Components of rat diet and rat chow

	Standard chow		High fat diet	
Ingredients	g kg^{-1}	kcal kg^{-1}	g kg^{-1}	kcal kg^{-1}
Cornstarch (Q.S.P.)	397.5	1590	115.5	462
Casein	200	800	200	800
Sucrose	100	400	100	400
Dextrinated starch	132	528	132	528
Lard	—	—	312	2808
Soybean Oil	70	630	40	360
Cellulose	50	—	50	—
Mineral Mix	35	—	35	—
Vitamin Mix	10	—	10	—
L-Cystine	3	—	3	—
Choline	2.5	—	2.5	—
Total	1000	3948	1000	5358

in insulin signalling are not fully understood. Exercise training is also associated with enhanced AMP-activated protein kinase (AMPK) signalling. AMPK activation can modulate NO production through down-regulation of iNOS protein expression (Pilon *et al.* 2004). Treatment with AICAR, an AMPK agonist, improves glucose homeostasis and insulin sensitivity (Winder, 2000; Fiedler *et al.* 2001).

In the light of these previous data, we investigated whether the improvement in insulin signalling, associated with acute exercise, could be associated with the down-regulation of iNOS protein expression and reduced *S*-nitrosation of IRβ, IRS1 and Akt, and accompanied by AMPK activation.

Methods

Animals and diet

Male Wistar rats from the University of Campinas Central Animal Breeding Center were used in the experiments. All experiments were approved by the Ethics Committee of the State University of Campinas (UNICAMP).

The 4-week-old Wistar rats were divided into three groups, control rats (C) fed standard rodent chow (composition, see Table 1), obese rats, fed on an obesity-inducing diet for 3 months (DIO) (composition, see Table 1), and a third group, which also received an obesity-inducing diet, but was submitted to a single bout of exercise (DIO + EXE).

Exercise protocol

Rats were accustomed to swimming for 10 min for 2 days. The animals swam in groups of three in plastic barrels of 45 cm in diameter that were filled to a depth of 60 cm, for two 3 h-long bouts, separated by a 45 min rest period, and the water temperature was maintained at ∼34°C. This exercise protocol was adaptated from a previously published procedure (Chibalin *et al.* 2000). Two and 16 h after the exercise protocol, or as indicated in the time course experiments, the rats were anaesthetized with an intraperitoneal (I.P.) injection of sodium thiopental (40 mg (kg body weight)$^{-1}$). In all experiments the appropriateness of anaesthesia depth was tested by evaluating pedal and corneal reflexes, throughout the experimental procedure. Following the experimental procedures, the rats were killed under anaesthesia (thiopental 200 mg kg^{-1}) following the recommendations of the NIH publication n°85–23.

S-Nitrosoglutathione treatment

S-Nitrosoglutathione (GSNO) was prepared by the reaction of glutathione with sodium nitrite in acidic solution, as previously reported (Shishido *et al.* 2003). The rats received an intraperitoneal (I.P.) injection of GSNO (0.1 mol l^{-1}) or phosphate-buffered saline every 2 h, until completing four doses in 8 h. Immediately after the last dose the animals were submitted to the same exercise protocol, and 2 h or 16 h after the last bout of exercise, the rats were anaesthetized with an I.P. injection of sodium thiopental (40 mg (kg body weight)$^{-1}$), and then skeletal muscle (gastrocnemius) was taken for biochemical analyses.

L-NIL treatment

The rats received an intraperitoneal injection of the iNOS inhibitor L-N^6-(l-iminoethyl)lysine (L-NIL; 80 mg (kg body weight)$^{-1}$) or phosphate-buffered saline twice (every 12 h) daily for 10 days. This treatment protocol with L-NIL was adaptated from a previously published procedure (Sugita *et al.* 2005). One hour after the last dose of L-NIL, the animals were submitted to the protocol of acute exercise previously described, and 2 h and 16 h after the last bout of exercise, the rats were anaesthetized with an I.P. injection of sodium thiopental (40 mg (kg body weight)$^{-1}$), and then skeletal muscle (gastrocnemius) was extracted for biochemical analyses.

Insulin tolerance test (ITT) and serum insulin determination

Two hours and 16 h after the exercise protocol, the rats were submitted to an insulin tolerance test (ITT; 9.0 ml kg^{-1} of a solution 10^{-6} mol l^{-1} of insulin). Briefly, 9.0 ml kg^{-1} of a solution 10^{-6} mol l^{-1} of human recombinant insulin (Humulin R) from Eli Lilly (Indianapolis, IN, USA) was injected I.P. in anaesthetized rats, the blood samples were collected from the tail at 0, 5, 10, 15, 20, 25 and 30 min, for serum glucose determination. The rate constant for plasma glucose disappearance (K_{ITT}) was calculated using

the formula $0.693/(t_{1/2})$. The plasma glucose $t_{1/2}$ was calculated from the slope of least square analysis of the plasma glucose concentration during the linear phase of decline (Bonora *et al.* 1989). Plasma glucose level was determined by colorimetric method using a glucosemeter (Advantage. Boehringer Mannheim, USA). Plasma was separated by centrifugation (1100 *g*) for 15 min at 4°C and stored at −80°C until assay. Radioimmunoassay (RIA) was employed to measure serum insulin, according to a previous description (Scott *et al.* 1990).

Protein analysis by immunoblotting

As soon as anaesthesia was assured by the loss of pedal and corneal reflexes, the abdominal cavity was opened, the portal vein was exposed and 0.2 ml of normal saline with or without insulin (10^{-6} mol l^{-1}) was injected. In preliminary experiments, we determined that this dose of insulin can reach peripheral levels that are 3–4 times higher than the dose that can induce the maximal insulin effect on insulin signalling proteins in muscle. At 90 s after the insulin injection, both portions of gastrocnemius (red and white fibres) were ablated, pooled, minced coarsely and homogenized immediately in extraction buffer (1% Triton X-100, 100 mM Tris, pH 7.4, containing 100 mM sodium pyrophosphate, 100 mM sodium fluoride, 10 mM EDTA, 10 mM sodium vanadate, 2 mM PMSF and 0.1 mg ml^{-1} aprotinin) at 4°C with a Polytron PTA 20S generator (Brinkmann Instruments model PT 10/35) operated at maximum speed for 30 s. The extracts were centrifuged at 9000 *g* and 4°C in a Beckman 70.1 Ti rotor (Palo Alto, CA, USA) for 40 min to remove insoluble material, and the supernatants of these homogenates were used for protein quantification, performed by the Bradford method. Proteins were denatured by boiling in Laemmli sample buffer containing 100 mM DTT, run on SDS-PAGE, transferred to nitrocellulose membranes, which were blocked, probed and developed as previously described (Laemmli, 1970; Saad *et al.* 1997). The IRβ and IRS1 were immunoprecipitated from rat muscle with or without previous insulin infusion in the portal vein. Antibodies used for immunoblotting were antiphosphotyrosine (pY) (sc-508, mouse monoclonal) anti-IR (sc-711, rabbit polyclonal), anti-IRS1 (sc-559, rabbit polyclonal), anti-Akt (sc-1618, goat polyclonal), antiphospho [Ser^{473}] Akt (sc-7985-R, rabbit polyclonal), anti-iNOS (sc-7271, mouse monoclonal), antiphospho-c-jun N-terminal kinase (JNK) (sc-6254, mouse polyclonal), anti-protein tyrosine phosphate 1B (PTP1B) (sc-1719 goat polyclonal) (Santa Cruz Biotechnology, CA, USA), antiphospho [Ser^{79}] acetyl CoA carboxylase (ACC) (rabbit polyclonal, 07-184), antiphosphoserine-IRS-1307 (rabbit polyclonal, no 7247) was from Upstate Biotechnology (Charlottesville, VA, USA). Anti-ACC (rabbit polyclonal, no 3662), anti-AMPK (rabbit polyclonal, no 2757), antiphospho [Thr^{172}] AMPK (rabbit polyclonal, no. 2531), antip85-PI3-kinase (phosphatidylinositol 3-kinase, PI3-K) (rabbit polyclonal, no 4292) antibodies were from Cell Signalling Technology (Beverly, MA, USA). Blots were exposed to preflashed Kodak XAR film with Cronex Lightning Plus intensifying screens at 80°C for 12–48 h. Band intensities were quantified by optical desitometry (Scion Image software, ScionCorp, Frederick, MD, USA) of the developed autoradiographs.

Detection of *S*-nitrosated proteins by the biotin-switch method

The biotin-switch assay was performed essentially as previously described (Jaffrey & Snyder, 2001; Martinez-Ruiz & Lamas, 2004). Muscle tissue was extracted and homogenized in extraction buffer (250 mM Hepes, pH 7.7, 1 mM EDTA, 0.1 mM neucuproine). After centrifugation at 9000 *g* for 20 min, insoluble material was removed and extracts were adjusted to 0.5 mg ml^{-1} of protein, and equal amounts were blocked with four volumes of blocking buffer (225 mM Hepes, pH 7.7, 0.9 mM neucuproine, 2.5% SDS, and 20 mM methylmethanethiosulphonate) at 50°C for 30 min with agitation. After blocking, extracts were precipitated with two volumes of cold acetone (−20°C), chilled at −20°C for 10 min, centrifuged at 2000 *g* at 4°C for 5 min, washed with acetone, dried out, and resuspended in 0.1 ml HENS buffer (250 mM Hepes, pH 7.7, 1 mM EDTA, 0.1 mM neucoproine, and 1% SDS) per milligram of protein. Until this point, all operations were carried out in the dark. A one-third volume of biotin-HPDP 4 mM and 2.5 mM ascorbic acid was added and incubated for 1 h at room temperature. Proteins were acetone-precipitated again and resuspended in the same volume of HENS buffer.

For purification of biotinylated proteins, samples from the biotin-switch assay were diluted with two volumes of neutralization buffer (20 mM Hepes, pH 7.7, 100 mM NaCl, 1 mM EDTA, and 0.5% Triton X-100), and 15 μl neutravidin-agararose per milligram of protein in the initial extract was added and incubated for 1 h at room temperature with agitation. Beads were washed five times with washing buffer (20 mM Hepes, pH 7.7, 600 mM NaCl, 1 mM EDTA, and 0.5% Triton X-100) and incubated with elution buffer (20 mM Hepes, pH 7.7, 100 mM NaCl, 1 mM EDTA, and 100 mM 2-mercaptoethanol) for 20 min at 37°C with gentle stirring. Supernatants were collected, Laemmli buffer was added, and proteins were separated by SDS-PAGE.

Table 2. Characteristics of Wistar rats after 3 months on a high-fat diet (DIO), DIO rats submitted to exercise (DIO + EXE-2 h and DIO + EXE-16 h) and their age-matched controls

	Control	DIO	DIO + EXE-2 h	DIO + EXE-16 h
Body weight (g)	412.3 ± 17.4	536.8 ± 28.8*	539.1 ± 29.6*	575,1 ± 26,5*
Epididymal fat (g)	5.67 ± 1.2	11.34 ± 1.6*	11.41 ± 1.4*	12,63 ± 1.3*
Plasma glucose (mg dl^{-1})	81.80 ± 5.9	89.70 ± 7.1	90.63 ± 8.5	85,63 ± 9,6*
Insulin (ng ml^{-1})	3.33 ± 0.8	6.84 ± 0.66*	6.12 ± 1.8*	6.41 ± 1,8*
FFA (mmol l^{-1})	0.63 ± 0.16	1.72 ± 0.27*	2.92 ± 0.4*#	ND
TNFα (pg ml^{-1})	42.6 ± 19.8	122.6 ± 14.1*	129.7 ± 17.4*	ND
K_{itt} (% min^{-1})	4.67 ± 0,14	2.4 ± 0,6*	4.89 ± 0,8#	4.72 ± 0.6#

$n = 8$ in each group. *$P < 0.001$ *versus* control group and #$P < 0.001$ *versus* DIO #P < 0.001 *versus* DIO, ND, not determined.

Other assays

Serum free fatty acids (FFA) levels were analysed in rats using the NEFA-kit-U (Wako Chemical GmBH, Neuss, Germany) with oleic acid as a standard. Serum levels of tumour necrosis factor α (TNF-α) was determined in rats using ELISA kits from Pierce Biotechnology (Rockford, IL, USA), according to the instructions of the manufacturer. Both analyses were determined 2 h after the acute exercise.

Statistical analysis

Where appropriate, the results were expressed as means ± S.E.M. Differences between the lean group and sedentary obese group and between the sedentary obese and the group submitted to the exercise protocol were evaluated using one-way analysis of variance (ANOVA). When ANOVA indicated significance, a Bonferroni *post hoc* test was performed.

Results

Physiological and metabolic parameters

Table 2 shows comparative data regarding controls (C), diet-induced obesity rats (DIO) and DIO rats submitted to exercise protocol (DIO + EXE-2 h and DIO + EXE-16 h). Rats fed on the high-fat diet for 12 weeks had a higher body weight, epididymal fat and fasting serum insulin than age-matched controls (C). No significant variations were found in body weight, epididymal fat and fasting serum insulin in DIO rats after a single session of exercise, compared to DIO rats. The fasting glucose concentrations were similar between the groups; however, the reduction in the glucose disappearance rate (K_{ITT}), induced by the high-fat diet, was restored 2 h and 16 h after acute exercise.

As expected, the plasma FFA levels were higher in obese rats, and acute exercise induced a marked increase in the levels of this substrate. Plasma levels of TNF-α were also higher in DIO rats, but there was not a clear increase in this cytokine after a bout of exercise.

A single bout of exercise improves insulin signalling in the muscle of DIO rats

The effect of *in vivo* I.V. insulin infusion on IR tyrosine phosphorylation was examined in the gastrocnemius muscle of controls, DIO rats and DIO rats submitted to exercise (after 2 h and 16 h). Fragments of muscle tissue were immunoprecipitated with anti-IR antibody and then blotted with antiphosphotyrosine antibody. In the control animals, insulin increased IR tyrosine phosphorylation by 6.9-fold over basal, compared with 2.4-fold over basal in the muscle of DIO rats. Insulin increased IR tyrosine phosphorylation by 7.6-fold and 4.8-fold over basal in the muscle from DIO + EXE-2 h and DIO + EXE-16 h rats, respectively, showing that exercise improves insulin-induced IR tyrosine phosphorylation in these rats (Fig. 1*A*). There was no difference in basal levels of IR tyrosine phosphorylation or in IR protein levels between the groups (Fig. 1*A*).

IRS1 tyrosine phosphorylation and IRS1/PI3–K association were observed to increase in control animals by 8.0-fold and 8.6-fold over basal following insulin administration, respectively, compared with 2.4-fold and 1.9-fold increases in the muscle of DIO rats over basal. Insulin increased IRS1 tyrosine phosphorylation and IRS1/PI3–K association by 7.1-fold and 7.5-fold and 5.3-fold and 5.8-fold in the muscle from DIO + EXE-2 h and DIO + EXE-16 h rats, respectively, over basal, showing that exercise improves insulin-induced IRS1 tyrosine phosphorylation in these rats (Fig. 1*B* and *C*). There was no difference in basal levels of IRS1 tyrosine phosphorylation or in IRS1 protein levels between the groups (Fig. 1*B*).

Finally, in gastrocnemius muscle from control rats, insulin increased Akt serine phosphorylation by 7.7-fold over basal, compared with a 2.4-fold increase in the muscle from DIO rats over basal. Similar to insulin-induced IR and IRS1 tyrosine phosphorylation, there was an increase of 7.9-fold and 5.2-fold in the muscle of DIO + EXE-2 h and DIO + EXE-16 h rats, respectively, over basal, showing that exercise improves insulin-induced

Akt phosphorylation in these rats (Fig. 1*D*). There were no differences between the basal levels of Akt serine phosphorylation or in Akt protein levels between the groups (Fig. 1*D*).

Acute physical exercise reverses *S*-nitrosation and restores insulin signalling in the muscle of diet-induced obesity rats.

In order to determine the time-course of the exercise-induced reduction in iNOS expression, we measured iNOS protein levels by immunoblotting in the muscle of obese rats that were submitted to the exercise protocol at 1, 2, 4 and 16 h after exercise. Results show that 2 h after exercise there is greater decrease in iNOS protein expression and that after 16 h this expression is still decreased compared to controls (Fig. 2*A*). In the muscle of DIO rats an enhanced expression of iNOS was found (Fig. 2*B*). We demonstrated an enhanced *S*-nitrosation of IRβ, IRS1, and Akt in the muscle of DIO rats, and this nitrosation was significantly reduced 2 h and 16 h after exercise in DIO rats (Fig. 2*C–E*).

The increase in AMPK phosphorylation induced by acute physical exercise inhibits iNOS and reverses insulin resistance in the muscle

In order to investigate the time-course of the exercise-induced increase in AMPK phosphorylation, we measured

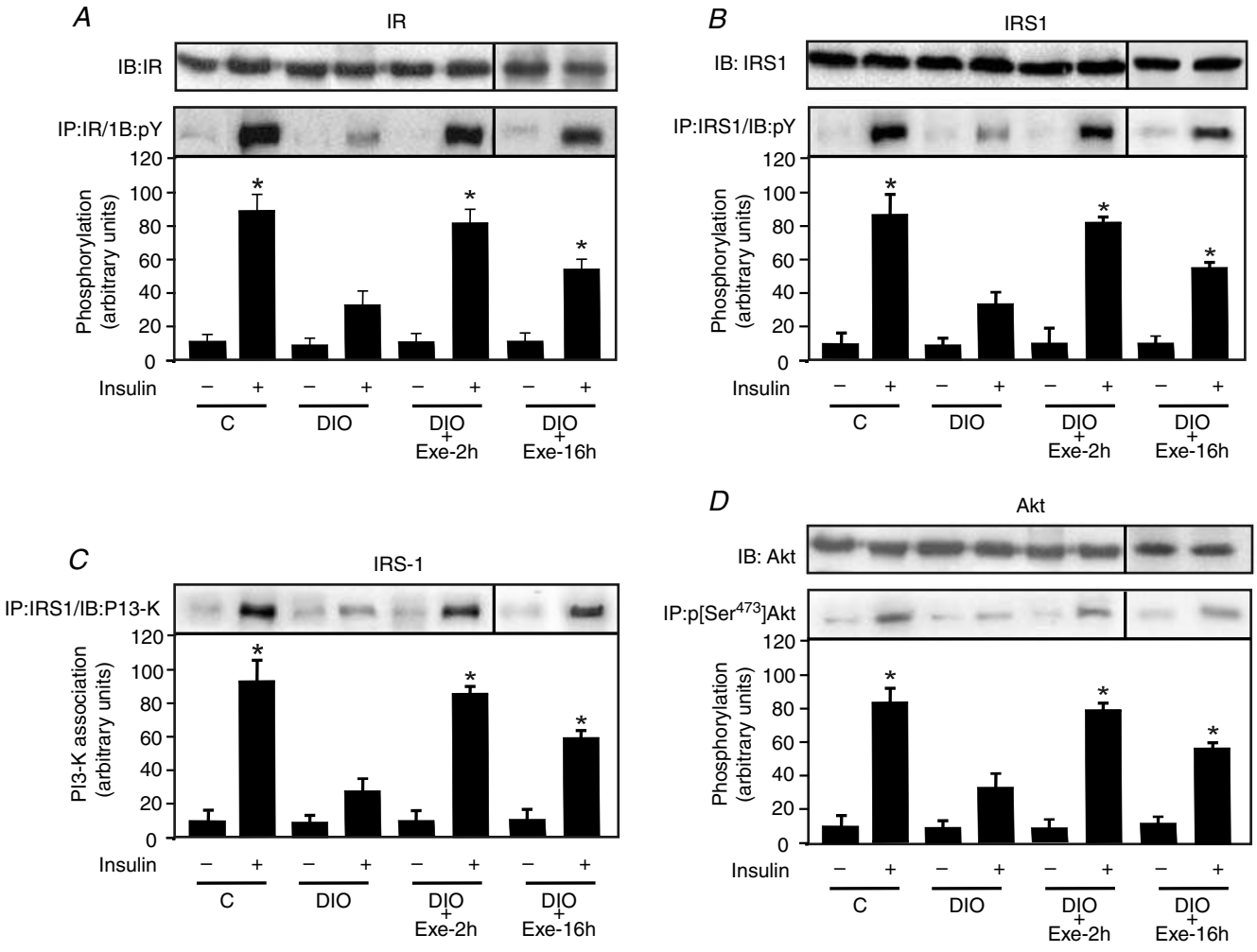

Figure 1. Insulin signalling in the muscle of controls, DIO and DIO rats submitted to exercise
Muscle extracts from rats injected with saline or insulin were prepared as described in Methods. *A*, tissue extracts were immunoprecipitated (IP) with anti-IRβ antibody and immunoblotted (IB) with anti-PY antibody or anti-IRβ antibody. *B*, tissue extracts were also IP with anti-IRS1 antibody and IB with anti-PY antibody and anti-IRS1 antibody, or *C*, anti-PI3-K antibodies. *D*, muscle extracts were IB with anti-Akt or antiphospho-[Ser^{473}] Akt antibodies. The results of scanning densitometry are expressed as arbitrary units. Bars represent means ± S.E.M. of eight rats. $^{*}P < 0.05$, *versus* DIO rats.

p-AMPK levels by immunoblotting. Physical exercise stimulated AMPK phosphorylation, which peaked at 1 h and then decreased, but phosphorylation at 16 h was still higher than basal (Fig. 3*A*). Two hours after exercise, in obese animals, in parallel with an increase in AMPK phosphorylation there was also an important increase in ACC phosphorylation, a downstream target of AMPK and a good correlate of its activation (Winder 2000). However, in obese animals (DIO) there was a decreased in AMPK and ACC phosphorylation when compared with control and DIO rats submitted to acute exercise protocol (Fig. 3*B* and *C*).

GSNO induces insulin resistance in muscle gastrocnemius *in vivo* by means of *S*-nitrosation

In order to investigate whether supplementation with a NO donor could abolish the effect of exercise in DIO rats, we administrated GSNO to obese rats for 8 h (every 2 h), and these animals were then submitted to the exercise protocol. Results showed that, in animals treated with GSNO, the effect of exercise on insulin sensitivity was abolished, as indicated by a lower plasma glucose disappearance rate during the insulin tolerance test (K_{ITT}) (Fig. 4*A*), suggesting that the reduction in nitrosation may be an important mechanism for the improvement of insulin

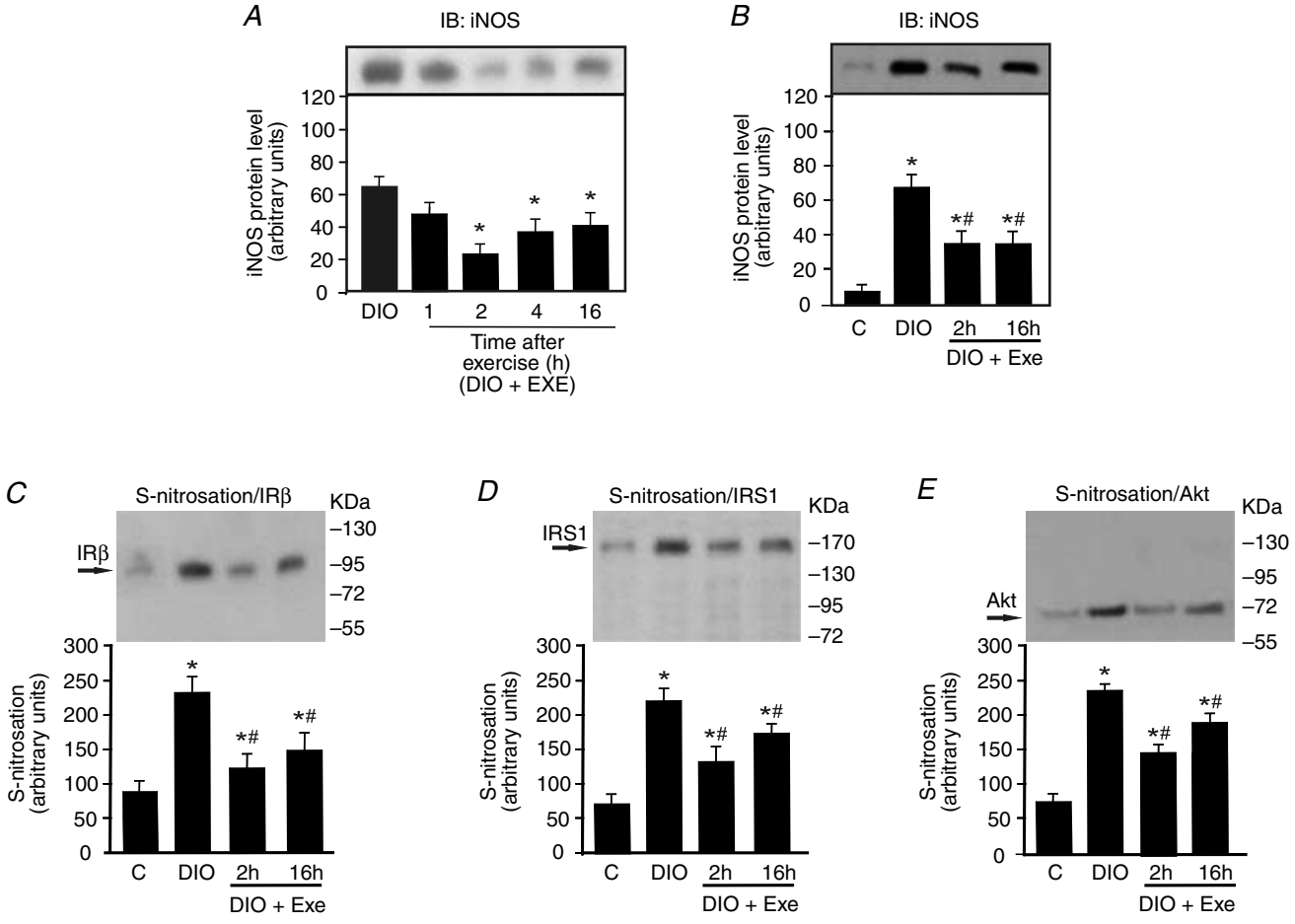

Figure 2. The protein iNOS expression and *S*-nitrosation of the proteins of the insulin signalling pathway in the gastrocnemius muscle of controls, DIO and DIO rats submitted to exercise
A, iNOS expression decreased 2 h after acute exercise, as demonstrated in the time course. However, the iNOS expression remained decreased for 16 h as compared to the DIO rats. *B*, iNOS expression was assessed by iNOS protein levels using Western blot, as described in Methods. *C–E*, *S*-nitrosation of IRβ (*C*), IRS1 (*D*), and Akt (*E*) is shown, as determined by the biotin-switch method. Bars represent means ± S.E.M. of eight rats. $^*P < 0.05$, *versus* control and $\#P < 0.05$, DIO + EXE *versus* DIO.

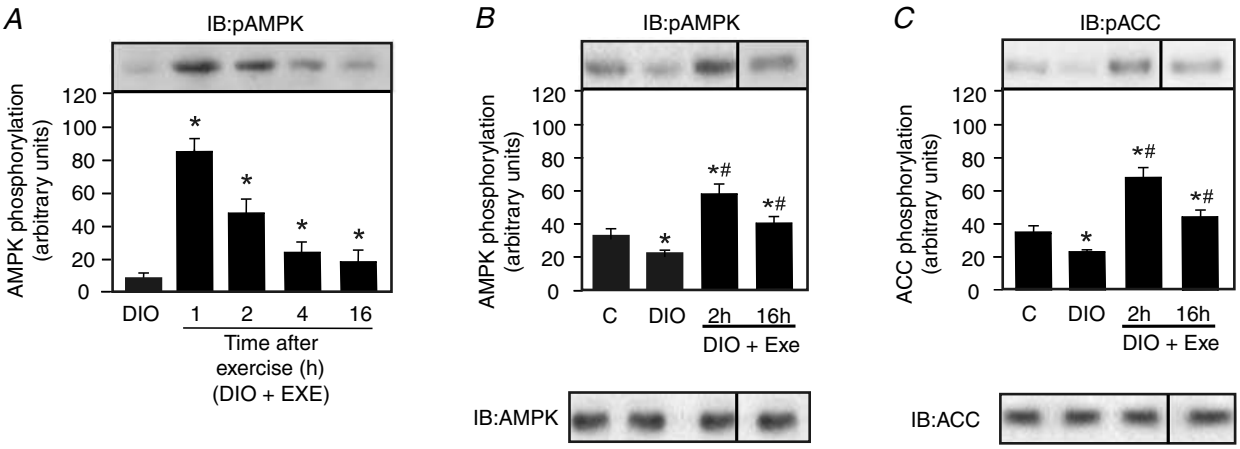

Figure 3. Expression and phosphorylation of AMPK and ACC in rat gastrocnemius muscles
A, physical exercise stimulated AMPK phosphorylation which peaked at 1 h and then decreased, but at 16 h it was still higher than basal. *B* and *C*, the results show that, in obese animals, 2 h after exercise, in parallel to an increase in AMPK phosphorylation there was also a significant important increase in ACC phosphorylation, a downstream target of AMPK and a good correlate of its activation (Winder 2000). Bars represent means ± S.E.M. of 16 rats (C and DIO) and 8 rats (DIO + EXE) $*P < 0.05$, *versus* control and $\#P < 0.05$, DIO + EXE *versus* DIO.

sensitivity induced by exercise. In accordance with these data, insulin-induced IR, IRS1 and Akt phosphorylation did not increase in GSNO-treated animals after exercise (Fig. 4*B–D*).

In the muscle of DIO rats, we found an enhanced expression of iNOS, and acute exercise reduces iNOS expression in GSNO-treated rats. (Fig. 4*E*). As expected, nitrosation of IRβ, IRS1, and Akt was not reduced after

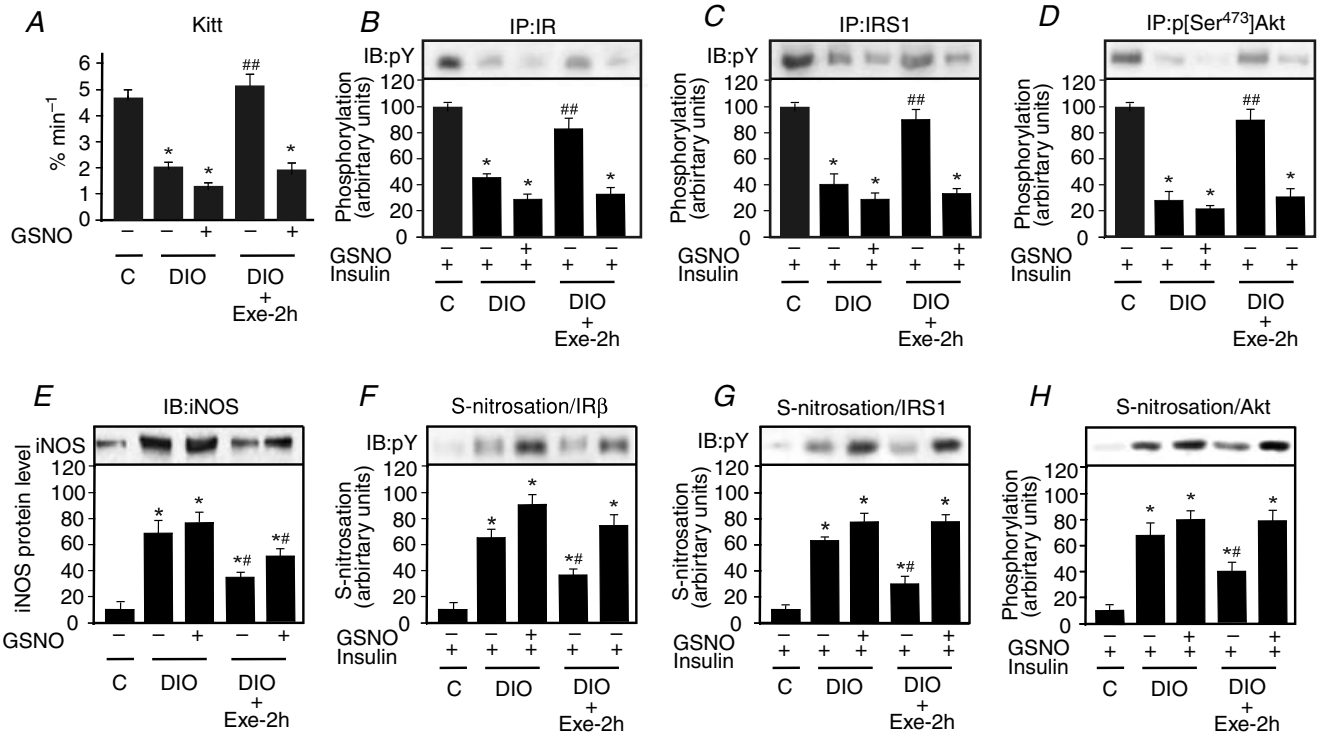

Figure 4. Effect of GSNO on insulin sensitivity and *S*-nitrosation in muscle of controls, DIO and DIO rats submitted to exercise
A, effect of GSNO treatment on glucose disappearance rates, measured by the 30-min insulin tolerance test (K_{ITT}). *B–D*, insulin-induced tyrosine phosphorylation of IRβ (*B*), IRS1 (*C*) and serine phosphorylation of Akt (*D*) followed by immunoprecipitation are shown. *E*, iNOS protein expression assessed by immunoblot is indicated. *F–H*, *S*-nitrosation of IRβ (*F*), IRS1 (*G*) and Akt (*H*) in muscle of animals, determined by the biotin switch method are shown. Bars represent means ± S.E.M. of six rats. $*P < 0.05$, *versus* control; $\#P < 0.05$, DIO + EXE *versus* DIO; $\#\#P < 0.05$, *versus* DIO or DIO + EXE-2 h plus GSNO injection.

exercise in GSNO-treated rats (Fig. 4*F–H*). These data suggest that the maintenance of nitrosation of IR, IRS1 and Akt by GSNO precludes the effect of exercise on insulin sensitivity.

The effects of an iNOS inhibitor on insulin resistance and *S*-nitrosation of proteins of the insulin signalling pathway

We next investigated whether an inhibitor of iNOS (L-NIL) could mimic the effect of exercise on insulin sensitivity and signalling in DIO rats. The administration of L-NIL for 10 days improved insulin sensitivity in DIO rats, as measured by the glucose disappearance rate during the insulin tolerance test, K_{ITT}, and no additive effect was observed in DIO animals that were treated with this drug and that exercised (Fig. 5*A*). In these experiments, insulin-induced IR, IRS1 and Akt phosphorylation was improved by L-NIL, furthermore, no additive effect was observed with exercise (Fig. 5*B–D*). L-NIL inhibits iNOS activity, but our results show that L-NIL has no effect on iNOS protein expression. As expected, L-NIL reduced IR, IRS1 and Akt *S*-nitrosation in DIO rats, and again no additive effect was observed with exercise (Fig. 5*E–H*).

Effect of treatment with GSNO or l-NIL on PTP1B protein levels, JNK activity and IRS1 serine phosphorylation in the muscle of controls, DIO and DIO + EXE rats

Diet-induced obesity is associated with an increased expression of PTP1B in muscle, and 2 h after an acute bout of exercise there is no change in this protein expression (Fig. 6*A*). The previous administration of a NO donor, GSNO, did not modify this increased expression of PTP1B.

JNK activation was determined by monitoring phosphorylation of JNK (Thr 183 and Tyr 185) (Fig. 6*B*). The high-fat diet induced an increase in JNK phosphorylation in the muscle of DIO rats when compared with control rats. Two hours after the exercise protocol is not sufficient to reverse the increase in JNK phosphorylation in the muscle of DIO rats. This phenomenon is not affected by a previous administration

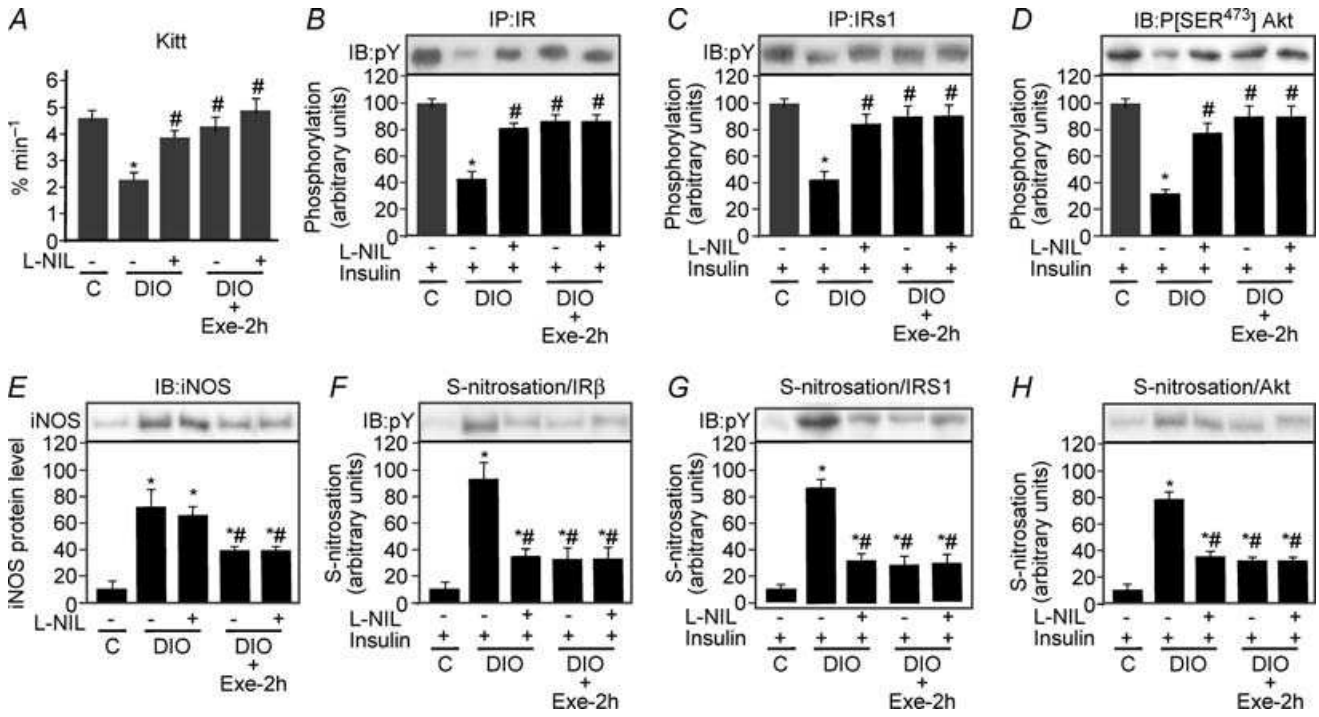

Figure 5. Effect of iNOS inhibitor (L-NIL) on insulin sensitivity and *S*-nitrosation in muscle of controls, DIO and DIO rats submitted to exercise
A, effect of treatment for 10 days with L-NIL on glucose disappearance rates, measured by the 30-min insulin tolerance test (K_{ITT}). *B–D*, insulin-induced tyrosine phosphorylation of IRβ (*B*), IRS1 (*C*) and serine phosphorylation of Akt (*D*) followed by immunoprecipitation are shown. *E*, iNOS protein expression assessed by immunoblot is indicated. *F–H*, *S*-nitrosation of IRβ (*F*), IRS1 (*G*) and Akt (*H*) in muscle of animals, determined by the biotin switch method are shown. Bars represent means ± S.E.M. of six rats. $^*P < 0.05$, *versus* control and $\#P < 0.05$, DIO + EXE *versus* DIO without GSNO injection.

of GSNO. Similar results were observed for IRS1 Ser307 phosphorylation (Fig. 6*C*).

The administration of L-NIL, which is an inhibitor of iNOS, did not affect the increase in PTP1B protein expression (Fig. 6*D*), JNK phosphorylation (Fig. 6*E*), or IRS1 Ser307 phosphorylation (Fig. 6*F*), induced by high-fat diet.

Discussion

The impaired insulin action on whole-body glucose uptake is a hallmark feature of type 2 diabetes mellitus. Physical exercise has been linked to improved glucose homeostasis and enhanced insulin sensitivity after an acute bout of exercise in humans (Devlin *et al.* 1987; Zierath, 1995) and rodents (Richter *et al.* 1982; Wallberg-Henriksson, 1987; Wallberg-Henriksson *et al.* 1988). In this study, we demonstrated that a high-fat diet leads to an increase in the iNOS protein level and *S*-nitrosation of IRβ, IRS1 and Akt. Interestingly, an acute bout of exercise reduces iNOS expression and *S*-nitrosation of proteins involved in the early steps of insulin action and improves insulin sensitivity in DIO rats.

Several mechanisms may be involved in insulin resistance in the muscle of DIO rats, including serine phosphorylation of IR or IRSs (induced by serine kinases such as mTOR, and the stress kinases, JNK and IKKβ IAB kinase), by an increase in the activity or amount of the enzymes that normally reverse insulin action (e.g. PTP1B) or by an increase in iNOS (Hotamisligil *et al.* 1996; Bedard *et al.* 1997; Elchebly *et al.* 1999; Perreault & Marette, 2001; Hirosumi *et al.* 2002; Carvalho-Filho *et al.* 2005; Ropelle *et al.* 2006). In several situations of insulin resistance, such as diet-induced or genetic obesity, and endotoxaemia, iNOS is induced in tissues classically related to insulin signalling (Bedard *et al.* 1997; Kapur *et al.* 1997; Kapur *et al.* 1999). Perreault & Marette (2001) demonstrated that the genetic disruption of iNOS protects against obesity-linked insulin resistance, preventing impairments in PI3-K and Akt activation by insulin in muscle.

We recently demonstrated that the insulin resistance associated with iNOS induction is mediated by

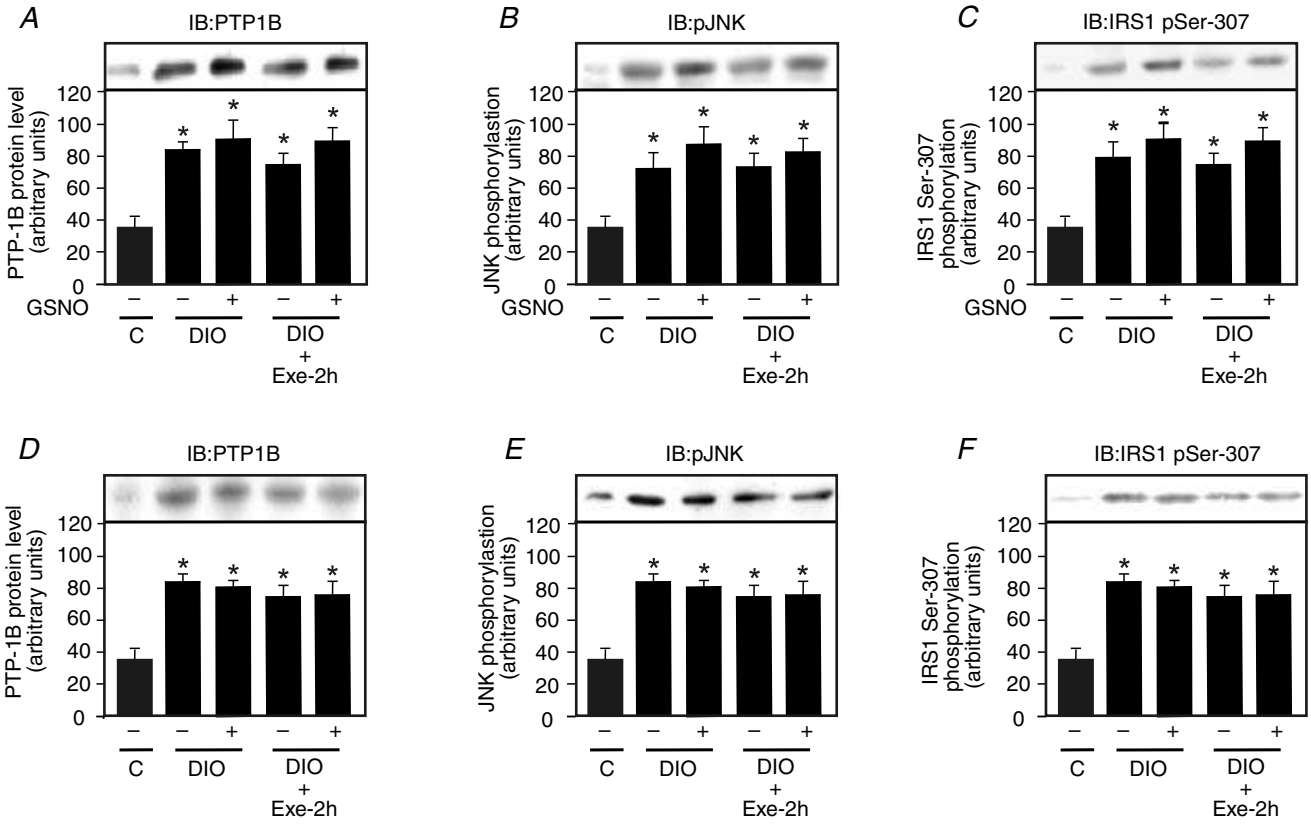

Figure 6. Effect of GSNO or L-NIL on PTP1B protein levels, JNK activity and IRS1 serine phosphorylation in the muscle of controls, DIO and DIO rats submitted to exercise
Tissue extracts were immunoblotted (IB) with anti-PTP1B antibody (*A* and *D*), antiphospho-JNK antibody (*B* and *E*), anti-IRS1307 phosphoserine antibody (*C* and *F*). Bars represent means ± S.E.M. of eight rats. $^*P < 0.05$, *versus* control.

S-nitrosation of proteins involved in insulin signal transduction, i.e, insulin receptor β-subunit, insulin receptor substrate 1 (IRS1), and Akt. *S*-nitrosation of IRβ reduces its autophosphorylation and tyrosine-kinase activity and *S*-nitrosation of IRS1 is associated with its reduced tissue expression (Carvalho-Filho *et al.* 2005; Carvalho-Filho *et al.* 2006). In addition, *S*-nitrosation of Akt is associated with a decreased serine kinase activity of this enzyme in basal states and after insulin stimulation. *S*-nitrosation of these proteins is associated with the down-regulation of the IRβ/IRS1/PI3-K/Akt pathway. Since this pathway plays a central role in the metabolic actions of insulin in the muscle, including stimulation of glucose uptake and glycogen synthesis, down-regulation of this pathway in muscle by *S*-nitrosation may be an important mechanism of iNOS-induced insulin resistance. Interestingly, our data show that a single bout of exercise in DIO rats reduced iNOS expression and the *S*-nitrosation of IRβ/IRS1/Akt in skeletal muscle. In accordance, it has recently been demonstrated in muscle biopsies that a regular exercise programme reduces the local expression of cytokines and iNOS (Gielen *et al.* 2003). Our data show that the effect of exercise, in reducing iNOS expression and decreasing *S*-nitrosation of proteins involved in early steps of insulin action, was accompanied by an improvement in insulin sensitivity and an increase in insulin-induced IRβ, IRS1 and Akt phosphorylation. In addition, our data reinforce this mechanism by showing, first, that treatment with a NO donor (GSNO) prevents the beneficial effect of exercise on insulin sensitivity and, secondly, by showing that upon inhibition of this latter situation there is no additive effect of exercise.

Some of our results differ from other studies on acute exercise (Chibalin *et al.* 2000; Arias *et al.* 2007), which showed unchanged serine phosphorylated Akt, but increased threonine phosphorylated Akt. The reasons for these differences are not completely clear, but certainly methodological differences may contribute to these discrepancies. In previous reports (Chibalin *et al.* 2000; Arias *et al.* 2007), insulin signalling was investigated in isolated muscle after *in vitro* incubation; however, our results were obtained after *in vivo* insulin stimulation. In addition, these previous studies investigated control rats, while in the present study we investigated the effect of exercise on DIO rats.

Exercise and muscle contraction have been shown to enhance NO production and NOS expression in muscle (Balon & Nadler, 1997). Previous data show that low doses of NO donors can increase glucose uptake and improve insulin action (McGrowder *et al.* 2006). We also investigated whether administration of low doses of GSNO (1 μM) can induce improved glucose uptake and/or changes in *S*-nitrosation of proteins during the early steps of insulin action in the muscle of rats. These results showed that at low doses, an NO donor (GSNO) improved glucose uptake, but did not induce *S*-nitrosation of IR, IRS1, PI3-K or Akt in muscle (data not shown). Although the mechanisms by which administration of low doses of NO can improve insulin sensitivity are not well established, our data suggest that changes in the *S*-nitrosation status of proteins involved in the insulin signalling pathway are not involved. In addition, it is important to emphasize that exercise induces neuronal and endothelial nitric-oxide synthase (nNOS and eNOS, also termed NOS1 and NOS3, respectively) and not iNOS (also termed NOS2) expression. We can, thus, suggest that the effect of NO on insulin sensitivity is dose dependent and also depends on the enzyme that generates NO, which is expressed in different sites.

The mechanism by which exercise reduces iNOS expression in DIO rats is not completely understood, but it may be mediated, at least in part, by an increase in AMPK. It is well known that exercise activates AMPK, and this is believed to contribute to its insulin-sensitizing action in situations of insulin resistance (Wojtaszewski *et al.* 2005). Data from different sources indicate that AMPK activation reduces iNOS induction and blunts iNOS-mediated NO production (Bedard *et al.* 1997; Kapur *et al.* 1997; Pilon *et al.* 2004). In accordance with these previous data, we show that, in the muscle of DIO rats, an acute bout of exercise is accompanied by an increase in AMPK activation and a reduction in iNOS expression.

In addition, it should be taken into consideration that insulin resistance is a metabolic situation that is related to several molecular mechanisms that act in parallel to down-regulate insulin signalling. Since exercise is an efficient way to improve insulin sensitivity, it is possible that it may also act in other mechanisms of insulin resistance. In this regard, we recently verified an attenuation of the increase in the expression and activity of the PTP1B 16 h after a single session of exercise (Ropelle *et al.* 2006). In this same exercise protocol, we also observed the reverse of JNK activation and the increase of serine phosphorylation of IRS1 in muscle of DIO rats.

Taking these data together with our data, we can suggest that exercise reverses the multiple mechanisms that can contribute to insulin resistance. However, the present data show that GSNO, which induces insulin resistance and impairs exercise-induced improvement in insulin action, does not affect JNK phosphorylation, PTP1B expression or IRS1 serine phosphorylation. In addition L-NIL, an inhibitor of iNOS improves insulin action and insulin signalling in DIO rats without influencing JNK phosphorylation, PTP1B expression or IRS1 serine phosphorylation. These data suggest that *S*-nitrosation is an important mechanism of insulin resistance, and reversal of this mechanism is sufficient to improve insulin action and signalling.

It is possible that common upstream events could mediate the increased activation of JNK, *S*-nitrosation

and iNOS expression in DIO rats, and that this common mechanism is reversed by exercise. We investigated some candidates and our data showed that 2 h after exercise there is a marked increase in FFA levels and almost no change in TNF-α levels, suggesting that these are probably not common upstream events in DIO and are not reversed by exercise. It is important to emphasize that JNK, *S*-nitrosation and iNOS can be activated by toll-like receptor 4 (TLR4), which is a pattern recognition receptor also present in muscle (Shi *et al.* 2006; Tsukumo *et al.* 2007). It was recently demonstrated in humans that exercise down-regulates TLR4 in monocytes (Lancaster *et al.* 2005), suggesting that this receptor may be a candidate for the activation of JNK, iNOS and *S*-nitrosation in obesity, and may be reversed by exercise.

It has been recently demonstrated that in humans, 15–18 h after a single session of exercise there is protection against fatty acid-induced insulin resistance and that this protective effect of exercise is accompanied by an increased lipogenic capacity of muscle and a resulting increase in partitioning of excess fatty acids toward triglyceride synthesis in muscle. This repartitioning of fatty acids after exercise toward intramyocellular triglyceride (IMTG) synthesis and oxidation reduced the accumulation of bioactive fatty acid metabolites, which are known to increase the activation of proinflammatory pathways in skeletal muscle and induce insulin resistance (Schenk & Horowitz, 2007). Similar results were obtained by transgenic overexpression of diacylglycerol acyltransferase (DGAT1) in mouse skeletal muscle, which mitigated the detrimental effect of fatty acids, and protected mice against high-fat diet-induced insulin resistance (Liu *et al.* 2007).

Our data show that, at 2 h after exercise in DIO rats, insulin sensitivity and insulin signalling were completely normalized; however, at 16 h after exercise, despite the normal insulin sensitivity there is only a partial restoration of insulin signalling. These data suggest that the complete normalization, by acute exercise, of the insulin action in obesity induced by diet may be caused by other factors and may involve other pathways. It is important to mention that the doses of insulin used were 3–4 times higher than the dose required for maximal insulin signalling, suggesting a possibility of spare insulin signalling under these conditions. This may involve proteins of the insulin signalling pathway not investigated, such as aPKC (protein kinase C), or other pathways such as cbl associated protein (CAP)/Casitas b lineage lymphoma (Cbl), which have a controversial role in insulin-induced glucose uptake in skeletal muscle. Another possibility may be associated with the haemodynamic changes induced by exercise. It is known that a single bout of exercise decreases sympathetic activity and increases muscle blood flow during the postexercise period. It is interesting that, during hyperinsulinaemia after a single bout of exercise, sympathetic activity is lower and muscle vasodilation is higher. These haemodynamic changes may also contribute to the reversion of the insulin resistance (Bisquolo *et al.* 2005). These data are in accordance with previous data demonstrating that exercise improves insulin-induced glucose uptake, at least in part, as a result of haemodynamic adaptations.

One limitation of the proposed theory of exercise-induced insulin sensitization in this study is that iNOS is normally not expressed in muscle (Kapur *et al.* 1997), and its expression is only induced in states of insulin resistance. However, exercise can also improve insulin action in healthy muscle. Therefore, this theory may not provide a universal explanation and, hence, is probably only one of several factors involved in the improvement of insulin sensitivity induced by exercise in DIO.

In summary, a single bout of exercise reverses insulin sensitivity in DIO rats by improving the insulin signalling pathway, in parallel with a decrease in iNOS expression and in the *S*-nitrosation of IR/IRS1/Akt. These results provide new insights into the mechanism by which exercise restores insulin sensitivity in DIO rats.

References

Arias EB, Kim J, Funai K & Cartee GD (2007). Prior exercise increases phosphorylation of Akt substrate of 160 kDa (AS160) in rat skeletal muscle. *Am J Physiol Endocrinol Metab* **292**, E1191–E1200.

Balon TW & Nadler JL (1997). Evidence that nitric oxide increases glucose transport in skeletal muscle. *J Appl Physiol* **82**, 359–363.

Bedard S, Marcotte B & Marette A (1997). Cytokines modulate glucose transport in skeletal muscle by inducing the expression of inducible nitric oxide synthase. *Biochem J* **325**, 487–493.

Betts JJ, Sherman WM, Reed MJ & Gao JP (1993). Duration of improved muscle glucose uptake after acute exercise in obese Zucker rats. *Obes Res* **1**, 295–302.

Bisquolo VA, Cardoso CG Jr, Ortega KC, Gusmao JL, Tinucci T, Negrao CE, Wajchenberg BL, Mion D Jr & Forjaz CL (2005). Previous exercise attenuates muscle sympathetic activity and increases blood flow during acute euglycemic hyperinsulinemia. *J Appl Physiol* **98**, 866–871.

Bonora E, Moghetti P, Zancanaro C, Cigolini M, Querena M, Cacciatori V, Corgnati A & Muggeo M (1989). Estimates of *in vivo* insulin action in man: comparison of insulin tolerance tests with euglycemic and hyperglycemic glucose clamp studies. *J Clin Endocrinol Metab* **68**, 374–378.

Broillet MC & Firestein S (1996). Direct activation of the olfactory cyclic nucleotide-gated channel through modification of sulfhydryl groups by NO compounds. *Neuron* **16**, 377–385.

Bruce CR, Lee JS & Hawley JA (2001). Postexercise muscle glycogen resynthesis in obese insulin-resistant Zucker rats. *J Appl Physiol* **91**, 1512–1519.

Carvalho-Filho MA, Ueno M, Carvalheira JB, Velloso LA & Saad MJ (2006). Targeted disruption of iNOS prevents LPS-induced *S*-nitrosation of IRbeta/IRS-1 and Akt and insulin resistance in muscle of mice. *Am J Physiol Endocrinol Metab* **291**, E476–E482.

Carvalho-Filho MA, Ueno M, Hirabara SM, Seabra AB, Carvalheira JB, de Oliveira MG, Velloso LA, Curi R & Saad MJ (2005). *S*-nitrosation of the insulin receptor, insulin receptor substrate 1, and protein kinase B/Akt: a novel mechanism of insulin resistance. *Diabetes* **54**, 959–967.

Chibalin AVYuM, Ryder JW, Song XM, Galuska D, Krook A, Wallberg-Henriksson H & Zierath JR (2000). Exercise-induced changes in expression and activity of proteins involved in insulin signal transduction in skeletal muscle: differential effects on insulin-receptor substrates 1 and 2. *Proc Natl Acad Sci U S A* **97**, 38–43.

Devlin JT, Hirshman M, Horton ED & Horton ES (1987). Enhanced peripheral and splanchnic insulin sensitivity in NIDDM men after single bout of exercise. *Diabetes* **36**, 434–439.

Elchebly M, Payette P, Michaliszyn E, Cromlish W, Collins S, Loy AL, Normandin D, Cheng A, Himms-Hagen J, Chan CC, Ramachandran C, Gresser MJ, Tremblay ML & Kennedy BP (1999). Increased insulin sensitivity and obesity resistance in mice lacking the protein tyrosine phosphatase-1B gene. *Science* **283**, 1544–1548.

Fiedler M, Zierath JR, Selen G, Wallberg-Henriksson H, Liang Y & Sakariassen KS (2001). 5-aminoimidazole-4-carboxy-amide-1-beta-D-ribofuranoside treatment ameliorates hyperglycaemia and hyperinsulinaemia but not dyslipidaemia in KKAy-CETP mice. *Diabetologia* **44**, 2180–2186.

Gielen S, Adams V, Mobius-Winkler S, Linke A, Erbs SYuJ, Kempf W, Schubert A, Schuler G & Hambrecht R (2003). Anti-inflammatory effects of exercise training in the skeletal muscle of patients with chronic heart failure. *J Am Coll Cardiol* **42**, 861–868.

Gross SS & Wolin MS (1995). Nitric oxide: pathophysiological mechanisms. *Annu Rev Physiol* **57**, 737–769.

Hirosumi J, Tuncman G, Chang L, Gorgun CZ, Uysal KT, Maeda K, Karin M & Hotamisligil GS (2002). A central role for JNK in obesity and insulin resistance. *Nature* **420**, 333–336.

Hotamisligil GS, Peraldi P, Budavari A, Ellis R, White MF & Spiegelman BM (1996). IRS-1-mediated inhibition of insulin receptor tyrosine kinase activity in TNF-alpha- and obesity-induced insulin resistance. *Science* **271**, 665–668.

Jaffrey SR & Snyder SH (2001). The biotin switch method for the detection of *S*-nitrosylated proteins. *Sci STKE* **2001**(86), PL1.

Kapur S, Bedard S, Marcotte B, Cote CH & Marette A (1997). Expression of nitric oxide synthase in skeletal muscle: a novel role for nitric oxide as a modulator of insulin action. *Diabetes* **46**, 1691–1700.

Kapur S, Marcotte B & Marette A (1999). Mechanism of adipose tissue iNOS induction in endotoxemia. *Am J Physiol Endocrinol Metab* **276**, E635–E641.

Laemmli UK (1970). Cleavage of structural proteins during the assembly of the head of bacteriophage T4. *Nature* **227**, 680–685.

Lancaster GI, Khan Q, Drysdale P, Wallace F, Jeukendrup AE, Drayson MT & Gleeson M (2005). The physiological regulation of toll-like receptor expression and function in humans. *J Physiol* **563**, 945–955.

Lander HM, Ogiste JS, Pearce SF, Levi R & Novogrodsky A (1995). Nitric oxide-stimulated guanine nucleotide exchange on p21ras. *J Biol Chem* **270**, 7017–7020.

Lane P & Gross SS (1999). Cell signaling by nitric oxide. *Semin Nephrol* **19**, 215–229.

Liu L, Zhang Y, Chen N, Shi X, Tsang B & Yu YH (2007). Upregulation of myocellular DGAT1 augments triglyceride synthesis in skeletal muscle and protects against fat-induced insulin resistance. *J Clin Invest* **117**, 1679–1689.

Martinez-Ruiz A & Lamas S (2004). Detection and proteomic identification of S-nitrosylated proteins in endothelial cells. *Arch Biochem Biophys* **423**, 192–199.

McGrowder D, Ragoobirsingh D & Brown P (2006). Modulation of glucose uptake in adipose tissue by nitric oxide-generating compounds. *J Biosci* **31**, 347–354.

Molina y Vedia L, McDonald B, Reep B, Brune B, Di Silvio M, Billiar TR & Lapetina EG (1992). Nitric oxide-induced *S*-nitrosylation of glyceraldehyde-3-phosphate dehydrogenase inhibits enzymatic activity and increases endogenous ADP-ribosylation. *J Biol Chem* **267**, 24929–24932.

Perreault M & Marette A (2001). Targeted disruption of inducible nitric oxide synthase protects against obesity-linked insulin resistance in muscle. *Nat Med* **7**, 1138–1143.

Pilon G, Dallaire P & Marette A (2004). Inhibition of inducible nitric-oxide synthase by activators of AMP-activated protein kinase: a new mechanism of action of insulin-sensitizing drugs. *J Biol Chem* **279**, 20767–20774.

Richter EA, Garetto LP, Goodman MN & Ruderman NB (1982). Muscle glucose metabolism following exercise in the rat: increased sensitivity to insulin. *J Clin Invest* **69**, 785–793.

Ropelle ER, Pauli JR, Prada PO, de Souza CT, Picardi PK, Faria MC, Cintra DE, Fernandes MF, Flores MB, Velloso LA, Saad MJ & Carvalheira JB (2006). Reversal of diet-induced insulin resistance with a single bout of exercise in the rat: the role of PTP1B and IRS-1 serine phosphorylation. *J Physiol* **577**, 997–1007.

Saad MJ, Maeda L, Brenelli SL, Carvalho CR, Paiva RS & Velloso LA (1997). Defects in insulin signal transduction in liver and muscle of pregnant rats. *Diabetologia* **40**, 179–186.

Schenk S & Horowitz JF (2007). Acute exercise increases triglyceride synthesis in skeletal muscle and prevents fatty acid-induced insulin resistance. *J Clin Invest* **117**, 1690–1698.

Scott MD, Kuypers FA, Butikofer P, Bookchin RM, Ortiz OE & Lubin BH (1990). Effect of osmotic lysis and resealing on red cell structure and function. *J Lab Clin Med* **115**, 470–480.

Shi H, Kokoeva MV, Inouye K, Tzameli I, Yin H & Flier JS (2006). TLR4 links innate immunity and fatty acid-induced insulin resistance. *J Clin Invest* **116**, 3015–3025.

Shishido SM, Seabra AB, Loh W & Ganzarolli de Oliveira M (2003). Thermal and photochemical nitric oxide release from *S*-nitrosothiols incorporated in Pluronic F127 gel: potential uses for local and controlled nitric oxide release. *Biomaterials* **24**, 3543–3553.

Stamler JS, Simon DI, Osborne JA, Mullins ME, Jaraki O, Michel T, Singel DJ & Loscalzo J (1992). *S*-nitrosylation of proteins with nitric oxide: synthesis and characterization of biologically active compounds. *Proc Natl Acad Sci U S A* **89**, 444–448.

Stamler JS, Toone EJ, Lipton SA & Sucher NJ (1997). (S) NO signals: translocation, regulation, and a consensus motif. *Neuron* **18**, 691–696.

Sugita H, Fujimoto M, Yasukawa T, Shimizu N, Sugita M, Yasuhara S, Martyn JA & Kaneki M (2005). Inducible nitric-oxide synthase and NO donor induce insulin receptor substrate-1 degradation in skeletal muscle cells. *J Biol Chem* **280**, 14203–14211.

Tsukumo DM, Carvalho-Filho MA, Carvalheira JB, Prada PO, Hirabara SM, Schenka AA, Araujo EP, Vassallo J, Curi R, Velloso LA & Saad MJ (2007). Loss-of-function mutation in Toll-like receptor 4 prevents diet-induced obesity and insulin resistance. *Diabetes* **56**, 1986–1998.

Wallberg-Henriksson H (1987). Glucose transport into skeletal muscle. Influence of contractile activity, insulin, catecholamines and diabetes mellitus. *Acta Physiol Scand Suppl* **564**, 1–80.

Wallberg-Henriksson H, Constable SH, Young DA & Holloszy JO (1988). Glucose transport into rat skeletal muscle: interaction between exercise and insulin. *J Appl Physiol* **65**, 909–913.

Winder WW (2000). AMP-activated protein kinase: possible target for treatment of type 2 diabetes. *Diabetes Technol Ther* **2**, 441–448.

Wojtaszewski JF, Birk JB, Frosig C, Holten M, Pilegaard H & Dela F (2005). 5′AMP activated protein kinase expression in human skeletal muscle: effects of strength training and type 2 diabetes. *J Physiol* **564**, 563–573.

Zierath JR (1995). In vitro studies of human skeletal muscle: hormonal and metabolic regulation of glucose transport. *Acta Physiol Scand Suppl* **626**, 1–96.

Acknowledgements

The authors thank Mr Luiz Janeri, Mr Jósimo Pinheiro and Márcio Alves da Cruz for their technical assistance. This work was supported by Grants from Fundação de Amparo à Pesquisa do Estado de São Paulo (FAPESP) and Conselho Nacional de Pesquisa (CNPq).